UNIVERSITEIT VAN PRETORIA
UNIVERSITY OF PRETORIA
YUNIBESITHI YA PRETORIA

Anti-inflammatory and anti-diabetic properties of plant extracts and compounds from *Scabiosa columbaria* and *Sclerocarya birrea*

by

CHIDINMA CHRISTIANA EZEOFOR

U17395918

Submitted in partial fulfilment of the requirements for the degree

PHILOSOPHIAE DOCTOR **CHEMISTRY**

Department of Chemistry

In the Faculty of Natural and Agricultural Sciences

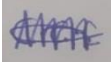**UNIVERSITY OF PRETORIA**

SOUTH AFRICA

Supervisor: Dr Dashnie Naidoo-Maharaj

Co-supervisor: Professor Vinesh Maharaj

December 2023

Submission declaration

I, <u>Chidinma Christiana Ezeofor</u>, declare that the thesis which I hereby submit for the degree of *Philosophiae Doctor* in the Department of Chemistry, at the University of Pretoria, is my own work and has not previously been submitted by me for a degree at this or any other tertiary institution.

Signature: …………………

Date: 29/2/2024………..

Plagiarism declaration
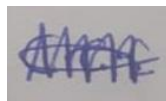
Full names of student: Chidinma Christiana Ezeofor

Student number: 17395918

Title of work: Anti-inflammatory and anti-diabetic properties of plant extracts and compounds from *Scabiosa columbaria* and *Sclerocarya birrea*

Declaration

1. I understand what plagiarism is and I am aware of the University's policy in this regard.
2. I declare that this thesis is my own original work. Where other people's work has been used (either from a printed source, internet or any other source), due acknowledgement was given, and reference was made according to departmental requirements.
3. I did not make use of another student's previous work and submit it as my own.
4. I did not allow and will not allow anyone to copy my work with the intention of presenting it as his or her own work.

Signature   Date: 29/2/2024

Dedication

This thesis is dedicated to my beloved parents Mr. and Mrs. Jonathan Ezeofor for their support and contributions towards my studies, my beloved husband Dr K.G Akpomie for his support and encouragement all through this program, my children Eseoghene and Oghenetega, my precious gifts from God and finally my siblings for their encouragement and advice.

Acknowledgements

Summary

Given that South Africa is home to around 10% of all flowering plant species known to humans, the country is blessed with an abundance of natural resources. About 24,000 plant species have yet to be fully uncovered for the benefit of humanity, making this a significant resource. The use of traditional medicine to cure illnesses is still widespread in South Africa despite the country's rapid urban and infrastructure development, more westernization, and accessibility to typical western medical institutions. Intricately woven within South African culture, the use of medicinal plants to heal illnesses is still prevalent. Additionally, due to Africa's failing healthcare system, using medicinal plants for health reasons is a well-accepted alternative that is practiced by all races, classes, and socio-economic classes. Bio-active extracts, fractions, and compounds have been identified as effective treatments for inflammatory and diabetic disorders based mostly on ethnomedicinal and empirical knowledge on traditional applications of plants. South Africa is a country with a high plant diversity of over 30,000 species of higher plants and 3,000 of these plant species have been found to be used in the traditional medicine for anti-inflammatory purposes. Inspired by the traditional uses of plant species, various scientists have studied the anti-inflammatory activities of South African plant species.

Current cosmeceutical and drug discoveries rely on the massive screening of natural product libraries against various extracellular and intracellular molecular targets to find novel chemotypes with the desired mode of action. In the pharmaceutical and cosmeceutical industries, there is an increasing interest in the demand for natural ingredients with potential health benefits, such as anti-inflammatory, anti-diabetic, and anti-cancer properties, in an effort to replace or lessen the usage of synthetic products. With 60% of marketed pharmaceuticals and cosmeceuticals, natural ingredients have long been a key source of medicinal and cosmeceutical scaffolds. Nature continues to prove to be a source of new bioactive molecules with high safety profiles, despite the fact that many synthetic chemists are focused on synthesizing potent compounds with high toxicity profiles for pharmaceutical and cosmeceutical goals. Therefore, natural product chemists keep looking for novel leads. As a continuation of these efforts, this study aimed to identify and develop new natural anti-inflammatory ingredients from selected South African plant species for commercial application in different market sectors based on their traditional uses and literature data and

to isolate and characterize biologically active compounds using modern hyphenated analytical techniques from biologically active plant species.

A literature survey was carried out to identify South African plants based on their traditional uses to include in this study. A scoring system was applied to rank them and 3 plant species (*Scabiosa columbaria*, *Commiphora pyracanthoides* and *Pelargonium capitatum*) belonging to three families were selected. The 3 plant species were collected from the University of Pretoria Experimental farm, KwaZulu Natal and Limpopo and extracted singly using cosmetic acceptable solvents (acetone, ethanol water/ethanol (1:1) and water). The extracts were tested in different assays (anti-inflammatory and skin even tone). After testing different extracts of the plant species, the ethanol extract of *S. columbaria* roots was selected for further evaluation to identify the compound/s responsible for the anti-inflammatory activity and development as a potential active herbal ingredient based on good anti-inflammatory efficacy data and no anti-inflammatory reports in the literature.

UPLC-QTOF-MS analysis of the ethanol extract of *S. columbaria* roots led to the tentative identification of fifteen compounds which are loganic acid (**53**) scrophuloside A1 (**peak 2**), 3,4-dicaffeoylquinic acid (**peak 3**), cantleyoside (**peak 4**), sylvestroside III (**peak 5**), triplostoside A (**54**), hederagenin (**55**), maslinic acid (**peak 8**), 2-isoursolic acid (**56**), glycyrrhetaldehyde (**peak 10**), pomaceic acid (**57**), euscaphic acid (**58**) and 3-oxoglycyrrhetinic acid (**61**).

The presence of loganic acid (**62**), cantleyoside -dimethyl-acetal (**63**), ursolic acid (**64**), 2-isoursolic acid (**65**), 24-nor-2α,3β-dihydroxyolean-4(23),12-ene (**66**) and hederagenin (**67**) in the ethanol extract of *S. columbaria* roots was confirmed by isolation and structure elucidation of the compounds using MS and NMR data. Significant reduction of nitric oxide levels in RAW 264.7 macrophages was observed for ursolic acid (**64**) (12.5, 25 and 50 µg mL^{-1}; 0.0702, 0.0558 and 0.0357 µg/mLrespectively), 24-nor-2α,3β-dihydroxyolean-4(23),12-ene (**66**) (12.5, 25 and 50 µg mL^{-1}; 0.0543, 0.0327 and 0.0231 µg/mLrespectively) and hederagenin (**67**) (12.5 and 25 µg mL^{-1}; 0.0735 and 0.0513 µg/mLrespectively) compared to the positive control aminoguanidine (12.5 µg mL^{-1}; 0.0336 µg mL^{-1}). At a concentration of 25 and 50 µg mL^{-1}, 24-nor-2α,3β-dihydroxyolean-4(23),12-ene (**66**) demonstrated a potent reduction in nitric oxide level in RAW 264.7 macrophages. The compounds identified in the ethanol extract of *S. columbaria* roots will be used as chemical markers for quality control

purposes, for batch-to-batch reproducibility that is required for commercializing the herbal ingredient. The anti-inflammatory activity of 24-nor-2α,3β-dihydroxyolean-4(23),12-ene (**66**) has been reported for the first time in this work. The active compounds (ursolic acid (**64**), 24-nor-2α,3β-dihydroxyolean-4(23),12-ene (**66**) and hederagenin (**67**)) were structurally similar and contained a β-hydroxy group at C-3. The compound 2- isoursolic acid (**65**) was inactive and had a hydroxy group at C-2 instead of C-3, which suggests that the position of the β-hydroxy group may play a role in the nitric oxide inhibition activity. A concentrated form of the ethanol extract of *S. columbaria* roots can be developed to have a higher concentration of the active compounds for commercial application as an anti-inflammatory ingredient.

Diabetes is a global health problem and a national economic burden. Although there are many anti-diabetic medications on the market, there is still a need for innovative treatment agents with increased efficacy and less side effects. Because they are more diverse and have minimal side effects than synthetic medications, pharmaceuticals made from natural products are more appealing. In line with this quest, the Department of Science and Innovation (DSI) established the African Traditional Medicines collaboration, where research was carried out to find and create a new natural anti-diabetic ingredient. *S. birrea* was chosen because its leaves and stem bark have historically been used to treat conditions including diabetic mellitus. Although type-2 diabetes mellitus was reportedly inhibited by *S. birrea* leaf extract, the compounds responsible for the anti-diabetic activity have not yet been identified, and their discovery will be helpful for commercial use. In order to discover the chemical compounds in *S. birrea* that are responsible for the anti-diabetic activity and to employ them as chemical markers for quality control purposes, this Ph.D. research was carried out.

Of all the extracts of *S. birrea* leaves tested, aqueous extract 4 showed statistically significant activity including at the lowest test concentration (0.01 µg mL^{-1}) and was selected to isolate and identify the compounds responsible for the anti-diabetic activity (glucose uptake activity).

UPLC-QTOF-MS analysis of the spray-dried aqueous leaf extracts of *S. birrea* (aqueous extracts 1 and 4) led to the tentative identification of sixteen compounds which are quinic acid (**peak 1**), gallic acid (**peak 2**), procyanidin B2 (**peak 3**), gallocatechin (**peak 4**), Pistafolin A (**peak 5**), epicatechin (**peak 6**), myricetin-3-O-β-D-glucuronide (**88**), gossypin (**peak 8**), quercetin-3-*O*-(6''-galloyl)-β-D-glucopyranoside (**peak 9**), myricetin-3-*O*-α-L-

rhamnopyranoside (**peak 10**), quercetin-3-O-β-D-glucuronide (**89**), quercetin-3-O-arabinoside (**peak 12**), quercetin-3-O-α-L-rhamnopyranoside (**peak 13**), kaempferol-3-O-α-L-rhamnopyranoside (**peak 14**), myricetin (**90**) and quercetin (**peak 16**). The presence of myricetin (**91**), myricetin-3-O-β-D-glucuronide (**92**) and quercetin-3-O-β-D-glucuronide (**93**) in the aqueous leaf extract of *S. birrea* was confirmed by isolation and structure elucidation of the compounds using MS and NMR data. Myricetin-3-O-α-L-rhamnopyranoside (**peak 10**), gallic acid (**peak 2**), quercetin-3-O-arabinoside (**peak 12**) and quercetin-3-O-α-L-rhamnopyranoside (**peak 13**) were previously reported to occur in *S. birrea*. Quinic acid (**peak 1**), myricetin (**90**) and quercetin (**peak 16**) were previously reported to have anti-diabetic activity. Myricetin-3-O-β-D-glucuronide (**92**) and quercetin-3-O-β-D-glucuronide (**93**) have not been previously reported to occur in *S. birrea*. Myricetin (**91**), myricetin-3-O-β-D-glucuronide (**92**) and quercetin-3-O-β-D-glucuronide (**93**) significantly increased the glucose uptake in differentiated C2C12 myocyte cells at different test concentrations; myricetin (**91**) (0.1 and 10 µg mL^{-1}; 85.7 and 109.1%, respectively), myricetin-3-O-β-D-glucuronide (**92**) (0.1 and 10 µg mL^{-1}; 61.6 and 88.8%, respectively) and quercetin-3-O-β-D-glucuronide (**93**) (0.1 and 10 µg mL^{-1}; 40.9 and 43.9%, respectively) compared to the treatment of insulin (0.1 µM; 100%). At a concentration of 10 µg mL^{-1}, myricetin (**91**) demonstrated both a potent and concentration-dependent stimulatory action on glucose uptake in the C2C12 myocytes, matching that of insulin, the positive control. Myricetin-3-O-β-D-glucuronide (**92**) has not been previously reported to have anti-diabetic activity, and the combination of this compound with other known anti-diabetic compounds in *S. birrea* contributes to the plant's anti-diabetic efficacy. These anti-diabetic compounds will be used as chemical markers for quality control purposes required for commercializing the herbal ingredient. This study provides scientific data to support the commercial application of the aqueous extract of *S. birrea* leaves as an anti-diabetic ingredient.

By finding novel active components and molecules responsible for the biological efficacy to be exploited as chemical markers for commercial application, the project's ultimate purpose was accomplished. The indigenous knowledge on the use of medicinal plants proves to be useful for identifying ingredients and developing products for the various market sectors, and this research provides scientific evidence on the value of South Africa's plant biodiversity as a continuing source of biologically active ingredients. Secondly the bioassay guided isolation method used in the isolation of active compounds proved to be a useful technique with the bioassay acting as a specific detector at every purification step. Though it can be criticized for

being time consuming and resource intensive compared to the conventional method of isolation, the approach compensates for these shortcomings by its effectiveness.

Table of Contents

xi

List of Figures

List of Tables

Abbreviations

AG	Aminoguanidine
ARC	Agricultural research council
B. cereus	*Bacillus cereus*
cNOS	Constitutive nitric oxide synthase
COSY	Correlation spectroscopy
COX	Cyclooxygenase
COXIBs	Cyclooxygenase inhibitors
CSIR	Council for scientific and industrial research
DCM	Dichloromethane
DMEM	Dulbecco's modified eagle medium
2DG	2-deoxyglucose
DG6P	Deoxy-D-glucose-6-phosphate
EGCG	Epigallocatechin-3-gallate
ELISA	Enzyme-linked immunosorbent assay
EMA	European medical agency
eNOS	Endothelial nitric oxide synthase
EtOAc	Ethyl acetate
ERK1/2	Extracellular signal-regulated kinase ½
E. faecalis	*Enterococcus faecalis*
E. coli	*Escherichia coli*
FBS	Fetal bovine serum
FDA	Food and drug administration
FMLP	*N*-formyl methionyl-leucyl-phenylalanine
GC-FID	Gas chromatography-flame ionization detector
GC-MS	Gas chromatography-mass spectrometry
GC-TOF-MS	Gas chromatography-time of flight-mass spectrometry
G6PDH	Glucose-6-phosphate dehydrogenase
GLP-1	Glucagon-like peptide 1

xxii

GLUT4	Glucose transporter 4
HIV/AIDS	Human immunodeficiency virus/acquired immunodeficiency syndrome
HMBC	Heteronuclear multiple bond correlation
HSQC	Heteronuclear single quantum coherence
HPLC-MS	High performance liquid-chromatography-mass spectrometry
HPLC-MS-SPE-NMR	High performance liquid-chromatography-mass spectrometry-solid phase extraction-nuclear-magnetic resonance
HPLC-QDA	High performance liquid chromatography-quantitative descriptive analysis
IBD	Inflammatory bowel disease
IDF	International diabetes federation
IFN-γ	Interferon-gamma
IL	Interleukin
iNOS	Inducible nitric oxide synthase
KRBH	Krebs ringer bicarbonate
LOX	Lipoxygenase
LPS	Lipopolysaccharide
MAPK	Mitogen-activated protein kinase
MMP-2	Matrix metallopeptidase 2
MIC	Minimum inhibitory concentration
NADP	Nicotinamide adenine dinucleotide phosphate
NED	N-1-naphthylethylenediamine dihydrochloride
NF-kB	Nuclear factor kappa-B
NO	Nitric oxide
nNOS	Neuronal nitric oxide synthase
NOESY	Nuclear over hauser effect spectroscopy
Nrf2	Nuclear factor erythroid 2-related factor 2
NSAIDs	Non-steroidal anti-inflammatory drugs
PAF	Platelet activating factor
PAMPS	Pathogen-associated molecular pattern molecules
PDA	Photodiode array

PGD	Prostaglandin D2
PGE	Prostaglandin E
PGF	Prostaglandin F
PIP3	Phosphatidylinositol (3,4,5)-trisphosphate
PI3K/Akt	Phosphatidylinositol 3-kinase/protein kinase B
PPARγ	Peroxisome proliferator-activated receptor γ
PTLC	Preparative thin layer chromatography
P. vulgaris	*Proteus vulgaris*
RIA	Radioimmunoassay
ROS	Reactive oxygen species
RPMI	Roswell park memorial institute medium
SANBI	South African national biodiversity institute
SAMRC	South African medical research council
S. columbaria	*Scabiosa columbaria*
S. birrea	*Sclerocarya birrea*
S. typhimurium	*Salmonella typhimurium*
S. flexneri	*Shigella flexneri*
S. aureus	*Staphylococcus aureus*
SLGT2	Sodium-glucose transport protein 2
STAT 3	Signal transducer and activator of transcription 3
T1DM	Type 1 diabetes mellitus
T2DM	Type 2 diabetes mellitus
TLC	Thin layer chromatography
TH-2	T-Helper 2
TNF-α	Tumour necrosis factor
UPLC-QTOF-MS	Ultra-pure liquid-chromatography-Q time of flight-mass spectrometry
UV	Ultraviolet
WHO	World

Supplementary data

xxvi

xxx

Chapter 1: General introduction

1.1   The value of natural products as a source of new medicinal and cosmeceutical ingredients

Natural products have long been a traditional source of medicine and are currently considered the most successful supply of potential drug leads with more than a million novel chemical entities discovered so far.[1, 2] Most people from developing countries depends on drugs of natural origin. However, several plant metabolites have been used as precursors in the synthesis to improve their biological potential. Sixty percent of the drugs currently on the market have originated from nature.[3] Successful drugs derived from natural sources include, but are not limited to, morphine (the analgesic from *Papaver somniferum*), penicillin (the antibiotic from *Penicillium notatum*), doxorubicin (from *Streptomyces peucetius*), tetracycline (from *Streptomyces aureofaciens*), cyclosporine (from *Tolypocladium inflatum*), metformin (an anti-diabetic drug from *Galega officinalis*), taxol (an anti-cancer drug from *Taxus brevifolia*), vinblastine (an anti-cancer drug from *Catharanthus roseus*), quinine (an anti-malarial drug from *Cinchona spp.)* and artemisinin (an anti-malarial drug from *Artemesia annua*).[2, 3]

The existence of communicable and non-communicable diseases and the challenges faced in discovering drug leads that can cure these diseases with minimal or no side effects is a major challenge. Irrespective of drug development for managing and treating diseases such as malaria, hypertension, HIV/AIDS, diabetes, inflammation and cancer, these diseases continuously affect different populations worldwide with significant fatalities. There is a need for innovative drug discovery strategies. In the past few decades, there has been an increase in the use of medicinal plants for health promotion and treatment of diseases in many countries including developed countries (UK, China, Germany, France).[4, 5] About a quarter of drugs approved by the Food and Drug Administration (FDA) and the European Medical Agency (EMA) and South African Medicines Control Council (SAMCC) are plant-based.[6, 7]

The cosmetic industry is focusing efforts on identifying new natural ingredients from plants. Consumers are more conscious of the products they use with a preference to the use of natural products instead of products containing synthetic ingredients. Undesirable ingredients include silicone, artificial colours, parabens and retinoids which may cause skin irritation, dryness,

1

burning, or tingling. Skin-lightening ingredients such as hydroquinone have been reported to have severe side effects leading to skin cancer. Plants are rich in bioactive ingredients with potential cosmetic and pharmaceutical applications.[8, 9] As a result, different plants have been explored by the cosmetic industry in search of natural active ingredients which show anti-aging, and UV protective effects in combination with medicinal properties such as anti-microbial, anti-inflammatory, anti-allergy and anti-oxidant.[10] These cosmetic ingredients with medicinal or drug-like properties are called cosmeceuticals.[11] Cosmeceuticals derived from natural sources include soy, azelaic acid, ascorbic acid, licorice, emblica and belides.[12]

1.2 Bioprospecting natural product libraries for medicinal and cosmeceutical discoveries

Natural products (NP) have evolved millions of years to elicit precisely tuned biological effects. As a result, many natural products occupy chemical space that is different from and complementary to that in synthetic libraries making natural product libraries attractive for medicinal and cosmeceutical discovery. Large screening campaigns have demonstrated the need for high quality molecular libraries in order to promote drug and cosmeceutical discovery. A major goal for developing libraries was to address the issues that have made natural products less amenable to the high throughput paradigm. These include the complexity of crude extracts, dereplication time, and a lag in prioritization of lead compounds compared to synthetic libraries. However, advances in approaches to natural product drug and cosmeceutical discovery incorporating new technologies have helped to overcome these difficulties. The pioneering work by researchers at Sequoia sciences set the stage for combining MS analyses with the generation of large natural product libraries.[13]

Natural product libraries became the approach adopted by different countries. In the United States of America, PhytoPharmacon is one of the largest natural product library/repositories. It has over 30,000 plant derived extracts and compounds collected from ethnobotanical based plants including 4000 plant extracts from different plant species, 25,000 semi-purified phytochemicals and 500 pure compounds based on bioassay guided fractionation and purification.[14] PharmaMar is the first company in the world to possess a large library of marine organisms with over 350,000 samples.[15] Analyticon have assembled a 25,000 pure natural product library over the last 20 years based on about 2000 different chemotypes that are available in a ready for screening format.[16]

2

One of the largest and most varied collections of natural products is found at the Natural Product Repository of the National Cancer Institute (NCI). It includes more than 230,000 different extracts made from plants, marine and microbial organisms that were obtained from biodiverse places across the world. It has created pre-fractionated library from over 125,000 natural product extracts with the aim of producing a publicly accessible, High throughput screening (HTS)-amenable library of > 1,000,000 fractions. Over 300, 000 fractions are now available for screening. It currently has 326,656 pure compounds.[17]

Currently, in South Africa, the University of Pretoria has a repository of ~11000 dry plant samples and 4000 samples comprising of extracts and fractions formatted in 96-well plates and stored for easy replication for evaluation in different screening programmes. Hyphenated analytical technologies such as HPLC-MS, HPLC-MS-NMR and UPLC-QTOF-MS were used for chemical characterization of the plant samples in the library. This library of extracts, fractions and compounds represents the South African plant biodiversity, and through collaborations can serve as a backbone for the discovery of potential hits for medicinal and cosmeceutical industries.[18]

1.3   Inflammation and anti-inflammatory ingredients

The term inflammation is coined from the latin word "inflammare" meaning "to burn".[19] Inflammation is a biological function triggered by harmful chemical, physical or biological agents and auto-immune responses.[20] Most times these agents are classified as pathogens (bacteria, fungi, viruses), pollutants (toxic compounds), hypersensitivity and shock or burn (trauma).[21] It is a complex process during which the body repairs tissue damage and protects itself against harmful stimuli. Inflammation is characterized by different symptoms such as redness, swelling, itching, heat and pain.[22] It can be defined as acute and chronic based on the type of response and competence of the action to get rid of the foreign agent or injured tissue. Acute inflammation occurs rapidly with the association of plasma protein, fluid and migration of neutrophils while chronic inflammation is a lengthy process associated with vascular proliferation, fibrosis, macrophage and tissue damage.[23] It is characterized by the enhancement of deteriorating sicknesses including, diabetes, inflammation, heart disease, etc. Most of the organs affected during inflammation are the skin, kidney, intestinal tract, heart, liver, lungs, pancreas, brain and reproductive organs.[20]

3

Monocytes and macrophages produce cytokines. The basic roles of cytokines in inflammatory processes include the activation of cells involved in inflammation (such as mast cells, macrophages and neutrophils), enabling communication between them, inducing synthesis of prostaglandin and affecting C-reactive protein synthesis.[24] There are two types of cytokines: proinflammatory cytokines (such as interleukins and nitric oxide) and anti-inflammatory cytokines. The predominance of proinflammatory cytokines leads to systemic inflammatory reaction while that of anti-inflammatory cytokines gives rise to anti-inflammatory response.[24] Regulation of inflammatory process and cellular response also involves eicosanoids which include prostaglandins (PGD, PGE and PGF), thromboxanes, prostacyclins, leukotrienes (LTB, LTC, LTD), mediators which arise as a response to stimuli from arachidonic acid connected with the cell membrane in the form of phospholipids.[24]

Prolonged inflammation plays a significant role in the progression of many diseases including cardiovascular diseases, cancer, autoimmune diseases, etc. These diseases are slowly disabling or fatal and affect a high percentage of the population.[25] The inhibiting inflammatory response has become one focus of treating these diseases. Many researchers have demonstrated that macrophages, the key inflammatory cells are closely associated with the pathologic process of inflammation.[26] Macrophages release an array of mediators including proinflammatory and cytotoxic cytokines, reactive oxygen intermediates and nitric oxide (NO) all of which have been implicated in the pathogenesis of tissue injury. Activated macrophages transcriptionally express inducible nitric oxide synthase (iNOS), which catalyzes the oxidative deamination of L-arginine to produce NO and is responsible for the prolonged and profound production of NO.[27] High-output NO by iNOS can provoke deleterious consequences such as septic shock and inflammatory diseases. Based on these observations, it has been hypothesized that inhibiting high-output NO production in macrophages, by blocking iNOS expressions or their activities, could serve as the basis for the potential development of anti-inflammatory drugs.[27]

1.3.1 Types of inflammation

Inflammation occurs in two stages: acute and chronic inflammation.[28] The acute inflammatory response is a complex but highly coordinated series of events involving cellular, molecular and physiological changes.[29] It is characterized by early vascular leakage with the extraction of

4

fluid and plasma components and massive recruitment of neutrophils that absorb invading pathogens and release proinflammatory mediators and reactive oxygen species (ROS) leading to damage of tissues and membrane lipid oxidation; neutrophils subsequently undergo apoptosis (cell death) an important step in the resolution of inflammation. As a result, certain monocytes begin to infiltrate and mature into macrophages, which are then responsible for clearing out germs, cellular debris, fibrin, protein clots and apoptotic cells. In addition, proinflammatory mediators are dissipated and anti-inflammatory pro-resolving mechanisms are initiated, finally, normal vascular permeability is restored leading to a termination of leukocyte emigration and restoration to normal tissue function.[30] However, if defects arise during any part of this highly conserved pathway, inflammation persists and becomes chronic lasting for longer periods (days, months or years) leading to excessive tissue damage.[29]

Chronic inflammation is therefore characterized by prolonged duration caused by persistent infections, immune-mediated inflammatory diseases, or prolonged exposure to toxic reagents. This results in severe tissue destruction caused predominantly by mononuclear macrophages.[31] Macrophages are dominant cellular players in chronic inflammation with a lifespan of several months to years. Chronic inflammation results in the pathogenesis of various prevalent diseases in modern western civilization such as rheumatoid arthritis; cardiovascular diseases such as myocardial infarction and atherosclerosis; various neuropathological disorders such as alzheimer's disease, diabetes, stroke and cancer through dysregulation of various signaling pathways such as nuclear factor kappa-B (NF-$_k$B), signal transducer and activator of transcription 3 (STAT 3), etc.[29] Hence targeting the inflammatory pathways has a high potential in preventing and eradicating these deadly diseases.[28]

1.3.2 Inflammatory pathways
1.3.2.1 Role of macrophages in inflammation

Macrophages are innate immune cells present in the tissue and necessary for homeostasis. They can be generated from monocytes in the blood after their activation and tissue infiltration. They also play a key role in regulating the response to inflammation through the transition of their phenotypes.[32] There are two phenotypes of macrophages namely: classical activated (M1) phenotype which promotes inflammation and the alternatively activated (M2) phenotype which terminates inflammation for tissue repair. These phenotypes are two extremes of a continuum of macrophage function.[33] Several mediators can orchestrate macrophages to differentiate into

5

M1-macrophages, they include lipopolysaccharide (LPS) and inflammatory cytokine such as interferon (IFN)-γ.[34] Furthermore, macrophages activated by IL-4 and IL-13 develop into alternatively (M2) activated macrophages which suppress inflammatory reactions and adaptive immune responses. The important role of macrophages in inflammation response may be a novel target for developing therapeutic pathways to treat a wide range of inflammatory diseases.[32]

1.3.2.2   Role of nitric oxide in inflammation

The role of nitric oxide (NO) in the skin has been the focus of considerable attention during the past years. NO play a key role in orchestrating the skin's response to external stimuli such as ultraviolet (UV) light, heat, response to infection, wound healing as well as possible underlying pathological conditions.[35] The free radical nitric oxide is synthesized by the oxidation of $_L$-arginine by a family of enzymes called NO synthase (NOS). Three isoforms of NOS have been described: Endothelial NOS (eNOS) and Neuronal NOS (nNOS) are constitutive NOS (cNOS) isoforms, and they produce picomolar to nanomolar quantities of NO for short periods and have homeostatic roles such as limiting UV-induced epidermal apoptosis, maintaining blood pressure, inhibiting platelet aggregation and leukocyte adhesion. Conversely, the third type of NOS Inducible NOS (iNOS) is inducible by noxious conditions such as injury, infection and inflammation. It is expressed by stimulation of inflammatory cytokines and UV radiation and generates significantly greater and more sustained amounts of NO.[36] While moderate levels of iNOS-derived NO are beneficial in contrast expression of iNOS has been linked with most acute and chronic inflammatory disorders eg. tumors, alzheimer's disease, liver injury, septic and hemorrhagic shock. Although all three NOS isoforms are involved to a greater or lesser extent during inflammation, the role of iNOS appears to be dominant.

Inducible high level of NO production mediates several inflammatory diseases either by having a direct effect or as a regulation of inflammatory pathways. Therefore, the balance between induction and suppression of iNOS may underlie much of the physiology and pathology of inflammation.[37] Although scientific evidence involves NO in the pathophysiology of inflammatory processes, there are contradictory reports in the literature concerning its role as an anti-inflammatory or proinflammatory agent. These properties of NO have led it to be called a "double-edged sword".[37] NO from eNOS likely play a role in the early stages of inflammation

whereas NO from iNOS contributes to many aspects of chronic inflammation. Therefore, the use of suitable iNOS inhibitors may be beneficial for the treatment of inflammatory diseases.[37]
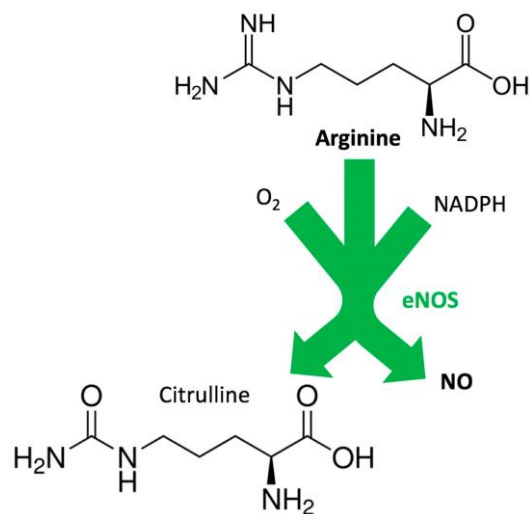
Figure 1.1: Biosynthesis of Nitric oxide (NO).[38]

1.3.3 Natural anti-inflammatory ingredients

The role of natural products as herbal remedies (and traditional medicine) has been recognized over centuries to combat human diseases such as cancer, cardiovascular disease and inflammatory diseases.[39, 37] Plants offer chemically diverse compounds which can be developed into drugs for the treatment of inflammatory diseases. The widely used drug aspirin was derived from salicylic acid which occurs naturally in the bark of the willow tree. Aspirin has analgesic and anti-pyretic properties and is used to treat rheumatic diseases.[40] Since then, the exploration of natural bioactive compounds has led to the discovery of numerous secondary metabolites with potent anti-inflammatory activity.[41] Plants reported to have anti-inflammatory activity include *Allium sativa*, *Aloe vera*, *Boswellia serrata*, *Ficus carica*, *Nigella sativa*, *Rosmarinus officinalis*, *Zingiber officinale*, *Verbena officinalis*, *Curcuma longa* L, *Vitis vinifera* L. and *Eriobotrya japonica*.[42] Literature reports on bioactive compounds confirmed the anti-inflammatory potential of various classes of metabolites such as terpenoids, polyphenols, alkaloids, steroids and macrolides.[20] The potent bioactive entities isolated from the plants namely curcumin, epigallocatechin-3-gallate and andrographolide have been proven to be active against inflammation and inflammatory mediators.[43]

Curcumin (**1**) is a polyphenol derived from the rhizome of *Curcuma longa* (turmeric). It exhibits different pharmacological activities through its interaction with a wide range of molecular targets, therefore, exhibiting anti-oxidant, anti-inflammatory and anti-cancer activity in different models of diseases. An *in vitro* study revealed the inhibitory effect of curcumin against lipoxygenase (LOX) and cyclooxygenase (COX) at non-toxic concentrations through nrf2-mediated gene transcription. These findings propose that curcumin possesses pleiotropic anti-inflammatory and cytoprotective actions that confer protection against microbial sepsis and other diseases.[44] Nevertheless, curcumin has low water solubility, poor absorption, elimination and rapid metabolism which limits its utilization.[45]

Epigallocatechin-3-gallate (EGCG) (**2**) is the most abundant catechin found in green tea (*Camella sinensis*). It protects against inflammation in prostate cancer cells by inhibiting gene induction of proinflammatory cytokines and chemokines, the activity of MMP-2 and -9 and cell migration. It also exhibits an anti-neuroinflammatory effect on atopic dermatitis thereby inhibiting IL-1β+Aβ induced IL-6, IL-8 and COX-2 expression in human astrocytoma cells. Its treatment for early-stage atopic dermatitis has entered phase II and III clinical trials.[43] On the other hand, the pro-oxidant nature of EGCG has been questioned, due to excess intake of EGCG which induced toxicity in animal models and human subjects. High-dose EGCG overproduces ROS, resulting in the damage of anti-oxidant defence in the body.[46] This limits its use in some patients.

Andrographolide (**3**) is the active labdane diterpenoid constituent isolated from *Andrographis paniculata* which occurs in South China and is used extensively in traditional Chinese medicine for detoxicating and heat-clearing. Studies have shown that inhibition of cell migration is a major contributor to the anti-inflammatory activity of andrographolide.[47] In another study, andrographolide exhibited its anti-inflammatory effects thus reducing the expression of COX-2.[48] According to previously published studies, the adverse drug reaction of andrographolide derivative injections include those of skin mucous membrane (itching, edema, rash, flushing), digestive system (vomiting, nausea, abdominal pain) and blood system (leukopenia and thrombocytopenia). This calls for caution in the use of compounds as it can cause life-threatening diseases.[49]

Curcumin (**1**)

Epigallocatechin-3-gallate (**2**)
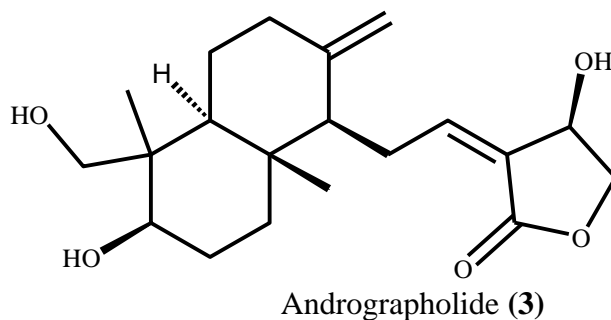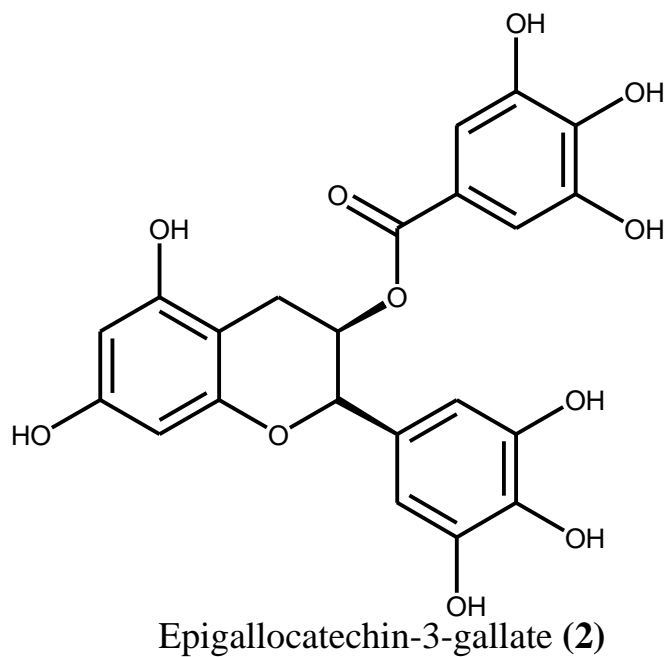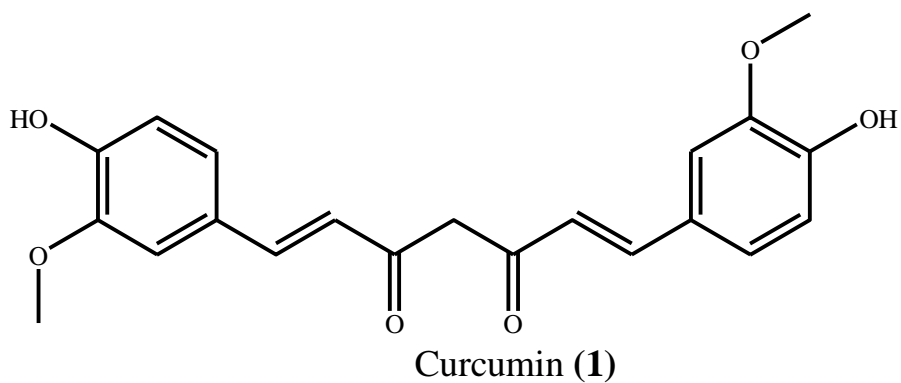
Andrographolide (**3**)

Figure 1.2: Chemical structures of curcumin (**1**), epigallocatechin-3-gallate (**2**) and andrographolide (**3**).

1.3.4 Current anti-inflammatory drugs/ medicines

Currently, steroidal and non-steroidal anti-inflammatory drugs (NSAIDS) with anti-inflammatory, analgesic and other curative effects are the most commonly used classical

treatments for inflammation in clinical practice. However, long-term use of these drugs can cause adverse reactions such as gastrointestinal damage, liver and kidney dysfunction and skin diseases. Therefore, finding natural compounds without toxic effects and good curative effects to replace anti-inflammatory drugs is an urgent issue to be solved in the clinical treatment of inflammation-related diseases.[50] Later, advances in molecular, chemical, cellular, biological and technological development led to the discovery of numerous drug targets like AMP-activated protein kinase (AMPK) for anti-inflammatory drug discovery.[51] Anti-inflammatory drugs are described in this section.

Aspirin is the most successfully used anti-inflammatory agent. It is a non-selective COX inhibitor having more selectivity towards COX-1. It inhibits the production of thromboxane A_2 in platelets and that of PGI_2, therefore, enhancing its use in coronary blockades. Furthermore, it acts at the hypothalamus causing an increase in peripheral blood flow, sweating and therefore cooling. Though, aspirin is an important drug in the management of inflammation, it is also associated with gastrointestinal side effects resulting in distress, nausea and vomiting.[52] Ibuprofen is an aryl propionic acid derivative widely used as an analgesic. It is also a non-selective COX inhibitor. Its efficacy is comparable to that of aspirin in anti-inflammatory assays with a lower side effect. It is associated with headaches, dizziness, nauseous and indigestion.[53] Sulindac is an indene acetic acid derivative used as an anti-inflammatory analgesic. It has a half-life of 8 hours and is used in the treatment of rheumatoid arthritis, ankylosing spondylitis and osteoarthritis. Its anti-inflammatory effects could be due to the inhibition of COX-1 and COX-2 which leads to the inhibition of prostaglandin synthesis. It is also associated with adverse effects such as gastric bleeding, nausea and dizziness.[53]

Indomethacin is an indole acetic acid derivative introduced in 1965 as anti-inflammatory analgesic used in rheumatoid arthritis, osteoarthritis and spondylitis. The anti-inflammatory activity of indole acetic acid analogs increases with an increase in the acidity of carboxylic acid while the amide analogs are devoid of activity. It is associated with dose-dependent effects such as gastric distress, headache and peptic ulcer.[53] Rofecoxib is the first diaryl furanone marketed in 1999 as a selective COX-2 inhibitor. It possesses anti-inflammatory, analgesic and anti-pyretic activity. It is used in the treatment of rheumatoid arthritis, acute pain and primary dysmenorrhea. Gastric injury is the side effect reported on the long-term use of this drug. It was withdrawn from the market in September 2004 as studies showed that it is associated with thrombotic and cardiovascular adverse side effects.[53, 54]

10

1.4 Diabetes mellitus and anti-diabetic ingredients

Diabetes is a complex, chronic, fast-growing and non-communicable endocrine disorder of global concern associated with a high risk of developing metabolism-related complications in patients. It is characterized by hyperglycemia, hyperlipidemia and oxidative stress.[55] Diabetes is associated with various complications caused by damage to body organs such as vision impairment, renal failure, cardiovascular disease, diabetic foot ulcer and mortality.[56] The world health organization (WHO) has expressed considerable concern over the global burden of diabetes. In 1980, WHO estimated the cases of diabetes to be 108 million worldwide but by 2017, this figure had spontaneously increased to 425 million people with diabetes, an increase of about 400% across that period. This figure equates to approximately 9% of the adult population over 18 years of age globally with equal representation from both males and females. The growing rate of diabetes is mostly observed in low-middle-income developing countries. The number of people with this disease is expected to rise exponentially and it is estimated that more than 642 million people will be diagnosed with diabetes by 2040.[57] Diabetes mellitus is estimated to be responsible for 3.2-5 million deaths globally and this high death rate places an increasing burden on the healthcare system with the global cost of diabetes estimated to be 727 billion US dollars in 2017. This cost is prone to increase with an increase in diabetes levels in the future.[57]

1.4.1 Types of Diabetes mellitus

Diabetes comprises 3 types which include Type 1 diabetes, Type 2 diabetes and Gestational diabetes. Among these, Type 2 diabetes is the most common type of diabetes.[55]

1.4.1.1 Type 2 Diabetes mellitus (T2DM)

T2DM is the most common class of DM with adult onset. In T2DM, the body develops an insulin resistance, resulting in a decrease in the amount of glucose that can be removed from the blood and stored as glycogen. Initially, the body produces higher amounts of insulin to compensate for this resistance but subsequently, quantity of insulin becomes unsustainable eventually leading to the damage of pancreatic β-cells. This gives rise to insufficient insulin action leading to hyperglycemia.[58] Insulin resistance gives rise to increased production of

11

glucose in the liver and reduced consumption of glucose by skeletal muscle and adipose tissue.[59] This together with pancreatic β-cell dysfunction gives rise to hyperglycemia. Studies have shown that people with T2DM possess lack of glucose transporter 4 (GLUT4) vesicles on the plasma membrane which is the result of resistance developed in the signaling cascade of the individual.[60]

T2DM is a complex form of DM and accounts for more than 90% of the estimated cases of diabetes impacting the quality of life, life expectancy and individual health. There is no cure for T2DM and its prevalence is largely increasing with an increased risk of complications such as diabetic retinopathy, neuropathy, kidney damage, microvascular and cardiovascular complications. T2DM can be managed by changes in diet and lifestyle that help to control plasma glucose levels which can be achieved by stimulating the secretion of insulin through medication and or dietary control.[61]

Figure 1.3: Pathophysiology of hyperglycemia in Type 2 diabetes mellitus.[62]

1.4.2   Natural anti-diabetic agents

Several studies have reported ethnomedicinal approaches for diabetes treatment and the use of plant-based natural products.[55] The multifactorial pathogenicity of diabetes mellitus requires a multi-modal therapeutic approach. Future treatment strategies might require the combination of different types of anti-diabetic agents including a strategy to use multicomponent-based natural products.[63] The use of natural substances especially plants to alleviate illnesses is an ancient practice. Many medicinal plants remain relevant in present-day medicine not only due to their application as crude drug preparations and formulas but also because they are the source of novel chemical entities that have become a mainstay of modern therapy. About 50% of the drugs in the market are from plant origin.[64] For example, Metformin, a less toxic biguanide and potent oral glucose-lowering agent was obtained from *Galenga officinalis* and is being used as a first-line drug for the treatment of diabetes mellitus.[65] About 400 plant species having hypoglycemic activity have been reported in the literature. Some of these promising natural anti-diabetic plant species include *Camellia sinensis*, *Curcuma longa*, *Gymnema sylvestre*, *Panax ginseng*, *Capsicum annum*, *Glycine max*, *Rhizoma coptidis*, *Silybum marianum*, *Carica papaya* and *Zingiber officinale*.[66] Most plants contain bioactive components such as alkaloids, flavonoids, terpenoids, glycosides, phenolics, etc. that were scientifically proven to have anti-diabetic activities.[67] With the rapid advancement of novel technologies and increased research on anti-diabetic natural products, many new plants, their extracts and active principles have been found to exhibit anti-diabetic effects which may provide valuable chemical entities to develop as novel anti-diabetic agents to supplement existing chemotherapies.[68] Some of them include curcumin, epigallocatechin-3-gallate, genistein and *Momordica charantia*.

Curcumin (**1**) is a bioactive component found in the rhizomes of *Curcuma longa* commonly known as turmeric. Curcumin significantly reduces the level of blood glucose and glycosylated hemoglobin (HbA1C) and improves the sensitivity of insulin. Curcumin also regulates diabetic neuropathy.[69] Due to the limitation of curcumin stated in section 1.2.3, it reduces its use as an anti-diabetic agent. Epigallocatechin-3-gallate (EGCG) (**2**) is a bioactive polyphenol found in green tea. Reports have shown its stimulation of glucose uptake to inhibit gluconeogenesis in skeletal muscle cells. It suppresses hepatic gluconeogenesis in isolated hepatocytes and attenuates insulin signaling blockade in HEPG2 cells. The anti-inflammatory and anti-oxidant properties of EGCG enable it to reduce the formation of free radicals and cause beneficial effects in diabetic mice. The prooxidant nature of this compound as stated in section 1.2.3 limits

its use in patients. Genistein (**4**) is one of the most common isoflavones found in *Glycine max* and have been reported to prevent diabetes. Genistein is known to have several beneficial effects on pancreatic beta cells such as increased insulin secretion, cell proliferation and the prevention of pancreatic beta cell apoptosis.[66] A combination of genistein and guggulsterone or green tea catechin and capsaicin suppressed adipogenesis and lipid deposition and increased lipolysis in 3T3-L1 adipocyte cells. Genistein is also reported to protect human pancreas cells that expressed estrogen receptor-b against high glucose-stimulated cell apoptosis and the prevention of their propagation through estrogen-receptor and Bcl-2 pathways.[55] However, genistein has also been reported to exert adverse effects by favoring cancer cell proliferation in patients with breast cancer.[70] *Momordica charantia* (MC) also known as bitter gourd or melon is a native shrub of Asia, Africa and Australia. It has a long history of use in traditional medicine in these regions and has been more recently incorporated into Chinese medicine.[71] Extracts from MC have demonstrated insulin-mimetic and insulin-secreting properties. It has also been shown to increase glucose consumption in the liver and decrease glucogenesis.[72] MC acts in synergism with common oral hypoglycemic agents such as metformin and glibenclamide. Its synergistic effect while potentially beneficial in the management of DM may also increase the risk of hypoglycemic episodes in patients taking both MC and oral hypoglycemic medication.[73]
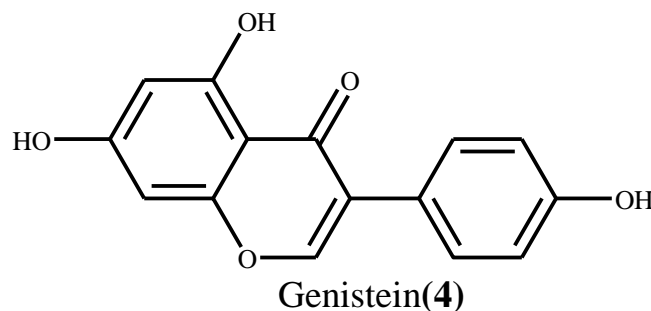
Genistein(**4**)

Figure 1.4: Chemical structure of genistein (**4**).

In addition to diet and physical activity, emerging evidence for several natural products has shown potential benefit in the treatment of diabetes mellitus and its applications. Natural products are appealing due to their multitude of effects and minimal side effect profile compared to conventional medications. However, some of these natural products have known drug interactions and the most common side effects attached to them. Some of these side effects are still unknown due to undiscovered metabolites that are the result of microbial degradation in the human body.[73] As a result, pharmaceutical studies on natural products are continuing to

discover and explore lead structures that may facilitate the development of new anti-diabetic drugs as a useful template.[74]

1.4.3 Current anti-diabetic drugs/ medicines

Different classes of compounds have been discovered that can modify metabolic processes to reduce plasma glucose levels. The list of approved hypoglycemic agents is shown in table 1.1. These agents are chosen based on different factors such as blood glucose level, nature of diabetes, age, other medical situations of the individual, or use of drugs.[55]

Table 1.1: List of commonly used glucose-lowering agents and their mechanism of action [55]

Chemical class	Drugs	Mechanism of action	Adverse effect
Biguanides	Metformin	Decrease in hepatic glucose production through AMPK kinase activation	Abdominal discomfort Diarrhea
α-glucosidase inhibitors	Acarbose Miglitol	Inhibition of α-glucosidase enzyme which gives rise to controlled or slow metabolism and absorption of carbohydrate	Flatulence Diarrhea Meteorism
Sulfonylureas	Glimepiride Glyburide Glipizide	Stimulates insulin secretion by pancreatic β-cells through the closure of K_{ATP} channel	Hypoglycemia Weight gain
Thiazolidinediones	Pioglitazone Troglitazone Rosiglitazone	Enhanced insulin sensitivity through activation of nuclear transcription factor and peroxisome proliferator receptor-γ	Edema Increased risk of bone fracture
Meglitinides	Nateglinide Repaglinide	Stimulates insulin secretion by pancreatic β-cells through the closure of K_{ATP} channel	Hypoglycemia Weight gain
Dipeptylpeptidase-4 (DPP-4) inhibitors	Linagliptin Sitagliptin Alogliptin Saxagliptin	Inhibits dipeptidyl peptidase enzyme and increased concentration of propandial incretin giving rise to decreased glucagon secretion and increased insulin secretion	Rare clinically significant side effect
Dopamine agonist	Bromocriptine	Increased insulin sensitivity mediated by activation of dopaminergic receptors and modulation of hypothalamic regulation of metabolism	Headache Nausea Dizziness Diarrhea Vomiting

15

Sodium-glucose cotransporter-2 (SLGT2) inhibitors	Dapagliflozin Canagliflozin Empagliflozin	Decreased reabsorption of glucose by kidney due to inhibition of SLGT2 in the proximal nephron	Urinary and genital tract infections Hypotension
Glucagon-like peptide-1 (GLP-1)	Liraglutide Albiglutide Lixisenatide Dulaglutide-Exenatide	Increased insulin secretion and decreased glucagon secretion through activation of GLP-1 receptor	Vomiting Nausea Diarrhea
Amylin analogs	Pramlintide	Secretion of glucagon through activation of amylin receptors	Nausea
Insulin	Aspart Glulisine Lispro Glargine Detemir	Binds to the insulin receptor and activates glucose transport GLUT4. PIP3 (Phosphatidylinositol-3,4,5-triphosphate) and tyrosinase phosphorylated guanine nucleotide exchange proteins enhance GLUT4 translocation from the cytosol to the plasma membrane	Hypoglycemia Weight gain

Based on these factors, the health care provider may prescribe one medication or a combination of medications to achieve a normal blood glucose level. Metformin, a member of the biguanide group is the first line glucose-lowering agent in type 2 diabetes. Other second-line hypoglycemic medications include α-glucosidase inhibitors, sulfonylureas, thiazolidinedione, meglitinides, etc.[55] Many of these oral anti-diabetic agents have serious adverse effects (table 1.1); thus, managing diabetes without any side effect is still a challenge. Therefore, the search for more effective and safer hypoglycemic agents has continued to be an important area of investigation.[75]

1.5   Melanogenesis and antimelanogenesis ingredients

Melanin is a pigment that occurs in humans, fungi and plants. It is responsible for the colour of eyes, hair and skin in humans.[76] The pigment is secreted and produced by the melanocytes cells which are distributed in the basal layer of the dermis through a physiological process called melanogenesis.[77, 78] Melanocyte cells produce two different types of melanin pigments: eumelanin, which is black or brown, and pheomelanin, which is red or yellow.[78] Each individual of a different racial group has roughly the same number of melanocyte cells;

16

therefore, the type of melanin produced depends on how well the melanocytes work, for example melanin production is genetically predisposed to be higher in people with darker skin.[79, 80] The size and clustering of melanosomes, which are organelles found within melanocyte cells, are the primary structural pigmentation differences between dark and light skin. Melanosomes are larger solitary organelles in dark skin and smaller and clustered in light skin.[80, 81] Through the absorption of UV radiation and the elimination of reactive oxygen species, melanin serves as the skin's defence against UV light damage.[76] Tyrosinase is a crucial enzyme involved in the synthesis of melanin.[82] Tyrosinase overactivity causes hyperpigmentation of the skin, and its underactivity causes hypopigmentation of the hair. The enzyme's underactivity can happen in any age group based on a person's genes, but the enzyme's overactivity is linked to aging.[76] Tyrosinase, also known as polyphenol oxidase, is a monooxygenase that contains copper and catalyzes two different processes involving molecular oxygen: hydroxylation of tyrosinase to 3,4-dihydroxyphenylalanine (DOPA) by the action of monophenolase and oxidation of DOPA to DOPA-quinone by action of diphenolase.[82]

Melanogenesis alterations may be responsible for various skin disorders, causing both aesthetic problems and dermatological issues. Senile lentigo, post-inflammatory melanoderma, melasma, pigmented freckles, and acne scars are examples of hyperpigmentation phenomena that are defined by the darkening of a skin area brought on by the overproduction of melanin. Hyperpigmentation is a rather frequent and typically unharmful condition that can be influenced by both external (UV radiation, medications including antibiotics, non-steroidal anti-inflammatory drugs, psychiatric drugs, pain relievers, birth control pills, etc.) and internal (hormones, inflammation, etc.) causes.[83] Contrarily, hypopigmentation refers to the loss of skin pigment brought on by a reduction in melanocytes, melanin, or the amino acid L-Tyrosine, which is necessary for the production of melanin.

1.5.1   Natural antimelanogenesis ingredients

Currently, most cosmetic products contain various types of skin even tone ingredients either found in natural, semi-synthetic or synthetic forms. In addition to resulting in a brighter and even complexion skin tone, it is claimed that skin even tone agents are used to prevent hyperpigmentation by reducing melanin production.[84] The use of available skin even tone products commercialized in a market has some controversial and doubtful safety issues to the users. This is a result of dangerous even tone compounds like hydroquinone and mercury being

17

added to cosmetic goods to produce an immediate and stronger even tone effect.[84] According to a survey, customers are seriously concerned about the safety of these chemicals due to their numerous negative impacts on the body's health and the skin, such as skin irritation, contact dermatitis, depigmentation, ochronosis and toxicity of the organs.[85, 86] To protect consumers, the Ministry of Health has strongly forbidden the use of these dangerous compounds as skin even tone agents in cosmetic items. However, due to their safety, affordability, and lack of side effects, natural skin even tone solutions are a superior option to those chemical substances.[87] Soy, kojic acid, arbutin, and azelaic acid are natural skin-even tone ingredients that can prevent hyperpigmentation with minimal side effects on the skin.

Soy (*Glycemic max*) is a legume that is high in protein and fibre. Soymilk contains 3.5% protein, 2% fat, 0.5% ash, 2.9% carbohydrates and a high amount of isoflavones that scavenge free radicals released by UV exposure to prevent skin aging and protects against UV-induced skin damage.[88] Natural soybeans contain small proteins, Bowman-Birk inhibitor and soybean trypsin inhibitor. This depigmenting effect is available only with fresh soymilk and not pasteurized soymilk.[89] Total soy is now being added to skin care products to help with solar lentigines and patchy hyperpigmentation, which are common side effects of photodamage.[90] However, soy can result in moderate gastrointestinal side effects such as nausea, bloating, and constipation. In certain people, it can also result in allergic reactions that include rashes, itching, and breathing difficulties.[88]

Kojic acid (**5**) is a tyrosinase inhibitor derived from various fungal species such as Aspergillus and Penicillium. It exhibited mushroom tyrosinase inhibition activity with an IC_{50} value of 0.014.[89] It functions as an anti-oxidant and blocks the conversion of dopamine and *O*-quinone into their respective melanin and DL-DOPA, respectively.[91] Additionally, kojic acid blocks tyrosinase's catecholase activity, which is necessary and the rate-limiting enzyme in the manufacture of the skin pigment melanin.[92] According to a study, kojic acid has a significant potential for sensitization and can result in irritating contact dermatitis.[89] Arbutin (**6**) isolated from the fresh fruit of the California buckeye, *Aesculus california* is reported by various researchers to inhibit the oxidation of L-DOPA catalyzed by mushroom tyrosinase with an IC_{50} value of 0.04.[89] It is effective in the topical treatment of various cutaneous hyperpigmentation characterized by hyperactive melanocyte function.[93] A recent study indicated that arbutin inhibits melanin synthesis by inhibiting tyrosinase activity. Nevertheless, arbutin is reported to have side effects such as redness, itchiness, dryness, blisters and contact dermatitis.[89] A

18

naturally occurring dicarboxylic acid produced from Pitysporum ovale is azelaic acid (**7**). Its lightening effect appears to be selective and most noticeable in highly active melanocytes, with minimal effects in normally pigmented skin [89]. Azelaic acid (**7**) was successfully used by Fitton and Goa in a study to treat rosacea, solar keratosis, and hyperpigmentation linked to burns and herpes labialis. They applied azelaic acid at concentrations of 15% or 20% twice daily for 3– 12 months. This treatment produced clinical and histological resolution in facial lentigo maligna.[94] Transient erythema and skin irritation marked by scaling, itching, redness and burning are some of its most common side effects [89].
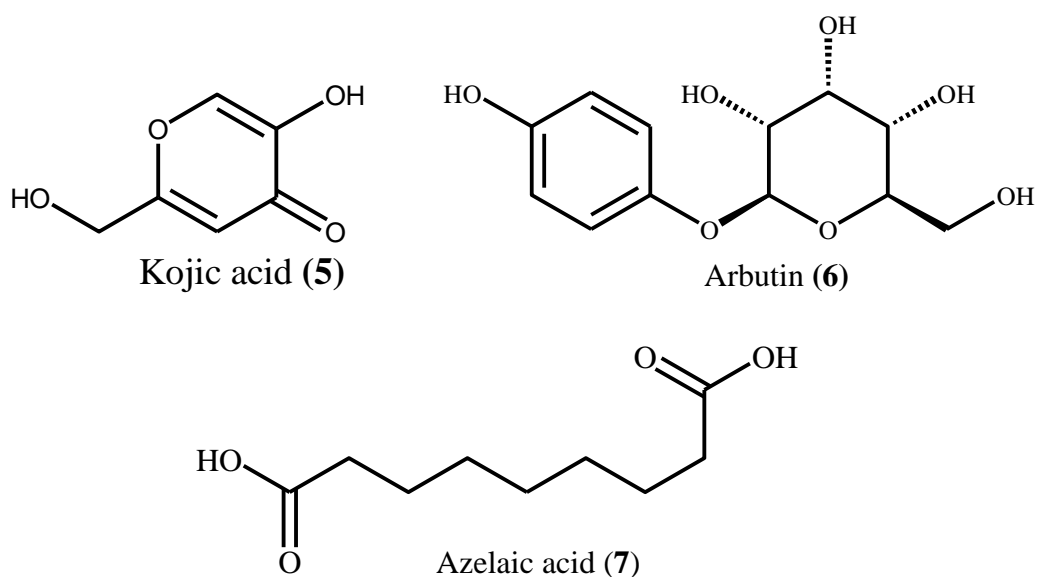
Figure 1.5: Chemical structures of kojic acid (**5**), arbutin (**6**) and azelaic acid (**7**).

1.5.2   Current antimelanogenesis ingredients

As the population ages, dyspigmentation due to photoaging will become more common and consumers are increasingly requesting treatment for this cosmetic problem.[95] While hydroquinone monotherapy and other prescription-strength topicals are fairly effective, they have drawbacks, including high cost, possible skin irritation and the need to limit the duration of use. It is therefore likely that in the future, more products containing effective but less irritating ingredients will continue to be developed as skin even tone ingredients. The following are some currently used skin depigmentation and lightening agents and their adverse effects.[89]

19

For skin whitening, hydroquinone (**8**), a common chemical, is easily accessible in cosmetic and over-the-counter forms. It is frequently used to treat melanosis and other hyperpigmentary illnesses and is regarded as one of the most powerful inhibitors of melanogenesis both *in vitro* and *in vivo*.[96] Melasma, post-inflammatory hyperpigmentation, and other hyperpigmentation problems have all been successfully treated with this phenolic chemical (hydroquinone).[97] The development of exogenous ochronosis, sooty hyperpigmentation in the treatment area that may be difficult to reverse, and skin irritation or contact dermatitis are among hydroquinone's frequent adverse effects, according to Kamau et al.[98]

Corticosteroids (**9**) are classified according to their potencies from class I (most potent) to class VII (least potent) and are most frequently used in combination with hydroquinone and/or mercurial in skin lightener solutions. Licensed in 1973, clobetasol propionate is a class I fluorinated corticosteroid that produces hypopigmentation or skin whitening as well as vasoconstriction and immunosuppression. Clobetasol propionate was quickly included in skin-lightening treatments and found widespread use in many African and Afro-Caribbean communities because it is highly stable and capable of penetrating the epidermal and dermal skin layers. Unfortunately, long-term usage of this extremely strong corticosteroid can have serious side effects such as cutaneous atrophy and clinical signs of thin, fragile skin.[99] Today, the vast majority of skin even tone agents include a form of retinoid (**10**). All trans-retinoic acids, 13-cis retinoic acid (isotretinoin), retinol, retinaldehyde, and tazarotene are examples of topical retinoids. Retinoids, which are well known for their anti-aging properties, lighten hyperpigmented skin by reducing melanosome transfer from epidermal melanocytes and obstructing the transcription of tyrosinase and the manufacture of melanin. Dryness, irritability, skin colour changes, photosensitivity, redness, swelling, crusting, and blistering are some of its negative effects.[99] Glycolic acid (**11**) is an alpha-hydroxy acid derived from sugarcane, and it may have two skin even tone effects. At low concentrations, glycolic acid has an epidermal discohesive effect, which results in more rapid desquamation of pigmented keratinocytes. At higher concentrations, glycolic acid results in epidermolysis. When glycolic acid is used in the treatment of post inflammatory hyperpigmentation, it has been suggested that it should be initiated at low concentrations to avoid skin irritation and exacerbated hyperpigmentation. Common side effects of glycolic acid include dry skin, erythema, burning sensations, itching, skin irritation and skin rashes [89].
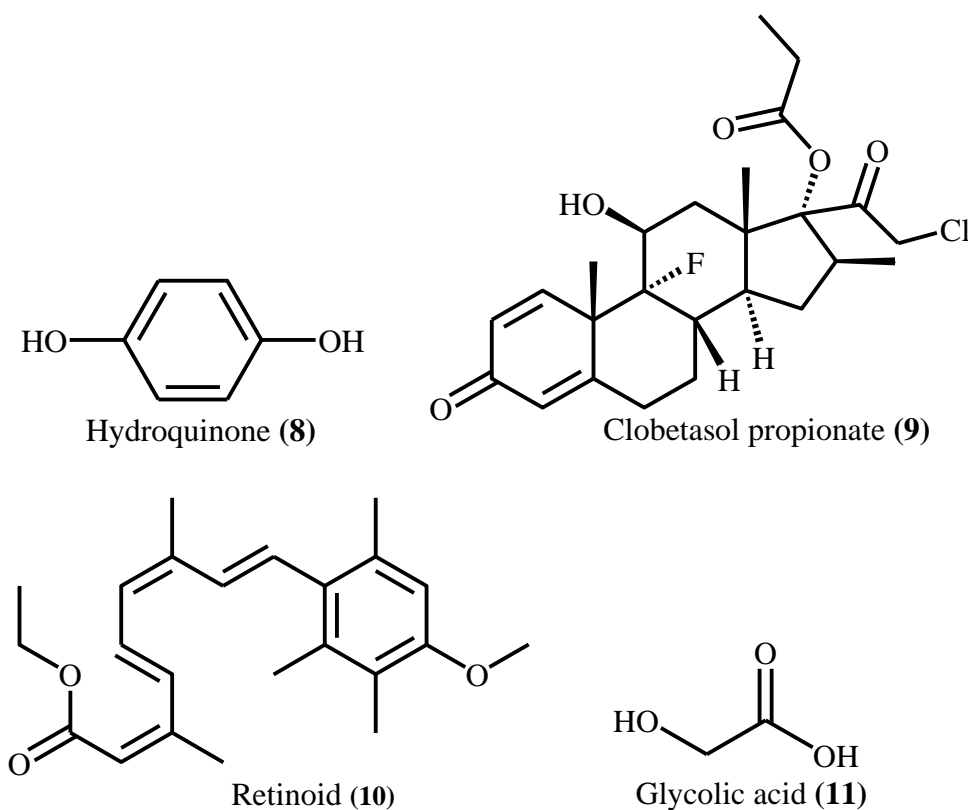
Figure 1.6: Chemical structures of hydroquinone (**8**), clobetasol propionate (**9**) retinoid (**10**) and glycolic acid (**11**).

1.6   Problem statement and justification

It has been well established that inflammation contributed to the pathological processes of various chronic diseases such as inflammatory bowel disease, atherosclerosis and alzheimer's disease. Anti-inflammation has been a promising strategy to suppress or delay these diseases.[100] The currently available repertoire of approved anti-inflammatory agents mainly consists of non-steroidal anti-inflammatory drugs (NSAIDs), glucocorticoids, immunosuppressant drugs and biologicals. Despite this arsenal, therapy is often not effective enough or is accompanied by intolerable side effects which weaken the overall potential of anti-inflammatory treatment. Thus, the identification of substances with an inhibitory effect on iNOS expression would hold tremendous potential in advancing the treatment of inflammatory or chronic immune disorders.[101]

The use of medicinal plant therapies to treat chronic inflammatory illnesses such as skin inflammation, rheumatoid arthritis and inflammatory bowel diseases (IBD) is prevalent and on

21

the rise. Plants are an important source of biologically active natural products and could be considered a promising means for the discovery of new drugs due to easy access and low cost. Despite the therapeutic benefits of aspirin (as mentioned earlier), it is associated with upper gastrointestinal (GI) side effects including ulcer and bleeding.[102] The development of standardized herbal medicines with proven efficacy and safety of use is therefore of great importance not only for increasing access to medicines but also for offering new therapeutic "hits".[103]

One of the parts of the global beauty market with the quickest growth is the skin even tone sector. According to global industry analysts (GIA), the market for universal skin even tone will reach \$23 billion by 2020.[104] A recent meta-analysis reported an estimate of 27.7%, with Africa having a current estimated frequency of 27.1%, showing the ubiquity of skin even tone use on a global scale.[105] The need for lighter skin tones has been fuelled by a long history of social divisions, including cultural pressures and stigmas. Injections, creams, lotions, soaps, and other products used to treat hyperpigmentation conditions are frequently misused as self-medication to lighten the skin's tone. Steroids, mercury, hydroquinone (HQ), which is regarded as the gold standard, and its derivatives are among the most frequently utilized substances.

Exogenous ochronosis and viral dermatosis are two health issues linked to the long-term usage of these skin-lightening chemicals. These substances have been prohibited as skin even tone agents in a number of African nations, including South Africa, Nigeria, Kenya, and the Ivory Coast, due to their toxicity. Despite this ban, these harmful substances are frequently illegally added to cosmetic formulations, and the public continues to have access to them through unofficial means such as street sellers, markets, and non-pharmaceutical stores.[106, 107] Botanicals and natural substances, on the other hand, present safer choices because they could not be as hazardous as synthetic ones and might result in less negative side effects.[108] In many cultures, utilizing plant extracts as cosmetics to promote skin health is a standard practice in traditional medicine. This may be explained by the fact that plant extracts are a rich source of vitamins, anti-oxidants, essential oils, and other bioactive substances that give the body the nutrition required for good skin.[109] The significant advancement of research using plant extracts in cosmetics demonstrates the growing interest of researchers and pharmaceutical companies in developing natural skin even tone products.[110]

Several local plants in South Africa such as *Scabiosa columbaria* have been traditionally used for the treatment of skin-related diseases such as acariosis, dermatitis, eczema, follicular acne, measles and rash.[111, 112] Despite their traditional use, the anti-inflammatory activity of S. *columbaria* and *P. capitatum* have not been reported in the literature, furthermore, though the anti-inflammatory activity of *C. pyracanthoides* have been reported, its bioactive constituents have not been identified, therefore this study investigated *S. columbaria, C. pyracanthoides and P. capitatum* as sources of anti-inflammatory ingredients. In addition, though the skin even tone activity of *S. columbaria* has been reported, the compounds responsible for the activity have not been investigated. Therefore, this study examines the skin even tone activity of *S. columbaria*.

Due to growth in population, urbanization, aging, lifestyle alterations, increasing prevalence of obesity and inadequate exercise, the past two decades have experienced a tremendous increase worldwide in the number of people diagnosed with diabetes mellitus (DM). DM and its complications are costly to manage not only for affected individuals but also for the healthcare system around the world. According to IDF, DM accounts for 5-10% of the total healthcare budget in many countries.[113] The increasing prevalence of DM has motivated the development of many new approaches such as oral hypoglycemic agents and insulin therapy to treat hyperglycemia to maintain a normal glucose concentration and prevent the development of complications.[114] Although oral hypoglycemic agents and insulin are the therapeutic approach for the treatment of DM and are effective in controlling hyperglycemia, these chemical drugs are complicated by many factors inherent to the disease process, typically insulin resistance, hyperinsulinemia, hypertension, impaired insulin secretion and cholesterol abnormalities. Most of them have prominent side effects and fail to significantly eliminate the course of diabetic complications. As the presently available therapeutic approaches have limitations concerning systemic efficacy, patient compliance and adverse effects, it has prompted a tremendous effort worldwide in the search for alternative treatment strategies for this metabolic disease.[115]

Before the advancement of modern medicine, plant-based therapies were used for the treatment and maintenance of diabetes mellitus. The Egyptian Papyrus Ebers records the use of various grains in the treatment of diabetes mellitus and numerous texts have described the use of herbs, spices and other plant materials for the same purpose.[116, 117] Because of the adverse effects and cost associated with the current anti-diabetic drugs, the use of natural products as alternative therapies are dramatically increasing. It has been estimated that more than 1000 plant remedies

are used globally for the treatment and maintenance of diabetes mellitus. One such medicinal plant with reported anti-diabetic properties is *Sclerocarya birrea*. This plant has been traditionally used to treat diabetes and some of these uses were documented in literature.[118] Both its stembark and leaves were shown to possess glucose-lowering properties in several *in vitro* studies.[119-121] However, information on the compounds that contribute to the anti-diabetic activities of the plant species remains scanty. The present study primarily examines the anti-diabetic activity of *S. birrea* leaf extract and targeted the isolation and identification of chemical compounds responsible for the biological activity through bioassay-guided fractionation.

1.7   Aim and Objectives

The aims of the study were:

To identify plant species with anti-inflammatory, anti-diabetic and skin even tone activity and to characterize new and known anti-inflammatory and anti-diabetic compounds using modern hyphenated analytical techniques from the selected plant species as well as develop standardized ingredients for commercial application.

The overall objectives of the study were:

- Selection of plants based on traditional uses for treating inflammation, skin even tone, diabetes mellitus and related symptoms (information obtained from the University of Pretoria repository).
- Literature searches on reported scientific uses of the selected plants.
- Collection, extraction, *in vitro* anti-inflammatory, skin even tone and anti-diabetic biological efficacy testing of extracts.
- Obtaining chemical profiles of plant extracts using UPLC-QTOF-MS.
- Identification, isolation and purification of bioactive compounds using UPLC-QTOF-MS, silica gel chromatography, LC-MS-SPE-NMR and mass directed preparative HPLC.
- Structure elucidation of biologically active compounds using UPLC-QTOF-MS and NMR.
- *In vitro* anti-inflammatory and anti-diabetic screening of bio-active compounds.

The subdivision of the work were as follows:

Chapter 1 presents the general introduction of the work.

Chapter 2 provides the selection of South African plants from University of Pretoria repository, literature searches on scientific uses of plants, collection and extraction of the selected plants using industry-accepted solvents, *in vitro* anti-inflammatory (selected proinflammatory cytokines inhibition assay) and melanin inhibition assays of extracts and chemical profiling of the active extracts.

Chapter 3 is a continuation of chapter 2 that describes collection, extraction and *in vitro* anti-inflammatory screening (nitric oxide inhibition assay) of the selected plant species (*S. columbaria*) from Chapter 2, chemical profiling of the active extracts, fractionation of the active extracts, biological screening of the fractions, isolation of compounds from the active fraction/s, their structural elucidation and *in vitro* anti-inflammatory screening (nitric oxide inhibition assay) of the bio-active compounds.

Chapter 4 discusses the *in vitro* glucose uptake activity of different collections of a plant species (*S. birrea*) based on the reported traditional use, chemical profiling and fractionation of the active extracts, biological screening of the fractions, isolation of compounds from the active fractions and their structural elucidation and *in vitro* glucose uptake activity of the bio-active compounds.

Chapter 5 provides an overall conclusion of the study.

1.8   References

1.   Dias, D. A.; Urban, S.; Roessner, U., A historical overview of natural products in drug discovery. *Metabolites* **2012,** *2* (2), 303-36.
2.   Carter, G. T., Natural products and Pharma 2011: strategic changes spur new opportunities. *Nat Prod Rep* **2011,** *28* (11), 1783-9.
3.   Thomford, N. E.; Senthebane, D. A.; Rowe, A.; Munro, D.; Seele, P.; Maroyi, A.; Dzobo, K., Natural Products for Drug Discovery in the 21st Century: Innovations for Novel Drug Discovery. *Int J Mol Sci* **2018,** *19* (6).
4.   Banjari, I.; Misir, A.; Šavikin, K.; Jokić, S.; Molnar, M.; De Zoysa, H. K. S.; Waisundara, V. Y., Antidiabetic Effects of Aronia melanocarpa and Its Other Therapeutic Properties. *Front Nutr* **2017,** *4*, 53-53.
5.   Yatoo, D. M.; Dimri, U.; Gopalakrishnan, A.; Karthik, K.; M, G.; Khandia, R.; M, S.; Saxena, A.; Alagawany, M.; Farag, M.; Munjal, A.; Dhama, K., Beneficial health

applications and medicinal values of Pedicularis plants: A review. *Biomedicine & Pharmacotherapy* **2017,** *95*, 1301-1313.

6. Patridge, E.; Gareiss, P.; Kinch, M. S.; Hoyer, D., An analysis of FDA-approved drugs: natural products and their derivatives. *Drug Discov Today* **2016,** *21* (2), 204-7.

7. Wani, M. C.; Taylor, H. L.; Wall, M. E.; Coggon, P.; McPhail, A. T., Plant antitumor agents. VI. The isolation and structure of taxol, a novel antileukemic and antitumor agent from Taxus brevifolia. *J Am Chem Soc* **1971,** *93* (9), 2325-7.

8. Armendáriz-Barragán, B.; Zafar, N.; Badri, W.; Galindo-Rodríguez, S. A.; Kabbaj, D.; Fessi, H.; Elaissari, A., Plant extracts: from encapsulation to application. *Expert Opin Drug Deliv* **2016,** *13* (8), 1165-75.

9. Działo, M.; Mierziak, J.; Korzun, U.; Preisner, M.; Szopa, J.; Kulma, A., The Potential of Plant Phenolics in Prevention and Therapy of Skin Disorders. *Int J Mol Sci* **2016,** *17* (2), 160.

10. Georgiev, V.; Slavov, A.; Vasileva, I.; Pavlov, A., Plant cell culture as emerging technology for production of active cosmetic ingredients. *Eng Life Sci* **2018,** *18* (11), 779-798.

11. Mohd Nasir, H.; Mohd-Setapar, S., Natural Ingredients in Cosmetics from Malaysian Plants: A Review. *Sains Malaysiana* **2018,** *47*, 951-959.

12. Murphy, M. J.; Dow, A. A., Natural Cosmeceutical Ingredients for the Management of Hyperpigmentation in Hispanic and Latino Women. *J Clin Aesthet Dermatol* **2021,** *14* (8), 52-56.

13. Bugni, T. S.; Richards, B.; Bhoite, L.; Cimbora, D.; Harper, M. K.; Ireland, C. M., Marine Natural Product Libraries for High-Throughput Screening and Rapid Drug Discovery. *Journal of Natural Products* **2008,** *71* (6), 1095-1098.

14. Library/PhytoPharmacon, N. P. PhytoPharmacon 2018. https://phytopharmacon.com/targeted_library.html.

15. Mar, P., Pharma Mar 2022. **2022.**

16. Butler, M. S.; Fontaine, F.; Cooper, M. A., Natural product libraries: assembly, maintenance, and screening. *Planta Med* **2014,** *80* (14), 1161-70.

17. Wilson, B. A. P.; Thornburg, C. C.; Henrich, C. J.; Grkovic, T.; O'Keefe, B. R., Creating and screening natural product libraries. *Nat Prod Rep* **2020,** *37* (7), 893-918.

18. Mokoka, T. A.; Xolani, P. K.; Zimmermann, S.; Hata, Y.; Adams, M.; Kaiser, M.; Moodley, N.; Maharaj, V.; Koorbanally, N. A.; Hamburger, M.; Brun, R.; Fouche, G., Antiprotozoal screening of 60 South African plants, and the identification of the antitrypanosomal germacranolides schkuhrin I and II. *Planta Med* **2013,** *79* (14), 1380-4.

19. Abdulkhaleq, L. A.; Assi, M. A.; Abdullah, R.; Zamri-Saad, M.; Taufiq-Yap, Y. H.; Hezmee, M. N. M., The crucial roles of inflammatory mediators in inflammation: A review. *Vet World* **2018,** *11* (5), 627-635.

20. Kishore, N.; Kumar, P.; Shanker, K.; Verma, A. K., Human disorders associated with inflammation and the evolving role of natural products to overcome. *Eur J Med Chem* **2019,** *179*, 272-309.

21. Ashley, N.; Weil, Z.; Nelson, R., Inflammation: Mechanisms, Costs, and Natural Variation. *Annual Review of Ecology Evolution and Systematics* **2012,** *43*, 385-406.

22. Ikeda, Y.; Murakami, A.; Ohigashi, H., Ursolic acid: an anti- and pro-inflammatory triterpenoid. *Mol Nutr Food Res* **2008,** *52* (1), 26-42.

23. Riegsecker, S.; Wiczynski, D.; Kaplan, M. J.; Ahmed, S., Potential benefits of green tea polyphenol EGCG in the prevention and treatment of vascular inflammation in rheumatoid arthritis. *Life Sci* **2013,** *93* (8), 307-312.

24. Dawid-Pać, R., Medicinal plants used in treatment of inflammatory skin diseases. *Postepy Dermatol Alergol* **2013,** *30* (3), 170-177.

25. He, X.; Shu, J.; Xu, L.; Lu, C.; Lu, A., Inhibitory Effect of Astragalus Polysaccharides on Lipopolysaccharide-Induced TNF-a and IL-1β Production in THP-1 Cells. *Molecules* **2012,** *17* (3), 3155-3164.

26. Jakobsson, P.-J., How macrophages mediate inflammatory pain via ATP signaling. *Nature Reviews Rheumatology* **2010,** *6* (12), 679-681.

27. Zhou, H. Y.; Shin, E. M.; Guo, L. Y.; Youn, U. J.; Bae, K.; Kang, S. S.; Zou, L. B.; Kim, Y. S., Anti-inflammatory activity of 4-methoxyhonokiol is a function of the inhibition of iNOS and COX-2 expression in RAW 264.7 macrophages via NF-κB, JNK and p38 MAPK inactivation. *European Journal of Pharmacology* **2008,** *586* (1), 340-349.

28. Kunnumakkara, A. B.; Sailo, B. L.; Banik, K.; Harsha, C.; Prasad, S.; Gupta, S. C.; Bharti, A. C.; Aggarwal, B. B., Chronic diseases, inflammation, and spices: how are they linked? *Journal of Translational Medicine* **2018,** *16* (1), 14.

29. Stables, M. J.; Gilroy, D. W., Old and new generation lipid mediators in acute inflammation and resolution. *Prog Lipid Res* **2011,** *50* (1), 35-51.

30. Kadl, A.; Leitinger, N., The role of endothelial cells in the resolution of acute inflammation. *Antioxid Redox Signal* **2005,** *7* (11-12), 1744-54.

31. Gosslau, A.; Li, S.; Ho, C. T.; Chen, K. Y.; Rawson, N. E., The importance of natural product characterization in studies of their anti-inflammatory activity. *Mol Nutr Food Res* **2011,** *55* (1), 74-82.

32. Su, Y.; Gao, J.; Kaur, P.; Wang, Z., Neutrophils and Macrophages as Targets for Development of Nanotherapeutics in Inflammatory Diseases. *Pharmaceutics* **2020,** *12* (12), 1222.

33. Mantovani, A.; Sozzani, S.; Locati, M.; Allavena, P.; Sica, A., Macrophage polarization: tumor-associated macrophages as a paradigm for polarized M2 mononuclear phagocytes. *Trends Immunol* **2002,** *23* (11), 549-55.

34. Mosser, D. M.; Edwards, J. P., Exploring the full spectrum of macrophage activation. *Nature Reviews Immunology* **2008,** *8* (12), 958-969.

35. Virág, L.; Szabó, E.; Bakondi, E.; Bai, P.; Gergely, P.; Hunyadi, J.; Szabó, C., Nitric oxide-peroxynitrite-poly(ADP-ribose) polymerase pathway in the skin. *Exp Dermatol* **2002,** *11* (3), 189-202.

36. Mowbray, M.; Tan, X.; Wheatley, P. S.; Morris, R. E.; Weller, R. B., Topically Applied Nitric Oxide Induces T-Lymphocyte Infiltration in Human Skin, but Minimal Inflammation. *Journal of Investigative Dermatology* **2008,** *128* (2), 352-360.

37. Tunctan, B.; Altug, S., The Use of Nitric Oxide Synthase Inhibitors in Inflammatory Diseases: A Novel Class of Anti-Inflammatory Agents. *Current Medicinal Chemistry - Anti-Inflammatory & Anti-Allergy Agents* **2004,** *3* (3), 271-301.

38. Gambardella, J.; Khondkar, W.; Morelli, M. B.; Wang, X.; Santulli, G.; Trimarco, V., Arginine and Endothelial Function. *Biomedicines* **2020,** *8* (8).

39. Yuan, G.; Wahlqvist, M. L.; He, G.; Yang, M.; Li, D., Natural products and anti-inflammatory activity. *Asia Pac J Clin Nutr* **2006,** *15* (2), 143-52.

40. Vane, J. R., Inhibition of prostaglandin synthesis as a mechanism of action for aspirin-like drugs. *Nat New Biol* **1971,** *231* (25), 232-5.

41. Attiq, A.; Jalil, J.; Husain, K.; Ahmad, W., Raging the War Against Inflammation With Natural Products. *Frontiers in pharmacology* **2018,** *9*, 976-976.

42. Azab, A.; Nassar, A.; Azab, A. N., Anti-Inflammatory Activity of Natural Products. *Molecules* **2016,** *21* (10).

43. Wang, R. X.; Zhou, M.; Ma, H. L.; Qiao, Y. B.; Li, Q. S., The Role of Chronic Inflammation in Various Diseases and Anti-inflammatory Therapies Containing Natural Products. *ChemMedChem* **2021,** *16* (10), 1576-1592.

44. Li, J.; Zhang, H.; Huang, W.; Qian, H.; Li, Y., TNF-α inhibitors with anti-oxidative stress activity from natural products. *Curr Top Med Chem* **2012,** *12* (13), 1408-21.

45. Peng, Y.; Ao, M.; Dong, B.; Jiang, Y.; Yu, L.; Chen, Z.; Hu, C.; Xu, R., Anti-Inflammatory Effects of Curcumin in the Inflammatory Diseases: Status, Limitations and Countermeasures. *Drug Design, Development and Therapy* **2021,** *Volume 15*, 4503-4525.

46. Ouyang, J.; Zhu, K.; Liu, Z.; Huang, J., Prooxidant Effects of Epigallocatechin-3-Gallate in Health Benefits and Potential Adverse Effect. *Oxidative Medicine and Cellular Longevity* **2020,** *2020*, 9723686.

47. Tsai, H.-R.; Yang, L.-M.; Tsai, W.-J.; Chiou, W.-F., Andrographolide acts through inhibition of ERK1/2 and Akt phosphorylation to suppress chemotactic migration. *European Journal of Pharmacology* **2004,** *498* (1), 45-52.

48. Hidalgo, M. A.; Romero, A.; Figueroa, J.; Cortés, P.; Concha, II; Hancke, J. L.; Burgos, R. A., Andrographolide interferes with binding of nuclear factor-kappaB to DNA in HL-60-derived neutrophilic cells. *Br J Pharmacol* **2005,** *144* (5), 680-6.

49. Shang, Y.-x.; Shen, C.; Stub, T.; Zhu, S.-j.; Qiao, S.-y.; Li, Y.-q.; Wang, R.-t.; Li, J.; Liu, J.-p., Adverse Effects of Andrographolide Derivative Medications Compared to the Safe use of Herbal Preparations of Andrographis paniculata: Results of a Systematic Review and Meta-Analysis of Clinical Studies. *Frontiers in Pharmacology* **2022,** *13*.

50. Deng, W.; Du, H.; Liu, D.; Ma, Z., The Role of Natural Products in Chronic Inflammation. *Frontiers in Pharmacology* **2022**, 1521.

51. Rainsford, K. D., Anti-inflammatory drugs in the 21st century. *Subcell Biochem* **2007,** *42*, 3-27.

52. Wu, K. K., Aspirin and other cyclooxygenase inhibitors: new therapeutic insights. *Semin Vasc Med* **2003,** *3* (2), 107-12.

53. Kulkarni, R. G.; Achaiah, G.; Sastry, G. N., Novel targets for antiinflammatory and antiarthritic agents. *Curr Pharm Des* **2006,** *12* (19), 2437-54.

54. Davies, N. M.; Jamali, F., COX-2 selective inhibitors cardiac toxicity: getting to the heart of the matter. *J Pharm Pharm Sci* **2004,** *7* (3), 332-6.

55. Jugran, A. K.; Rawat, S.; Devkota, H. P.; Bhatt, I. D.; Rawal, R. S., Diabetes and plant-derived natural products: From ethnopharmacological approaches to their potential for modern drug discovery and development. *Phytother Res* **2021,** *35* (1), 223-245.

56. Dehvan, F.; Qasim Nasif, F.; Dalvand, S.; Ausili, D.; Hasanpour Dehkordi, A.; Ghanei Gheshlagh, R., Self-care in Iranian patients with diabetes: A systematic review and meta-analysis. *Prim Care Diabetes* **2021,** *15* (1), 80-87.

57. Cock, I. E.; Ndlovu, N.; Van Vuuren, S. F., The use of South African botanical species for the control of blood sugar. *J Ethnopharmacol* **2021,** *264*, 113234.

58. Nawaz, A.; Zhang, P.; Li, E.; Gilbert, R. G.; Sullivan, M. A., The importance of glycogen molecular structure for blood glucose control. *iScience* **2021,** *24* (1), 101953.

59. Stumvoll, M.; Goldstein, B. J.; van Haeften, T. W., Type 2 diabetes: principles of pathogenesis and therapy. *Lancet* **2005,** *365* (9467), 1333-46.

60. Joshi, D. M.; Patel, J.; Bhatt, H., In silico study to quantify the effect of exercise on surface GLUT4 translocation in diabetes management. *Network Modeling Analysis in Health Informatics and Bioinformatics* **2021,** *10* (1), 1.

61. Gebrie, D.; Getnet, D.; Manyazewal, T., Cardiovascular safety and efficacy of metformin-SGLT2i versus metformin-sulfonylureas in type 2 diabetes: systematic review and meta-analysis of randomized controlled trials. *Sci Rep* **2021,** *11* (1), 137.

62. Zheng, Y.; Ley, S. H.; Hu, F. B., Global aetiology and epidemiology of type 2 diabetes mellitus and its complications. *Nature Reviews Endocrinology* **2018,** *14* (2), 88-98.

63. Halimi, S.; Schweizer, A.; Minic, B.; Foley, J.; Dejager, S., Combination treatment in the management of type 2 diabetes: focus on vildagliptin and metformin as a single tablet. *Vasc Health Risk Manag* **2008,** *4* (3), 481-492.

64. Koehn, F. E.; Carter, G. T., The evolving role of natural products in drug discovery. *Nature Reviews Drug Discovery* **2005,** *4* (3), 206-220.

65. Makwana, A. R.; Sameja, K.; Rao, S., A review on medicinal plants of Gujarat with anti-diabetic potential. **2016,** *8*, 167-173.

66. Oh, Y. S., Plant-Derived Compounds Targeting Pancreatic Beta Cells for the Treatment of Diabetes. *Evid Based Complement Alternat Med* **2015,** *2015*, 629863.

67. Tran, N.; Pham, B.; Le, L., Bioactive Compounds in Anti-Diabetic Plants: From Herbal Medicine to Modern Drug Discovery. *Biology (Basel)* **2020,** *9* (9).

68. Hung, H. Y.; Qian, K.; Morris-Natschke, S. L.; Hsu, C. S.; Lee, K. H., Recent discovery of plant-derived anti-diabetic natural products. *Nat Prod Rep* **2012,** *29* (5), 580-606.

69. Xu, L.; Li, Y.; Dai, Y.; Peng, J., Natural products for the treatment of type 2 diabetes mellitus: Pharmacology and mechanisms. *Pharmacol Res* **2018,** *130*, 451-465.

70. Russo, M.; Russo, G. L.; Daglia, M.; Kasi, P. D.; Ravi, S.; Nabavi, S. F.; Nabavi, S. M., Understanding genistein in cancer: The "good" and the "bad" effects: A review. *Food Chemistry* **2016,** *196*, 589-600.

71. Leatherdale, B. A.; Panesar, R. K.; Singh, G.; Atkins, T. W.; Bailey, C. J.; Bignell, A. H., Improvement in glucose tolerance due to Momordica charantia (karela). *Br Med J (Clin Res Ed)* **1981,** *282* (6279), 1823-4.

72. Sarkar, S.; Pranava, M.; Marita, R., Demonstration of the hypoglycemic action of Momordica charantia in a validated animal model of diabetes. *Pharmacol Res* **1996,** *33* (1), 1-4.

73. Schultz, W. M.; Varghese, T.; Heinl, R. E.; Dhindsa, D. S.; Mahlof, E. N.; Cai, H. C.; Southmayd, G.; Sandesara, P. B.; Eapen, D. J.; Sperling, L. S., Natural Approaches in Diabetes Management: A Review of Diet, Exercise, and Natural Products. *Curr Pharm Des* **2018,** *24* (1), 84-98.

74. Alam, F.; Islam, M. A.; Kamal, M. A.; Gan, S. H., Updates on managing type 2 diabetes mellitus with natural products: towards antidiabetic drug development. *Current Medicinal Chemistry* **2018,** *25* (39), 5395-5431.

75. Saxena, A.; Vikram, N. K., Role of selected Indian plants in management of type 2 diabetes: a review. *J Altern Complement Med* **2004,** *10* (2), 369-78.

76. Mapunya, M. B.; Nikolova, R. V.; Lall, N., Melanogenesis and antityrosinase activity of selected South african plants. *Evid Based Complement Alternat Med* **2012,** *2012*, 374017.

77. Rangkadilok, N.; Sitthimonchai, S.; Worasuttayangkurn, L.; Mahidol, C.; Ruchirawat, M.; Satayavivad, J., Evaluation of free radical scavenging and antityrosinase activities of standardized longan fruit extract. *Food and Chemical Toxicology* **2007,** *45* (2), 328-336.

78. Wang, K.-H.; Lin, R.-D.; Hsu, F.-L.; Huang, Y.-H.; Chang, H.-C.; Huang, C.-Y.; Lee, M.-H., Cosmetic applications of selected traditional Chinese herbal medicines. *Journal of ethnopharmacology* **2006,** *106* (3), 353-359.

79. Kim, Y.-J.; Uyama, H., Tyrosinase inhibitors from natural and synthetic sources: structure, inhibition mechanism and perspective for the future. *Cellular and molecular life sciences CMLS* **2005,** *62*, 1707-1723.

80. Summers, B., A lightening tour of skin-brightening options. *Pharm. Cosmet. Rev* **2006,** *33*, 29-30.

81. Bulpitt, C.; Markowe, H.; Shipley, M., Why do some people look older than they should? *Postgraduate medical journal* **2001,** *77* (911), 578-581.

82. Nerya, O.; Vaya, J.; Musa, R.; Izrael, S.; Ben-Arie, R.; Tamir, S., Glabrene and isoliquiritigenin as tyrosinase inhibitors from licorice roots. *Journal of Agricultural and Food Chemistry* **2003,** *51* (5), 1201-1207.

83. Fernandez, X.; Michel, T.; Azoulay, S., Actifs cosmétiques à effet blanchissant-Nature, efficacité et risques. **2015**.

84. Hanif, N.; Al-Shami, A. M. A.; Khalid, K. A.; Hadi, H., Plant-based skin lightening agents: A review. *J. Phytopharm* **2020,** *9*, 54-60.

85. Chaowattanapanit, S.; Silpa-Archa, N.; Kohli, I.; Lim, H. W.; Hamzavi, I., Postinflammatory hyperpigmentation: A comprehensive overview: Treatment options and prevention. *Journal of the American Academy of Dermatology* **2017,** *77* (4), 607-621.

86. Agrawal, S.; Mazhar, M., Adulteration of mercury in skin whitening creams–A nephrotoxic agent. *Current Medicine Research and Practice* **2015,** *5* (4), 172-175.

87. Gupta, S.; Gautam, A.; Kumar, S., Natural skin whitening agents: a current status. *Adv Biol Res (Rennes)* **2014,** *8* (6), 257-259.

88. Haron, H.; Jamil, A.; Besar, N. A. A., Photoprotection and skin whitening effect of dietary soy milk in healthy young female adults. *Journal of Pakistan Association of Dermatologists* **2020,** *30* (3), 412-417.

89. Parvez, S.; Kang, M.; Chung, H. S.; Cho, C.; Hong, M. C.; Shin, M. K.; Bae, H., Survey and mechanism of skin depigmenting and lightening agents. *Phytotherapy Research: An International Journal Devoted to Pharmacological and Toxicological Evaluation of Natural Product Derivatives* **2006,** *20* (11), 921-934.

90. Paine, C.; Sharlow, E.; Liebel, F.; Eisinger, M.; Shapiro, S.; Seiberg, M., An alternative approach to depigmentation by soybean extracts via inhibition of the PAR-2 pathway. *Journal of investigative dermatology* **2001,** *116* (4), 587-595.

91. Burdock, G. A.; Soni, M. G.; Carabin, I. G., Evaluation of health aspects of kojic acid in food. *Regulatory toxicology and pharmacology* **2001,** *33* (1), 80-101.

92. Cabanes, J.; Chazarra, S.; Garcia-Carmona, F., Kojic acid, a cosmetic skin whitening agent, is a slow-binding inhibitor of catecholase activity of tyrosinase. *Journal of Pharmacy and Pharmacology* **1994,** *46* (12), 982-985.

93. Hori, I.; Nihei, K. i.; Kubo, I., Structural criteria for depigmenting mechanism of arbutin. *Phytotherapy Research: An International Journal Devoted to Pharmacological and Toxicological Evaluation of Natural Product Derivatives* **2004,** *18* (6), 475-479.

94. Fitton, A.; Goa, K. L., Azelaic acid: a review of its pharmacological properties and therapeutic efficacy in acne and hyperpigmentary skin disorders. *Drugs* **1991,** *41*, 780-798.

95. Briganti, S.; Camera, E.; Picardo, M., Chemical and instrumental approaches to treat hyperpigmentation. *Pigment cell research* **2003,** *16* (2), 101-110.

96. Palumbo, G.; Fanini, D.; Pantaleoni, G.; Carlucci, G., Pharmacological studies on furprofen-its pharmokinetic profile and antiinflammatory action following oral-adminstration. *International Journal of Immunopathology and Pharmacology* **1991,** *4* (2), 85-90.

97. Yang, C., Tea and health. *Nutrition (Burbank, Los Angeles County, Calif.)* **1999,** *15* (11-12), 946-949.

98. Kamau, P.; Jordan, R., Kinetic study of the oxidation of catechol by aqueous copper (II). *Inorganic chemistry* **2002,** *41* (12), 3076-3083.

99. Davids, L. M.; Van Wyk, J.; Khumalo, N. P.; Jablonski, N. G., The phenomenon of skin lightening: Is it right to be light? *South African Journal of Science* **2016,** *112* (11-12), 1-5.

100. Wu, X.; Gao, H.; Sun, W.; Yu, J.; Hu, H.; Xu, Q.; Chen, X., Nepetoidin B, a Natural Product, Inhibits LPS-stimulated Nitric Oxide Production via Modulation of iNOS Mediated by NF-κB/MKP-5 Pathways. *Phytotherapy Research* **2017,** *31* (7), 1072-1077.

101. Hsieh, I. N.; Chang, A. S.-Y.; Teng, C.-M.; Chen, C.-C.; Yang, C.-R., Aciculatin inhibits lipopolysaccharide-mediated inducible nitric oxide synthase and cyclooxygenase-2 expression via suppressing NF-κB and JNK/p38 MAPK activation pathways. *Journal of Biomedical Science* **2011,** *18* (1), 28.

102. Lanas, A.; Scheiman, J., Low-dose aspirin and upper gastrointestinal damage: epidemiology, prevention and treatment. *Current Medical Research and Opinion* **2007,** *23* (1), 163-73.

103. Recio, M. C.; Andujar, I.; Rios, J. L., Anti-inflammatory agents from plants: progress and potential. *Curr Med Chem* **2012,** *19* (14), 2088-103.

104. Opperman, L.; De Kock, M.; Klaasen, J.; Rahiman, F., Tyrosinase and melanogenesis inhibition by indigenous African plants: A review. *Cosmetics* **2020,** *7* (3), 60.

105. Sagoe, D.; Pallesen, S.; Dlova, N. C.; Lartey, M.; Ezzedine, K.; Dadzie, O., The global prevalence and correlates of skin bleaching: a meta-analysis and meta-regression analysis. *International journal of dermatology* **2019,** *58* (1), 24-44.

106. Kamagaju, L.; Morandini, R.; Gahongayire, F.; Stévigny, C.; Ghanem, G.; Pirotte, G.; Duez, P., Survey on skin-lightening practices and cosmetics in Kigali, Rwanda. *International Journal of Dermatology* **2016,** *55* (1), 45-51.

107. Gbetoh, M. H.; Amyot, M., Mercury, hydroquinone and clobetasol propionate in skin lightening products in West Africa and Canada. *Environmental research* **2016,** *150*, 403-410.

108. Di Petrillo, A.; González-Paramás, A. M.; Era, B.; Medda, R.; Pintus, F.; Santos-Buelga, C.; Fais, A., Tyrosinase inhibition and antioxidant properties of Asphodelus microcarpus extracts. *BMC complementary and alternative medicine* **2016,** *16* (1), 1-9.

109. Ribeiro, A. S.; Estanqueiro, M.; Oliveira, M. B.; Sousa Lobo, J. M., Main benefits and applicability of plant extracts in skin care products. *Cosmetics* **2015,** *2* (2), 48-65.

110. Ali, S., Recent advances in treatment of skin disorders using herbal products. *Journal of Skin* **2017,** *1* (1), 6-7.

111. Otang-Mbeng, W.; Sagbo, I. J., Anti-Melanogenesis, Antioxidant and Anti-Tyrosinase Activities of Scabiosa columbaria L. *Processes* **2020,** *8* (2).

112. Maroyi, A., Scabiosa columbaria: A review of its medicinal uses, phtochemistry and biological activities. *Asian Journal of Pharmaceutical and Clinical Research* **2019**, 10-14.

113. Wild, S.; Roglic, G.; Green, A.; Sicree, R.; King, H., Global prevalence of diabetes: estimates for the year 2000 and projections for 2030. *Diabetes Care* **2004,** *27* (5), 1047-53.

114. Munhoz, A. C. M.; Frode, T. S., Isolated Compounds from Natural Products with Potential Antidiabetic Activity - A Systematic Review. *Curr Diabetes Rev* **2018,** *14* (1), 36-106.

115. Qi, L. W.; Liu, E. H.; Chu, C.; Peng, Y. B.; Cai, H. X.; Li, P., Anti-diabetic agents from natural products--an update from 2004 to 2009. *Curr Top Med Chem* **2010,** *10* (4), 434-57.

116. Ryan, E. A.; Pick, M. E.; Marceau, C., Use of alternative medicines in diabetes mellitus. *Diabet Med* **2001,** *18* (3), 242-5.

117. Peesa, J., Herbal medicine for diabetes mellitus: A Review. *International Journal of Phytopharmacy* **2013,** *3*.

118. Ojewole, J. A.; Mawoza, T.; Chiwororo, W. D.; Owira, P. M., Sclerocarya birrea (A. Rich) Hochst.['Marula'](Anacardiaceae): a review of its phytochemistry, pharmacology and toxicology and its ethnomedicinal uses. *Phytotherapy Research: An International Journal Devoted to Pharmacological and Toxicological Evaluation of Natural Product Derivatives* **2010,** *24* (5), 633-639.

119. Xu, D. P.; Li, Y.; Meng, X.; Zhou, T.; Zhou, Y.; Zheng, J.; Zhang, J. J.; Li, H. B., Natural Antioxidants in Foods and Medicinal Plants: Extraction, Assessment and Resources. *Int J Mol Sci* **2017,** *18* (1).

120. Iwu, M.; Duncan, A.; Okunji, C., New Antimicrobials of Plant Origin. *Perspectives on new crops and new uses* **1999**.

121. Dimo, T.; Rakotonirina, S. V.; Tan, P. V.; Azay, J.; Dongo, E.; Kamtchouing, P.; Cros, G., Effect of *S. birrea* (Anacardiaceae) stem bark methylene chloride/methanol extract on streptozotocin-diabetic rats. *J Ethnopharmacol* **2007,** *110* (3), 434-8.

Chapter 2: Evaluation of South African plant species for anti-inflammatory activity and skin even tone

2.1 Introduction

2.1.1 The role of ethnobotany in the selection of plants

Herbal medicine is still utilized in the healthcare system, especially in the underdeveloped countries. This traditional medicine is passed down through generations based on the experiences that was there long before any written records existed.[1] Numerous drugs including morphine, artemisinin, quinine, aspirin and many others, are derived from traditional uses.[2] This traditional use of plants for health care is called ethnobotanical medicine.[3] Traditional medicine encompasses all alternative medical philosophies, typically excluding so-called "Western" medicine. In general, plants employed in diverse kinds of traditional medicine have varying potential therapeutic properties, depending on the level of authenticity of the associated medical practice. Traditional Chinese, Ayurvedic, and Unani medical systems, for instance, are all founded on theories (beliefs may vary), formal education, and a written historically accurate past. The systems are frequently updated in light of experience and contemporary thinking. In these activities, the apprentice system is used to pass on knowledge from one person to another, from father to son, or from guru to disciple. These systems generally lack a formal teaching component, and the information is frequently treated as highly confidential and not recorded in writing. Despite the doubts of western-trained medical professionals and scientists regarding the value of information resulting from any of these systems, collectively they are currently providing for the primary healthcare requirements of the majority of the world's population, and this source must not be disregarded in any program of rational drug development, starting with plant materials.[4]

2.1.2 Plant collection approaches and selection criteria

For researchers conducting phytochemical analysis of medicinal plants with the goal of isolating and identifying the active ingredients, it is important that the right choice of plant species must be made. This decision is challenging given the variety of plants that haven't been thoroughly investigated from a phytochemical and pharmacological standpoint.[5] A variety of methods or selection criteria can be used to choose plant materials. These criteria include

details on their traditional or folk medical uses, high taxonomic diversity of the source material, chemotaxonomic relationships of previously known biological activity in an organism, promising biological test results (published or unpublished) on a particular plant in a previous study, toxicity of plant and field observation on signs of interaction between organisms.[6]

It is widely accepted that folk or traditional medicinal uses of plants indicate the presence of biologically active constituent(s) in a plant. The prolonged and continuing use of a particular plant in an indigenous culture to treat certain ailment should provide a demonstration of efficacy. Collecting plants with such uses for drug testing is believed to increase the odds in discovering new medicines.[6] The screening of a huge collection of varied plant samples for one or more biological activities is a second and extremely popular method for discovering new plants. This strategy is justified by the observation that a broad range or array of taxonomic variety reflects a great diversity of chemical compounds, as each species of plant produces a unique set of chemicals as a result of millions of years of biological evolution. The term "random collection" is frequently used to describe this screening technique. Compared to an ethnobotanically based drug discovery approach, the discovery reservoir is much deeper in biodiversity-based search, however in view of the large number of plants to be looked at, and the large number of therapeutic categories against which tests have to made, biodiversity-based drug discovery approach is considered a very expensive process while the chances of discovery are very low.[6]

Related plant taxa tend to produce similar chemical compounds. The closer the taxonomic relationships, the better are the chances that similar or related compounds may occur in these taxa. In cases where a molecule or compounds have significant medical or pharmaolgical implications, efforts are undertaken to locate analogous or comparable compounds among allied taxa. Different forms belonging to the same species, different species in the same genus and even different genera in the same family. Such knowledge is the basis of chemotaxonomy.[7] Positive and promising laboratory (*in vitro*) test results for an extract provide a strong basis to go back to the field to recollect samples of the same taxon of plant in a large quantity for further studies. Data on such activity may be obtained from unpublished laboratory test of samples originally collected based on the criteria described above or from published literature sources. This criterion is important to guide on the plant species to be selected especially if it has been reported for the biological activity of interest.[6] Another criteria to take into account when

choosing a plant species is the toxicity of the species. Reported toxicity (low or high toxicity) of a plant species can reduce the chances of selecting a plant species.

During plant collecting expeditions, field observations are obviously very important. A species which grows in a hostile environment (such as tropical forest) in which there is a danger of attack from insects, bacteria, fungi or virus will attempt to protect itself by synthesizing insecticidal, anti-bacterial, fungicidal or virucidal constituents. Queiroz et al. reported that the berries of *Phytolacca dodecandra,* were used as a traditional soap to kill snails. This allowed the discovery of a new class of molluscicidal compounds, the saponins. Field observation have been increasingly recognized to be an important criterion in selecting plant(s) for collection of biomedical evaluation. Unfortunately, examples of cosmeceuticals that have been discovered through this approach are not available while the reservoir for discovery through this approach is scarce.[5]

A multifactorial plant selection method employing various criteria (as discussed above) was applied in order to select plant species that were screened for anti-inflammatory and anti-melanogenesis activity. For each criterion (traditional medicinal uses, published scientific findings and toxicity), an arbitrary score system was ascribed to the species and the sum of these enabled the comparison of potential candidates.

2.1.3   Inflammation, cosmeceuticals used for skin inflammation and bioassays used in assessing anti-inflammatory agents

The skin encounters daily onslaught by exogenous stimuli. Noxious stimuli sometimes result in injuries and/or infections, leading to wound, inflammatory dermatoses, skin ageing or skin carcinogenesis. Inflammation takes place in response to these damages to the normal skin barrier. At the molecular level, the inflammatory response participates in a series of complex repair pathways related to the innate immune response, cutaneous differentiation and skin barrier repair.[8] Initially, upon inflammatory response, the keratinocytes and the innate immune cells are activated.[9] Secreted cytokines such as IL-1α, TNF-α and IL-6 induce the chemokines of chemotaxis that attract the immune cells to the site of injury and infection. Reactive oxygen species are produced by activated keratinocytes and immune cells.[8] The inflammatory microenvironment contributes to tissue repair and infection prevention/control. However, the chemokines produced by activated keratinocytes and immune cells are also able to damage the

skin tissue in proximity to the target of the inflammatory response. Therefore, the intensity of inflammation and the time to resolution are critical in avoiding or at least limiting damage to normal skin tissue.[9] Thus, modulation of inflammation is important in maintaining skin homeostasis. If the initial acute response fails to resolve the causative factor, then the inflammatory response will continue, and the subsequent inflammatory microenvironment will disrupt skin homeostasis. If the dysregulation of inflammatory skin response persists, chronic inflammation dermatoses such as atopic dermatitis, psoriasis, skin ageing and other skin disorders arises.[10]

Considering the increased vulnerability to environmental damage and the development of skin diseases, skin disorders caused by inflammation have gained increased attention from dermatologist. Skin disorders such as psoriasis, atopic dermatitis, acne, eczema and skin lesions associated with inflammation have thus led patients to consider the use of cosmetic products for improved skin condition.[11] Cosmeceuticals have gained popularity because of widespread acceptance of the apparent safety and reduced side effects of compounds isolated from natural sources. The role of some cosmeceutical products in the treatment of skin inflammation disorders is described as follows: Chronic inflammation has been closely linked with skin ageing.[12] Skin ageing is influenced both by intrinsic and extrinsic factors that result in the loss of structural integrity and physiological function.[13] Chronic inflammation as a result of sun exposure occurs in response to the release of proteolytic enzyme including TNF-α and IL-6 from keratinocytes that disrupt the permeability of the stratum corneum.[13, 14] Pharmaceuticals targeted at reversing chronic inflammation have been recommended as plausible regimes for the treatment of skin aging.[12] They are described in section 2.1.4.

Atopic dermatitis (AD) is associated with excess immunoglobin E production and inflammation is a characteristic indication of the disorder.[16] Topical steroids are used as standard treatment to reduce inflammation in patients suffering with AD. Although, topical steroids provide rapid relief, their use has been associated with significant adverse effect including acne, excessive hair growth, atrophy and hypopigmentation.[17] The anti-inflammatory properties of aloe including their role in atopic dermatitis are well documented. Finberg and colleagues evaluated the anti-inflammatory activity of *A. ferox* and *A. vera* gel extracts and reported a reduction in cutaneous inflammatory responses in 2,4-dintirochlorobenzene challenged mice models after topical treatment through a reduction in serum immunoglobulin E (IgE) levels which is an important antibody that has been linked with AD.[16] The

36

phytochemical constituents of *A. vera* may thus be promising alternatives to topical corticosteroids in the treatment of AD. Therefore, looking for high performance anti-inflammatory ingredients for skin care products from plants is considered to be a promising strategy for preventing skin diseases and inflammation associated disorders.

There are several models to test the anti-inflammatory effects of topically applied agents. The *in vitro* models currently used in screening for cosmeceutical ingredients are as follows: Relatively simple and easy to produce two-dimensional (2D) skin cell cultures that allow assessment of response to a given stimulus. It can be considered the simplest *in vitro* model for analysing the cellular phenomena involved in the epidermal inflammatory process. Though this model do not take into account the complex structures and interactions within the tissues, they have an advantage of being able to assess the response of specific cells to a given stimulus.[19] Another commonly used cell culture for anti-inflammatory studies is RAW 264.7 from LPS stimulated murine macrophages which was used by Mokdad et al. to demonstrate the anti-inflammatory effects of free and liposome encapsulated thermal water on the skin. A significant reduction in the production of nitric oxide (NO) and a modulation of the production of TNF-α were observed.[20] Wu et al. established a coculture of HaCaT and U937 cell lines to find bromodomain and extra-terminal domain (BET) antagonists for the inhibition of skin inflammatory genes. Effective BET inhibitors were tested in a mouse model of imiquimod-induced psoriasis form dermatitis. This *in vitro* selection accurately predicted therapeutic efficacy *in vivo*.[21] The second *in vitro* model is three-dimensional (3D) cell culture that better mimic human skin physiology by more accurately replicating mechanical and chemical signals. This model is used to evaluate chemicals and other constituents such as skin irritation, corrosion, absorption and penetration.[18] The third *in vitro* model is skin on a chip which plays a role in mediating inflammatory response because it is the pathway by which immune cells migrate between lymphoid organs and peripheral tissues.[22, 23] Skin on a chip device have numerous biomedical applications including skin disease modelling, cosmetic development, skin health monitoring and cosmetic delivery efficiency studies.[24]

In vivo testing is the most reliable means to evaluate the anti-inflammatory effects of topically applied agent. However, due to the sensitivity of the animals used for in vivo testing and the potential harm that they get exposed to during experimental use, substituting the use of animals for *in silico* and *in vitro* techniques with the use of tissues of ethical origin is what is currently in use.[18] The *in vitro* models have the potential to aid in the search for effective therapeutics

for skin inflammation and are promising tools for future investigations. For the purpose of this study, the two-dimensional cell culture *in vitro* model was used to screen for anti-inflammatory ingredients from the selected plant species (*S. columbaria*, *C. pyracanthoides* and *P. capitatum)*.

2.1.4 South African plants researched for skin inflammation

Many South African plants are used traditionally for their anti-inflammatory properties. Four selected plant species, namely *Acokanthera oppositifolia*, *Plantago lanceolata*, *Conyza canadensis* and *Artemisia vulgaris* were reported to be part of plant species used in South Africa to treat infection and inflammation-related diseases.[25] The use of rooibos and honeybush in the treatment of skin disease has gained popularity worldwide. In addition to their rich anti-oxidant content, the anti-inflammatory properties of these species have bolstered their pharmaceutical appeal. Magcwebeba et al. described the anti-inflammatory activity of methanolic and aqueous rooibos and honeybush extracts in terms of their ability to inhibit UVB-induced accumulation of IL-α and the promoted apoptosis of cells that accumulate excess IL-α. [15] Fermented honeybush extracts displayed similar activity against UVB-induced damage in HaCaT keratinocytes where the expression of IL-1β, IL-6 and IL-8 were suppressed.[15] The extract was capable of upregulating the activity of epidermal barrier proteins including involucrin, filaggrin and loricrin and as the barrier function of the skin is improved so is the structural integrity of the skin.

Very little is known about the effects of South African medicinal plants in cytokine assays. Aqueous leaf extracts of *Adansonia digitata* induce a significant decrease of IL-6 and IL-8 *in vitro*.[26] The methanol leaf extract of *Ximenia caffra* inhibits mRNA expression of proinflammatory genes (IL-6, iNOS and TNF-α) using RT-qPCR *in vitro*. The extract significantly decreased the NF-kβ transcription activity in a dose-dependent manner by approximately 60% compared to the control. Furthermore, a significant decline was observed in the expression of IL-6, up to almost 100-fold compared to the untreated LPS induced cells. [27] *Aspalathus linearis* significantly decreased TNF-α and IL-6 levels in the liver of mice.[28]

The capacity of extracts of selected South African plants to inhibit NO synthesis and release in LPS stimulated RAW cells *in vitro* was reported by Adebayo et al. The leaf acetone extract of *Leucaeria leucocephala* (Lam.)de wit, Lippia javanica (Burm. f.) Spreng., *Maesa lanceolata*

Forssk had 97-99% inhibition on NO production at 25-30 µg mL^{-1}. The leaf ethanol extract of *Ocimium labiatum* had 100% inhibition on NO production at 25 µg mL^{-1}.[29]

Some of the Eastern Cape plant species used for various skin care have been identified to possess anti-inflammatory effects. These plants include *Acokanthera oppositifolia*, *Acacia karoo*, *Bowiea volubilis*, *Dodonaea viscosa*, *Elephantorrhiza elephantina*, *Erythrina lysistemon*, *Coreyia flanaganii*, *Grewia occidentalis*, *Pelargonium sidoides* and *Protex simplex* They were reported to inhibit skin inflammation.[30]

Further investigation of species with promising anti-inflammatory activity resulted in the isolation of several bio-active compounds. Root and seed extracts of *Ziziphus spinachristi* inhibited NF-kB-DNA binding. The active compounds epigallocatechin (**12**), gallocatechin (**13**), spinosin (**14**), 6''feruloylspinosin (**15**) and 6''sinapoylspinosin (**16**) contributed to the activity.[31] From the DCM fraction of the methanolic extract of the root of *Jatropha curcas*, two lathyrane diterpenoids, jatrocurcasenone H (**17**) and jatrocurcasenone I (**18**) exhibited potent inhibitory activities against LPS-induced nitric oxide (NO) production in RAW 264.7 cells with IC$_{50}$ values of 11.28 and 7.71 µM, respectively.[32] Totarol (**19**) a compound isolated from many *Podocarpus* species inhibit linoleic acid autooxidation, mitochondrial and microsomal lipid peroxidation induced by Fe (III)-ADP/NADPH. Totarol is now commercially produced from *Podocarpus totara* as Totarol^{TM} and is effective as a topical anti-inflammatory agent.[33] Plumbagin (**20**), a napthoquinone compound had an IC$_{50}$ of 0.39 µM on NO production and a significant suppression of proinflammatory cytokine release. Another important plant derived anti-inflammatory compound is resveratrol (**21**). At 100 µg mL^{-1}, it significantly inhibited lipopolysaccharide (LPS) induced IL-6 and IL-8 secretion by human gingival fibroblast.[29]

Epigallocatechin (**12**)   Gallocatechin (**13**)

Spinosin (**14**)

6" feruloylspinosin (**15**)

6" sinapoylspinosin (**16**)

Jatrocurcasenone H (**17**)   Jatrocurcasenone I (**18**)

Totarol (**19**)   Plumbagin (**20**)

Resveratrol (**21**)
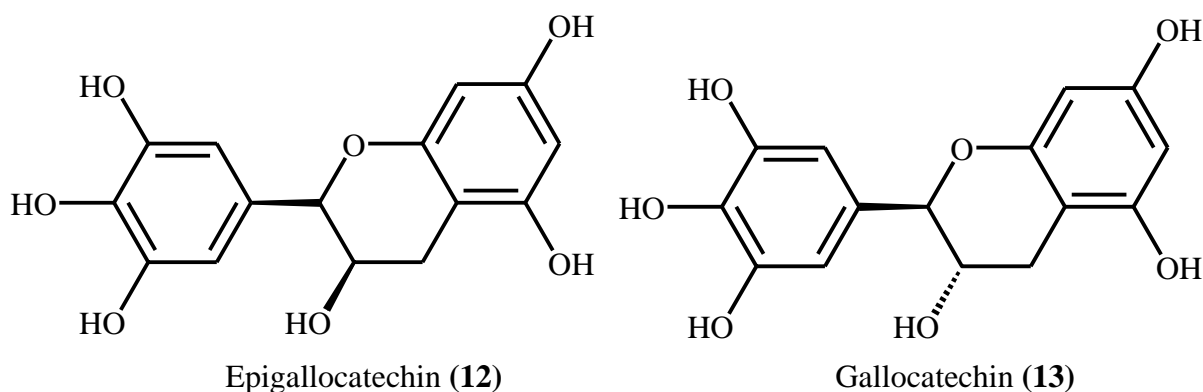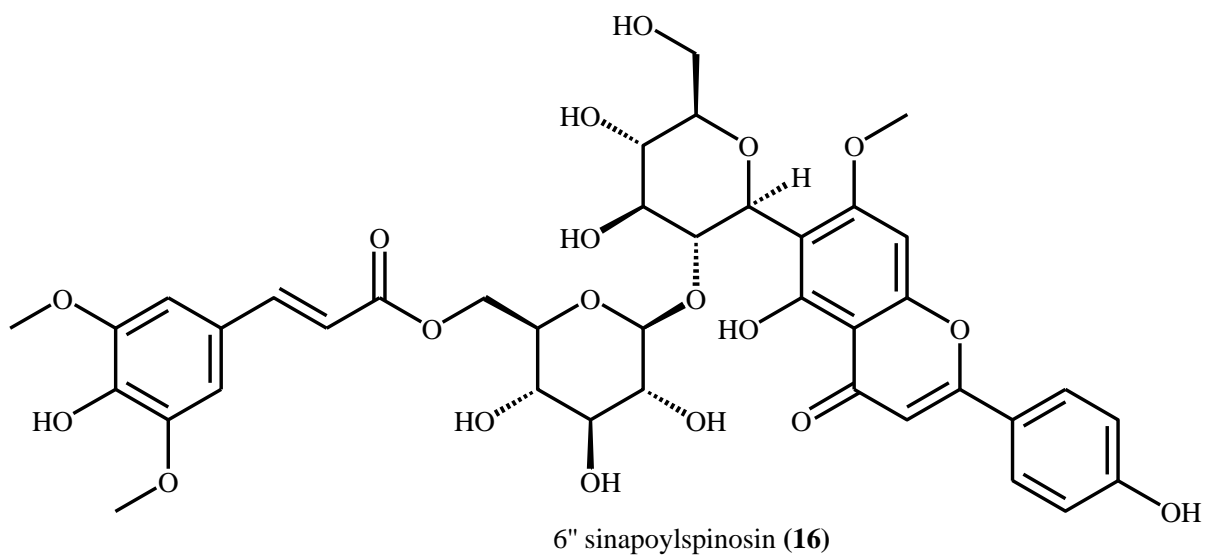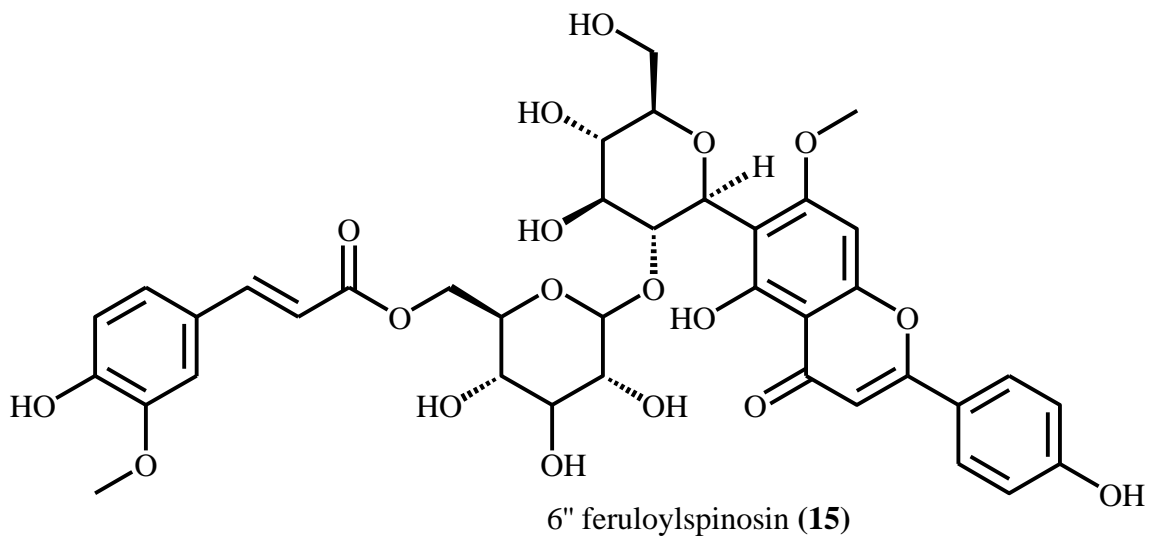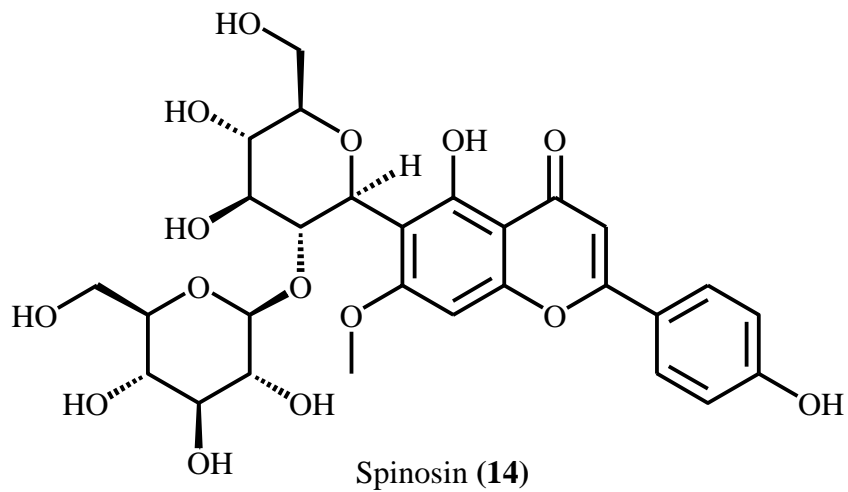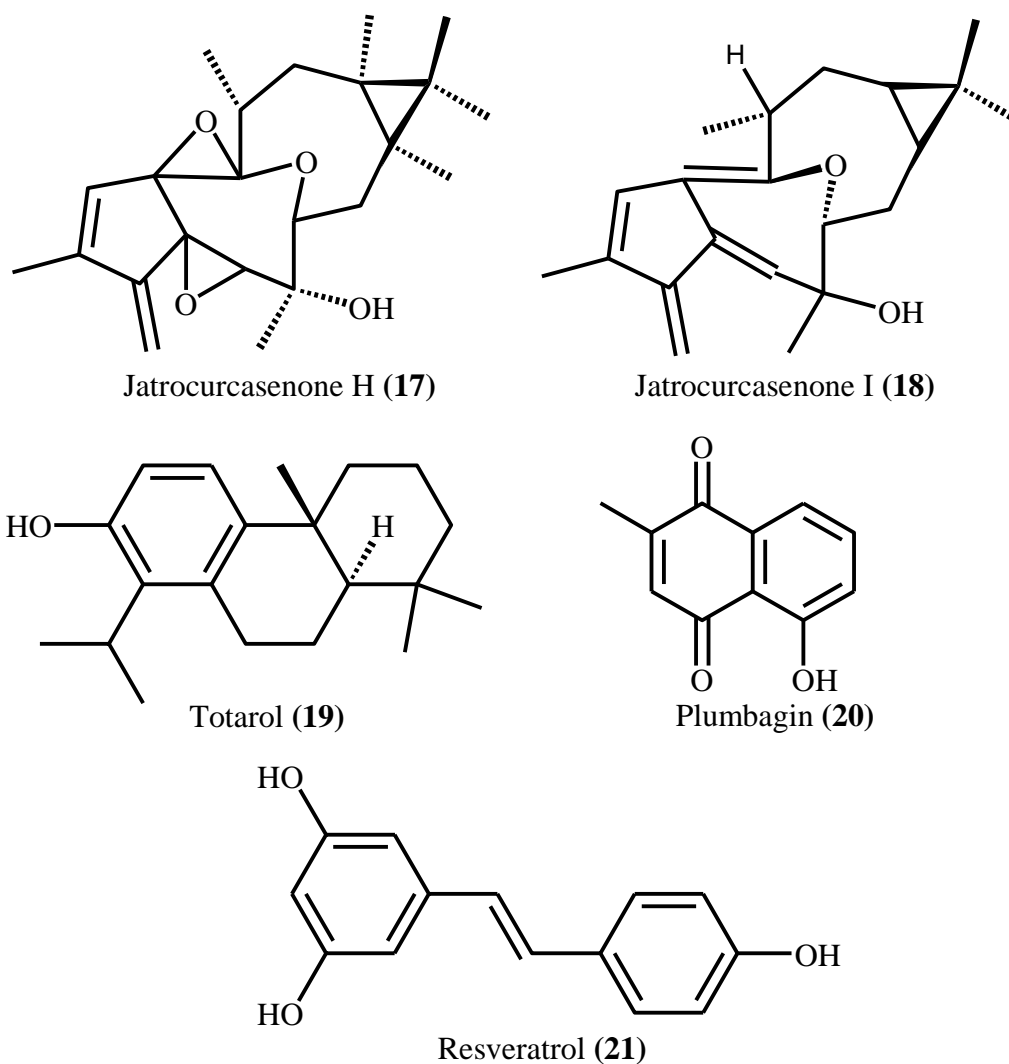
Figure 2.1: Chemical structures of anti-inflammatory compounds isolated from South African plants.

2.1.5   Skin even tone and bioassays used in assessing skin even tone agents

Melanin pigments in skin play a key role in determining skin colour and are synthesized by large dendritic cells known as melanocytes which are located at the epidermal-dermal junction. [34] Tyrosinase in melanocytes is a key enzyme in the synthesis of melanin pigments. [35] Melanocytes transfer melanin pigments to neighbouring cells such as keratinocytes. Melanin production and transport is increased by factors such as UV rays, hormones and chemicals resulting in darkening of the skin and development of age spots, freckles, melasma and other disorders of hyperpigmentation. [36] In different parts of the world, skin whitening products are very popular and are used to lighten the skin and to treat freckles and skin hyperpigmentation.

[37] The development of successful skin even tone products depend on the use of effective skin even tone ingredients that inhibit melanin formation in melanocytes.

A number of *in vitro* screening methods for assessing skin even tone agents are available and they include tyrosinase inhibition assay which involves inhibition of tyrosinase which is an enzyme that is engaged in the most important rate determining step in melanin biosynthesis. Melanogenesis is initiated by tyrosine that is metabolised into DOPA and then dopaquinone by tyrosinase. Therefore, studies on tyrosinase inhibitors are highly important for the development of new ingredients for the treatment of abnormal melanin coloration as well as functional cosmetics intended to produce a depigmenting effect.[38]

Another *in vitro* screening method is DOPA autooxidation inhibition assay used to measure the DOPA oxidation inhibited by tyrosinase. This method is similar to the aforementioned tyrosinase inhibition assay except it includes the use of DOPA as a substrate.[38] Dopachromeautomerase inhibition assay is another *in vitro* screening method which measure the inhibition of dopachrometautomerase enzyme which is a major enzyme that correlates with the melanogenesis pathway by catalysing the transformation of dopachrome into 5,6-dihydroxyindole-2-carboxylic acid (DHICA). The production of DHICA eventually leads to the brown DHICA-eumlanin which is followed by further oxidation and polymerization thereby stimulating epidermal melanogenesis.[39]

Evaluation of depigmenting effect using melanocytes is another *in vitro* screening method used for the evaluation of the depigmenting effect using melanocytes. It is a screening system that simulates condition similar to intracellular conditions compared with *in vitro* test of enzyme activity or autooxidation and has the advantage of being able to analyse overall effects on melanin biosynthesis by melanocytes. However, as this method is complex and time consuming, it is believed that this method is appropriate for the confirmatory evaluation of samples that are preliminary screened with an enzyme activity assay. Evaluation of the depigmenting effect using melanocytes can be performed by measuring the intracellular tyrosinase activity or the amount of intracellular melanin produced. Various methods are used depending on the type of cell line culture conditions and method of evaluation.[38] For the purpose of this study, human melanoma cell line was used in the evaluation of depigmenting effect of *S. columbaria* roots to ascertain if it can inhibit the production of melanin.

2.1.6 South African plants researched for skin even tone

Mapunya et al. investigated the melanogenesis and anti-tyrosinase activity of South African plants. The work presented the following species as traditionally utilized for the inhibition of melanin: *Aloe aculeata*, *Aloe pretoriensis*, *Calodendrum capensis* and *Sclerocarya birrea*.[40] Several plant extracts were tested for their inhibitory action on melanogenesis in mouse melanoma cells. The leaves and bark extracts of *Harpephyllum caffrum* showed 26% melanin inhibition at 6.25 µg mL^{-1}. The leaf extract of *Greyia flanaganii* exhibited 20% melanin inhibition at 6.25 µg mL^{-1}. The leaf extract of *Greyia radlkoferi* exhibited significant tyrosinase inhibition with an IC$_{50}$ value of 17.96 µg/mL with an isolated compound 2,4,6-trihydroxydihydroxychalcone (**22**) exhibiting a tyrosinase inhibition with an IC$_{50}$ value of 17.70 µg mL^{-1}. The shoot of *Myrsine africana* exhibited an 18% melanin inhibition with an IC$_{50}$ value of 12.50 µg mL^{-1}. *Garcinia mangostane* leaf extract showed tyrosinase inhibitory activity in a dose dependent manner without any significant effect on cell proliferation.[41] The stem bark extract of *Sideroxylon inerme* was reported to exhibit 37% melanin inhibition at an IC$_{50}$ value of 6.2 µg mL^{-1}.[42]

Antityrosinase compounds were also identified from South African plant species. Mikayoulou et al. isolated anthraquinones from two *Aloe* species (*Aloe ferox* and *Aloe plicatilis*) leaves methanol extracts, which displayed moderate to weak antityrosinase activity against mushroom tyrosinase with IC$_{50}$ values ranging from 31.5 to 84.1 µM.[43] The most active components were aloesin (**23**) and plicataloside (**24**) with IC$_{50}$ values of 31.5 and 84.1 µM, respectively. Mulholland et al. extracted twelve compounds in addition to triterpenoids from the stem bark and fruit of *Garcinia livingstonei*. and tested them for their impact on melanin levels of the melanocytes, from which three compounds, morelloflavone (**25**), morelloflavone-7"-sulphate (**26**) and sargaol (**27**) elicited a concentration-dependent decrease in melanin content with morelloflavone-7"-sulphate (**26**) having the most promising profile with IC$_{50}$ value of 8.6 µM.[44] Unfortunately, they also displayed cytotoxicity towards the melanocyte cells. From the methanolic and acetone stem bark extracts of *Sideroxylon inerme*, two compounds epigallocatechin gallate (**28**) and procyanidin B2 (**29**) were isolated and screened against monophenolase. They both displayed excellent tyrosinase activities with IC$_{50}$ values of 30 and >200 µg mL^{-1}, respectively.[42] Langat et al. isolated fifteen compounds from the stem bark of *Cassipourea flanaganii* and tested them for their skin even tone properties from which five compounds ent-atis-16-en-19-al (**30**), ent-kaur-16-en-19-al (**31**), 19-acetoxy-ent-atis-16-ene

43

(**32**), guinesine C (**33**) and β-amyrin (**34**) showed a concentration dependent effect on melanin content which did not appear to be dependent on their inhibition of tyrosinase.[42b]

2,4,6-trihydroxydihydroxychalcone (**22**)

Aloesin (**23**)

Plicataloside (**24**)
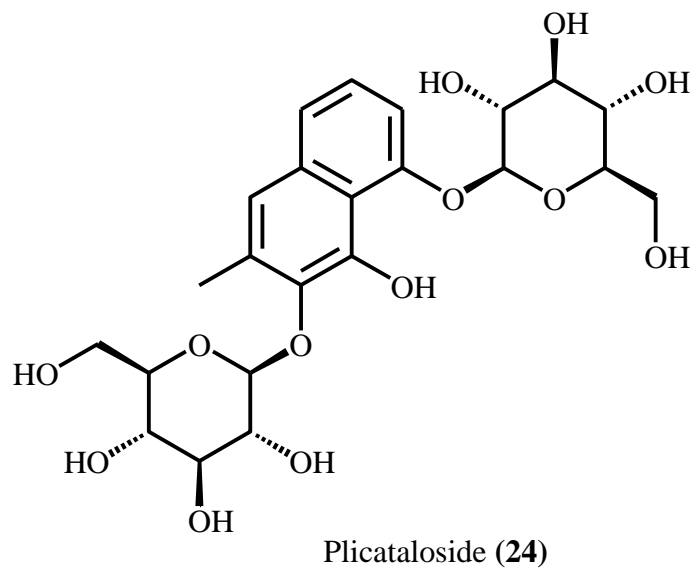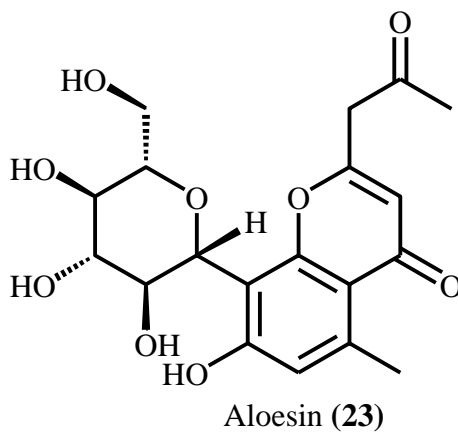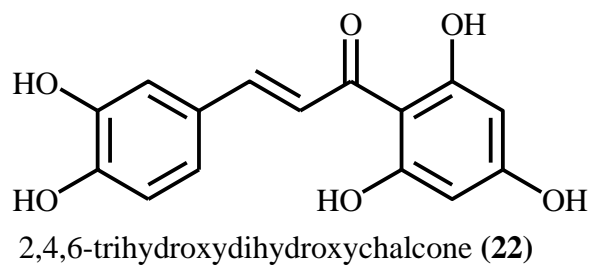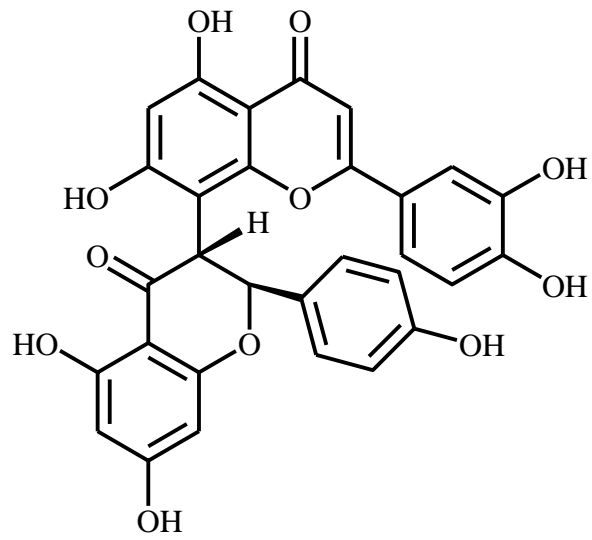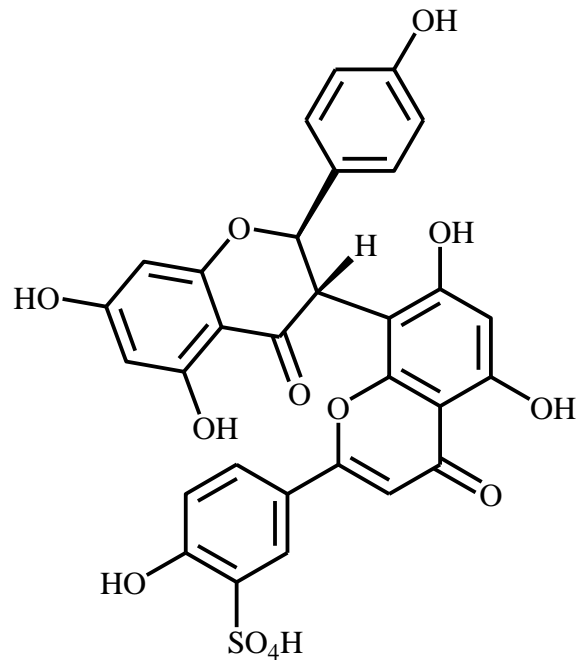
Morelloflavone (**25**)

morelloflavone-7"-sulphate (**26**)
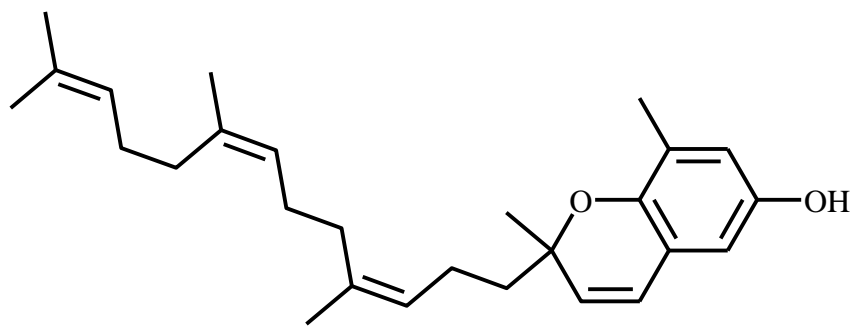
Sargaol (**27**)
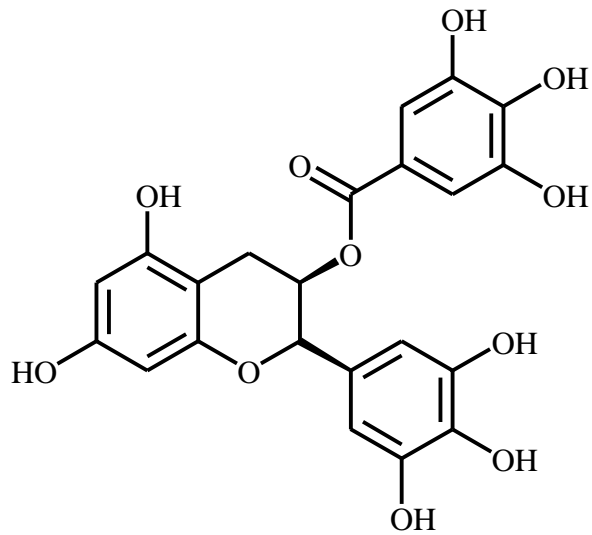
Epigallocatechin gallate **(28)**
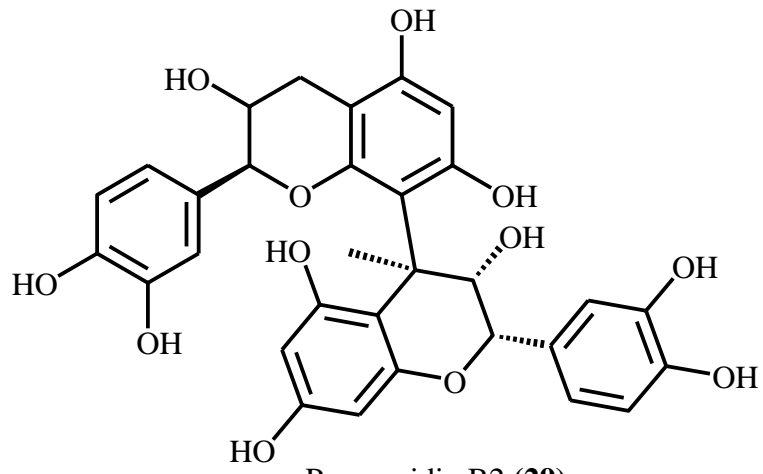
Procyanidin B2 **(29)**
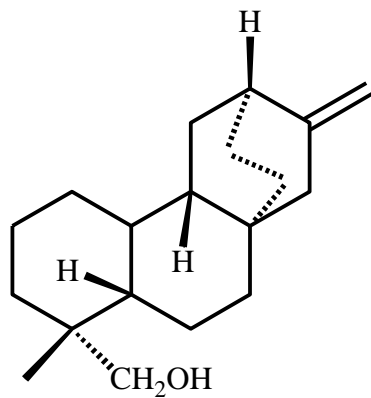
ent-atis-16-en-19-al **(30)**
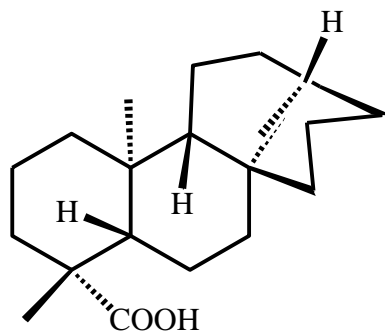
ent-kaur-16-en-19-al (**31**)
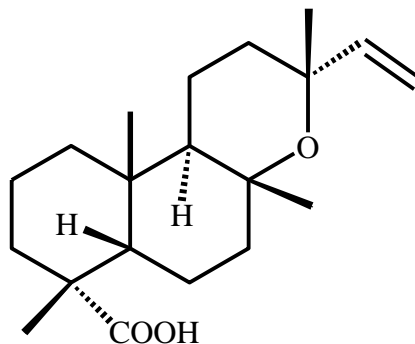
19-acetoxy-ent-atis-16-ene (**32**)
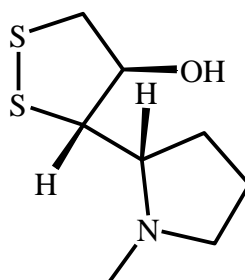
guinesine C (**33**)
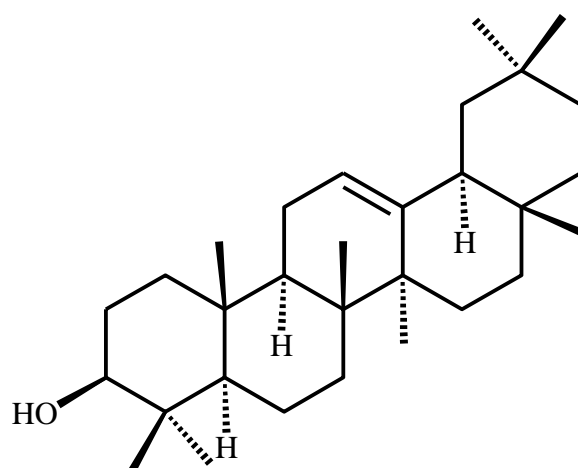
Beta-amyrin (**34**)

Figure 2.2: Chemical structures of antityrosinase and anti-melanogenesis compounds isolated from South African plants.

47

South Africa is known for its floral diversity. Many plants have been explored for their potential in the management and treatment of various inflammatory and skin even tone effects. However, a large number of plant species growing in South Africa remain untapped for potential anti-inflammatory and skin even tone discovery.[45] There is a need for exploration of South African plant species in cosmeceutical discovery in search of anti-inflammatory and skin even tone lead compounds.

This study investigates selected plants obtained from the University of Pretoria repository, linked to traditional uses associated with inflammation, skin even tone and topical applications, by screening extracts of different plant parts against selected pro-inflammatory cytokines and normal human melanocyte cells, respectively, to identify ingredients with anti-inflammatory and skin even tone properties.

2.2   Material and methods

2.2.1   Selection of plants based on traditional uses and literature searches

A survey of relevant literature on ethnomedicinal use of plants in South Africa revealed approximately 57 plant species associated with skin problems. Keywords and phrases that were used included inflammation, swelling, topical use, skin irritation, eczema, dandruff, rheumatism, skin repair, wound healing, hair growth and hair straightening. To aid in the selection of plants, the inclusion criteria were that:

➢ The literature has ethnobotanical or ethnopharmacological contexts, and articles should be ethnobotanical field studies/surveys reporting on plant(s) with an indication as used for treating inflammation, skin repair and related conditions mentioned above.

➢ The study must be focused on plants.

➢ The plants must be indigenous to South Africa.

➢ The study must be written in English.

➢ All plant species with traditional use relevant for treating inflammation, skin repair and related conditions mentioned above but has not been reported scientifically for that use were flagged as potential candidates for selection.

2.2.2 Selection of plants based on scoring system

A literature search on reported scientific uses of the selected plants using Google scholar, Pubmed and the University of Pretoria library was carried out. The keywords were made up of traditional medicinal plants used for treating inflammation, skin even tone and related symptoms. The identified plants were ranked by a scoring system of 1, 2 and 3 where 1 represents strong, 2 medium and 3 weak. The criteria used for scoring were as follows:

- ➢ Strength of the traditional uses for inflammatory disease and skin even tone: A score of 1 was given to plants utilized traditionally for the two diseases mentioned. A score of 2 was given to plants utilized traditionally for one of the diseases mentioned and a score of 3 was given to the plant if no knowledge of its traditional application has been reported.
- ➢ Strength of the published use for inflammatory and skin even tone: Plants with published potent anti-inflammatory and skin even tone activity was given a score of 1, plants with moderate and no published anti-inflammatory and skin even tone activity were given scores of 2 and 3 respectively.
- ➢ Plant toxicity: Plants with no toxicity were given score of 1 and plants with unknown toxicity were given score of 2 while plants with toxicity were given score of 3.

2.2.3 Collection and extraction of plant material

The first collection of plant species (*S. columbaria* and *P. peltatum*) was obtained from Random Harvest Indigenous Nursery (This is a wholesale indigenous nursery located at college road Muldersdrift Krugersdorp, 1739, South Africa. The nursery grows and sells plants indigenous to South Africa, herbs and a few seasonal vegetables to the general public) and transferred to University of Pretoria Experimental Farm Plant Nursery Gauteng, South Africa, by a curator named Jason Sampson in April 2018 (Autumn season). The extract quantities were not sufficient for further research, and additional plant material was collected. The second collection of plant species (*S. columbaria*, *C. pyracanthoides* and *P. capitatum)* were obtained from Vryheid, Shongololo Pass, KwaZulu Natal, South Africa, by a botanist named J. Vahrmeijer after replacing one of the previous plant species *Pelargonium peltatum* with *Pelargonium capitatum* in July 2018 (winter season). The plants were identified at the H.G.W.J Schweickerdt Plant Herbarium at the University of Pretoria, where the plant specimens were deposited. The plant parts were cleaned to remove soil and debris, after which they were sliced

into small pieces and oven-dried at 40-60ºC. Dried plant materials were ground to powder using a grinder (Polymix, PX-MFC 90 D, Lasec, Gauteng, South Africa) and stored at room temperature.

For the first collection of *S. columbaria* and *P. peltatum*, ground plant materials (0.9-1.8g) were extracted separately using ethanol and acetone, water/ ethanol (1:1) and water by adding each solvent (60 mL) to an Erlenmeyer flask containing the plant material and stirring for 24 hours using a magnetic stirrer. The extraction was carried out three times, with filtration in between each extraction. The mixture was filtered under vacuum while the extracts obtained from different extractions were combined and evaporated to dryness using a rotary evaporator and freeze drier (specifically for water) (figure 2.3). All the extracts were stored in a cold room before the biological screening.
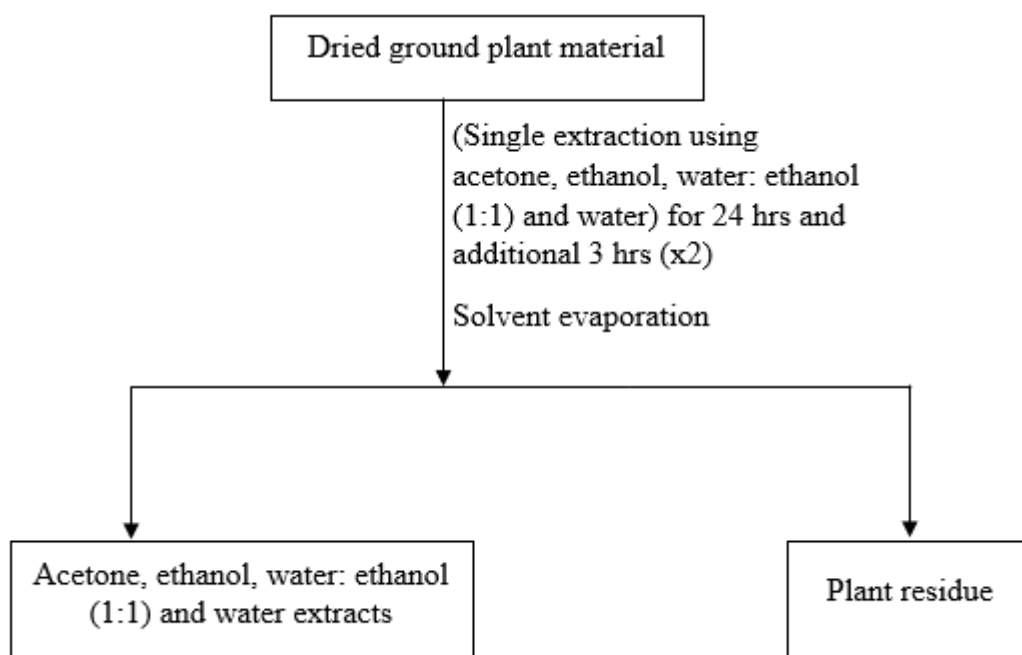
Figure 2.3: Flow diagram for the single extraction of the two batches of *S. columbaria* roots and leaves, *C. pyracanthoides* stem bark and *P. capitatum* leaves using acetone, ethanol, water/ ethanol (1:1) and water.

For the second collection of *S. columbaria, C. pyracanthoides* and *P. capitatum*, ground plant materials (15-100g) were extracted separately using ethanol and acetone, while 2-100g of ground plant materials were extracted using water/ethanol (1:1) and water by adding each solvent (50-1000 mL) to an Erlenmeyer flask containing the plant material and stirring for 24

50

hours using a magnetic stirrer. The extraction, filtration and storage procedures were carried out as described for the single extraction of the first batch of plant material.

2.2.4 Biological screening of extracts from selected plant materials for their anti-inflammatory and skin even tone activity

The biological screening was undertaken by a commercial company as part of a collaboration and due to agreements, the identity cannot be disclosed.

Roots and leaves of *S. columbaria*, stem barks of *C. pyracanthoides* and leaves of *P. capitatum* were screened against selected proinflammatory cytokines to determine their anti-inflammatory activity while the root of *S. columbaria* was screened against normal human melanocytes to ascertain its skin even tone activity.

2.2.4.1 Anti-inflammatory screening

The U937 cell line is used in this protocol to model the monocyte/macrophage immune response *in vitro*. Treatment with phorbol-12-myristate-13-acetate (PMA) and lipopolysaccharide (LPS) induced the secretion of proinflammatory mediators and cytokines. Co-treatment with anti-inflammatory agents allows the identification of intrinsic regulatory activity of proinflammatory reactions *in vitro*. The human myeloid U937 cell line (ATCC: CRL-1593.2) was treated with the extracts in a culture medium RPMI 1640 (42401-018, GIBCO-Invitrogen) supplemented with L-glutamine, penicillin, *streptomycin* (G11146, Sigma-Aldrich), heat-treated 10% foetal calf serum, 10 µg/mLof Phorbol 12-myristate 13-acetate (PMA, P8139-1MG, Sigma-Aldrich), and 60 µg/mLof lipopolysaccharides for *E. Coli* (LPS, L4391-1MG, Sigma-Aldrich). Seven doses of the extracts were tested: 1, 3, 10, 30, 100, 300, and 1000 µg mL^{-1}. Twenty-four hours after treatment at 37°C in a humidified 5% CO_2 atmosphere, cell viability was measured using AlamarBlue® (DAL1025, Life Technologies) for each condition. Supernatants were then collected, and the PGE2, IL-6, IL-1β, IL-8 and TNF-α are quantified using immunoassays. Dose-response curves were generated, and the IC$_{50}$ for each analyte was determined (dose corresponding to 50% inhibition of the quantity of the proinflammatory mediator).

2.2.4.2 Inhibition of melanin production assay

Melanocyte culture medium (M154) and human melanocyte growth supplement (HMGS supplements) from Thermo Fischer and normal human melanocytes (NHM) were purchased from Tebu-Bio (C-002-5C). Extracts evaluated were solubilized in dimethyl sulfoxide (DMSO) at 30 mM and diluted in culture medium in a 2-fold serial dilution manner to obtain 10 doses starting from 200 µM. NHM were cultivated as described by Duval et al.[46] NHM were seeded in 384-well microtiter plates at 20 000 cells in 80 µL culture medium per well. The raw materials were added after 24 hours of incubation while replacing the culture medium, and cells were incubated at 37°C with 5% CO_2 and saturated humidity for 72 hours. Optical density was measured at 340 nm and the data normalized in comparison with untreated cells. Dose-response curves were generated. IC_{50} was determined (dose corresponding to 50% inhibition of the melanin signal).

2.2.5 UPLC-QTOF-MS analysis of extracts

The crude extracts were analyzed on a Waters acquity ultra-performance liquid chromatography-quadrupole time of flight mass spectrometer (UPLC-QTOF-MS). The extracts were prepared at a concentration of 1 mg/mL in MeOH. They were analyzed on a Waters Acquity UPLC system equipped with a binary solvent delivery system and an autosampler. The Waters BEH C_{18} (2.1 mm x 100 mm, 1.7 µM) column was used. The mobile phase consisted of solvents A = H_2O + 0.1% formic acid (FA) and B = Acetonitrile + 0.1% FA, applied in a gradient mode (0 min 3% B, 0.10 min 3% B, 14 min 100% B, 16 min 100% B, 16.5 min 3% B, 20 min 3% B) with a flow rate of 0.3 mL/min. The injection volume was 5 µL. The separated compounds were analyzed by a Waters Synapt G2 high-definition QTOF mass spectrometer, which was run in electrospray ionization positive and negative modes. The compounds in the samples were tentatively identified by obtaining the molecular formula of compounds from Masslynx based on the best iFit value, mass error and %Fit Conf comparing their MS/MS fragmentation pattern with that of best suggested matched compounds from ChemSpider, Metfrag, Metlin, Metfusion, Dictionary of Natural Products, PubChem and Waters UNIFY® Scientific Information System (version 1.9.2) assessing the Chinese Natural Product database. The iFit value compares the isotopic ion ratio to the theoretical ion ratio. The closer the iFit value is to zero, the lower the difference between the isotopic ion ratio and the theoretical ion ratio and the more accurate the suggested molecular formula. The accepted mass

error range is between 0 to 5 ppm. Additionally, known compounds reported in the genus or species of a plant of interest can be identified by comparing their accurate masses and fragments although this might not be able to distinguish between isomers.

2.3   Results and Discussion

2.3.1 Selection of plants based on traditional uses and literature searches

Using traditional uses of South African plant species with set key words obtained from literature searches, thirty three plant species were identified as candidates for anti-inflammatory screening, nine plant species were identified as candidates for anti-irritant screening, two plant species were identified as candidates with hair straightening properties, two plant species were identified as candidates for anti-dandruff screening and eleven plant species were identified as candidates with wound healing properties as shown in table 2.1.

Table 2.1: Plant selection based on traditional uses and scientific information

Genus/Species	Properties based on traditional uses	Scientific information
Plants with anti-inflammatory properties		
Acacia polyacantha	Anti-inflammatory[47]	
Acacia sieberiana	Anti-inflammatory[48]	
Albizia adianthifolia	Anti-inflammatory, body wash, skin problems[49]	
Boerhavia diffusa	Anti-inflammatory[50]	
Cissus quadrangularis	Wound healing, treatment of burns and swellings[51]	
Conyza scabrida	Anti-inflammatory[52]	
Crinum macowanii	Treatment of swelling, itchy rashes, rheumatism and arthritis[53]	
Croton gratissimus	Anti-inflammatory, treatment of swelling, topical use as deodorants, perfumes and hair washes[54]	Anti-inflammatory properties reported[55]
Croton sylvaticus	Anti-inflammatory, treatment of swelling[56]	Analgesic, anti-oxidant, anti-microbial properties reported[56]
Datura stramonium	Treatment of rheumatism, swelling, boils, gout, abscesses and wounds[57]	
Euphorbia ingens	Treatment of swelling[58]	Related species and compounds have anti-inflammatory properties[59]
Galenia africana	Wound healing, anti-inflammatory, treatment of skin disorders and syphilis[60]	
Grewia retinervis	Anti-inflammatory[61]	
Helichrysum gerberifolium	Wound healing, treatment of swelling, muscle relaxant[62]	
Hibiscus surattensis	Anti-inflammatory and anti-irritant[63]	
Lantana camara	Wound healing, anti-irritant, treatment of swelling, eczema, has antiseptic properties[64]	
Nymania capensis	Wound healing, anti-inflammatory[65]	

53

Osmitopsis asteriscoides	Anti-inflammatory, treatment of swelling, cuts and scars[66]	
Ozoroa engleri	Anti-inflammatory, hair application[67]	
Ozoroa sphaerocarpa	Anti-inflammatory[68]	
Physalis peruviana	Anti-inflammatory[69]	
Pollichia campestris	Treatment of rheumatism, bruises and swelling[70]	
Pterocarpus angolensis	Anti-inflammatory, wound healing, treatment of sores, venereal diseases and ring worm[71]	
Schotia brachypetala	Treatment of acne, tropical ulcer, swelling, used as body wash[72]	
Ficus lutea	Treatment of skin problems[73]	
Jatropha curcas	Treatment of sores, venereal diseases, herpes, boils, baldness, sprain, wounds, rheumatism, skin complaints, used for hair growth[74]	
Kigelia africana	Treatment of cuts, sores, rheumatism, wounds, infected bites, stings, syphilitic ulcers[75]	
Lippia javanica	Treatment of febrile rashes, chest ailments, scars on sprained joints, scabies, hair lice, measles and rashes[76]	
Melianthus major	Treatment of septic wound, sores, bruises, rheumatism, boils, stretch marks, scars and skin problems[77]	
Pelargonium luridum	Treatment of sores[78]	
Tarchonanthus camphoratus	Anti-dandruff, anti-inflammatory, treatment of hair lice, sore feet, massage legs[79]	
Widdringtonia nodiflora	Used as a fumigation in gout, rheumatism and oedematous swelling[80]	
Ximenia caffra	Anti-inflammatory[81]	
Plants with anti-irritant properties		
Achillea millefolium	Treatment of skin irritation and burns[82]	
Aloe arborescens	Treatment of skin irritation and burns[83]	
Aloe mutabilis	Treatment of skin irritation and burns[84]	
Cussonia spicata	Treatment of skin irritation, acne, relieve cramps and muscle spasm[85]	
Diospyros whyteana	Treatment of skin irritation and rashes[86]	
Dombeya rotundifolia	Anti-irritant[87]	
Leonotis leonurus	Treatment of muscle cramps, skin diseases, sores, bee and scorpion sting, boils, eczema, itching and muscle cramps[88]	
Phyllanthus reticulatus	Treatment of sores, burns and skin irritation[89]	
Vernonia hirsute	Treatment of rectal sores, rashes, skin irritation[90]	
Plants with anti-dandruff properties		
Scabiosa columbaria	Anti-dandruff, skin soothing effect, wound healing[91]	
Tarchonanthus camphoratus	Anti-inflammatory, treatment of sore feet, hair lice and dandruff, massage legs[79]	
Plants with hair straightening properties		
Cassytha ciliolate	Hair straightening, hair growth[92]	
Commiphora pyracanthoides	Hair straightener[93]	
Plants with wound healing properties		
Athrixia phylicoides	Treatment of acne, boils, wound and cuts[94]	Anti-inflammatory and anti-microbial properties reported[94]

54

Carpobrotus edulis	Treatment of eczema, ringworm, burns, scalds, sunburn, sting and skin infections[95]	Skin regeneration on flat worm and anti-oxidant properties reported[96]
Grewia occidentalis	Treatment of wound, boils and sores, preventing greying hair[97]	Anti-bacterial properties reported [97]
Opuntia ficus-indica	Treatment of soothing burns, rashes, ulcer, furuncles and wounds[98]	Wound healing and skin repair properties reported[99]
Pelargonium capitatum	Wound healing, soothing effect for cracked skin, rashes[100]	Anti-microbial (bacterial and fungal) properties reported[101]
Pelargonium peltatum	Wound healing, antiseptic for scratches, wash greasy skin[102]	
Peltophorum africanum	Treatment of wounds, rashes and eye complaints[103]	Anti-aging properties reported[104]
Withania somnifera	Wound healing, skin problems, sores, rash [105]	Anti-cancer, anti-microbial (wound infections) properties reported[106, 107]
Hydnora africana	Wound healing, anti-inflammatory[108]	Anti-oxidant and anti-bacterial properties reported[108]
Equisetum ramosissimum	Wound healing, anti-inflammatory[109]	Anti-oxidant and anti-bacterial properties reported[110]
Capparis tomentosa	Treatment of wound, leprosy, scrofula, anti-inflammatory[111]	Anti-oxidant, anti-bacterial and anti-inflammatory (weak) properties[112, 113]

2.3.2   Selection of plants based on scoring system

Using traditional uses and database searches, 10 South African plant species were identified as candidates for anti-inflammatory and skin even tone screening as shown in table 2.2. These plants were ranked according to the scoring system (score -1, 2 and 3 as described in section 2.2.1) adapted from previous studies.[5, 6] The likelihood of selecting a given plant species will be decreased in cases where a given selection criterion could not be used because the information was not easily accessible online. For example, if a plant species' toxicity, one of the criteria used for selection, was not reported in literature, it decreased the chances of choosing that plant species. This was done in case the plant species later displayed any toxicity.

Table 2.2: Scoring for selection of plant species

Genus and species	Properties based on traditional use related to inflammation and skin even tone (A)	Previously reported bioassays related to inflammation and skin even tone (B)	Toxicity (C)	Total score (A)+(B)+(C)	Selected/Not selected
Grewia retinervis	Roots are chewed and the content rubbed on skin inflammation.[114] **Score-2**	No reported anti-inflammatory and skin even tone activity. **Score -3**	Unknown toxicity. **Score-2**	7	Not selected
Scabiosa columbaria	The roots and leaves of the plant are used traditionally to treat skin-related diseases. The leaves, roots and stems are used to treat skin infections such as acariosis, dermatitis, eczema, measles and follicular acne rash.[115] Dried leaves and roots are made into wound healing ointment.[116] **Score-1**	Methanol leaf extract of *S. columbaria* effectively decreased melanin content in B16F10 (mouse melanoma) cells with moderate inhibition of tyrosinase enzyme in a dose-dependent manner.[91] **Score-2**	No toxicity was observed in the human dermal fibroblast (MHRF) cell line at the tested concentrations (25-200 µg mL^{-1}).[91] **Score-1**	4	Selected

56

Cassytha ciliolate	No reported traditional use of *C. ciliolate* on skin inflammation and skin even tone disease. **Score -3**	No reported anti-inflammatory and skin even tone activity. **Score-3**	Unknown toxicity. **Score-2**	8	Not selected
Commiphora pyracanthoides	The resin of *Commiphora* species is reported as a good source of traditional medicine for the treatment of inflammation.[117] **Score-2**	The stem extract of *C. pyracanthoides* exhibited potent *in vitro* 5-lipoxygenase (5-LOX) inhibitory activity at IC_{50} = 27.86 ± 4.45 µg mL^{-1}.[118] **Score-1**	Minimal cytotoxicity against human kidney epithelium cells. **Score-3**	6	Selected
Pelargonium capitatum	*Pelargonium* species are used as traditional remedies for wounds and abscesses.[119] **Score-2**	No reported anti-inflammatory and skin even tone activity. **Score-3**	Low toxicity against transformed human kidney epithelial (Graham) cells, IC_{50} = 101.59 µg mL^{-1}.[119] **Score-3**	8	Selected
Pelargonium peltatum	*Pelargonium* species are used as traditional remedies for wounds and abscesses.[119] **Score-2**	No reported anti-inflammatory and skin even tone activity. **Score-3**	Low toxicity against the Madin-Darby canine kidney (MDCK) cell line of the root, leaves and stem extracts of *P. peltatum* at 100 µg mL^{-1}.[120] **Score 3**	8	Selected

57

Persicaria serrulate	No reported traditional use of *P. serrulata* on skin inflammation and skin even tone disease. **Score-3**	No reported anti-inflammatory and skin even tone activity. **Score-3**	Unknown toxicity. **Score-2**	8	Not selected
Withania somnifera	*W. somnifera* leaves are used for carbuncles, inflammation and swelling. Its roots are used in the treatment of rheumatic pain, inflammation of joints, nervous disorders and epilepsy.[105] **Score-2**	Oral administration of *Withania somnifera* roots at a dose of 300 mg/kg.wt. appreciably attenuated the production of these proinflammatory cytokines: TNF-α, IL-1β, IL-6, and IL-10. **Score-1**	Reported toxicity causing liver damage.[121] **Score-3**	6	Not selected
Hydnora africana	Infusions of *Hydnora africana* are used as a face wash to treat acne.[122] **Score-3**	The root extract of *Hydnora africana* exhibited potent *in vitro* COX-1 and COX-2 inhibitory activity at $IC_{50} = 250$ µg mL^{-1}.[123] **Score-1**	Unknown toxicity. **Score-2**	6	Not selected
Equisetum ramosissimum subsp. *ramosissimum*	The aerial part of *E. ramosissimum* is used as a diuretic, an antitussive and an astringent. It is	Aqueous methanol and ethanol extracts of *E. ramosissimum* exhibited good	Reported maternal toxicity of aerial parts of	5	Not selected

	also used to treat swelling. It also acts as a protective agent against melanoma and melanogenesis.[110] **Score-1**	antityrosinase activity at IC_{50} values of 1.125 and 2.500 mg/mL respectively.[110] Crude butanolic and methanolic extracts exhibited significant inhibition of rat paw oedema and ear oedema at a dose of 400 mg/kg.[124] **Score-1**	*E. ramosissimum* extract on pregnant Sprague-Dawley rats.[125] **Score-3**		

59

According to the criteria used, the plant species with the best scores representing the highest priority was *Scabiosa columbaria* with a score of 4, the plant species *Equisetum ramosissimum* had a score of 5, three plant species, *Commiphora pyracanthoides*, *Withania somnifera* and *Hydnora Africana* had a score of 6, one plant species, *Grewia retinervis* had a score of 7 and four plant species, *Cassytha ciliolate*, *Pelargonium capitatum*, *Pelargonium peltatum*, *Persicaria serrulate* had a score of 8. The toxicity of four plant species (*Grewia retinervis*, *Cassytha ciliolate*, *Persicaria serrulate* and *Hydnora africana*) were not available in literature, therefore they were not selected for further studies. Two plant species (*Withania somnifera* and *Equisetum ramosissimum*) were reported to be toxic on liver and pregnant rats, with this information, they were not selected despite their previous report on their traditional uses to treat inflammation and acne and their reported anti-inflammatory and anti-tyrosinase activity. The four plant species (*S. columbaria*, *C. pyracanthoides*, *P. capitatum* and *P. peltatum*) that had little to minimal toxicity, traditional uses on the skin, anti-inflammatory and anti-melanogenesis activity were thereby selected for collection, extraction and biological screening. The four plant species belonged to three families, Caprifoliaceae, Burseraceae and Geraniaceae. One of the selected plant species *Pelargonium peltatum* was replaced by *Pelargonium capitatum*.

2.3.3 Collection and extraction of plant material

The first and second collections of the selected plant species (*S. columbaria*, *C. pyracanthoides*, *P. peltatum* and *P. capitatum*) were obtained from different locations and different seasons as stated in section 2.2.2. This was to enable sufficient collection of plant materials. *P. peltatum* was replaced with *P. capitatum* to evaluate other species of the *Pelargonium* genus. Each plant material was individually extracted with acceptable solvents (acetone, ethanol, water/ethanol (1:1) and water) for the cosmetics industry. The wet and dry masses of ground plant materials for different collections were as follows; the first collection of *S. columbaria* roots and leaves were 322.90g and 4.90g respectively, the second collection of *S. columbaria* roots were 594.78g and 220.09g respectively, the second collection of *S. columbaria* leaves were 194.16g and 34.76g respectively, the first collection of *C. pyracanthoides* stem bark were 936.40g and 475.60g respectively, the first collection of *P. peltatum* leaves were 151.80g and 9.90g respectively, the first collection of *P. capitatum* leaves were 1104.43g and 250.52g respectively.The masses of all the extracts obtained are given in table 2.3. The extraction yields

© University of Pretoria

of all the extracts were calculated based on the dry weight of the extracted plant material. The voucher specimens of the plant species are shown in table 2.3.

Table 2.3: Plant extraction, yields and voucher specimen numbers of the selected plant species

Type of extract	Mass of dry ground plant material used for extraction	Mass of extract obtained	% extraction yield from dry plant material
Scabiosa columbaria L. roots, first collection (voucher specimen number: PRU 124542)			
Acetone extract	0.90g	0.03g	3.33%
Ethanol extract	0.90g	0.12g	13.33%
Water/ethanol (1:1) extract	0.90g	0.18g	20.00%
Water extract	0.90g	0.15g	16.67%
Scabiosa columbaria leaves, first collection (voucher specimen number: PRU 124542)			
Acetone extract	1.80g	0.10	5.55%
Ethanol extract	1.80g	0.23	12.78%
Water/ethanol (1:1) extract	1.80g	0.36	20.00%
Water extract	1.80g	0.33	18.33%
Scabiosa columbaria roots, second collection (voucher specimen number: PRU124670)			
Acetone extract	60.00g	2.84g	4.73%
Ethanol extract	60.00g	3.51g	5.85%
Water/ethanol (1:1) extract	40.00g	8.26g	20.65%
Water extract	45.00g	13.83g	30.73%
Scabiosa columbaria leaves, second collection (voucher specimen number: PRU124670)			
Acetone extract	7.00g	0.44g	6.28%
Ethanol extract	7.00g	0.55g	7.86%
Water/ethanol (1:1) extract	2.00g	0.70g	35.00%
Water extract	2.00g	0.64g	32.00%
Commiphora pyracanthoides Engl. stem bark, first collection (voucher specimen number: PRU124669)			
Acetone extract	100.00g	4.81g	4.81%
Ethanol extract	100.00g	4.78g	4.78%
Water/ethanol (1:1) extract	100.00g	12.67g	12.67%
Water extract	100.00g	4.56g	4.56%
Pelargonium peltatum (L.) leaves, first collection (voucher specimen number: PRU 124541)			

61

Acetone extract	1.80g	0.16g	8.89%
Ethanol extract	1.80g	0.29g	16.11%
Water/ethanol (1:1) extract	1.80g	0.60g	33.33%
Water extract	1.80g	0.54g	30.00%
Pelargonium capitatum (L.) leaves, first collection (voucher specimen number: PRU124671)			
Acetone extract	60.00g	7.99g	13.32%
Ethanol extract	60.00g	5.81g	9.68%
Water/ethanol (1:1) extract	50.00g	10.78g	21.56%
Water extract	60.00g	8.47g	14.12%

Following extraction, with solvents acceptable to the cosmetic industry (acetone, ethanol, water/ethanol (1:1) and water), a total of 28 extracts were prepared for the different plant species and their plant parts. Based on the weights of the wet and dry plant materials of all the plant species, it was observed that the percentage loss of water during the process of drying the plant materials was in the descending order as follows (*P. peltatum* leaves (93.0%)> *S. columbaria* leaves (82.0%)> *P. capitatum* leaves (77.0%)> *S. columbaria* roots (63.0%)> *C. pyracanthoides* stem bark (49.0%)). This showed that leaves tend to lose more water during the process of drying followed by roots and stem bark. This also gives information on quantity of fresh plant material to be collected in terms of commercialization. The extraction yield of the 28 plant extracts ranged from 3.3% to 35.0%. The variation in the extraction yield depended on the plant species and plant part collected. Based on the extraction yield, the acetone, ethanol, water/ethanol (1:1) and water extracts of the leaves of *S. columbaria* (second collection) and *P. peltatum* gave the highest yield (ranging from 6.3% to 35.0% for *S. columbaria* and 8.9% to 33.3% for *P. peltatum*) compared to the other extracts. The four extracts (acetone, ethanol, water/ethanol (1:1) and water extracts) of *S. columbaria* leaves also had a higher yield (ranging from 5.5% to 20.0% for first collection and 6.3% to 35.0% for the second collection) than those of *S. columbaria* roots both in the first and second collections (ranging from 3.3% to 20.0% for the first collection and 4.7% to 30.7% for the second collection). The four extracts of the stem bark of *C. pyracanthoides* had the lowest extraction yield (ranging from 4.6% to 12.7%). This showed that based on the extraction of different plant parts, leaves give the highest yield followed by the roots and lastly the stem bark. The solvent that had the highest extraction yield for all the plant extracts both for the first and second collection was water/ethanol (1:1) except for *S. columbaria* roots (second collection) where water extract had the highest yield (30.7%)

suggesting that the plant species have abundance of polar compounds than moderately to nonpolar compounds. Extracts (acetone, ethanol, water/ethanol (1:1) and water) from the second collection of *S. columbaria* roots and leaves, *C. pyracanthoides* stem barks and *P.capitatum* leaves were screened for their anti-inflammatory properties while acetone extract of *S. columbaria* roots was screened for skin even tone activity.

2.3.4   The effect of plant extracts on selected proinflammatory cytokines

Table 2.4 shows the anti-inflammatory results of the acetone, ethanol, water/ethanol (1:1) and water extracts of *Scabiosa columbaria* (roots and leaves), *Pelargonium capitatum* (leaves) and *Commiphora pyracanthoides* (stem bark) from the second collection of plant materials against the human myeloid U937 cell line. The anti-inflammatory activity of the extracts was ranked by the efficacy index ranging from 4 to 0 where 4 and 3 represent good activity, 2 and 1 represent moderate activity and 0 represent no or minimal activity. Based on the results, the efficacy index includes:

- a) **Good activity**:

    $IC_{50} \leq 1$ µg/mL– 4

    1 µg/mL$< IC_{50} \leq 10$ µg/mL- 3

- b) **Moderate activity**:

    10 µg/mL$< IC_{50} \leq 100$ µg/mL- 2

    100 µg/mL$< IC_{50} \leq 1000$ µg/mL- 1

- c) **No or minimal activity**:

    $IC_{50} > 1000$ µg/mL– 0

    Other terms in the results and their descriptions include:

    NA – Not Applicable

    NC – No Class: cytotoxic effect at the lowest tested dose

    + - IR > 150 with a clear dose-response

    (+) – IR > 150 without clear dose-response

Table 2.4: Extraction yield from selected plant materials (*S. columbaria* roots and leaves, *C. pyracanthoides* and *P. capitatum*) and *in vitro* anti-inflammatory activity of extracts against selected proinflammatory cytokines (PGE2, IL-6, IL-8, TNF-α and IL-1β). Penicillin and streptomycin were used as control compounds. Fractions highlighted in red showed good activity, those highlighted in orange were moderately active while those highlighted in yellow displayed minimal or no activity

Plant species	Cmax µg mL⁻¹	Viability CV75 µg mL⁻¹	PGE2		IL-6		IL-8		TNF-α		IL-1β	
			IC$_{50}$ µg mL⁻¹	Index	IC$_{50}$ µg mL⁻¹	Index	IC$_{50}$ µg mL⁻¹	Index	IC$_{50}$ µg mL⁻¹	Index	IC$_{50}$ µg mL⁻¹	Index
Scabiosa columbaria, acetone extract	1000	62	2	3	< 1	4	21	2	< 1	4	< 1	4
Scabiosa columbaria, ethanol Extract	1000	57	2	3	3	3	8	3	6	3	6	3
Scabiosa columbaria, water/ ethanol (1:1) extract	1000	430	4	3	2	3	50	2	14	2	9	3
Scabiosa columbaria, water extract	1000	> 1000	40	2	67	2	245	1	129	1	99	2
Scabiosa columbaria, acetone extract	1000	17	3	3	2	3	9	3	9	3	9	3
Scabiosa columbaria, ethanol Extract	1000	80	28	2	5	3	NA	0	NA	0	NA	0

Scabiosa columbaria, water/ ethanol (1:1) extract	1000	391	+	INC	2	3	122	1	96	2	130	1
Scabiosa columbaria, water extract	1000	> 1000	>1000	INC	187	1	(+)	(+)	>1000	0	>1000	0
Commiphora pyracanthoides acetone extract	1000	6	3	3	< 1	4	NA	0	3	3	3	3
Commiphora pyracanthoides ethanol extract	1000	20	7	3	< 1	4	NA	0	(+)	(+)	(+)	(+)
Commiphora pyracanthoides water/ ethanol (1:1) extract	1000	52	8	3	1	3	23	2	8	3	15	2
Commiphora pyracanthoides water extract	1000	120	16	2	22	2	70	2	56	2	45	2
Pelargonium capitatum, acetone extract	1000	620	+	INC	1	3	(+)	(+)	292	1	252	1
Pelargonium capitatum, ethanol extract	100	> 100	(+)	(+)	22	2	> 100	0	> 100	INC	(+)	(+)
Pelargonium capitatum, water/ ethanol (1:1) extract	100	> 100	(+)	(+)	24	2	> 100	0	> 100	0	> 100	0
Pelargonium capitatum, water extract	1000	> 1000	463	1	546	1	922	1	>1000	0	>1000	0

Index: Legend of Efficacy index

0: $IC_{50} > 1000$ µg mL^{-1}

1: 100 µg/mL$< IC_{50} \leq 1000$ µg mL^{-1}

2: 10 µg/mL$< IC_{50} \leq 100$ µg mL^{-1}

3: 1 µg/mL$< IC_{50} \leq 10$ µg mL^{-1}

4: $IC_{50} \leq 1$ µg mL^{-1}

In the study, the acetone and ethanol extracts of *S. columbaria* roots and the acetone extract of *S. columbaria* leaves displayed the best activity with IC_{50} ranging from < 1 to 2 µg mL^{-1}, 2 to 8 µg/mL and 2 to 9 µg/mL for all the cytokines, except for one of the cytokines IL-8, where the acetone extract of *S. columbaria* roots displayed moderate activity with IC_{50} 21 µg mL^{-1}. Water/ ethanol (1:1) extract of *S. columbaria* roots displayed good activity on PGE2, IL-6 and IL-1β with IC_{50} ranging from 2 to 9 µg/mL except for IL-8 and TNF-α where it displayed moderate activity with IC_{50} 50 and 14 µg mL^{-1}, respectively. Water extract of *S. columbaria* roots displayed moderate activity on all the cytokines with IC_{50} values ranging from 40 to 245 µg mL^{-1}. Ethanol and water/ ethanol (1:1) extracts of *S. columbaria* leaves displayed good activity on the cytokines IL-6 with IC_{50} of 5 and 2 µg mL^{-1}, respectively while water/ ethanol (1:1) extract of *S. columbaria* leaves displayed moderate activity on IL-8, TNF-α and IL-1β with IC_{50} values ranging from 96 to 130 µg mL^{-1}.

In Lesotho and South Africa, *S. columbaria* is used in the treatment of inflammation.[115] From the screenings carried out by Mhlongo et al. the acetone and hexane extracts of *S. columbaria* showed good activity against murine macrophages (RAW 264.7) in a concentration-dependent manner.[116] Significant inhibition of nitric oxide (NO) was observed at 50 and 100 µg/mL in the acetone extract and 100 µg/mL in the hexane extract in the same study. This indicated that the active ingredients might be non-polar compounds that can be extracted with acetone and partitioned with hexane. The published results were in agreement with the result in this study, as the acetone extract of *S. columbaria* showed the best activity. Thus far, no compound has been reported to be isolated from *S. columbaria* roots and tested for its anti-inflammatory activity providing the motivation for further investigating the root, which is described in Chapter 3, for the isolation and identification of the anti-inflammatory ingredients.

In the current study, acetone and water/ ethanol (1:1) extracts of *C. pyracanthoides* showed good activity with the IC_{50} ranging from < 1 to 3 µg/mL and 1 to 8 µg/mL for all the cytokines except for cytokines IL-8, where the acetone extract displayed no activity as well as IL-8 and IL-1β, where the water/ ethanol (1:1) extract showed moderate activity with IC_{50} values of 23 µg/mL and 15 µg mL^{-1}, respectively. The ethanol extract showed good activity for the cytokines PGE2 and IL-6, with IC_{50} ranging from <1 to 7 µg mL^{-1}. *Commiphora* species are widely used in traditional medicine for the treatment of various diseases, including inflammation.[117] The anti-inflammatory potency of *C. pyracanthoides* has been reported whereby a study reported by Paraskeva et al., the DCM/MeOH (1:1) stem extract of *C. pyracanthoides* exhibited

67

moderate to good 5-LOX inhibitory activity with an IC_{50} value of 27.86 ± 4.45 µg mL^{-1}.[118] There is no report on the identification of active ingredients. Further investigation of this species and identification of the compounds responsible for the observed anti-inflammatory effect is therefore warranted.

In this study, all the extracts (acetone, ethanol, water/ ethanol (1:1) and water) of *P. capitatum* exhibited good to moderate activity with IC_{50} ranging from 1 to 546 µg/mLfor one of the cytokines, IL-6. The sweet-scented leaves of *Pelargonium capitatum* is used traditionally to treat cracked skin. It can be tied to a piece of muslin and used in the bath as a skin and wash treatment, which also soothes rashes.[126] There are no reports on the anti-inflammatory activity of *P. capitatum*, indicating that the plant species needs to be investigated to identify the compounds responsible for the observed activity.

2.3.5   The effect of plant extract on melanin production

Figure 2.4 shows the skin even tone activity of the acetone extract of *S. columbaria* (roots) from the second collection of plant materials against the M154 normal human melanocytes (NHM).
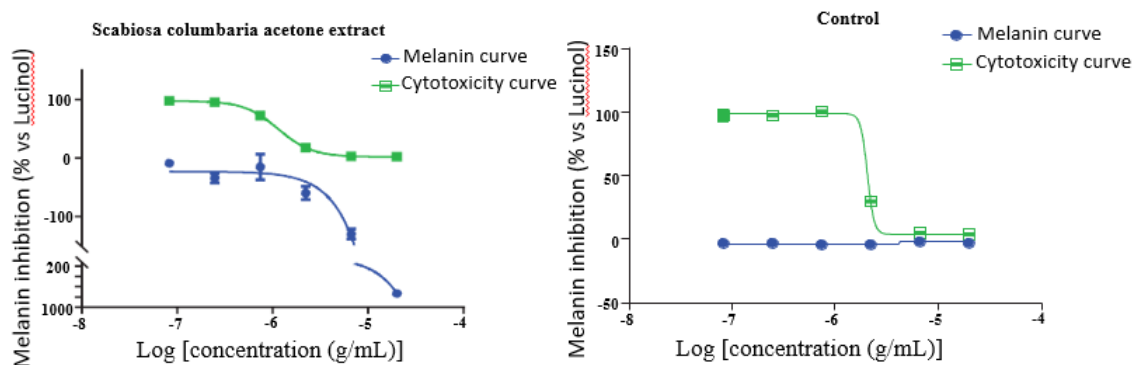
Figure 2.4: Whitening 2D co-culture model (melanin global) of acetone extract of *S. columbaria* roots.

The acetone extract of *S. columbaria* roots was tested at different concentrations (0.08-20 µg mL^{-1}) for skin even tone activity. The extract did not show any decreasing trend in melanin signal at these concentrations (0.08-2.1 µg mL^{-1}) but showed cytotoxicity at concentrations (2.2-20 µg mL^{-1}). As a result, the acetone extract of *S. columbaria* root was not considered to

© University of Pretoria

have skin even tone activity. In contradiction to the results found in this study, the anti-melanogenesis activity of *S. columbaria* has been reported.[91] In the study, methanol extract of *S. columbaria* leaves at 25-100 µg/mLeffectively decreased melanin content in α-MSH-stimulated B16F10 (mouse melanoma cells) in a dose-dependent manner. The reason may be attributed to the leaves being studied rather than the roots. Additionally, methanol was used as an extraction solvent in the reported case, while the acetone extract was tested in this study, and finally, the activity reported was tested against mouse melanoma cells (B16F10), whereas in our study, normal human melanocytes (NHM) were used. Moreover, the acetone extract of *S. columbaria* roots showed activity using the 1D model (HTS melanin global) but failed to show activity in the 2D coculture test model. Overall, *S. columbaria* may still be considered for further investigation to identify the active constituents responsible for the activity in the 1D model.

2.3.6 Identification of chemical markers from the acetone extract of *S. columbaria* leaves

The acetone extract of *S. columbaria* leaves showed good anti-inflammatory potential, therefore chemical markers were analysed from the extract for quality control and commercialization purposes.

Figure 2.5 shows the UPLC-QTOF-MS chemical profile of the acetone extract of *S. columbaria* leaves (second collection) operating in negative electrospray (ESI) ionization mode.
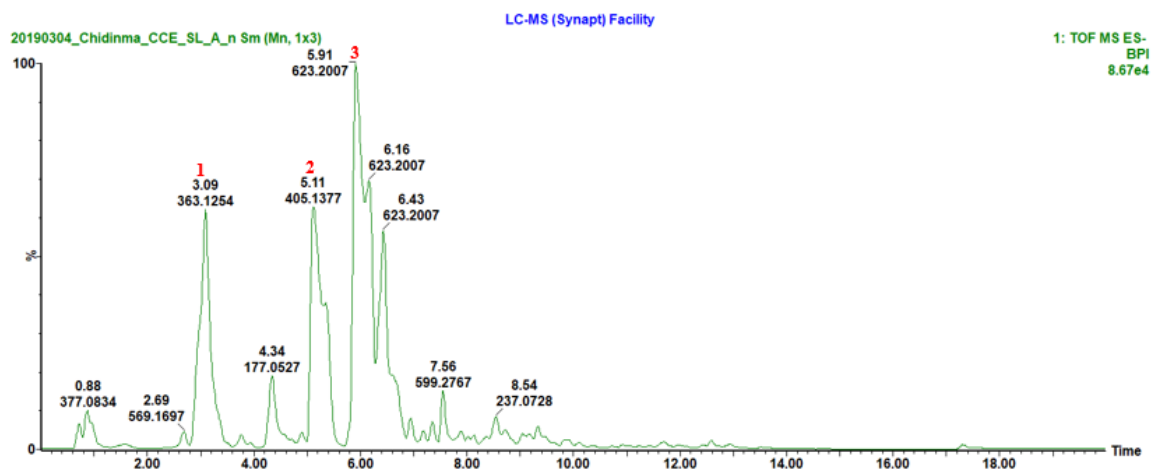
Figure 2.5: ESI negative mode BPI chromatogram of the acetone extract of *S. columbaria* leaves (second collection).

Three compounds were tentatively identified from the UPLC-QTOF-MS analysis in ESI negative mode using accurate mass data and mass fragmentation patterns as described in section 2.2.4. The corresponding peaks are labelled in the chromatogram (figure 2.5). Table 2.5 shows accurate mass, formula and MS/MS data for compound fragments tentatively identified from the acetone extract of *S. columbaria* leaves.

Table 2.5: Compounds tentatively identified using UPLC-QTOF-MS analysis of the acetone extract of *S. columbaria* leaves

Peak No	RT (min)	Acquired [M-H] *m/z*	Formula	Calculated [M-H] *m/z*	Possible structure	Mass error (ppm)	MS/MS Data (fragments)		Reference
1	3.09	363.1274	$C_{15}H_{24}O_{10}$	363.1291	harpagide **(Iridoid glycoside)**	4.7	184.0644	$[M-H]^-$-$C_6H_{11}O_6$	[127]
							179.0545	$[M-H]^-$-$C_9H_{13}O_4$	
							165.0527	$[M-H]^-$-$C_6H_{11}O_6$-H_2O	
							139.0370	$[M-H]^-$-$C_6H_{11}O_6$-H_2O-CO	
							85.0267	$[M-H]^-$- $C_6H_{11}O_6$-$C_4H_5O_2$	
2	5.11	405.1389	$C_{17}H_{26}O_{11}$	405.1397	10-hydroxyloganin **(Isoprenoid)**	2.0	345.1169	$[M-H]^-$-$C_2H_6O_2$	[128]
							179.0535	$[M-H]^-$-$C_{11}H_{15}O_5$	
							165.0527	$[M-H]^-$-$C_{11}H_{15}O_6$	
3	5.91	623.1987	$C_{29}H_{36}O_{15}$	623.1978	forsythiaside **(Polyphenol)**	1.3	461.1653	$[M-H]^-$-$C_6H_7O_3$	[129]
							161.0220	$[M-H]^-$-$C_{20}H_{29}O_{11}$-H_2O	
							135.0432	$[M-H]^-$-$C_{20}H_{29}O_{12}$-CHO	
							113.0222	$[M-H]^-$-$C_6H_{11}O_5$-$C_9H_7O_4$-$C_8H_9O_3$-H_2O	

The structures of the tentatively identified compounds are shown in figure 2.6.

Harpagide (**35**)

10-hydroxyloganin (**36**)

Forsythiaside (**32**)
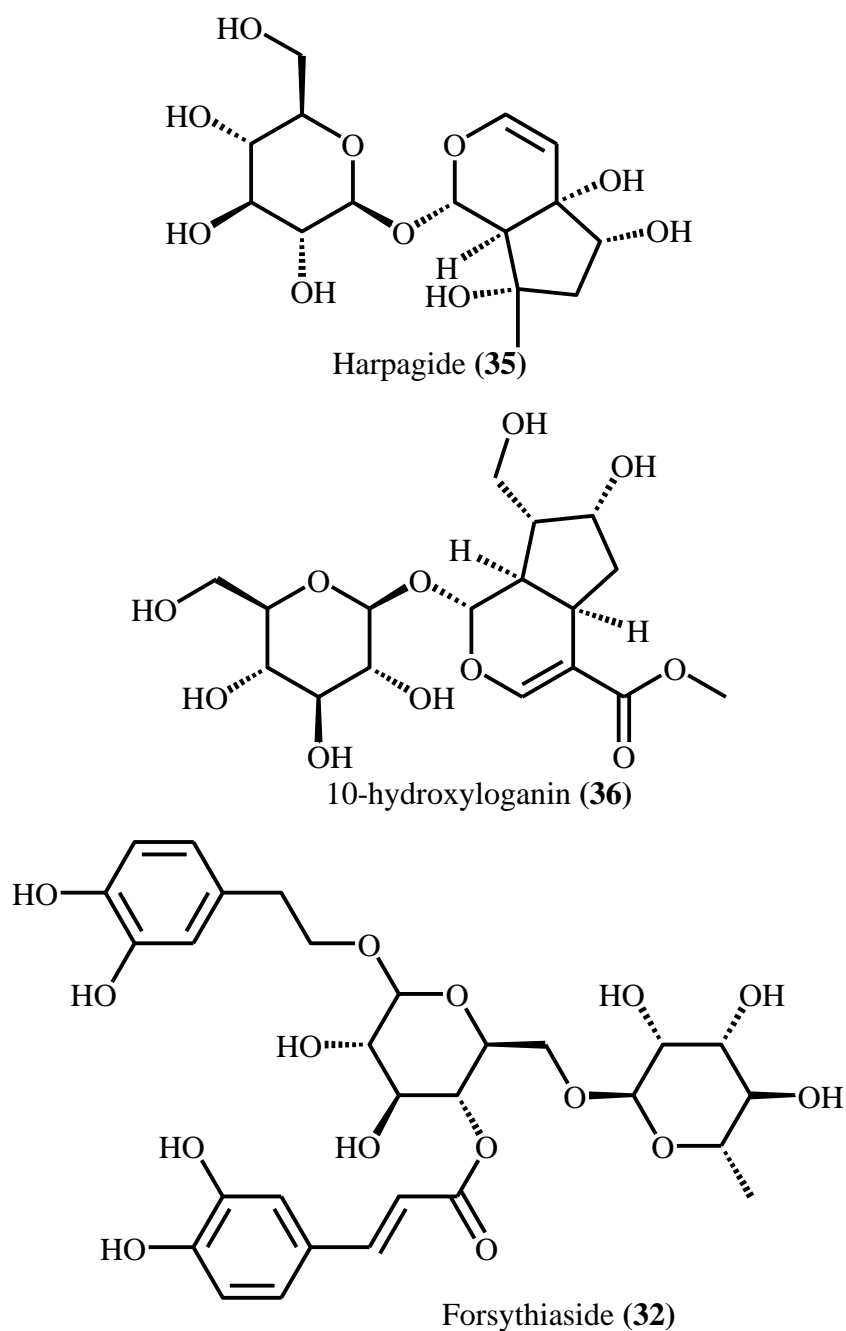
Figure 2.6: Structures of chemical markers tentatively identified from *S. columbaria* leaves.

In the first order mass spectrum of peak 2, the [M-H]⁻ ion was observed with *m/z* 363.1274 [M-H]⁻ at the retention time 3.09 minutes. It had a molecular formula of $C_{15}H_{23}O_{10}^{-}$ with a normalized iFit value of 0.0. The fragmentation pattern observed was in agreement with that reported for harpagide (**35**).[127] Harpagide (**35**) was reported to decrease TNF-α secretion in

phorbol myristate acetate-differentiated THP-1 cells, while it induced the mRNA-expression of certain proteins involved in leukocyte transmigration in undifferentiated cells.[130] Zhang et al. also reported on the significant inhibitory effects of the hydrolysed product of harpagide with β-glucosidase treatment on COX-2 activity at 2.5-100 µM in a concentration-dependent manner.[131] These reported activities may contribute to the fact that harpagide may be responsible for the anti-inflammatory activity observed in *S. columbaria*. The MS spectrum of peak 4 was observed at the retention time 5.11 mins with *m/z* 405.1389 [M-H]$^-$. The molecular formula obtained was $C_{17}H_{25}O_{11}^-$ with a normalized iFit value of 0.0. The analysis of the MS/MS data revealed that the compound was an isoprenoid which matched 10-hydroxyloganin (**36**).[128]

Peak 5 represents a precursor ion with *m/z* 623.1987 [M-H]$^-$ at the retention time 5.91 minutes. The molecular formula of the compound was given as $C_{29}H_{36}O_{15}^-$ with a normalized iFit value of 0.0. The analysis of MS/MS data indicated that it was a polyphenol, matching forsythiaside (**37**).[129] Forsythiaside (**37**) was reported to significantly inhibit LPS-induced inflammatory mediators TNF-α, IL-1β, NO and PGE2 production through inhibition of NF-κB activation and activation of the Nrf2/HO-1 signaling pathway.[132] Tong et al. also reported that forsythiaside effectively inhibited LPS-induced mammary inflammation in mice by attenuating the activation of the NF-κB and p38 MAPK signaling pathways.[133] These reported activities may contribute to the fact that forsythiaside may be responsible for the anti-inflammatory activity observed in *S. columbaria*.

2.3.7 Identification of chemical markers in the acetone extract of *C. pyracanthoides* stem bark

The acetone extract of *C. pyracanthoides* stem bark showed good anti-inflammatory potential, therefore chemical markers were analysed from the extract for quality control and commercialization purposes.

Figure 2.7 shows the UPLC-QTOF-MS chemical profile of the acetone extract of *C. pyracanthoides* stem bark (second collection) operating in negative electrospray (ESI) ionization mode.
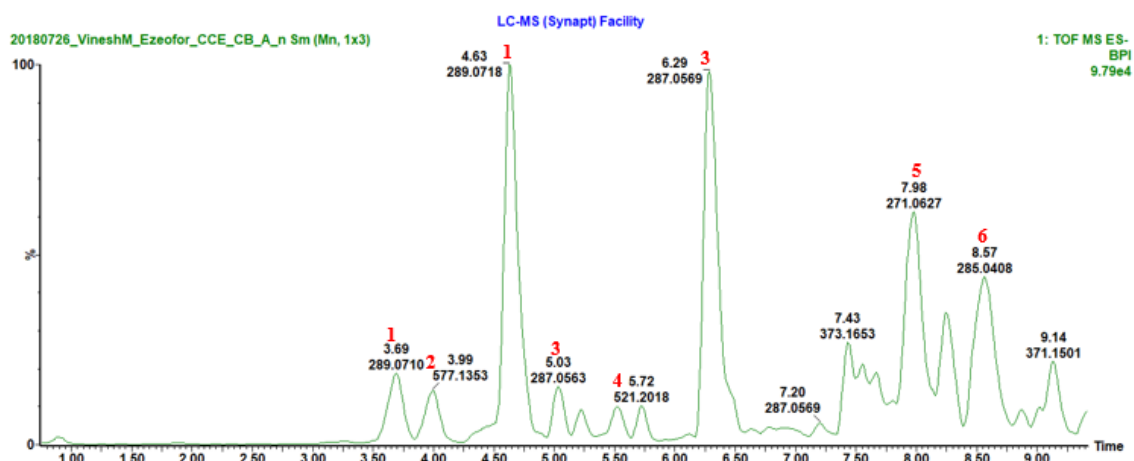
Figure 2.7: ESI negative mode BPI chromatogram of the acetone extract of *C. pyracanthoides* stem bark (second collection) with the expansion of region 1 to 10 mins.

Six compounds were tentatively identified from the UPLC-QTOF-MS analysis in ESI negative mode using accurate mass data and mass fragmentation patterns as described in section 2.2.4. The corresponding peaks are labelled in the chromatogram (figure 2.7). Table 2.6 shows accurate mass, formula and MS/MS data for compound fragments tentatively identified from the acetone extract of *C. pyracanthoides* stem bark.

Table 2.6: Compounds tentatively identified using UPLC-QTOF-MS analysis of the acetone extract of *C. pyracanthoides* stem bark

Peak No	RT (min)	Acquired [M-H] *m/z*	Formula	Calculated [M-H] *m/z*	Possible structure	Mass error (ppm)	MS/MS Data (fragments)		Reference
1	3.69/4.63	289.0710	$C_{15}H_{14}O_6$	289.0712	Epicatechin (**Flavonoid**)	0.7	125.0236	$[M-H]^-$-$C_9H_8O_3$	[134]
							123.0450	$[M-H]^-$-$C_9H_{10}O_3$	
							137.0243	$[M-H]^-$-$C_8H_8O_3$	
							169.0126	$[M-H]^-$-$C_7H_4O_2$	
2	3.99	577.1345	$C_{30}H_{26}O_{12}$	577.1340	procyanidin B2 (**Proanthocyanidin**)	0.2	125.0250	$[M-H]^-$-$C_{24}H_{20}O_9$	[135]
							169.0167	$[M-H]^-$-$C_{22}H_{16}O_8$	
							289.0725	$[M-H]^-$-$C_{15}H_{12}O_6$	
							407.0773	$[M-H]^-$-$C_8H_8O_3$-H_2O	
							109.0296	$[M-H]^-$-$C_{24}H_{20}O_{10}$	
3	5.03/6.29	287.0561	$C_{15}H_{12}O_6$	287.0555	Dihydrokaempferol (**Flavanol**)	1.7	125.0259	$[M-H]^-$-$C_8H_8O_2$-CHO	[136]
							152.0125	$[M-H]^-$-$C_8H_8O_2$-	
							107.0137	$[M-H]^-$-$C_9H_8O_4$	
							135.0402	$[M-H]^-$-$C_7H_4O_4$	
4	5.51	303.0511	$C_{15}H_{12}O_7$	303.0505	Dihydroquercetin (**Flavonoid**)	2.0	125.0252	$[M-H]^-$-$C_9H_8O_4$	[137]
							177.0178	$[M-H]^-$-$C_6H_4O_3$	
							193.0508	$[M-H]^-$-$C_6H_7O_2$	
							109.0295	$[M-H]^-$-$C_9H_7O_5$	
5	7.98	271.0625	$C_{15}H_{12}O_5$	271.0606	Naringenin (**Flavanone**)	2.0	243.0667	$[M-H]^-$-CO	[138]
							151.0054	$[M-H]^-$-C_8H_8O	
							119.0512	$[M-H]^-$-C_8H_8O-$2H_2O$	
							107.0149	$[M-H]^-$-C_8H_8O-CO_2	
6	8.57	285.0403	$C_{15}H_{10}O_6$	285.0399	Kaempferol (**Flavonoid**)	1.4	151.0051	$[M-H]^-$-$C_8H_6O_2$	[139]
							135.0081	$[M-H]^-$-$C_7H_4O_4$	
							163.0027	$[M-H]^-$-C_6H_5O-H_2O-O	
							93.0347	$[M-H]^-$-$C_9H_5O_5$	

The structures of the tentatively identified compounds are shown in figure 2.8.

Epicatechin (**38**)

Procyanidin B2 (**39**)

Dihydrokaempferol (**40**)

Dihydroquercetin (**41**)

Naringenin (**42**)

Kaempferol (**43**)
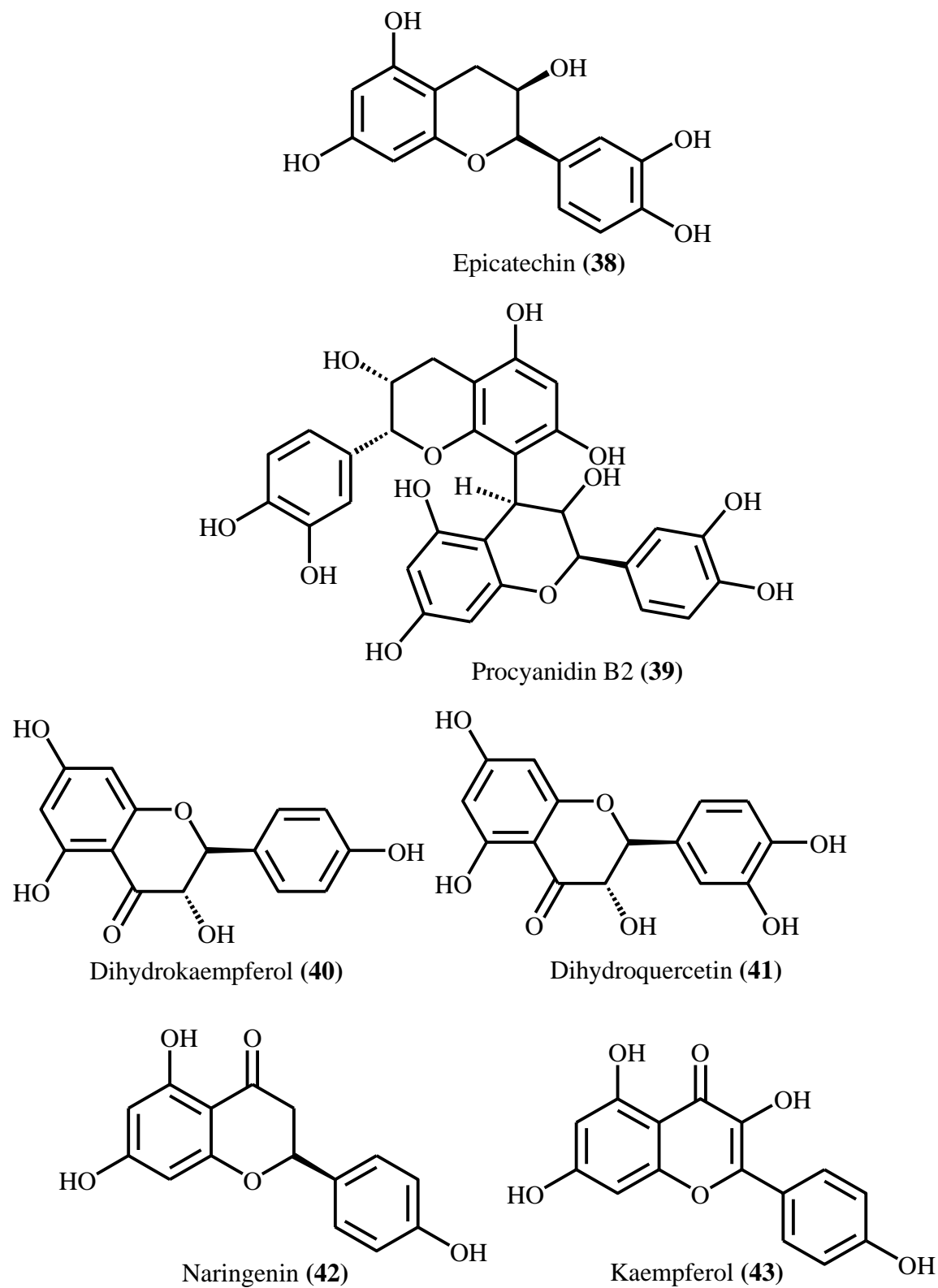
Figure 2.8: Structures of chemical markers tentatively identified from *C. pyracanthoides* stem bark.

The first order mass spectrum of peak 1 showed an [M-H]$^-$ ion at m/z 289.0710 at retention times 3.69 and 4.63 minutes. The molecular formula generated was $C_{15}H_{13}O_6^-$ with normalized iFit value of 0.017. The MS/MS data analysis suggested that it was a flavonoid and was identified as epicatechin (**38**). Epicatechin (**38**) in doses of 5, 25 and 50 µM remarkably (p < 0.05) was reported to inhibit the production of proinflammatory mediators including nitric oxide (NO) and prostaglandin E2 (PGE2), as well as the production of proinflammatory cytokines including tumor necrosis factor (TNF)-alpha and interleukin (IL)-6 in LPS-induced Raw 264.7 macrophages.[140] This shows that epicatechin can inhibit inflammatory response and may be responsible for the anti-inflammatory activity observed in *C. pyracanthoides*.

The first order mass spectrum of peak 2 showed an [M-H]$^-$ ion with m/z 577.1345 at the retention time 3.99 minutes. The molecular formula was given as $C_{30}H_{25}O_{12}^-$ with a normalized iFit value of 0.10. Analysis of the MS/MS data revealed that it was a proanthocyanidin, identified as procyanidin B2 (**39**). Procyanidin B2 (**39**) was reported to inhibit the monosodiumurate (MSU)-induced inflammatory response in gout by inhibiting the NLRP3 inflammasome pathway, thereby reducing interleukin-1β (Il-1β) and cathepsin B release.[141] Procyanidin B2 was also reported to prevent LPS-induced tumor necrosis factor-α, interleukin-1β expression, NF-κB activation, and NLRP3 inflammasome activation.[142] These reported activities may contribute to the fact that procyanidin B2 may be responsible for the anti-inflammatory activity observed in *C. pyracanthoides*.

The first order mass spectrum of peak 3 showed an [M-H]$^-$ ion with m/z 287.0569 at retention times 5.03 and 6.29 minutes. The molecular formula was given as $C_{15}H_{11}O_6^-$ with a normalized iFit value of 0.147. The MS/MS data analysis suggested that it was a flavonol, tentatively identified as dihydrokaempferol (**40**).[136] Dihydrokaempferol (**40**) was reported to potently inhibit the secretion of TNF-α, PGE2, IL-1β and IL-6, and had a prominent inhibitory effect on the downregulation of the phosphorylated protein level of NF-κB p65.[143] This showed that dihydrokaempferol may be responsible for the anti-inflammatory activity observed in *C. pyracanthoides*.

The first order mass spectrum of peak 4 showed an [M-H]$^-$ ion with m/z 303.0511 at the retention times 5.51 minutes. The molecular formula was given as $C_{15}H_{11}O_7^-$ with a normalized iFit value of 0.101. Analysis of the MS/MS data revealed that it was a flavonoid, identified as

dihydroquercetin (**41**).[137] Dihydroquercetin (**41**) was reported to significantly inhibit mRNA expression levels of proinflammatory cytokines (IL-1α, IL-1-β, and IL-6) and chemokines (CXCL8 and CCL20) in TNF-α-induced HaCaT cells. It also inhibited expression levels of IL-1α/β, IL-6, CXCL8, and CCL20 by inhibiting IκB/STAT3 protein phosphorylation upon stimulation of TNF-α, IL-17A and IFN-γ.[144] This showed that dihydroquercetin may be responsible for the anti-inflammatory activity observed in *C. pyracanthoides*.

The first order mass spectrum of peak 5 showed an [M-H]$^-$ ion with *m/z* 271.0625 at the retention time 7.98 minutes. The molecular formula generated was $C_{15}H_{11}O_5^-$ with a normalized iFit value of 0.221. The MS/MS data analysis suggested that it was a flavonone, tentatively identified as naringenin (**42**). [138] Naringenin (**42**) presents therapeutic effects in several models of inflammatory pain. It inhibits the pain-like behaviour induced by inflammatory stimuli such as phenyl-p-benzoquinone, acetic acid, formalin, complete Freund's adjuvant, capsaicin, carrageenan, superoxide anion and LPS. It also inhibits UVB irradiation-induced skin inflammatory edema, cytokine production, myeloperoxidase activity, matrix metalloproteinase-9 activity, and oxidative stress.[145] This showed that naringenin may contribute to the anti-inflammatory activity observed in *C. pyracanthoides*.

In the ESI MS spectrum, peak 9 showed an [M-H]$^-$ ion with *m/z* 285.0403 at the retention time 8.57 minutes. The molecular formula was given as $C_{15}H_9O_6^-$ with a normalized iFit value of 0.116. Analysis of the MS/MS data revealed that it was a flavonoid, identified as kaempferol (**43**). [139] Different researchers have reported that kaempferol (**43**) is responsible for the inhibition of nitric oxide synthesis, which was induced by the administration of LPS to J77 cells and RAW264.7 cells and resulted in the reduction of inflammation. It was also demonstrated that the levels of TNF-α, nitric oxide and IL-1B were reduced by the treatment of kaempferol in diabetic neuropathy patients.[146] This showed that kaempferol may contribute to the anti-inflammatory activity observed in *C. pyracanthoides*.

2.3.8 Identification of chemical markers from the acetone extract of *P. capitatum* leaves

The acetone extract of *P. capitatum* leaves showed good anti-inflammatory potential, therefore chemical markers were analysed from the extract for quality control and commercialization purposes.

Figure 2.9 shows the UPLC-QTOF-MS chemical profile of the acetone extract of *P. capitatum* leaves (second collection) operating in negative electrospray (ESI) ionization mode.
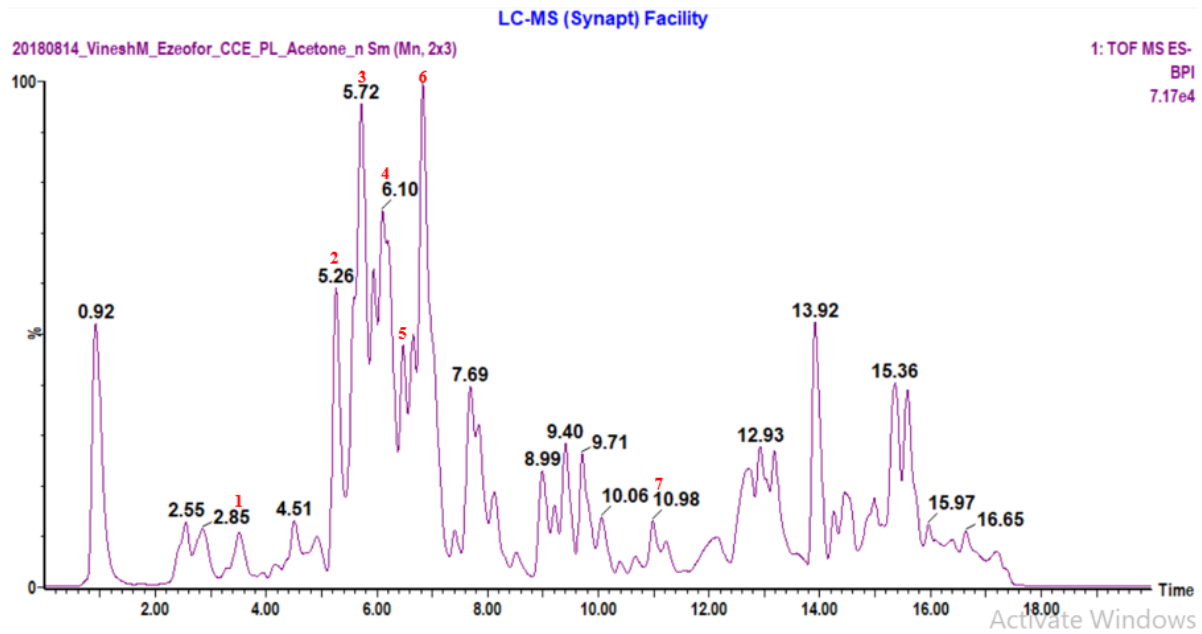
Figure 2.9: ESI negative mode BPI chromatogram of the acetone extract of *P. capitatum* leaves (second collection) with the expansion of region 2 to 12 mins.

Seven compounds were tentatively identified from the UPLC-QTOF-MS analysis in ESI negative mode using accurate mass data and mass fragmentation patterns as described in section 2.2.4. The corresponding peaks are labelled in the chromatogram (figure 2.9). The other peaks were not identified as their fragmentation pattern did not match those in the databases used in the identification process. Table 2.7 shows accurate mass, formula and MS/MS data for compound fragments tentatively identified from the acetone extract of *P. capitatum* leaves

Table 2.7: Compounds tentatively identified using UPLC-QTOF-MS analysis of the acetone extract of *P. capitatum* leaves

Peak No	RT (min)	Acquired [M-H] *m/z*	Formula	Calculated [M-H] *m/z*	Possible structure	Mass error (ppm)	MS/MS Data (fragments)		Reference
1	3.52	163.0378	$C_9H_8O_3$	163.0395	*p*-coumaric acid **(Hydroxycinnamic acid)**	-1.4	149.0064	$[M-H]^-$-O	[147]
							119.0484	$[M-H]^-$-CO_2	
							93.0294	$[M-H]^-$-$C_3H_3O_2$	
							71.0124	$[M-H]^-$-C_6H_5O	
2	5.26	625.1422	$C_{27}H_{30}O_{17}$	625.1405	quercetin-3-*O*-sophoroside **(Flavone)**	2.0	445.0859	$[M-H]^-$-$C_6H_{11}O_6$	[148]
							300.0263	$[M-H]^-$-$C_{12}H_{21}O_{10}$	
							271.0240	$[M-H]^-$- $C_{12}H_{21}O_{10}$-O-H_2O	
							178.9955	$[M-H]^-$-$C_{21}H_{19}O_{11}$	
3	5.72	609.1468	$C_{27}H_{30}O_{16}$	609.1456	Rutin **(Flavonoid glycoside)**	2.0	301.0305	$[M-H]^-$-$C_{12}H_{21}O_9$	[149]
							284.0312	$[M-H]^-$-$C_{12}H_{21}O_9$-H_2O	
							178.9969	$[M-H]^-$-$C_{15}H_9O_6$-$C_6H_{11}O_4$	
							151.0003	$[M-H]^-$-$C_{12}H_{21}O_9$-$C_8H_5O_3$	
4	6.10	463.0865	$C_{21}H_{20}O_{12}$	463.0877	Quercimeritrin **(Flavonoid)**	-2.4	300.0264	$[M-H]^-$-$C_6H_{10}O_5$	[150]
							271.0228	$[M-H]^-$-$C_6H_{11}O_5$-CO	
							255.0275	$[M-H]^-$-$C_6H_{11}O_5$-CO_2	
							151.0004	$[M-H]^-$-$C_6H_{11}O_5$-$C_8H_6O_3$	
5	6.46	433.0747	$C_{20}H_{18}O_{11}$	433.0771	quercetin-3-*O*-alpha-L-arabinopyranside **(Curcuminoids)**	3.5	300.0251	$[M-H]^-$-$C_5H_9O_4$	[151]
							271.0218	$[M-H]^-$-$C_6H_{10}O_5$	
							255.0274	$[M-H]^-$-$C_6H_{10}O_6$	
							151.0006	$[M-H]^-$-$C_{13}H_{14}O_7$	
6	6.83	447.0921	$C_{21}H_{20}O_{11}$	447.0927	Orientin **(Flavonoid glycoside)**	-1.3	284.0312	$[M-H]^-$-$C_6H_{11}O_5$	[152]
							271.0221	$[M-H]^-$-$C_6H_{11}O_5$-H_2O	
							255.0265	$[M-H]^-$-$C_6H_{11}O_5$-H_2O-O	

						151.0009	[M-H]$^-$-C$_6$H$_{11}$O$_5$-C$_8$H$_6$O$_2$	
7	10.98	169.1213	C$_{10}$H$_{18}$O$_2$	169.1229	citronellic acid **(Monoterpenoid)**	2.5	97.0643	[M-H]$^-$-C$_2$H$_3$O$_2$-CH$_3$	[153]
							152.9939	[M-H]$^-$-H$_2$O	
							143.0695	[M-H]$^-$-2CH$_3$	
							83.0476	[M-H]$^-$-C$_4$H$_7$O$_2$	

The structures of the compounds are shown in figure 2.10.
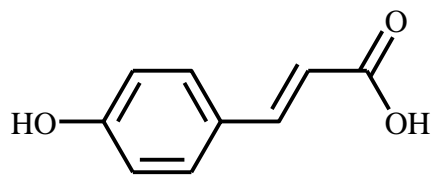
p-coumaric acid (**44**)
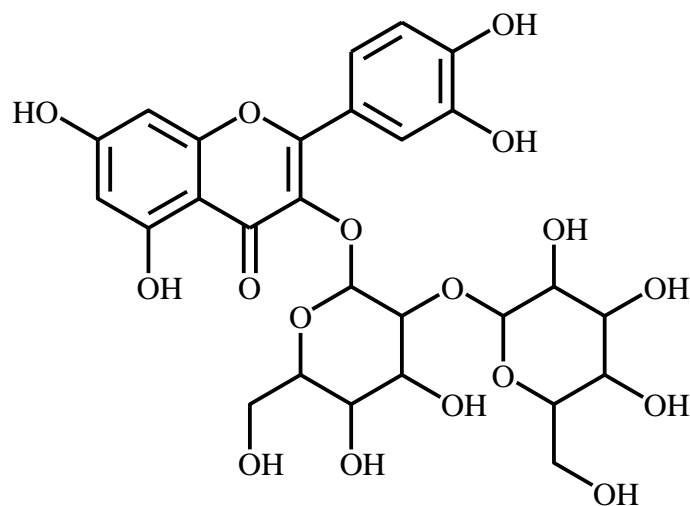
Quercetin-O-sophoroside (**45**)
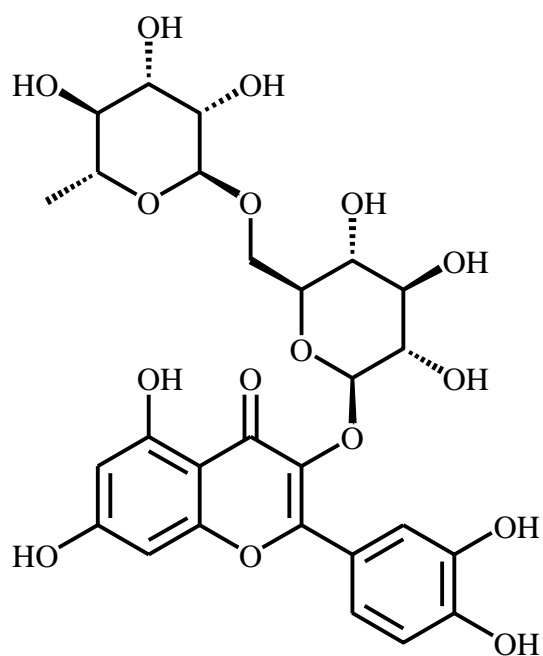
Rutin (**46**)
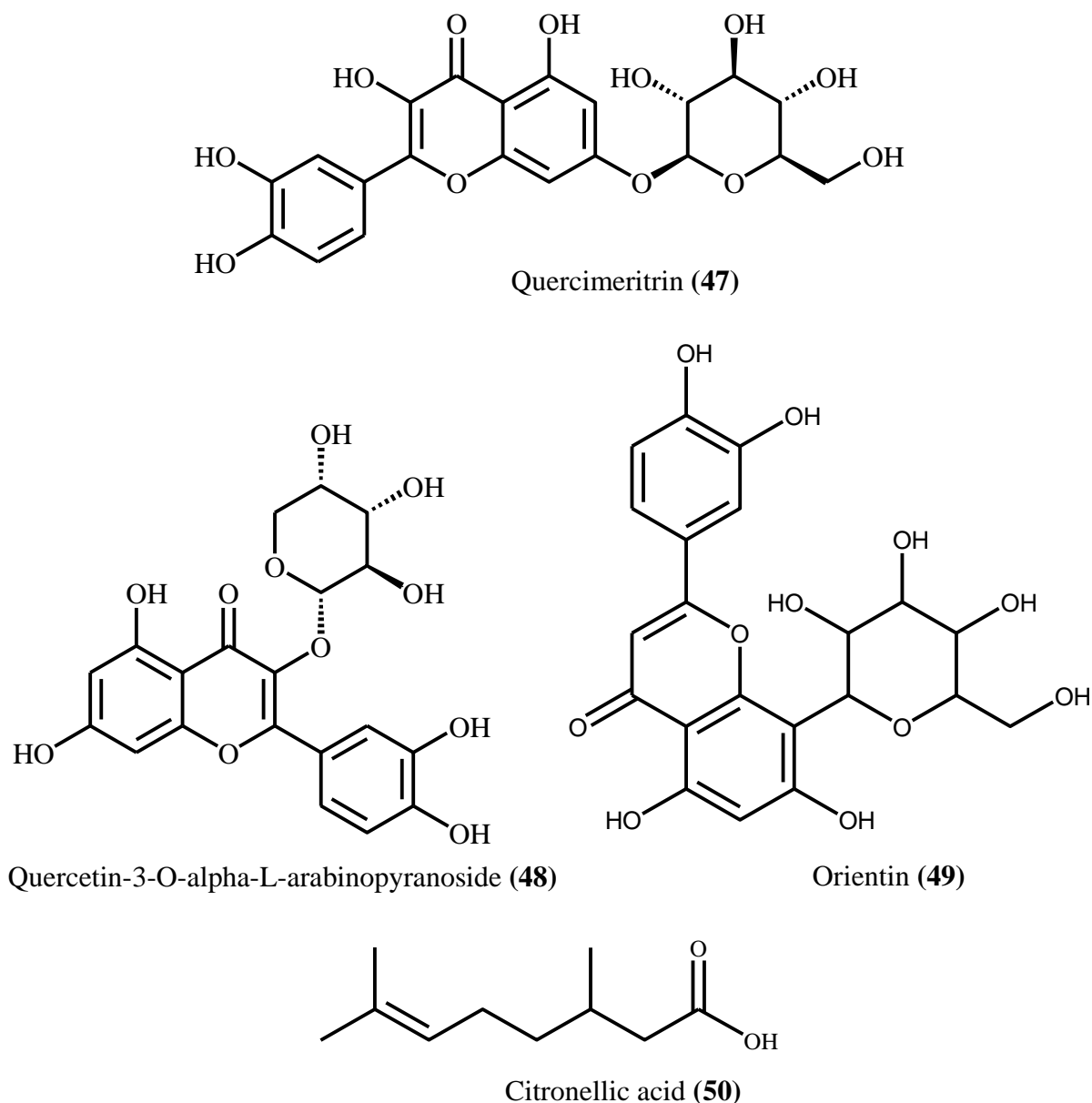
Figure 2.10: Structures of chemical markers tentatively identified from *P. capitatum* leaves.

The first order mass spectrum of peak 1 showed an [M-H]⁻ ion with *m/z* 163.0378 at the retention time 3.52 minutes. Analysis of elemental composition yielded the molecular formula $C_9H_7O_3^-$ with a normalized iFit value of 0.147. The fragmentation pattern observed was in agreement with that reported for *p*-coumaric acid (**44**). [147] Pragasam et al. reported that *p*-coumaric acid (**44**) showed significant ($p < 0.05$) anti-inflammatory effects in adjuvant-induced arthritic rats by effecting a decrease in the expression of the inflammatory mediator TNF-α and circulating immune complexes.[154] This showed that *p*-coumaric acid may contribute to the anti-inflammatory activity observed in *P. capitatum*.

83

The ESI MS spectrum of peak 2 showed an [M-H]$^-$ ion with m/z 625.1422 at the retention time 5.26 minutes. The molecular formula was given as $C_{27}H_{29}O_{17}^-$ with a normalized iFit value of 0.003. Analysis of the MS/MS data revealed that the compound was a flavone, identified as quercetin-3-O-sophoroside (**45**).[148] In the ESI MS spectrum, peak 3 showed an [M-H]$^-$ ion with m/z 609.1468 at the retention time 5.72 minutes. The molecular formula was given as $C_{27}H_{29}O_{16}^-$ with a normalized iFit value of 0.173. The analysis of the MS/MS data indicated that it was a flavonoid glycoside, matching rutin (**46**).[149] Previous studies have revealed that rutin (**46**) suppressed the production of tumour necrosis factor-α and IL-6 and the activation of nuclear factor-κB and extracellular regulated kinases 1/2 by high mobility group box 1 (HMGB1).[155] This showed rutin may contribute to the anti-inflammatory activity observed in *P. capitatum*.

Peak 4 observed with m/z 463.0865 [M-H]$^-$ at the retention time 6.10 minutes had a molecular formula of $C_{21}H_{19}O_{12}^-$ with a normalized iFit value of 0.003. Analysis of the MS/MS data revealed that the compound was a flavonoid, identified as quercimeritrin (**47**). Quercimeritrin (**47**) has been reported to possess anti-inflammatory activity by inhibiting the expression of inducible nitric oxide synthase and the release of nitric oxide by lipopolysaccharide-stimulated RAW 264.7 macrophages in a dose-dependent manner. Quercimeritrin also inhibited the overexpression of cyclooxygenase-2 and granulocyte- macrophage–colony-stimulating factor.[156] This showed that quercimeritrin may contribute to the anti-inflammatory activity observed in *P. capitatum*. In the first order mass spectrum of peak 5, the [M-H]$^-$ ion was observed with m/z 433.0747 [M-H]$^-$ at the retention time 6.46 minutes. It had a molecular formula of $C_{20}H_{17}O_{11}^-$ with a normalized iFit value of 0.001. The analysis of the MS/MS data indicated that it was a curcuminoid, matching quercetin-3-O-alpha-L-arabinopyranoside (**48**).[151]

In the first order mass spectrum of peak 6, the [M-H]$^-$ ion was observed with m/z 447.0921 [M-H]$^-$ at the retention time 6.83 minutes. It had a molecular formula of $C_{21}H_{19}O_{11}^-$ with a normalized iFit value of 0.039. Analysis of the MS/MS data revealed that the compound was a flavonoid glycoside, identified as orientin (**49**). [152] A study carried out by Yu et al. reported that orientin suppressed inflammatory responses through the modulation of the mitogen-activated protein kinase MAPK/NF-κB signaling pathway by suppressing NF-κB translocation.[157] This showed that orientin may contribute to the anti-inflammatory activity observed in *P. capitatum*.

The MS spectrum of peak 7 was observed at the retention time 10.98 mins with *m/z* 169.1213 [M-H]$^-$. The molecular formula obtained was $C_{10}H_{17}O_2^-$ with a normalized iFit value of 0.005. The analysis of the MS/MS data indicated that it was a monoterpenoid, matching citronellic acid (**50**). Citronellic acid, one of the constituents in Eucalyptus citriodora leaf extract inhibited the expression levels of TNF-α, IL-6, NO, iNOS and COX-2 in LPS- activated RAW 264.7 macrophages.[153] This showed that citronellic acid may contribute to the anti-inflammatory activity observed in *P. capitatum*.

2.4   Conclusion

Three plant species (*Scabiosa columbaria*, *Commiphora pyracanthoides* and *Pelargonium capitatum*) from 3 different families were selected for research, based on their traditional uses, and by applying criteria and a scoring system. Plant extracts were prepared and screened for anti-inflammatory activity against selected proinflammatory cytokines. Based on the screening results, one plant species (*Scabiosa columbaria*) was selected for screening against normal human melanocytes. Sixteen extracts were prepared from different plant parts of the 3 plants. Acetone and ethanol extracts of the roots of *Scabiosa columbaria*, acetone extract of the leaves of *S. columbaria* and acetone and water/ ethanol (1:1) extracts of the stem bark of *Commiphora pyracanthoides* potently (<1 to 9 µg mL^{-1}) decreased the levels of the selected proinflammatory cytokines (PGE2, TNF-α, IL-6, IL-8 and IL-1β). Extracts (acetone, ethanol, water/ ethanol (1:1) and water) from the leaves of *P. capitatum* displayed moderate activity (1 to 546 µg mL^{-1}) on one of the cytokines (IL-6) while no activity was obtained in the other cytokines. There is no scientific literature report on the anti-inflammatory activity of *P. capitatum*. *S. columbaria*, *C. pyracanthoides* and *P. capitatum* were traditionally used for the treatment of wound healing and skin inflammation. The extracts from these plant species were scientifically shown to exhibit proinflammatory cytokine inhibition activities, thus providing scientific evidence supporting their traditional uses and also exhibiting their potential to be developed into anti-inflammatory ingredients.

The chemical profiles for the most active extracts from the three plant species (*S. columbaria*, *C. pyracanthoides* and *P. capitatum*) were developed for quality control purposes. Three compounds were tentatively identified by UPLC-QTOF-MS analysis from the acetone extract of *S. columbaria* leaves which are harpagide (**30**), 10-hydroxyloganin (**31**) and forsythiaside

85

(**32**). These compounds were not previously reported to occur in *S. columbaria*. Six compounds were tentatively identified by UPLC-QTOF-MS analysis from the acetone extract of *C. pyracanthoides*, which are epicatechin (**33**), procyanidin B2 (**34**), dihydrokaempferol (**35**), dihydroquercetin (**36**) naringenin (**37**) and kaempferol (**38**). Seven compounds were tentatively identified by UPLC-QTOF-MS analysis from the acetone extract of *P. capitatum* which are *p*-coumaric acid (**39**), quercetin-3-*O*-sophoroside (**40**), rutin (**41**), quercimeritrin (**42**), quercetin-3-*O*-alpha-L-arabinopyranoside (**43**), orientin (**44**) and citronellic acid (**45**). The identified compounds can be used as chemical markers for batch-to-batch reproducibility, as a requirement for commercialization. Furthermore, *S. columbaria* root was the most bio-active. As no compounds have been isolated from *S. columbaria* and tested for its anti-inflammatory activity, it was selected for further investigation, (chapter 3) to identify and isolate the compound/s responsible for the observed activity.

The acetone extract of *S. columbaria* roots did not show any skin even tone activity in the even tone 2D coculture model, even though it exhibited a positive result in the 1D model (melanin global). An extract of a different plant part, the leaves, of *S. columbaria* has previously been reported to have an anti-melanogenesis effect. Since the acetone extract of *S. columbaria* roots were not active in the 2D skin even tone model, further research on this plant species for skin even tone was not conducted.

2.5   References

1.   Liana, D.; Rungsihirunrat, K., Phytochemical screening, antimalarial activities, and genetic relationship of 16 indigenous Thai Asteraceae medicinal plants: A combinatorial approach using phylogeny and ethnobotanical bioprospecting in antimalarial drug discovery. *Journal of Advanced Pharmaceutical Technology & Research* **2021,** *12* (3), 254.
2.   Buenz, E. J.; Verpoorte, R.; Bauer, B. A., The ethnopharmacologic contribution to bioprospecting natural products. *Annual review of pharmacology and toxicology* **2018,** *58*, 509-530.
3.   Hamburger, M.; Marston, A.; Hostettmann, K., Search for new drugs in plant origin in Advances in Drug Research. Vol. 20. London: B. Testa Editor. Academic Press: 1991.
4.   Mandal, V.; Gopal, V.; Mandal, S. C., An inside to the better understanding of the ethnobotanical route to drug discovery-the need of the hour. *Natural Product Communications* **2012,** *7* (11), 1934578X1200701134.
5.   Queiroz, E. F.; Wolfender, J.-L.; Hostettmann, K., Modern approaches in the search for new lead antiparasitic compounds from higher plants. *Current drug targets* **2009,** *10* (3), 202-211.
6.   Soejarto, D. D., Biodiversity prospecting and benefit-sharing: perspectives from the field. *Journal of Ethnopharmacology* **1996,** *51* (1-3), 1-15.

7. Harborne, J., Chemical data in practical taxonomy. *Current concepts in plant taxonomy. London* **1984**, 237-261.

8. Reinke, J. M.; Sorg, H., Wound repair and regeneration. *Eur Surg Res* **2012,** *49* (1), 35-43.

9. Lin, T. K.; Zhong, L.; Santiago, J. L., Anti-Inflammatory and Skin Barrier Repair Effects of Topical Application of Some Plant Oils. *Int J Mol Sci* **2017,** *19* (1).

10. Schmuth, M.; Blunder, S.; Dubrac, S.; Gruber, R.; Moosbrugger-Martinz, V., Epidermal barrier in hereditary ichthyoses, atopic dermatitis, and psoriasis. *J Dtsch Dermatol Ges* **2015,** *13* (11), 1119-23.

11. Działo, M.; Mierziak, J.; Korzun, U.; Preisner, M.; Szopa, J.; Kulma, A., The Potential of Plant Phenolics in Prevention and Therapy of Skin Disorders. *Int J Mol Sci* **2016,** *17* (2), 160.

12. Thornfeldt, C. R., Chronic inflammation is etiology of extrinsic aging. *J Cosmet Dermatol* **2008,** *7* (1), 78-82.

13. Farage, M. A.; Miller, K. W.; Elsner, P.; Maibach, H. I., Intrinsic and extrinsic factors in skin ageing: a review. *Int J Cosmet Sci* **2008,** *30* (2), 87-95.

14. Lee, S. J.; Lee, K. B.; Son, Y. H.; Shin, J.; Lee, J. H.; Kim, H. J.; Hong, A. Y.; Bae, H. W.; Kwon, M. A.; Lee, W. J.; Kim, J. H.; Lee, D. H.; Jeong, E. M.; Kim, I. G., Transglutaminase 2 mediates UV-induced skin inflammation by enhancing inflammatory cytokine production. *Cell Death Dis* **2017,** *8* (10), e3148.

15. Magcwebeba, T.; Swart, P.; Swanevelder, S.; Joubert, E.; Gelderblom, W., Anti-Inflammatory Effects of Aspalathus linearis and Cyclopia spp. Extracts in a UVB/Keratinocyte (HaCaT) Model Utilising Interleukin-1α Accumulation as Biomarker. *Molecules* **2016,** *21* (10).

16. Finberg, M. J.; Muntingh, G. L.; van Rensburg, C. E., A comparison of the leaf gel extracts of Aloe ferox and Aloe vera in the topical treatment of atopic dermatitis in Balb/c mice. *Inflammopharmacology* **2015,** *23* (6), 337-41.

17. Ellis, C.; Luger, T.; Abeck, D.; Allen, R.; Graham-Brown, R. A.; De Prost, Y.; Eichenfield, L. F.; Ferrandiz, C.; Giannetti, A.; Hanifin, J.; Koo, J. Y.; Leung, D.; Lynde, C.; Ring, J.; Ruiz-Maldonado, R.; Saurat, J. H., International Consensus Conference on Atopic Dermatitis II (ICCAD II): clinical update and current treatment strategies. *Br J Dermatol* **2003,** *148 Suppl 63*, 3-10.

18. Pérez-Salas, J. L.; Moreno-Jiménez, M. R.; Rocha-Guzmán, N. E.; González-Laredo, R. F.; Medina-Torres, L.; Gallegos-Infante, J. A., In Vitro and Ex Vivo Models for Screening Topical Anti-Inflammatory Drugs. *Scientia Pharmaceutica* **2023,** *91* (2), 20.

19. De Vuyst, E.; Salmon, M.; Evrard, C.; Lambert de Rouvroit, C.; Poumay, Y., Atopic Dermatitis Studies through In Vitro Models. *Front Med (Lausanne)* **2017,** *4*, 119.

20. Mokdad, R.; Seguin, C.; Fournel, S.; Frisch, B.; Heurtault, B.; Hadjsadok, A., Anti-inflammatory effects of free and liposome-encapsulated Algerian thermal waters in RAW 264.7 macrophages. *Int J Pharm* **2022,** *614*, 121452.

21. Wu, X.; Shi, Z.; Hsu, D. K.; Chong, J.; Huynh, M.; Mendoza, L.; Yamada, D.; Hwang, S. T., A monocyte-keratinocyte-derived co-culture assay accurately identifies efficacies of BET inhibitors as therapeutic candidates for psoriasiform dermatitis. *J Dermatol Sci* **2020,** *100* (1), 31-38.

22. Risueño, I.; Valencia, L.; Jorcano, J. L.; Velasco, D., Skin-on-a-chip models: General overview and future perspectives. *APL Bioeng* **2021,** *5* (3), 030901.

23. Zhang, Q.; Sito, L.; Mao, M.; He, J.; Zhang, Y. S.; Zhao, X., Current advances in skin-on-a-chip models for drug testing. *Microphysiol Syst* **2018,** *2*.

24. Cui, M.; Wiraja, C.; Zheng, M.; Singh, G.; Yong, K. T.; Xu, C., Recent Progress in Skin-on-a-Chip Platforms. *Advanced Therapeutics* **2021,** *5*, 2100138.

25. Adebayo, S. A.; Ondua, M.; Shai, L. J.; Lebelo, S. L., Inhibition of nitric oxide production and free radical scavenging activities of four South African medicinal plants. *J Inflamm Res* **2019,** *12*, 195-203.

26. Selvarani, V.; Hudson James, B., Multiple inflammatory and antiviral activities in Adansonia digitata (Baobab) leaves, fruits and seeds. *Journal of Medicinal Plants Research* **2009,** *3* (8), 576-582.

27. Zhen, J.; Guo, Y.; Villani, T.; Carr, S.; Brendler, T.; Mumbengegwi, D. R.; Kong, A. N.; Simon, J. E.; Wu, Q., Phytochemical Analysis and Anti-Inflammatory Activity of the Extracts of the African Medicinal Plant Ximenia caffra. *J Anal Methods Chem* **2015,** *2015*, 948262.

28. Oguntibeju, O. O., Medicinal plants with anti-inflammatory activities from selected countries and regions of Africa. *J Inflamm Res* **2018,** *11*, 307-317.

29. Adebayo, S. A.; Amoo, S. O., South African botanical resources: A gold mine of natural pro-inflammatory enzyme inhibitors? *South African Journal of Botany* **2019,** *123*, 214-227.

30. Sagbo, J.; Mbeng, W., *Indigenous Cosmetics Plants in the Eastern Cape Province of South Africa: A Case of Skin Care*. 2018.

31. Kadioglu, O.; Jacob, S.; Bohnert, S.; Naß, J.; Saeed, M. E. M.; Khalid, H.; Merfort, I.; Thines, E.; Pommerening, T.; Efferth, T., Evaluating ancient Egyptian prescriptions today: Anti-inflammatory activity of Ziziphus spina-christi. *Phytomedicine* **2016,** *23* (3), 293-306.

32. Ravindranath, N.; Reddy, M.; Ramesh, C.; Ramu, R.; Prabhakar, A.; Jagadeesh, B.; Das, B., New Lathyrane and Podocarpane Diterpenoids from Jatropha curcas. *Chemical & pharmaceutical bulletin* **2004,** *52*, 608-11.

33. Abdillahi, H. S.; Finnie, J. F.; Van Staden, J., Anti-inflammatory, antioxidant, anti-tyrosinase and phenolic contents of four Podocarpus speciess used in traditional medicine in South Africa. *J Ethnopharmacol* **2011,** *136* (3), 496-503.

34. Majmudar, G.; Jacob, G.; Laboy, Y.; Fisher, L., An in vitro method for screening skin-whitening products. *Journal of Cosmetic Science* **1998,** *49*, 361-368.

35. Tobin, D.; Quinn, A. G.; Ito, S.; Thody, A. J., The presence of tyrosinase and related proteins in human epidermis and their relationship to melanin type. *Pigment Cell Res* **1994,** *7* (4), 204-9.

36. Nakazawa, K.; Sahuc, F.; Damour, O.; Collombel, C.; Nakazawa, H., Regulatory effects of heat on normal human melanocyte growth and melanogenesis: comparative study with UVB. *J Invest Dermatol* **1998,** *110* (6), 972-7.

37. Rafal, E. S.; Griffiths, C. E.; Ditre, C. M.; Finkel, L. J.; Hamilton, T. A.; Ellis, C. N.; Voorhees, J. J., Topical tretinoin (retinoic acid) treatment for liver spots associated with photodamage. *N Engl J Med* **1992,** *326* (6), 368-74.

38. Son, K.; Heo, M., The evaluation of depigmenting efficacy in the skin for the development of new whitening agents in K orea. *International journal of cosmetic science* **2013,** *35* (1), 9-18.

39. Barber, J. I.; Townsend, D.; Olds, D. P.; King, R. A., Dopachrome oxidoreductase: a new enzyme in the pigment pathway. *Journal of Investigative Dermatology* **1984,** *83* (2), 145-149.

40. Mapunya, M. B.; Nikolova, R. V.; Lall, N., Melanogenesis and antityrosinase activity of selected South african plants. *Evid Based Complement Alternat Med* **2012,** *2012*, 374017.

41. Opperman, L.; de Kock, M.; Klaasen, J.; Rahiman, F., Tyrosinase and Melanogenesis Inhibition by Indigenous African Plants: A Review. *Cosmetics* **2020,** *7*, 60.

42. Momtaz, S.; Mapunya, B. M.; Houghton, P. J.; Edgerly, C.; Hussein, A.; Naidoo, S.; Lall, N., Tyrosinase inhibition by extracts and constituents of Sideroxylon inerme L. stem bark, used in South Africa for skin lightening. *Journal of Ethnopharmacology* **2008,** *119* (3), 507-512.

42b. Langat, M. K.; Dlova, N. C.; Mulcahy-Ryan, L. E.; Schwikkard, S. L.; Opara, E. I.; Crouch, N. R.; Hiles, J. D.; Mulholland, D. A., The effect of isolates from Cassipourea flanaganii (Schinz) alston, a plant used as a skin lightening agent, on melanin production and tyrosinase inhibition. *Journal of Ethnopharmacology* **2021**, 264, 113272.

43. Mikayoulou, M.; Mayr, F.; Temml, V.; Pandian, A.; Vermaak, I.; Chen, W.; Komane, B.; Stuppner, H.; Viljoen, A., Anti-tyrosinase activity of South African Aloe speciess and isolated compounds plicataloside and aloesin. *Fitoterapia* **2021,** *150*, 104828.

44. Mulholland, D. A.; Mwangi, E. M.; Dlova, N. C.; Plant, N.; Crouch, N. R.; Coombes, P. H., Non-toxic melanin production inhibitors from Garcinia livingstonei (Clusiaceae). *J Ethnopharmacol* **2013,** *149* (2), 570-5.

45. Lall, N.; Kishore, N., Are plants used for skin care in South Africa fully explored? *J Ethnopharmacol* **2014,** *153* (1), 61-84.

46. Duval, C.; Reginier, M.; Schmidt, R., Distinct melanogenic response of human melanocytes in mono-culture, in co-culture with keratinocytes and in reconstructed epidermis, to UV exposure. *Pigment cell research* **2001,** *14* (5), 348-355.

47. Ashu, F. A.; Na-Iya, J.; Wamba, B. E.; Kamga, J.; Nayim, P.; Ngameni, B.; Beng, V. P.; Ngadjui, B. T.; Kuete, V., Antistaphylococcal activity of extracts, fractions, and compounds of Acacia polyacantha wild (Fabaceae). *Evidence-Based Complementary and Alternative Medicine* **2020,** *2020*.

48. Ngaffo, C. M. N.; Tchangna, R. S. V.; Mbaveng, A. T.; Kamga, J.; Harvey, F. M.; Ngadjui, B. T.; Bochet, C. G.; Kuete, V., Botanicals from the leaves of Acacia sieberiana had better cytotoxic effects than isolated phytochemicals towards MDR cancer cells lines. *Heliyon* **2020,** *6* (11), e05412.

49. Maroyi, A., Albizia Adianthifolia: Botany, Medicinal Uses, Phytochemistry, and Pharmacological Properties. *ScientificWorldJournal* **2018,** *2018*, 7463584.

50. Mishra, S.; Aeri, V.; Gaur, P. K.; Jachak, S. M., Phytochemical, therapeutic, and ethnopharmacological overview for a traditionally important herb: Boerhavia diffusa Linn. *Biomed Res Int* **2014,** *2014*, 808302.

51. Hamid, H. S.; Patil, S. In *A Phytochemical and Pharmacological Review of an Indian Plant: Cissus quadrangularis*, Medical Sciences Forum, MDPI: 2023; p 20.

52. Thring, T.; Springfield, E.; Weitz, F., Antimicrobial activities of four plant speciess from the Southern Overberg region of South Africa. *African Journal of Biotechnology* **2007,** *6* (15).

53. PlantZAfrica.com, S., Crinum Macowanii.

54. Erhabor, J.; Oyenihi, O.; Erukainure, O.; Matsabisa, M., Croton gratissimus Burch. (Lavender croton): A Review of the Traditional Uses, Phytochemistry, Nutritional Constituents and Pharmacological Activities. **2022,** *6*, 842-855.

55. Rampa, K. M.; Van De Venter, M.; Koekemoer, T. C.; Swanepoel, B.; Venables, L.; Hattingh, A. C.; Viljoen, A. M.; Kamatou, G. P., Exploring four South African Croton speciess for potential anti-inflammatory properties: in vitro activity and toxicity risk assessment. *J Ethnopharmacol* **2022,** *282*, 114596.

56. Maroyi, A., Traditional usage, phytochemistry and pharmacology of Croton sylvaticus Hochst. ex C. Krauss. *Asian Pacific Journal of Tropical Medicine* **2017,** *10* (5), 423-429.

57. Srivastava, R.; Srivastava, P., The medicinal significance of Datura stramonium-A review. *Biomedical Journal of Scientific & Technical Research* **2020,** *29* (2), 22223-22226.

58. Okpako, I. O.; Kyama, M. C.; Njeru, S. N., Phytochemical screening and gas chromatography-mass spectrometry analysis of Euphorbia ingens organic root extract. *Journal of Medicinal Plants Research* **2023,** *17* (3), 100-105.

59. Abo-Dola, M. A.; Lutfi, M. F., Anti-inflammatory activity of Euphorbia aegyptiaca extract in rats. *Int J Health Sci (Qassim)* **2016,** *10* (1), 69-75.

60. Heredia, D.; Green, I.; Klaasen, J.; Rahiman, F., Importance and Relevance of Phytochemicals Present in <i>Galenia africana</i>. *Scientifica* **2022,** *2022*, 5793436.

61. PlantZAfrica.com, S., Grewia retinervis.

62. Lourens, A.; Viljoen, A. M.; Van Heerden, F., South African Helichrysum speciess: a review of the traditional uses, biological activity and phytochemistry. *Journal of Ethnopharmacology* **2008,** *119* (3), 630-652.

63. Sultana, S.; Al Faruq, A.; Nahid-Al-Rashid, D.; Nasim, T.; Ahsan, M., In-vitro antiinflammatory, anti-oxidant and in-vivo analgesic, anti-diarrheal activities of fractional leaf extracts of Hibiscus surattensis. *European Journal of Pharmaceutical and Medical Research* **2018,** *5* (4), 167-173.

64. Rana, S. K.; Chakraborthy, G. S.; Mazumder, A.; Das, S.; Sodhi, G.; Kumar, K.; Kumar, P., A review of Lantana Camara, A herbal medication with diverse clinical pharmacology. **2019**.

65. Oyedeji-Amusa, M. O.; Sadgrove, N. J.; Van Wyk, B. E., The Ethnobotany and Chemistry of South African Meliaceae: A Review. *Plants (Basel)* **2021,** *10* (9).

66. Viljoen, A.; Van Vuuren, S.; Ernst, E.; Klepser, M.; Demirci, B.; Başer, H.; Van Wyk, B.-E., Osmitopsis asteriscoides (Asteraceae)-the antimicrobial activity and essential oil composition of a Cape-Dutch remedy. *Journal of Ethnopharmacology* **2003,** *88* (2-3), 137-143.

67. De Wet, H.; Nciki, S.; van Vuuren, S. F., Medicinal plants used for the treatment of various skin disorders by a rural community in northern Maputaland, South Africa. *Journal of Ethnobiology and Ethnomedicine* **2013,** *9* (1), 1-10.

68. PlantZAfrica, S., Ozoroa Sphaerocarpa.

69. Kasali, F. M.; Tusiimire, J.; Kadima, J. N.; Tolo, C. U.; Weisheit, A.; Agaba, A. G., Ethnotherapeutic Uses and Phytochemical Composition of Physalis peruviana L.: An Overview. *ScientificWorldJournal* **2021,** *2021*, 5212348.

70. Chandra, S.; Rawat, D. S., Medicinal plants of the family Caryophyllaceae: a review of ethno-medicinal uses and pharmacological properties. *Integrative Medicine Research* **2015,** *4* (3), 123-131.

71. Chowdhury, S. R.; Haldar, S.; Bhar, R.; Das, S.; Saha, A.; Pal, K.; Bandyopadhyay, S.; Paul, J., Pterocarpus angolensis: Botanical, chemical and pharmacological review of an endangered medicinal plant of India. *J. Exp. Biol. Agric. Sci* **2022,** *10*, 150-156.

72. Sobeh, M.; ElHawary, E.; Peixoto, H.; Labib, R. M.; Handoussa, H.; Swilam, N.; El-Khatib, A. H.; Sharapov, F.; Mohamed, T.; Krstin, S., Identification of phenolic secondary metabolites from Schotia brachypetala Sond.(Fabaceae) and demonstration of their antioxidant activities in Caenorhabditis elegans. *PeerJ* **2016,** *4*, e2404.

73. Blom van Staden, A.; Lall, N., Chapter 20 - Ficus lutea. In *Underexplored Medicinal Plants from Sub-Saharan Africa*, Lall, N., Ed. Academic Press: 2020; pp 133-138.

74. Sharma, S.; Dhamija, H. K.; Parashar, B., Jatropha curcas: a review. *Asian Journal of Research in Pharmaceutical Science* **2012,** *2* (3), 107-111.

75. Bello, I.; Shehu, M. W.; Musa, M.; Asmawi, M. Z.; Mahmud, R., Kigelia africana (Lam.) Benth.(Sausage tree): Phytochemistry and pharmacological review of a

quintessential African traditional medicinal plant. *Journal of ethnopharmacology* **2016,** *189*, 253-276.

76. Maroyi, A., <i>Lippia javanica</i> (Burm.f.) Spreng.: Traditional and Commercial Uses and Phytochemical and Pharmacological Significance in the African and Indian Subcontinent. *Evidence-Based Complementary and Alternative Medicine* **2017,** *2017*, 6746071.

77. Maroyi, A., Melianthus major L.(Francoaceae): review of its medicinal uses, phytochemistry and biological activities. *Journal of Pharmaceutical Sciences and Research* **2019,** *11* (11), 3638-3642.

78. Brendler, T.; Van Wyk, B.-E., A historical, scientific and commercial perspective on the medicinal use of Pelargonium sidoides (Geraniaceae). *Journal of ethnopharmacology* **2008,** *119* (3), 420-433.

79. Nasr, F. A.; Noman, O. M.; Alqahtani, A. S.; Qamar, W.; Ahamad, S. R.; Al-Mishari, A. A.; Alyhya, N.; Farooq, M., Phytochemical constituents and anticancer activities of Tarchonanthus camphoratus essential oils grown in Saudi Arabia. *Saudi Pharmaceutical Journal* **2020,** *28* (11), 1474-1480.

80. Sadgrove, N. J.; Senbill, H.; Van Wyk, B.-E.; Greatrex, B. W., New labdanes with antimicrobial and acaricidal activity: Terpenes of Callitris and Widdringtonia (Cupressaceae). *Antibiotics* **2020,** *9* (4), 173.

81. Aremu, A. O.; Pendota, S. C., Medicinal Plants for Mitigating Pain and Inflammatory-Related Conditions: An Appraisal of Ethnobotanical Uses and Patterns in South Africa. *Front Pharmacol* **2021,** *12*, 758583.

82. Ali, S. I.; Gopalakrishnan, B.; Venkatesalu, V., Pharmacognosy, phytochemistry and pharmacological properties of Achillea millefolium L.: a review. *Phytotherapy Research* **2017,** *31* (8), 1140-1161.

83. Coopoosamy, R. M.; Naidoo, K. K., A comparative study of three Aloe speciess used to treat skin diseases in South African rural communities. *The Journal of Alternative and Complementary Medicine* **2013,** *19* (5), 425-428.

84. andongensis Baker, A., Aloe L.

85. Tetyana, P.; Prozesky, E.; Jäger, A.; Meyer, J.; Van Staden, J.; Van Wyk, B.-E., Some medicinal properties of Cussonia and Schefflera speciess used in traditional medicine. *South African Journal of Botany* **2002,** *68* (1), 51-54.

86. Elgorashi, E. E.; Taylor, J. L.; Maes, A.; van Staden, J.; De Kimpe, N.; Verschaeve, L., Screening of medicinal plants used in South African traditional medicine for genotoxic effects. *Toxicology letters* **2003,** *143* (2), 195-207.

87. Maroyi, A., Dombeya rotundifolia (Hochst.) Planch.: review of its botany, medicinal uses, phytochemistry and biological activities. *Journal of Complementary Medicine Research* **2018,** *9* (3), 74-74.

88. Nsuala, B. N.; Enslin, G.; Viljoen, A., "Wild cannabis": A review of the traditional use and phytochemistry of Leonotis leonurus. *Journal of Ethnopharmacology* **2015,** *174*, 520-539.

89. Sharma, S.; Kumar, S., Phyllanthus reticulatus Poir.-an important medicinal plant: A review of its phytochemistry, traditional uses and pharmacological properties. *International Journal of Pharmaceutical Sciences and Research* **2013,** *4* (7), 2528.

90. Pooley, E., *A field guide to wildflowers: KwaZulu-Natal and the eastern region*. Natal Flora Publ. Trust: 1998.

91. Otang-Mbeng, W.; Sagbo, I. J., Anti-Melanogenesis, antioxidant and anti-Tyrosinase activities of Scabiosa columbaria L. *Processes* **2020,** *8* (2), 236.

92. Reserve, H. B. S. F. N., Cassytha ciliolata.

93. PlantZAfrica.com, S., Commiphora Jacq.

94. Lerotholi, L.; Chaudhary, S.; Combrinck, S.; Viljoen, A., Bush tea (Athrixia phylicoides): A review of the traditional uses, bioactivity and phytochemistry. *South African Journal of Botany* **2017,** *110*, 4-17.

95. Mudimba, T. N.; Nguta, J. M., Traditional uses, phytochemistry and pharmacological activity of Carpobrotus edulis: A global perspective. *J. Phytopharm* **2019,** *8*, 111-116.

96. Akinyede, K. A.; Ekpo, O. E.; Oguntibeju, O. O., Ethnopharmacology, therapeutic properties and nutritional potentials of Carpobrotus edulis: A comprehensive review. *Scientia Pharmaceutica* **2020,** *88* (3), 39.

97. Grierson, D. S.; Afolayan, A. J., Antibacterial activity of some indigenous plants used for the treatment of wounds in the Eastern Cape, South Africa. *Journal of Ethnopharmacology* **1999,** *66* (1), 103-106.

98. Kaur, M.; Kaur, A.; Sharma, R., Pharmacological actions of Opuntia ficus indica: A Review. *Journal of Applied Pharmaceutical Science* **2012,** *2* (7), 15-18.

99. Koshak, A. E.; Algandaby, M. M.; Mujallid, M. I.; Abdel-Naim, A. B.; Alhakamy, N. A.; Fahmy, U. A.; Alfarsi, A.; Badr-Eldin, S. M.; Neamatallah, T.; Nasrullah, M. Z.; H, M. A.; Esmat, A., Wound Healing Activity of Opuntia ficus-indica Fixed Oil Formulated in a Self-Nanoemulsifying Formulation. *Int J Nanomedicine* **2021,** *16*, 3889-3905.

100. world, P species., Pelargonium capitatum, https://www.pelargonium species world.com/page19.html.

101. Rafiq, R.; Hayek, S. A.; Anyanwu, U.; Hardy, B. I.; Giddings, V. L.; Ibrahim, S. A.; Tahergorabi, R.; Kang, H. W., Antibacterial and Antioxidant Activities of Essential Oils from Artemisia herba-alba Asso., Pelargonium capitatum × radens and Laurus nobilis L. *Foods* **2016,** *5* (2).

102. PlantZAfrica.com, S., Pelargonium peltatum.

103. Mazimba, O., Pharmacology and phytochemistry studies in Peltophorum africanum. *Bulletin of Faculty of Pharmacy, Cairo University* **2014,** *52* (1), 145-153.

104. Ndlovu, G.; Fouche, G.; Tselanyane, M.; Cordier, W.; Steenkamp, V., In vitro determination of the anti-aging potential of four southern African medicinal plants. *BMC Complement Altern Med* **2013,** *13*, 304.

105. Umadevi, M.; Rajeswari, R.; Rahale, C. S.; Selvavenkadesh, S.; Pushpa, R.; Kumar, K. S.; Bhowmik, D., Traditional and medicinal uses of Withania somnifera. *The pharma innovation* **2012,** *1* (9, Part A), 102.

106. Ajand, N.; Roshanai, K., The Effect of Withania Somnifera Root Extract on Open Wound Healing in the Male Rats. *SSU_Journals* **2015,** *23* (9), 900-911.

107. Rai, M.; Jogee, P. S.; Agarkar, G.; Santos, C. A. d., Anticancer activities of Withania somnifera: Current research, formulations, and future perspectives. *Pharmaceutical biology* **2016,** *54* (2), 189-197.

108. Wintola, O. A.; Afolayan, A. J., The antibacterial, phytochemicals and antioxidants evaluation of the root extracts of Hydnora africanaThunb. used as antidysenteric in Eastern Cape Province, South Africa. *BMC Complementary and Alternative Medicine* **2015,** *15* (1), 307.

109. Szuman, K.; Lall, N., Chapter 13 - Equisetum ramosissimum. In *Underexplored Medicinal Plants from Sub-Saharan Africa*, Lall, N., Ed. Academic Press: 2020; pp 93-98.

110. Savaya, N. S. A.; Issa, R. A.; Talib, W. H., In vitro evaluation of the antioxidant, anti-Propioni bacterium acne and antityrosinase effects of Equisetum ramosissimum (Jordanian horsetail). *Tropical Journal of Pharmaceutical Research* **2020,** *19* (10), 2147-2152.

111. Gebrehiwot, S.; Chaithanya, K. K., Traditional uses, phytochemistry, and pharmacological properties of Capparis tomentosa Lam.: a review. *Drug Invent Today* **2020,** *13* (7), 1006-1011.

112. Tekulu, G. H.; Hiluf, T.; Brhanu, H.; Araya, E. M.; Bitew, H.; Haile, T., Anti-inflammatory and anti-nociceptive property of Capparis tomentosa Lam. root extracts. *Journal of Ethnopharmacology* **2020,** *253*, 112654.

113. Wangai, L. N.; Waithera, B. W.; Karau, G. M.; Koimburi, B. N.; Ndura, P. K.; Karanja, B. N.; Gitau, M. K.; Kirira, P., Investigation of the in vitro antioxidant activity, in vivo antidiabetic efficacy and safety of Capparis tomentosa aqueous roots extracts in male alloxanized mice. **2015**.

114. Van Wyk, A. E.; Van den Berg, E.; Coates Palgrave, M.; Jordaan, M., Dictionary of names for southern African trees. Scientific names of indigenous trees, shrubs and climbers with common names from 30 languages. **2011**.

115. Maroyi, A., Scabiosa columbaria: A review of its medicinal uses, phtochemistry and biological activities. *Asian Journal of Pharmaceutical and Clinical Research* **2019**, 10-14.

116. Mhlongo, F.; Cordero-Maldonado, M. L.; Crawford, A. D.; Katerere, D.; Sandasi, M.; Hattingh, A. C.; Koekemoer, T. C.; Van de Venter, M.; Viljoen, A. M., Evaluation of the wound healing properties of South African medicinal plants using zebrafish and in vitro bioassays. *Journal of Ethnopharmacology* **2022,** *286*, 114867.

117. Shen, T.; Li, G.-H.; Wang, X.-N.; Lou, H.-X., The genus Commiphora: A review of its traditional uses, phytochemistry and pharmacology. *Journal of Ethnopharmacology* **2012,** *142* (2), 319-330.

118. Paraskeva, M. P.; van Vuuren, S. F.; van Zyl, R. L.; Davids, H.; Viljoen, A. M., The in vitro biological activity of selected South African Commiphora speciess. *Journal of Ethnopharmacology* **2008,** *119* (3), 673-679.

119. Lalli, J. Y. Y.; Van Zyl, R. L.; Van Vuuren, S. F.; Viljoen, A. M., In vitro biological activities of South African Pelargonium (Geraniaceae) speciess. *South African Journal of Botany* **2008,** *74* (1), 153-157.

120. Coronado-López, S.; Caballero-García, S.; Aguilar-Luis, M. A.; Mazulis, F.; Del Valle-Mendoza, J., Antibacterial Activity and Cytotoxic Effect of Pelargonium peltatum (Geranium) against Streptococcus mutans and Streptococcus sanguinis. *Int J Dent* **2018,** *2018*, 2714350.

121. Siddiqui, S.; Ahmed, N.; Goswami, M.; Chakrabarty, A.; Chowdhury, G., DNA damage by Withanone as a potential cause of liver toxicity observed for herbal products of Withania somnifera (Ashwagandha). *Current Research in Toxicology* **2021,** *2*, 72-81.

122. Nethathe, B.; Ndip, R., Bioactivity of Hydnora africana on selected bacterial pathogens: Preliminary phytochemical screening. *Afr J Microbiol Res* **2011,** *5* (18), 2820-6.

123. Elgorashi, E. E.; McGaw, L. J., African plants with in vitro anti-inflammatory activities: A review. *South African Journal of Botany* **2019,** *126*, 142-169.

124. Sissi, S.; Loubna, A.; Ouhaddou, S.; Ahmed, O.; Larhsini, M.; Markouk, M., In vitro Antioxidant Potential and In vivo Analgesic and Anti-Inflammatory Activities of Moroccan Equisetum ramosissimum. *The Natural Products Journal* **2023,** *13* (3), 48-59.

125. Alebous, H.; Hudeb; Sober; Gray; Johnson, M., Assessing Effects of Equisetum Ramosissimum Extract on Hematological and Serum Biochemical Parameters in Pregnant Sprague-Dawley Rats. *African Journal of Traditional, Complementary and Alternative Medicines* **2016,** *13*.

126. Goldblatt, P.; Manning, J., *Cape plants: a conspectus of the Cape flora of South Africa*. National Botanical Institute: 2000.

127. Bleotu, A.; Mandravel, C.; Ciuculescu, C., Characterization of some glycoside iridoids by mass spectrometry. *Romanian Biotechnological letters* **2006**, *11* (2), 2643.

128. Veettil, V. N.; Elkahoui, S.; Adnan, M.; Patel, M.; Kadri, A.; Aouadi, K.; De Feo, V.; Badraoui, R., HR-LCMS-Based Metabolite Profiling, Antioxidant, and Anticancer Properties of Teucrium polium L. Methanolic Extract: Computational and In Vitro Study.

129. Cho, H.-E.; Ahn, S.-Y.; Son, I.-S.; Hwang, G.-H.; Kim, S.-C.; Woo, M.-H.; Lee, S.-H.; Son, J.-K.; Hong, J.-T.; Moon, D.-C., HPLC-tandem mass spectrometric analysis of the marker compounds in Forsythiae Fructus and multivariate analysis. *Natural Product Sciences* **2011**, *17* (2), 147-159.

130. Schopohl, P.; Grüneberg, P.; Melzig, M. F., The influence of harpagoside and harpagide on TNFα-secretion and cell adhesion molecule mRNA-expression in IFNγ/LPS-stimulated THP-1 cells. *Fitoterapia* **2016**, *110*, 157-165.

131. Zhang, L.; Feng, L.; Jia, Q.; Xu, J.; Wang, R.; Wang, Z.; Wu, Y.; Li, Y., Effects of β-glucosidase hydrolyzed products of harpagide and harpagoside on cyclooxygenase-2 (COX-2) in vitro. *Bioorganic & Medicinal Chemistry* **2011**, *19* (16), 4882-4886.

132. Wang, Y.; Zhao, H.; Lin, C.; Ren, J.; Zhang, S., Forsythiaside A Exhibits Anti-inflammatory Effects in LPS-Stimulated BV2 Microglia Cells Through Activation of Nrf2/HO-1 Signaling Pathway. *Neurochem Res* **2016**, *41* (4), 659-65.

133. Tong, C.; Chen, T.; Chen, Z.; Wang, H.; Wang, X.; Liu, F.; Dai, H.; Wang, X.; Li, X., Forsythiaside a plays an anti-inflammatory role in LPS-induced mastitis in a mouse model by modulating the MAPK and NF-κB signaling pathways. *Research in Veterinary Science* **2021**, *136*, 390-395.

134. Hou, A. J.; Peng, L. Y.; Liu, Y. Z.; Lin, Z. W.; Sun, H. D., Gallotannins and related polyphenols from Pistacia weinmannifolia. *Planta Med* **2000**, *66* (7), 624-6.

135. Rue, E. A.; Rush, M. D.; van Breemen, R. B., Procyanidins: a comprehensive review encompassing structure elucidation via mass spectrometry. *Phytochem Rev* **2018**, *17* (1), 1-16.

136. Xiao, X.; Xu, L.; Hu, H.; Yang, Y.; Zhang, X.; Peng, Y.; Xiao, P.-G., DPPH radical scavenging and postprandial hyperglycemia inhibition activities and flavonoid composition analysis of hawk tea by UPLC-DAD and UPLC-Q/TOF MSE. *Molecules* **2017**, *22*, 1622.

137. Yang, G.; Lang, Y., Extract identification and evaluation of the cytotoxic activity of Polygala fallax Hemsl in Heilongjiang ethnic medicine against tumors. *Technology and Health Care* **2023**, (Preprint), 1-11.

138. Xu, F.; Liu, Y.; Zhang, Z.; Yang, C.; Tian, Y., Quasi-MSidentification of flavanone 7-glycoside isomers in Da Chengqi Tang by high performance liquid chromatography-tandem mass spectrometry. *Chinese medicine* **2009**, *4*, 15.

139. Zhou, C.; Luo, Y.; Lei, Z.; Wei, G., UHPLC-ESI-MS Analysis of Purified Flavonoids Fraction from Stem of *Dendrobium denneaum Paxt.* and Its Preliminary Study in Inducing Apoptosis of HepG2 Cells. *Evidence-Based Complementary and Alternative Medicine* **2018**, *2018*, 8936307.

140. Wang, H.; Cao, Z., Anti-inflammatory effects of (-)-epicatechin in lipopolysaccharide-stimulated raw 264.7 macrophages. *Tropical Journal of Pharmaceutical Research* **2014**, *13* (9), 1415-1419.

141. Chen, H.; Wang, W.; Yu, S.; Wang, H.; Tian, Z.; Zhu, S., Procyanidins and Their Therapeutic Potential against Oral Diseases. *Molecules* **2022**, *27* (9).

142.   Jiang, Y.;   Wang, X.;   Yang, W.; Gui, S., Procyanidin B2 Suppresses Lipopolysaccharides-Induced Inflammation and Apoptosis in Human Type II Alveolar Epithelial Cells and Lung Fibroblasts. *J Interferon Cytokine Res* **2020,** *40* (1), 54-63.

143.   Yang, L.; He, J., Anti-inflammatory effects of flavonoids and phenylethanoid glycosides from Hosta plantaginea flowers in LPS-stimulated RAW 264.7 macrophages through inhibition of the NF-κB signaling pathway. *BMC Complementary Medicine and Therapies* **2022,** *22* (1), 1-9.

144.   Park, J. E.; Kwon, H. J.; Lee, H. J.; Hwang, H. S., Anti-inflammatory effect of taxifolin in TNF-α/IL-17A/IFN-γ induced HaCaT human keratinocytes. *Applied Biological Chemistry* **2023,** *66* (1), 8.

145.   Manchope, M. F.; Casagrande, R.; Verri, W. A., Jr., Naringenin: an analgesic and anti-inflammatory citrus flavanone. *Oncotarget* **2017,** *8* (3), 3766-3767.

146.   Alam, W.; Khan, H.; Shah, M. A.; Cauli, O.; Saso, L., Kaempferol as a Dietary Anti-Inflammatory Agent: Current Therapeutic Standing. *Molecules* **2020,** *25* (18).

147.   M. Sinosaki, N.; P. Tonin, A.; Ribeiro, M.; Poliseli, C.; Berton, S.; Silveira, R.; Visentainer, J.; O. Santos, O.; Meurer, E., Structural Study of Phenolic Acids by Triple Quadrupole Mass Spectrometry with Electrospray Ionization in Negative Mode and H/D Isotopic Exchange. *Journal of the Brazilian Chemical Society* **2019,** *31*.

148.   Wang, Y.; Berhow, M. A.; Black, M.; Jeffery, E. H., A comparison of the absorption and metabolism of the major quercetin in brassica, quercetin-3-O-sophoroside, to that of quercetin aglycone, in rats. *Food chemistry* **2020,** *311*, 125880.

149.   Abdulla, R.; Mansur, S.; Lai, H.; Aobuli, A.; Guangying, S.; Huang, G.; Aisa, H., Qualitative Analysis of Polyphenols in Macroporous Resin Pretreated Pomegranate Husk Extract by HPLC-QTOF-MS. *Phytochemical analysis : PCA* **2017,** *28*.

150.   Kumar, S.; Singh, A.; Kumar, B., Identification and characterization of phenolics and terpenoids from ethanolic extracts of Phyllanthus speciess by HPLC-ESI-QTOF-MS/MS. *J Pharm Anal* **2017,** *7* (4), 214-222.

151.   Gay, M.; Goh, E.; Ritchie, M., Flavonoids Identification in Complex Plant Extracts using Ion Mobility TOF MS and MSE. *STRUCTURAL ELUCIDATION*, 15.

152.   Doimo, L., Azulenes, Costols and Γ-Lactones from Cypress-Pines (Callitris columellaris, C. glaucophylla and C. intratropica) Distilled Oils and Methanol Extracts. *Journal of Essential Oil Research* **2001,** *13* (1), 25-29.

153.   Liu, J.; Yu, Y.; Dong, G.; Hao, C.; Liu, Y.; Chen, S., Identification and quantification of flavonoids in 207 cultivated lotus (Nelumbo nucifera) and their contribution to different colors. *PeerJ Analytical Chemistry* **2022,** *4*, e22.

154.   Pragasam, S. J.; Venkatesan, V.; Rasool, M., Immunomodulatory and Anti-inflammatory Effect of p-Coumaric Acid, a Common Dietary Polyphenol on Experimental Inflammation in Rats. *Inflammation* **2013,** *36* (1), 169-176.

155.   Yoo, H.; Ku, S. K.; Baek, Y. D.; Bae, J. S., Anti-inflammatory effects of rutin on HMGB1-induced inflammatory responses in vitro and in vivo. *Inflamm Res* **2014,** *63* (3), 197-206.

156.   Legault, J.; Perron, T.; Mshvildadze, V.; Girard-Lalancette, K.; Perron, S.; Laprise, C.; Sirois, P.; Pichette, A., Antioxidant and anti-inflammatory activities of quercetin 7-O-β-D-glucopyranoside from the leaves of Brasenia schreberi. *Journal of Medicinal Food* **2011,** *14* (10), 1127-1134.

157.   Yu, Y.; Pei, F.; Li, Z., Orientin and vitexin attenuate lipopolysaccharide-induced inflammatory responses in RAW264.7 cells: a molecular docking study, biochemical characterization, and mechanism analysis. *Food Science and Human Wellness* **2022,** *11* (5), 1273-1281.

CHAPTER 3: Anti-inflammatory screening, characterization and isolation of compounds from *Scabiosa columbaria* roots

3.1 Introduction

3.1.1 Background to the genus

The genus *Scabiosa* belongs to the family of Caprifoliaceae, although in previous reports, it appears to be included in the Dipsacaceae family. However, due to morphological and molecular phylogenetics analysis, Dipsacaceae is no longer recognized as a family and their species are currently placed in the family Caprifoliaceae.[1] The genus *Scabiosa* is considered to have 618 scientific plant names of species although only 62 species have accepted Latin binominal names.[1] The majority of the *Scabiosa* species are widely distributed in the Mediterranean region, Asia and Southern Africa.[2] *Scabiosa* species are annual plants with basal leaf rosettes and leafy stems. They are mostly shrubs with variations in size from 10 cm to 60 cm.[3] Their flowers have crowded small heads with colours ranging from white to purple which is why some are used as ornamental plants.[1] Several species of the genus *Scabiosa* are widely used in the food, cosmetic and pharmaceutical industries.[4] The class of compounds known to occur in this genus includes flavonoids, iridoids and terpenoids and their derivatives. Some of the species that occur in this genus include *Scabiosa stellata*, *Scabiosa atropurpurea*, *Scabiosa succisa*, *Scabiosa comosa*, *Scabiosa tschilliensis*, *Scabiosa hymettia*, *Scabiosa prolifera* L., *Scabiosa arenaria* Forssk, *Scabiosa argentea* L., *Scabiosa tenuis*, *Scabiosa columbaria*, etc.[1] The current study focuses on the species *Scabiosa columbaria*. It is a perennial herb widely used as herbal medicine throughout its distributional range in tropical Africa, Asia and Europe. Aerial parts, leaves, roots and stems of this plant are used as herbal medicine for eye problems, heartburn, respiratory problems, wounds, female infertility, venereal disease, skin infections and menstrual problems.[3]

3.1.2 Botany and geographical distribution

The Dipsacaceae family contains annual and perennial herbs or shrubs that occur mainly in the Mediterranean basin with about 20% distribution in Eastern Africa, Southern Africa and Asia.[5] *S. columbaria* is mainly found in Northeast, Southern Africa, Temperate Asia and Europe.[5] Its

distribution extends from Europe where it is recorded exclusively in semi-dry or dry grassland (a vegetation type that reduced drastically in Swiss lowlands as a result of land use changes and transformation process in the last decades) to Italy where it is recorded in grassland arid pastures nutrient poor habitat, grazed and mown calcareous grassland to Africa where it is recorded in open woodland, grassland, bushveld, sandy flats, rocky slopes, mountain slopes and valleys at an altitude ranging from 5 m to 3475 m above sea level.[6, 7] This plant is considered an endangered species in Netherlands, the Pre-alps and the Swiss Jura mountains in Northern Switzerland.[8, 9]

The genus name 'Scabiosa' is obtained from the word scabies which means 'to scratch' because of its use in ancient times as an herbal medicine for scabies, skin sores and other skin infection. The species name 'columbaria' is a latin word meaning dove-like or dove-colored in reference to some flower forms of the speciess.[10] S. columbaria is commonly called Wild scabious and Butterfly blue in English, Bitterwortel in Afrikaans, Makgha in Xhosa and Ibheka in Zulu.[11] Two species of S. columbaria are recognized which include S. columbaria subsp. banatica (Waldst and Kit) Diklic and S.columbaria subsp. Caespitosa Jamzad.[12] S. columbaria is a perennial evergreen herb that is 1m in height with the branches springing forth from persistent fleshy roots.[12] The leaves have an oblanceolate shape with thin-textured slightly hairy, characteristic lobed margin forming a rosette on the ground. The stems are long, slender, erect and seldomly branched with a terminal head of small flowers which are surrounded by bristly bracts. The flowers are pink, white or lilac.[3] This plant usually grows in soils with a pH of 6.5-7.2 and flowers in mid-summer.[13, 14]

Figure 3.1: Picture A shows the *S. columbaria* plant with flowers and picture B shows the *S. columbaria* plant without flowers (Picture A taken from www.plantinfo.co.za [15] and Picture B captured by Chidinma Ezeofor)

3.1.3 Traditional uses of *S. columbaria*

The decoction of the aerial part of the plant is used in Spain as a traditional remedy for diphtheria.[16] The aerial parts of the plant have also been used for the treatment of uterine disorders, high blood pressure and hepatic protector.[16, 17] The leaves and roots of the plant are used traditionally as an ointment for wound healing.[18] Studies revealed that the leaves and roots of *S. columbaria* are used commercially as colic and herbal medicine for heartburn in South Africa.[19] The roots and whole plants of *S. columbaria* are sold as herbal medicine in informal herbal medicine markets in 66.7% of the provinces in South Africa which include Eastern Cape, Limpopo, KwaZulu-Natal, Northern Cape, Gauteng and Mpumalanga.[3] This plant is commonly used in South Africa contributing to the primary health care of local communities. It is incorporated into the traditional material medica in South Africa and is included in the book 'Medicinal plants of South Africa.[3]

In Lesotho, the roots of the plant are mixed with the leaves of *Asclepias humilis* (E. Mey) Schltr and the rhizomes of *Gunnera perpensa* L. to address menstrual problems.[20, 21] The roots of *S. columbaria* in combination with *Cussonia paniculata* and *Saposhnikovia divaricata* are used for the treatment of colic.[22] *S. columbaria* roots are mixed with those of *Aster bakerianus* Burtt Davy ex C.A.Sm for the treatment of skin rashes.[23] Also, a mixture of the roots of *S. columbaria* with those of *Decoma anomala, Helichrysum caespititium* (DC) Sond ex Harr. and *Zantedeschia albomaculata* is used for the treatment of venereal diseases.[21, 24] Apart from being used as herbal medicine, it is also consumed as a leafy vegetable in Italy.[25] In the Iberian peninsula, Italy and South Africa, the leaves, stems and roots of this plant were applied on the skin for the treatment of skin infections like eczema, fungus-borne skin disease, acariasis, dermatitis, measles and rashes. An ointment produced from the mixture of charred roots of *S. columbaria* and kerosine is applied topically by the Sotho residents for the treatment of venereal sores. Dried and roasted roots of the plant mixed with animal fat were used as an ointment to heal wounds.[26] The powdered root of the plant is used to make baby powder.[11] In this study, *S. columbaria* was selected based on its extensive traditional uses for the treatment of skin-related diseases.

3.1.4 Previously reported biological efficacy of *S. columbaria*

Van Vuuren et al. showed that the aqueous and DCM/Methanol (1:1) extracts of *S. columbaria* leaves exhibited anti-bacterial activity (MIC from 2 mg/mL) against *Gardnerella vaginalis*, *Neisseria gonorrhoeae*, *Oligella ureolytica,* and *Ureaplasma urealyticum* bacteria associated with urogenital or sexually transmitted infections.[27] Aqueous and organic root extracts of *S. columbaria* showed anti-bacterial activities (MIC from 1.3 mg/mL to > 8 mg/mL) against pathogens such as *Citrobacter freundii*, *Enterobacter homaendis*, *Moraxella catarrhalis*, *Klebsiella pneumoniae* and *Staphylococcus aureus*.[28] Van Vuuren et al. reported the anti-fungal activity (MIC from 2 mg/mL to 8 mg/mL) of aqueous and DCM/Methanol (1:1) extracts of the leaves and roots of *S. columbaria* against *Candida albicans* (associated with urogenital or sexually transmitted diseases) using the microdilution technique.[27] The same study reported the anti-protozoal activity of aqueous and DCM/Methanol (1:1) extracts of the leaves and roots of *S. columbaria* against *Trichomonas vaginalis* (associated with urogenital or sexually transmitted infection). The DCM/Methanol (1:1) extract of the leaves showed good activity (3 mg/mL) compared to the positive control ciprofloxacin (0.01 mg/mL).[27] Otang-Mbeng et al. reported the anti-tyrosinase and anti-oxidant activities of the methanol extract of *S. columbaria* leaves at 25-100 µg/mLin a dose-dependent manner. The plant extract was not found to be cytotoxic at the concentration tested.[29]

3.1.5 Reported phytochemistry and biological efficacy of compounds found in *S. columbaria*

Phytochemical studies have shown the presence of triterpenes, triterpene saponins, triterpene glycosides, monoterpenoid glucoindole alkaloids, iridoids and flavonoids in the *Scabiosa* genus.[1, 30] The chemical constituents of *S. columbaria* are quite limited although it is known to contain tannins, saponins, iridoids and their glycosides.[14, 31]

Loganin (**51**) and sweroside (**52**) were isolated from the 95% 1:1 ethanol/trichloromethane extract of *S. columbaria* tubers.[14] Loganin (**51**) has been reported to have anti-inflammatory

activity as a COX-1 inhibitor (IC_{50} = 3.55 mM) and TNF-α suppression activity (IC_{50} = 154.6 mM).[32]

Loganin (**51**)

Sweroside (**52**)
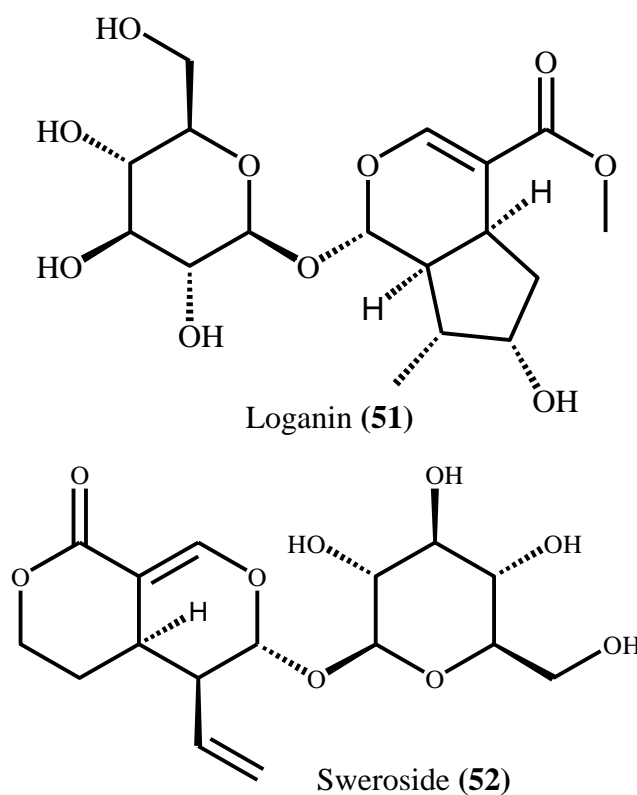
Figure 3.2: Structures of compounds reported from *Scabiosa columbaria*.

3.2   Materials and methods

3.2.1   Collection, processing and extraction of *S. columbaria* roots

The first and second collections of *S. columbaria* roots and the *in vitro* anti-inflammatory screening against selected proinflammatory cytokines of the extracts (acetone, ethanol, water/ethanol (1:1) and water) obtained from the second collection of the *S. columbaria* roots were discussed in chapter 2. Subsequent anti-inflammatory screenings (NO inhibition assay) were carried out at Bioassaix, Nelson Mandela University (NMU). The extract quantities obtained from the second collection of plant material were not sufficient for further research, and additional plant material was collected. The third collection of plant material was undertaken by J. Vahrmeijer from Nylstroom (Modimolle) in Limpopo, South Africa. The plant specimen was deposited at the H.G.W.J Schweickerdt Plant Herbarium (voucher specimen number PRU 125482). The plant material was dried and ground as described for the second collection in chapter 2 (section 2.2.3). Ground plant material (10g) was extracted separately

using acetone, water/ethanol (1:1) and water by adding each solvent (100 mL) in an Erlenmeyer flask containing the plant material and stirring for 24 hours using a magnetic stirrer while 1 kg of ground plant material was extracted using ethanol by adding 1000 mL of the solvent in an Erlenmeyer flask containing the plant material and stirring for 24 hours using a magnetic stirrer (figure 3.3). The extraction, filtration and storage procedure were carried out as described for the second collection of plant material in chapter 2 (section 2.2.3). The extracts (acetone, ethanol, water/ethanol (1:1) and water) obtained from second and third collection of *S. columbaria* roots were screened in the anti-inflammatory assay.
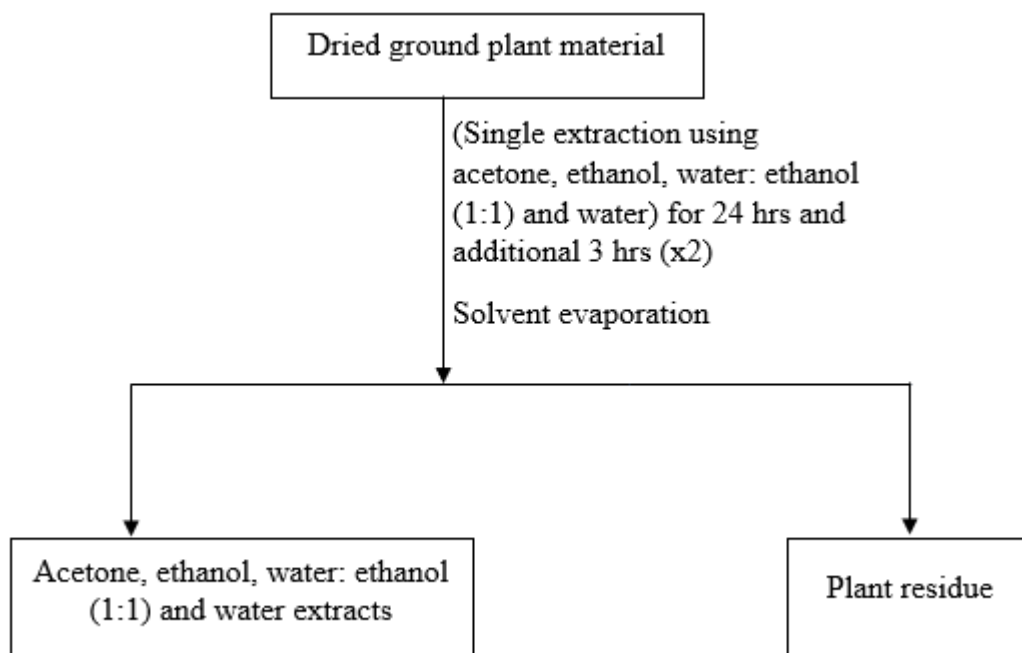
Figure 3.3: Flow diagram for the extraction of the second and third collection of *S. columbaria* roots using acetone, ethanol, water/ethanol (1:1) and water, separately.

3.2.2   Isolation and identification of pure compounds
3.2.2.1 Liquid-liquid partitioning of the ethanol extract

Liquid-liquid partitioning of the ethanol extract of *S. columbaria* roots (from the third collection of the plant) was carried out to separate the polar (defatted ethanol fraction) and non-polar (hexane fraction) parts of the crude extract. The ethanol extract (40 g) was defatted by

101

partitioning between 400 mL of ethanol/water (90:10) and 200 mL of hexane. After the separation of the two layers, the ethanol/water (defatted) fraction and the hexane fraction were evaporated to dryness using a rotary evaporator (figure 3.4). The process was repeated two times. The defatted ethanol fraction and the hexane fraction were screened for the anti-inflammatory activity.
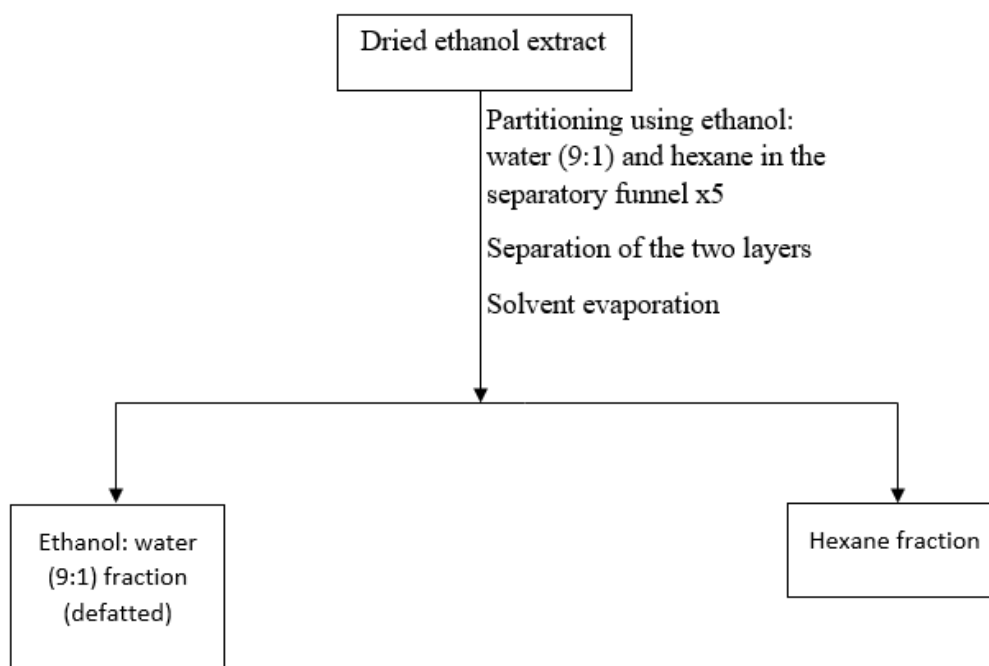
Figure 3.4: Flow diagram showing the liquid-liquid partitioning of the ethanol extract of the third batch of *S. columbaria* roots.

3.2.2.2 Fractionation of the defatted ethanol fraction

The defatted ethanol fraction of *S. columbaria* roots was fractionated to isolate and identify the chemical compounds. The defatted ethanol fraction (15g) was fractionated by column chromatography using silica gel (Merck silica gel 60 (0.063-0.20 mm)) and 73:24:3 ethyl acetate/methanol/water as the mobile phase (isocratic). The resulting 20 fractions were monitored by TLC analysis. The TLC plates (Merck silica gel plates 60 F_{254}) were viewed under a UV lamp at 256 nm and 366 nm (Spectroline®Model ENF-240C/FE, Spectronics Corporation Westbury, New York, USA), then stained by spraying with vanillin reagent. Fractions 11 to 13 and 17 to 19 were combined separately based on their similar TLC profiles. The 16 fractions were labelled as F_1 to F_{16}. Fractions 11 and 15 were selected for purification

using HPLC-QDA as they both were a good representation of all the compounds in the defatted ethanol fraction based on their TLC profiles.

3.2.2.3 Preparative HPLC fractionation of the defatted ethanol fraction

To facilitate the isolation of compounds from fraction 11 (500 mg) obtained from the silica gel column chromatography of the ethanol fraction, it was dissolved in 5 mL HPLC grade MeOH and then filtered through a 0.22 µm nylon syringe filter (13 mm diameter). The solution was subjected to analysis using an XBridge C18 analytical column (4.6 mm x 150 mm, 5 µm, Waters). Chromatographic conditions were optimized on an XBridge C18 analytical column (4.6 mm x 150 mm, 5 µm Waters) to achieve a well-resolved chromatogram within a short analysis time. The optimized method was upscaled to the Prep C18 column (19 mm x 250 mm, 5 µm, Waters) using Waters Prep calculator software. The mobile phase consisted of water + 0.1% Formic acid (FA) (solvent A) and MeOH + 0.1% FA (solvent B) at a flow rate of 17.06 mL/min (obtained from the calculator) and an injection volume of 200 µL for 50 mins. The gradient method used was as follows: 8%B (0.00-0.17 min), 8-38%B (0.17-30.00 mins), 38-100%B (30.00-43.33 minutes), 100-8%B, (43.33-50.00 mins). The preparative HPLC was interfaced with a 2998 PDA detector and a QDA mass spectrometer operated in a negative ion mode. The source temperature was 120°C, while the probe temperature was set at 600°C. The capillary and cone voltages were set to 800 and 10V respectively. Data between 100 and 900 *m/z* were collected. Using a fraction collector, the eluents were collected in 240 tubes, each holding roughly 2 mL. Fractions were subsequently combined based on their similar MS and UV data and concentrated to give six subfractions. A pure compound (**62**) and four semi-pure subfractions ($F_{11}SF_2$, $F_{11}SF_4$, $F_{11}SF_5$ and $F_{11}SF_6$) were collected based on their molecular ion mass in electrospray negative mode (figure 3.5). $F_{11}SF_5$ was purified in the same way as described above resulting in the isolation of a pure compound (**63**) (figure 3.5).

Fraction 15 (500 mg) from the silica gel column chromatography of the ethanol fraction was fractionated using the same instrument and conditions as above yielding ten subfractions that could not be further purified to obtain pure compounds due to their low quantities.

103
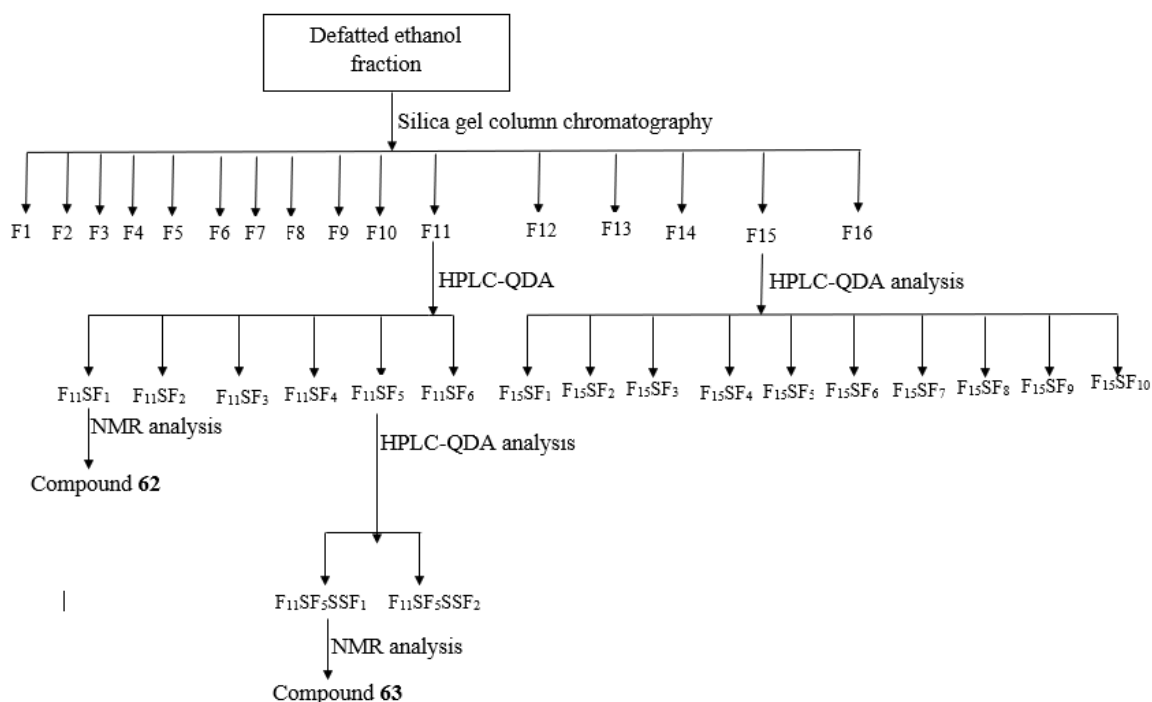
Figure 3.5: Flow diagram showing fractionation of the defatted ethanol fraction of *S. columbaria* roots.

3.2.2.4 Fractionation of the hexane fraction of the ethanol extract

Fractionation of the hexane fraction of the ethanol extract of *S. columbaria* roots was carried out to isolate and identify the compound(s) responsible for the potent activity observed for the hexane fraction. The hexane fraction (7g) was fractionated by column chromatography using silica gel (Merck silica gel 60 (0.063-0.20 mm)). The silica gel was loaded unto the column using hexane. The mobile phase increased in polarity in 5% increments of EtOAc in hexane to 100% EtOAc. Thereafter, 10, 20 and 30% MeOH in EtOAc was used to elute the remaining compounds from the column. The resulting 70 fractions were monitored by TLC (Merck silica gel plates 60 F_{254}). The solvent systems used for the TLC analysis were 9:1 Hex/ EtOAc, 8:2 Hex/ EtOAc, 7:3 Hex/ EtOAc, 1:9 Hex/EtOAc and 9:1 EtOAc/MeOH. The TLC plates were viewed under a UV lamp at 256 nm and 366 nm (Spectroline®Model ENF-240C/FE, Spectronics Corporation Westbury, New York, USA), then stained by spraying with vanillin reagent. Fractions 1-8, 9-23, 24-26, 27-32, 33-36, 37-43, 44-47, 48-53, 54-65 and 66-70 were combined separately based on their similar TLC profiles. A total of 10 fractions were finally obtained and labelled as F_1 to F_{10} (figure 3.6).
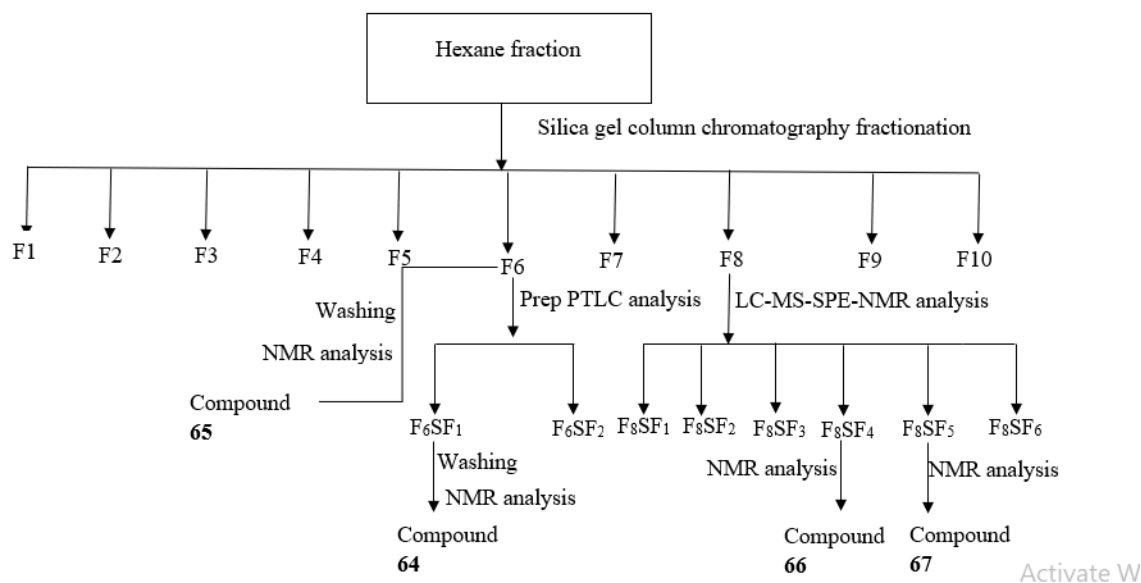
Figure 3.6: Flow diagram showing fractionation of the hexane fraction of *S. columbaria* roots.

3.2.2.5 Preparative thin layer chromatography (PTLC) of the hexane fraction

To facilitate the isolation of active compound(s) responsible for the potent activity observed for the hexane fraction, purification of active fraction 6 from the silica gel column chromatography of the hexane fraction was carried out. Fraction 6 (50 mg) above was subjected to purification using silica gel preparative thin layer chromatography (PTLC) (Silica gel 60 glass plates (Merck KGaA, Darmstadt, Germany) and 80: 15: 5 hexane/dichloromethane/methanol as the mobile phase (isocratic). The two resulting bands were monitored by TLC analysis. The PTLC plate (Silica gel 60 glass plates (Merck KGaA, Darmstadt, Germany) was viewed under a UV lamp at 256 nm and 366 nm (Spectroline®Model ENF-240C/FE, Spectronics Corporation Westbury, New York, USA). The two separated bands were scratched into two polytope vials respectively, and the compounds were eluted using dichloromethane and ethyl acetate simultaneously. The two eluted band(s)/compound(s) were analyzed by NMR which showed that they were still impure. One of the eluted bands/compounds was further subjected to purification by adding acetonitrile (5 mL) to the dried eluted band (appearing as a white solid powder) in a polytope vial and stirring for 10 minutes at room temperature. The resulting solution was allowed to settle after which the supernatant was carefully removed using a pasteur pipette without touching the settled solid. After removing the supernatant, 5 ml of methanol was added to the resulting residue obtained from above and the procedure for washing with acetonitrile above was

105

followed. The resulting supernatant was removed using a pasteur pipette while the residue (2 mg) obtained was evaporated to dryness by exposing it on a petri dish kept in a fume cupboard overnight. The dried residue resulted to a pure compound (**64**).

3.2.2.6 Purification of a compound from the hexane fraction

In line with the goal stated in section 3.2.2.5, purification of active fraction 6 from the silica gel column chromatography of the hexane fraction was carried out. Fraction 6 (10 mg) from the silica gel column chromatography of the hexane fraction was subjected to purification by washing with hexane, ethyl acetate, acetonitrile and methanol simultaneously. Hexane (5 mL) was added to 10 mg of fraction 6 (white precipitate) in a polytope vial and stirred for 10 mins at room temperature. The resulting solution was allowed to settle after which the supernatant was carefully removed using a pasteur pipette without touching the settled solid. After removing the supernatant, 5 ml of ethyl acetate was added to the resulting residue obtained from above and the procedure for washing with hexane above was followed. The same process was repeated with acetonitrile (5 mL) and methanol (5 mL) simultaneously. The final residue obtained was evaporated to dryness by exposing it on a petri dish kept in a fume cupboard overnight. The dried residue resulted to a pure compound (**65**) (figure 3.6).

3.2.2.7 LC-MS-SPE-NMR purification of compounds from fractions of the hexane fraction

In line with the goal stated in section 3.2.2.5, purification of active fraction 8 from the silica gel column chromatography of the hexane fraction was carried out. Fraction 8 (100 mg) from above was subjected to mass directed purification using hyphenated liquid chromatography-mass spectrometry-solid phase extraction-nuclear magnetic resonance spectroscopy (LC-MS-SPE-NMR). The solution was dissolved in 1.5 mL of tetrahydrofuran and filtered on an AcrodiscR syringe filters. The separation was achieved on a Phenomenex C18 column (150 x 4.6 mm, 5µm Luna® Omega). The mobile phase consisted of water + 0.1% FA (solvent A) and ACN + 0.1% FA (solvent B) at a flow rate of 0.6 mL/min and injection volume of 15 µL for 25 mins. The gradient method used was as follows: 45%B (0.00-1.00 min), 45-100%B (1.00-22.00 mins), 100-45%B (22.00-25.00 mins). Peaks were detected by the PDA detector as they eluted from the column and then trapped in individual allocated SPE cartridges. The loaded cartridges were dried using pressurized nitrogen gas. The trapped peaks were eluted

from the cartridges to pre-weighed vials using the SamplePro Tube liquid handler. Data collected using HyStarTM software package. Two pure compounds (**66**) and (**67**) and four semi-pure subfractions (F$_8$SF$_1$, F$_8$SF$_2$, F$_8$SF$_3$ and F$_8$SF$_6$) were collected based on their molecular ion mass in electrospray negative mode (figure 3.6).

3.2.3   UPLC-QTOF-MS analysis of extracts, fractions and compounds

The crude extracts, fractions and compounds were analyzed on Waters acquity ultra-performance liquid chromatography-quadrupole time of flight mass spectrometer (UPLC-QTOF-MS) operating in both positive and negative mode as described in Chapter 2 (section 2.2.5)

3.2.4   NMR analysis of pure compounds

NMR analysis of pure compounds was conducted using Bruker Avance III 400 MHz and 500 MHz spectrophotometers equipped with a prodigy probe. Compounds were dissolved in deuterated solvents (250 µl for 500 MHz and 400 µl for 400 MHz instruments) CDCl$_3$ (Aldrich Chemistry, Sigma-Aldrich, USA), CD$_3$OD (Merck, Switzerland) and DMSO-d$_6$ (Sigma-Aldrich, USA) in NMR tubes for analysis. The chemical shifts were reported in ppm (δ-scale) reference to residual solvent resonances (CD$_3$OD δ_H 3.31, δ_C 49.0 ppm; CDCl$_3$ δ_H 7.26, δ_C 77.16 ppm; DMSO-d$_6$ δ_H 2.50, δ_C 39.52 ppm). Data were processed using Topspin 4.0.9 software from Bruker. The coupling constants "J" were given in Hertz (Hz). The signal multiplicity was reported with the corresponding letter in Italics as follows: s = singlet, d = doublet, dd = doublet of doublet, q = quartet, m = multiplet. The structures of the compounds were elucidated by interpretation of the 1D (^{1}H, ^{13}C) and 2D (HSQC, HMBC, COSY) NMR data.

3.2.5   Biological screening of extracts, fractions and compounds from *Scabiosa columbaria* roots

The biological screening was carried out at the Bioassaix laboratory, NMU, under the supervision of Professor Maryna van de Venter.

3.2.6 Nitric oxide (NO) inhibition assay

Raw 264.7 cells were seeded into 96 well plates at a density of $1x\ 10^5$ cells per well overnight for proper attachment. The spent culture medium was removed the next day and the samples (diluted in Roswell Park Memorial Institute Medium (RPMI) supplemented with 10 % Fetal Bovine Serum (FBS)) were added to give final concentrations of 25, 50, 100 and 200 µg/mL(50 µg/mLper well at double the desired final concentration). 50 µg/mLof LPS (final concentration of 500 ng/mL) containing medium was added to the corresponding wells to assess the anti-inflammatory activity. Aminoguanidine (AG) (100 µM) was used as the positive control for this assay. Cells were incubated for further 24 hrs. To quantify the production of nitric oxide, 50 µl of the spent culture medium was transferred to a new 96 well plate and 50 µl Greiss reagent (containing 50 µl of sulfanilamide and 50 µl of N-1-naphthylethylenediamine dihydrochloride (NED) solution) was added. Absorbance was measured at 540 nm using a BioTek® PowerWave XS spectrophotometer (Winooski, VT, USA) and the result expressed relative to the appropriate untreated control. A standard curve using sodium nitrite dissolved in the culture medium was used to determine the concentration of nitric oxide in each sample.

3.2.7 Cytotoxicity assay

Cell viability was assessed using 3-[4,5-dimethylthiazol-2-yl]-2,5-diphenyltetrazolium-bromide (MTT) to confirm that the test samples were not toxic to the cells. This was done by replacing the existing medium and treatments in each well with medium containing 0.5 mg/mL MTT and further incubating it for 30 minutes at 37°C. MTT was further removed and 200 µL of DMSO was added to each well to solubilize the formazan crystals. Absorbance was read at 540 nm using a BioTek® PowerWave XS spectrophotometer (Winooski, VT, USA).

3.3 Results and discussion
3.3.1 Collection, processing and extraction of *S. columbaria* roots

The third collection of wet roots of *S. columbaria* was 3649.6g and after drying and grinding, 2768.30g of the ground roots was obtained. The extraction yields for the acetone, ethanol, water/ethanol (1:1) and water extracts were 3.5% (0.0705g), 14.5% (0.29g), 39.7% (0.80g) and 18.15% (0.36g), respectively based on the dry weight of extracted plant material.

3.3.2 Anti-inflammatory screening of extracts

The four extracts (acetone, ethanol, water/ethanol (1:1) and water) from second and third collections of plant material were screened against LPS stimulated nitric oxide production in Raw 264.7 macrophages to determine their anti-inflammatory potential (figure 3.7).
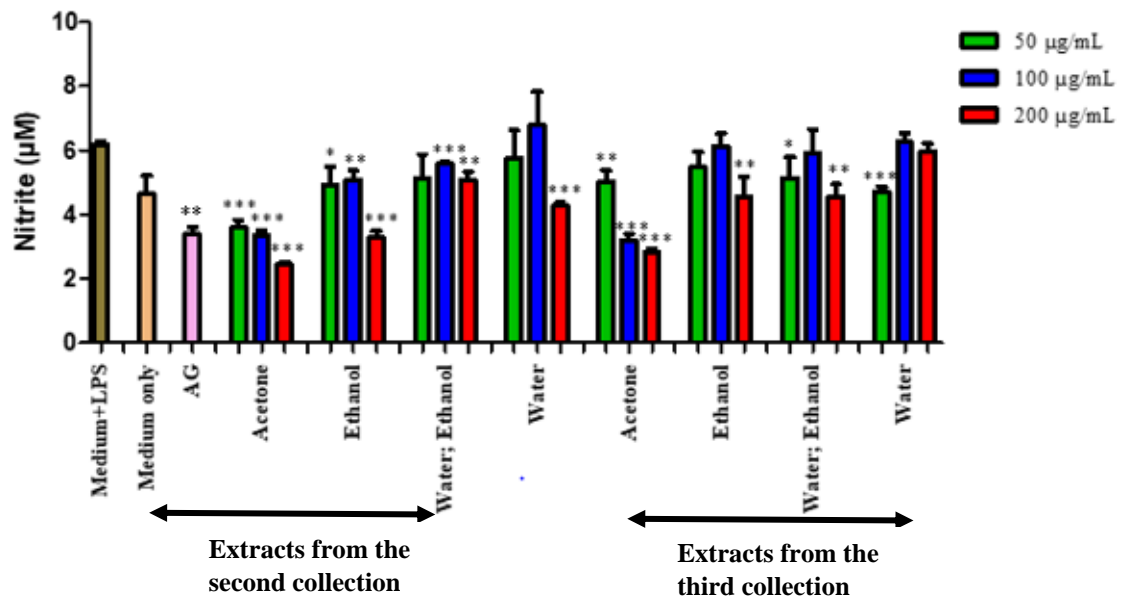
Figure 3.7: Nitric oxide production in LPS activated macrophages treated with different concentrations of extracts. Bar graphs represent triplicate values of one experiment. Error bars represent the standard deviation of the mean. The p values are relative to the negative control (medium + LPS). Aminoguanidine (AG) was included as the positive control. p value < *$p < 0.05$, **$p < 0.01$, ***$p < 0.001$.

The results showed that the acetone extract from the second collection significantly ($P < 0.001$) reduced LPS-stimulated nitric oxide production in Raw 264.7 macrophages at all tested concentrations (50, 100 and 200 μg mL^{-1}), relative to the negative control (medium + LPS) (50 μg mL^{-1}). The ethanol extract of the second collection also showed significant inhibitory effect on nitric oxide production at all tested concentrations (50 [$P < 0.05$], 100 [$P < 0.01$] and 200 [$P < 0.001$] μg mL^{-1}) relative to the negative control (medium + LPS) (50 μg mL^{-1}). Additionally, water/ethanol (1:1) and water extracts from the second collection showed significant inhibitory effect on the production of nitric oxide at 100 [$P < 0.001$] and 200 μg/mL[$P < 0.01$] for water/ethanol (1:1); 200 μg/mL[$P < 0.001$] for water relative to the negative control (medium + LPS) (50 μg/mL). The acetone extract of the third collection

significantly reduced LPS-stimulated nitric oxide production at all tested concentrations (50 [P < 0.01], 100 and 200 [P <0.001] µg/mLrelative to the negative control (medium + LPS) (50 µg mL^{-1}). The ethanol extract of the third collection also showed a significant reduction in the production of LPS stimulated nitric oxide in Raw 264.7 macrophages at 200 µg/mL[P<0.05] relative to the negative control (medium + LPS) (50 µg/mL). The water/ethanol (1:1) extract of the same collection also showed significant inhibitory effect on nitric oxide production at 50 [P<0.05] and 200 µg/mL[P<0.01] relative to the negative control (medium + LPS) (50 µg mL^{-1}). In addition, significant inhibition of LPS stimulated nitric oxide production was observed at 50 µg/mL[P<0.001] for water extract of the third collection relative to the negative control (medium + LPS) (50 µg mL^{-1}). Extracts from the second collection of plant material showed better activity than the extracts from the third collection. Differences in seasons, age and locations could have played a role in the differences observed with the biological activities because of the different ratios of chemical compounds plants produce in different conditions.[33] The anti-inflammatory activity of *S. columbaria* roots acetone, ethanol, water/ethanol (1:1) and water extracts observed in this study are consistent with a previous study on the anti-inflammatory activity of *S. columbaria* leaves prepared with acetone and hexane. The acetone extract of *S. columbaria* leaves displayed anti-inflammatory activity at high test concentrations (50 µg/mL[P < 0.05] and 100 µg/mL[P < 0.01]) while the hexane extract displayed anti-inflammatory activity at the test concentration (100 µg/mL[P < 0.05].[34] Although the acetone extracts from the second collection showed better activity, the quantities obtained were insufficient for further research. The ethanol extract from the third collection was selected for fractionation to target the active compound/s since ethanol is a more industry-acceptable solvent than acetone and easier to isolate compounds than the water/ethanol (1:1) or water extracts.

3.3.3 Cell viability of extracts

The cell viability assay was carried out for the four extracts (acetone, ethanol, water/ethanol (1:1) and water) from second and third collection to confirm that the extracts were not toxic to the RAW 264.7 cells (figure 3.8).
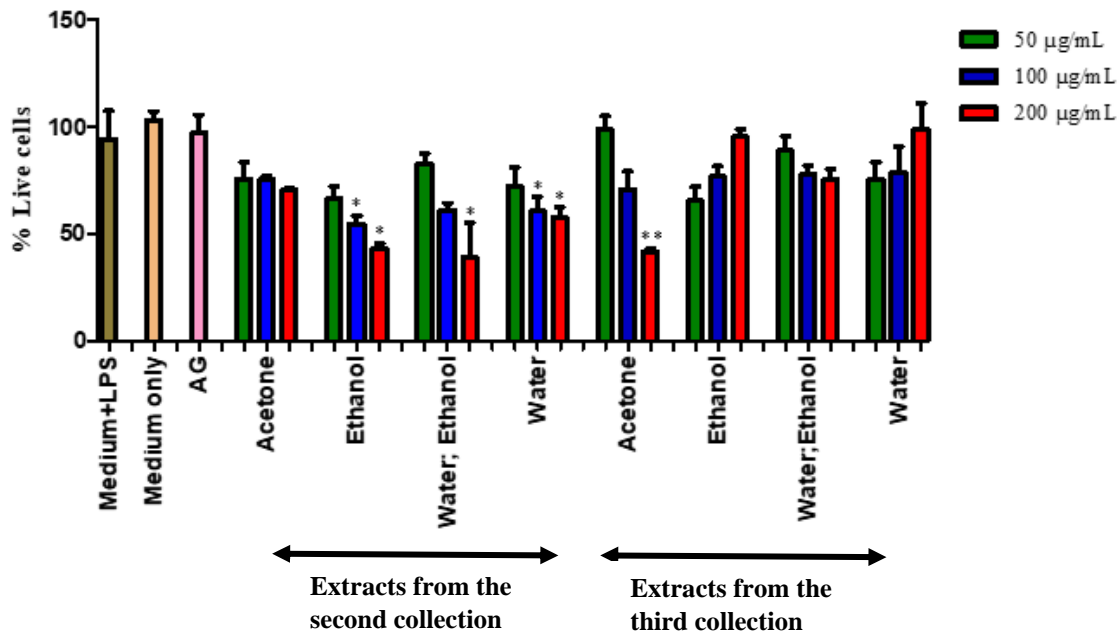
Figure 3.8: Cell viability (%) of LPS activated macrophages after 24 hours of exposure to extracts. Bar graphs represent triplicate value of one experiment. Error bars represent the standard deviation of the mean. The p values are relative to the negative control (medium + LPS). Aminoguanidine (AG) was included as the positive control. p value < *p < 0.05, **p < 0.01, ***p < 0.001.

The third collection of extracts (ethanol, ethanol/water (1:1), water) showed less cytotoxicity effect on the LPS activated macrophages at the tested concentrations than the second collection of extracts (ethanol, ethanol/water (1:1), water). A noticeable difference observed is that the less polar acetone extract of the third collection showed statistically significant cytotoxicity at 200 µg/mLcompared to the second collection acetone extract. This implies that the activity observed in ethanol, ethanol/water (1:1) and water extracts from the second collection and acetone extract from the third collection were as a result of the death of RAW 264.7 cells. Therefore, those extracts at the observed concentrations (100 and 200 µg/mLfor ethanol and water extracts from the second collection; 200 µg/mLfor ethanol/water (1:1) extract from the second collection and acetone extract from the third collection) were not considered to have anti-inflammatory potential.

3.3.4 UPLC-QTOF-MS analysis of active extracts of *S. columbaria* roots from second and third collections

A comparison of the UPLC-QTOF-MS chemical profiles of acetone extracts from second and third collection and ethanol extracts from second and third collections was carried out to identify common peaks in the extracts which could be responsible for the observed biological activity as these extracts were the most active in both collections (figure 3.9 and 3.10).
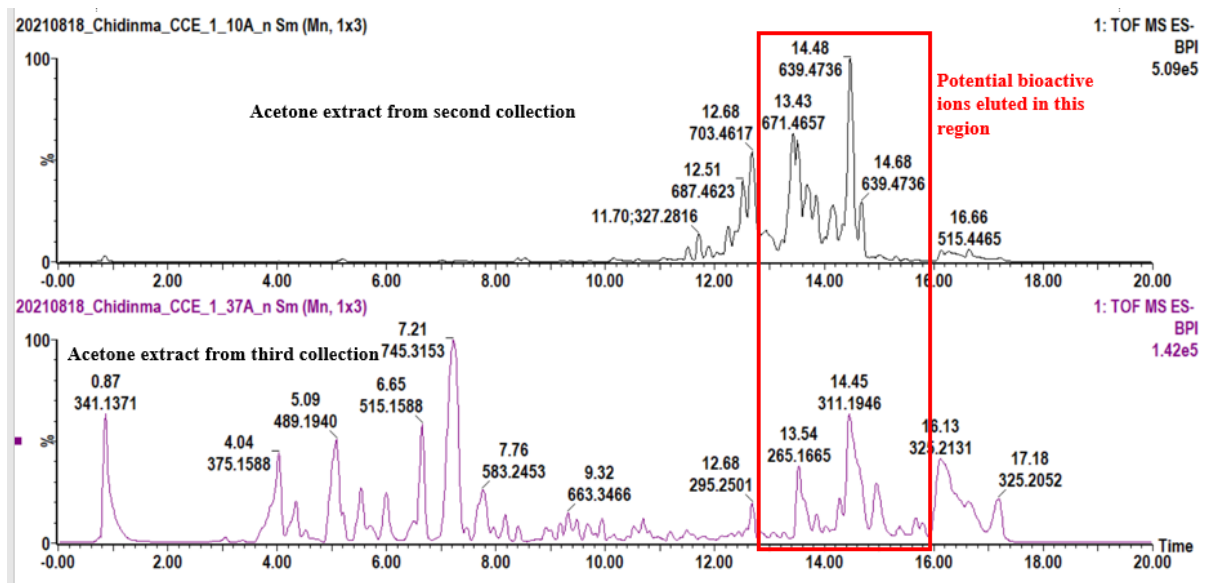
Figure 3.9: ESI negative mode BPI chromatogram of active acetone extracts of *S. columbaria* roots (second and third collection) showing the probable range that contained the bioactive compounds.
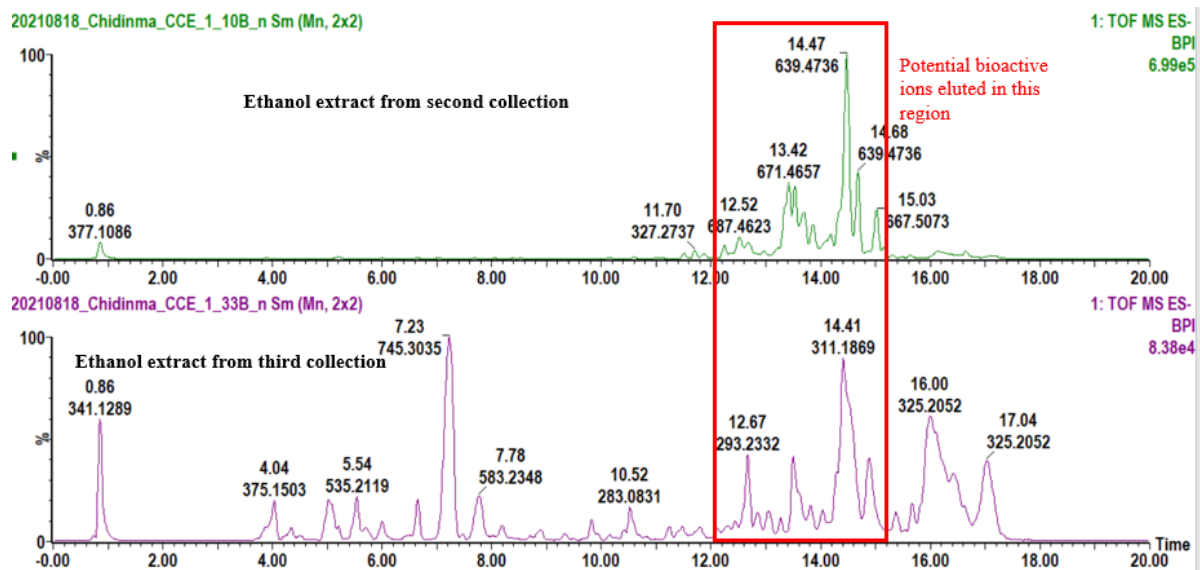
Figure 3.10: ESI negative mode BPI chromatogram of ethanol extracts of *S. columbaria* roots (second and third collection) showing the probable range that contained the bioactive compounds.

The acetone extract from the second collection showed peaks mainly within the 11 to 15-minute range of the 20-minute chromatogram. This distribution of peaks reveals that the extract is composed of non-polar compounds. In comparison, the acetone extract from the third collection was constituted of both polar and non-polar compounds as shown by the retention times of the peaks distributed in the 1 to 17-minute range. The limited anti-inflammatory activity exhibited by the acetone extract from the third collection can be attributed to the active compounds in the non-polar region of the extract having been diluted by the polar inactive compounds in the extract. This trend was also observed in the ethanol extract of both second and third collections. The chemical profiles of the acetone extracts from both collections and the ethanol extracts from both collections showed differences in their chemical composition. Differences could be attributed to climatic changes such as temperature, soil humidity, rainfall, age of the plant as well as different stages of plant metabolism, since plant collections were from different locations and seasons (winter for the second collection and autumn for the third collection).[35] Despite the difference observed in their chemical profiles, acetone and ethanol extracts from both collections showed significant inhibitory effects on nitric oxide production. This could be due to the presence of common class of compounds that are responsible for the anti-inflammatory activity. Analysis of compounds in the region of the chromatograms highlighted above using databases (MetFrag, PubChem, Dictionary of natural products) after generating the molecular formula through MassLynx revealed the class of compounds as

113

triterpenoids. Triterpenoids have been reported to have ant-inflammatory activity. This gave an insight as to what class of compounds would be targeted for isolation.

3.3.5 Tentative identification of compounds from the ethanol extract of *S. columbaria* roots

The ethanol extract of *S. columbaria* roots displayed good anti-inflammatory activity and was selected for identification and isolation of compounds responsible for the activity. The ethanol extract was subsequently analysed by UPLC-QTOF-MS for tentative identification of the compounds which will give more information on the class of compounds present in the extract that could contribute to the anti-inflammatory activity. Figure 3.11 shows the UPLC-QTOF-MS chemical profiles of the ethanol extract of *S. columbaria* roots (third collection) operating in negative electrospray (ESI) ionization mode.
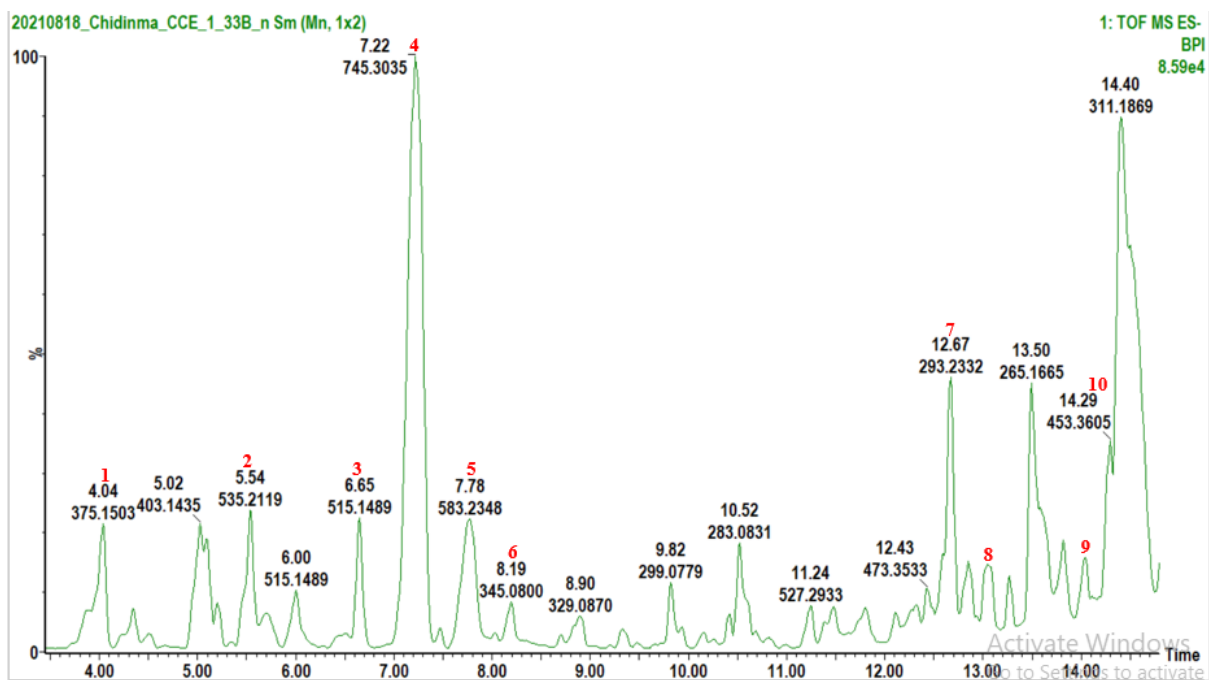
Figure 3.11: ESI negative mode BPI chromatogram of the ethanol extract of *S. columbaria* roots (third collection) with the expansion of region 4 to 15 mins.

Ten compounds were tentatively identified from the UPLC-QTOF-MS analysis in ESI negative mode using accurate mass data and mass fragmentation patterns as described in Chapter 2

114

(section 2.2.5). Table 3.1 shows accurate mass, formula and MS/MS data for compound fragments tentatively identified from the ethanol extract of *S. columbaria* roots.

Table 3.1: Compounds tentatively identified from the ethanol extract of *S. columbaria* roots using data obtained from UPLC-QTOF-MS analysis

Peak No.	RT (min)	Acquired [M-H]⁻ m/z	Formula	Calculated [M-H]⁻ m/z	Possible compound	Mass error (ppm)		MS/MS Data (fragments)	Reference
1	4.04	375.1298	$C_{16}H_{24}O_{10}$	375.1 291	loganic acid (**Iridoid glycoside**)	1.9	213.0773	$[M-H]^-$-$C_6H_{11}O_6$	[36, 37]
							169.0887	$[M-H]^-$-$C_6H_{11}O_6$-CO_2	
							151.0756	$[M-H]^-$-$C_6H_{11}O_6$-CO_2-H_2O	
2	5.53	535.1801	$C_{26}H_{32}O_{12}$	535.1816	scrophuloside A₁ (**Phenylpropanoid glycoside**)	2.8	461.1030	$[M-H]^-$-CO_2-CH_3O	[38]
							417.1550	$[M-H]^-$-CO_2-$2CH_3O$-CH_3	
							373.1275	$[M-H]^-$-$C_6H_{11}O_5$	
							269.0819	$[M-H]^-$-$C_{10}H_9O_3$-CO_2-CH_3-$2H_2O$	
							254.0572	$[M-H]^-$-$C_{10}H_9O_3$-CO_2-CH_3-$3H_2O$	
3	6.63	515.1188	$C_{25}H_{24}O_{12}$	515.1190	3,4-dicaffeoylquinic acid (**Quinic acid**)	0.4	353.0386	$[M-H]^-$-$C_{16}H_{17}O_9$	[39]
							191.0549	$[M-H]^-$-$C_{16}H_{17}O_9$-$C_7H_{11}O_6$	
							179.0347	$[M-H]^-$-$C_{16}H_{17}O_9$-$C_9H_7O_4$	
							161.0228	$[M-H]^-$-$C_{16}H_{17}O_9$-$C_9H_7O_4$-H_2O	
							135.0443	$[M-H]^-$-$C_{16}H_{17}O_9$-$C_9H_7O_4$-CO_2	
4	7.19	745.2553	$C_{33}H_{46}O_{19}$	745.2555	Cantleyoside (**Bis-iridoid glycoside**)	0.3	583.2027	$[M-H]^-$-$C_6H_{11}O_5$	[37, 40]
							513.1609	$[M-H]^-$-$C_6H_{11}O_5$-C_2H_3-C_2H_3O	
							141.0186	$[M-H]^-$-$2C_6H_{11}O_5$-C_2H_3-C_2H_3O-$C_{11}H_{14}O_4$	
5	7.78	583.2029	$C_{27}H_{36}O_{14}$	583.2027	sylvestroside III (**Bis-iridoid glycoside**)	0.3	495.1464	$[M-H]^-$-$C_2H_3O_2$-CH_3O	[41]
							373.1093	$[M-H]^-$-$C_{11}H_{15}O_4$	
							193.0500	$[M-H]^-$-$C_{11}H_{15}O_4$-$C_6H_{11}O_6$	
							149.0600	$[M-H]^-$-$C_{11}H_{15}O_4$-$C_6H_{11}O_6$-C_2H_3O	
6	8.19	791.2983	$C_{35}H_{52}O_{20}$	791.2974	triplostoside A (**Bis-iridoid glycoside**)	1.1	629.2430	$[M-H]^-$-$C_6H_{11}O_5$	[37]
							495.1506	$[M-H]^-$-$C_6H_{11}O_5$-$C_6H_{14}O_3$	
							419.1523	$[M-H]^-$-$C_{17}H_{25}O_9$	
							345.0598	$[M-H]^-$-$2C_6H_{11}O_6$-$C_4H_9O_2$	
							287.0165	$[M-H]^-$-$C_{18}H_{25}O_{11}$-$C_4H_9O_2$	
7	12.65	471.3330	$C_{30}H_{48}O_4$	471.3318	Hederagenin (**Triterpenoid**)	2.6	457.3371	$[M-H]^-$-CH_3	[42, 43]
							427.3568	$[M-H]^-$-CO_2-H_2	
							407.3294	$[M-H]^-$- CO_2-$2H_2$-H_2O	
							295.2426	$[M-H]^-$-$7CH_3$-CO_2H-$2H_2O$	
8	13.01	471.3455	$C_{30}H_{48}O_4$	471.3474	maslinic acid (**Triterpenoid**)	4.0	453.2974	$[M-H]^-$-H_2O	[44, 45]
							423.3198	$[M-H]^-$-CH_3-$2H_2O$	
							405.2812	$[M-H]^-$-$2CH_3$-$2H_2O$	

9	14.04	455.3511	$C_{30}H_{48}O_3$	455.3525	2-isoursolic acid (**Triterpenoid**)	3.1	437.3203	$[M-H]^-$-H_2O	45, 46
							407.3495	$[M-H]^-$-HCHO-H_2O	
							391.3392	$[M-H]^-$-HCHO-H_2O-CH_4	
							377.3038	$[M-H]^-$-HCHO-H_2O-C_2H_6	
10	14.27	453.3355	$C_{30}H_{46}O_3$	453.3369	glycyrrhetaldehyde (**Triterpenoid**)	3.1	407.3324	$[M-H]^-$-CHO-H_2O	47
							309.1721	$[M-H]^-$-CHO-H_2O-O-$7CH_3$	
							279.2390	$[M-H]^-$-CHO-H_2O-O-$5CH_3$	

The structures of the compounds tentatively identified are shown in figure 3.12.

Loganic acid (53)

Triplostoside A (54)

118

Hederagenin (**55**)

2-isoursolic acid (**56**)
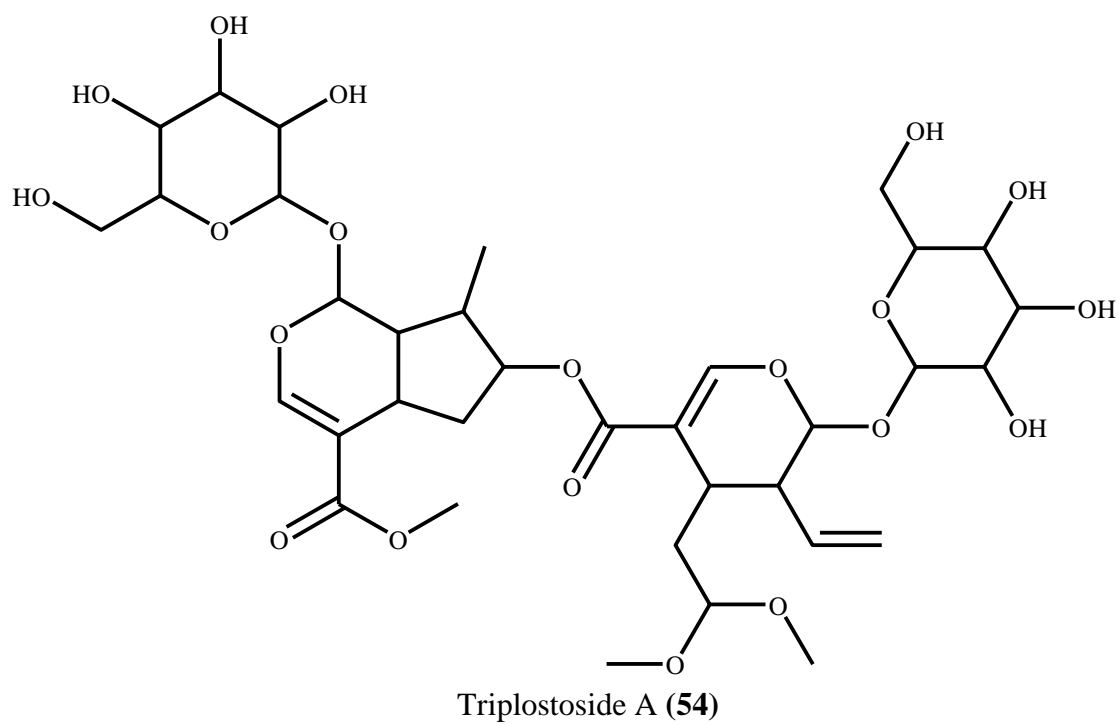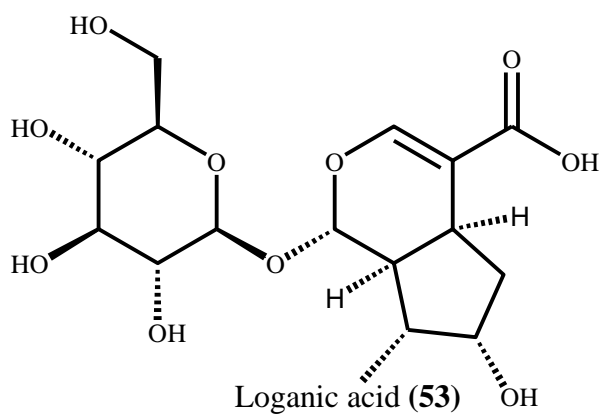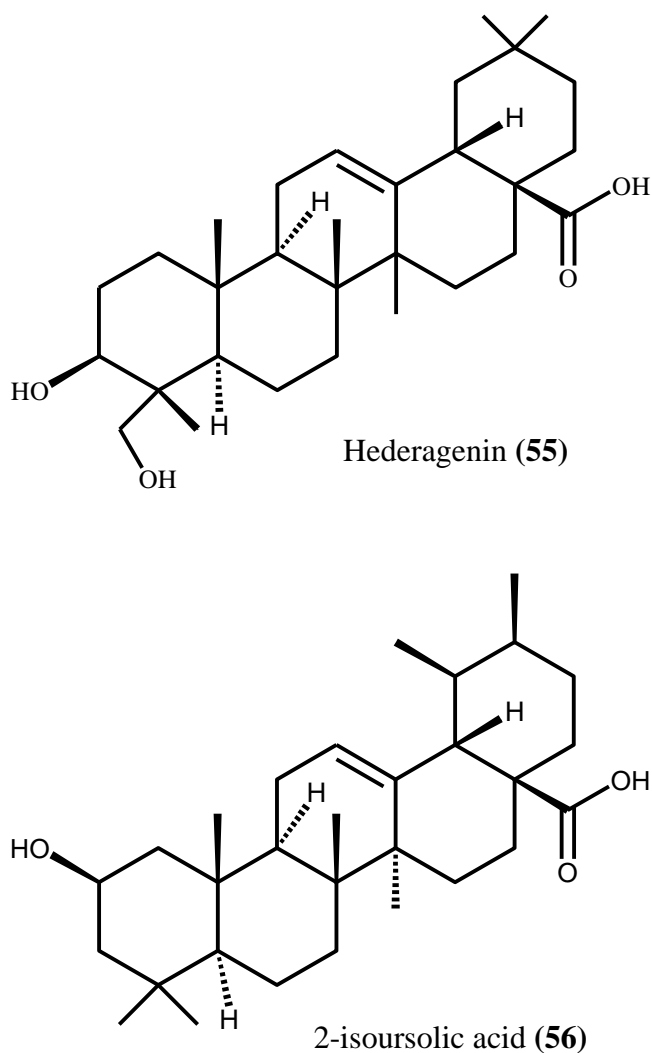
Figure 3.12: Structures of compounds tentatively identified (peaks 1, 6, 7 and 9).

The ten compounds tentatively identified include one iridoid glycoside, one phenylpropanoid glycoside, one quinic acid, three bis-iridoid glycosides and four triterpenoids.

The peak at *m/z* 375.1298 (peak 1), at a retention time 4.04 minutes, had a molecular formula $C_{16}H_{23}O_{10}^{-}$ with a normalized iFit value of 0.001, which corresponded to the [M-H]$^{-}$ ion. The fragmentation pattern observed was in agreement with that reported for loganic acid (**53**) previously identified in *Scabiosa species*.[1, 48]

The peak at *m/z* 535.1801 (peak 2), at a retention time 5.53 minutes, had a molecular formula $C_{26}H_{31}O_{12}^{-}$ with a normalized iFit value of 0.001, which corresponded to the [M-H]$^{-}$ ion. The fragmentation pattern observed was in agreement with that reported for scrophuloside A1.[38]

In the first order mass spectrum, peak 3 exhibited an [M-H]$^-$ ion with *m/z* 515.1188 at the retention time 6.63 minutes. It had a molecular formula of $C_{25}H_{23}O_{12}^-$ with a normalized iFit value of 0.000. Analysis of the MS/MS data revealed that the compound was a quinic acid which matched 3,4-dicaffeoylquinic acid previously identified in *Scabiosa species*.[39, 49]

Peak 4 had an [M-H]$^-$ ion with *m/z* 745.2553 in the ESI MS spectrum at the retention time 7.19 minutes. It had a molecular formula of $C_{33}H_{45}O_{19}^-$ with a normalized iFit value of 0.000. Analysis of the MS/MS data revealed that the compound was a bis iridoid glycoside which matched cantleyoside previously identified in *Scabiosa species*.[1, 37]

In the first order mass spectrum, peak 5 exhibited an [M-H]$^-$ ion with *m/z* 583.2029 at the retention time 7.78 minutes. It had a molecular formula of $C_{27}H_{35}O_{14}^-$ with a normalized iFit value of 0.000. Analysis of the MS/MS data revealed that the compound was a bis iridoid glycoside which matched sylvestroside III.[41]

In the ESI-MS spectrum, peak 6 had an [M-H]$^-$ ion observed with *m/z* 791.2983 at the retention time 8.19 minutes. It had a molecular formula of $C_{35}H_{51}O_{20}^-$ with a normalized iFit value of 0.002. Analysis of the MS/MS data revealed that the compound was a bis iridoid glycoside which matched triplostoside A (**54**).[37]

The ESI-MS spectrum of peak 7 showed an [M-H]$^-$ ion with *m/z* 471.3330 at the retention time 12.65 minutes. It had a molecular formula of $C_{30}H_{47}O_4^-$ with a normalized iFit value of 0.003. Analysis of the MS/MS data revealed that the compound was a triterpenoid which matched hederagenin (**55**).[42, 43]

In the ESI-MS spectrum, peak 8 had an [M-H]$^-$ ion with *m/z* 471.3455 at the retention time 13.01 minutes. It had a molecular formula of $C_{30}H_{47}O_4^-$ with a normalized iFit value of 0.061. Analysis of the MS/MS data revealed that the compound was a triterpenoid which matched maslinic acid.[44, 45]

In the first order mass spectrum of peak 9, the [M-H]$^-$ ion was observed with *m/z* 455.3511 at the retention time 14.04 minutes. It had a molecular formula of $C_{30}H_{47}O_3^-$ with normalized iFit value of 0.001. Analysis of the MS/MS data revealed that the compound was a triterpenoid which matched 2-isoursolic acid (**56**).[45, 46]

The ESI-MS spectrum of peak 10 showed an [M-H]$^-$ ion with *m/z* 453.3355 at the retention time 14.27 minutes. It had a molecular formula of $C_{30}H_{45}O_3^-$ with a normalized iFit value of 0.009. Analysis of the MS/MS data revealed that the compound was a triterpenoid which matched glycyrrhetaldehyde.[47]

3.3.6 Liquid-liquid partitioning of the ethanol extract

The liquid-liquid partitioning of the ethanol extract was carried out to separate the polar compounds in the extract from the non-polar compounds to ascertain where the activity of the extract is coming from. Liquid-liquid partitioning of the ethanol extract yielded 77% of the defatted ethanol fraction and 22% of the hexane fraction. This indicates that the plant is rich in polar compounds.

3.3.7 Anti-inflammatory activity of the defatted ethanol and hexane fractions

The inhibitory effects of the defatted ethanol (polar) and hexane (non-polar) fractions on nitric oxide production in Raw 264.7 macrophages were evaluated over a concentration range of 25-200 µg/mLto ascertain where the anti-inflammatory activity of the ethanol extract came from. Figure 3.13 shows the biological screening results.
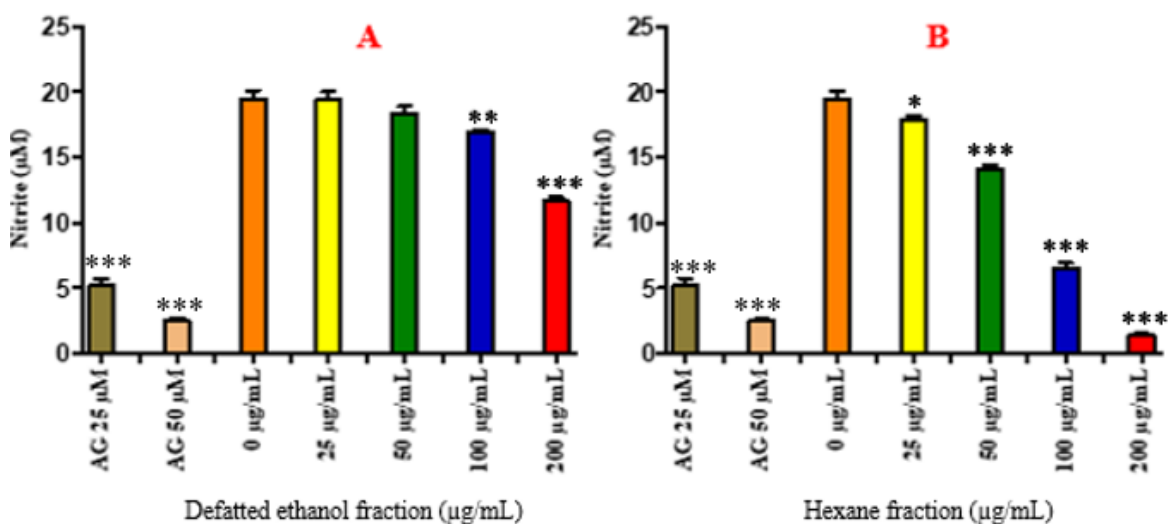
Figure 3.13: Nitric oxide production in LPS activated macrophages treated with different concentrations of defatted ethanol (A) and hexane (B) fractions. Bar graphs represent the value of the experiment at the tested concentration. Error bars

121

represent the standard deviation of the mean. The p values are relative to the negative control (0 µg mL^{-1}). Aminoguanidine (AG) was included as the positive control. p value < *p < 0.05, **p < 0.01, ***p < 0.001.

The dose-response effect of the hexane fraction can be seen as statistically significant reduction of LPS-stimulated nitric oxide production was observed in Raw 264.7 macrophages at test concentrations 50, 100 and 200 µg/mL[P<0.001] relative to the negative control (blank), while at 25 µg/mL[P < 0.05] there was not much significant reduction of LPS-stimulated nitric oxide production observed in Raw 264.7 macrophages. This showed that the anti-inflammatory activity of the hexane fraction was observed at higher test concentrations (50, 100 and 200 µg mL^{-1}). The defatted ethanol fraction showed a significant inhibitory effect on nitric oxide production at the higher test concentrations (100 and 200 µg/mL[P < 0.01 and P<0.001 respectively]) relative to the negative control (blank). The lower test concentrations (25 and 50 µg mL^{-1}) did not show any significant reduction of LPS-stimulated nitric oxide production observed in Raw 264.7 macrophages. This suggests that the less polar compounds of the ethanol extract are responsible for the activity. The hexane fraction from the ethanol extract of *S. columbaria* root was further fractionated targeting the active compounds.

3.3.8 Effect of defatted ethanol and hexane fractions on cell viability

In order to confirm that the activity of the defatted ethanol and hexane fractions was not due to cytotoxicity of the fractions to the Raw 264.7 cells, cell viability test was carried out on the defatted ethanol and hexane fractions. Figure 3.14 shows the result.
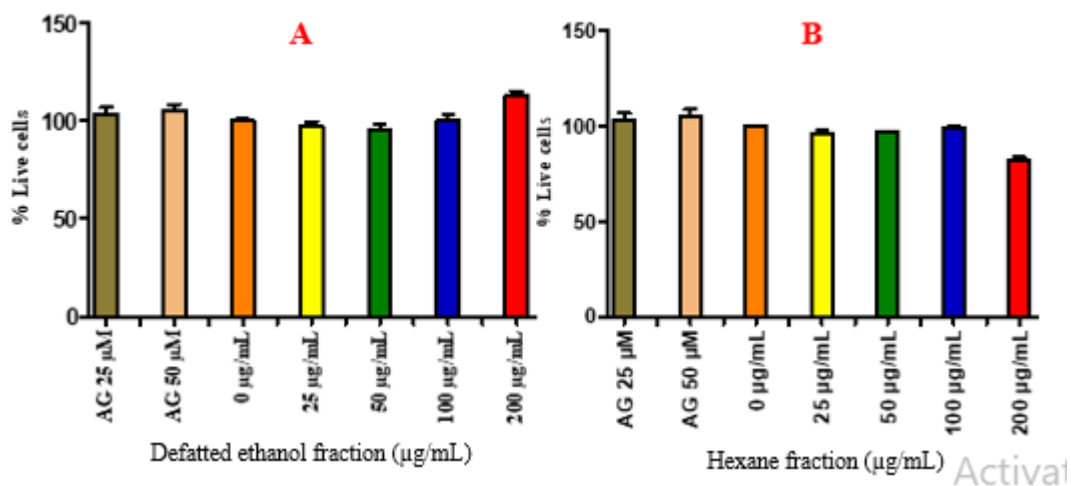
Figure 3.14: Cell viability (%) of LPS activated macrophages after 24 hours of exposure to treatments with different concentrations of defatted ethanol (A) and hexane (B) fractions Bar graphs represent the value of the experiment at the tested concentration. Error bars represent the standard deviation of the mean. The p values are relative to the negative control ($0\,\mu g\,mL^{-1}$). Aminoguanidine (AG) was included as the positive control. p value < *p < 0.05, **p < 0.01, ***p < 0.001.

Both fractions, at all test concentrations (25-200 µg mL^{-1}) were not considered toxic to the cells, although the percentage of live cells were less in the presence of the hexane faction (at 200 µg mL^{-1}). Therefore, the activity observed for defatted ethanol and hexane fraction was not as a result of its cytotoxicity to the Raw 264.7 cells but due to the active chemical compounds present in the fractions.

3.3.9 Comparison of the chemical profiles of the crude ethanol extract and the active hexane fraction

In order to determine the efficiency of the liquid-liquid partitioning, a comparison of the UPLC MS profiles was done between the ethanol extract of *S. columbaria* roots and the hexane fraction obtained from the fractionation of the ethanol extract. UPLC-QTOF-MS chemical profiles of the crude ethanol extract and the hexane fraction are shown in figure 3.15.

123
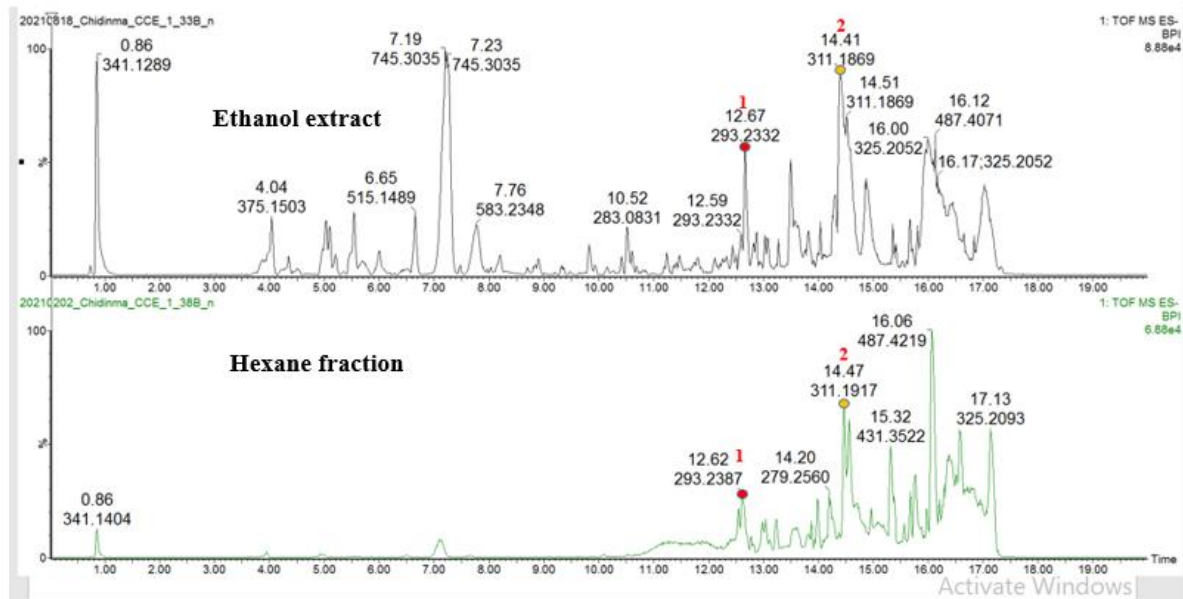
Figure 3.15: ESI negative mode BPI chromatogram of the ethanol extract and the hexane fraction of *S. columbaria* roots (third collection).

A comparison of their respective chromatograms showed that many compounds in the polar region of the ethanol extract were not present in the hexane fraction. Peak 1 observed in the non-polar region of the ethanol extract with *m/z* 293.2332 (at the retention time 12.67 minutes) was present in the hexane extract with *m/z* 293.2387 (at the retention time 12.62 minutes). The compound corresponding to this peak was tentatively identified as hederagenin as described in section 3.3.5. Peak 2 observed in the ethanol extract with *m/z* 311.1869 (at the retention time 14.41 minutes) was present in the hexane extract with *m/z* 311.1917 (at the retention time 14.47 minutes). The compound corresponding to this peak was tentatively identified as 2-isoursolic acid as described in section 3.3.5. These two compounds could be responsible for the anti-inflammatory activity, however, they need to be isolated and tested to confirm that they are the biologically active compounds. The UPLC MS profiles showed the successful separation of the non-polar compounds from the polar compounds with two non-polar compounds tentatively identified as hederagenin and 2-isoursolic acid and possibly contributing to the activity. These were targeted during the purification of the hexane fraction purification.

3.3.10 Isolation of compounds from the defatted ethanol fraction

Compounds were isolated from the defatted ethanol fraction to confirm the structures of compounds tentatively identified by UPLC-QTOF-MS of the ethanol extract and to purify

other compounds that could possibly contribute to the anti-inflammatory activity of the defatted ethanol fraction as it showed moderate anti-inflammatory activity (figure 3.13). Silica gel column chromatography of the defatted ethanol fraction (10g) using a single solvent system (73:24:3 ethyl acetate/methanol/water) resulted in the collection of 16 fractions (F_1-F_{16}). Fraction 11 which represent most of the compounds in the fractions was chosen for further isolation of compounds using preparative HPLC-QDA. Fraction 11 was subjected to purification using preparative HPLC-QDA. The separation resulted in six subfractions $F_{11}SF_1$ to $F_{11}SF_6$ (figure 3.16) which were targeted for isolation.

Figure 3.16: LC-UVmax-QDA chromatogram of Fraction 11 from HPLC-QDA.

The subfractions were analyzed by NMR spectroscopy. They were all mainly mixtures of compounds except the first subfraction (labelled as $F_{11}SF_1$) which was pure (compound (**62**) with sufficient quantity (12 mg). Insufficient quantities were obtained for other subfractions $F_{11}SF_2$ (5 mg), $F_{11}SF_3$ (4 mg), $F_{11}SF_4$ (6 mg) and $F_{11}SF_6$ (4 mg), therefore could not purify further. $F_{11}SF_5$ was collected in sufficient quantity (46 mg). It was subjected to purification using preparative HPLC-QDA. The two sub subfractions labelled $F_{11}SF_5SSF_1$ and $F_{11}SF_5SSF_2$ (figure 3.5) were collected in fraction collector tubes. $F_{11}SF_5SSF_2$ was collected in small quantity (0.4 mg) while $F_{11}SF_5SSF_1$ the major peak was collected in pure form and sufficient quantity for further analysis (15mg) compound (**63**). Two compounds (compounds **62** and **63**) were successfully purified from the defatted ethanol extract. These compounds will be tested for their anti-inflammatory potential.

3.3.11 Fractionation of the hexane fraction and biological screening of fractions

The hexane fraction (7g) was subjected to column chromatography using silica gel as the stationary phase to target and isolate the active compounds present in it. Seventy fractions were collected and monitored by thin-layer chromatography (TLC). Similar fractions were combined to give ten fractions as described above (section 3.2.2.4 and figure 3.6). These fractions were evaluated for their inhibition of nitric oxide production together with the crude ethanol extract. The hexane fraction was not evaluated for its anti-inflammatory potential alongside the fractions obtained from it as a result of insufficient quantity that remained after its silica gel column chromatography.

Figure 3.17 shows the anti-inflammatory potential of the crude ethanol extract and the fractions obtained from the hexane fraction against LPS stimulated nitric oxide production in Raw 264.7 macrophages.
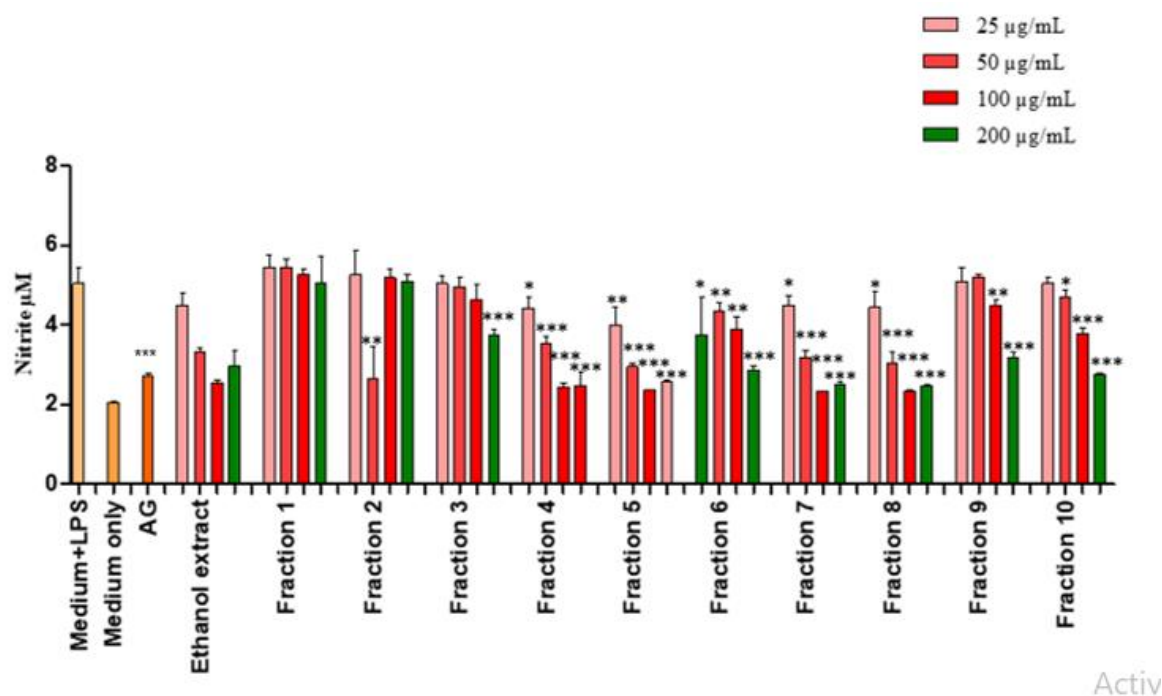
Figure 3.17: Nitric oxide production in LPS activated macrophages treated with different concentrations of fractions. Bar graphs represent triplicate values of one experiment. Error bars represent the standard deviation of the mean. The p values are relative to the negative control (medium + LPS). Aminoguanidine (AG) was included as the positive control. p value < *$p < 0.05$, **$p < 0.01$, ***$p < 0.001$.

The activity of the ethanol extract was again observed as in the initial study (significantly reduced LPS-stimulated nitric oxide production in Raw 264.7 macrophage relative to the negative control (medium +LPS)). Nine out of the ten fractions (fractions 2 to 10) showed anti-inflammatory activity in the nitric oxide production assay at different concentrations. Five fractions (fractions 4 to 8) exhibited significant inhibition on nitric oxide production in Raw 264.7 macrophages at 25 and 50 µg/mLrelative to the negative control (medium + LPS) which are lower test concentrations and therefore show good activity; fractions 4, 6, 7 and 8 (25 µg/mL[P<0.05]); fraction 5 (25 µg/mL[P<0.01]); fractions 4, 5, 7 and 8 (50 µg/mL[P<0.001]); fraction 6 (50 µg mL^{-1}[P<0.01]). Additionally, fraction 10 showed significant inhibition of nitric oxide production at one test concentration (50 µg/mL[P<0.05]) while fractions 1, 2, 3

126

and 9 showed no or minimal activity especially at high test concentrations (100 and 200 µg mL^{-1}) This indicates that the fractionation concentrated most of the active compounds in fractions 4 to 8 and these are the moderately polar region (eluted with 60% hexane and 40% ethyl acetate). Overall, the fractions were less effective than the positive control (aminoguanidine). To confirm that the activity of the fractions was as a result of the active compounds present in the fractions, cell viability test was carried out on the fractions.

3.3.12   Effect of the fractions on cell viability

Figure 3.18 shows the effect of fractions from the active hexane fraction on Raw 264.7 cell viability to ascertain if the fractions were cytotoxic to the cells.
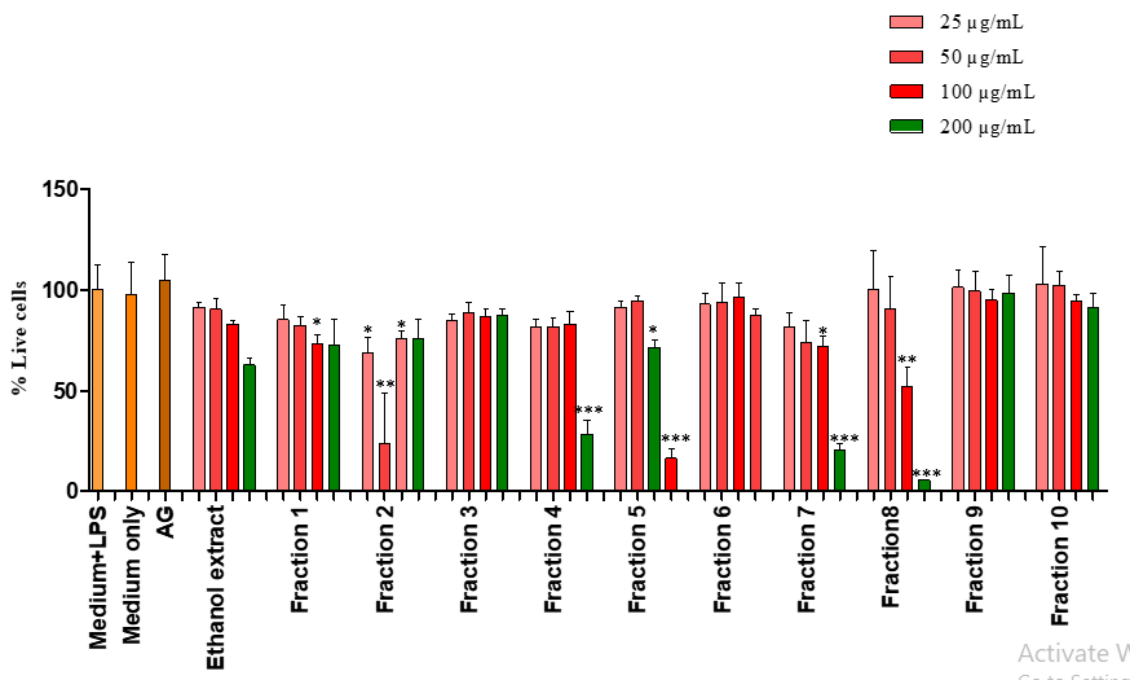
Figure 3.18: Cell viability (%) of LPS activated macrophages after 24 hours of exposure to fractions. Bar graphs represent triplicate value of one experiment. Error bars represent the standard deviation of the mean. P value: *p < 0.05, **p < 0.01, ***p < 0.001.

Fractions 3, 6, 9 and 10 were considered not toxic to the cells. This showed that the anti-inflammatory activity observed in these fractions (fractions 3, 6, 9 and 10) were as a result of presence of active compounds in the fractions. Other fractions showed an effect on cell viability. This was specifically observed for fractions 4, 5, 7 and 8 at the higher test

127

concentration of 200 µg mL^{-1}. Although, these fractions showed an effect on cell viability, the observed cytotoxicity could be as a result of inactive compounds present in these fractions. As a result of this, these fractions were still targeted for isolation of active compounds. Fraction 2 showed a greater cytotoxic effect at 50 µg/mL[P<0.01] than at other test concentrations (25 and 100 µg/mL[P<0.01]) and it also showed significant inhibition of nitric oxide production at this test concentration (50 µg/mL[P<0.01]). This indicated that the observed activity in this test concentration (50 µg/mL) was as a result of cytotoxicity of the fraction (fraction 2) on the Raw 264.7 cells. As a result of this, fraction 2 was not considered for isolation of active compounds. As mentioned in section 3.3.11, fractions 4 to 8 exhibited good anti-inflammatory activity even though they were less effective than the positive control (aminoguanidine). Fractions 6 and 8 were selected for chemical analysis and isolation of active compounds as the fractions (fractions 6 and 8) had the best anti-inflammatory activity and less complex chemical profiles compared to the other active fractions (fractions 4, 5 and 7)

3.3.13 UPLC-QTOF-MS analysis and tentative identification of bioactive compounds from active fraction 6

The active fraction 6 showed the best anti-inflammatory activity and therefore was analyzed using UPLC-QTOF-MS to get an indication of its chemical profile in assisting the targeted purification of the active compounds. Figure 3.19 shows this profile.
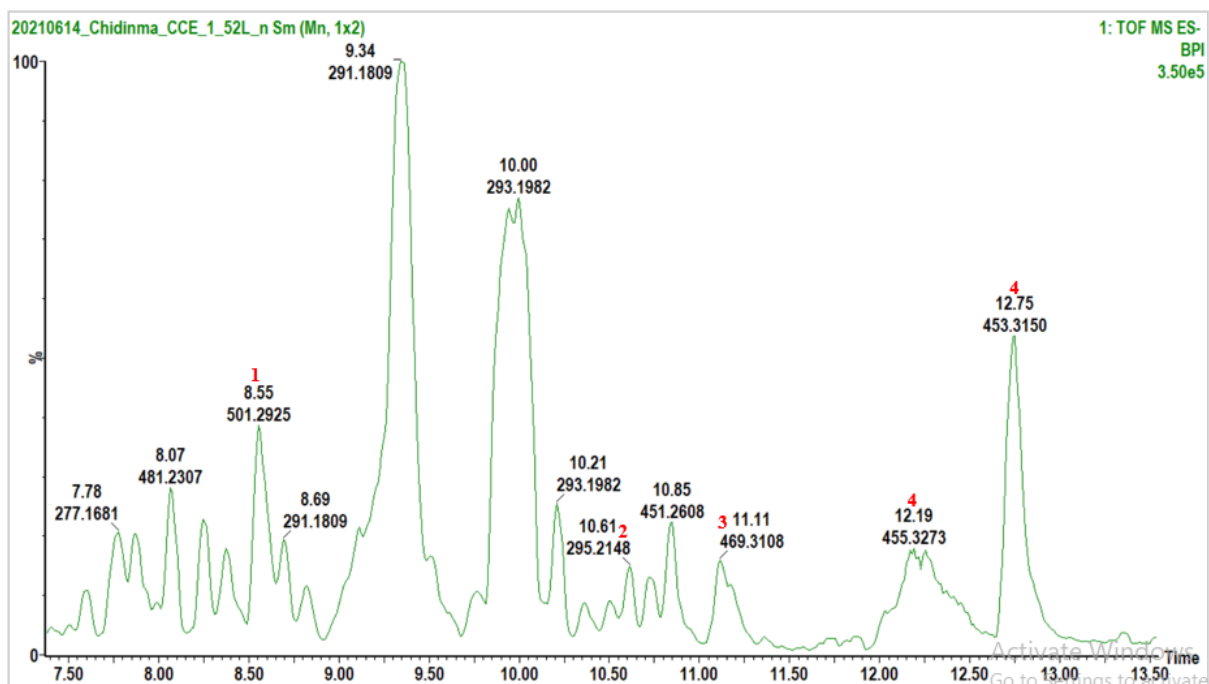
Figure 3.19: ESI negative mode BPI chromatogram of active fraction 6 from the hexane fraction of the ethanol extract (third collection).

The online databases (MetFrag, PubChem, Metlin and Dictionary of Natural Products) were used to tentatively identify the compounds in the active fraction 6 from the hexane fraction of the ethanol extract (figure 3.19). Triterpenoids was the class of compound identified in this active fraction and a total of five compounds were tentatively identified as pomaceic acid, euscaphic acid, hederagenin, 2-isoursolic acid and glycyrrhetaldehyde. Table 3.2 shows accurate mass, formula and MS/MS data for compound fragments tentatively identified from the active fraction 6 from the hexane fraction of the ethanol extract (third collection).

Table 3.2: Compounds tentatively identified from fraction 6 of the hexane fraction using data obtained from UPLC-QTOF-MS analysis

Peak No.	RT (min)	Acquired [M-H]⁻ *m/z*	Formula	Calculated [M-H]⁻ *m/z*	Possible structure	Mass error (ppm)	MS/MS Data (fragments)		Reference
1	8.55	501.3203	$C_{30}H_{46}O_6$	501.3194	pomaceic acid (**Triterpenoid**)	1.8	483.3008	$[M-H]^-H_2O$	[45]
							457.3300	$[M-H]^-CO_2$	
							439.3207	$[M-H]^-CO_2-H_2O$	
							407.3305	$[M-H]^-C_2H_2O_4$	
2	10.60	487.3423	$C_{30}H_{48}O_5$	487.3423	euscaphic acid (**Triterpenoid**)	0.0	469.2981	$[M-H]^-H_2O$	[45, 50]
							453.3150	$[M-H]^-H_2O-O$	
							425.3053	$[M-H]^-H_2O-CO_2$	
							407.3294	$[M-H]^-2H_2O-CO_2$	
3	11.11	471.3372	$C_{30}H_{48}O_4$	471.3318	Hederagenin (**Triterpenoid**)	2.5	457.3438	$[M-H]^-CH_3$	[42, 43]
							427.3481	$[M-H]^-CO_2-H_2$	
							407.3294	$[M-H]^-CO_2-2H_2-H_2O$	
							295.2249	$[M-H]^-7CH_3-CO_2H-2H_2O$	
4	12.19	455.3526	$C_{30}H_{48}O_3$	455.3525	2-isoursolic acid (**Triterpenoid**)	0.2	437.3005	$[M-H]^-H_2O$	[45, 46]
							407.3319	$[M-H]^-HCHO-H_2O$	
							391.3059	$[M-H]^-HCHO-H_2O-CH_4$	
							377.3378	$[M-H]^-HCHO-H_2O-C_2H_6$	
5	12.73	453.3369	$C_{30}H_{46}O_3$	453.3369	glycyrrhetaldehyde (**Triterpenoid**)	0.0	407.3309	$[M-H]^-CHO-H_2O$	[47]
							309.3204	$[M-H]^-CHO-H_2O-O-7CH_3$	
							279.2296	$[M-H]^-CHO-H_2O-O-5CH_3$	

130

The structures of the compounds tentatively identified (peaks 1-5) are shown in figure 3.20.

Pomaceic acid (**57**)

Euscaphic acid (**58**)

Hederagenin (**59**)

131

2-isoursolic acid (**60**)

Glycyyrhetaldehyde (**61**)
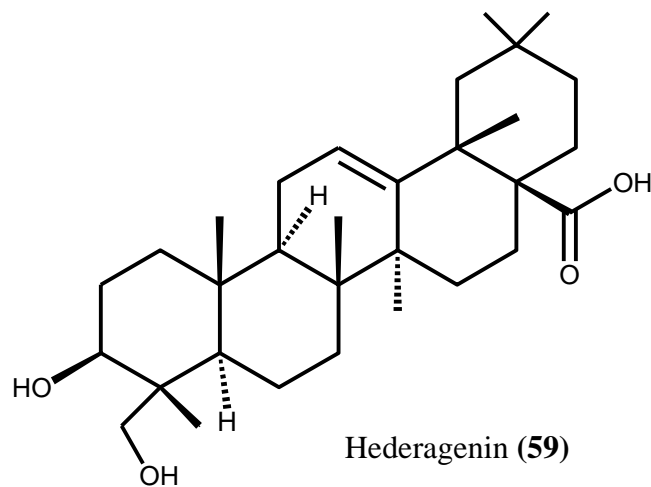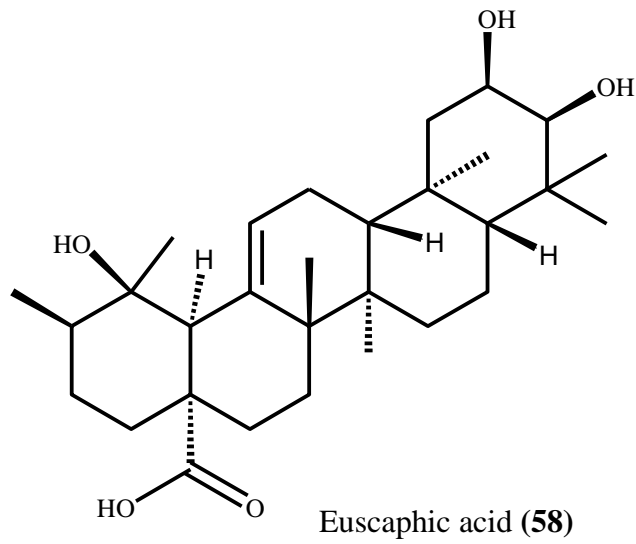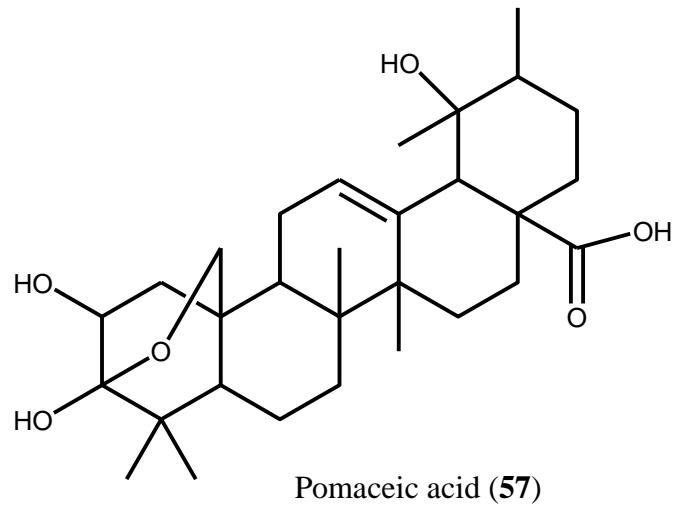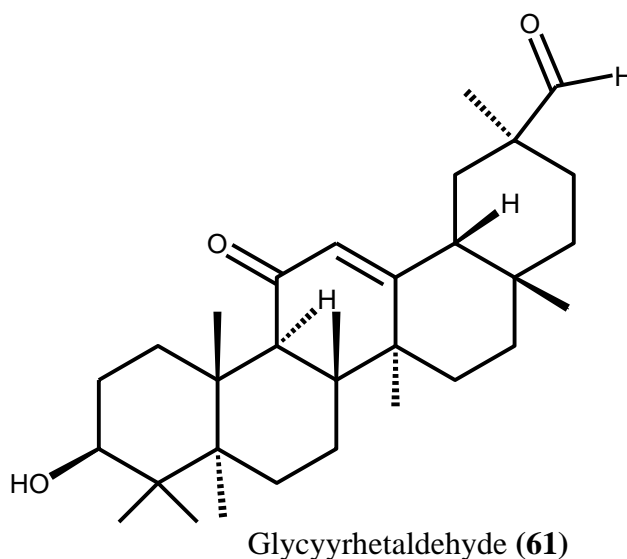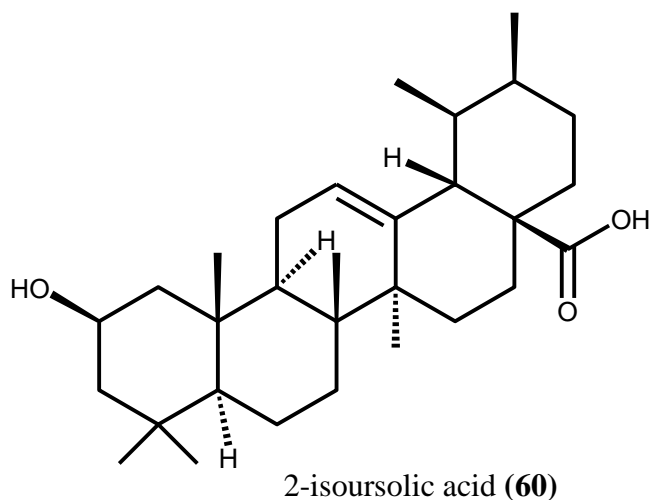
Figure 3.20: Structures of chemical markers tentatively identified.

The peak at *m/z* 501.3203 (Peak 1), at a retention time 8.55 minutes, had a molecular formular $C_{30}H_{45}O_6^-$ with a normalized iFit value of 0.000, which corresponded to the [M-H]⁻ ion. The fragmentation pattern observed was in agreement with that reported for pomaceic acid (**57**).[45] The peak at *m/z* 487.3423 (Peak 2), at a retention time 10.60 minutes, had a molecular formular $C_{30}H_{47}O_5^-$ [M-H]⁻ with a normalized iFit value of 0.000. Analysis of the MS/MS data revealed that the compound was a triterpenoid which matched euscaphic acid (**58**).[50] The compound euscaphic acid is likely to contribute to the anti-inflammatory activity of the active fractions (fractions 4-8) from the hexane fraction of the ethanol extract based on its reported anti-inflammatory activity.[51] The compound corresponding to peak 3 was tentatively identified as hederagenin as described in section 3.3.5. Hederagenin is likely to be one of the compounds contributing to the anti-inflammatory activity of the active fractions (fractions 4-8) from the

132

hexane fraction of the ethanol extract based on its reported anti-inflammatory activity.[52] The compounds corresponding to peaks 4 and 5 were tentatively identified as 2-isoursolic acid and glycyrrhetaldehyde respectively as described in section 3.3.5. 2-isoursolic acid was common in both the ethanol extract and active hexane fraction suggesting that it might possibly be contributing to the anti-inflammatory activity observed in the active fractions (fractions 4-8). Analysis of the UPLC-MS profile of the active fraction 6 tentatively showed that triterpenoid was the likely class of compound contributing to the anti-inflammatory activity and it also suggested the compounds (euscaphic acid, hederagenin and 2-isoursolic acid) that could be contributing to the observed activity. This class of compounds were targeted during the purification of the active fractions (fractions 6 and 8) from the hexane fraction.

3.3.14   Isolation of compounds from the hexane fractions

Fractions 6 and 8 from the silica gel column chromatography of the hexane fraction showed good activity and less complexity of their chemical profiles and were therefore subjected to chromatographic techniques to isolate compounds. Fraction 6 (50 mg) (white solid) from the silica gel column chromatography of the hexane fraction was subjected to purification using silica gel preparative thin layer chromatography (PTLC) and 80:15:5 hexane/dichloromethane/methanol as the mobile phase (isocratic). The detail of the purification is given in section 3.2.2.5 above. The purification resulted to a pure compound (**64**).

Fraction 6 (10 mg) (white solid) from the silica gel column chromatography of the hexane fraction was subjected to purification by washing the solid. The detail of the purification was given in section 3.2.2.6 above. The purification resulted in a pure compound (**65**).

Fraction 8 (100 mg) was subjected to purification using hyphenated liquid chromatography-mass spectrometry-solid phase extraction-nuclear magnetic resonance (LC-MS-SPE-NMR). A total of six subfractions were collected. The subfractions labelled F_8SF_1-F_8SF_6 shown in figure 3.21 were trapped in SPE cartridges through multiple trapping.

133
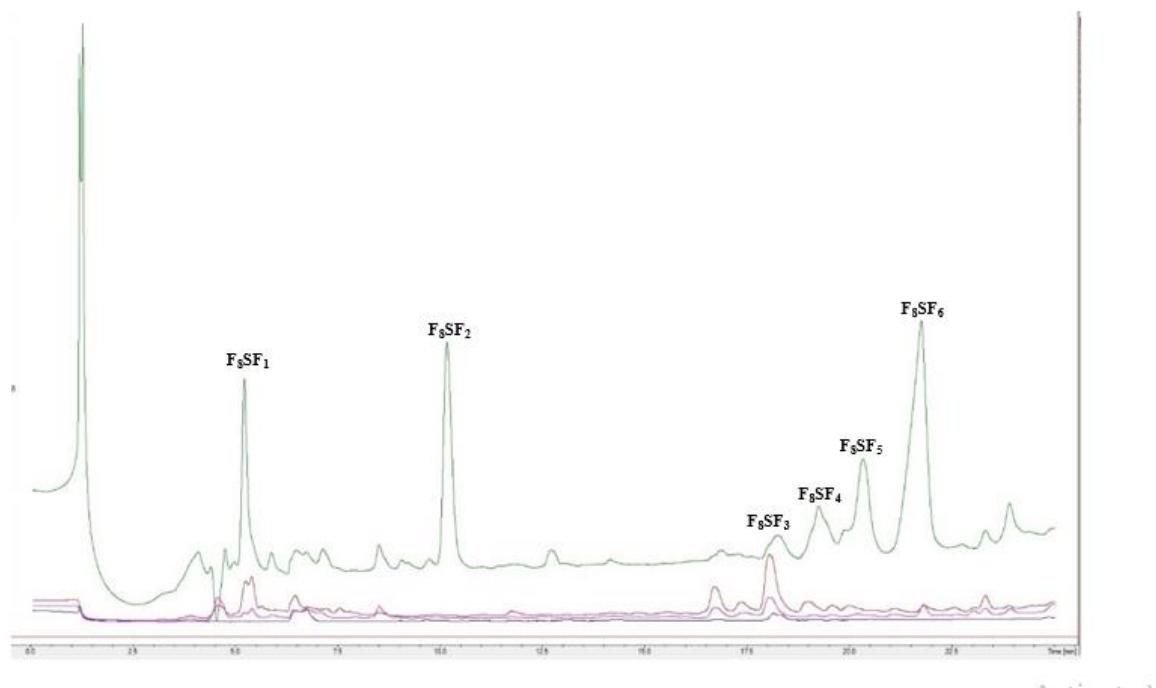
Figure 3.21: LC-UV$_{max}$ plot chromatogram of Fraction 8 from LC-MS-SPE-NMR.

Subfractions F$_8$SF$_4$ and F$_8$SF$_5$ were collected in pure forms (compounds (**66**) and (**67**)) in sufficient quantities of 0.9 mg and 1.5 mg, respectively while the quantity of other subfractions (F$_8$SF$_1$ (0.2 mg), F$_8$SF$_2$ (0.3 mg), F$_8$SF$_3$ (0.2 mg) and F$_8$SF$_6$ (0.4 mg)) were insufficient to be analyzed on NMR.

3.3.15   Structure elucidation of compounds isolated from *S. columbaria*
3.3.15.1 Loganic acid (62)

Compound **62** was isolated as a brown solid and was identified as loganic acid by the interpretation of NMR spectroscopy, mass data and comparison to literature.[53] The molecular formula of the compound is $C_{16}H_{25}O_{10}$ as deduced from its monoprotonated molecular ion at *m/z* 377.1490 [M+H]$^+$ (calculated for $C_{16}H_{25}O_{10}$, *m/z* 377.1448, M+H) based on the QTOF mass spectrum with five degrees of unsaturation. The ^{13}C NMR spectrum had a total of sixteen carbon signals which were assigned as eleven methines (five glucopyranosyl methines at δ_C 99.5, 75.15, 77.97, 74.71, 78.32), two methylene carbons (one oxygenated at δ_C 62.71), one methyl and two quaternary carbons (one carboxylic acid at δ_C 162.67) as deduced from its DEPT 135 spectrum. The methine signal at δ_C 97.51 was assigned to C-1, δ_C 114.56 was assigned to C-4 olefinic carbon, δ_C 162.67 was assigned to C-11 carboxylic acid group, two prominent signals at δ_C 13.45 assigned to C-10 and δ_C 71.55 assigned to C-7 indicated the

134

position of methyl carbon and carbon attached to a hydroxyl group respectively. The ^{1}H NMR spectrum showed the presence of one methyl resonating at δ_H 0.95 (3H, d, J = 6.96 Hz, H-10), two methylene at δ_H 2.09 (2H, dd, J = 8.17, 13.82 Hz, H-6) and 3.75 ({2H, d, J = 11.99 Hz, H-6a'}, 3.51 {2H, dd, J = 5.43, 11.83 Hz, H-6b'}), four methines at δ_H 2.95 (1H, q, J = 7.72 Hz, H-5), 3.22 (1H, m, H-7), 1.73 (1H, m, H-8) and 1.88 (1H, ddd, J = 9.18, 8.94, 4.64 Hz, H-9) and an α, β-unsaturated acetal groups at δ_H 5.29 (1H, d, J = 4.38 Hz, H-1), 7.39 (1H, s, H-3) together with a β-D-glucopyranosyl anomeric proton at δ_H 4.68 (1H, d, J = 7.92 Hz, H-1'). All these assignments confirmed the presence of an iridoid skeleton. One anomeric carbon at δ_C 99.95 was assigned to C-1'. The HMBC correlation between the proton at δ_H 7.39 (H-3) with δ_C 162.67 (C-11) confirmed the position of the carboxylic acid. HMBC correlation also established the point of attachment of the glucopyranosyl moiety to the aglycone based on the correlation between δ_H 5.29 (H-1) to δ_C 99.95 (C-1'). The carbon at δ_C 75.15 (C-2') correlating with δ_H 4.68 (H-1') and 3.05 (H-3'); carbon at δ_C 78.32 (C-5') correlating with δ_H 3.15 (H-4') and 3.75 (H-6') confirmed the presence of a sugar moiety.

There was a COSY correlation between the proton at δ_H 2.95 (H-5) and the proton at δ_H 1.88 (H-9) while another correlation was observed between the proton at δ_H 1.73 (H-8) and another proton at δ_H 0.95 (H-10) indicating that position 5 was adjacent to 9 while 8 was adjacent to 10. The anomeric proton at δ_H 4.68 (H-1') showed a COSY correlation with the proton at δ_H 3.90 (H-2'). The proton at δ_H 3.75 (H-6') also showed a COSY correlation with the proton at δ_H 3.31 (H-5') indicating that position H-1' was adjacent to H-2' while H-5' was adjacent to H-6'. The structure of compound **62** is shown in figure 3.22, and the selected HMBC and COSY correlations are shown in figure 3.23.

Figure 3.22: Chemical structure of loganic acid (**62**).

——— COSY correlation

⟶ HMBC correlation

Figure 3.23: Selected HMBC and COSY correlations of loganic acid (**62**).

The proposed structure was confirmed by comparing the NMR data to the literature data of loganic acid (**62)** (table 3.3).

Table 3.3: ^{1}H (500 MHz), ^{13}C (125 MHz), HMBC and COSY NMR data of Compound (**62**) compared to the literature ^{1}H and ^{13}C NMR data of loganic acid

Position	Isolated loganic acid (CD₃OD)	Published NMR for loganic acid ((DMSO-d₆) (^{1}H, 500 MHz ^{13}C, 125 MHz) [53]	Isolated loganic acid (CD₃OD)	Isolated loganic acid (CD₃OD)

	δ_C	δ_H (m, J in Hz, no of hydrogens)	δ_C	δ_H (m, J in Hz, no of hydrogens)	HMBC correlation	COSY correlation
1	97.51, [CH]	5.29, d, J = 4.38 Hz, 1H	96.48, [CH]	5.09, d, J = 4.90 Hz, 1H	C3, C5, C6, C8, C11, C1'	H9
2						
3	151.76, [CH]	7.39, s, 1H	150.55, [CH]	7.29, s, 1H	C1, C4, C5, C11	H5
4	114.56, [C]		113.05, [C]			
5	32.20, [CH]	2.95, q, J = 7.72 Hz, 1H	31.34, [CH]	2.92, q, J = 7.9 Hz, 1H	C1, C3, C4, C6, C7, C8, C9, C1'	H6, H9
6	42.66, [CH$_2$]	2.09, dd, J = 8.17, 13.82 Hz, 2H	42.21, [CH$_2$]	2.07, dd, J = 13.2, 7.9 Hz, 2H	C4, C5, C10	H7, H5
7	71.55, [CH]	3.22, m, 1H	72.64 [CH]	3.15, dd, J = 9.00 Hz, 8.60 Hz, 1H	C1, C5, C7, C9	H8, H6
8	42.12, [CH]	1.73, m, 1H	40.97, [CH]	1.71, m, 1H	C4, C10, C1'	H10
9	46.49, [CH]	1.88, ddd, J = 9.18, 8.94, 4.68 Hz, 1H	45.20, [CH]	1.81, ddd, J = 8.60, 7.90, 4.90, 1H	C4, C5, C7, C10	H1, H5
10	13.45, [CH$_3$]	0.95, d, J = 6.96 Hz, 3H	14.01, [CH$_3$]	0.98, d, J = 6.80 Hz, 3H		H9, H8
11	162.67, [C]		168.56, [C]			
1'	99.95, [CH]	4.68, d, J = 7.92 Hz, 1H	98.97, [CH]	4.48, d, J = 7.90 Hz, 1H	C2', C3', C4', C5'	H2'
2'	75.15, [CH]	3.90, t, J = 4.60 Hz, 1H	73.61, [CH]	3.88, t, J = 4.70 Hz, 1H	C1, C9 , C2', C3', C4', C5', C6'	
3'	77.97, [CH]	3.05, t, J = 8.12 Hz, 1H	77.22, [CH]	2.97, t, J = 8.60 Hz, 1H	C1, C1', C2', C3', C4', C5', C6'	
4'	74.71, [CH]	3.15, m, 1H	70.54, [CH]	3.05, dd, J = 9.40, 9.00Hz, 1H	C1', C2', C3', C4', C5', C6'	
5'	78.32, [CH]	3.31, m, 1H	77.66, [CH]	3.14, m, 1H	C1, C6'	
6'	62.71, [CH$_2$]	3.75, d, J = 11.99 Hz, 1H 3.51, dd, J = 5.43, 11.83 Hz, 1H	61.60, [CH$_2$]	3.66, d, J = 11.70 Hz, 1H 3.44, dd, J = 11.70 Hz, 6.40 Hz, 1H	C1, C3, C1', C2', C3', C4', C5'	H5'

Loganic acid, a conjugate acid of loganate was previously isolated from the flowering plants of *S. hymettia* [58], *S. atropurpurea* [59] and whole plant of *S. variifolia* [60]. This is the first report on its isolation from *S. columbaria*.

3.3.15.2 Cantleyoside-dimethyl-acetal (63)

Compound **63** was isolated as a brown solid and was identified as cantleyoside-dimethyl-acetal by the interpretation of the NMR spectroscopy, mass data and comparison to literature data.[61] The molecular formula of the compound is $C_{35}H_{53}O_{20}$ as deduced from its monoprotonated molecular ion at *m/z* 793.3092 [M+H]$^+$ (calculated for $C_{33}H_{53}O_{20}$, *m/z* 793.3130, M+H) based on the QTOF mass spectrum with ten degrees of unsaturation. The ^{13}C-NMR spectrum showed the presence of thirty-five carbon signals which were assigned as twenty-two methines (ten glucopyranosyl methines at δ_C 100.13, 74.69, 78.36, 71.56, 78.36, 100.04, 74.59, 77.96, 71.50, 78.36), five methylenes (two oxygenated appearing at one chemical shift δ_C 62.73 and 62.73, one olefinic at δ_C 119.73), four methyls and four quaternary carbons (two carboxylic appearing at one chemical shift δ_C 169.36) as deduced from its DEPT 135 spectrum. The ^{1}H NMR spectrum showed the presence of two anomeric protons at δ_H 4.71 (1H, d, *J* = 7.8 Hz, H-1″) and 4.70 (1H, d, *J* = 7.8 Hz, H-1‴). Additionally, the ^{1}H NMR spectrum showed signals for two olefinic protons at δ_H 7.45 (2H, s, H-3, H-3′), two acetal proton resonances at δ_H 5.22 (1H, m, H-1) and 5.54 (1H, d, *J* = 5.2 Hz, H-1′), a doublet for a secondary methyl group at δ_H 1.10 (3H, d, *J* = 5.6 Hz, H-10), resonances for a terminal vinyl group at δ_H 5.33 (2H, m, H-10′) and δ_H 2.90 (1H, m, H-9′) and signals corresponding to one carbomethoxy group at δ_H 3.71 (3H, s, CH$_3$O-11) and two carbomethoxy groups at δ_H 3.31 (6H, m, CH$_3$O-7′) indicating the presence of an iridoid glucoside unit and a seco-iridoid glucoside unit in the molecule. The spectroscopic features were similar to those of cantleyoside-methyl-hemiacetal except for the replacement of one carbomethoxy group with a hydroxyl group in the ^{1}H NMR spectrum.[62] The chemical shifts of all the individual protons of the two sugar units were ascertained from the ^{1}H NMR data and the ^{13}C NMR chemical shifts of their attached carbons were assigned unambiguously from the HSQC spectrum. These data demonstrated the presence of two terminal β-glucopyranosyl units. In the HMBC spectrum, the proton signals at δ_H 7.45 (H-3), 3.71 (11-O-CH$_3$) and 3.15 (H-5) showed long-range correlation with the carbon resonance at δ_C 169.36 (C-11), while the carbon signals at δ_C 47.02 (C-6′), 53.59 (CH$_3$O-7′) and 52.66 (CH$_3$O-7′) displayed long-range correlation with proton resonances at δ_H 5.77 (H-8′) indicating the location of a methoxy group at C-11 and two methoxy groups at C-7′ respectively. This evidence suggested that compound **63** was made up of a loganin unit and a secologanoside unit. The site of linkage among the two units was confirmed by the HMBC experiment which showed correlations between the proton signals at δ_H 7.45 (H-3′), 5.32 (H-7) and 3.00 (H-5′) and the carbon chemical shift at δ_C 169.36 (C-11′). These data indicated that the C-11′ carboxylic acid group of the secologanoside moiety

was linked to the C-7 hydroxyl group of loganin component. Thus, compound **63** differs from cantleyoside-methyl-hemiacetal reported in *Pterocephalus pinardii* by the replacement of a methoxy group with an OH group at C-7' position. HMBC correlation also established the point of attachment of the two glucopyranosyl moiety to the aglycones based on the correlations between δ_H 4.70 (H-1''') to δ_C 97.75 (C-1) and δ_H 4.71 (H-1'') to δ_C 97.45 (C-1'). There was a COSY correlation between the proton at δ_H 2.15 (H-8) and the proton at δ_H 1.10 (H-10) indicating that position 8 was adjacent to 10.[62] The structure of compound **63** is shown in figure 3.24, and the selected HMBC and COSY correlations are shown in figure 3.25.
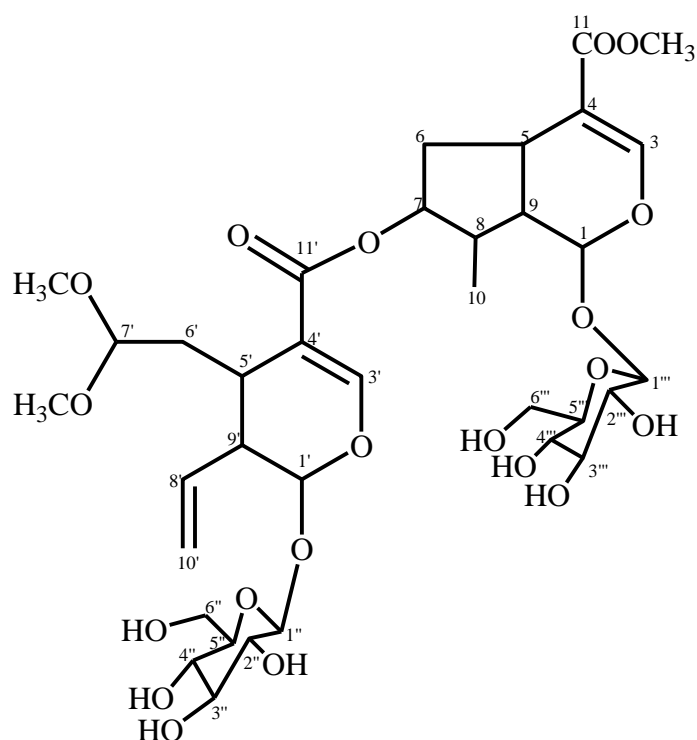
Figure 3.24: Chemical structure of cantleyoside-dimethyl-acetal (**63**).
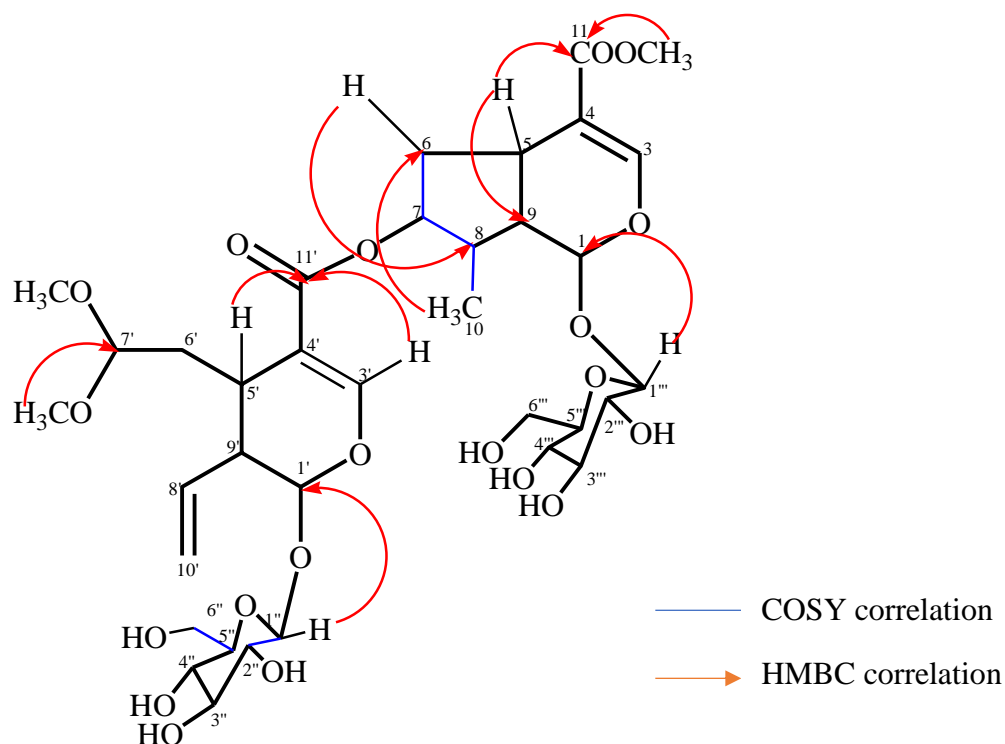
Figure 3.25: Selected HMBC and COSY correlations of cantleyoside-dimethyl-acetal (**63**).

The proposed structure was confirmed by comparing the NMR data to the literature data of cantleyoside-dimethyl-acetal (**63**) (table 3.4).

Table 3.4: ^{1}H (500 MHz), ^{13}C (125 MHz), HMBC and COSY NMR data of Compound (**63**) compared to the literature ^{1}H and ^{13}C NMR data of cantleyoside-dimethyl-acetal

Position	Isolated cantleyoside-dimethyl-acetal (CD₃OD)		Published NMR for cantleyoside-dimethyl acetal ((CD₃OD) (^{1}H, 500 MHz ^{13}C, 125 MHz) [61]		Isolated cantleyoside-dimethyl acetal (CD₃OD)	Isolated cantleyoside-dimethyl acetal (CD₃OD)
	δ$_C$	δ$_H$ (m, *J* in Hz, no of hydrogens)	δ$_C$	δ$_H$ (m, *J* in Hz, no of hydrogens)	HMBC correlation	COSY correlation
1	97.75 [CH]	5.22, m, 1H	98.3 [CH]	5.28, m, 1H		
2						
3	153.24 [CH]	7.45, s, 1H	154.2 [CH]	7.44, s, 1H	C1, C4, C5, C11, C1'	
4	113.25 [C]		114.2 [C]			
5	33.19 [CH]	3.15, m, 1H	33.4 [CH]	3.15, m, 1H	C3, C4, C9, C11	H6

140

Position	δC	δH	δC	δH	HMBC	COSY
6	40.28 [CH₂]	2.33, m, 1H 1.77, m, 1H	41.2 [CH₂]	2.32, m, 1H 1.78, m, 1H	C4, C5, C7, C8, C9, C4'	H6a-H6b
7	78.36 [CH]	5.32, t, J = 3.2 Hz, 1H	79.3 [CH]	5.22, t, J = 3.7 Hz, 1H	C1, C3, C5, C9, C11'	H8, H6
8	40.99 [CH]	2.15, m, 1H	41.9 [CH]	2.05-2.15, m, 1H	C1, C4, C5, C6, C9, C10	H10
9	47.02 [CH]	3.33, m, 1H	47.9 [CH]	2.05-2.15, m, 1H		
10	13.86 [CH₃]	1.10, d, J = 5.6 Hz, 3H	14.7 [CH₃]	1.09, d, J = 6.2 Hz, 3H	C6, C7, C8,	
11	169.36 [C]		170.3 [C]			
CH₃O-11	51.76 [CH₃]	3.71, s, 3H	52.6 [CH₃]	3.72, s, 3H	C11	
1'	97.45 [CH]	5.54, d, J = 5.2 Hz, 1H	98.7 [CH]	5.53, d, J = 5.4 Hz, 1H	C3', C5', C1"	
2'						
3'	152.56 [CH]	7.45, s, 1H	153.4 [CH]	7.46, s, 1H	C4', C5', C11'	H5'
4'	111.96 [C]		112.9 [C]			
5'	29.46 [CH]	3.00, m, 1H	30.4 [CH]	2.93, m, 1H	C1', C4', C9', C11'	
6'	31.8 [CH₂]	2.10, m, 1H 1.68, m, 1H	34.1 [CH₂]	2.05, m, 1H 1.65, m, 1H		
7'	47.02 [CH]	3.33, m, 1H	46.3 [CH]	2.70, m, 1H		
CH₃O-7'	53.59 [CH₃]	3.31, m, 3H	54.5 [CH₃]	3.18-3.40, m, 3H		
CH₃O-7'	52.66 [CH₃]	3.31, m, 3H	53.6 [CH₃]	3.18-3.40, m, 3H		
8'	135.78 [CH]	5.77, m, 1H	136.7 [CH]	5.76, m, 1H	C6', CH₃O-7'	
9'	47.3 [CH]	2.90, m, 1H	46.3	2.70, m, 1H	C1'	
10'	119.73 [CH₂]	5.33, m, 2H	120.7 [CH₂]	5.28, m, 2H	C1', C3', C5', C6', C9'	
11'	169.36 [C]		169.2 [C]			
1"	100.13 [CH]	4.71, d, J = 7.8 Hz, 1H	101.1 [CH]	4.71, d, J = 7.8 Hz, 1H	C1', C2", C3", C4", C5"	H2"
2"	74.69 [CH]	3.33, 3.39, m, 1H	75.5 [CH]	3.18-3.40, m, 1H	C1", C3", C4", C5", C6"	
3"	78.36 [CH]	3.33, 3.39, m, 1H	78.9 [CH]	3.18-3.40, m, 1H	C1", C2", C4", C5", C6"	
4"	71.56 [CH]	3.23, m, 1H	72.5 [CH]	3.18-3.40, m, 1H	C1", C2", C3", C5"	
5"	78.36 [CH]	3.33, 3.39, m, 1H	79.3 [CH]	3.18-3.40, m, 1H	C1", C2", C3", C4", C6"	
6"	62.73 [CH₂]	3.69, m, 1H 3.92, d, J = 11.48 Hz, 1H	63.6 [CH₂]	3.65, m, 1H 3.90, d, J = 11.6 Hz, 1H	C3", C4", C5"	H5", H6a"-H6b"

1'''	100.04 [CH]	4.70, d, J = 7.8 Hz, 1H	101.1 [CH]	4.70, d, J = 7.9 Hz, 1H	C1, C2''', C3''', C4''', C5'''	
2'''	74.59 [CH]	3.39, 3.33, m, 1H	75.5 [CH]	3.18-3.40, m, 1H	C1''', C3''', C4''', C5''', C6'''	
3'''	77.96 [CH]	3.39, 3.33, m, 1H	78.9 [CH]	3.18-3.40, m, 1H	C1''', C2''', C4''', C5''', C6'''	
4'''	71.50 [CH]	3.23, m, 1H	72.5 [CH]	3.18-3.40, m, 1H	C1''', C2''', C3''', C5'''	
5'''	78.36 [CH]	3.39, 3.33, m, 1H	79.3 [CH]	3.18-3.40, m, 1H	C1''', C2''', C3''', C4''', C6'''	
6'''	62.73 [CH$_2$]	3.69, m, 1H 3.92, d, J = 11.48 Hz, 1H	63.6 [CH$_2$]	3.65, m, 1H 3.90, d, J = 11.6 Hz, 1H	C3''', C4''', C5'''	H6a'''-H6b'''

Cantleyoside-dimethyl-acetal was previously isolated from the aerial part of *Scaevola montana* from the tropical Goodinaceae family and was subsequently found to be present in the aerial part of *Pterocephalus perennis* [61], however, this is the first report on its isolation from *S. columbaria*.

3.3.15.3 Ursolic acid (64)

Compound **64** was isolated as a white crystalline solid and was identified as ursolic acid by the interpretation of NMR spectroscopy, mass data and comparison to literature.[63] The molecular formula of the compound is $C_{30}H_{47}O_3$ as deduced from its monoprotonated molecular ion at *m/z* 455.3546 [M+H]$^+$ (calculated for $C_{30}H_{47}O_3$, *m/z* 455.3525, M+H) based on the QTOF mass spectrum with seven degrees of unsaturation. ^{13}C NMR spectrum had a total of thirty signals and the assignments were done together with DEPT 135 spectra. It consisted of seven methines (one oxygenated at δ_C 79.18), nine methylenes, seven methyls and seven quaternary carbons (one carboxylic at δ_C 180.28). Three signals at δ_C 180.28 (C-28), 138.09 (C-13) and 126.04 (C-12) were identified for carboxylic and olefinic function moieties based on their chemical shifts. One signal at δ_C 79.18 (C-3) indicated the presence of carbinol carbon based on its downfield chemical shift. Apart from one carboxylic and one olefinic group, the other elements of unsaturation were attributed to five rings suggesting a pentacyclic triterpenoid. The ^{1}H NMR spectrum revealed the presence of seven methyl groups at δ_H 0.80-0.95 (3H, s, H-24), 0.80-0.95 (3H, s, H-25), 0.82-0.89 (3H, s, H-26), 0.82-0.89 (3H, d, J = 6.30 Hz, H-29), 0.97 (3H, d, J = 12.04 Hz, H-30), 1.11 (3H, s, H-27), 1.01 (3H, s, H-23), an olefinic methine group at δ_H 5.28 (1H, t, H-12), and oxygenated methine group at δ_H 3.24 (1H, dd, J = 11.19, 4.80 Hz, H-3). In addition, one proton resonance at δ_H 2.20-2.22 (1H, d, J = 11.78 Hz, H-18) from one

methine group was seen. Several protons for methylene and methine groups overlap in the range between 0.76 and 1.95. The ursane-12- skeleton of compound **64** was established by the characteristic ^{1}H NMR signals of the two doublet methyl protons for 29-H and 30-H at 0.82-0.89 (3H, d, J = 6.30 Hz) and 0.97 (3H, d, J = 12.04 Hz), the 12-H vinyl proton at 5.28 (t), and the doublet methine proton (for 18-H) at 2.20-2.22 (1H, d, J = 11.78 Hz). In the HMBC spectrum, the methyl hydrogens at δ_H 0.80-0.95 (H-25) showed correlations with the methylene carbon at δ_C 38.76 (C-1), methine carbons at δ_C 79.18 (C-3),55.45 (C-5) and 47.69 (C-9), methyl carbons at δ_C 28.29 (C-23) and 15.63 (C-24) and quaternary carbons at δ_C 39.63 (C-8) and 39.22 (C-10), thus structural unit (a) was proposed. The HMBC correlations were also observed between the methyl hydrogens at δ_H 1.01 (H-23) and 0.80-0.95 (H-24) with the methine carbons at δ_C 79.18 (C-3), 55.45 (C-5), 47.69 (C-9), methyl carbon at δ_C 28.29 (C-23) and quaternary carbon at δ_C 39.22 (C-10). This indicated that the two methyl groups at positions 23 and 24 are attached to the quaternary carbon at position 4. The chemical shift of the methine carbon at δ_C 79.18 indicated that a hydroxyl group is attached to it. Therefore, this accounted for one hydroxyl group. These HMBC correlations supported the closure of ring A. This was further supported by the COSY correlations between the methine hydrogen at δ_H 3.24 (H-3) and the methylene hydrogen at δ_H 1.64 (H-2) indicating that position 2 was adjacent to position 3. HMBC correlations were observed between methylene hydrogen at δ_H 1.68-1.95 (H-11) and quaternary carbons at δ_C 39.63 (C-8), 138.09 (C-13) and methine carbons at δ_C 47.69 (C-9) and 126.04 (C-12). These correlations suggested an extension of ring (a) to (b), and it was further supported by the COSY correlations where the methine hydrogen at δ_H 0.74-0.76 (H-5) showed correlations with the methylene hydrogen at δ_H 1.56 (H-6). In addition, the methylene hydrogen (H-6) showed a correlation with another methylene hydrogen at δ_H 1.69-1.78 (H-7). HMBC correlations were observed between the methyl group at δ_H 1.11 (H-27) with the quaternary carbons at δ_C 39.63 (C-8), 138.09 (C-13), 42.19 (C-14) and methylene carbon at δ_C 30.75 (C-15). These correlations accounted for the extension of structural unit (b) to (c) as well as suggested the assignment of the methyl group at position 27. The extension of structural unit (d) to (e) was sorted in a similar manner where quaternary carbon at δ_C 138.09 (C-13) showed HMBC correlation with the methine hydrogens at δ_H 2.20-2.22 (H-18) and 1.07-1.36 (H-19 and 20). The HMBC correlations between the methyl hydrogen at δ_H 0.82-0.89 (H-29) and methine carbons at δ_C 52.97 (C-18), 38.91 (C-19) and 38.98 (C-20) as well as the methylene carbons at δ_C 28.16 (C-21) and 33.13 (C-22) assisted in the assignment of the methyl group at 29 position. In addition, the HMBC correlations between the methyl group at δ_H 0.97 (H-30) and the methine carbons at δ_C 38.91 (C-19) and 38.98 (C-20) also suggested the assignment of

143

the methyl group at position 30. These HMBC correlations supported the closure of ring (e). The assignment of the carboxylic acid at position 28 was suggested by the HMBC correlation between the methylene hydrogen at δ_H 1.68-1.95 (H-16) and the quaternary carbon at δ_C 180.28 (C-28). The structure of compound **64** is shown in figure 3.26, and the selected HMBC and COSY correlations are shown in figure 3.27.
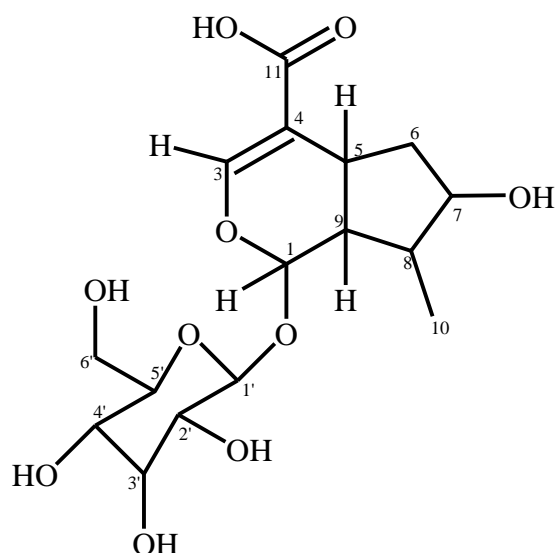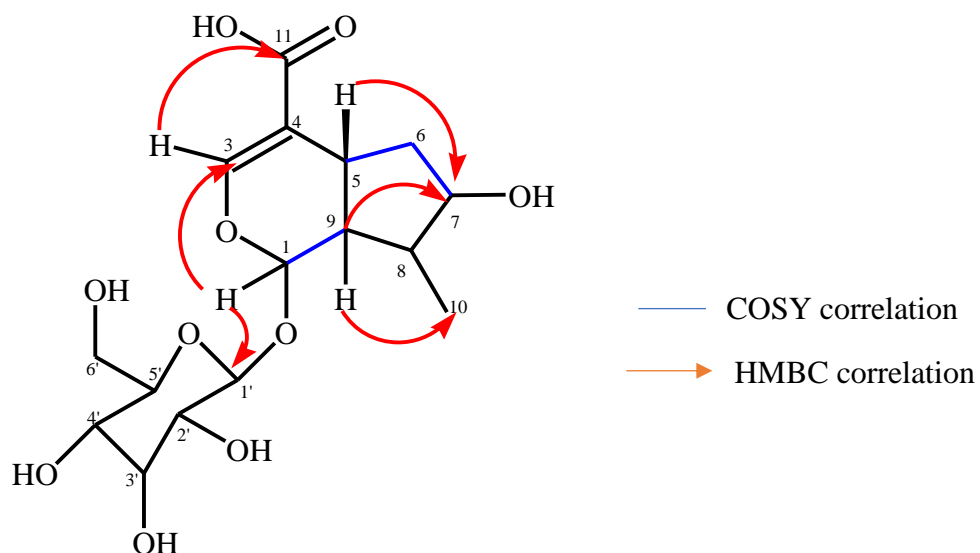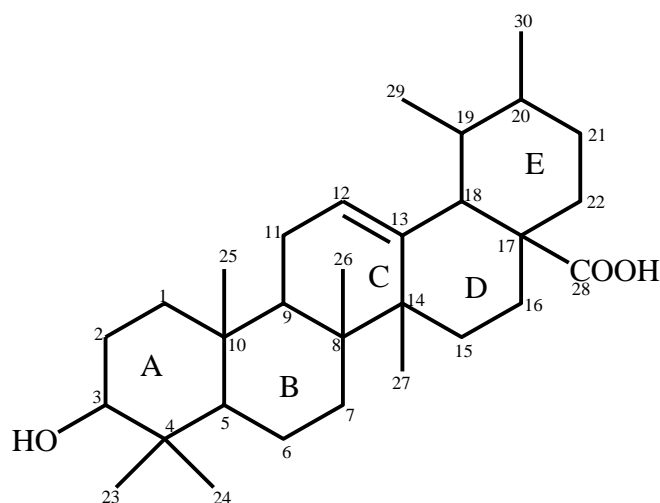

Figure 3.26: Chemical structure of ursolic acid (64).
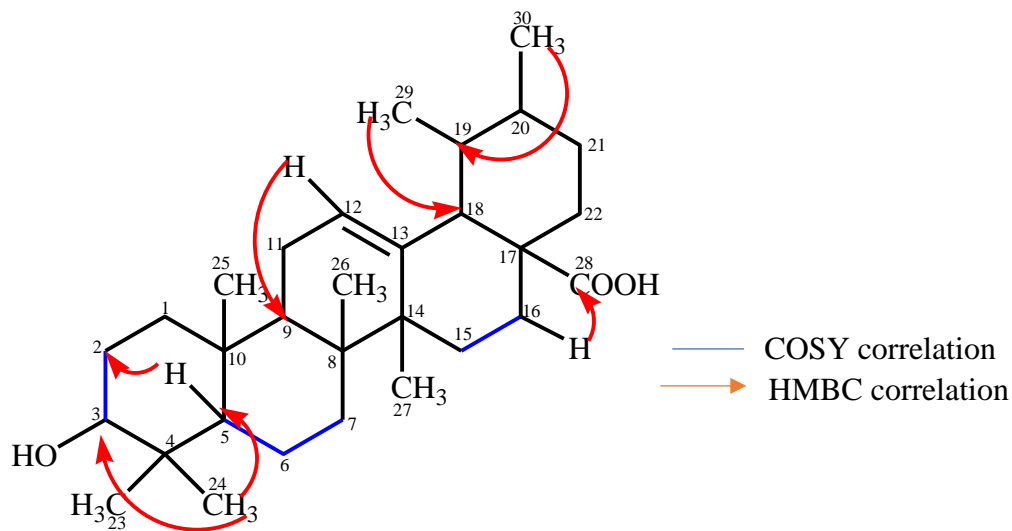
Figure 3.27: Selected HMBC and COSY correlations of ursolic acid (64).

The proposed structure was confirmed by comparing the NMR data to the literature data of ursolic acid (**64**) (table 3.5).

Table 3.5: ^{1}H (500 MHz), ^{13}C (125 MHz), HMBC, and COSY NMR data of Compound (**64**) compared to the literature ^{1}H and ^{13}C NMR data of ursolic acid

Position	Isolated ursolic acid (CDCl$_3$)		Published NMR for ursolic acid ((Pyridine-d_5) (^{1}H, 500 MHz ^{13}C, 125 MHz) [63]		Isolated ursolic acid (CDCl$_3$)	Isolated ursolic acid (CDCl$_3$)
	δ$_C$	δ$_H$ (m, J in Hz, no of hydrogens)	δ$_C$	δ$_H$ (m, J in Hz, no of hydrogens)	HMBC correlation	COSY correlation
1	38.76, CH$_2$	1.68, m, 2H	39.2, CH$_2$	1.58, 1.00, 2H		
2	27.38, CH$_2$	1.64, m, 2H	28.2, CH$_2$	1.81, 1.81, 2H	C1	
3	79.18, CH	3.24, dd J =11.19 4.8 Hz, 1H	78.2, CH	3.44, dd, 1H	C24, C25	H2
4	37.14, C		39.6, C			
5	55.45, CH	0.76, 0.74, m, 1H	55.9, CH	0.88, d, 1H	C2, C3, C4, C8, C9, C24, C25	
6	18.45, CH$_2$	1.56, m, 2H	18.8, CH$_2$	1.58, 1.39, 2H		H5
7	36.83, CH$_2$	1.78, 1.75, 1.69, m, 2H	33.7, CH$_2$	1.59, 1.39, 2H		H6
8	39.63, C		40.1, C			
9	47.69, CH	1.53, m, 1H	48.1, CH	1.65, 1H	C4, C26	
10	39.22, C		37.5, C			
11	23.44, CH$_2$	1.95, 1.68, 1.70, m, 2H	23.7, CH$_2$	1.96, 2H	C8, C9, C12, C13	
12	126.04, CH	5.28, t, 1H	125.7, CH	5.49, s, 1H	C9, C11, C14, C18	
13	138.09, C		139.3, C			
14	42.19, C		42.6, C			

145

15	30.75, CH$_2$	1.28, t, 2H	28.8, CH$_2$	1.22, 2.33 t, 2H	C11	H16
16	24.36, CH$_2$	1.95, 1.68, 1.70, t, 2H	23.8, CH$_2$	2.14 t, 2.01, 2H	C28	
17	48.04, C		48.1, C			
18	52.97, CH	2.22, 2.20, d, J = 11.78 Hz, 1H	53.6, CH	2.63, d, 1H	C13	H22
19	38.91, CH	1.36, 1.07, m, 1H	39.5, CH	1.49, 1H	C13, C30	
20	38.98, CH	1.36, 1.07, m, 1H	39.4, CH	1.05, 1H	C13, C30	
21	28.16, CH$_2$	1.14, m, 2H	31.1, CH$_2$	1.40, 1.49, 2H		
22	33.13, CH$_2$	1.36, 1.34, m, 2H	37.4, CH$_2$	1.97, 2H		
23	28.29, CH$_3$	1.01, s, 3H	28.8, CH$_3$	1.24, s, 3H	C3, C5, C9, C10, C24	
24	15.63, CH$_3$	0.95, 0.80, s, 3H	16.5, CH$_3$	1.02, s, 3H	C3, C5, C9, C10, C23, C25, C27	
25	15.74, CH$_3$	0.95, 0.80, s, 3H	15.7, CH$_3$	0.92, s, 3H	C1, C3, C5, C8, C9, C10, C23, C27	
26	17.22, CH$_3$	0.89, 0.82, s, 3H	17.5, CH$_3$	1.06, s, 3H	C23, C25, C27	
27	23.70, CH$_3$	1.11, s, 3H	24.0, CH$_3$	1.24, s, 3H	C8, C13, C14, C15	
28	180.28, C		179.7, C			
29	17.13, CH$_3$	0.89, 0.82, d J = 6.30 Hz, 3H	17.5, CH$_3$	1.02, d, 3H	C18, C19, C20, C21, C22	
30	21.31, CH$_3$	0.97, d, J = 12.04 Hz, 3H	21.4, CH$_3$	0.97, d, 3H	C19, C20	

Ursolic acid, a natural pentacyclic triterpenoid was previously isolated from the whole plant of

S. stellata.[1] It is a common compound present in different plant species eg, it has been isolated

146

from the leaves of *A. scholaris* [65], *O. lamiifolium* [66] and *O. gratissimum* [67], however, this is the first report of its isolation from *S. columbaria*.

3.3.15.4 2-Isoursolic acid (65)

Compound **65** was isolated as a white crystalline solid and was identified as 2-isoursolic acid by the interpretation of NMR spectroscopy, mass data and comparison to literature.[68] The molecular formula of the compound is $C_{30}H_{47}O_3$ as deduced from its monoprotonated molecular ion at *m/z* 457.3727 [M+H]$^+$ (calculated for $C_{30}H_{47}O_3$, *m/z* 457.3682, M+H) based on the QTOF mass spectrum with seven degrees of unsaturation. The ^{13}C NMR spectrum had a total of thirty signals assigned to seven methines (one oxygenated methine at δ_C 76.85), nine methylene, seven methyl and seven quaternary carbons (one carboxylic acid at δ_C 178.6) as deduced from DEPT 135 spectra. Three signals at δ_C 178.6 (C-28), 138.26 (C-13) and 124.57 (C-12) were identified for carboxylic and olefinic function moieties based on their chemical shifts. Apart from one carboxylic acid and one olefinic moiety, the remaining elements of unsaturation were attributed to five ring system. The ^{1}H NMR spectrum of this compound revealed signals for seven singlet methyl at δ_H 0.69 (3H, s, H-24), 0.77-0.82 (3H, s, H-25), 0.77-0.82 (3H, d, *J* = 6.40 Hz, H-29), 0.87 (3H, s, H-30), 0.90 (3H, s, H-23), 0.92 (3H, s, H-26), 1.05 (3H, s, H-27), one oxygenated methine group at δ_H 3.01 (1H, m, H-2), the presence of an olefinic methine group at δ_H 5.12 (1H, t, H-12) and a proton resonance at δ_H 2.10 (1H, d, *J* = 11.55 Hz, H-18) for a methine group. Several proton resonances for methylenes and methyls are embedded in the overlapping range between 0.68 and 1.86. The HMBC correlations between the methyl hydrogens at δ_H 0.90 (H-23) and 0.69 (H-24) and the methylene carbon at δ_C 38.43 (C-1) and methine carbons at δ_C 76.85 (C-2) and 54.77 (C-5), suggested the presence of structural unit (a). This indicated that the two methyl groups at positions 23 and 24 are likely to be attached to the quaternary carbon at position 4. HMBC correlations were further observed between methyl hydrogen at δ_H 0.77-0.82 (H-25) and methylene carbons at δ_C 38.43 (C-1). The chemical shift of the methine carbon at δ_C 76.85 (C-2) indicated that a hydroxyl group is attached to it. Therefore, it accounted for one hydroxyl group. In addition, HMBC correlations were observed between methine carbon at δ_C 54.77 (C-5) and methylene hydrogens at δ_H 1.28-1.45 (H-3), methyl hydrogens δ_H at 0.90 (H-23) and 0.69 (H-24). These HMBC correlations supported the closure of ring (a). This was further supported by the COSY correlations between the methylene hydrogen at δ_H 1.53 (H-1) and the methine hydrogen at δ_H 3.01 (H-2) while the methine hydrogen (H-2) showed COSY

correlation with the methylene hydrogen at δ_H 1.28-1.95 (H-3) indicating that position 1 was adjacent to 2 while 2 was adjacent to 3. HMBC correlations were observed between the methylene carbon at δ_C 38.43 (C-1) and the methylene hydrogen at δ_H 1.31-1.47 (H-6). This correlation is a weak one as it is a 4J correlation. This correlation supported the extension of ring (a) to (b). The methine carbon at δ_C 47.04 (C-9) showed HMBC correlation with the methylene hydrogens at δ_H 1.29-1.57 (H-7), 1.00 (H-11), methine hydrogen at δ_H 5.12 (H-12) and methyl hydrogen at δ_H 0.77-0.82 (H-25). These correlations accounted for the extension of structural unit (b) to (c).

HMBC correlations were observed between methyl hydrogen at δ_H 0.77-0.82 (H-25) with methylene carbons at δ_C 38.43 (C-1) as well as the methine carbon at δ_C 47.09 (C-9). These correlations suggested the assignment of the methyl group at position 25. The extension of structural unit (c) to (d) to (e) was sorted in a similar manner where quaternary carbon at δ_C 41.68 (C-14) showed HMBC correlations with the methine hydrogens at δ_H 1.47-1.86 (H-9), 5.12 (H-12), 2.10 (H-18), methylene hydrogens at δ_H 0.92 (H-15), 1.53 (H-16) and the methyl hydrogen at δ_H 1.05 (H-27). The HMBC correlations between the quaternary carbon at δ_C 178.6 (C-28) and the methine hydrogen at δ_H 2.10 (H-18) assisted in the assignment of the carboxylic acid at position 28. Additionally, the HMBC correlations between the methyl carbon at δ_C 17.09 (C-29) and the methine hydrogens at δ_H 2.10 (H-18), 0.93 (H-19) and 0.83-1.32 (H-20) suggested the assignment of two methyl groups at positions 29 and 30. This was further supported by the COSY correlations between the methine hydrogen at δ_H 0.83-1.32 (H-20) and the methyl hydrogens at δ_H 0.77-0.82 (H-29) and 0.87 (H-30).

A big difference in chemical shift was observed in the C-2 resonance of compound **65**(δ_c 76.85 observed in the study and δ_c 66.90 published value) and this can be attributed to the influence on solvent type, solvent concentration and temperature at the time of the analysis.

The only difference between compounds **64** and **65** was that while the former has a hydroxyl group attached at position C-3, the hydroxyl group was attached at position C-2 on the latter which accounts for the multiplicity of multiplet observed for the methine hydrogen at position 2 which is between two methylene hydrogens (H-1) and (H-3). The structure of compound **65** is shown in figure 3.28, and the selected HMBC and COSY correlations are shown in figure 3.29.
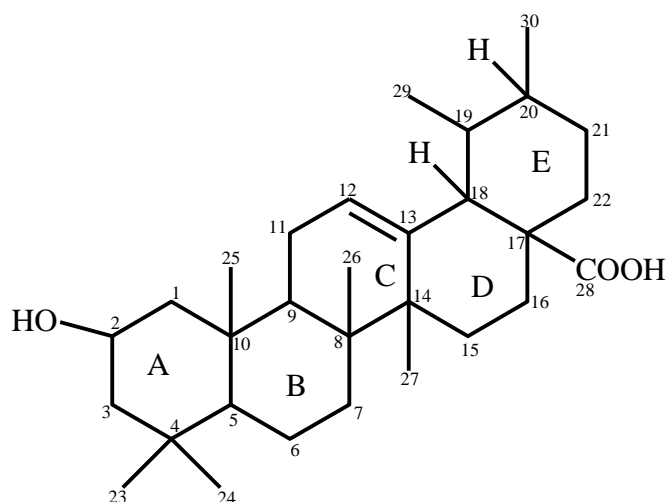
Figure 3.28: Chemical structure of 2-isoursolic acid (**65**).

COSY correlation
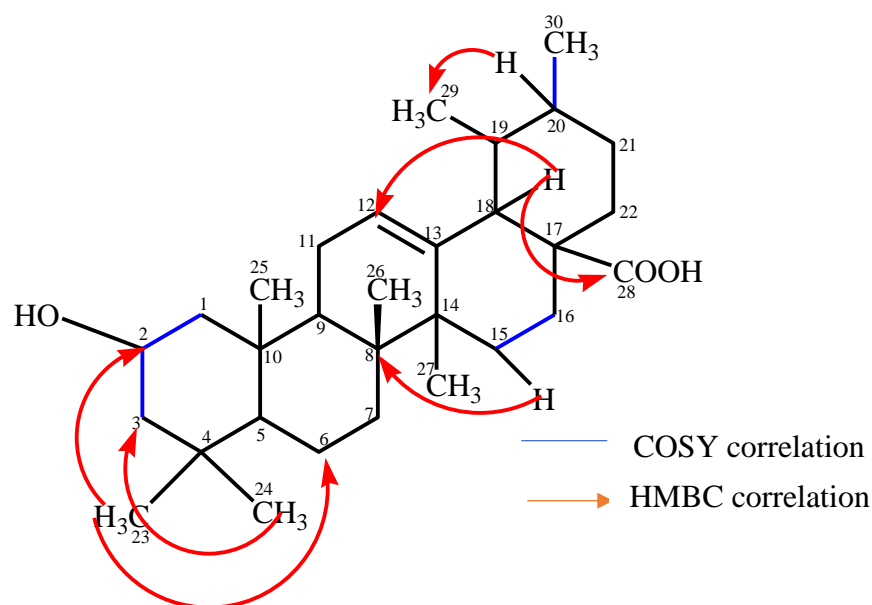
HMBC correlation

Figure 3.29: Selected HMBC and COSY correlation of 2-isoursolic acid (**65**).

The proposed structure was confirmed by comparing the NMR data to the literature data of 2-Isoursolic acid (**65**) (table 3.6).

Table 3.6: ^{1}H (500 MHz), ^{13}C (125 MHz), HMBC, and COSY NMR data of Compound (**65**) compared to the literature ^{1}H and ^{13}C NMR data of 2-Isoursolic acid

Position	Isolated 2-Isoursolic acid (DMSO-d₆)	Published NMR for 2-Isoursolic acid (Pyridine d_5) (^{1}H, 500 MHz ^{13}C, 125 MHz) [68]	Isolated 2-Isoursolic acid (DMSO-d₆)	Isolated 2-Isoursolic acid (DMSO-d₆)

	δ_C	δ_H (m, *J* in Hz, no of hydrogens)	δ_C	δ_H (m, *J* in Hz, no of hydrogens)	HMBC correlation	COSY correlation
1	38.43, [CH$_2$]	1.53, m, 2H	40.4		C2	H2
2	76.85, [CH]	3.01, m, 1H	66.9, [CH]			H3, H1
3	32.73, [CH$_2$]	1.28-1.45, m, 2H	37.5		C2, C5, C6	H2
4	-[C] (chemical shift possibly in the region of the solvent peak)		-[C] (not reported)			
5	54.77, [CH]	0.68, s, 1H	54.8			
6	18.04, [CH$_2$]	1.31-1.47, m, 2H	18.4		C1, C7, C9, C24	
7	36.57, [CH$_2$]	1.29, 1.53-1.57, m, 2H	39.5		C9	H9, H26
8	38.24, [C]		39.6			
9	47.04, [CH]	1.47-1.86, m, 1H	48.6		C10, C11, C14, C16, C25, C27	H12, H26, H27
10	36.36, [C]		38.0			
11	27.57, [CH$_2$]	1.00, m, 2H	33.0		C9	
12	124.57, [CH]	5.12, t, 1H	126.0, [CH]	5.28, brs, 1H	C9, C14, C18	
13	138.26, [C]		139.3			
14	41.68, [C]		47.8			
15	30.23, [CH$_2$]	0.92, 1.27, 1.44, 1.54, m, 2H	33.8		C8, C9, C14, C16	
16	23.84, [CH$_2$]	1.53, m, 2H	28.7		C14	H15
17	46.86, [C]		48.2			
18	52.41, [CH]	2.10, d, *J* = 1.55, 1H	53.8		C12, C13, C14, C16, C17, C20, C28, C29	
19	38.47, [CH]	0.93, s, 1H	42.9		C15, C16, C17, C20, C29	
20	38.55, [CH]	0.83, 1.32, m, 1H	47.7		C12, C16, C18, C19, C28, C29	H29, H30
21	22.89, [CH$_2$]	1.05, m, 2H	24.8		C13	
22	27.03, [CH$_2$]	1.45, m, 2H	31.2			
23	28.30, [CH$_3$]	0.90, s, 3H	33.5, [CH$_3$]	0.99, s, 3H	C1, C2, C5, C6, C10, C24	

150

24	16.15, [CH$_3$]	0.69, s, 3H	19.3, [CH$_3$]	0.79, s, 3H	C1, C2, C3, C5, C8, C23, C25	
25	16.97, [CH$_3$]	0.77-0.82, s, 3H	21.4, [CH$_3$]	0.92, s, 3H	C1, C3, C9, C14, C23, C24, C26	
26	21.16, [CH$_3$]	0.92, s, 3H	24.0, [CH$_3$]	0.92, s, 3H	C25	
27	23.32, [CH$_3$]	1.05, s, 3H	25.1, [CH$_3$]	1.25, s, 3H	C11, C14, C26	
28	178.6, [C]		179.9			
29	17.09, [CH$_3$]	0.77-0.82, d, $J = 6.40$ Hz, 3H	23.9, [CH$_3$]	0.87, s, 3H	C17	
30	15.28, [CH$_3$]	0.87, s, 3H	17.6, [CH$_3$]	0.85, s, 3H		

2-isoursolic acid is an isomer of a natural pentacyclic triterpenoid ursolic acid. It has not been reported from a plant species. It was first synthesized through a novel one pot conversion of 2,3-dihydroxytriterpene to 3-deoxy-2-oxotriterpenes[63].This is the first report of its isolation from *S. columbaria*.

3.3.15.5   24-nor-2α,3β-dihydroxyolean-4(23)-12-ene (66)

Compound **66** was isolated as a white crystalline solid and was identified as 24-nor-2α,3β-dihydroxyolean-4(23)-12-ene by the interpretation of NMR spectroscopy, mass data and comparison to literature.[69] The molecular formula of the compound is $C_{29}H_{45}O_2$ as deduced from its monoprotonated molecular ion at *m/z* 425.3482 [M-H]$^-$ (calculated for $C_{29}H_{45}O_2$, *m/z* 425.3420, M-H) based on the QTOF mass spectrum with seven degrees of unsaturation. ^{13}C NMR spectrum had a total of twenty-nine signals and the assignments were done together with DEPT 135 spectra. It consists of six methine carbons (two oxygenated methines at δ_C 73.66 and 79.16), ten methylene (one exocyclic methylene at δ_C 104.72), six methyl carbons and seven quaternary carbons. All these resonances accounted for a partial molecular formula $C_{29}H_{43}$. The four sp^2 carbons (δ_C 149.55, 104.72, 125.96 and 138.45,) attributable to C-4, C-23, C-12 and C-13 positions respectively indicated two double bond functionality which accounts for two degrees of unsaturation. This suggested that the compound contained five rings. ^{13}C NMR spectrum confirmed the existence of two methine carbons attached to hydroxyl groups (δ_C 73.66 and 79.16) attributable to the C-2 and C-3 positions based on their chemical shifts. The ^{1}H NMR spectrum revealed the presence of six singlet methyl groups at δ_H 0.97-1.37 (3H, s, H-29), 1.14 (3H, s, H-27), 0.98 (3H, s, H-26), 0.89 (3H, s, H-25), 0.89 (3H, s, H-

28) and 0.81 (3H, s, H-24), an olefinic methine group at δ_H 5.32 (1H, s, H-12), an exocyclic methylene group with protons at δ_H 5.17 (1H, s, H-23a) and 4.77 (1H, s, H-23b), two oxygenated methine groups with protons at δ_H 3.56 (1H, m, H-2) and 3.87 (1H, d, J = 8.54 Hz, H-3). In addition, one resonance at δ_H 1.71 (1H, m, H-5) from one methine group was seen. Several protons for methylene and methine overlap in the range between δ_H 1.54 and 2.10. In the HMBC spectrum, the exocyclic methylene hydrogens at δ_H 4.77 and 5.17 (H-23) showed correlations with the methine carbons at δ_C 50.37 (C-5) and 79.16 (C-3). This confirmed the presence of an exocyclic methylene group at the 23 position and thus the structural unit (a) was proposed. The structural unit (a) was confirmed by the long-range HMBC correlations of the methyl hydrogen at δ_H 0.81 (H-24) with methylene carbon at δ_C 46.65 (C-1), methine carbon at δ_C 50.37 (C-5) and the quaternary carbon at δ_C 42.47 (C-10). This was further supported by the COSY correlations between one of the exocyclic methylene protons at δ_H 5.17 (H-23a) and the other methylene proton at δ_H 4.77 (H-23b) as well as the methine protons at δ_H 1.71 (H-5) and 3.87 (H-3). The COSY correlations between methylene proton at δ_H 2.10 (H-1) and methine proton at δ_H 3.56 (H-2) and the correlation between methine proton at δ_H 3.56 (H-2) and another methine proton at δ_H 3.87 (H-3) confirmed the presence of the methine proton at δ_H 3.56 (H-2) in ring (a). The extension of structural unit (a) to (b) was sorted out similarly by the long-range correlations in the HMBC spectrum where the methyl hydrogen at δ_H 0.81 (H-24) showed contour peaks with the methine carbon at δ_C 45.03 (C-9) and another quaternary carbon at δ_C 42.47 (C-10). COSY correlation between methylene proton at δ_H 1.72-2.06 (H-11) and methine proton at δ_H 5.32 (H-12) was observed confirming that they were beside each other. This information gave an extension of structural unit (b) to (c). The extension of structural unit (c) to (d) was seen in the HMBC correlation of methine proton at δ_H 2.22-2.25 (H-18) to the quaternary carbon at δ_C 39.20 (C-14) and the HMBC correlations between the methyl proton at δ_H 0.98 (H-26) to methylene carbon at δ_C 31.60 (C-15). This also confirmed the position of the methyl proton at the 26 positions. The confirmation of the methyl group at the 27 position was confirmed by the long-range HMBC correlations of the methyl group at δ_H 1.14 (H-27) to the quaternary carbons at δ_C 138.45 (C-13) and 38.78 (C-17) and to the methylene carbon at δ_C 20.94 (C-21). It also gave an extension of (d) to (e). The HMBC correlations between the methylene protons at δ_H 0.98-1.54 (H-21) and 1.47 (H-19) and the methyl carbon at δ_C 17.25 (C-28); and the correlations between the two methyl protons at δ_H 1.14 (H-27) and 0.89 (H-28) and the methylene proton at δ_H 0.98-1.54 (H-21) with the methyl carbon at δ_C 38.98 (C-29) assisted in the assignment of the two methyl groups in the 28 and 29 positions. A big difference in chemical shift was observed in the C-22 resonance of compound

66 (δ_c 31.60 observed in the study and δ_c 46.80 published value). The plausible reason is mentioned above.

The structure of compound **66** is shown in figure 3.30, and the selected HMBC and COSY correlations are shown in figure 3.31.

Figure 3.30: Chemical structure of 24-nor-2α,3β-dihydroxyolean-4(23)-12-ene (**66**).
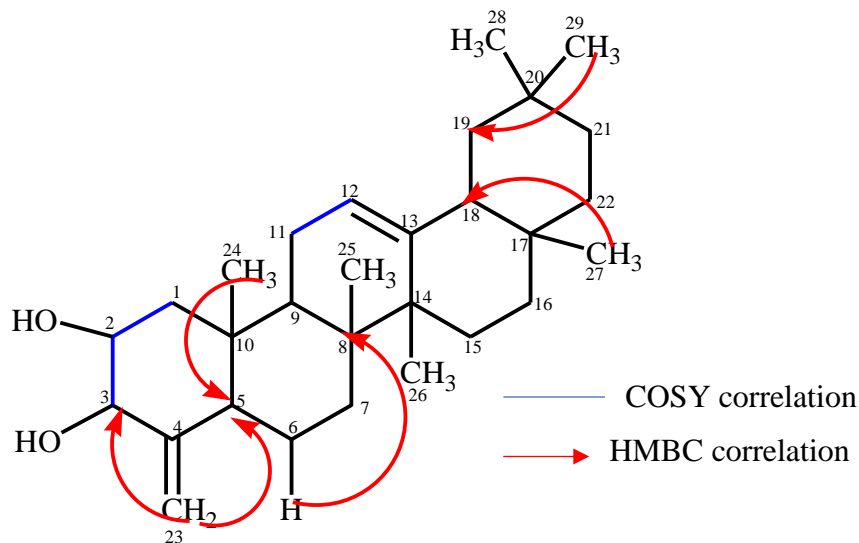
Figure 3.31: Selected HMBC and COSY correlation of 24-nor-2α,3β-dihydroxyolean-4(23)-12-ene (**66**).

The proposed structure was confirmed by comparing the NMR data to the literature data of 24-nor-2α,3β-dihydroxyolean-4(23)-12-ene (**66**) (table 3.7).

153

Table 3.7: ¹H (500 MHz), ¹³C (125 MHz), HMBC and COSY NMR data of Compound (**66**) compared to the literature ¹H and ¹³C NMR data of 24-nor-2α,3β-dihydroxyolean-4(23)-12-ene

Position	Isolated 24-nor-2α,3β-dihydroxyolean-4(23)-12-ene (CDCl₃)		Published NMR for 24-nor-2α,3β-dihydroxyolean-4(23)-12-ene ((CD₃OD) (¹H, 500 MHz ¹³C, 125 MHz) [69]		Isolated 24-nor-2α,3β-dihydroxyolean-4(23)-12-ene (CDCl₃)	Isolated 24-nor-2α,3β-dihydroxyolean-4(23)-12-ene (CDCl₃)
	δ$_C$	δ$_H$ (m, *J* in Hz, no of hydrogens)	δ$_C$	δ$_H$ (m, *J* in Hz, no of hydrogens)	HMBC correlation	COSY correlation
1	46.65, [CH₂]	2.10, m, 2H	43.8, [CH₂]		C3, C5	H24
2	73.66, [CH]	3.56, m, 1H	70.0, [CH]	3.69, ddd, *J* = 12.5, 10.0, 4.0 Hz, 1H		H1
3	79.16, [CH]	3.87, d, *J* = 8.54 Hz, 1H	78.9, [CH]	4.16, d, *J* =10 Hz, 1H		H2
4	149.55, [C]		144.0, [C]			
5	50.37, [CH]	1.71, d, *J* = 10 Hz, 1H	46.0, [CH]	2.19, d, *J* = 11 Hz, 1H		
6	28.03, [CH₂]	1.17-1.91, m, 2H	21.0, [CH₂]		C2, C8, C10, C14	
7	36.79, [CH₂]	1.70-1.75, m, 2H	34.0, [CH₂]		C8	
8	39.84, [C]		40.0, [C]			
9	45.03, [CH]	1.72, m, 1H	46.5, [CH]			
10	42.47, [C]		38.9 [C]			
11	24.39, [CH₂]	1.72-2.06, m, 2H	25.3, [CH₂]		C13, C17	
12	125.96, [CH]	5.32, s, 1H	123.0, [CH]	5.29, t, *J* = 3.7 Hz, 1H	C10	H11

154

13	138.45, [C]		145.9, [C]			
14	39.20, [C]		41.0, [C]			
15	29.84, [CH$_2$]	1.29, m, 2H	27.3, [CH$_2$]		C13, C19, C22	
16	24.32, [CH$_2$]	2.06, m, 2H	26.2, [CH$_2$]		C14	
17	38.78, [C]		31.0, [C]			
18	52.90, [CH]	2.22-2.25, m, 1H	47.8, [CH]		C14, C29	
19	30.75 [CH$_2$]	1.47, m, 2H	37.2, [CH$_2$]			
20	48.05, [C]		31.5, [C]			
21	20.94, [CH$_2$]	0.98-1.54, m, 2H	34.8, [CH$_2$]		C17, C19, C29	
22	31.60, [CH$_2$]	1.56, m, 2H	46.8, [CH$_2$]			
23	104.72, [CH$_2$]	5.17, s 4.77, s (geminal protons), 2H	110.0, [CH$_2$]	4.71-5.05, brs, 2H	C3, C5	H3, H23, H5
24	15.13, [CH$_3$]	0.81, s, 3H	14.0, [CH$_3$]		C1, C5, C8, C9, C10, C14	
25	17.15, [CH$_3$]	0.89, s, 3H	18.0, [CH$_3$]	0.79, s, 3H	C14, C15, C26	
26	21.31, [CH$_3$]	0.98, s, 3H	26.0, [CH$_3$]	0.90, s, 3H	C14, C15, C17, C24	
27	23.65, [CH$_3$]	1.14, s, 3H	27.5, [CH$_3$]	1.20, s, 3H	C13, C17, C20, C29	
28	17.25, [CH$_3$]	0.89, s, 3H	24.0, [CH$_3$]	0.99, s, 3H	C18, C21, C22, C29	
29	38.98, [CH$_3$]	0.97-1.37, s, 3H	33.0, [CH$_3$]	0.96, s, 3H	C19, C22, C27	

155

24-nor-2α,3β-dihydroxyolean-4(23)-12-ene is a triterpenoid which was isolated for the first time from the leaves of *Salvia hierosolymitana*.[69] It is not commonly found in other plant species, however, this is the first report of its isolation from *S. columbaria*.

3.3.15.6 Hederagenin (67)

Compound **67** was isolated as a white crystalline solid and was identified as hederagenin by the interpretation of NMR spectroscopy, mass data and comparison to literature.[65, 66] The molecular formula of the compound is $C_{30}H_{47}O_4$ as deduced from its monoprotonated molecular ion at *m/z* 471.3473 [M-H]⁻ (calculated for $C_{30}H_{47}O_4$, *m/z* 471.3474, M-H) based on the QTOF mass spectrum with seven degrees of unsaturation. The ¹³C NMR spectrum had a total of thirty signals and the assignments were done together with DEPT 135 spectrum. It consists of five methines (one oxygenated methine at δ_C 76.94), eleven methylene carbons (one oxygenated methylene at δ_C 72.37), six methyl carbons and eight quaternary carbons (one carboxylic acid at δ_C 181.37). Three ¹³C signals at δ_C 181.37, 138.09 and 125.91 ppm were identified for carboxylic and olefinic function moieties based on their chemical shifts. Two signals at δ_C 76.94 and 72.37 ppm indicated the presence of carbinol carbons based on their chemical shifts. Apart from one carboxylic acid and one olefinic group, the remaining elements of unsaturation were attributed to five rings suggesting a pentacyclic triterpenoid. The ¹H NMR spectrum revealed the presence of six singlet methyl groups at δ_H 0.93-1.00 (3H, s, H-30), 0.98 (3H, s, H-25), 0.94 (3H, s, H-29), 0.81-0.96 (3H, s, H-24), 0.79-0.86 (3H, s, H-26) and 0.79-0.86 (3H, s, H-27), one olefinic methine group at δ_H 5.26 (1H, brs, H-12), one oxygenated methine group with a proton at δ_H 3.64 (1H, t, *J* = 7.5, 15.3 Hz, H-3) and one oxygenated methylene group with protons at δ_H 3.74 (1H, d, *J* = 10.50 Hz, H-23a) and 3.44 (1H, d, *J* = 10.19 Hz, H-23b). In addition, one proton resonance at δ_H 2.19 (1H, d, *J* = 11.93 Hz, H-18) from one methine was seen. Several protons for methylene and methine overlap in the range between δ_H 0.86 and 2.00. In the HMBC spectrum, methylene carbon at δ_C 72.37 (C-23) correlated with methylene proton at δ_H 3.74 (H-23) and 3.44 (H-23). The methylene protons at δ_H 3.74 and 3.44 (H-23) also showed long-range correlations with methine carbon at δ_C 76.94 (C-3) and methyl carbon at 11.53 (C-24) and thus the structural unit (a) was proposed. The structural unit (a) was confirmed by the long-range correlation of methine proton at δ_H 3.64 (H-3) with methylene carbon at δ_C 72.37 (C-23) and methyl carbon at 11.53 (C-24). This was further confirmed by the contour peaks of methyl proton at δ_H 0.81-0.96 (H-24) with methine carbons at δ_C 76.94 (C-3) and 47.67 (C-5), quaternary carbon at 39.20 (C-4) and methylene

carbon at 72.37 (C-23). The structural unit (a) was further supported by the COSY correlation between the methine proton at δ_H 3.64 (H-3) and methylene proton at δ_H 1.63 (H-2). The extension of the structural unit (a) to (b) was sorted out similarly by the long-range correlation method in the HMBC experiment where methine proton at δ_H 1.53 (H-5) showed contour peaks with quaternary carbon at δ_C 39.20 (C-4) and 37.03 (C-10), methylene carbon at 18.61 (C-6), and methyl carbon at 15.99 (C-25). In addition, methyl proton at δ_H 0.98 (H-25) showed connectivity to methylene carbon at δ_C 38.44 (C-1) and methine carbon at 47.67 (C-5). An extension of structural unit (b) to (c) was shown in the HMBC experiment where methine proton at δ_H 0.86 (H-9) showed contour peaks with methylene carbons at δ_C 32.90 (C-7) and 23.41 (C-11), quaternary carbons at 41.97 (C-8), 37.03 (C-10) and 42.16 (C-14) and methyl carbon at 17.13 (C-26), methyl proton at δ_H 0.79-0.86 (H-26) also showed connectivity with methylene carbon at δ_C 32.90 (C-7), quaternary carbons at 41.97 (C-8) and 42.16 (C-14) while methylene protons at δ_H 0.91 (H-7) showed contour peaks with quaternary carbon at δ_C 41.97 (C-8) and methine carbon at 49.95 (C-9). A further extension to the structural unit (c) was complicated due to the overlap of peaks. Another approach from the olefinic center with methine proton at δ_H 5.26 (H-12) was adopted as it gave contour peaks with methylene carbon at δ_C 23.41 (C-11), quaternary carbon at 42.16 (C-14) and methine carbon at 52.82 (C-18) while methylene proton at δ_H 1.85-1.91 (H-11) gave contour peaks with quaternary carbon at δ_C 41.97 (C-8) and methine carbon at 125.91 (C-12) according to the HMBC experiment. All these correlations led to the structural unit (d). The extension of the structural unit (d) to (e) was sorted out in a similar manner where methine proton at δ_H 2.19 (H-18) showed connectivity with methylene carbons at δ_C 36.83 (C-19) and 30.75 (C-21) and quaternary carbon at 39.63 (C-20) according to the HMBC experiment. This was further confirmed by the correlation of methyl protons at δ_H 0.93-1.00 (H-30) and 0.94 (H-29) with methylene carbons at δC 36.83 (C-19), 30.75 (C-21) and 29.72 (C-22) and quaternary carbon at 39.63 (C-20) and assisted in the assignment of two methyl groups at C-29 and C-30 positions. Furthermore, quaternary carbon at δ_C 181.37 (C-28) showed long-range HMBC correlations with methylene protons at δ_H 1.85 (H-15) and 1.08-2.00 (H-16) which assisted in the assignment of the carboxylic acid group at the 28 position.

A big difference in chemical shift was observed in the C-18, C-19, C-20 resonance of compound **67** (δ_c 52.82 observed in the study and δ_c 41.30 and 42.40 published value for C-18; δ_c 36.83 observed in the study and δ_c 45.90 and 46.90 published value for C-19 and δ_c 39.63 observed in the study and δ_c 30.70 and 31.30 published value for C-20). The plausible reason is mentioned above.

The structure of compound **67** is shown in figure 3.32, and the selected HMBC and COSY correlations are shown in figure 3.33.
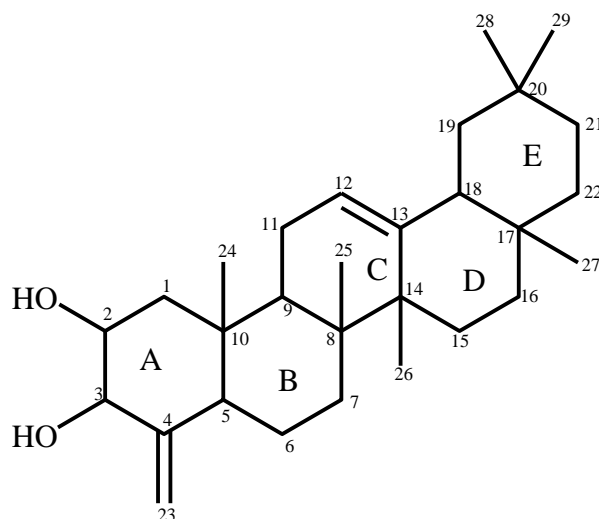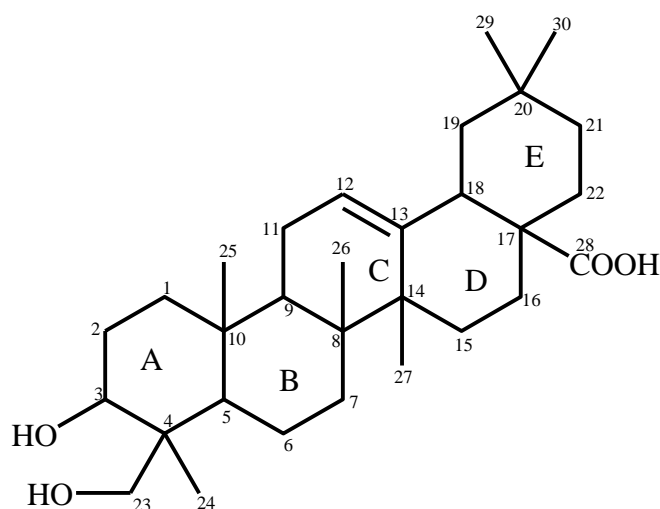

Figure 3.32: Structure of hederagenin (**67**).
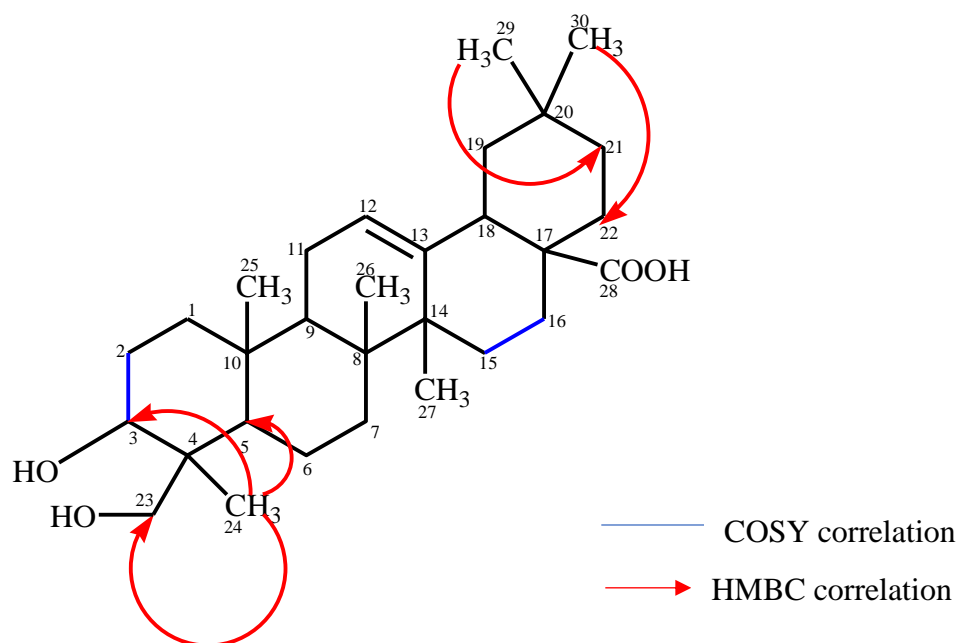
Figure 3.33: Selected HMBC and COSY correlation of hederagenin (**67**).

The proposed structure was confirmed by comparing the NMR data to the literature data of hederagenin (**67**) (table 3.8).

Table 3.8: ^{1}H (500 MHz), ^{13}C (125 MHz), HMBC and COSY NMR data of Compound (**67**) compared to the literature ^{1}H and ^{13}C NMR data of hederagenin

158

Position	Isolated hederagenin (CDCl₃)		Published NMR for hederagenin ((CDCl₃, Pyridine-d₅) (¹H, 500 MHz ¹³C, 125 MHz) [65],[66]			Isolated hederagenin (CDCl₃)	Isolated hederagenin (CDCl₃)
	δ_C	δ_H (m, J in Hz, no of hydrogens)	δ_C	δ_C	δ_H (m, J in Hz, no of hydrogens)	HMBC Correlation	COSY correlation
1	38.44, [CH₂]	1.64, m, 2H	38.1, [CH₂]	39.1, [CH₂]	1.12-1.61, m, 2H		
2	26.99, [CH₂]	1.63, m, 2H	26.4, [CH₂]	28.1, [CH₂]	1.91, m, 2H		
3	76.94, [CH]	3.64, t, J = 7.5 Hz, 15.3 Hz, 1H	76.4, [CH]	73.7, [CH]	4.24, m, 1H	C9, C23, C24	H-2
4	39.20, [C]		41.7, [C]	43.3, [C]			
5	47.67, [CH]	1.53, m, 1H	49.7, [CH]	48.9, [CH]	1.56, m, 1H	C1, C4, C6, C8, C10, C25	
6	18.61, [CH₂]	1.38, m, 2H	18.50, [CH₂]	18.9, [CH₂]	1.43, m, 2H	C1, C10, C14	
7	32.90, [CH₂]	0.91, m, 2H	32.4, [CH₂]	Not provided	0.95-1.30, m, 2H	C4, C8, C9, C10, C26, C27	
8	41.97, [C]		39.3, [C]	40.1, [C]			
9	49.95, [CH]	0.86, m, 1H	47.5, [CH]	48.5, [CH]	1.80, m, 1H	C1, C4, C7, C8, C10, C11, C14, C25, C26, C27	
10	37.03, [C]		36.9, [C]	37.6,			
11	23.41, [CH₂]	1.85-1.91, m, 2H	23.1, [CH₂]	24.1, [CH₂]	1.99, m, 2H	C5, C8, C12	
12	125.91, [CH]	5.26, brs, 1H	122.2, [CH]	122.9, [CH]	5.52, d, J = 3.7 Hz, 1H	C5, C8, C11, C14, C17, C18	
13	138.09, [C]		143.6, [C]	145.2, [C]			
14	42.16, [C]		41.7, [C]	42.6, [C]			
15	28.15, [CH₂]	1.85, m, 2H	27.7, [CH₂]	28.7, [CH₂]	1.19-2.19, m, 2H	C27, C28	
16	24.30, [CH₂]	1.08-2.00, m, 2H	23.4, [CH₂]	24.1, [CH₂]	1.98-2.16, m, 2H	C8, C13, C14, C15, C17, C20, C28	H-15
17	48.04, [C]		46.7, [C]	47.0, [C]			
18	52.82 [CH]	2.19, d, J = 11.93 Hz, 1H	41.3, [CH]	42.4, [CH]	3.32, dd, J = 14.0, 4.9 Hz, 1H	C16, C19, C20, C21	
19	36.83, [CH₂]	1.68, m, 2H	45.9, [CH₂]	46.9, [CH₂]	1.83-2.06, m, 2H		
20	39.63, [C]		30.7, [C]	31.3, [C]			

159

21	30.75, [CH$_2$]	1.50, m, 2H	33.9, [CH$_2$]	Not provided	1.20-1.46, m, 2H		
22	29.72, [CH$_2$]	1.27, m, 2H	32.4, [CH$_2$]	Not provided	1.31-1.81, m, 2H		
23	72.37, [CH$_2$]	3.74, d, J =10.50 3.44, d, J =10.19 Hz, 2H	71.3, [CH$_2$]	68.2, [CH$_2$]	4.21, d, J = 8.2 Hz 3.74, d, J = 8.2 Hz, 2H	C3, C24	
24	11.53, [CH$_3$]	0.89, s, 3H	11.6, [CH$_3$]	13.5, [CH$_3$]	1.07, s, 3H	C3, C4, C5, C23, C25	
25	15.99, [CH$_3$]	0.98, s, 3H	15.7, [CH$_3$]	16.3, [CH$_3$]	0.99, s, 3H	C1, C4, C5, C6	
26	17.13, [CH$_3$]	0.83, s, 3H	16.9, [CH$_3$]	17.9, [CH$_3$]	1.07, s, 3H	C5, C6, C7, C8, C9, C14, C25	
27	17.25, [CH$_3$]	0.83, s, 3H	26.0, [CH$_3$]	26.5, [CH$_3$]	1.26, s, 3H	C6, C7, C8, C9, C14, C17, C18	
28	181.37, [C]		178.2, [C]	180.1, [C]			
29	23.75, [CH$_3$]	0.94, s, 3H	33.1, [CH$_3$]	Not provided	0.94, s, 3H	C17, C19, C20, C21	
30	21.32, [CH$_3$]	0.97, s, 3H	23.6, [CH$_3$]	24.2, [CH$_3$]	1.02, s, 3H	C17, C19, C20, C21, C22	

Hederagenin is a water insoluble pentacyclic triterpenoid. It was first isolated from the leaves of English ivy *Hedera helix*, a species of flowering plant of the family Araliaceae. Subsequently it has been identified from the fruit of *Fructus Akebiae,* the leaves of *Cyclocarya paliuru,* the fruit of *Sapindus saponaria* and the roots of *Clematis mandshurica*, however, this is the first report on its isolation in *S. columbaria*.[67]

3.3.16 The inhibitory effect of isolated compounds on nitric oxide production

The first batch of isolated compounds, loganic acid (**62**), cantleyoside-dimethyl-acetal (**63**) and 2-isoursolic acid (**65**) and the second batch of isolated compounds, ursolic acid (**64**), 24-nor-2α,3β-dihydroxyolean-4(23),12-ene (**66**) and hederagenin (**67**) were assessed for their inhibitory activities on nitric oxide production in LPS-induced Raw 264.7 macrophages in anti-inflammatory assays. Figures 3.34 and 3.35 show the results. The first batch of isolated compounds (loganic acid (**62**), cantleyoside-dimethyl-acetal (**63**) and 2-isoursolic acid (**65**)) were screened in a quadruplicate assay while the second batch of isolated compounds (ursolic acid (**64**), 24-nor-2α,3β-dihydroxyolean-4(23),12-ene (**66**) and hederagenin (**67**)) were screened in a triplicate assay.
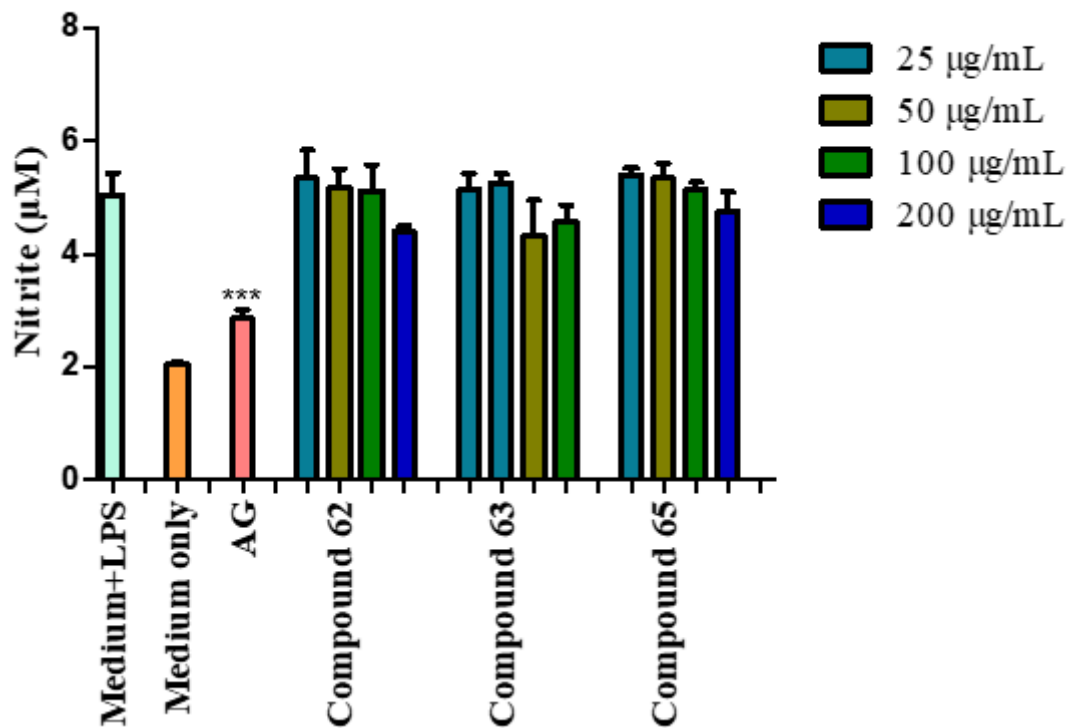
Figure 3.34: Nitric oxide production in LPS activated macrophages treated with different concentrations of pure compounds, loganic acid (**62**), cantleyoside-dimethyl-acetal (**63**) and 2-isoursolic acid (**65**). Bar graphs represent triplicate values of one experiment. Error bars represent the standard deviation of the mean. The p values are relative to the negative control (medium + LPS). Aminoguanidine (AG) was included as the positive control. p value < *p < 0.05, **p < 0.01, ***p < 0.001.
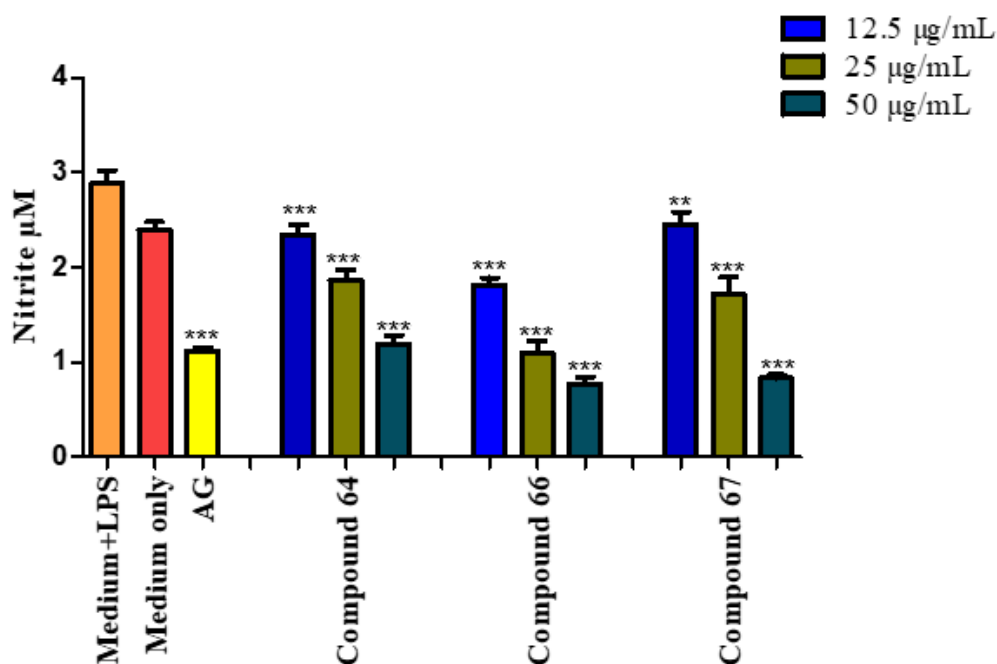
Figure 3.35: Nitric oxide production in LPS activated macrophages treated with different concentrations of pure compounds, ursolic acid (**64**), 24-nor-2α,3β-dihydroxyolean-4(23),12-ene (**66**) and hederagenin (**67**). Bar graphs represent triplicate values of one experiment. Error bars represent the standard deviation of the mean. The p values are relative to the negative control (medium + LPS). Aminoguanidine (AG) was included as the positive control. p value < *p < 0.05, **p < 0.01, ***p < 0.001.

The cytotoxic effect of the first batch of isolated compounds, loganic acid (**62**), cantleyoside-dimethyl-acetal (**63**) and 2-isoursolic acid (**65**) and the second batch of isolated compounds, ursolic acid (**64**), 24-nor-2α,3β-dihydroxyolean-4(23),12-ene (**66**) and hederagenin (**67**) was also determined to accurately establish potential anti-inflammatory activity. The isolated compounds (loganic acid (**62**), cantleyoside-dimethyl-acetal (**63**) and 2-isoursolic acid (**65**) from the first batch and ursolic acid (**64**), 24-nor-2α,3β-dihydroxyolean-4(23),12-ene (**66**) and hederagenin (**67**) from the second batch) were treated at different concentrations on RAW 264.7 macrophage viability (figures 3.36 and 3.37) respectively.

162
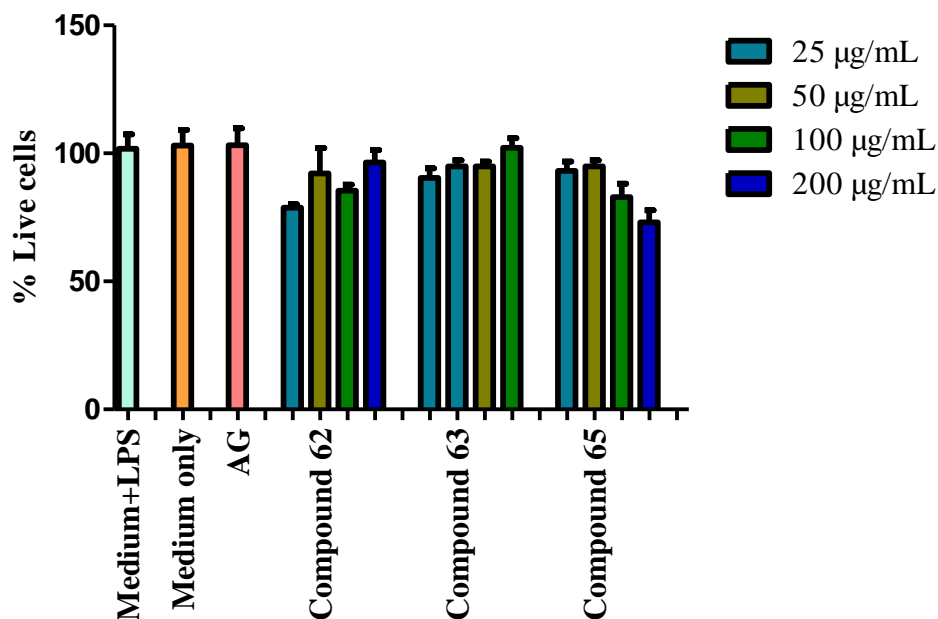
Figure 3.36: Cell viability (%) of LPS activated macrophages after 24 hours of exposure to pure compounds, loganic acid (**62**), cantleyoside-dimethyl-acetal (**63**) and 2-isoursolic acid (**65**). Bar graphs represent triplicate values of one experiment. Error bars represent the standard deviation of the mean. The p values are relative to the negative control (medium + LPS). Aminoguanidine (AG) was included as the positive control. p value < *p < 0.05, **p < 0.01, ***p < 0.001.
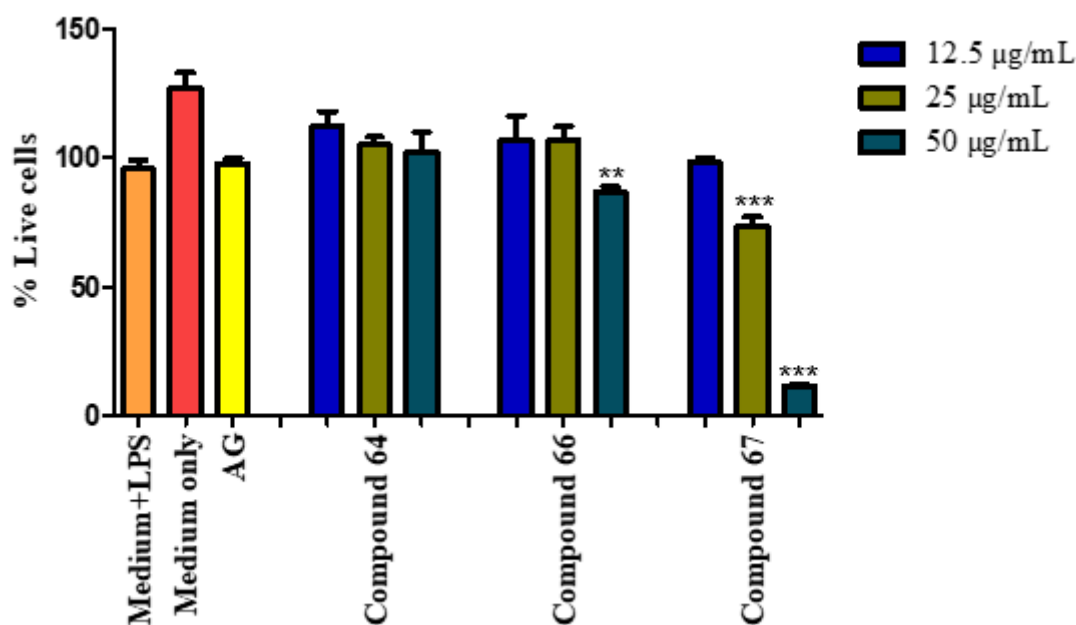
Figure 3.37: Cell viability (%) of LPS activated macrophages after 24 hours of exposure to pure compounds, ursolic acid (**64**), 24-nor-2α,3β-dihydroxyolean-4(23),12-ene (**66**) and hederagenin (**67**). Bar graphs represent triplicate values of one experiment. Error bars represent the standard deviation of the mean. The p values are relative to the negative control (medium + LPS). Aminoguanidine (AG) was included as the positive control. p value < *p < 0.05, **p < 0.01, ***p < 0.001.

The screening result of the first batch of isolated compounds showed that loganic acid (**62**) did not show any significant reduction in the LPS-stimulated nitric oxide production in Raw 264.7 cells at all the tested concentrations 25, 50, 100 and 200 µg/mL(5.34 ± 0.50, 5.16 ± 0.34, 5.13 ± 0.46 and 4.39 ± 0.10 µM) relative to the negative control (medium + LPS) (4.95 ± 0.39 µM at 25 µg mL^{-1}) (figure 3.34). The cytotoxicity result showed that loganic acid (**62**) was not toxic to the RAW 264.7 cells (figure 3.36). Cantleyoside-dimethyl-acetal (**63**) also did not show any significant reduction in the LPS-stimulated nitric oxide production in Raw 264.7 cells at all the tested concentrations 25, 50, 100 and 200 µg/mL(5.14 ± 0.30, 5.25 ± 0.16, 4.33 ± 0.62 and 4.58 ± 0.29 µM) relative to the negative control (medium + LPS) (4.95 ± 0.39 µM at 25 µg/mL) (figure 3.34). The cytotoxicity result showed that cantleyoside-dimethyl-acetal (**63**) was not toxic to the RAW 264.7 cells (figure 3.36). The compound 2-isoursolic acid (**65**) also did not show any significant reduction in the LPS-stimulated nitric oxide production in Raw 264.7

164

cells at all the tested concentrations 25, 50, 100 and 200 µg/mL(5.40 ± 0.12, 5.34 ± 0.26, 5.14 ± 0.14 and 4.74 ± 0.37 µM) relative to the negative control (medium + LPS) (4.95 ±0.39 µM at 25 µg/mL) (figure 3.34). The cytotoxicity result also showed that 2-isoursolic acid (**65**) was not toxic to the RAW 264.7 cells (figure 3.36). These results showed that the first batch of isolated compounds loganic acid (**62**), cantleyoside-dimethyl-acetal (**63**) and 2-isoursolic acid (**65**) did not have any anti-inflammatory activity as they did not show any significant reduction of the LPS-stimulated nitric oxide production in RAW 264.7 macrophages relative to the negative control (medium + LPS).

The screening result of the second batch of isolated compounds shows that ursolic acid (**64**) significantly decreased LPS-stimulated nitric oxide production in RAW 264.7 macrophages by 2.34 ± 0.10, 1.86 ± 0.11 and 1.19 ± 0.10 µM at concentrations 12.5, 25 and 50 µg/mLrespectively relative to the negative control (2.95 ± 0.14 µM at 12.5 µg mL^{-1}) (figure 3.35). The cytotoxicity result revealed that ursolic acid (**64**) was not toxic to the Raw 264.7 cells (figure 3.37). Ursolic acid (**64**) has previously been reported to show significant inhibition on LPS-stimulated nitric oxide production in RAW 264.7 macrophage by 9, 7.5 and 3.5 µM at concentrations 10, 20 and 40 µg/mLthree times lower activity than what was observed in this study (anti-inflammatory assay).[68] 24-nor-2α,3β-dihydroxyolean-4(23),12-ene (**66**) significantly decreased LPS-stimulated nitric oxide production in RAW 264.7 macrophages by 1.81 ± 0.07, 1.09 ± 0.13 and 0.77 ± 0.07 µM at the concentrations 12.5, 25 and 50 µg/mLrespectively relative to the negative control (2.95 ± 0.14 at 12.5 µg/mL) (figure 3.35). The cytotoxicity result revealed 24-nor-2α,3β-dihydroxyolean-4(23),12-ene (**66**) induced decreased cell viability at 50 µg/mLby 25 %. Though the decreased cell viability showed death of the RAW 264.7 cells at 50 µg/mL, the compound still showed good activity at the lower test concentrations (12.5 and 25 µg/mL) (figure 3.37). It is therefore established that 24-nor-2α,3β-dihydroxyolean-4(23),12-ene become cytotoxic to the cells above a concentration of 25 µg/mL.

The inhibitory activity of nitric oxide production for 24-nor-2α,3β-dihydroxyolean-4(23)-12-ene (**66**) was presented for the first time in this study and is regarded as being good (1.81, 1.09 and 0.77 µM at 12.5, 25 and 50 µg/mLrespectively). Hederagenin (**67**) significantly decreased LPS-stimulated nitric oxide production in RAW 264.7 macrophages by 2.45 ± 0.14 and 1.71 ± 0.19 µM at concentrations 12.5 and 25 µg/mLrelative to the negative control (2.95 ± 0.14 at 12.5 µg/mL) (figure 3.35). The cytotoxicity result showed that hederagenin (**67**) induced decreased cell viability at 25 µg/mLby 35 % and at 50 µg/mLby 80 %. This shows that the

165

activity of hederagenin (**67**) observed at 50 µg/mLwas a result of the death of the macrophage cells exposed to this compound and therefore was not considered. It is also established that the hederagenin become cytotoxic to the cells above a concentration of 12.5 µg/mL. The inhibitory activity of hederagenin (**67**) in nitric oxide production in RAW 264.7 macrophage has previously been reported with an IC_{50} value of 22.6 ± 0.21µM (IC_{50} value of quercetin (positive control) 7.14 ± 0.38µM) eleven times lower activity than what was observed in this study (anti-inflammatory assay).[69]. 24-nor-2α,3β-dihydroxyolean-4(23),12-ene (**66**) exhibited the best anti-inflammatory potential as it showed the highest reduction in nitrite concentration (1.81 ± 0.07, 1.09 ± 0.13 and 0.77 ± 0.07 µM respectively) at all three tested sample concentrations (12.5, 25 and 50 µg/mL) relative to the negative control (2.95 ± 0.14 µM at 12.5 µg/mL) with an effect on cell viability at the concentration (50 µg/mL). This was followed by ursolic acid (**64**) (2.34 ± 0.10, 1.86 ± 0.11 and 1.19 ± 0.10 µM respectively) at the above tested concentrations. The decrease in nitrite concentration of hederagenin (**67**) at 25 and 50 µg/mLcannot be considered as it proved to be highly cytotoxic at both concentrations however at 12.5 µg/mL, the decrease in nitric oxide concentration can be considered as anti-inflammatory activity as no effect in cytotoxicity was evident. The results indicated that the isolated compounds (ursolic acid (**64**), 24-nor-2α,3β-dihydroxyolean-4(23),12-ene (**66**) and hederagenin (**67**) from the active fractions were responsible for the inhibition of nitric oxide production. The structures of the three active compounds ursolic acid (**64**), 24-nor-2α,3β-dihydroxyolean-4(23),12-ene (**66**), and hederagenin (**67**) show they are pentacyclic triterpenoids with ursane and oleanane skeletons and this class of compounds has been reported to have anti-inflammatory activity.[70] Further preliminary structure activity relationship analysis of ursane and oleanane triterpenoids disclosed that the β-hydroxy group at the C-3 position was essential for the nitric oxide inhibitory activity.[70] All three active compounds in this study had a β-hydroxy group at the C-3 position which confirmed the above assumption. However, 2-isoursolic acid (**65**) which had a hydroxy group at the C-2 position was not active. This also supports the above assumption although it is subject to confirmation and can be further verified.

This is the first report of loganic acid (**62**), cantleyoside-dimethyl-acetal (**63**), ursolic acid (**64**), 2-isoursolic acid (**65**) 24-nor-2α,3β-dihydroxyolean-4(23),12-ene (**66**) and hederagenin (**67**) from *S. columbaria*. This is also the first report of the anti-inflammatory activity of 24-nor-2α,3β-dihydroxyolean-4(23),12-ene (**66**) and could be potentially developed into an anti-inflammatory ingredient.

3.4   Conclusion

The four extracts (acetone, ethanol, water/ethanol (1:1), water) of *S. columbaria* showed good anti-inflammatory activity, however, based on commercial suitability and easier to isolate compounds from ethanol than water, the ethanol extract was selected for research and isolation of active compounds. Liquid-liquid partitioning of the ethanol extract using hexane led to the concentration of actives in the hexane fraction. The chemical profile of the ethanol extract of *S. columbaria* was carried out to identify compounds in the extract. Ten compounds were tentatively identified by UPLC-QTOF-MS analysis which are loganic acid, schrophuloside A1, 3,4-dicaffeoylquinic acid, cantleyoside, sylvestroside III, triplostoside A, hederagenin, maslinic acid, 2-isoursolic acid, glycyrrhetaldehyde. The presence of loganic acid, triplostoside A, hederagenin and 2-isoursolic acid was confirmed through isolation, purification and structure elucidation using MS and NMR data. These compounds have been identified for the first time in *S. columbaria*. Fractionation of the hexane fraction led to the isolation of 4 compounds: ursolic acid (**64**), 2-isoursolic acid (**65**), 24-nor-2α,3β-dihydroxyolean-4(23) (**66**),12-ene and hederagenin (**67**). Fractionation of the defatted ethanol fraction led to the isolation of 2 compounds: loganic acid (**62**) and cantleyoside-dimethyl-acetal (**63**). The three pentacyclic triterpenoids ursolic acid (**64**) 24-nor-2α,3β-dihydroxyolean-4(23),12-ene (**66**), and hederagenin (**67**) significantly decreased the nitric oxide levels in RAW 264.7 macrophages at 12.5, 25 and 50 µg/mLrelative to the negative control (medium + LPS (2.95 ± 0.14 at 12.5 µg/mL)) by 1.81 ± 0.07, 1.09 ± 0.13 and 0.77 ± 0.07 µM; 2.34 ± 0.10, 1.86 ± 0.11 and 1.19 ± 0.10 µM; 2.45 ± 0.14 and 1.71 ± 0.19 µM respectively. 24-nor-2α,3β-dihydroxyolean-4(23),12-ene (**66**) was the most active compound showing potent activity at the two tested concentrations (1.09 µM at 25 µg/mLand 0.07 µM at 50 µg/mL) relative to the negative control (medium + LPS (2.95 ± 0.14 at 12.5 µg/mL)). This is the first report of the anti-inflammatory activity of 24-nor-2α,3β-dihydroxyolean-4(23),12-ene (**66**) and could be potentially developed into an anti-inflammatory ingredient. All the active compounds (**64**, **66** and **67**) were structurally similar and contained a β-hydroxy group at C-3. Compound (**65**) was inactive and had a hydroxy group at C-2 instead of C-3 which indicated that the β-hydroxy group at C-3 increased the nitric oxide inhibition activity of the compounds. This study shows the potential for the ethanol extract of *S. columbaria* to be developed as an anti-inflammatory ingredient and used as a complementary medicine to reduce swelling.

3.5   References

1.   Pinto, D. C. G. A.; Rahmouni, N.; Beghidja, N.; Silva, A. M. S., Scabiosa Genus: A Rich Source of Bioactive Metabolites. *Medicines (Basel)* **2018,** *5* (4), 110.

2.   Carlson, S. E.; Linder, H. P.; Donoghue, M. J., The historical biogeography of Scabiosa (Dipsacaceae): implications for Old World plant disjunctions. *Journal of Biogeography* **2012,** *39*.

3.   Maroyi, A., Scabiosa columbaria: A review of its medicinal uses, phtochemistry and biological activities. *Asian Journal of Pharmaceutical and Clinical Research* **2019**, 10-14.

4.   Al-Qudah, M.; Otoom, N.; Al-Jaber, H.; Tashtoush, H.; Mayyas, A. S.; Tarawneh, I.; Lahham, J.; Orabi, S., Chemical Composition of Essential Oil of Jordanian Scabiosa prolifera at Different Flowering Stages. *Jordan Journal of chemistry* **2016**.

5.   Manning, J. C.;   Goldblatt, P.; Johns, A., A taxonomic review of Cephalaria (Dipsacaceae) in the Cape Floristic Region. *South African Journal of Botany* **2014,** *94*, 195-203.

6.   Germishuizen, G.; Meyer, N. L. In *Plants of southern Africa: an annotated checklist*, 2003.

7.   Bruyns, P. V., *Plant Systematics and Evolution* **2005,** *252* (3/4), 249-251.

8.   Angeloni, F.; Vergeer, P.; Wagemaker, C. A. M.; Ouborg, N. J., Within and between population variation in inbreeding depression in the locally threatened perennial Scabiosa columbaria. *Conservation Genetics* **2014,** *15* (2), 331-342.

9.   Niemelä, J.; Baur, B., Threatened species in a vanishing habitat: Plants and invertebrates in calcareous grasslands in the Swiss Jura mountains. *Biodiversity and Conservation* **1998,** *7*, 1407-1416.

10.   South African National Biodiversity Institute Scabiosa columbaria. http://pza.sanbi.org/scabiosa-columbaria (accessed November 25, 2021).

11.   Sagbo, J., Anti-Melanogenesis, Antioxidant and Anti-Tyrosinase Activities of Scabiosa columbaria L. *Processes* **2020,** *8*, 236.

12.   Van Wyk, B.-E.; Van Oudtshoorn, B.; Gericke, N., *Medicinal plants of South Africa*. 2nd ed. ed.; Briza Publications: Pretoria, 2009.

13.   Basto, S.; Dorca, C.; Thompson, K.; Rees, M., Effect of pH buffer solutions on seed germination of Hypericum pulchrum, Campanula rotundifolia and Scabiosa columbaria. *Seed Science and Technology* **2013,** *41*.

14.   Horn, M. M.; Drewes, S. E.; Brown, N. J.; Munro, O. Q.; Meyer, J. J. M.; Mathekga, A. D. M., Transformation of naturally-occurring 1,9-trans-9,5-cis sweroside to all trans sweroside during acetylation of sweroside aglycone. *Phytochemistry* **2001,** *57* (1), 51-56.

15.   Plants, R. s., Scabiosa columbaria.

16.   Rigat, M.; Bonet, M. À.; Garcia, S.; Garnatje, T.; Vallès, J., Studies on pharmaceutical ethnobotany in the high river Ter valley (Pyrenees, Catalonia, Iberian Peninsula). *Journal of Ethnopharmacology* **2007,** *113* (2), 267-277.

17.   Seleteng Kose, L.; Moteetee, A.; Van Vuuren, S., Ethnobotanical survey of medicinal plants used in the Maseru district of Lesotho. *J Ethnopharmacol* **2015,** *170*, 184-200.

18.   Wyk, B. E.; Oudtshoorn, B.; Gericke, N., *Medicinal Plants of South Africa*. 2009.

19.   Van Wyk, B. E., The potential of South African plants in the development of new food and beverage products. *South African Journal of Botany* **2011,** *77* (4), 857-868.

20.   Maroyi, A., From Traditional Usage to Pharmacological Evidence: Systematic Review of Gunnera perpensa L. *Evidence-Based Complementary and Alternative Medicine* **2016,** *2016*, 1-14.

21.   Maroyi, A., Dicoma anomala sond.: A review of its botany, ethnomedicine, phytochemistry and pharmacology. *Asian Journal of Pharmaceutical and Clinical Research* **2018,** *11*, 70.

22.   Flora of Lesotho. *Taxon* **1972,** *21* (1), 182-184.

23.   Mhlongo, L. S.; Van Wyk, B. E., Zulu medicinal ethnobotany: new records from the Amandawe area of KwaZulu-Natal, South Africa. *South African Journal of Botany* **2019,** *122*, 266-290.

24.   Maroyi, A., Phytochemical and ethnopharmacological review of Heterophyxis Natalensis. *Asian Journal of Pharmaceutical and Clinical Research* **2019**, 8-15.

25.   Guarrera, P. M.; Savo, V., Wild food plants used in traditional vegetable mixtures in Italy. *Journal of Ethnopharmacology* **2016,** *185*.

26.   Besbes Hlila, M.; Mosbah, H.; Majouli, K.; Ben Nejma, A.; Ben Jannet, H.; Mastouri, M.; Aouni, M.; Selmi, B., Antimicrobial Activity of Scabiosa arenaria Forssk. Extracts and Pure Compounds Using Bioguided Fractionation. *Chem Biodivers* **2016,** *13* (10), 1262-1272.

27.   van Vuuren, S. F.; Naidoo, D., An antimicrobial investigation of plants used traditionally in southern Africa to treat sexually transmitted infections. *Journal of Ethnopharmacology* **2010,** *130* (3), 552-558.

28.   Kose, L. E. M. S., *Evaluation of Commonly Used Medicinal Plants of Maseru District in Lesotho for Their Ethnobotanical Uses, Antimicrobial Properties and Phytochemical Compositions*. University of Johannesburg: 2017.

29.   Otang-Mbeng, W.; Sagbo, J., Anti-Melanogenesis, Antioxidant and Anti-Tyrosinase Activities of Scabiosa columbaria L. *Processes* **2020,** *8*, 236.

30.   Corradi, E.; De Mieri, M.; Gafner, F.; Hamburger, M.; Potterat, O., A New Secoiridoid Glucoside, and a Metabolite Profile of Scabiosa lucida. *Natural Product Communications* **2016,** *11* (7), 1934578X1601100705.

31.   Vinnitska, R. B., Studies of phthalates pigeon scabious (Scabiosa columbaria L.). *Farmatsevtychnyi zhurnal* **2018,** *0* (1), 59-63.

32.   Carrillo-Ocampo, D.; Bazaldúa-Gómez, S.; Bonilla-Barbosa, J. R.; Aburto-Amar, R.; Rodríguez-López, V., Anti-Inflammatory Activity of Iridoids and Verbascoside Isolated from Castilleja tenuiflora. *Molecules* **2013,** *18* (10), 12109-12118.

33.   Soni, U.; Brar, S.; Gauttam, V., Effect of seasonal variation on secondary metabolites of medicinal plants. *Int J Pharm Sci Res* **2015,** *6*, 3654-3662.

34.   Mhlongo, F.; Cordero-Maldonado, M. L.; Crawford, A. D.; Katerere, D.; Sandasi, M.; Hattingh, A. C.; Koekemoer, T. C.; Van de Venter, M.; Viljoen, A. M., Evaluation of the wound healing properties of South African medicinal plants using zebrafish and in vitro bioassays. *Journal of Ethnopharmacology* **2022,** *286*, 114867.

35.   Prinsloo, G.; Nogemane, N., The effects of season and water availability on chemical composition, secondary metabolites and biological activity in plants. *Phytochemistry Reviews* **2018,** *17* (4), 889-902.

36.   Wu, J.; Zhao, Z.; Wu, L.; Wang, Z., Authentication of Gentiana straminea Maxim. and its substitutes based on chemical profiling of iridoids using liquid chromatography with mass spectrometry. *Biomed Chromatogr* **2016,** *30* (12), 2061-2066.

37.   Sun, X.; Zhang, Y.; Yang, Y.; Liu, J.; Zheng, W.; Ma, B.; Guo, B., Qualitative and quantitative analysis of furofuran lignans, iridoid glycosides, and phenolic acids in Radix Dipsaci by UHPLC-Q-TOF/MS and UHPLC-PDA. *Journal of Pharmaceutical and Biomedical Analysis* **2018,** *154*, 40-47.

38. Kim, I.; Kaneko, N.; Uchiyama, N.; Lee, J.; Takeya, K.; Kawahara, N.; Goda, Y., Two Phenylpropanoid Glycosides from Neopicrorhiza scrophulariiflora. *Chemical & pharmaceutical bulletin* **2006,** *54*, 275-7.

39. Fu, Y.; Sun, R.; Yang, J.; Wang, L.; Zhao, P.; Chen, S., Characterization and Quantification of Phenolic Constituents in Peach Blossom by UPLC-LTQ-Orbitrap-MS and UPLC-DAD. *Natural Product Communications* **2020,** *15*.

40. Oszmiański, J.; Wojdyło, A.; Juszczyk, P.; Nowicka, P., Roots and Leaf Extracts of Dipsacus fullonum L. and Their Biological Activities. *Plants (Basel)* **2020,** *9* (1), 78.

41. Kuhtinskaja, M.; Bragina, O.; Kulp, M.; Vaher, M., Anticancer Effect of the Iridoid Glycoside Fraction from Dipsacus fullonum L. Leaves. *Natural Product Communications* **2020,** *15* (9), 1934578X20951417.

42. Xia, Y.; Wei, G.; Si, D.; Liu, C., Quantitation of ursolic acid in human plasma by ultra performance liquid chromatography tandem mass spectrometry and its pharmacokinetic study. *J Chromatogr B Analyt Technol Biomed Life Sci* **2011,** *879* (2), 219-24.

43. Balkrishna, A.; Verma, S.; Sharma, P.; Tomer, M.; Srivastava, J.; Varshney, A., Comprehensive and Rapid Quality Evaluation Method for the Ayurvedic Medicine Divya-Swasari-Vati Using Two Analytical Techniques: UPLC/QToF MS and HPLC–DAD. *Pharmaceuticals* **2021,** *14* (4), 297.

44. Asteggiano, A.; Occhipinti, A.; Capuzzo, A.; Mecarelli, E.; Aigotti, R.; Medana, C., Quali–Quantitative Characterization of Volatile and Non-Volatile Compounds in Protium heptaphyllum (Aubl.) Marchand Resin by GC–MS Validated Method, GC–FID and HPLC–HRMS2. *Molecules* **2021,** *26* (5), 1447.

45. Sut, S.; Poloniato, G.; Malagoli, M.; Dall'Acqua, S., Fragmentation of the main triterpene acids of apple by LC-APCI-MSn. *Journal of Mass Spectrometry* **2018,** *53* (9), 882-892.

46. Chen, Q.; Zhang, Y.; Zhang, W.; Chen, Z., Identification and quantification of oleanolic acid and ursolic acid in Chinese herbs by liquid chromatography-ion trap mass spectrometry. *Biomed Chromatogr* **2011,** *25* (12), 1381-8.

47. España, M. D.; Arboleda, J. W.; Ribeiro, J. A.; Abdelnur, P. V.; Guzman, J. D., Eucalyptus leaf byproduct inhibits the anthracnose-causing fungus Colletotrichum gloeosporioides. *Industrial Crops and Products* **2017,** *108*, 793-797.

48. Li, S.; Wan, C.; He, L.; Yan, Z.; Wang, K.; Yuan, M.; Zhang, Z., Rapid identification and quantitative analysis of chemical constituents of Gentiana veitchiorum by UHPLC-PDA-QTOF-MS. *Revista Brasileira de Farmacognosia* **2016,** *27*.

49. Ma, J. N.; Bolraa, S.; Ji, M.; He, Q. Q.; Ma, C. M., Quantification and antioxidant and anti-HCV activities of the constituents from the inflorescences of Scabiosa comosa and S. tschilliensis. *Nat Prod Res* **2016,** *30* (5), 590-4.

50. Chen, F.; Li, H.-l.; Tan, Y.; Lai, W.-Y.; Qin, Z.-M.; Cai, H.-D.; Li, Y.-h.; Zhang, j.; Xiaopo, Z., Sensitive and cost-effective LC–ESI–MS/MS method for quantitation of euscaphic acid in rat plasma using optimized formic acid concentration in mobile phase. *Anal. Methods* **2014,** *6*.

51. Kim, I. T.; Ryu, S.; Shin, J. S.; Choi, J. H.; Park, H. J.; Lee, K. T., Euscaphic acid isolated from roots of Rosa rugosa inhibits LPS-induced inflammatory responses via TLR4-mediated NF-κB inactivation in RAW 264.7 macrophages. *J Cell Biochem* **2012,** *113* (6), 1936-46.

52. Li, Y.; Dong, J.; Shang, Y.; Zhao, Q.; Li, P.; Wu, B., Anti-inflammatory effects of hederagenin on diabetic cardiomyopathy via inhibiting NF-κB and Smads signaling pathways in a type-2 diabetic mice model. *RSC Advances* **2019,** *9* (45), 26238-26247.

53. Szumny, D.; Sozański, T.; Kucharska, A. Z.; Dziewiszek, W.; Piórecki, N.; Magdalan, J.; Chlebda-Sieragowska, E.; Kupczynski, R.; Szeląg, A.; Szumny, A., Application of Cornelian Cherry Iridoid-Polyphenolic Fraction and Loganic Acid to Reduce Intraocular Pressure. *Evidence-Based Complementary and Alternative Medicine* **2015,** *2015*, 939402.

54. Christopoulou, C.; Graikou, K.; Chinou, I., Chemosystematic value of chemical constituents from Scabiosa hymettia (Dipsacaceae). *Chem Biodivers* **2008,** *5* (2), 318-23.

55. Polat, E.; Alankus-Caliskan, O.; Karayildirim, T.; Bedir, E., Iridoids from Scabiosa atropurpurea L. subsp. maritima Arc. (L.). *Biochemical Systematics and Ecology* **2010,** *SCI*, 253-55.

56. Papalexandrou, A.; Magiatis, P.; Perdetzoglou, D.; Skaltsounis, A. L.; Chinou, I.; Harvala, C., Iridoids from Scabiosa variifolia (Dipsacaceae) growing in Greece. *Biochemical Systematics and Ecology - BIOCHEM SYST ECOL* **2003,** *31*, 91-93.

57. Graikou, K.; Aligiannis, N.; Chinou, I. B.; Harvala, C., Cantleyoside-dimethyl-acetal and other iridoid glucosides from Pterocephalus perennis--antimicrobial activities. *Z Naturforsch C J Biosci* **2002,** *57* (1-2), 95-9.

58. Gülcemal, D.; Masullo, M.; Alankuş-Calişkan, O.; Karayildirim, T.; Senol, S. G.; Piacente, S.; Bedir, E., Monoterpenoid glucoindole alkaloids and iridoids from Pterocephalus pinardii. *Magn Reson Chem* **2010,** *48* (3), 239-43.

59. Werner, S.; Simic, N.; Robert, W.; Robert, S.; Kunert, O., Complete assignments of 1H and 13C NMR resonances of oleanolic acid, 18a-oleanolic acid, ursolic acid and their 11-oxo derivatives. *Magn. Reson. Chem.* **2003,** *41*.

60. Suhagia, B. N.; Rathod, I. S.; Ezhava, S. B.; Patel, J., A simple method for the isolation and estimation of ursolic acid in Alstonia Scholaris R. BR. *Int J Pharm Sci Res* **2013,** *4* (7), 2807.

61. Birhanu, G., Isolation of ursolic acid from the leaves of Ocimum lamiifolium collected from Addis Ababa Area, Ethiopia. *African Journal of Biotechnology* **2020,** *19* (2), 65-70.

62. Tshilanda, D. D.; Onyamboko, D. N.; Babady-Bila, P.; Ngbolua, K.-t.-N.; Tshibangu, D. S.; dia Fita Dibwe, E.; Mpiana, P. T., Anti-sickling Activity of Ursolic Acid Isolated from the Leaves of Ocimum gratissimum L. (Lamiaceae). *Natural Products and Bioprospecting* **2015,** *5* (4), 215-221.

63. Hao, J.; Zhang, P.; Wen, X.; Sun, H., Efficient Access to 2-Isobetulinic Acid, 2-Isooleanolic Acid, and 2-Isoursolic Acid. *The Journal of Organic Chemistry* **2008,** *73* (18), 7405-7408.

64. De Felice, A.; Bader, A.; Leone, A.; Sosa, S.; Loggia, R. D.; Tubaro, A.; De Tommasi, N., New polyhydroxylated triterpenes and anti-inflammatory activity of Salvia hierosolymitana. *Planta Med* **2006,** *72* (7), 643-9.

65. Tori, K.; Seo, S.; Shimaoka, A.; Tomita, Y., Carbon-13 NMR spectra of olean-12-enes. Full signal assignments including quaternary carbon signals assigned by use of indirect 13C, 1H spin couplings. *Tetrahedron Letters* **1974,** *15* (48), 4227-4230.

66. Nkouayeb, B. M. N.; Azebaze, A. G. B.; Tabekoueng, G. B.; Tsopgni, W. D. T.; Lenta, B. N.; Frese, M.; Sewald, N.; Vardamides, J. C., Chemical Constituents of Nauclea vanderguchtii. *Natural Product Sciences* **2020,** *26* (2), 144-150.

67. Zeng, J.; Huang, T.; Xue, M.; Chen, J.; Feng, L.; Du, R.; Feng, Y., Current knowledge and development of hederagenin as a promising medicinal agent: a comprehensive review. *RSC advances* **2018,** *8* (43), 24188-24202.

68.   Kim, D.; Lee, S. K.; Park, K.-S.; Kwon, N.-Y.; Park, H.-J., Isolation of constituents with nitric oxide synthase inhibition activity from Phryma leptostachya var. asiatica. *Natural Product Sciences* **2019,** *25* (1), 34-37.

69.   Zhang, L. J.; Cheng, J. J.; Liao, C. C.; Cheng, H. L.; Huang, H. T.; Kuo, L. M.; Kuo, Y. H., Triterpene acids from Euscaphis japonica and assessment of their cytotoxic and anti-NO activities. *Planta Med* **2012,** *78* (14), 1584-90.

70.   Han, J. S.; Kim, J. G.; Le, T. P. L.; Cho, Y. B.; Lee, M. K.; Hwang, B. Y., Pentacyclic triterpenes with nitric oxide inhibitory activity from Potentilla chinensis. *Bioorg Chem* **2021,** *108*, 104659.

CHAPTER 4: Anti-diabetic screening, characterization and isolation of compounds from *Sclerocarya birrea* leaves

4.1 Introduction

4.1.1 Background to the genus

The genus *Sclerocarya* belongs to the Anacardiaceae family, which comprises of 800 species distributed in 81 genera and occurs in tropical and subtropical areas.[1] Several species of this family show significant economic importance due to their woods for carpentry, fruits, and edible seeds, all of them with expressive commercial value.[1] From its hard seed or nut, the genus *Sclerocarya* was derived from the Greek words which are Sklero meaning hard and Karyon meaning nut.[2] The genus *Sclerocarya* has two species that are endemic to sub-Saharan Africa, Madagascar and eastern Kenya namely, *Sclerocarya birrea* and *Sclerocarya gilettii*.[3]

The class of compounds known to occur in this genus includes polysaccharides, essential oil, lipids, resins and phenolic compounds.[4] The current study focuses on the species *S. birrea* (A. Rich) Hoscht commonly referred to as Marula. It is one of the most recognized indigenous trees belonging to the Anacardiaceae family.[5] It is in this family because of its dioecy nature, resin canals in the outer covering as well as its production of plumpy fruits by female trees.[3] *S. birrea* is one of the commonly utilized indigenous wild fruits in Africa.[6] It is a multipurpose tree highly appreciated by rural communities, mainly for its fruits but also for its cosmetic oil from the seed and medicinal properties from the bark and leaves.[7]

4.1.2 Botany and geographical distribution

S. birrea is a deciduous medium size tree that can grow up to 18 m in height (figure 4.1). It bears fruit from January to March, flowers from September to November and is leafless for several months of the year.[8,9] The fruits are edible yellow oblong shaped (3-4 cm in diameter) with plain tough skin and juicy mucilaginous flesh.[9] It produces seeds that encloses 2-3 soft white edible kernels which are rich in oil and protein.[10] It is commonly known as Cider tree or Marula in English; Maroela in Afrikaans and Umganu in Zulu.[11] The *S. birrea* tree has a spreading crown, and the leaves are 8 to 38 cm long with elliptic shape and smooth margins.[12,13] They are imparipinnate and alternate with 3-18 pairs of leaflets which are dark green above and pale bluish-green below.[14]

S. birrea occurs on a wide variety of soil types such as deep sands on granite and basaltic clays. It prefers well-drained soils in areas with a mean annual rainfall of 200-1500 mm.[14] It has variable fruit size but is roughly plum sized. *S. birrea* abscises before ripening at which stage the skin color is green and the fruit firm. The ripe fruits have a thick yellow peel and translucent whitish flesh.[15] The *S. birrea* tree is present in most parts of Africa, particularly in the lowland of KwaZulu Natal (South Africa) from where it projects northwards through tropical Africa into Sudan and Ethiopia. In South Africa, the tree is also present in Swaziland, Botswana, Angola, Zimbabwe, Namibia and Malawi.[8] In West Africa, the tree is found in Cameroon, Nigeria, Gambia, and Central African Republic. The tree thrives in various woodland habitats and on sandy loam soils but is more often found in semi-arid and savannah regions of Sub-Saharan Africa.[16] Three subspecies of *S. birrea* are well known: *S. birrea* subsp. *caffra* (Sond) Kokwaro; *S.birrea* subsp. *multifoliolata* (Engl) Kokwaro and *S. birrea* subsp. *birrea*.[17] In Southern Africa, the most common subspecies is caffra which is found in Swaziland, Zimbabwe, Namibia, Botswana and South Africa. In South Africa, it is common in the savannah areas of Northern KwaZulu Natal, Northwest and Mpumalanga provinces.[17]

Figure 4.1: Picture A shows *S. birrea* tree and picture B shows *S. birrea* leaves with fruits. [18, 19](Picture A and B taken from Encyclopedia, W.T.F and PlantZAfrica.com).

4.1.3   Traditional uses of *S. birrea*

Fresh fruit of *S. birrea* can be eaten as well as fermented to make a beer.[20] Jam, wine and fruit juice are products made by processing the fruit.[21, 22] The oil obtained from *S. birrea* kernel is used for different purposes. In the Limpopo region of South Africa, the oil is used to massage babies' face, feet, and hands to prevent dryness of skin, it is also used as a shampoo for fragile,

dry and damaged hair as well as a soap and nose drop for children. In some rural areas in South Africa, it is used to treat leather and preserve meat.[23] The kernels can either be consumed as a snack or mixed with wild spinach and served with maize meal while the oil can be extracted from the kernel using the cold-press method.[21, 22] *S. birrea* leaves are eaten by both wildlife and livestock.[22] The wood carving produces utilitarian items such as plates, spoons, and decorative animal figures. Amarula cream liquor is a commercial alcoholic drink produced from the fermented fleshy part of *S. birrea* fruit and traded worldwide.[24] Fruit, kernel and beer (fermented from *S. birrea*) are sold to generate fees, uniforms and books thereby reducing poverty for poor households.[25] The barks and leaves are used medicinally.[21, 22] Bapedi traditional healers practicing in the Capricon, Sekhukhune and Waterberg districts of the Limpopo province (South Africa) use the bark and fruit juice of *S. birrea* in the treatment of Asthma and related symptoms.[26] *S. birrea* bark is traditionally used in Limpopo province in South Africa in the treatment of Sexually Transmitted Infections specifically HIV/AIDS.[27] The bark is also pounded and mixed with warm water and the infusion is administered as a treatment for diarrhea.[28]

Runyoro et al. reported the traditional use of *S. birrea* root and stem bark in the treatment of oral and oesophageal candidiasis.[29] The bark decoction has been utilized as an anti-cough remedy. The leaves, pulp, fruit and mistletoe are used for hypertension.[30] The Zulus use the fruit as an insecticide also the stem bark decoction is used as a remedy for diarrhea.[24, 31]. Powdered bark is given to pregnant women to regulate the sex of babies.[31] In Cameroon, the stem bark is used in the treatment of diabetes mellitus.[32] *S. birrea* leaves, stem bark, roots and fruits are used in Ghana in the treatment of snake bite, splenomegaly, goiter and pharyngitis.[32] Some South African communities use the leaves and stem bark in the management of diarrhea, dysentery, stomach ailment, inflammation, ulcer, hypertension, skin disease, fever, diabetes mellitus and malaria.[11] Venda inhabitants of South Africa use the stem bark in the treatment of fever, stomach ailment and ulcer.[24] In East Africa, *S. birrea* roots are utilized as an ingredient in an alcoholic, phytomedicine for the treatment of an internal ailment called 'Kati' while the bark is used to manage stomach disorder.[33] The Hausa native of West Africa uses the cold infusion of *S. birrea* stem bark as a treatment for dysentery.[34] The gum obtained from the tree is rich in tannins and therefore is employed in ink substitute production.[31] *S. birrea* wood is used by South Africans and Zimbabweans in the production of drums, toys, dishes, carvings and divining bowls.[35] The fruit peel from *S. birrea* is used in the manufacture of oil for cosmetic purposes.[36] The Vharenda people of South Africa use the stem bark for treating ulcer, fever

and stomach ailment.[24] The smoke produced by burning dried seeds of the *S. birrea* plant has been used to repel mosquitoes in the uMkhanyakude district, KwaZulu Natal province and South Africa.[37]

The disadvantage of using bark as a source of medicinal components is that the injudicial removal of bark can lead to the death of the plant. Leaves are a more sustainable resource than bark, they could be used without any detrimental effect on the plant.[24]

4.1.4 Previously reported biological efficacy of *S. birrea* as an anti-diabetic agent

S. birrea (A. Rich) Hoscht also known as the tree of life is a popular member of the Anacardiaceae family. Different biological activities have arisen from various parts of *S. birrea* including anti-diabetic properties thereby providing scientific evidence to support the traditional medicinal uses of the plant.[11, 31, 38] Ojewole et al. studied the use of the aqueous extract of *S. birrea* stem bark in the management of pain, arthritis, inflammation and adult-onset type 2 diabetes mellitus (T2DM) in rat and mice models. The aqueous extract produced dose-dependent and significant protection against electrical heat- induced pain as well as production of dose and time-related significant and sustained reduction in the fresh egg albumin-induced acute inflammation of the rat hind paw edema. In addition, moderate to high doses of the aqueous extract gave rise to dose-dependent and a significant reduction in the level of blood glucose of both fasted diabetic and normal rats.[39] *In-vitro* anti-diabetic activity of aqueous and methanol extracts of *S. birrea* was investigated. The extracts showed *in-vitro* anti-diabetic activity by inhibiting α-amylase and α-glucosidase activity in a dose-dependent manner comparable to the positive control acarbose. The methanol extract had better anti-diabetic activity than the aqueous extract by reducing elevated serum glucose levels in T2DM. Furthermore, both extracts also significantly increased glucose uptake in C2C12 myotubes, 3T3-L1adipocytes and HepG2 hepatocarcinoma cells.[40] The use of *S. birrea* stem bark in the management of diabetes was investigated by Ojewole et al.[11] The aqueous extract of the stem bark restored lipidemia, glucose tolerance, hepatic function, oxidative stress and prevention of high blood pressure induced by the application of oxidized palm oil and sucrose in rat's diet.[41]

Dimo et al. showed that the 1:1 methanol/methylene chloride extract of *S. birrea* stem bark exhibited hypoglycemic activity and an increase in plasma insulin levels in streptozotocin-induced diabetic rats. The effective concentration of the plant extract (300 mg/kg) also reduced

urea, triglyceride, and plasma cholesterol levels. Furthermore, the oral glucose tolerance in rats treated with the plant extract was improved significantly.[32] This study suggests that *S. birrea* stem bark extract can improve the glucose level balance in streptozotocin-induced diabetes which is associated with increased secretion of insulin.

Victoria-Montesinos et al. investigated how prediabetic participants' glucose metabolism was affected by a nutraceutical supplement based on a natural extract of *S. birrea*. The study was conducted over a ninety-day period with thirty-three subjects assigned to the experimental group (daily administration of 100 mg of the supplement based on a natural extract of *S. birrea*) and thirty-four patients assigned to the placebo group. The oral glucose tolerance test (OGTT) area under the curve (AUC) showed a statistically significant decrease in the experimental group after 40 and 90 days as compared with baseline in this study. Additionally, individuals in the experimental group also experienced a greater fall in systolic blood pressure. In participants with verified prediabetes, this exploratory clinical research suggests the anti-diabetic efficacy of a nutraceutical supplement based on a natural extract of *S. birrea*.[42]

The therapeutic efficacy of *S. birrea* leaves aqueous extract on hepatic steatosis in diabetic mice was assessed by Mabasa et al. When compared to obese control and metformin-treated mice, mice administered with the aqueous extract of *S. birrea* leaves showed significantly lower body and liver weight ($P < 0.05$). Furthermore, hepatic steatosis was considerably reduced in mice given an aqueous extract of *S. birrea* leaves in comparison to mice given metformin and an obese control group ($P < 0.05$). In comparison to the obese control mice, there was a decrease in the expression of fatty acid synthase and an increase in the fatty acid oxidation gene carnitine palmitoyltransferase, which was linked to the decreased lipid buildup. The findings suggest that in diabetic mice, the aqueous extract of *S. birrea* leaves prevents hepatic steatosis.[43]

4.1.5   Reported phytochemistry and biological efficacy of compounds found in *S. birrea* leaves

Phytochemical analysis of *S. birrea* leaves showed the presence of flavonoids, tannins, polyphenols, saponoside, alkaloids and anthocyanins.[44] The flavonoid found in *S. birrea* leaves include quercetin (**68**) and its derivatives (quercetin-3-*O*-α-(5''-galloyl) arabinofuranoside (**69**), quercetin-3-*O*-β-D-(6''-galloyl)galactopyranoside (**70**), quercetin-3-*O*-β-D-(6'-

177

galloyl)glucopyranoside (**71**), quercetin-3-*O*-α-L-rhamnopyranoside (**72**) and quercetin-3-*O*-β-D-glucopyranoside (**73**), myricetin-3-*O*-α-L-rhamnopyranoside (**74**), kaempferol and its derivatives kaempferol-3-*O*-β-D-(6'-galloyl)glucopyranoside (**75**), kaempferol-3-*O*-α-L-rhamnopyranoside (**76**).[45] The same study also reported the presence of (-)-epigallocatechin-3-*O*-galloylester (**77**), gallic acid (**78**) and (-)-epicatechin-3-*O*-galloyl ester (**79**) (figure 4.2).

Quercetin has been reported to control blood glucose levels through elevation of the expression of GLUT-4 and enhances the uptake of glucose on the skeletal muscle cell surface through the stimulation of the adenosine monophosphate activated protein kinase (AMPK) pathway.[46] Zhang et al. reported that quercetin-3-O-α-L-rhamnopyranoside exhibited moderate α-glucosidase inhibitory activity with an IC_{50} value of 374.94 ± 4.35 µg/mL.[47] Kaempferol has been reported to inhibit α-amylase and α-glucosidase with an IC_{50} values of 51.24 and 29.37 µg/mLrespectively.[48] Prasad et al. reported that gallic acid increases GLUT4 translocation and glucose uptake activity in an Akt-independent manner.[49] The chemical composition and seasonal variation of essential oil of *S. birrea* leaves cultivated in Benin were studied using steam distillation, Gas Chromatography-Flame Ionization Detector (GC-FID) and Gas Chromatography-Mass Spectrometry (GC-MS) method. A total of 49 compounds were identified, and they represented 98% of the hydro-distillate. The oil is composed of about 96% sesquiterpene. The percentage oil content varied between the cold and hot seasons of which 7-epi-α-selinene (**80**) (38%), α-muurolene (**81**) (25%), valencene (**82**) (17%), β-selinene (**83**) (4.3%), β-caryophyllene (**84**) (3.2%), allo-aromadendrene-epoxide (**85**) (1.5%) and 14-hydroxy-α-humulene (**86**) (1.5%) were the major compounds observed in the hot season while 7-epi-α-selinene (**80**) (51%), β-selinene (**83**) (15%), valencene (**82**) (12%), α-selinene (**87**) (8.1%) and β-caryophyllene (**84**) (1.8%) were observed in the cold season.[50]
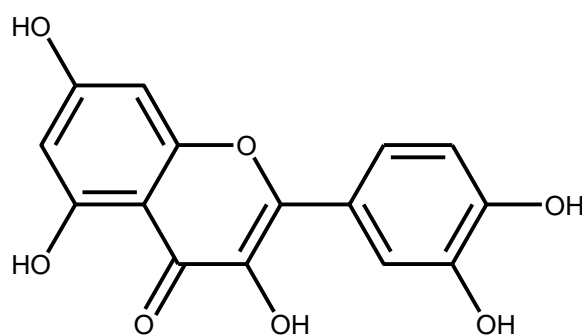
Quercetin (**68**)

178
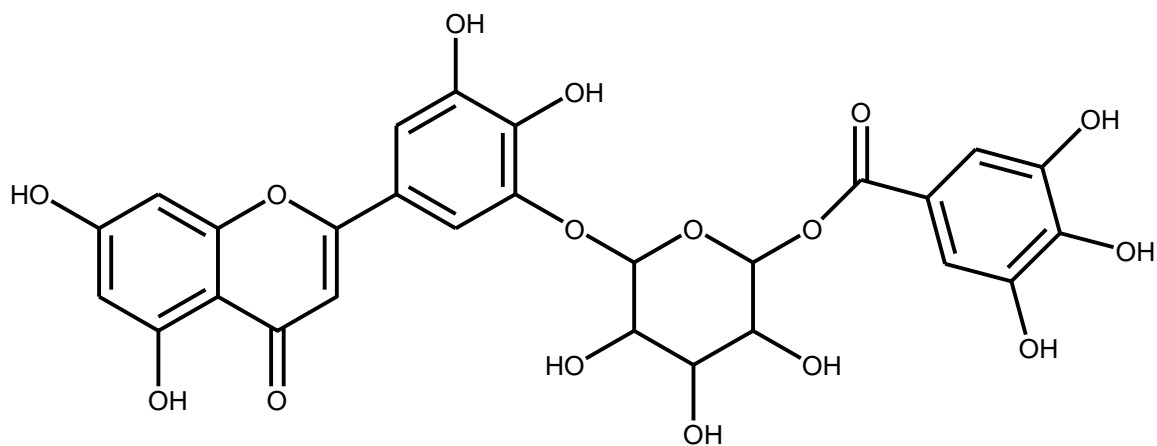
Quercetin-3-O-alpha-(5''-galloyl) arabinofuranoside **(69)**
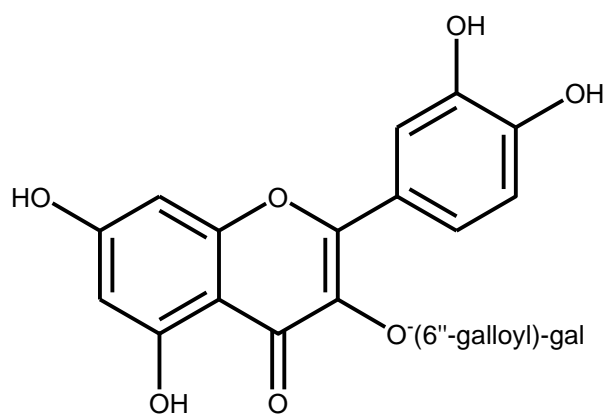
Quercetin-3-O-beta-D-(6''-galloyl)galactopyranoside **(70)**
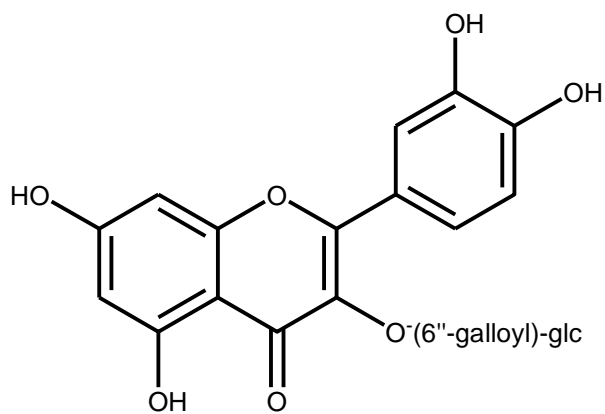
Quercetin-3-O-beta-D-(6'-galloyl)glucopyranoside **(71)**
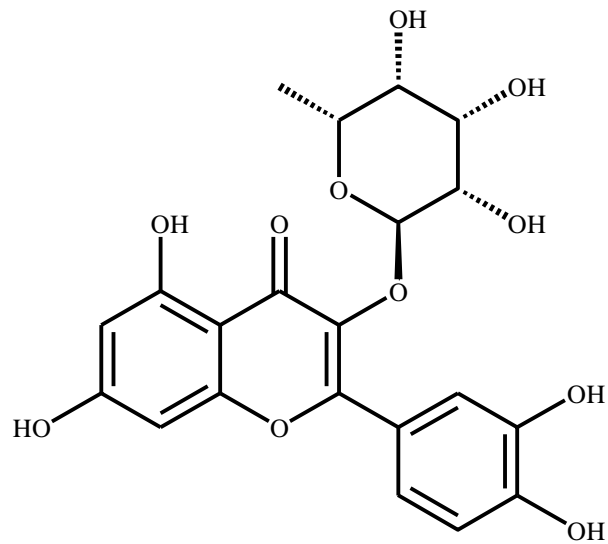
Quercetin-3-O-alpha-L-rhamnopyranoside **(72)**
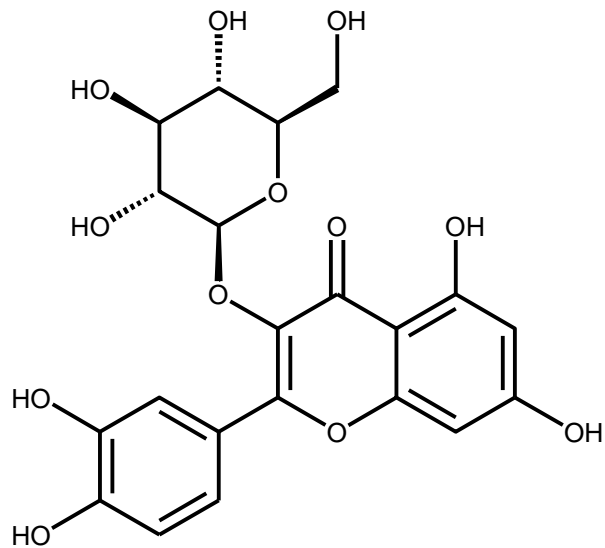
Quercetin-3-*O*-beta-D-glucopyranoside **(73)**
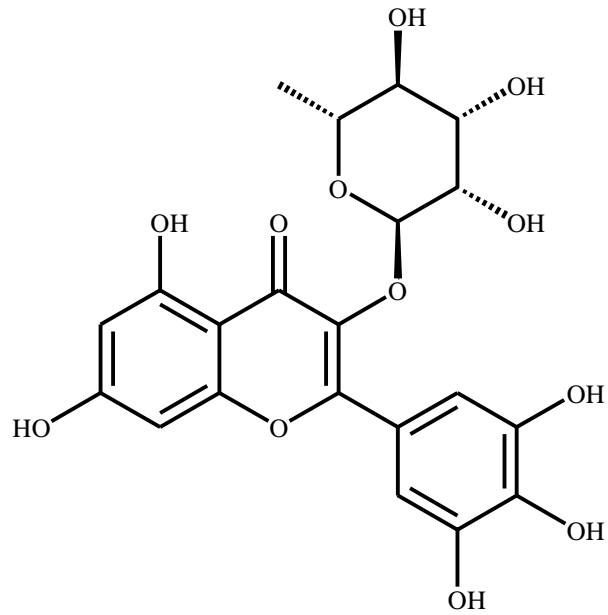
Myricetin-3-O-alpha-L-rhamnopyranoside **(74)**
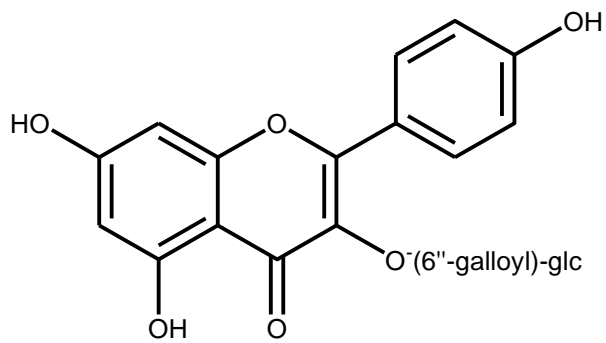
Kaempferol-3-O-beta-D-(6'-galloyl)glucopyranoside **(75)**
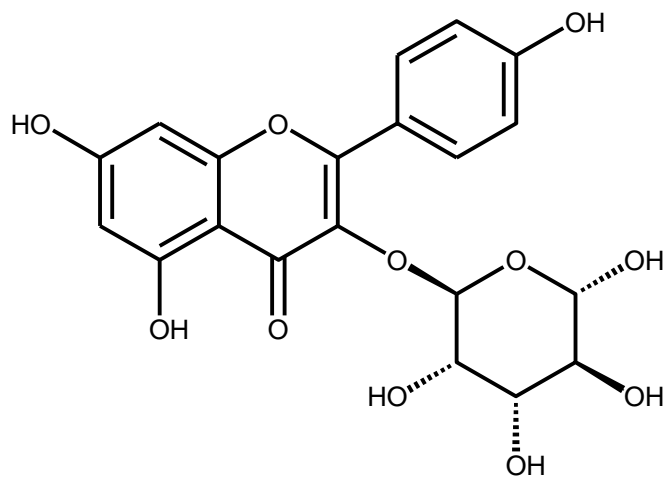
Kaempferol-3-O-alpha-rhamnopyranoside **(76)**
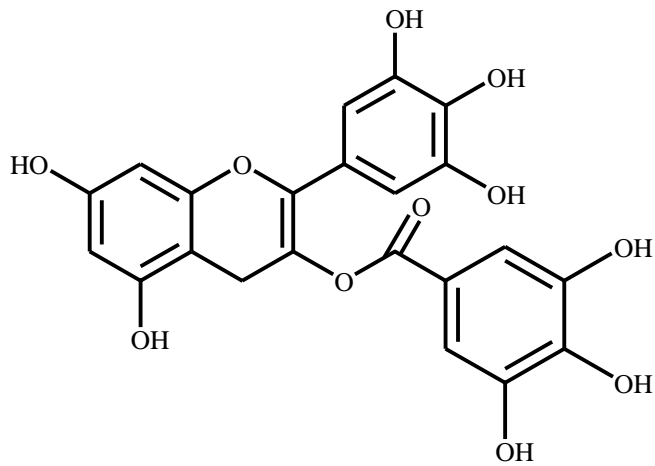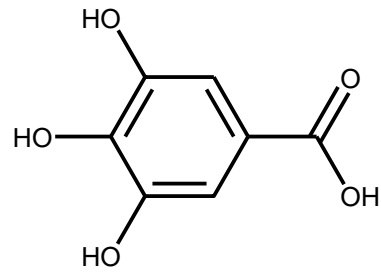
(-)-Epigallocatechin-3-O-galloylester (**77**)   Gallic acid (**78**)
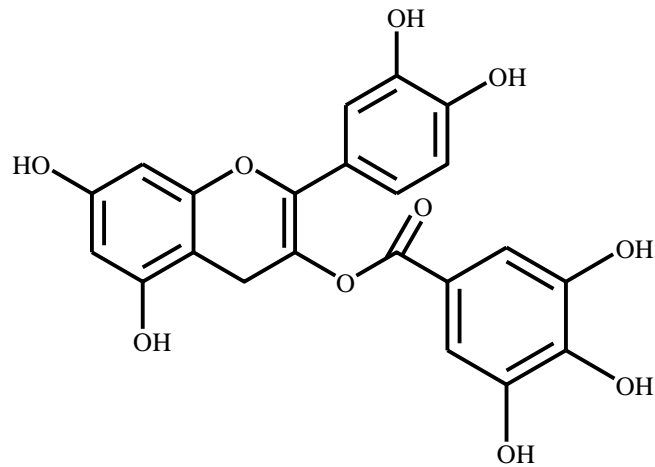
(-)-Epicatechin-3-O-galloyl-ester (**79**)
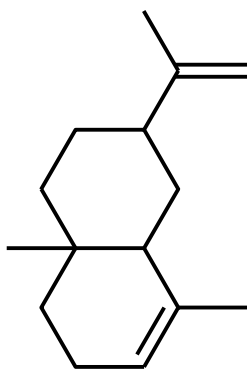
7 epi-alpha-selinene (**80**)   alpha-muurolene (**81**)   Valencene (**82**)
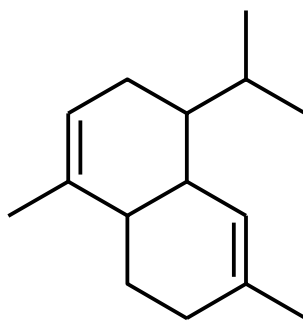
Beta selinene **(83)**   Beta-caryophyllene **(84)** allo-aromadendrene-epoxide **(85)**

14-hydroxy-alpha-humulene **(86)**   alpha-selinene **(87)**
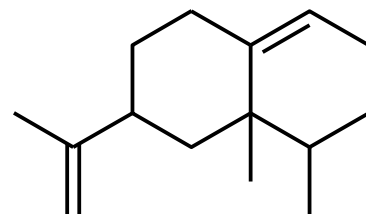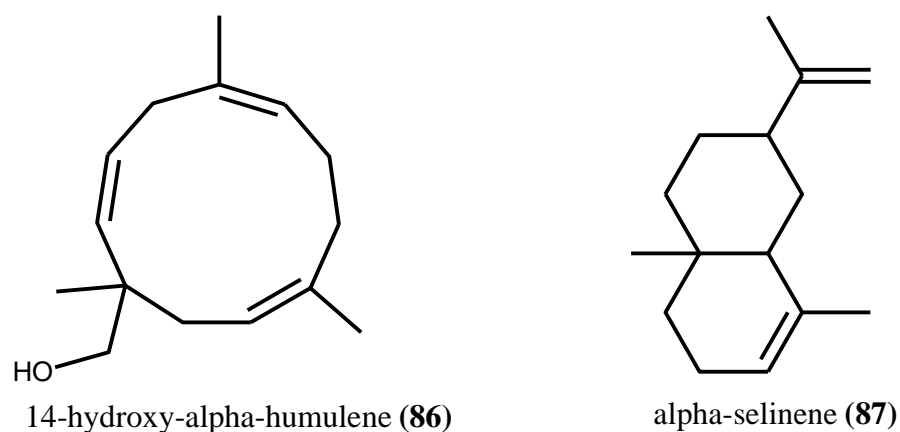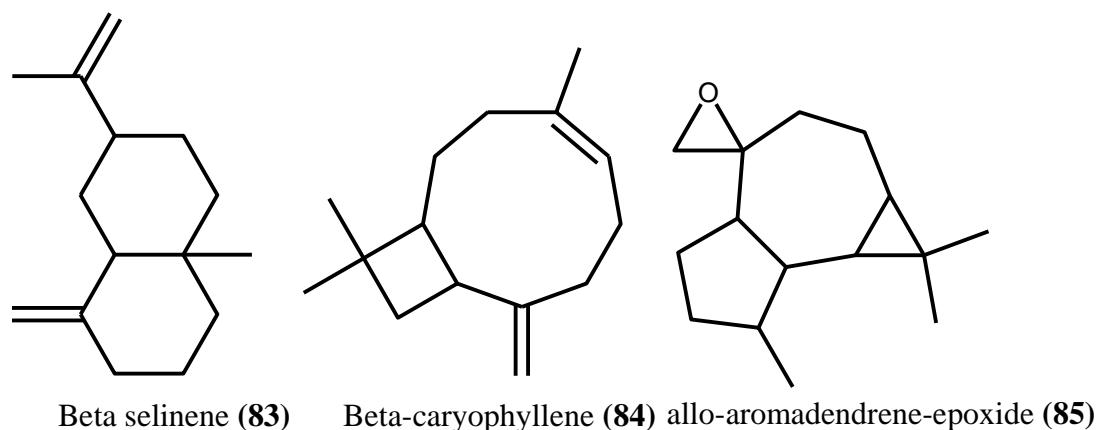
Figure 4.2: Structures of compounds reported from *S. birrea* leaves.

4.2   Materials and methods

4.2.1   Collection and extraction of *S. birrea* leaves

Four batches of *S. birrea* leaves were collected from Limpopo and Mpumalanga provinces in South Africa by the Agricultural Research Council (ARC) and voucher specimens (Organism ID 48536, specimen numbers P25796, P25362, P25359, P25361) were prepared and deposited at the South African Biodiversity Institute (SANBI). Extraction and spray drying were carried out by the Council for Scientific and Industrial Research (CSIR). Aqueous extracts 1, 2, 3 and 4 were separately prepared from the four plant batches and spray-dried. Extraction was carried out in a 50L stainless steel vessel electric operated stirrer running at a slow speed using de-ionized water. The slurry was transferred into a hydraulic press to separate the biomass from liquid through a 50-micron filter bag at the highest pressure of 300 bars. The filtrate from the filtration process was spray-dried using a GEA Niro Pharmaceutical spray drier. All four spray

183

-dried extracts (aqueous extracts 1, 2, 3 and 4) were stored in a room before biological screening.

4.2.2 Fractionation of the spray-dried extract (aqueous extract 4)

The most active spray-dried extract (aqueous extract 4) was fractionated using a positive pressure Solid Phase Extraction (ppSPE) workstation on a reverse phase C8 cartridge (figure 4.3). The flow rate was 5 ml/min. Fractionation was carried out to identify the active compound(s) in the active fraction. Aqueous extract 4 (4.0 kg) was dissolved in 4.5ml of water and adsorbed on cotton wool. It was frozen at -45°C and freeze-dried by the freeze dryer at -56°C and 151 mT. The SPE cartridge (hypersep C8) was equilibrated using 100% methanol and 100% water simultaneously and conditioned using the first solvent system (95:5 water: methanol). The freeze-dried cotton wool containing the sample was placed in an empty cartridge and placed on top of the conditioned SPE cartridge (hypersep C8) and was fractionated into seven fractions (fractions 1-7) using different solvent systems (95:5 water: methanol, 80:20 water: methanol, 60:40 water: methanol, 40:60 water: methanol, 20:80 water: methanol, 0:100 water: methanol and 50:50 acetonitrile: methanol).

Spray dried aqueous extract 4 of *S. birrea* leaves

Dissolve in water (4.5 ml)

Adsorb on cotton wool

Freeze for 3hrs

Freeze-dry

Equilibrate and condition hypersep C8 SPE cartridge

Place the freeze- dried cotton wool containing the sample on top of the conditioned hypersep C8 SPE cartridge

X 10

F1   F2   F3   F4   F5   F6   F7

Active fractions

UPLC-QTOF-MS analysis

3 active compounds tentatively identified and targeted for purification using HPLC-QDA and LC-MS-SPE-NMR

Figure 4.3: Flow diagram showing the bioassay-guided fractionation of the spray-dried aqueous leaf extract of *S. birrea* (Aqueous extract 4).

4.2.3   Chemical analysis of extracts, fractions and compounds
4.2.3.1 UPLC-QTOF-MS analysis of extracts, fractions and compounds

The crude extracts, fractions and compounds were analyzed on Waters acquity ultra-performance liquid chromatography-quadrupole time of flight mass spectrometer (UPLC-QTOF-MS) operating in both positive and negative mode as described in Chapter 2 (section 2.2.5)

4.2.4   Isolation and identification of pure compounds
4.2.4.1 Preparative HPLC fractionation of the active fraction 4

Fraction 4 (1 mg) was dissolved in 1 mL HPLC grade MeOH and then filtered through a 0.22 μm nylon syringe filter (13 mm diameter). The solution was subjected to analysis using an XBridge C18 analytical column (4.6 mm x 150 mm, 5 μm, Waters) for optimization of the

chromatographic conditions. The mobile phase consisted of water + 0.1% FA (solvent A) and MeOH + 0.1% FA (solvent B) at a flow rate of 1.00 mL/min and an injection volume of 10 µL for 27 mins. The gradient method used was as follows: 70.% B (0.00 min), 50% B (1.00 min), 40% B (12.00 mins), 30% B (19.00 mins), 0% B (21.00 mins) and 70% B (27.00 mins). The optimized method was upscaled to the Prep C18 column (19 mm x 250 mm, 5 µm, Waters) using Waters Prep calculator software. Fraction 4 (250 mg) was dissolved in 2.5 mL HPLC grade MeOH and then filtered through a 0.22 µm nylon syringe filter (13 mm diameter). The mobile phase was the same as stated above at a flow rate of 20.00 mL/min (obtained from the calculator) and an injection volume of 200 µL for 45 mins. The gradient method used was as follows: 70% B (0.00 min), 60% B (20.00 mins), 40% B (31.67 mins), 0% B, (35.00 mins) and 70%B (45.00 mins). The preparative HPLC was interfaced with a 2998 PDA detector and a QDA mass spectrometer detector (Waters, Milford, MA, USA) operated in a positive ion mode. The source temperature was 120°C, while the probe temperature was set at 600°C. The capillary and cone voltages were set to 800 and 10V respectively. Targeted masses (m/z 495, 479 and 319) were collected in test tubes (approximately 8 mL capacity) using the waters 2767 fraction collector, which placed the targeted peaks based on their m/z in various separate test tubes. After six injections, the collected peaks with the same m/z were combined and subsequently concentrated to dryness under vacuum by using a Genevac HT series evaporating system. The purity of the collected peaks was checked using proton NMR.

4.2.4.2 LC-MS-SPE-NMR purification of compounds from active fraction 3

Fraction 3 (40 mg) was subjected to mass directed purification using hyphenated liquid chromatography-mass spectrometry-solid phase extraction-nuclear magnetic resonance (LC-MS-SPE-NMR) (figure 4.4). The solution was dissolved in 1 mL HPLC grade MeOH and the resulting solution was filtered through a 0.22 µm nylon syringe filter (13 mm diameter). The separation was achieved on a Phenomenex C18 column (150 x 4.6 mm, 5µm Luna® Omega). The mobile phase consisted of water + 0.1% FA (solvent A) and MeOH+ 0.1% FA (solvent B) at a flow rate of 0.5 mL/min and injection volume of 15 µL for 25 mins. The gradient method used was as follows: 8% B (0.00 min), 50% B (10 mins), 65% B (18 mins) and 100% B (22 mins). Peaks were detected by the PDA detector as they eluted from the column and then trapped in individual allocated SPE cartridges. The loaded cartridges were dried using pressurized nitrogen gas. The two trapped peaks were eluted from the cartridges to pre-weighed vials using the SamplePro Tube liquid handler. Data collected using HyStarTM software

186

package. The solvents were evaporated to dryness using a Genevac HT series evaporating system. The two peaks were analysed by proton NMR to check for their purity.
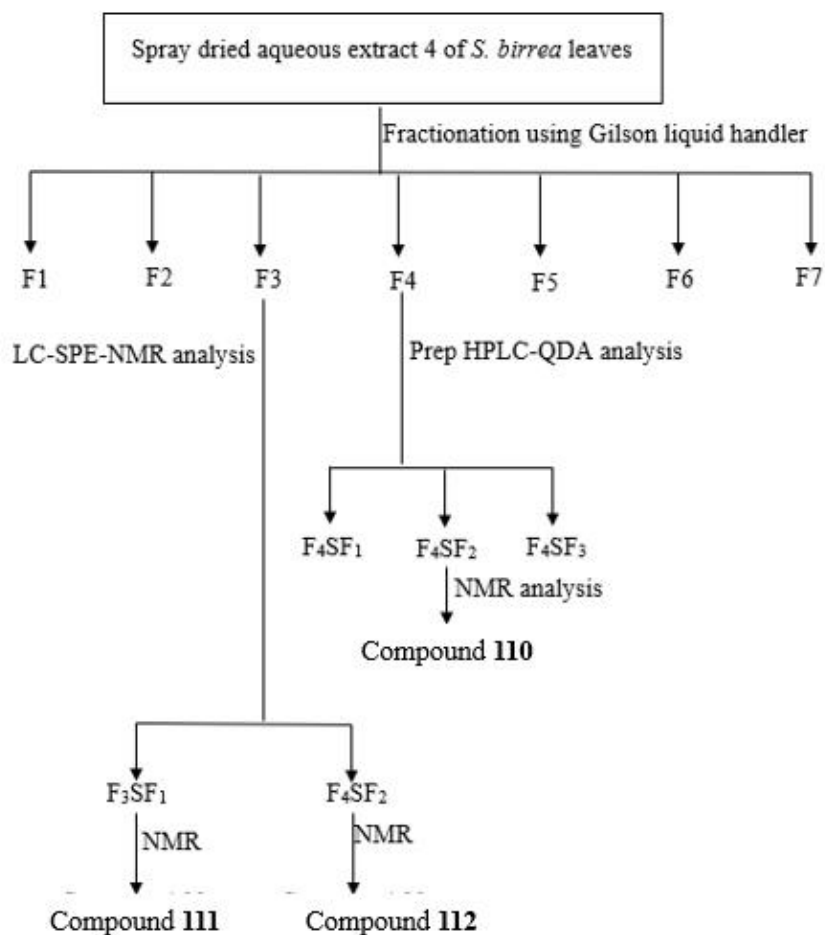
Figure 4.4: Flow diagram showing the purification of the active fractions from spray-dried aqueous extract 4 of *S. birrea* leaves.

4.2.5 NMR analysis of pure compounds

NMR analysis of pure compounds was conducted using Bruker Avance III 400 MHz and 500 MHz spectrophotometers equipped with a prodigy probe as described in Chapter 3 (section 3.2.4).

4.2.6   Biological screening of extracts, fractions and compounds from *S. birrea* leaves

The biological screening was carried out at the Biomedical Research and Innovation Platform, South African Medical Research Council (SAMRC).

187

4.2.6.1 Glucose uptake assay

A glucose uptake assay kit (Promega Glucose Uptake -GLO Assay, Maidson, WI, USA) was used to estimate glucose uptake according to the described technique.[51] C2C12 mouse skeletal muscle cells (American Type Culture Collection (ATCC), cat CRL 1722 (Manassas, VA, USA)), were sub-cultured and differentiated using a modified method of Muller et al. (2012). [52] C2C12 muscle cells were seeded into 24-well plates (25,000 cells/well). The C2C12 cells were maintained in DMEM supplemented with 10% FCS at 37 °C in 5% CO2 in humidified air for 3 days (to 80–90% confluency). Thereafter, the 10% FCS was substituted with 2% horse serum for a further 2 days to induce myocytic differentiation before performing the assay. Briefly, C2C12 myocytes were exposed for 40 min to test samples prepared in Krebs ringer bicarbonate HEPES buffer (KRBH) and 2 percent BSA without glucose before being treated for one hour with relevant fraction concentrations ranging from 0.01 to 100 µg/mLof the test samples. The intracellular build-up of 2-deoxyglucose-6-phosphate (2DG6P) after a 30 min treatment was used to determine 2-deoxyglucose uptake measured by the luminescent signal proportional to 2DG6P concentration using a SpectraMax® i3x Multi-Mode Microplate Reader (Molecular Devices, San Jose, CA, USA). The means and standard deviations of three different experiments were used to calculate all of the data. Statistical differences between groups were assessed using one-way ANOVA with Dunnett's post hoc test. For graphic depiction and statistical analysis, GraphPad 6 software was employed. Statistical significance was defined as a value of $p = 0.05$.

4.2.6.2 Cytotoxicity assay

Mosman et al. established a colorimetric-based assay for detecting cell metabolic activity called 3-[4,5-dimethylthiazol-2-yl]-2,5-diphenyltetrazolium-bromide (MTT) for determining cell viability.[53] C2C12 muscle cells were seeded into 96-well plates (5000 cells/well). Briefly, 10 µL of stock MTT solution was added to the assay wells and incubated for 4 hr at 37 °C. To dissolve the dark blue formazan precipitate, 100 µL of 0.04N HCL in isopropanol was added to each well and carefully mixed. To determine MTT activity, the absorbance of each well was measured at 570 nm on a SpectraMax® i3x Multi-Mode Microplate Reader after a few minutes at room temperature to guarantee full dissolution of the crystals.

188

4.3 Results and discussion

4.3.1 Collection and extraction of *S. birrea* leaves

The plant leaves were harvested in four batches from various locations and seasons. Plants were collected over different years (2014–2017) from Limpopo and Mpumalanga. Extraction and spray drying were carried out by the Council for Scientific and Industrial Research (CSIR). Aqueous extracts 1, 2, 3 and 4 were separately prepared from the four plant batches and spray-dried over different years (2014–2017). Aqueous extract 2 was prepared and spray-dried from plant material that was in storage for two to three years while aqueous extracts, 1, 3 and 4 were prepared and spray-dried after receiving harvested plant material (table 4.1).

Table 4.1: Plant harvesting, extraction, spray drying and yields of *S. birrea* (Marula) leaves

Extract	Harvesting date by Year	Extraction/Spray drying date by year	Harvest Location (Province)	Mass of Leaves Extracted	Mass of spray dried extract	% Extraction yield
Aqueous extract 1	Ending of 2013	Beginning 2014	Limpopo	9.4 kg	1.070 Kg	11%
Aqueous extract 2	2014	2017	Mpumalanga	4.0 Kg	0.521 Kg	13%
Aqueous extract 3	Ending of 2014	Beginning 2015	Mpumalanga	4.0 kg	0.348 Kg	9%
Aqueous extract 4	2017	2017	Mpumalanga	4.0 Kg	0.783 Kg	20%

The plant material collected from Limpopo produced a lower yield (11%) of aqueous extract than the plant material collected from Mpumalanga (20% yield). The result of the percentage yield of extraction of all the plant collections shows that a higher extraction yield (20%) was obtained for the recent collection of *S. birrea* leaf material carried out in 2017 (aqueous extract 4) as compared to 11.4% and 13.03% for the 2014 harvest (aqueous extracts 1 and 2, respectively) (table 4.1). The lower extraction yield from the 2014 collection (aqueous extracts 1 and 2) could be attributed to seasonal variation, rainfall received during the harvest season in addition to storage conditions of the plant material over time. The age of the plant material in the different seasons can also be a contributing factor. The lower extraction efficiency (13.03%) of the 2014 harvest (aqueous extract 2) as compared to the extraction efficiency (20%) for the

189

2017 plant collection (aqueous extract 4) can also be attributed to not extracting the plant material immediately after harvest. The storage condition would have contributed to its low extraction yield. As a result, it is recommended that the plant material be extracted as soon as possible following harvest.

4.3.2 Effect of plant extracts on glucose uptake

The four aqueous spray-dried extracts were evaluated for their effect on glucose uptake in differentiated C2C12 myocytes. *In vitro,* differentiated C2C12 myocytes are representative of skeletal muscle, the major insulin-responsive tissue responsible for more than 75% of insulin-mediated glucose disposal from the peripheral circulation. The glucose uptake results for aqueous extracts 1, 2, 3 and 4 tested at different concentrations (0.01, 0.1, 1, 10, 100 µg/mL) are shown in figure 4.5.
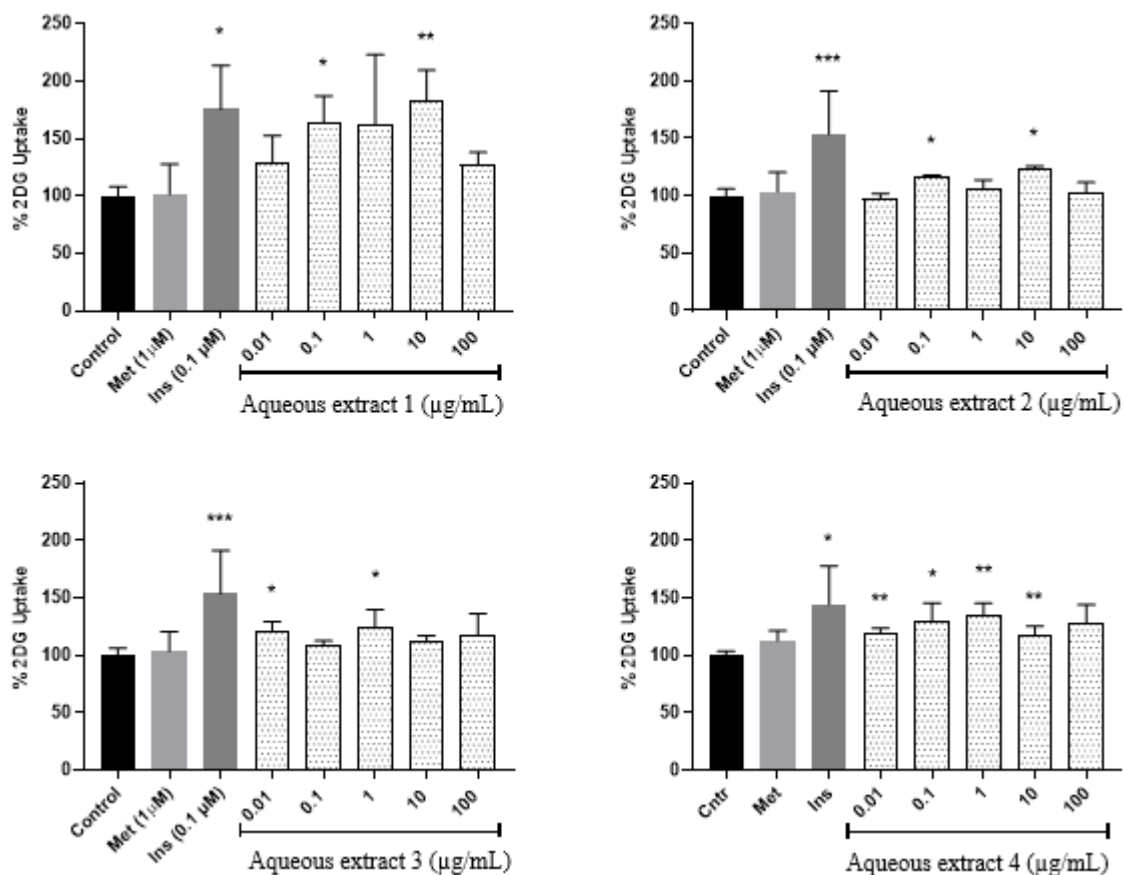
Figure 4.5: Glucose uptake in C2C12 myocytes. Glucose uptake activity % estimated from 2-deoxy-D-glucose uptake in C2C12 myocytes exposed to the *S. birrea* leaf extracts at different concentrations over one hour. The percentage is expressed

relative to the control set at 100%. Insulin (Ins) and metformin (Met) were included as positive and drug reference controls respectively. *p* value < **p* < 0.05, **p < 0.01, ***p < 0.001.

Both aqueous extracts 1 and 4 caused significant increases in glucose uptake in C2C12 cells. Aqueous extract 1 significantly increased glucose uptake in C2C12 cells (p < 0.5) at 0.1 µg/mLand at 10 µg/mL(p < 0.01) while aqueous extract 4 significantly increased glucose uptake in C2C12 cells (p < 0.01) at 0.01, 1 and 10 µg/mLand (p < 0.5) at 0.1 µg/mL, respectively. At 10 µg/mL, aqueous extract 1 exhibited higher glucose uptake (180%) compared to the glucose uptake stimulated by the positive control insulin (170%) (untreated control is measured as 100% uptake) whilst at 0.1 µg/mLit was marginally lower (140%). Similarly, aqueous extract 4 increased glucose uptake by 130% at 0.1 µg/mL, 120% at 1 µg/mL, 120% at 0.01 µg/mLand 110% at 10 µg/mL, albeit slightly lower than the positive control insulin (140%) but higher than the reference drug metformin (figure 4.5). This showed the presence of compound(s) with the potential to stimulate glucose uptake comparable to that of insulin in both extracts. A similar glucose absorption pattern was demonstrated in a study conducted by Da Costa Mousinho et al. on the aqueous extract of *S. birrea* bark which revealed the dose-dependent glucose uptake by the C2C12 cell line with significant glucose absorption (p < 0.05) at 1.56–6.25 µg/mLwhich is comparable to the glucose uptake activity result obtained in this study.[54] Another study has reported that an aqueous extract of *S. birrea* stem bark increased glucose uptake in treated RIN-m5F pancreatic beta cells at concentrations ranging from 3.12–50 µg/mLin a dose-dependent manner with substantial glucose uptake observed at 25, 50 and 100 µg/mL(p < 0.001).[55]

4.3.3   Cell viability of active extracts

The MTT cell viability assay was carried out for the two most active extracts (aqueous extracts 1 and 4) to confirm that the test samples were not toxic to the cells (figure 4.6).
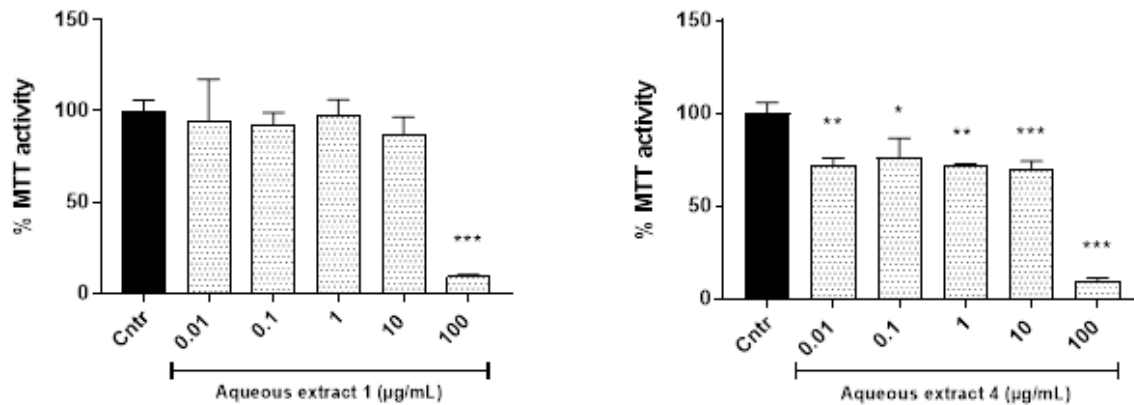
Figure 4.6: MTT cell viability assay of C2C12 myocytes treated with extract for 72 hours. The data are presented as mean $\pm$ SD, expressed relative to the control at 100%. p value $<$ *$p < 0.05$, **$p < 0.01$. ***$p < 0.001$.

Aqueous extract 1 only decreased cell viability at the highest concentration of 100 µg/mLAfter 72 h of exposure. Aqueous extract 4 induced decreased cell viability at all tested concentrations by 25% while it also significantly induced decreased cell viability at 100 µg/mLby 80%. It is therefore established that the extracts become cytotoxic to the cells above a concentration of 10 µg/mL.

4.3.4 Identification of chemical markers from the active spray-dried aqueous extracts of *S. birrea* leaves

A chemical analysis of aqueous extracts 1 and 4 was undertaken to identify common peaks in the extracts which could be responsible for the observed biological activity. Figures 4.7 and 4.8 show the UPLC-QTOF-MS chemical profiles of the active spray-dried aqueous extracts 1 and 4 operating in negative and positive electrospray (ESI) ionization modes, respectively.

192
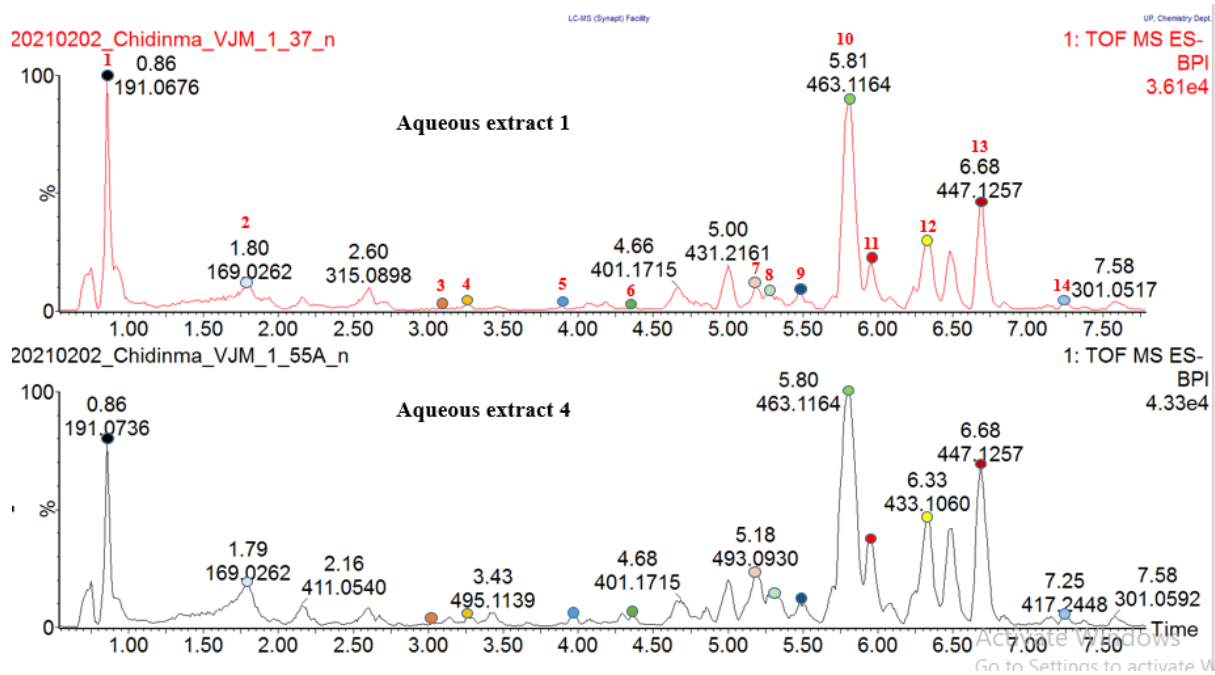
Figure 4.7: ESI negative mode BPI chromatogram of active spray-dried aqueous extracts 1 and 4.

Fourteen compounds were tentatively identified by comparing their accurate masses and MS/MS fragmentation patterns with compounds in databases such as Metlin, Metfusion, Chemspider, Pubchem, Dictionary of Natural Products and Waters UNIFY ® Scientific Information System.
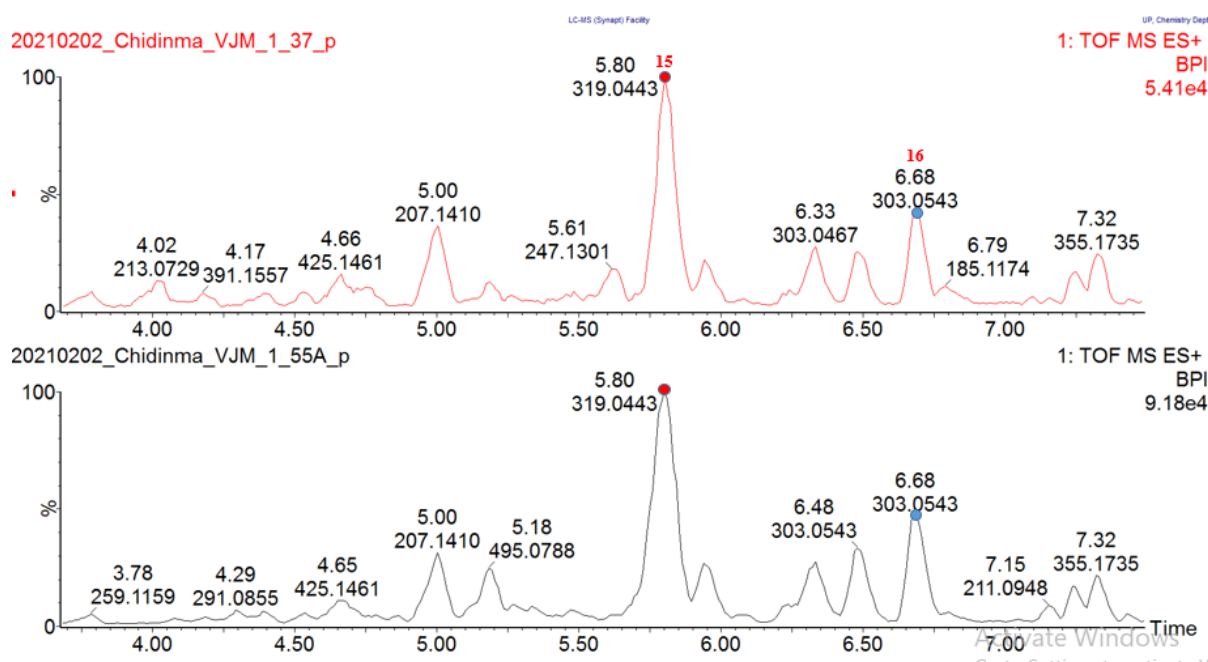
Figure 4.8: ESI positive mode BPI chromatogram of active spray-dried aqueous extracts 1 and 4.

Two compounds were tentatively identified by comparing their accurate masses and MS/MS fragmentation pattern with compounds in databases such as Metlin, Metfusion, Chemspider, Pubchem, Dictionary of Natural Products and Waters UNIFY® Scientific Information System (version 1.9.2) accessing the Chinese Natural Products database. The sixteen compounds tentatively identified (which include two organic acids, one proanthocyanidin, five flavonoids, one gallotannin, two flavonoid glucuronides and five flavonoid glycosides) were common in both extracts (aqueous extracts 1 and 4), indicating the two extracts are chemically similar and these compounds may be responsible for the glucose uptake activity observed in the two extracts. Compounds tentatively identified by UPLC-QTOF-MS analysis of the spray-dried aqueous extract 4 are shown in table 4.2.

A minor peak (peak 11) with *m/z* 477.1037 (at the retention time 5.94 minutes) was present in both active extracts in the negative mode. Another minor peak (peak 6) with *m/z* 289.0920 (at the retention time 4.29 minutes) was present in both active extracts in the negative mode. A very minor peak (peak 2) with *m/z* 169.0262 (at retention times 1.69-1.80 minutes) was present in both active extracts in the negative mode. The major peak (peak 15) with *m/z* 319.0443 (at the retention time 5.80 minutes) was present in both active extracts in the positive mode. The intense peak (peak 16) with *m/z* 303.0543 (at the retention time 6.68 minutes) was present in

194

both active extracts in the positive mode. The structures of the compounds corresponding to the labelled peaks (2, 6, 11, 15 and 16) were tentatively identified using accurate mass data and mass fragmentation patterns as described in this section below. These common compounds could be responsible for the anti-diabetic activity of the extracts. Confirmation of the compounds requires isolation and purification, and biological screening of the compounds will confirm if they are responsible for the activities of the extracts.

Table 4.2 shows accurate mass, formula and MS/MS data for compound fragments tentatively identified from the active spray-dried aqueous extracts of *S. birrea* leaves (aqueous extracts 1 and 4).

Table 4.2: Compounds tentatively identified using UPLC-QTOF-MS analysis of the spray-dried aqueous extract of *S. birrea* leaves

Peak No.	RT (min)	Acquired [M-H]⁻ m/z	Formula	Calculated [M-H]⁻ m/z	Possible structure	Mass error (ppm)		MS/MS Data (fragments)	Reference
1	0.86	191.0582	$C_7H_{12}O_6$	191.0556	quinic acid **(Organic acid)**	2.1	96.9628	$[M-H]^-$-$2H_2O$-$4H_2$-CO_2-O	[56]
							85.0324	$[M-H]^-$-CO_2-H_2O-$C_2H_4O_2$	
							169.0149	$[M-H]^-$-H_2O-$2H_2$	
							125.0267	$[M-H]^-$-H_2O-$4H_2$-CO_2	
2	1.79	.169.0166	$C_7H_6O_5$	169.0137	gallic acid **(Organic acid)**	4.1	125.0273	$[M-H]^-$-CO_2	[56]
							151.0037	$[M-H]^-$-H_2O	
							79.0213	$[M-H]^-$-CO_2-H_2O-CO	
3	3.03	577.1329	$C_{30}H_{26}O_{12}$	577.1346	procyanidin B2 **(Proanthocyanidin)**	-2.4	125.0284	$[M-H]^-$-$C_{24}H_{20}O_9$	[57]
							169.0152	$[M-H]^-$-$C_{22}H_{16}O_8$	
							289.0711	$[M-H]^-$-$C_{15}H_{12}O_6$	
							407.0763	$[M-H]^-$-$C_8H_8O_3$-H_2O	
							451.0951	$[M-H]^-$-$C_6H_6O_3$	
							109.0325	$[M-H]^-$-$C_{24}H_{20}O_{10}$	
4	3.29	305.0664	$C_{15}H_{14}O_7$	305.0661	gallocatechin **(Flavonoid)**	1.0	125.0251	$[M-H]^-$-$C_9H_8O_4$	[58]
							137.0260	$[M-H]^-$-$C_8H_8O_4$	
							165.0231	$[M-H]^-$-$C_6H_2O_3$-H_2O	
							169.0153	$[M-H]^-$-$C_7H_4O_3$	
							109.0320	$[M-H]^-$-$C_9H_8O_5$	
5	3.96	647.0889	$C_{28}H_{24}O_{18}$	647.0884	pistafolin A **(Gallotannin)**	0.3	169.0165	$[M-H]^-$-$C_{21}H_{18}O_{13}$	[59]
							125.0267	$[M-H]^-$-$C_{22}H_{18}O_{15}$	
							343.0704	$[M-H]^-$-$C_{14}H_8O_8$	

196

#	RT		Formula		Name		Fragment	Assignment	Ref
							173.0495	[M-H]⁻-C$_{21}$H$_{10}$O$_{13}$	
							495.0775	[M-H]⁻-C$_7$H$_4$O$_4$	
6	4.29	289.0735	C$_{15}$H$_{14}$O$_6$	289.0712	epicatechin **(Flavonoid)**	1.4	125.0267	[M-H]⁻-C$_9$H$_8$O$_3$	[60]
							123.0114	[M-H]⁻-C$_9$H$_{10}$O$_3$	
							137.0247	[M-H]⁻-C$_8$H$_8$O$_3$	
							108.0248	[M-H]⁻-C$_9$H$_9$O$_4$	
							152.0139	[M-H]⁻-C$_7$H$_5$O$_3$	
							169.0180	[M-H]⁻-C$_7$H$_4$O$_2$	
7	5.18	493.0631	C$_{21}$H$_{18}$O$_{14}$	493.0618	myricetin-3-O-β-D-glucuronide **(Flavonoid glucuronide)**	0.8	317.0317	[M-H]⁻-C$_6$H$_8$O$_6$	[61, 62]
							151.0060	[M-H]⁻-C$_{14}$H$_{14}$O$_{10}$	
							137.0261	[M-H]⁻-C$_{14}$H$_{12}$O$_{11}$	
							179.0005	[M-H]⁻-C$_{13}$H$_{14}$O$_9$	
							107.0153	[M-H]⁻-C$_{15}$H$_{14}$O$_{12}$	
8	5.26	479.0834	C$_{21}$H$_{20}$O$_{13}$	479.0826	gossypin **(Flavonoid)**	0.4	316.0238	[M-H]⁻-C$_6$H$_{11}$O$_5$	
							151.0051	[M-H]⁻-C$_{13}$H$_{12}$O$_{10}$	
							271.0272	[M-H]⁻-C$_9$H$_4$O$_6$	
							287.0200	[M-H]⁻-C$_9$H$_4$O$_5$	
9	5.50	615.0966	C$_{28}$H$_{24}$O$_{16}$	615.0986	quercetin 3-O-(6"-galloyl)-Beta-D-glucopyranoside **(Flavonoid glycoside)**	0.2	463.0871	[M-H]⁻-C$_7$H$_4$O$_4$	[45]
							300.0294	[M-H]⁻-C$_{13}$H$_{15}$O$_9$	
							316.0228	[M-H]⁻-C$_{15}$H$_7$O$_7$	
							271.0255	[M-H]⁻-C$_{13}$H$_{12}$O$_{11}$	
							151.0063	[M-H]⁻-C$_{21}$H$_{20}$O$_{12}$	
10	5.80	463.0876	C$_{21}$H$_{20}$O$_{12}$	463.0877	myricetin-3-O-alpha-L-	1.9	316.0236	[M-H]⁻-C$_6$H$_{11}$O$_4$	[45]
							151.0056	[M-H]⁻-C$_{14}$H$_{16}$O$_8$	

197

No.	RT	[M-H]⁻ measured	Formula	[M-H]⁻ calc	Identification	Error (ppm)	Fragment m/z	Fragment assignment	Ref
					rhamnopyranoside		179.0000	[M-H]⁻-C$_{13}$H$_{16}$O$_7$	
					de		271.0252	[M-H]⁻-C$_6$H$_{11}$O$_5$-2H$_2$O	
					(Flavonoid glycoside)		287.0211	[M-H]⁻-C$_6$H$_{11}$O$_5$-H$_2$O	
11	5.94	477.0679	C$_{21}$H$_{18}$O$_{13}$	477.0669	quercetin-3-O-beta-D-glucuronide **(Flavonoid glucuronide)**	1.7	301.0366	[M-H]⁻-C$_6$H$_8$O$_6$	[63, 64]
							151.0056	[M-H]⁻-C$_{14}$H$_{14}$O$_9$	
							179.0002	[M-H]⁻-C$_{15}$H$_{18}$O$_{10}$	
							255.0325	[M-H]⁻-C$_7$H$_{10}$O$_8$	
							271.0258	[M-H]⁻-C$_7$H$_{10}$O$_7$	
12	6.33	433.0780	C$_{20}$H$_{18}$O$_{11}$	433.0771	quercetin-3-O-arabinoside **(Flavonoid glycoside)**	0.0	300.0290	[M-H]⁻-C$_5$H$_9$O$_4$	[64]
							151.0043	[M-H]⁻-C$_{13}$H$_{14}$O$_7$	
							271.0269	[M-H]⁻-C$_6$H$_{10}$O$_5$	
							255.0307	[M-H]⁻-C$_6$H$_{10}$O$_6$	
13	6.68	447.0932	C$_{21}$H$_{20}$O$_{11}$	447.0927	quercetin-3-O-alpha-L-rhamnopyranoside **(Flavonoid glycoside)**	3.4	300.0297	[M-H]⁻-C$_6$H$_{11}$O$_4$	[65]
							151.0060	[M-H]⁻-C$_{14}$H$_{16}$O$_7$	
							255.0310	[M-H]⁻-C$_7$H$_{12}$O$_6$	
							271.0260	[M-H]⁻-C$_7$H$_{12}$O$_5$	
							179.0016	[M-H]⁻-C$_{15}$H$_{20}$O$_8$	
14	7.38	431.0977	C$_{21}$H$_{20}$O$_{10}$	431.0978	kaempferol-3-O-alpha-L-rhamnopyranoside **(Flavonoid glycoside)**	0.0	285.0436	[M-H]⁻-C$_6$H$_{10}$O$_4$	[66, 67]
							125.0257	[M-H]⁻-C$_{15}$H$_{14}$O$_7$	
							227.0390	[M-H]⁻-C$_8$H$_{12}$O$_6$	
							255.0323	[M-H]⁻-C$_7$H$_{12}$O$_5$	
							151.0050	[M-H]⁻-C$_{14}$H$_{16}$O$_6$	

Peak No.	RT (min)	Acquired $[M+H]^+$ m/z	Formula of possible structure	Theoretical $[M+H]^+$ m/z	Possible structure	Mass error (ppm)	MS/MS Data (fragments)		Reference
15	5.80	319.0463	$C_{15}H_{11}O_8$	319.0454	myricetin **(Flavonoid)**	-1.3	153.0194	$[M+H]^+$-$C_8H_6O_4$	[61, 68]
							165.0195	$[M+H]^+$-$C_7H_6O_4$	
							273.0418	$[M+H]^+$-H_2O-CO	
							217.0499	$[M+H]^+$-H_2O-3CO	
							245.0447	$[M+H]^+$-H_2O-2CO	
							137.0236	$[M+H]^+$-$C_7H_6O_4$-CO	
16	6.48	303.0497	$C_{15}H_{10}O_7$	303.0505	quercetin **(Flavonoid)**	-2.6	153.0188	$[M+H]^+$-$C_8H_6O_3$	[69]
							229.0505	$[M+H]^+$-H_2O-2CO	
							285.0414	$[M+H]^+$-H_2O	
							257.0463	$[M+H]^+$-H_2O-CO	
							201.0552	$[M+H]^+$-H_2O-3CO	

The structures of the compounds are shown in figure 4.9.
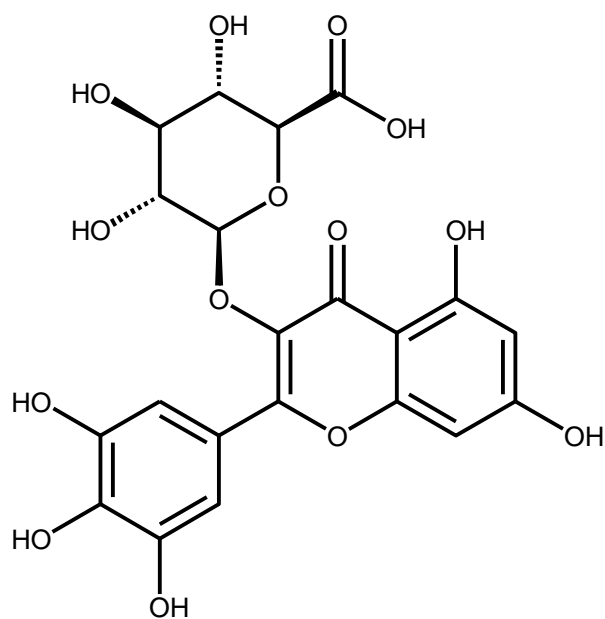
Myricetin-3-*O*-beta-D-glucuronide (**88**)
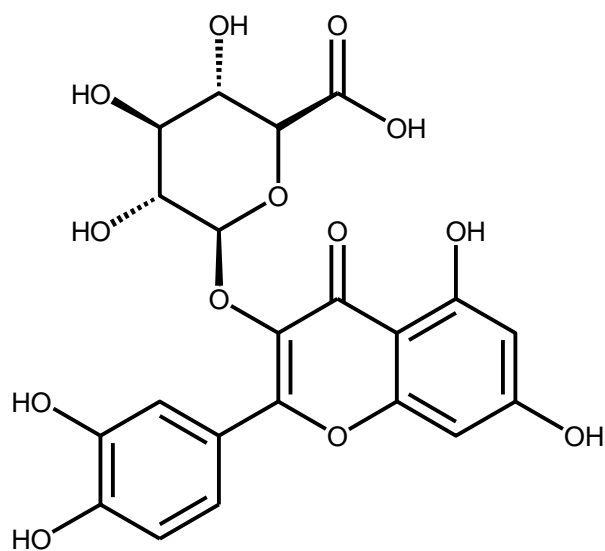
Quercetin-3-O-beta-D-glucuronide(**89**)

Myricetin (**90**)

Figure 4.9: Structures of chemical markers (myricetin-3-O-β-D-glucuronide (**88**), quercetin-3-O-β-D-glucuronide (**89**) and myricetin (**90**) tentatively identified.

In the first order mass spectrum of peak 1, the [M-H]$^-$ ion was observed with *m/z* 191.0582 [M-H]$^-$ at the retention time 0.86 minutes. It had a molecular formula of $C_7H_{11}O_6^-$ with a normalized iFit value of 0.000. Analysis of the MS/MS data revealed that the compound was an organic acid, tentatively identified as quinic acid.[56]
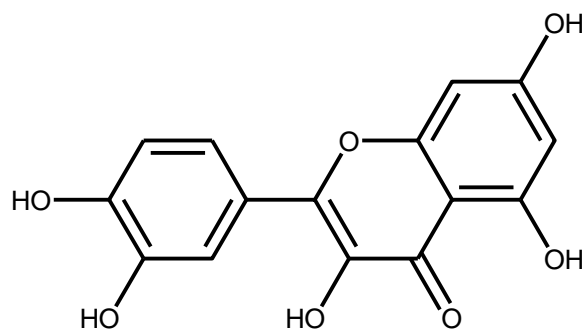
The MS spectrum of peak 2 was observed at the retention time 1.79 mins with *m/z* 169.0166 [M-H]$^-$. The molecular formula obtained was $C_7H_5O_5^-$ with a normalized iFit value of 0.000. The analysis of the MS/MS data indicated that it was an organic acid, matching gallic acid. Gallic acid has also been reported for its anti-diabetic activity.[70]

The first order mass spectrum of peak 3 showed an [M-H]$^-$ ion with *m/z* 577.1329 at the retention time 3.03 minutes. The molecular formula was given as $C_{30}H_{26}O_{12}^-$ with a normalized iFit value of 0.114. Analysis of the MS/MS data revealed that the compound was an proanthocyanidin tentatively identified as procyanidin B2.[57]

Peak 4 represents a precursor ion with *m/z* 305.0664 [M-H]$^-$ at the retention time 3.29 minutes. The molecular formula of the compound was given as $C_{15}H_{13}O_7^-$ with normalized iFit value of 0.075. The analysis of the MS/MS data indicated that it was a flavonoid, matching gallocatechin.

The first order mass spectrum of peak 5 showed an [M-H]$^-$ ion with *m/z* 647.0889 at the retention time 3.96 minutes. The molecular formula was given as $C_{28}H_{24}O_{18}^-$ with normalized iFit value of 0. 043. Analysis of the MS/MS data revealed that the compound was a gallotannin tentatively identified as Pistafolin A.

The first order mass spectrum of peak 6 showed an [M-H]$^-$ ion with *m/z* 289.0735 at the retention time 4.29 minutes. The molecular formula generated was $C_{15}H_{13}O_6^-$ with normalized iFit value of 0.017. The analysis of the MS/MS data indicated that it was a flavonoid, matching epicatechin. Studies by Yuzuak et al. identified epicatechin in the berries of two muscadine grape hybrids FLH 13-11 and FLH 17-66.[58] Epicatechin has been reported for its anti-diabetic activity.[71]

In the ESI MS spectrum, peak 7 showed an [M-H]$^-$ ion with *m/z* 493.0631 at the retention time 5.18 minutes. The molecular formula was given as $C_{21}H_{17}O_{14}^-$ with normalized iFit value of

0.006. Analysis of the MS/MS data revealed that the compound was a flavonoid glucuronide tentatively identified as myricetin 3-O-β-D-glucuronide (**88**).[61,62].

The first order mass spectrum of peak 8 showed an [M-H]$^-$ ion with *m/z* 479.0834 at the retention time 5.26 minutes. Analysis of elemental composition yielded the molecular formula $C_{21}H_{19}O_{13}^-$ with normalized iFit value of 0. The analysis of the MS/MS data indicated that it was a flavonoid, matching gossypin.

The ESI MS spectrum of peak 9 showed an [M-H]$^-$ ion with *m/z* 615.0966 at the retention time 5.50 minutes. The molecular formula was given as $C_{28}H_{23}O_{16}^-$ with a normalized iFit value of 0.000. Analysis of the MS/MS data revealed that the compound was a flavonoid glycoside tentatively identified as quercetin 3-O-(6"-Galloyl)-beta-D-glucopyranoside.[45]

Peak 10 represents a precursor ion with *m/z* 463.0876 [M-H]$^-$ at the retention time 5.80 minutes. The molecular formula of compound $C_{21}H_{19}O_{12}^-$ was obtained with a normalized iFit value of 0.000. The analysis of the MS/MS data indicated that it was a flavonoid glycoside, matching myricetin-3-O-alpha-L-rhamnopyranoside.[61,45]

The first order mass spectrum of peak 11 showed an [M-H]$^-$ ion with *m/z* 477.0679 at the retention time 5.94 minutes. The molecular formula obtained was $C_{21}H_{17}O_{13}^-$ with a normalized iFit value of 0.000. Analysis of the MS/MS data revealed that the compound was a flavonoid glucuronide tentatively identified as quercetin-3-O-beta-D-glucuronide (**89**).[63, 64] Quercetin-3-O-β-D-glucuronide has previously been reported to attenuate 25 mM HG-induced suppressed nuclear factor erythroid 2-related factor 2 and anti-oxidant enzyme expression in mouse glomerular mesangial cells (MES-13).[72]

In the ESI MS spectrum, peak 12 showed an [M-H]$^-$ ion with *m/z* 433.0780 at the retention time 6.33 minutes. The molecular formula was given as $C_{20}H_{17}O_{11}^-$ with a normalized iFit value of 0.000. The analysis of the MS/MS data indicated that it was a flavonoid glycoside, matching quercetin-3-O-arabinoside.[64]

Peak 13 observed with *m/z* 447.0932 [M-H]$^-$ at the retention time 6.68 minutes had a molecular formula of $C_{21}H_{19}O_{11}^-$ with a normalized iFit value of 0.000. Analysis of the MS/MS data

revealed that the compound was a flavonoid glycoside tentatively identified as quercetin-3-O-alpha-L-rhamnopyranoside.

The ESI MS spectrum of peak 14 showed an $[M-H]^-$ ion with *m/z* 431.0977 at the retention time 7.38 minutes. The molecular formula was given as $C_{21}H_{19}O_{10}^-$ with a normalized iFit value of 0.000. Analysis of the MS/MS data revealed that the compound was a flavonoid glycoside tentatively identified as kaempferol-3-O-alpha-L-rhamnopyranoside.[66, 67]

Peak 15 represents a precursor ion with *m/z* 319.0463 $[M+H]^+$ at the retention time 5.80 minutes. The molecular formula of compound $C_{15}H_{11}O_8^+$ was generated from Masslynx software with a normalized iFit value of 0.000. Analysis of the MS/MS data revealed that the compound was a flavonoid tentatively identified as myricetin (**90**).[61] Myricetin has been reported for its anti-diabetic activity.[73]

The first order mass spectrum of peak 16 showed an $[M+H]^+$ ion with *m/z* 303.0497 at the retention time 6.48 minutes. The molecular formula obtained was $C_{15}H_{11}O_7^+$ with a normalized iFit value of 0.000. Analysis of the MS/MS data revealed that the compound was a flavonoid tentatively identified as quercetin. Quercetin has been reported for its anti-diabetic effect in streptozocin-induced diabetic rats.[74]

4.3.5 Fractionation targeting the biologically active compounds

Since both aqueous extracts 1 and 4 were chemically similar, and the aqueous extract 4 showed statistically significant biological activity at all test concentrations including at 0.01 µg/mL, aqueous extract 4 was selected for fractionation to isolate the compounds responsible for the glucose uptake activity. Aqueous extract 4 (4.0 kg) was fractionated using a GX-241 liquid handler Gilson instrument on a solid phase extraction (SPE) cartridge (hypersep C8) with the eluent of water (H_2O), MeOH and acetonitrile (MeCN) in the following ratios: H_2O: MeOH (95:5, 80:20, 60:40, 40:60, 20:80, 0:100) for fractions 1 to 6, respectively, and MeOH: MeCN 50:50 for fraction 7. The fractions were collected (8 mL each) in preweighed polytope vials. The solvents were evaporated to dryness using a Genevac HT series. The seven fractions were tested for their glucose uptake activity in the C2C12 cell line.

4.3.6 Biological screening of fractions for glucose uptake activity in the C2C12 cell line

The positive control insulin and seven fractions from aqueous extract 4 were screened over a concentration range of 0.01-100 µg/mLto ascertain the *in vitro* glucose uptake in the C2C12 cell line. Differentiated C2C12 cell (myotubules) enhances the insulin-sensitive glucose uptake mechanism by increasing the translocation of glucose transporter 4 (GLUT 4) to the surface of the cell.[75] Based on this, insulin was selected as a positive control to ascertain maximal glucose uptake. The biological screening results are shown in figure 4.10.
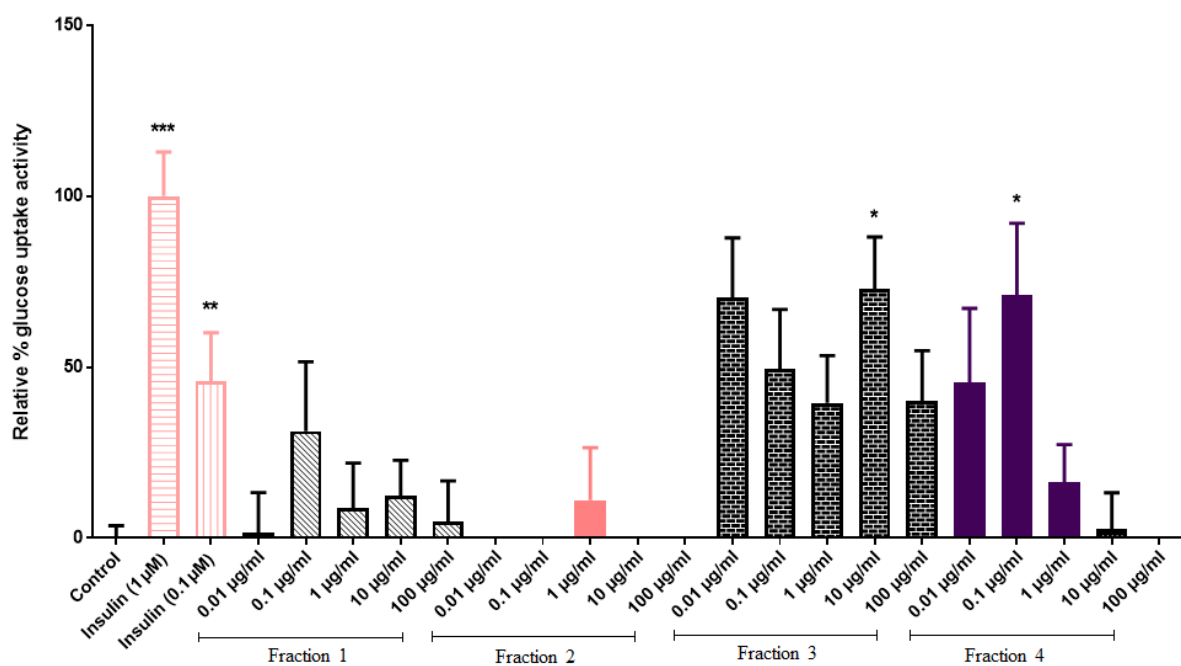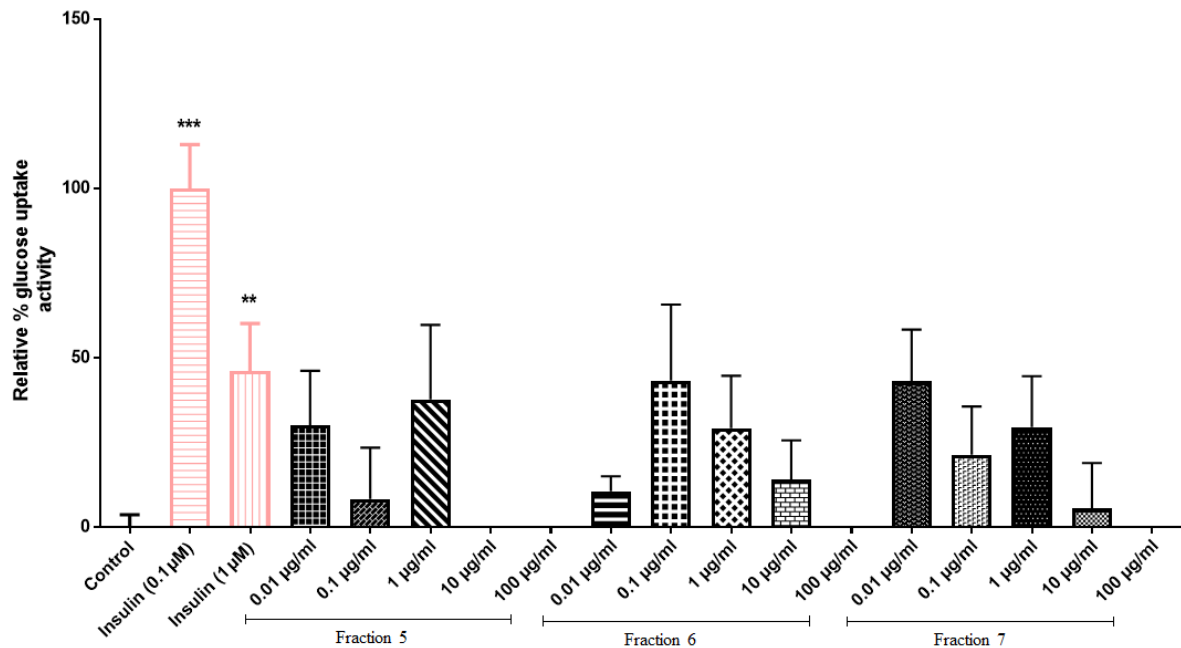
Figure 4.10: Relative Glucose uptake activity of *S. birrea* fractions in C2C12 myocytes over a range of 0.01-100 µg/mL. Activity is expressed relative % to the baseline glucose uptake (control) set at 0% and the positive control insulin (Ins) set at 100%. Active fraction (fraction 3) exhibited comparable potency to Insulin. P value $< *p < 0.05$, $**p < 0.01$. $***p < 0.001$.

Activity is expressed in relative % to the baseline glucose uptake (control) set at 0% and the positive control insulin (Ins) set at 100%. This was used as a reference to select the active fraction. Out of the tested fractions, fractions 3 and 4 (H_2O: MeOH (60:40 and 40:60) respectively) with activity ranges of 24-73% and 46-54% respectively significantly increased glucose uptake ($p < 0.05$) in C2C12 skeletal myocytes. Overall, the fractions were less effective than the positive control (Insulin). A common observation was a decrease in glucose uptake for most of the fractions at 100 µg/mL. Fractions 3 and 4 exhibited good activity in the glucose uptake assay even though they were less effective than the positive control therefore the two active fractions were considered for chemical analysis and isolation of active compounds.

4.3.7 UPLC-QTOF-MS analysis of active fractions

The active fractions (fractions 3 and 4) were analyzed using UPLC-QTOF-MS to identify the active compounds (figure 4.11).
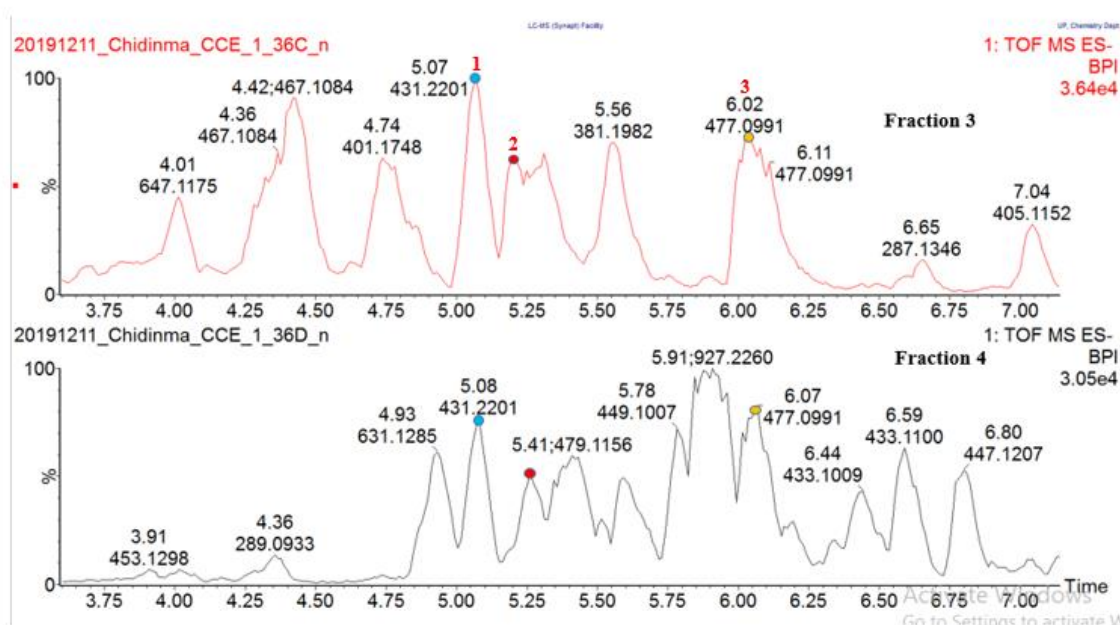
Figure 4.11: ESI negative mode BPI chromatogram of fractions 3 and 4 from spray-dried aqueous extract 4 of *S. birrea* leaves. Unidentified (at *m/z* 431.2201 [M-H]⁻ retention time 5.07 minutes), myricetin-3-*O*-β-D-glucuronide (at *m/z* 493.0886 [M-H]⁻ retention time 5.26 minutes), quercetin-3-*O*-β-D-glucuronide (at *m/z* 477.0991 [M-H]⁻ retention time 6.02 minutes).

Peak 1 with *m/z* 431.2201 (at the retention time 5.07 minutes) in fraction 3 was present (at the retention time 5.08 minutes) in fraction 4. The compound corresponding to this peak was not identified. Peak 2 with *m/z* 493.0886 (at the retention time 5.31 minutes) in fraction 3 was present (at the retention time 5.26 minutes) in fraction 4. The compound was tentatively identified as myricetin-3-*O*-β-D-glucuronide (**88**) as described in section 4.3.4 (table 4.2). The presence of myricetin-3-*O*-β-D-glucuronide in the active fractions 3 and 4 indicates that this flavonoid glucuronide contributes to the glucose uptake potential of the extracts. Peak 3 with *m/z* 477.0991 (at the retention time 6.02 minutes) in fraction 3 was present (at the retention time 6.07 minutes) in fraction 4. The compound was tentatively identified as quercetin-3-*O*-β-D-glucuronide (**89**) as described in section 4.3.4 (table 4.2). Its presence in the two active fractions 3 and 4 indicates that it contributes to the glucose uptake activity of the extracts. Isolation and biological screening of these two pure compounds will confirm their anti-diabetic activity.

4.3.8 Isolation of compounds from active fraction 3

Isolation of compounds from the active fraction 3 was carried out to identify the active compound(s). Fraction 3 was subjected to purification by hyphenated liquid chromatography-mass spectrometry-solid phase extraction-nuclear magnetic resonance (LC-MS-SPE-NMR) analysis. The two peaks labelled in figure 4.12 were trapped in SPE cartridges through multiple trapping. Compound (**92**) (F_3SF_1) and compound (**93**) (F_3SF_2) were collected in pure forms in sufficient quantities of 1.6 mg and 0.9 mg respectively. They were screened for their glucose uptake assay in C2C12 myocytes.
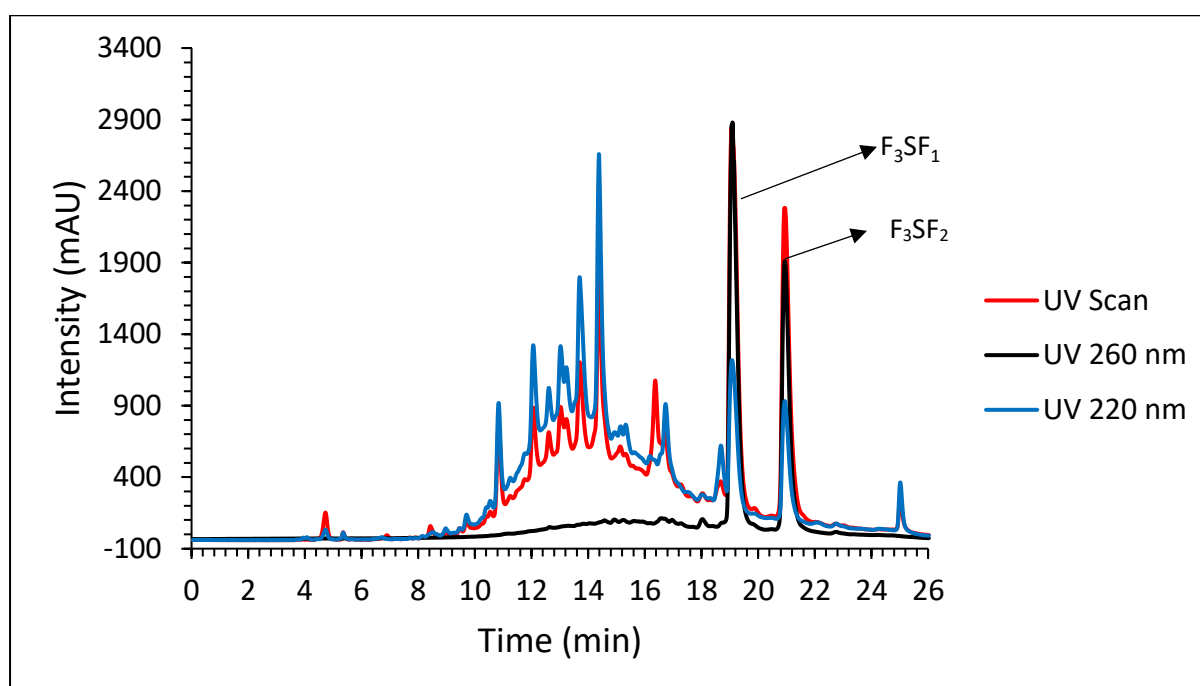
Figure 4.12: LC-UV $_{max}$ plot chromatogram of fraction 3 from LC-MS-SPE-NMR.

4.3.9   Isolation of compounds from active fraction 4

Isolation of compounds from the active fraction 4 was carried out to identify the active compounds. Fraction 4 was purified using mass-directed preparative high-performance liquid chromatography-qualitative data analysis (HPLC-QDA). The purification was carried out in a positive mode (figure 4.13).
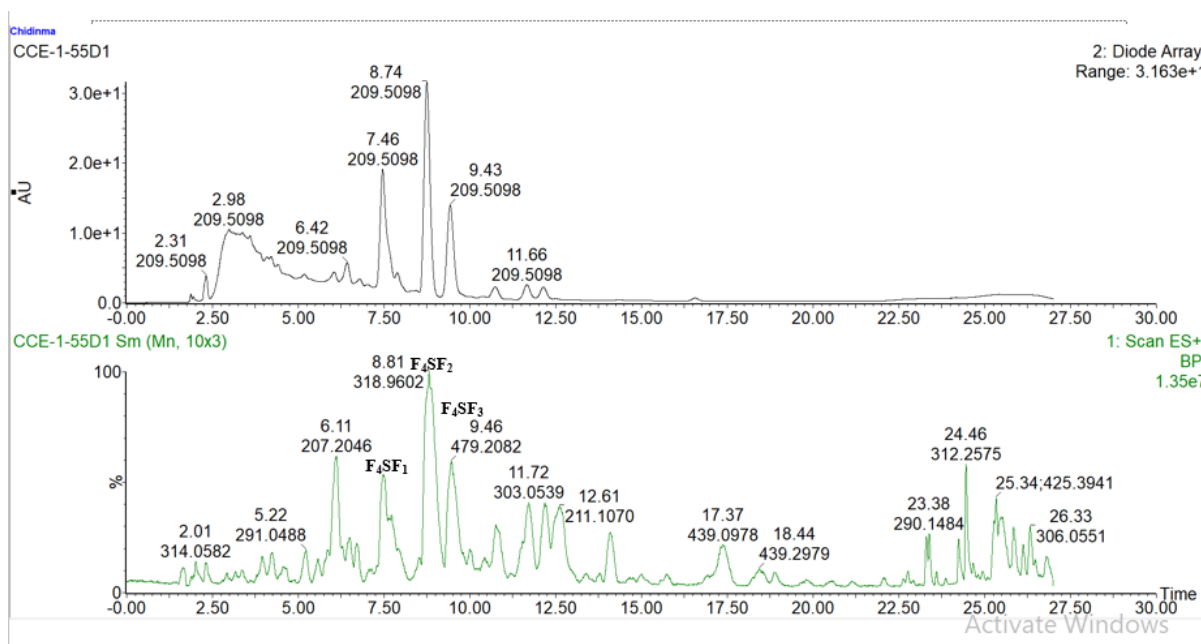
Figure 4.13: HPLC-UV$_{max}$ plot and MS positive mode chromatogram of fraction 4.

Three peaks were collected in sufficient quantities to allow further analysis. They were labelled as F$_4$SF$_1$ (8.21 mg), F$_4$SF$_2$ (compound (**91**), 9 mg) and F$_4$SF$_3$ (3.63 mg). The compounds were analyzed by NMR spectroscopy. The ^{1}H NMR spectra of compound (**91**) showed it was pure with minor impurities therefore 1D and 2D NMR spectroscopy together with UPLC MS analysis were carried out for the structure to be elucidated (section 4.3.10) while F$_4$SF$_1$and F$_4$SF$_3$ confirmed that they were still mixtures and needed further purification. The two compounds were purified from fraction 3 where they were also present using hyphenated liquid chromatography-mass spectrometry-solid phase extraction-nuclear magnetic resonance (LC-MS-SPE-NMR) analysis (section 4.3.8).

4.3.10 Structure elucidation of compounds isolated from *S. birrea*
4.3.10.1 Myricetin (91)

Compound **91** was isolated as a light-yellow solid and was identified as myricetin by the interpretation of the NMR spectroscopy, mass data and comparison to literature data.[76] The molecular formula of the compound is C$_{15}$H$_{11}$O$_8$ as deduced from its monoprotonated molecular ion at *m/z* 319.0443 [M+H]$^+$ (calculated for C$_{15}$H$_{11}$O$_8$, *m/z* 319.0454, M+H) based on the QTOF mass spectrum with eleven degrees of unsaturation. The ^{13}C NMR spectrum exhibited fifteen carbon signals, which were assigned as four aromatic methines and eleven quaternary carbons (one carbonyl, six O-bearing and four aliphatic) using the DEPT spectrum.

208

This suggested the compound had a flavonoid structure. The ^{1}H NMR spectrum showed the presence of four aromatic protons resonating at δ_H 6.22 (1H, d, $J_{H-6-H-8}$ = 2.13 Hz, H-6) and δ_H 6.39 (1H, d, $J_{H-6-H-8}$ = 2.13 Hz, H-8) consistent with the meta coupled protons at H-6 and H-8 positions on the A-ring, and a signal at δ_H 6.97 (2H, s, H-2', H-6') indicating the presence of two protons appearing as a singlet due to their para substituted ring B which led to their symmetrical pattern. The position of these protons was assigned through HMBC correlation between δ_H 6.97 (H-2' and H-6') with δ_C 145.5 (C-2) and HMBC correlation between δ_H 6.22 (H-6) and δ_H 6.39 (H-8) with δ_C 102.2 (C-10). Furthermore HMBC correlation was observed between δ_H 6.22 (H-6) with δ_C 161.8 (C5) and δ_C 93.3 (C8), between δ_H 6.39 (H-8) with δ_C 98.4 (C6), δ_C 164.5 (C7) and δ_C 157.1 (C9) and between δ_H 6.97 (H-2' and H-6') with δ_C 120.5 (C-1'), δ_C 145.5 (C-3'), δ_C 145.5 C-5' and δ_C 108.1 (C-6') which supported their assignment. There were no COSY correlations observed. The structure of compound **91** is shown in figure 4.14, and the selected HMBC correlations are shown in figure 4.15.

Figure 4.14: Chemical structure of myricetin (**91**).

Figure 4.15: Selected HMBC correlation of myricetin (**91**).

The proposed structure was confirmed by comparing the NMR data to the literature data of myricetin (**91**) (table 4.3).

Table 4.3: [1]H (500 MHz), ^{13}C (125 MHz) and HMBC NMR data of Compound (**91**) compared to the literature ^{1}H and ^{13}C NMR data of myricetin

Position	Isolated myricetin (CD₃OD)		Published NMR for myricetin ((DMSO-d₆) (^{1}H, 500 MHz ^{13}C, 125 MHz) [76]		Isolated myricetin (CD₃OD)
	δ_C	δ_H (m, *J* in Hz, no of hydrogens)	δ_C	δ_H (m, *J* in Hz, no of hydrogens)	HMBC correlation
2	145.5		146.8		
3	136.5		135.9		
4	178.3		175.7		
5	161.8		160.7		
6	98.4	6.22, d, *J* = 2.09 Hz, 1H	98.2	6.18, d, *J* = 2.40 Hz, 1H	C8, C10, C5
7	164.5		164.1		
8	93.3	6.39, d, *J* = 2.17 Hz, 1H	93.2	6.37, d, *J* = 1.8 Hz, 1H	C6, C10, C9, C7
9	157.1		156.1		
10	102.2		102.9		
1'	120.5		120.7		
2'6'	108.1	6.97, s, 2H	107.1	7.24, s, 2H	C2, C6', C1', C3', C5'
3'	145.5		145.7		
4'	134.9		135.8		
5'	145.5		145.7		

Myricetin was first isolated from the bark of the *Myrica nagi* and subsequently was found to be present in the leaves of *Rhus coriaria*, *Rhus cotinus*, *Rhus metopium* and *Myrica gale* [77]. This is the first report of its isolation from *S. birrea*.

4.3.10.2 Myricetin-3-O-β-D-glucuronide (92)

Compound **92** was isolated as a light-yellow solid and was identified as myricetin-3-O-β-D-glucuronide by the interpretation of the NMR spectroscopy, mass data and comparison to literature data.[78] The molecular formula of the compound is $C_{21}H_{19}O_{14}$ as deduced from its monoprotonated molecular ion at m/z 495.0886 [M+H]$^+$ (calculated for $C_{21}H_{19}O_{14}$, m/z 495.0775, M+H) based on the QTOF mass spectrum with thirteen degrees of unsaturation. The ^{13}C-NMR spectrum showed the presence of twenty-one carbon signals which were assigned as nine methines (four aromatic methines and five glucuronic acid methines) and twelve quaternary carbons (one carbonyl, one carboxylic acid, six O-bearing, four aliphatic) as deduced from its DEPT spectrum. The ^{1}H NMR spectrum showed the presence of four aromatic protons (δ_H 6.21-7.29). Two protons resonating at δ_H 6.21 (1H, d, J = 2.05 Hz, H-6) and δ_H 6.39 (1H, d, J = 2.00 Hz, H-8) consistent with the meta coupled protons at H-6 and H-8 positions on the A-ring and a signal at δ_H 7.29 (2H, s, H-2', H-6') indicating the presence of two protons at 2'and 6' positions appearing as a singlet due to their *para* substituted ring B which led to their symmetrical pattern. Similar signals were observed for compound **92**. Additional signals were observed in the carbon and proton NMR for the sugar moiety. A sequential *trans*-1,2-diaxial relationship of H-1"- H-5" (δ_H 5.39-3.49, J = 7.9-9.6 Hz) indicated the presence of a β-D-glucuropyranosyl moiety.[79] Attachment of the sugar moiety to the flavonoid skeleton at δ_C 134.1 (C-3) was confirmed from the HMBC correlation of the anomeric proton signal at δ_H 5.39 (H-1") with δ_C 134.1 (C-3) of ring C in the myricetin aglycone. Furthermore, HMBC correlation was observed in the sugar moiety between δ_H 3.49-3.61 (H-2") with δ_C 71.6 (C-4"), δ_H 3.49-3.61 (H-3") with δ_C 104.2 (C-1") and δ_C 171.7 (C-6"), δ_H 3.75 (H-5") with δ_C 104.2 (C-1"), δ_C 71.6 (C-4") and δ_C 171.7 (C-6"). This supported their assignments. All the other HMBC correlations observed were similar to those in compound **92**.

COSY correlation was observed between δ_H 5.39 (H-1") and δ_H 3.49-3.61 (H-2") which confirmed that they were adjacent to each other. This supported their assignment. The downfield chemical shift of the anomeric proton H-1" (δ_H 5.39) suggests that it was between two oxygens. The relative configuration at the anomeric position was deduced from the ^{1}H NMR spectrum by analyzing the coupling constant at H-1"(J = 7.88 Hz) which established the configuration as a axial-configuration. The structure of compound **92** is shown in figure 4.16, and the selected HMBC correlations are shown in figure 4.17.
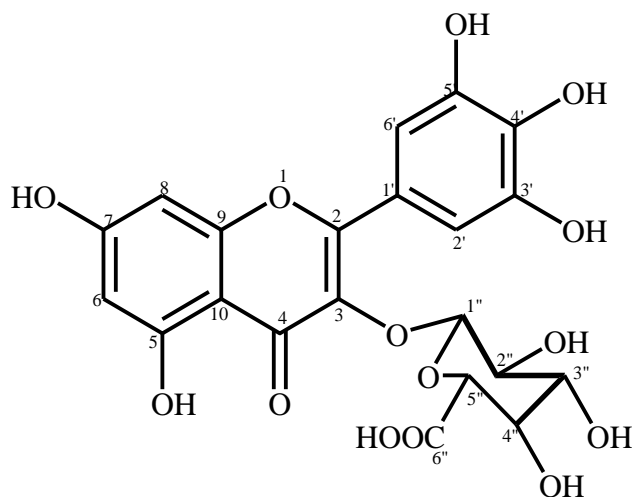
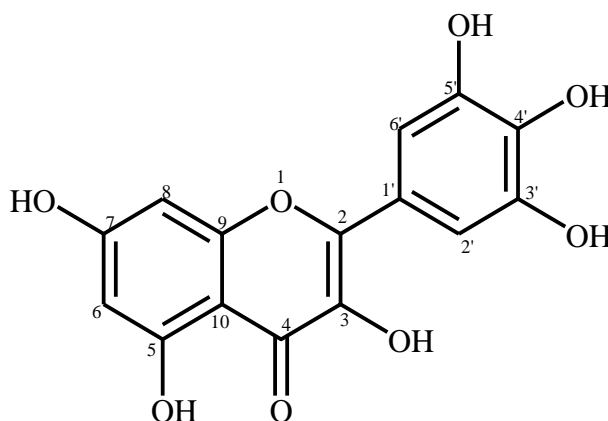**Figure 4.16**: Chemical structure of myricetin-3-*O*-*β*-D-glucuronide (**92**).
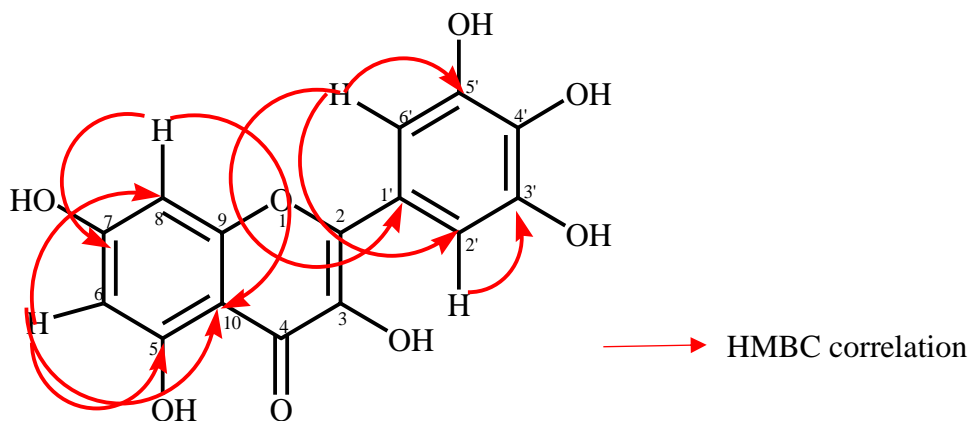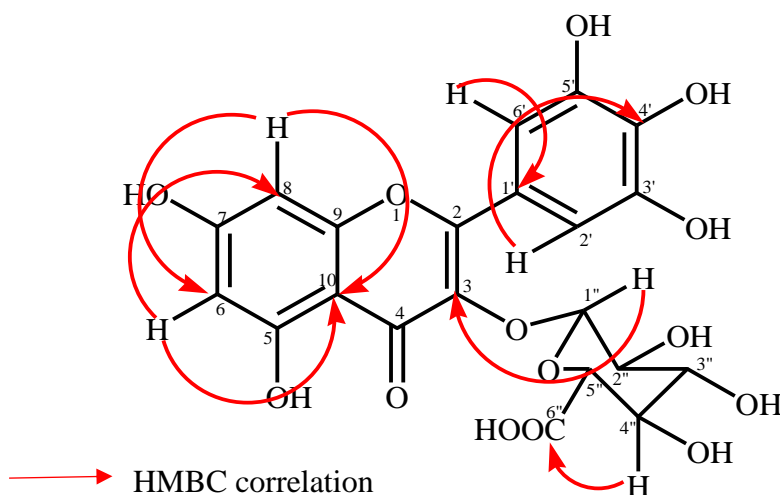

→ HMBC correlation

Figure 4.17: Selected HMBC correlation of myricetin-3-*O*-*β*-D-glucuronide (**92**).

The proposed structure was confirmed by comparing the NMR data to the literature data of myricetin-3-O-β-D-glucuronide (**92**) (table 4.4).

Table 4.4: ^{1}H (500 MHz), ^{13}C (125 MHz) and HMBC NMR data of Compound (**92**) compared to the literature ^{1}H and ^{13}C NMR data of myricetin-3-*O*-β-D-glucuronide

Position	Isolated myricetin-3-*O*-*β*-D-glucuronide (CD₃OD)	Published NMR for myricetin-3-*O*-*β*-D-glucuronide ((DMSO-d₆) (¹H, 500 MHz ¹³C, 125 MHz) [78]	Isolated myricetin-3-*O*-*β*-D-glucuronide (CD₃OD)	Isolated myricetin-3-*O*-*β*-D-glucuronide (CD₃OD)

	δ_C	δ_H (m, *J* in Hz, no of hydrogens)	δ_C	δ_H (m, *J* in Hz, no of hydrogens)	HMBC correlation	COSY correlation
2	157.5		156.2			
3	134.1		133.2			
4	177.8		177.1			
5	161.7		161.2			
6	98.5	6.21, d, *J* = 2.05 Hz, 1H	98.7	6.20, d, *J* = 1.90 Hz, 1H	C5, C7, C8, C10	
7	164.6		164.2			
8	93.2	6.39, d, *J* = 2.00 Hz, 1H	93.4	6.38, d, *J* = 1.90 Hz, 1H	C6, C7, C9, C10	
9	157.0		156.2			
10	102.7		101.1			
1'	120.3		119.7			
2', 6'	108.5	7.29, s, 2H	108.5	7.28, s, 2H	C2, C1', C2', C3', C4', C5'	
3'	145.0		145.4			
4'	136.7		136.8			
5'	145.0		145.4			
1''	104.2	5.39, d, *J* = 7.88 Hz, 1H	103.8	5.36, d, *J* = 7.60 Hz, 1H	C3	H-2''
2''	73.9	3.49-3.61, m, 3H	73.6	3.66-3.43, m, 3H	C4''	
3''	76.3	3.49-3.61, m, 3H	76.0	3.66-3.43, m, 3H	C1'', C3'', C6''	
4''	71.6	3.49-3.61, m, 3H	71.2	3.66-3.43, m, 3H		
5''	75.8	3.75, d, *J* = 9.68 Hz, 1H	75.9	3.77, d, *J* = 9.50 Hz, 1H	C1'', C4'', C6''	

213

6''	171.7		169.8			

Myricetin-3-*O*-β-D-glucuronide, a glucuronide conjugate of myricetin was isolated for the first time from the leaves of *Schinus terebinthifolius Raddi* and then from other sources including the leaves of *Epilobium angustifolium* [80], the leaves of *Cyclocarya paliurus* [81].This is the first report of its isolation from *S. birrea*

4.3.10.3 Quercetin-3-*O*-β-D-glucuronide (93)

Compound **93** was isolated as a light-yellow solid and identified as quercetin-3-*O*-β-D-glucuronide by the interpretation of NMR spectroscopy, mass data and previously published studies.[78] The molecular formula of the compound is $C_{21}H_{18}O_{13}$ as deduced from its monoprotonated molecular ion at *m/z* 479.0952 [M+H]$^+$ (calculated for $C_{21}H_{18}O_{13}$, *m/z* 479.0826, M+H) based on the QTOF mass spectrum with thirteen degrees of unsaturation. The ^{13}C NMR spectrum showed the presence of twenty-one carbon signals which were assigned as ten methine groups (five aromatic methines and five glucuronic acid methine) and eleven quaternary carbons (one carbonyl, one carboxylic acid, five O-bearing and four aliphatic) as deduced from its DEPT spectrum. The ^1H NMR spectrum showed signals corresponding to five aromatic protons (δ_H 6.10-7.78). Two proton signals at δ_H 6.10 (1H, d, *J* = 2.05 Hz, H-6) and 6.30 (1H, d, *J* = 2.05 Hz, H-8) attributable to the A ring of quercetin which were assigned to H-6 and H-8 positions respectively. Additionally, three proton signals at δ_H 7.78 (1H, bs, H-2'), 6.75 (1H, d, *J* = 8.48 Hz, H-5') and 7.44 (1H, dd, *J* = 2.15 and 0.78 Hz, H-6') were assigned to the B ring of quercetin as H-2', H-5' and H-6' respectively. These proton signals confirmed that the structure of the aglycone moiety was quercetin. Similar signals were observed in the carbon and proton NMR spectra for compound **92**. The only difference between compounds **92** and **93** is that the former has an extra proton and molecular mass oxygen which is one less hydroxyl group in compound **93**. HMBC correlations were observed between δ_H 7.78 (H-2') and δ_C 125.8 (C-1'), δ_C 148.5 (C-4') and δ_C 121.5 (C-6'); between δ_H 6.75 (H-5') and δ_C 125.8 (C-1'), δ_C 144.5 (C-3') and δ_C 121.5 (C-6') and between δ_H 7.44 (H-6') and δ_C 148.5 (C-4') and δ_C 116.4 (C-5') which supported their assignment. In addition, HMBC correlations were observed in the sugar moiety between δ_H 5.32 (H-1'') and δ_C 134.5 (C-3), δ_C 76.6 (C-3'') and δ_C 76.5 (C-5''); between δ_H 3.38-3.49 (H-2'' and H-4'') and δ_C 103.9 (C-1''), δ_C 76.6 (C-3''), δ_C 73.7 (C-4''), δ_C 76.5 (C-5'') and δ_C 174.9 (C-6'') which supported their assignment. COSY correlation

214

was observed between δ_H 6.75 (H-5') and δ_H 7.44 (H-6') showing that they were adjacent to each other. All the other HMBC and COSY correlations observed were similar to those in compound **92**. The structure of compound **93** is shown in figure 4.18, and the selected HMBC and COSY correlations are shown in figure 4.19.
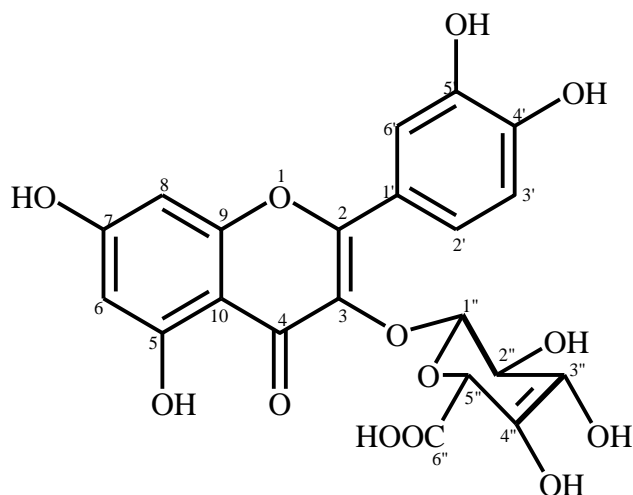

Figure 4.18: Chemical structure of quercetin-3-*O*-β-D-glucuronide (**93**).
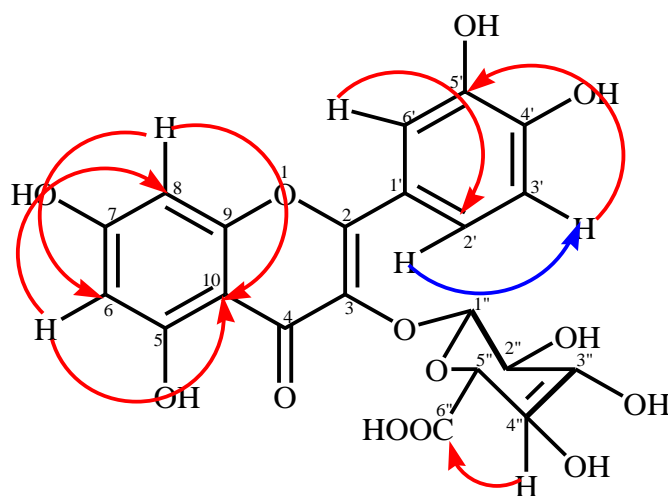

Figure 4.19: Selected HMBC and COSY correlations of quercetin-3-*O*-β-D-glucuronide (**93**).

The proposed structure was confirmed by comparing the NMR data to the literature data of quercetin-3-*O*-β-D-glucuronide (**93**) (table 4.5).

Table 4.5: ¹H (500 MHz), ¹³C (125 MHz) and HMBC NMR data of Compound (**93**) compared to the literature ¹H and ¹³C NMR data of quercetin-3-*O*-β-D-glucuronide

Position	Isolated quercetin-3-*O*-β-D-glucuronide (CD₃OD)		Data published for quercetin-3-*O*-β-D-glucuronide ((DMSO-d₆) (¹H, 500 MHz ¹³C, 125 MHz) [78]		Isolated quercetin-3-*O*-β-D-glucuronide (CD₃OD)	Isolated quercetin-3-*O*-β-D-glucuronide (CD₃OD)	Isolated quercetin-3-*O*-β-D-glucuronide (CD₃OD)
	δ_C	δ_H (m, *J* in Hz, no of hydrogens)	δ_C	δ_H (m, *J* in Hz, no of hydrogens)	HMBC correlation	COSY Correlation	NOESY correlation
2	161.6		159.2				
3	134.5		135.5				
4	177.9		179.4				
5	164.7		163.2				
6	101.6	6.10, d, *J* = 2.05 Hz, 1H	100.1	6.21, d, *J* = 2.00 Hz, 1H	C5, C8, C10		
7	168.2		166.2				
8	93.3	6.30, d, *J* = 2.05 Hz, 1H	94.9	6.40, d, *J* = 2.00 Hz, 1H	C5, C6, C9, C10		
9	157.7		158.6				
10	104.3		105.8				
1'	125.8		123.0				
2'	114.7	7.78, bs, 1H	116.2	7.60-7.67, m, 1H	C1', C4', C6'		
3'	144.5		146.1				
4'	148.5		150.0				
5'	116.4	6.75, d, *J* = 8.48 Hz, 1H	117.4	6.85, d, *J* = 8.48 Hz, 1H	C1', C3', C6'	H-6'	
6'	121.5	7.44, dd, *J* = 2.15,	123.6	7.60-7.67, m, 1H	C4', C5'		H-5'

216

		0.78 Hz, 1H)					
1"	103.9	5.32, d, $J =$ 7.57 Hz, 1H	104.4	5.34, d, $J =$ 7.40 Hz, 1H	C3 C3", C5"	H-2"	H-5", H-4"
2"	74.1	3.38-3.49, m, 3H	75.5	3.42-3.66, m, 3H	C1", C3", C4", C5", C6"		
3"	76.6	3.38-3.49, m, 3H	77.7	3.42-3.66, m, 3H	C1", C3", C4", C5", C6"		
4"	73.7	3.38-3.49, m, 3H	73.0	3.42-3.66, m, 3H	C1", C3", C4", C5", C6"		
5"	76.5	3.55, d, $J =$ 9.7 Hz, 1H	77.2	3.75, d, $J =$ 9.60 Hz, 1H	C1", C4", C6"		
6"	174.9		172.4				

Quercetin-3-*O*-β-D-glucuronide a glucuronide conjugate of quercetin was previously isolated from the leaves of *Polygonum perfoliatum* [82], the aerial part of *Polygonum aviculare* [83]and from the leaves of *Nelumbo nucifera* [84]. This is the first report of its isolation from *S. birrea*.

4.3.11 The effect of the isolated compounds on glucose uptake

To evaluate the glucose uptake activity of the isolated compounds (**91**-**93**), the uptake of 2-deoxyglucose (2DG) in C2C12 myocytes was measured. Figure 4.20 shows the cellular 2-deoxy-D-glucose uptake in C2C12 myocytes treated with compounds (**91**), (**92)** and (**93)** at different concentrations.
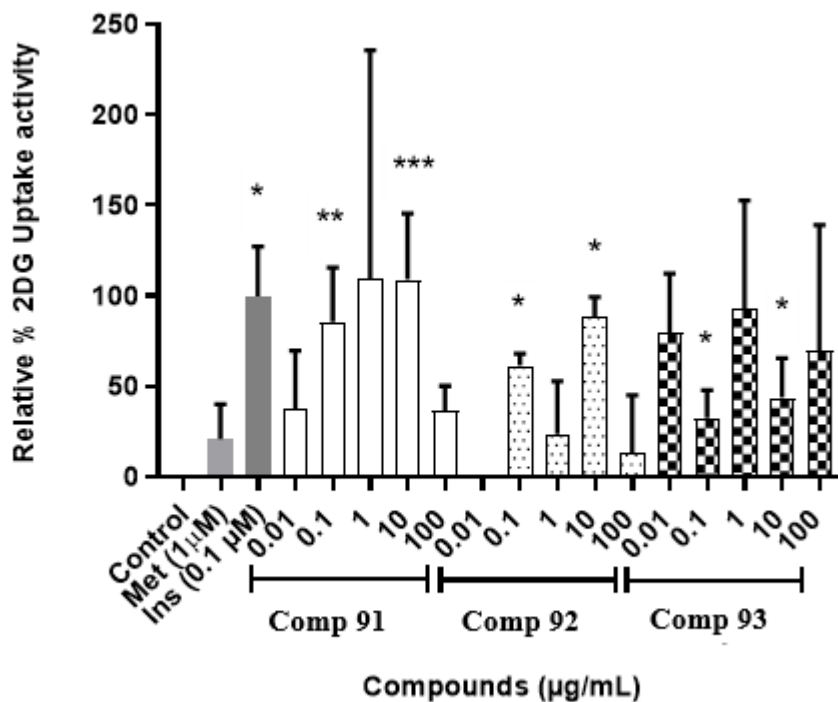
Figure 4.20: Glucose uptake activity was estimated from the cellular 2-deoxy-D-glucose uptake in C2C12 myocytes treated with compounds (**91**), (**92**) and (**93**) at different concentrations for 1 hour. 2-deoxy-D-glucose uptake estimated after 30 minutes. Activity is expressed as relative % to the baseline glucose uptake (untreated control) set at 0% and the positive control insulin (Ins) set at 100%. P value * $p < 0.05$, ** $p < 0.01$ and *** $p < 0.001$.

Significant glucose uptake was observed for compound (**91**) (0.1 and 10 µg/mL; 85.7 and 109.1%, respectively), compound (**92**) (0.1 and 10 µg/mL; 61.6 and 88.8%, respectively) and compound (**93**) (0.1 and 10 µg/mL; 40.9 and 43.9%, respectively) compared to the treatment of insulin (0.1 µM; 100%). At a concentration of 10 µg/mL, compound (**91**) demonstrated both a potent and concentration-dependent stimulatory action on glucose uptake in the C2C12 myocytes, matching that of insulin, the positive control. This suggests that these compounds may be able to stimulate cellular glucose uptake, at least in part by upregulating the expression and translocation of insulin-responsive glucose transporter 4 (GLUT 4), either via an insulin mimetic mechanism or via an insulin-independent mechanism(s) such as AMPK activation, which is largely responsible for glucose uptake in muscle and adipose tissue.[55, 85] This *in vitro* result further indicated that compounds (**92**) and (**93**) are also active and responsible for promoting glucose uptake in differentiated C2C12 myocytes and suggest that these compounds

may contribute at least in part to the anti-diabetic properties of *S. birrea*. The phytochemistry of *S. birrea* has been extensively researched with flavonoids and flavonoid glycosides reported as the main classes of compounds. Flavonoids improve α-glycosidase, glucose metabolism, glucose transport, aldose reductase and other targeted cellular signalling networks in various effector cells such as pancreatic β-cells, adipocytes, hepatocytes and skeletal muscle, thereby exhibiting versatile anti-diabetic activities. None of the reports in the documented literature report on the compounds responsible for the anti-diabetic activity in *S.birrea*. This is the first report showing compounds in *S. birrea* that are responsible for the anti-diabetic activity, which is useful for commercial application since these compounds can be utilized as chemical markers for quality control purposes.

This is the first report of the glucose uptake activity of myricetin-3-*O*-β-D-glucuronide (**92**). The activation of phosphoinositide 3-kinases/protein kinase B (PI3K/Akt) and the AMP-activated protein kinase (AMPK) signal pathways by myricetin has been shown to enhance glucose absorption in C2C12 myotubes. By activating the AMPK signal pathway, the compound could help mitigate hyperinsulinemia-induced insulin resistance. This represents a potential pathway through which myricetin regulates glucose utilization as well as prevents insulin resistance. Myricetin has been shown to have a therapeutic impact in patients with diabetes-related cardiovascular disease.[45] In the C2C12 cell line, myricetin-3-*O*-β-D-glucuronide (**92)** and quercetin-3-*O*-β-D-glucuronide (**93**) demonstrated considerable glucose absorption but the exact mechanism of action is unknown.[78][86] Quercetin-3-*O*-β-D-glucuronide has previously been reported to attenuate 25 mM HG-induced suppressed nuclear factor erythroid 2-related factor 2 and anti-oxidant enzyme expression in mouse glomerular mesangial cells (MES-13).[72] According to Eid et al. quercetin and its glycoside promote glucose absorption in skeletal muscle cells by stimulating the activation of the AMPK pathway.[51] The presence of sugar moiety on the flavonoid structure grants differences in physico-chemical properties over the aglycone. The molar mass increases, as well as its polar surface area and volume. The molecular structure becomes more flexible, due to the increased number of rotatable bonds, hydrogen bond acceptors and donors. These alterations could, on one hand, allow more favorable interactions with the active site of the C2C12 cell line, increasing the glucose uptake potential of the glycosides.[87] The three active compounds (**91**–**93**) were tentatively identified by UPLC-QTOF-MS analysis of spray-dried aqueous leaf extract of *S. birrea*, therefore purification, structure elucidation and biological screening of these

compounds in glucose uptake assay confirm the presence of these compounds in this extract as well as their activity.

4.4   Conclusion

Investigation of the leaves of *S. birrea*, as a more sustainable resource compared to the stems for supplying anti-diabetic ingredients, led to the isolation and identification of one flavonoid, myricetin (**91**), and two flavonoid glycosides, myricetin-3-*O*-β-D-glucuronide (**92**) and quercetin-3-*O*-β-D-glucuronide (**93**). This is the first report on the isolation of myricetin-3-*O*-β-D-glucuronide (**92**) and quercetin-3-*O*-β-D-glucuronide (**93**) from *S. birrea*. All three compounds significantly increased the glucose uptake in differentiated C2C12 myocyte cells at various test concentrations, indicating that these contribute holistically and, in all likelihood, synergistically to the anti-diabetic activity of the extract. This is the first report of the anti-diabetic activity of myricetin-3-*O*-β-D-glucuronide (**92)** and confirms the anti-diabetic properties of *S. birrea*, based on the *in vitro* glucose uptake assay, and supports the use of the leaves rather than the previously used stem bark to ensure sustainable harvesting for commercial supply of plant material. The chemical profile for the spray-dried aqueous extract of *S. birrea* leaves was developed for quality control purposes. Sixteen compounds were tentatively identified by UPLC-QTOF-MS analysis which are quinic acid, gallic acid, procyanidin B2, gallocatechin, pistafolin A, myricetin-3-*O*-β-D-glucuronide, quercetin-3-O-β-D-glucuronide, epicatechin, gossypin, quercetin 3-*O*-(6"-galloyl)-beta-D-glucopyranoside, myricetin-3-*O*-alpha-L-rhamnopyranoside, quercetin-3-*O*-arabinoside, quercetin-3-*O*-alpha-L-rhamnopyranoside, kaempferol-3-*O*-alpha-L-rhamnopyranoside, myricetin and quercetin. The presence of myricetin-3-*O*-β-D-glucuronide, quercetin-3-*O*-β-D-glucuronide and myricetin were confirmed through isolation, purification and structure elucidation using MS and NMR spectroscopy. This study provides scientific data to support the commercial application of the aqueous extract of *S. birrea* leaves as an anti-diabetic ingredient. However, further research needs to be carried out to ascertain the structure–activity relationship and mechanism of action of the isolated flavonoid glycosides (myricetin-3-*O*-β-D-glucuronide and quercetin-3-*O*-β-D-glucuronide) to develop an innovative and effective anti-diabetic therapy.

4.5 References

1. Schulze-Kaysers, N.; Feuereisen, M. M.; Schieber, A., Phenolic compounds in edible species of the Anacardiaceae family – a review. *RSC Advances* **2015,** *5* (89), 73301-73314.

2. Mkwezalamba, I.; Munthali, C. R. Y.; Missanjo, E., Phenotypic Variation in Fruit Morphology among Provenances of <i>Sclerocarya birrea</i> (A. Rich.) Hochst. *International Journal of Forestry Research* **2015,** *2015*, 735418.

3. Mashau, M. E.; Kgatla, T. E.; Makhado, M. V.; Mikasi, M. S.; Ramashia, S. E., Nutritional composition, polyphenolic compounds and biological activities of marula fruit (<i>Sclerocarya birrea</i>) with its potential food applications: a review. *International Journal of Food Properties* **2022,** *25* (1).

4. Tölke, E. D.; Lacchia, A. P. S.; Lima, E. A.; Demarco, D.; Ascensão, L.; Carmello-Guerreiro, S. M., Secretory ducts in Anacardiaceae revisited: Updated concepts and new findings based on histochemical evidence. *South African Journal of Botany* **2021,** *138*, 394-405.

5. Viljoen, A. M.; Kamatou, G. P. P.; Başer, K. H. C., Head-space volatiles of marula (Sclerocarya birrea subsp. caffra). *South African Journal of Botany* **2008,** *74* (2), 325-326.

6. Shackleton, S.; Shackleton, C.; Cunningham, T.; Lombard, C.; Sullivan, C.; Netshiluvhi, T., Knowledge on Sclerocarya birrea subsp. caffra with emphasis on its importance as a non-timber forest product in South and southern Africa: A summary. Part 1: Taxonomy, ecology and role in rural livelihoods. *School of Environmental Science and Management Papers* **2002,** *194*.

7. Hal, P., Processing of marula (Sclerocarya birrea subsp. Caffra) fruits : a case study on health-promoting compounds in marula pulp. **2013**.

8. Ngorima, G. T. In *Towards sustainable use of Marula (Sclerocarya birrea) in the Savannah woodlands of Zvishavane District, Zimbabwe*, 2007.

9. Ogbobe, O., Physico-chemical composition and characterisation of the seed and seed oil ofSclerocarya birrea. *Plant Foods for Human Nutrition* **1992,** *42* (3), 201-206.

10. Mizrahi, Y.; Nerd, A.; Janick, J. In *New crops as a possible solution for the troubled Israeli export market*, 1996.

11. Ojewole, J. A.; Mawoza, T.; Chiwororo, W. D.; Owira, P. M., Sclerocarya birrea (A. Rich) Hochst. ['Marula'] (Anacardiaceae): a review of its phytochemistry, pharmacology and toxicology and its ethnomedicinal uses. *Phytother Res* **2010,** *24* (5), 633-9.

12. Nghitoolwa, E.; Hall, J. B.; Sinclair, F. L., Population status and gender imbalance of the marula tree, Sclerocarya birrea subsp. caffra in northern Namibia. *Agroforestry Systems* **2003,** *59* (3), 289-294.

13. Mokgolodi, N. C.; Ding, Y.-f.; Setshogo, M. P.; Ma, C.; Liu, Y.-j., The importance of an indigenous tree to southern African communities with specific relevance to its domestication and commercialization: a case of the marula tree. *Forestry Studies in China* **2011,** *13* (1), 36-44.

14. Hall, J. B.; O'Brien, E. M.; Sinclair, F., Sclerocarya birrea: a monograph. *School of Agricultural and Forest Sciences Publication No. 19* **2002**, 1-157.

15. Chirwa, P.; Akinnifesi, F., Ecology, biology and distribution of Uapaca kirkiana Strychnos coculoides and Sclerocarya birrea in Southern Africa. 2008; pp 322-340.

16. Borochov-Neori, H.; Judeinstein, S.; Greenberg, A.; Fuhrman, B.; Attias, J.; Volkova, N.; Hayek, T.; Aviram, M., Phenolic antioxidants and antiatherogenic effects

of Marula (Sclerocarrya birrea Subsp. caffra) fruit juice in healthy humans. *J Agric Food Chem* **2008,** *56* (21), 9884-91.

17. Sinthumule, N. I.; Mzamani, L. C. M., Communities and Conservation: Marula Trees (Sclerocarya birrea subsp. caffra) Under Communal Management at Matiyane Village, Limpopo Province, South Africa. *Tropical Conservation Science* **2019,** *12*, 1940082919828969.

18. Encyclopedia, W. T. F., Sclerocarya birrea. **2016**.

19. PlantZAfrica.com, S., Sclerocarya birrea (A.Rich.) Hochst. subsp. caffra (Sond.) Kokwaro.

20. Shackleton, S.; Shackleton, C., Use of marula products for domestic and commercial purposes by households in the Bushbuckridge district, Limpopo Province, South Africa. **2002**.

21. Shackleton, C. M.; Botha, J.; Emanuel, P. L., Productivity and abundance of Sclerocarya birrea Subsp.Caffra in and around rural settlements and protected areas of the bushbuckridge lowveld, South Africa. *Forests, Trees and Livelihoods* **2003,** *13* (3), 217-232.

22. Nwonwu, F., The Socio-Cultural and Economic Relevance of the Marula Tree and its Sustainable Use in South Africa. *Africa Insight* **2007,** *36*.

23. Mariod, A.; MatthÄUs, B.; Eichner, K., Fatty acid, tocopherol and sterol composition as well as oxidative stability of three unusual Sudanese oils. *Journal of Food Lipids* **2005,** *11*, 179-189.

24. Eloff, J. N., Antibacterial activity of Marula (Sclerocarya birrea (A. rich.) Hochst. subsp. caffra (Sond.) Kokwaro) (Anacardiaceae) bark and leaves. *J Ethnopharmacol* **2001,** *76* (3), 305-8.

25. Shackleton, S.; Shackleton, C., The contribution of Marula (Sclerocarya birrea) fruit and fruit products to rural livelihoods in the bushbuckridge district, South Africa: Balancing domestic needs and commercialisation. *Forests, Trees and Livelihoods* **2005,** *15* (1), 3-24.

26. Semenya, S. S.; Maroyi, A., Plants Used by Bapedi Traditional Healers to Treat Asthma and Related Symptoms in Limpopo Province, South Africa. *Evidence-Based Complementary and Alternative Medicine* **2018,** *2018*, 2183705.

27. Semenya, S. S.; Potgieter, M.; Erasmus, L. J. C., Indigenous plant speciess used by Bapedi healers to treat sexually transmitted infections: Their distribution, harvesting, conservation and threats. *South African Journal of Botany* **2013,** *87*, 66-75.

28. Semenya, S. S.; Maroyi, A., Medicinal plants used by the Bapedi traditional healers to treat diarrhoea in the Limpopo Province, South Africa. *J Ethnopharmacol* **2012,** *144* (2), 395-401.

29. Runyoro, D.; Ngassapa, O.; Matee, M.; Joseph, C. C.; Moshi, M., Medicinal plants used by Tanzanian traditional healers in the management of Candida infections. *Journal of ethnopharmacology* **2006,** *106*, 158-65.

30. Prinsloo, G.; Street, R., Marula [Sclerocarya birrea (A.Rich) Hochst]: A Review of Traditional Uses, Phytochemistry, and Pharmacology. 2013; Vol. 1127, pp 19-32.

31. Ojewole, J. A., Evaluation of the anti-inflammatory properties of Sclerocarya birrea (A. Rich.) Hochst. (family: Anacardiaceae) stem-bark extracts in rats. *J Ethnopharmacol* **2003,** *85* (2-3), 217-20.

32. Théophile, D.; Rakotonirina, S.; Tan, P.; Azay, J.; Dongo, E.; Kamtchouing, P.; Cros, G., Effect of Sclerocarya birrea (Anacardidceae) stem bark methylene chloride/methanol extract on streptozotocin-diabetic rats. *Journal of ethnopharmacology* **2007,** *110*, 434-8.

33. Kokwaro, J. O., *Medicinal plants of East Africa*. 3rd ed. ed.; University of Nairobi Press: Nairobi, Kenya, 2009.

34. Prance, G. T., Medicinal plants in tropical West Africa. By Bep Oliver-Bever. *Brittonia* **1987,** *39*, 19-19.

35. Watt, J. M.; Breyer-Brandwijk, M. G., *The medicinal and poisonous plants of southern and eastern Africa : being an account of their medicinal and other uses, chemical composition, pharmacological effects and toxicology in man and animal*. Second edition. ed.; Livingstone: Edinburgh, 1962.

36. Hillman, Z.; Mizrahi, Y.; Beit-Yannai, E., Evaluation of valuable nutrients in selected genotypes of marula (Sclerocarya birrea ssp. caffra). *Scientia Horticulturae* **2008,** *117*, 321-328.

37. Mavundza, E. J.; Maharaj, R.; Finnie, J. F.; Kabera, G.; Van Staden, J., An ethnobotanical survey of mosquito repellent plants in uMkhanyakude district, KwaZulu-Natal province, South Africa. *J Ethnopharmacol* **2011,** *137* (3), 1516-20.

38. Ojewole, J., Anticonvulsant effect of Sclerocarya birrea (A. Rich.) Hochst. subsp. caffra (Sond.) Kokwaro (Anacardiaceae) stem-bark aqueous extract in mice. *J Nat Med* **2007,** *61*, 67-72.

39. Ojewole, J. A., Evaluation of the analgesic, anti-inflammatory and anti-diabetic properties of Sclerocarya birrea (A. Rich.) Hochst. stem-bark aqueous extract in mice and rats. *Phytother Res* **2004,** *18* (8), 601-8.

40. Da Costa Mousinho, N. M. H.; van Tonder, J. J.; Steenkamp, V., In Vitro Anti-diabetic Activity of Sclerocarya Birrea and Ziziphus Mucronata. *Natural Product Communications* **2013,** *8* (9), 1934578X1300800924.

41. Ngueguim, F. T.; Esse, E. C.; Dzeufiet, P. D.; Gounoue, R. K.; Bilanda, D. C.; Kamtchouing, P.; Dimo, T., Oxidised palm oil and sucrose induced hyperglycemia in normal rats: effects of Sclerocarya birrea stem barks aqueous extract. *BMC Complement Altern Med* **2016,** *16*, 47.

42. Victoria-Montesinos, D.; Sánchez-Macarro, M.; Gabaldón-Hernández, J. A.; Abellán-Ruiz, M. S.; Querol-Calderón, M.; Luque-Rubia, A. J.; Bernal-Morell, E.; Ávila-Gandía, V.; López-Román, F. J., Effect of dietary supplementation with a natural extract of Sclerocarya birrea on glycemic metabolism in subjects with prediabetes: a randomized double-blind placebo-controlled study. *Nutrients* **2021,** *13* (6), 1948.

43. Mabasa, L.; Kotze, A.; Shabalala, S.; Kimani, C.; Gabuza, K.; Johnson, R.; Sangweni, N. F.; Maharaj, V.; Muller, C. J. F., Sclerocarya birrea (Marula) Extract Inhibits Hepatic Steatosis in db/db Mice. *Int J Environ Res Public Health* **2022,** *19* (7).

44. Belemtougri, R. G.; Constantin, B.; Cognard, C.; Raymond, G.; Sawadogo, L., Effects of Sclerocarya birrea (A. rich) hochst (anacardiaceae) leaf extracts on calcium signalling in cultured rat skeletal muscle cells. *J Ethnopharmacol* **2001,** *76* (3), 247-52.

45. Braca, A.; Politi, M.; Sanogo, R.; Sanou, H.; Morelli, I.; Pizza, C.; De Tommasi, N., Chemical composition and antioxidant activity of phenolic compounds from wild and cultivated Sclerocarya birrea(Anacardiaceae) leaves. *J Agric Food Chem* **2003,** *51* (23), 6689-95.

46. Hamid, H.; Obaid, M. A., Role of Quercetin Flavonoid as Antidiabetic: A Review. **2021**, 1495-1500.

47. Zhang, Y.; Meng, J.; Wang, S.; Gu, D.; Lin, X.; Huang, D.; Yang, Y., Immobilized α-glucosidase using polydopamine-coated magnetic nanoparticles for targeted screening of an active component from Toona sinensis. *Journal of Liquid Chromatography & Related Technologies* **2021,** *44* (13-14), 674-681.

223

48. Ibitoye, O.; Uwazie, J.; Ajiboye, T., Bioactivity-guided isolation of kaempferol as the antidiabetic principle from Cucumis sativus L. fruits. *Journal of Food Biochemistry* **2018,** *42*.

49. Vishnu Prasad, C. N.; Anjana, T.; Banerji, A.; Gopalakrishnapillai, A., Gallic acid induces GLUT4 translocation and glucose uptake activity in 3T3-L1 cells. *FEBS Letters* **2010,** *584* (3), 531-536.

50. Salomé, K.; Gbaguidi, F.; Kossouoh, C.; Agbani, P.; Yayi, E.; Sinsin, B.; Moudachirou, M.; Accrombessi, G.; Quetin-Leclercq, J., Chemical composition and seasonal variation of essential oil of Sclerocarya birrea (A. Rich.) Hochst subsp birrea leaves from Benin. *Journal of medicinal plant research* **2011,** *5*, 4640-4646.

51. Eid, H. M.; Martineau, L. C.; Saleem, A.; Muhammad, A.; Vallerand, D.; Benhaddou-Andaloussi, A.; Nistor, L.; Afshar, A.; Arnason, J. T.; Haddad, P. S., Stimulation of AMP-activated protein kinase and enhancement of basal glucose uptake in muscle cells by quercetin and quercetin glycosides, active principles of the antidiabetic medicinal plant Vaccinium vitis-idaea. *Molecular Nutrition & Food Research* **2010,** *54* (7), 991-1003.

52. Nyirenda, K. K.; Saka, J. D. K.; Naidoo, D.; Maharaj, V. J.; Muller, C. J. F., Antidiabetic, anti-oxidant and antimicrobial activities of Fadogia ancylantha extracts from Malawi. *Journal of Ethnopharmacology* **2012,** *143* (1), 372-376.

53. Mosmann, T., Rapid colorimetric assay for cellular growth and survival: Application to proliferation and cytotoxicity assays. *Journal of Immunological Methods* **1983,** *65* (1), 55-63.

54. Mousinho, N. M.; van Tonder, J. J.; Steenkamp, V., In vitro anti-diabetic activity of Sclerocarya birrea and Ziziphus mucronata. *Nat Prod Commun* **2013,** *8* (9), 1279-84.

55. Kgopa, A. H., Effects of Sclerocarya birrea Stem-Bark Extracts on Glucose Uptake, Insulin Synthesis and Expression of Selected Genes Involved in the Synthesis and Secretion of Insulin in Rat Insulinoma Pancreatic Beta Cells. *Asian Journal of Chemistry* **2020,** *32*, 2195-2202.

56. Fathoni, A.; Saepudin, E.; Herry, C.; Rahayu, D. U. C.; Haib, J., *Identification of nonvolatile compounds in clove (Syzygium aromaticum) from Manado*. 2017; Vol. 1862, p 030079.

57. Rue, E. A.; Rush, M. D.; van Breemen, R. B., Procyanidins: a comprehensive review encompassing structure elucidation via mass spectrometry. *Phytochem Rev* **2018,** *17* (1), 1-16.

58. Yuzuak, S.; Ballington, J.; Xie, D. Y., HPLC-qTOF-MS/MS-Based Profiling of Flavan-3-ols and Dimeric Proanthocyanidins in Berries of Two Muscadine Grape Hybrids FLH 13-11 and FLH 17-66. *Metabolites* **2018,** *8* (4).

59. Yuzuak, S.; Ballington, J.; Xie, D.-Y., HPLC-qTOF-MS/MS-Based Profiling of Flavan-3-ols and Dimeric Proanthocyanidins in Berries of Two Muscadine Grape Hybrids FLH 13-11 and FLH 17-66. *Metabolites* **2018,** *8* (4), 57.

60. Hou, A. J.; Peng, L. Y.; Liu, Y. Z.; Lin, Z. W.; Sun, H. D., Gallotannins and related polyphenols from Pistacia weinmannifolia. *Planta Med* **2000,** *66* (7), 624-6.

61. Lin, Y.; Wu, B.; Li, Z.; Hong, T.; Chen, M.; Tan, Y.; Jiang, J.; Huang, C., Metabolite Identification of Myricetin in Rats Using HPLC Coupled with ESI-MS. *Chromatographia* **2012,** *75* (11), 655-660.

62. Hassan, W. H. B.; Abdelaziz, S.; Al Yousef, H. M., Chemical Composition and Biological Activities of the Aqueous Fraction of Parkinsonea aculeata L. Growing in Saudi Arabia. *Arabian Journal of Chemistry* **2019,** *12* (3), 377-387.

63. Dueñas, M.; Mingo-Chornet, H.; Pérez-Alonso, J.; Di Paola, R.; Gonzalez-paramas, A. M.; Santos Buelga, C., Preparation of quercetin glucuronides and characterization

by HPLC–DAD–ESI/MS. *European Food Research and Technology* **2008,** *227*, 1069-1076.

64. Kumar, S.; Singh, A.; Kumar, B., Identification and characterization of phenolics and terpenoids from ethanolic extracts of Phyllanthus species by HPLC-ESI-QTOF-MS/MS. *J Pharm Anal* **2017,** *7* (4), 214-222.

65. Saldanha, L. L.; Vilegas, W.; Dokkedal, A. L., Characterization of flavonoids and phenolic acids in Myrcia bella Cambess. using FIA-ESI-IT-MS(n) and HPLC-PAD-ESI-IT-MS combined with NMR. *Molecules* **2013,** *18* (7), 8402-16.

66. Piccinelli, A. L.; Veneziano, A.; Passi, S.; Simone, F. D.; Rastrelli, L., Flavonol glycosides from whole cottonseed by-product. *Food Chemistry* **2007,** *100* (1), 344-349.

67. March, R. E.; Miao, X.-S., A fragmentation study of kaempferol using electrospray quadrupole time-of-flight mass spectrometry at high mass resolution. *International Journal of Mass Spectrometry* **2004,** *231* (2), 157-167.

68. Yan, M.; Chen, M.; Zhou, F.; Cai, D.; Bai, H.; Wang, P.; Lei, H.; Ma, Q., Separation and analysis of flavonoid chemical constituents in flowers of Juglans regia L. by ultra-high-performance liquid chromatography-hybrid quadrupole time-of-flight mass spectrometry. *Journal of Pharmaceutical and Biomedical Analysis* **2019,** *164*, 734-741.

69. Scigelova, M.; Hornshaw, M.; Giannakopulos, A.; Makarov, A., Fourier Transform Mass Spectrometry. *Molecular & cellular proteomics : MCP* **2011,** *10*, M111.009431.

70. Variya, B. C.; Bakrania, A. K.; Patel, S. S., Antidiabetic potential of gallic acid from Emblica officinalis: Improved glucose transporters and insulin sensitivity through PPAR-γ and Akt signaling. *Phytomedicine* **2020,** *73*, 152906.

71. Chakravarthy, B. K.; Gupta, S.; Gode, K. D., Antidiabetic effect of (-)-epicatechin. *Lancet* **1982,** *2* (8292), 272-273.

72. Chen, H. W.; Yang, M. Y.; Hung, T. W.; Chang, Y. C.; Wang, C. J., Nelumbo nucifera leaves extract attenuate the pathological progression of diabetic nephropathy in high-fat diet-fed and streptozotocin-induced diabetic rats. *J Food Drug Anal* **2019,** *27* (3), 736-748.

73. Li, Y.; Zheng, X.; Yi, X.; Liu, C.; Kong, D.; Zhang, J.; Gong, M., Myricetin: a potent approach for the treatment of type 2 diabetes as a natural class B GPCR agonist. *FASEB J* **2017,** *31* (6), 2603-2611.

74. Bule, M.; Abdurahman, A.; Nikfar, S.; Abdollahi, M.; Amini, M., Antidiabetic effect of quercetin: A systematic review and meta-analysis of animal studies. *Food Chem Toxicol* **2019,** *125*, 494-502.

75. Nedachi, T.; Kanzaki, M., Regulation of glucose transporters by insulin and extracellular glucose in C2C12 myotubes. *Am J Physiol Endocrinol Metab* **2006,** *291* (4), E817-28.

76. He, D.; Gu, D.; Huang, Y.; Ayupbek, A.; Yang, Y.; Aisa, H.; Ito, Y., Separation and Purification of Phenolic Acids and Myricetin from Black Currant by High-Speed Countercurrent Chromatography. *Journal of liquid chromatography & related technologies* **2009,** *32*, 3077-3088.

77. Perkin, A. G., XXI.—Myricetin. Part II. *Journal of the Chemical Society, Transactions* **1902,** *81*, 203-210.

78. Granica, S.; Czerwińska, M. E.; Żyżyńska-Granica, B.; Kiss, A. K., Antioxidant and anti-inflammatory flavonol glucuronides from Polygonum aviculare L. *Fitoterapia* **2013,** *91*, 180-188.

79. Moon, J. H.; Tsushida, T.; Nakahara, K.; Terao, J., Identification of quercetin 3-O-beta-D-glucuronide as an antioxidative metabolite in rat plasma after oral administration of quercetin. *Free Radic Biol Med* **2001,** *30* (11), 1274-85.

80. Hiermann, A.; Schramm, H.; Laufer, S., Anti-inflammatory activity of myricetin-3-O-β-D-glucuronide and related compounds. *Inflammation research* **1998,** *47*, 421-427.

81. Zhang, J.; Shen, Q.; Lu, J.-C.; Li, J.-Y.; Liu, W.-Y.; Yang, J.-J.; Li, J.; Xiao, K., Phenolic compounds from the leaves of Cyclocarya paliurus (Batal.) Ijinskaja and their inhibitory activity against PTP1B. *Food Chemistry* **2010,** *119* (4), 1491-1496.

82. Fan, D.; Zhao, Y.; Zhou, X.; Gong, X.; Zhao, C., Simultaneous determination of esculetin, quercetin-3-O-β-D-glucuronide, quercetin-3-O-β-D-glucuronopyranside methyl ester and quercetin in effective part of Polygonum perfoliatum L. using high performace liquid chromatography. *Pharmacognosy Magazine* **2014,** *10* (39), 359.

83. Yang, H. H.; Hwangbo, K.; Zheng, M. S.; Cho, J. H.; Son, J.-K.; Kim, H. Y.; Baek, S. H.; Choi, H. C.; Park, S. Y.; Kim, J.-R., Quercetin-3-O-β-D-glucuronide isolated from Polygonum aviculare inhibits cellular senescence in human primary cells. *Archives of pharmacal research* **2014,** *37*, 1219-1233.

84. Yang, L.-L.; Xiao, N.; Li, X.-W.; Fan, Y.; Alolga, R. N.; Sun, X.-Y.; Wang, S.-L.; Li, P.; Qi, L.-W., Pharmacokinetic comparison between quercetin and quercetin 3-O-β-glucuronide in rats by UHPLC-MS/MS. *Scientific Reports* **2016,** *6* (1), 35460.

85. Polori, K. L.; Mashele, S. S.; Aremu, A. O., In vitro anti-diabetic effect and cytotoxicity of South African Ipomoea oblongata. *South African Journal of Botany* **2021,** *142*, 96-99.

86. Blahova, J.; Martiniakova, M.; Babikova, M.; Kovacova, V.; Mondockova, V.; Omelka, R., Pharmaceutical Drugs and Natural Therapeutic Products for the Treatment of Type 2 Diabetes Mellitus. *Pharmaceuticals* **2021,** *14* (8), 806.

87. Borges, P. H. O.; Pedreiro, S.; Baptista, S. J.; Geraldes, C. F. G. C.; Batista, M. T.; Silva, M. M. C.; Figueirinha, A., Inhibition of α-glucosidase by flavonoids of Cymbopogon citratus (DC) Stapf. *Journal of Ethnopharmacology* **2021,** *280*, 114470.

Chapter 5: General Conclusion

The research to identify and develop new natural anti-inflammatory ingredients was conducted for commercial application in the cosmetic industry. Based on the traditional uses and literature searches, South African plants were selected and tested for efficacy. *S. columbaria* was selected, based on good anti-inflammatory efficacy data and no anti-inflammatory reports in the literature.

After testing different extracts of *S. columbaria* during this Ph.D. research, the ethanol extract of *S. columbaria* roots was selected for further evaluation to identify the compound/s responsible for the anti-inflammatory activity and development as a potential active herbal ingredient. UPLC-QTOF-MS analysis of the ethanol extract of *S. columbaria* roots and NMR analysis of isolated compounds, led to the identification of compounds which include loganic acid (**62**), cantleyoside -dimethyl-acetal (**63**), ursolic acid (**64**), 2-isoursolic acid (**65**), 24-nor-2α,3β-dihydroxyolean-4(23),12-ene (**66**) and hederagenin (**67**). Significant reduction of nitric oxide levels in RAW 264.7 macrophages was observed for ursolic acid (**64**) (test concentrations: 12.5, 25 and 50 µg/mL; reduction by 0.0702, 0.0558 and 0.0357 µg/mLrespectively), 24-nor-2α,3β-dihydroxyolean-4(23),12-ene (**66**) (test concentration: 12.5, 25 and 50 µg/mL; reduction by 0.0543, 0.0327 and 0.0231 µg/mLrespectively) and hederagenin (**67**) (test concentration: 12.5 and 25 µg/mL; reduction by 0.0735 and 0.0513 µg/mLrespectively) compared to the positive control aminoguanidine (test concentration: 12.5 µg/mL; reduction by 0.0336 µg/mL). At concentrations of 25 and 50 µg/mL, 24-nor-2α,3β-dihydroxyolean-4(23),12-ene (**66**) demonstrated a potent reduction (0.0327 and 0.0231 µg/mL) in nitric oxide level in RAW 264.7 macrophages. The compounds identified in the ethanol extract of *S. columbaria* roots will be used as chemical markers for quality control purposes, for batch-to-batch reproducibility that is required for commercializing the herbal ingredient. The anti-inflammatory activity of *S. columbaria* roots and 24-nor-2α,3β-dihydroxyolean-4(23),12-ene (**66**) have been reported for the first time in this work. The active compounds (ursolic acid (**64**), 24-nor-2α,3β-dihydroxyolean-4(23),12-ene (**66**) and hederagenin (**67**)) were structurally similar and contained a β-hydroxy group at C-3. The compound 2-isoursolic acid (**65**) was inactive and had a hydroxy group at C-2 instead of C-3, which suggests that the position of the β-hydroxy group may play a role in the nitric oxide inhibition activity. A concentrated form of the ethanol extract of *S. columbaria* roots can be developed to have a

higher concentration of the active compounds for commercial application as an anti-inflammatory ingredient.

The research to identify and develop a new natural anti-diabetic ingredient was conducted as part of a project within the African Traditional Medicines consortium set-up by the Department of Science and Innovation (DSI). *S. birrea* was selected since the leaves and stem bark are used traditionally for the management of diabetes mellitus amongst other ailments. Although *S. birrea* leaf extract was reported to be active against type-2 diabetes mellitus, the compounds responsible for the anti-diabetic activity have not been reported and its identification will be useful for commercial application. This Ph.D. research was therefore conducted to identify the chemical compounds in *S. birrea* responsible for the anti-diabetic activity and to use these as chemical markers for quality control purposes. Of all the extracts of *S. birrea* tested, aqueous extract 4 showed statistically significant activity including at the lowest test concentration (0.01 µg/mL) and was selected to isolate and identify the compounds responsible for the anti-diabetic activity (glucose uptake activity).

UPLC-QTOF-MS analysis of the spray-dried aqueous leaf extracts of *S. birrea* (aqueous extracts 1 and 4) led to the tentative identification of sixteen compounds which are quinic acid (**peak 1**), gallic acid (**peak 2**), procyanidin B2 (**peak 3**), gallocatechin (**peak 4**), Pistafolin A (**peak 5**), epicatechin (**peak 6**), myricetin-3-*O*-β-D-glucuronide (**88**), gossypin (**peak 8**), quercetin-3-*O*-(6"-galloyl)-β-D-glucopyranoside (**peak 9**), myricetin-3-*O*-α-L-rhamnopyranoside (**peak 10**), quercetin-3-*O*-β-D-glucuronide (**89**), quercetin-3-*O*-arabinoside (**peak 12**), quercetin-3-*O*-α-L-rhamnopyranoside (**peak 13**), kaempferol-3-*O*-α-L-rhamnopyranoside (**peak 14**), myricetin (**90**) and quercetin (**peak 16**). The presence of myricetin (**91**), myricetin-3-*O*-β-D-glucuronide (**92**) and quercetin-3-*O*-β-D-glucuronide (**93**) in the aqueous leaf extract of *S. birrea* was confirmed by isolation and structure elucidation of the compounds using MS and NMR data. Gallic acid (**peak 2**), myricetin-3-*O*-α-L-rhamnopyranoside (**peak 10**), quercetin-3-*O*-arabinoside (**peak 12**) and quercetin-3-*O*-α-L-rhamnopyranoside (**peak 13**) were previously reported to occur in *S. birrea*. Quinic acid (**peak 1**), myricetin (**90**) and quercetin (**peak 16**) were previously reported to have anti-diabetic activity. Myricetin-3-*O*-β-D-glucuronide (**92**) and quercetin-3-*O*-β-D-glucuronide (**93**) have not been previously reported to occur in *S. birrea*. Myricetin (**91**), myricetin-3-*O*-β-D-glucuronide (**92**) and quercetin-3-*O*-β-D-glucuronide (**93**) significantly increased the glucose uptake in differentiated C2C12 myocyte cells at different test concentrations; myricetin (**91**) (0.1 and 10 µg/mL; 85.7 and 109.1%, respectively), myricetin-3-*O*-β-D-glucuronide (**92**) (0.1

228

and 10 µg/mL; 61.6 and 88.8%, respectively) and quercetin-3-O-β-D-glucuronide (**93**) (0.1 and 10 µg/mL; 40.9 and 43.9%, respectively) compared to the treatment of insulin (0.1 µM; 100%).

At a concentration of 10 µg/mL, myricetin (**91**) demonstrated both a potent and concentration-dependent stimulatory action on glucose uptake in the C2C12 myocytes, matching that of insulin, the positive control. Myricetin-3-O-β-D-glucuronide (**92**) has not been previously reported to have anti-diabetic activity, and the combination of this compound with other known anti-diabetic compounds in *S. birrea* contributes to the plant's anti-diabetic efficacy. These anti-diabetic compounds will be used as chemical markers for quality control purposes required for commercializing the herbal ingredient. This study provides scientific data to support the commercial application of the aqueous extract of *S. birrea* leaves as an anti-diabetic ingredient.

The overall goal of the project was achieved by identifying new active ingredients, and compounds responsible for the biological efficacy to be used as chemical markers for commercial application. This research provides scientific evidence on the value of South African plant biodiversity as a continued source of biologically active ingredients, and the indigenous knowledge on the use of medicinal plants proves to be beneficial for developing ingredients and products for the different market sectors.

SUPPLEMENTARY DATA
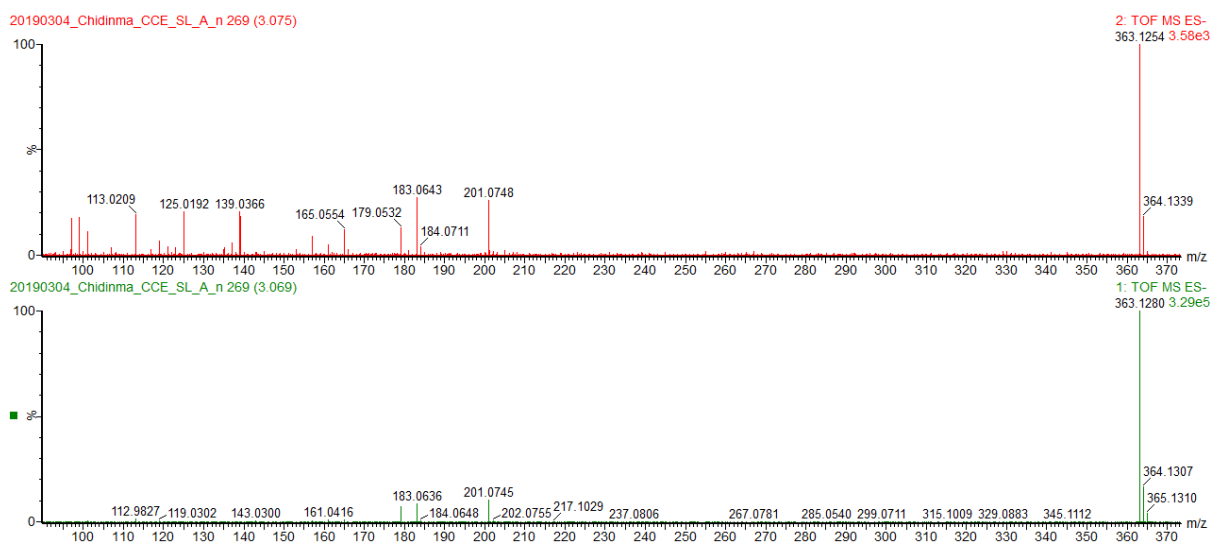
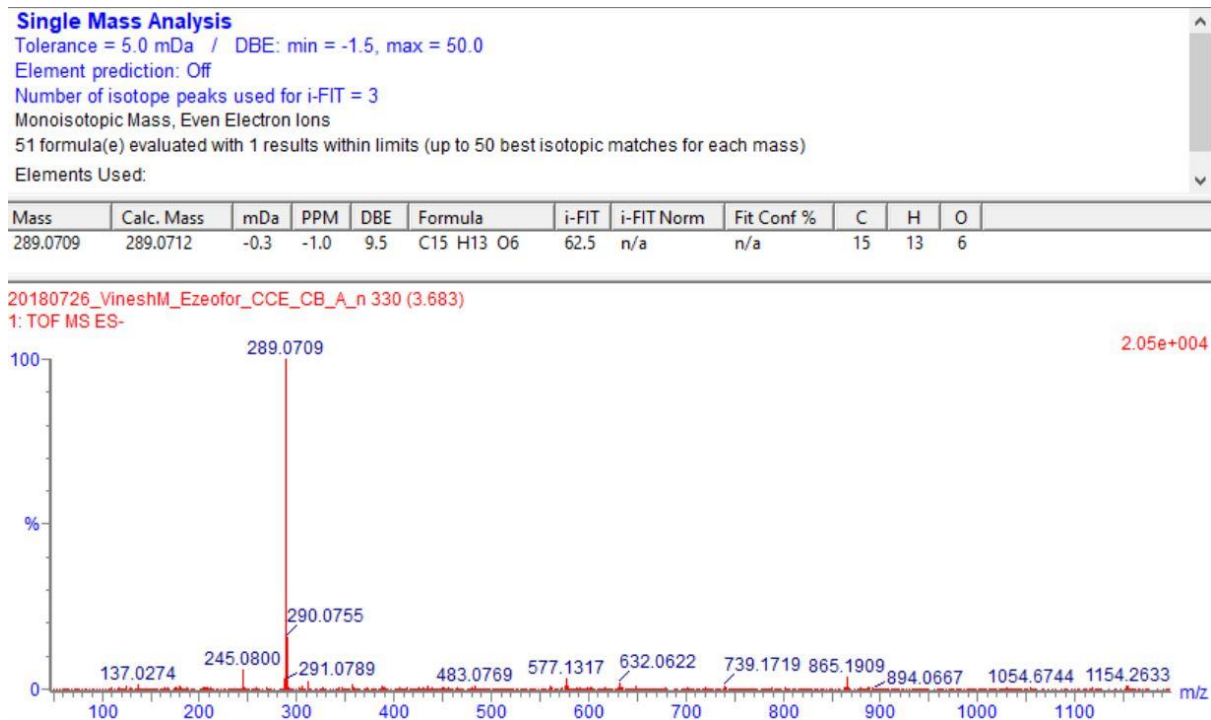**Supplementary data 1:** MS and MS/MS data of harpagide (**30**) in the acetone extract of *S. columbaria* leaves.
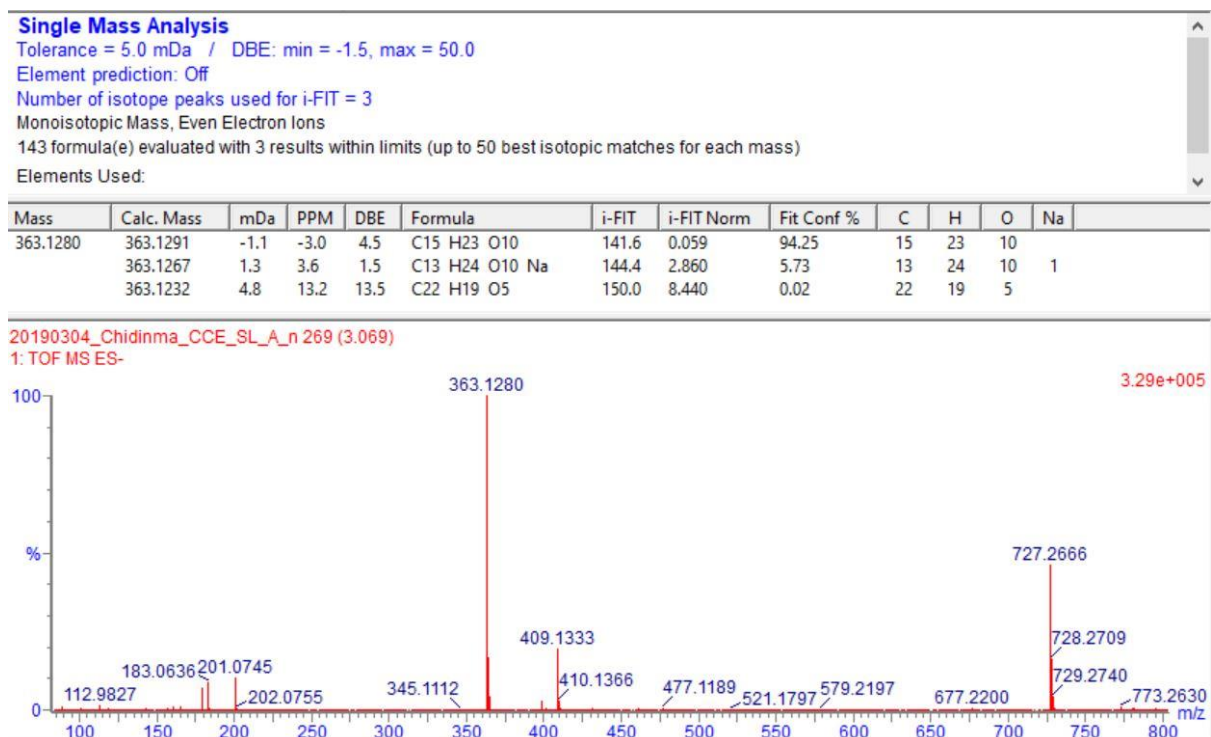

Supplementary data 2: iFit value of harpagide (**30**) in the acetone extract of *S. columbaria* leaves.
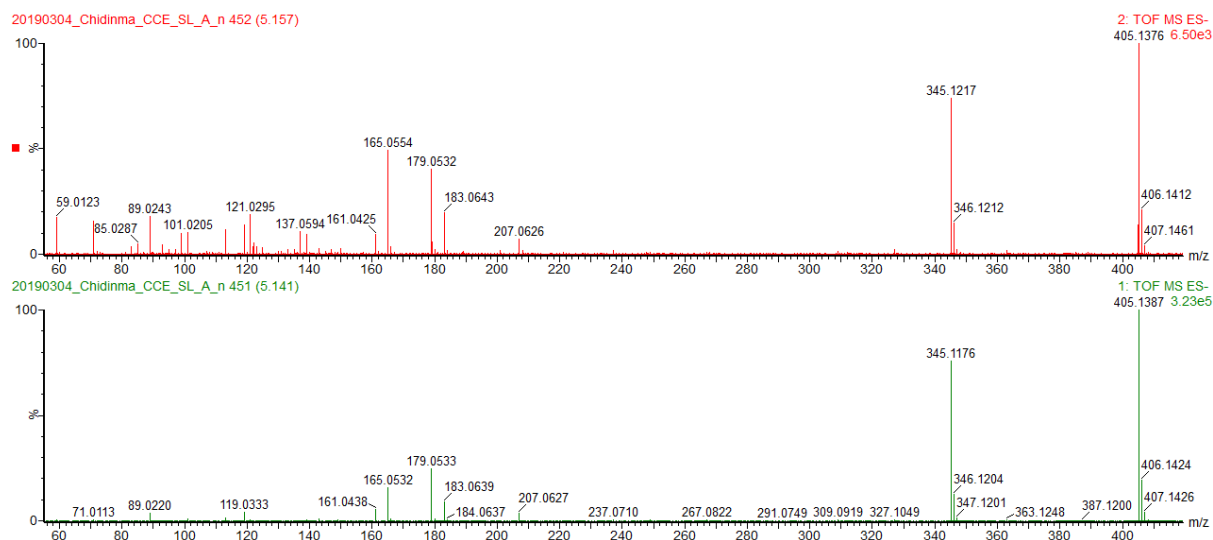
Supplementary data 3: MS and MS/MS data of 10-hydroxyloganin (**31**) in the acetone extract of *S. columbaria* leaves.

Single Mass Analysis
Tolerance = 5.0 mDa / DBE: min = -1.5, max = 50.0
Element prediction: Off
Number of isotope peaks used for i-FIT = 3
Monoisotopic Mass, Even Electron Ions
163 formula(e) evaluated with 3 results within limits (up to 50 best isotopic matches for each mass)
Elements Used:

Mass	Calc. Mass	mDa	PPM	DBE	Formula	i-FIT	i-FIT Norm	Fit Conf %	C	H	O	Na
405.1387	405.1397	-1.0	-2.5	5.5	C17 H25 O11	220.3	0.000	100.00	17	25	11	
	405.1373	1.4	3.5	2.5	C15 H26 O11 Na	230.3	10.041	0.00	15	26	11	1
	405.1338	4.9	12.1	14.5	C24 H21 O6	236.6	16.358	0.00	24	21	6	

Supplementary data 4: iFit value of 10-hydroxyloganin (**31**) in the acetone extract of *S. columbaria* leaves.
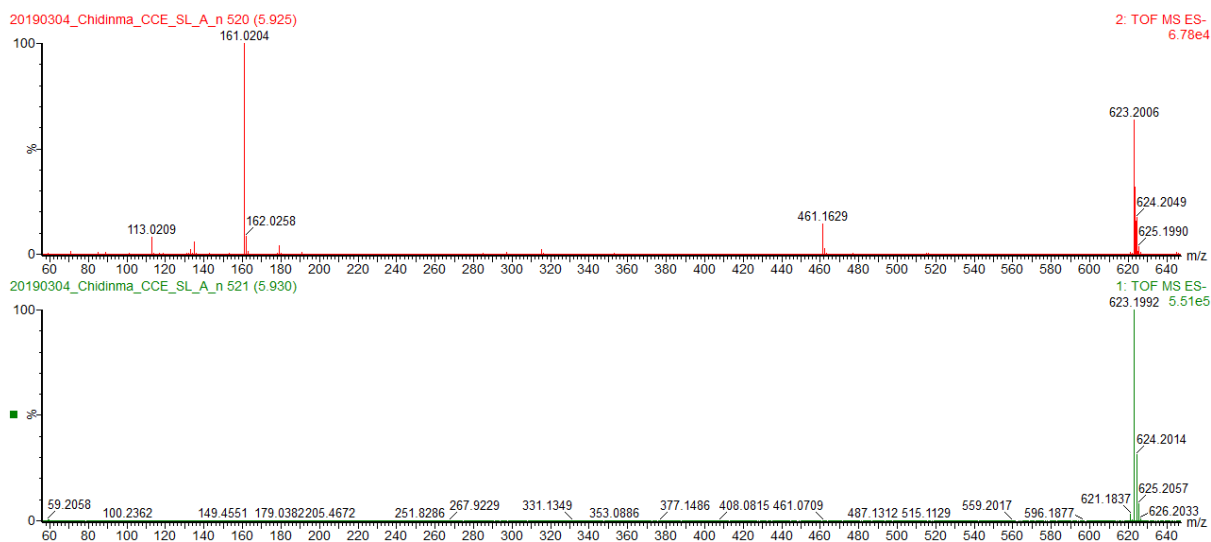
Supplementary data 5: MS and MS/MS data of forsythiaside (**32**) in the acetone extract of *S. columbaria* leaves.

Single Mass Analysis
Tolerance = 5.0 mDa / DBE: min = -1.5, max = 50.0
Element prediction: Off
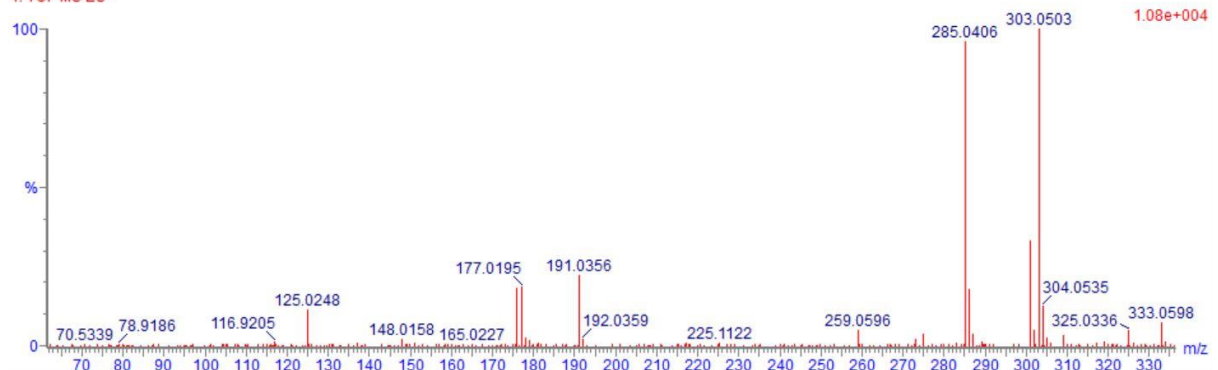Number of isotope peaks used for i-FIT = 3
Monoisotopic Mass, Even Electron Ions
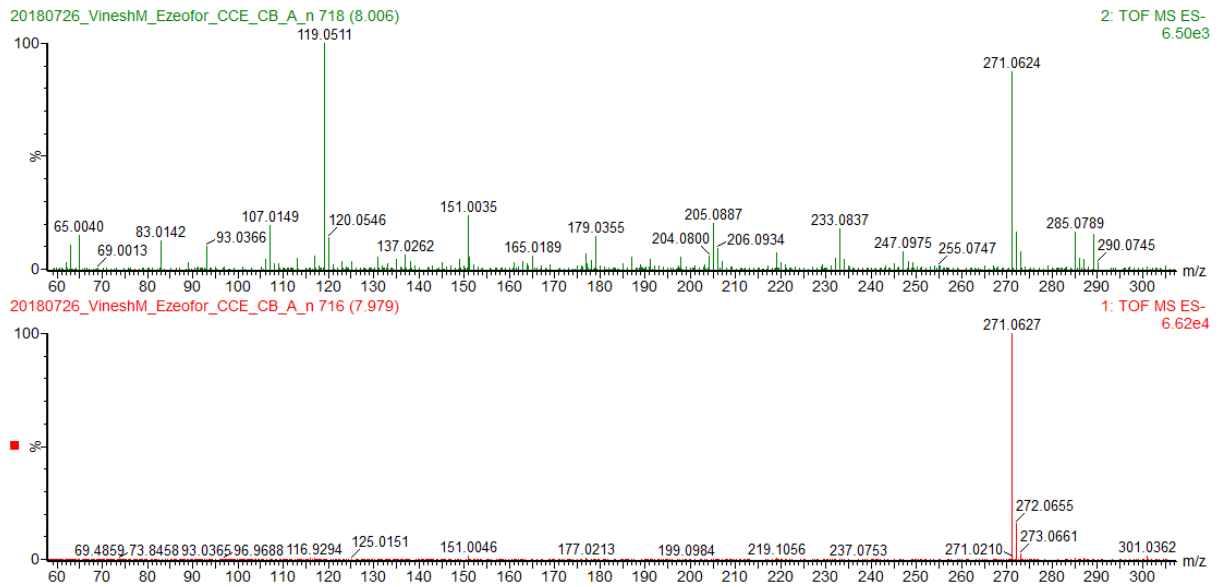365 formula(e) evaluated with 6 results within limits (up to 50 best isotopic matches for each mass)
Elements Used:

Mass	Calc. Mass	mDa	PPM	DBE	Formula	i-FIT	i-FIT Norm	Fit Conf %	C	H	O	Na
623.1992	623.1976	1.6	2.6	12.5	C29 H35 O15	140.2	0.026	97.48	29	35	15	
	623.1952	4.0	6.4	9.5	C27 H36 O15 Na	143.9	3.686	2.51	27	36	15	1
	623.2035	-4.3	-6.9	3.5	C22 H39 O20	150.2	9.947	0.00	22	39	20	
	623.1987	0.5	0.8	31.5	C45 H28 O2 Na	150.4	10.202	0.00	45	28	2	1
	623.2011	-1.9	-3.0	0.5	C20 H40 O20 Na	150.8	10.592	0.00	20	40	20	1
	623.2011	-1.9	-3.0	34.5	C47 H27 O2	151.6	11.353	0.00	47	27	2	
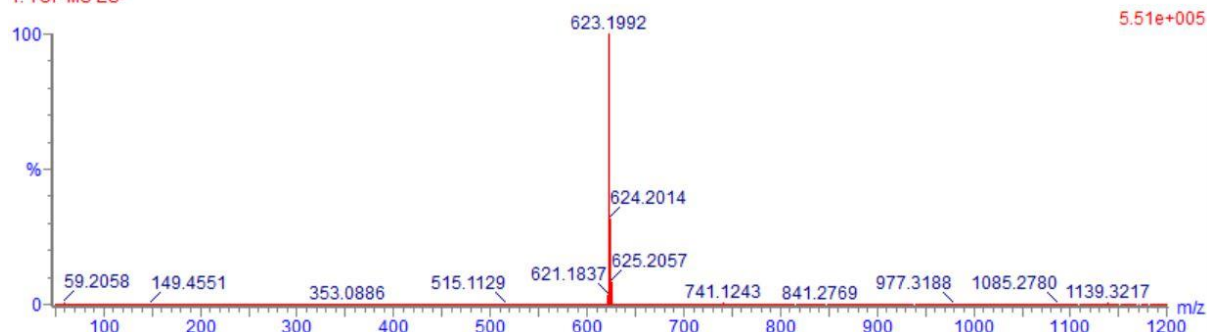
Supplementary data 6: iFit value of forsythiaside (**32**) in the acetone extract of *S. columbaria* leaves.
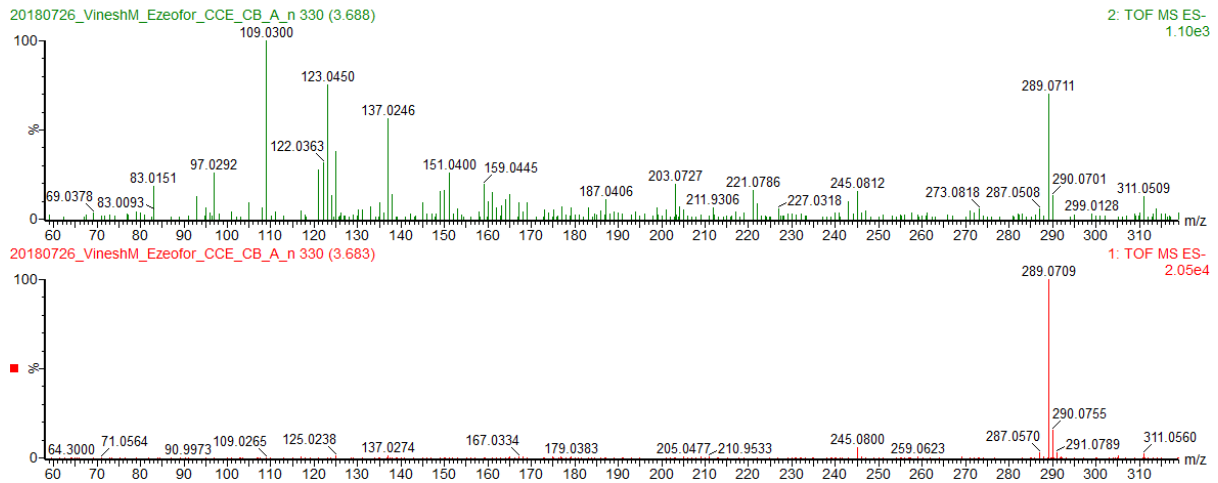
Supplementary data 7: MS and MS/MS data of epicatechin (**33**) in the acetone extract of *C. pyracanthoides* stem bark.


Supplementary data 8: iFit value of epicatechin (**33**) in the acetone extract of *C. pyracanthoides* stem bark.

233
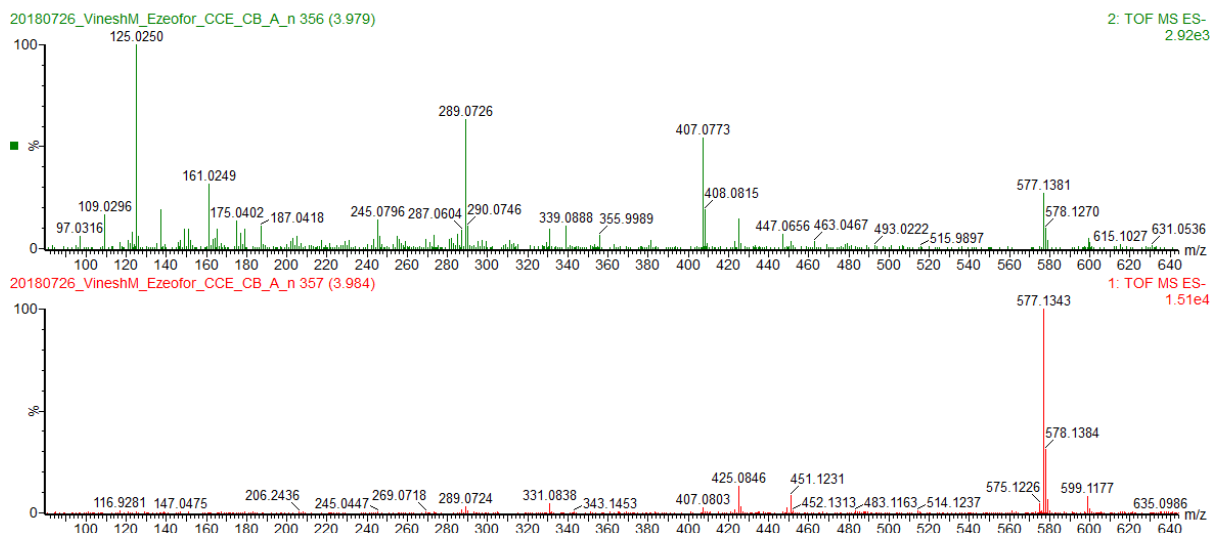
Supplementary data 9: MS and MS/MS data of procyanidin B2 (**34**) in the acetone extract of *C. pyracanthoides* stem bark.

Single Mass Analysis
Tolerance = 5.0 mDa / DBE: min = -1.5, max = 50.0
Element prediction: Off
Number of isotope peaks used for i-FIT = 3
Monoisotopic Mass, Even Electron Ions
162 formula(e) evaluated with 1 results within limits (up to 50 best isotopic matches for each mass)
Elements Used:

Mass	Calc. Mass	mDa	PPM	DBE	Formula	i-FIT	i-FIT Norm	Fit Conf %	C	H	O
577.1343	577.1346	-0.3	-0.5	18.5	C30 H25 O12	60.9	n/a	n/a	30	25	12
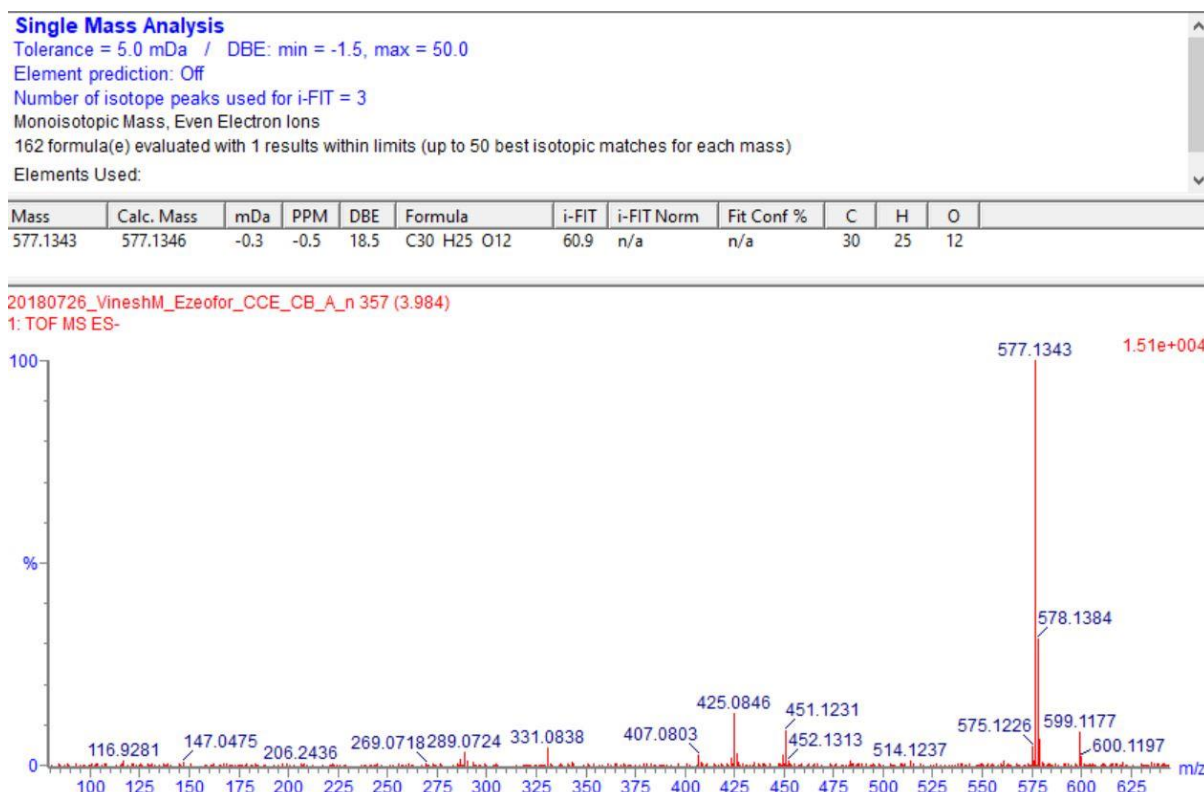
Supplementary data 10: iFit value of procyanidin B2 (**34**) in the acetone extract of *C. pyracanthoides* stem bark.
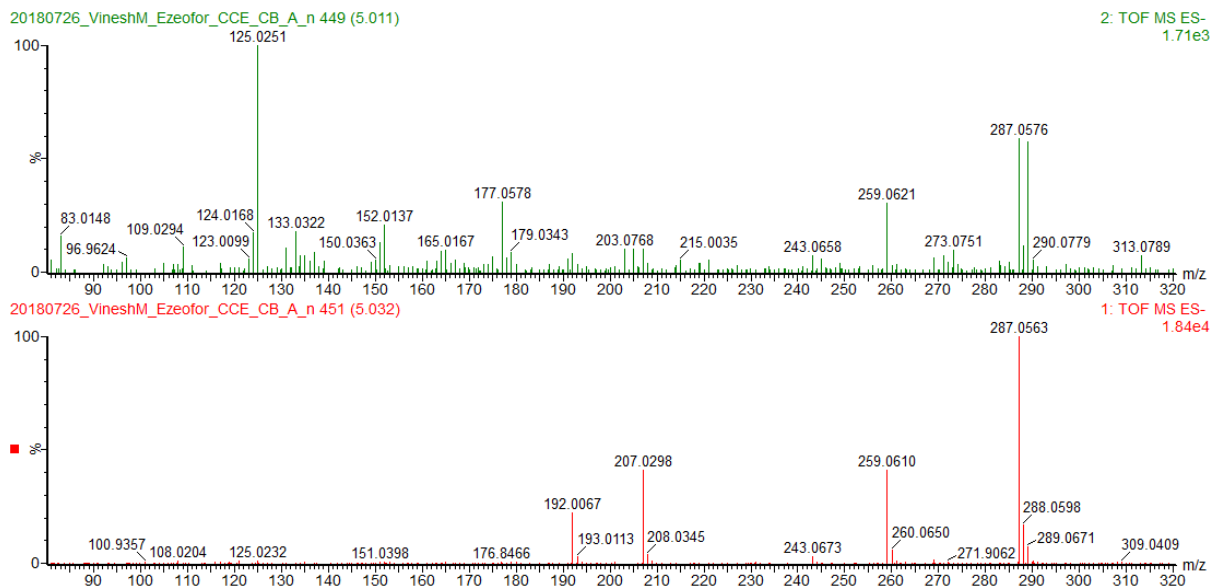
Supplementary data 11: MS and MS/MS data of dihydrokaempferol (**35**) in the acetone extract of *C. pyracanthoides* stem bark.
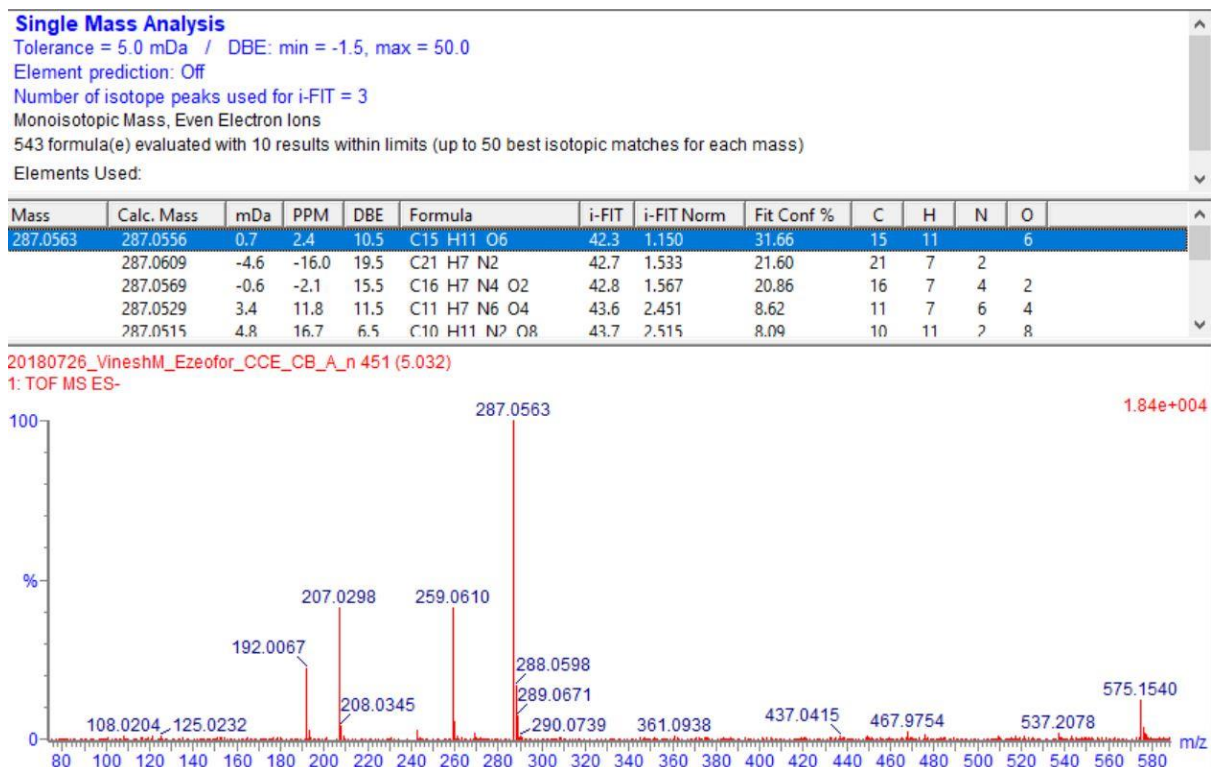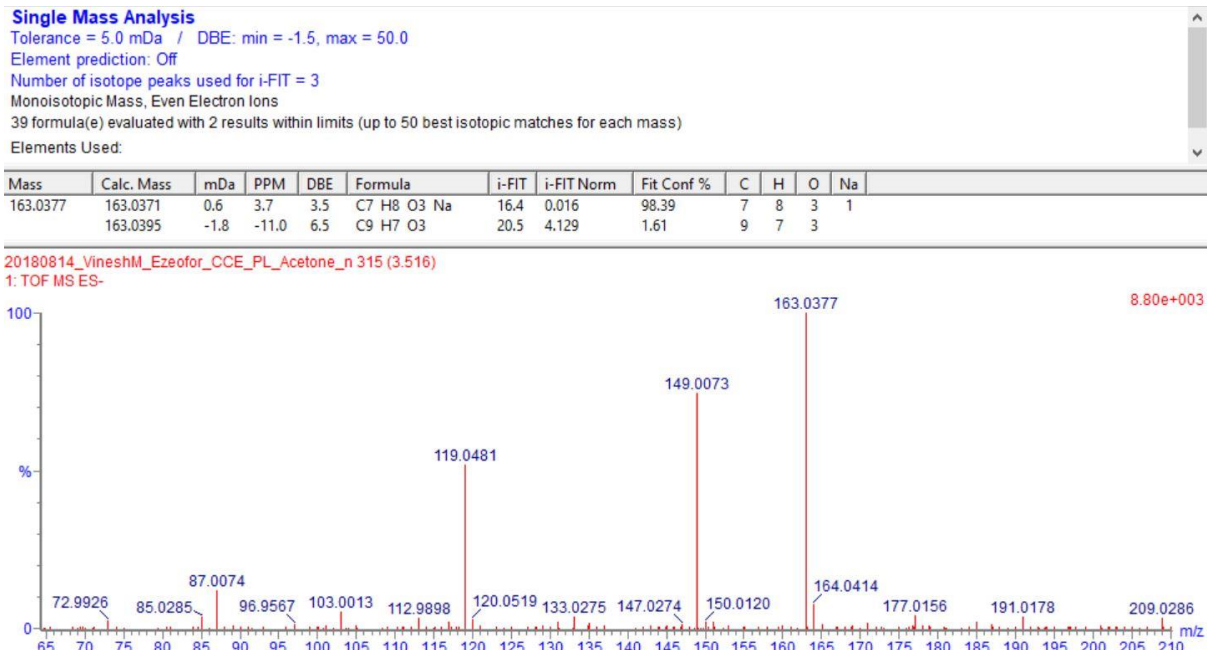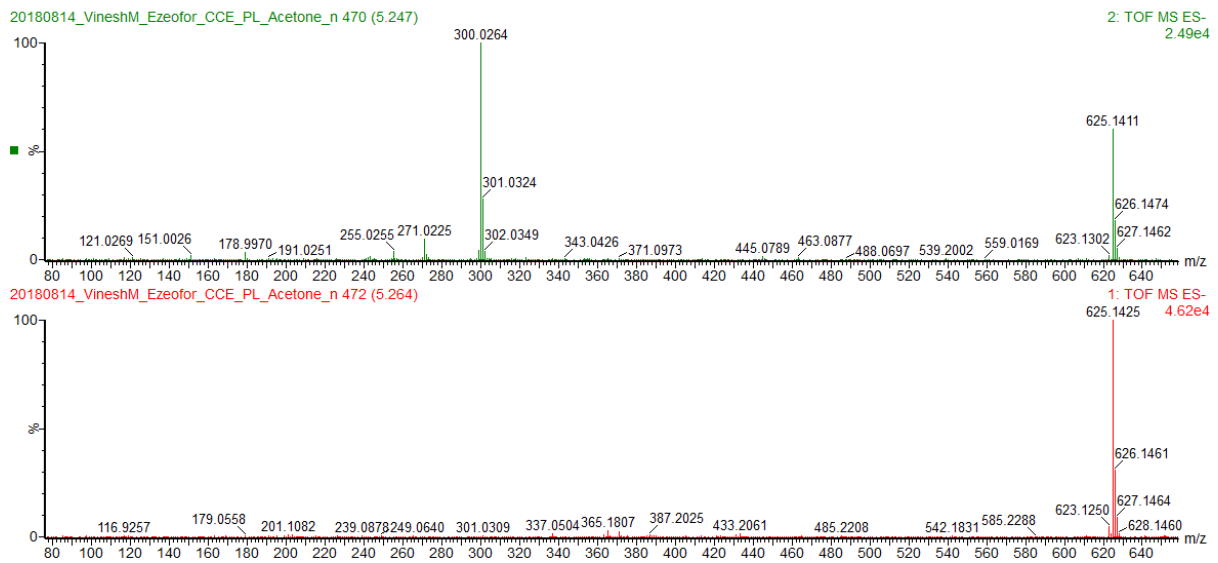

Supplementary data 12: iFit value of dihydrokaempferol (**35**) in the acetone extract of *C. pyracanthoides* stem bark.

235
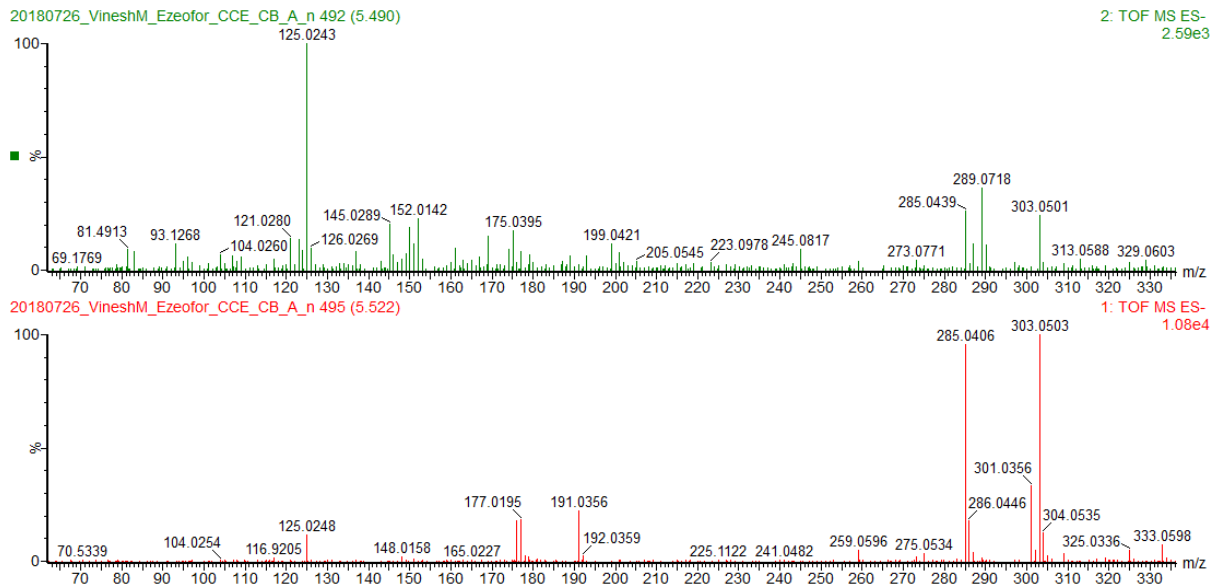
Supplementary data 13: MS and MS/MS data of dihydroquercetin (**36**) in the acetone extract of *C. pyracanthoides* stem bark.

Supplementary data 14: iFit value of dihydroquercetin (**36**) in the acetone extract of *C. pyracanthoides* stem bark.

Supplementary data 15: MS and MS/MS data of naringenin (**37**) in the acetone extract of *C. pyracanthoides* stem bark.

Single Mass Analysis
Tolerance = 5.0 mDa / DBE: min = -1.5, max = 50.0
Element prediction: Off
Number of isotope peaks used for i-FIT = 3
Monoisotopic Mass, Even Electron Ions
47 formula(e) evaluated with 2 results within limits (up to 50 best isotopic matches for each mass)
Elements Used:

Mass	Calc. Mass	mDa	PPM	DBE	Formula	i-FIT	i-FIT Norm	Fit Conf %	C	H	O
271.0627	271.0606	2.1	7.7	10.5	C15 H11 O5	72.7	0.001	99.93	15	11	5
	271.0665	-3.8	-14.0	1.5	C8 H15 O10	80.0	7.239	0.07	8	15	10

Supplementary data 16: iFit value of naringenin (**37**) in the acetone extract of *C. pyracanthoides* stem bark.
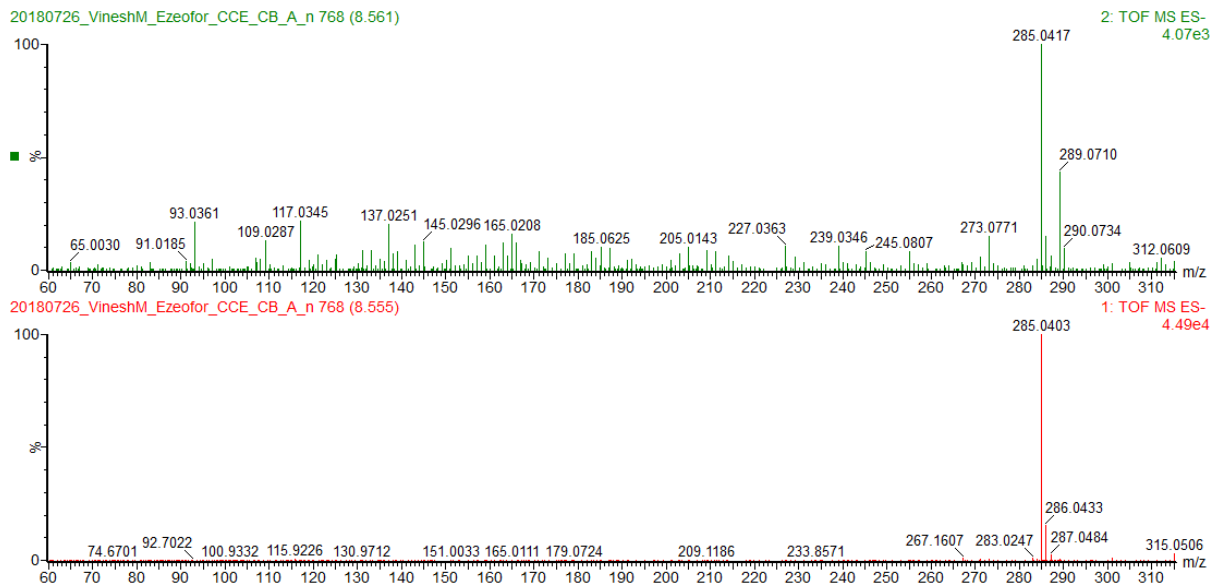
Supplementary data 17: MS and MS/MS data of kaempferol (**38**) in the acetone extract of *C. pyracanthoides* stem bark.

Single Mass Analysis
Tolerance = 5.0 mDa / DBE: min = -1.5, max = 50.0
Element prediction: Off
Number of isotope peaks used for i-FIT = 3
Monoisotopic Mass, Even Electron Ions
531 formula(e) evaluated with 11 results within limits (up to 50 best isotopic matches for each mass)
Elements Used:

Mass	Calc. Mass	mDa	PPM	DBE	Formula	i-FIT	i-FIT Norm	Fit Conf %	C	H	N	O
285.0403	285.0399	0.4	1.4	11.5	C15 H9 O6	120.8	0.092	91.17	15	9		6
	285.0372	3.1	10.9	12.5	C11 H5 N6 O4	123.6	2.851	5.78	11	5	6	4
	285.0413	-1.0	-3.5	16.5	C16 H5 N4 O2	124.6	3.913	2.00	16	5	4	2

20180726_VineshM_Ezeofor_CCE_CB_A_n 768 (8.555)
1: TOF MS ES-
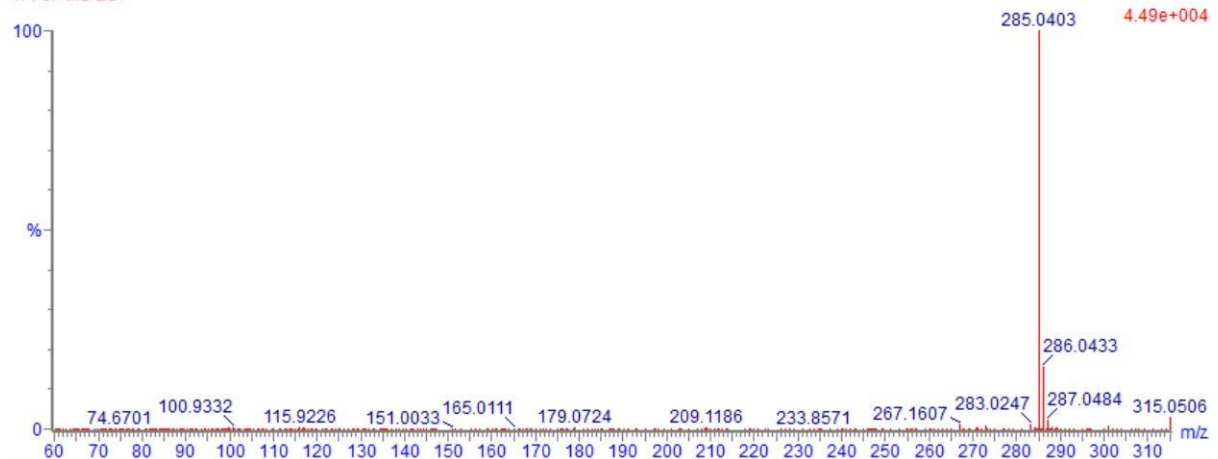
Supplementary data 18: iFit value of kaempferol (**38**) in the acetone extract of *C. pyracanthoides* stem bark.
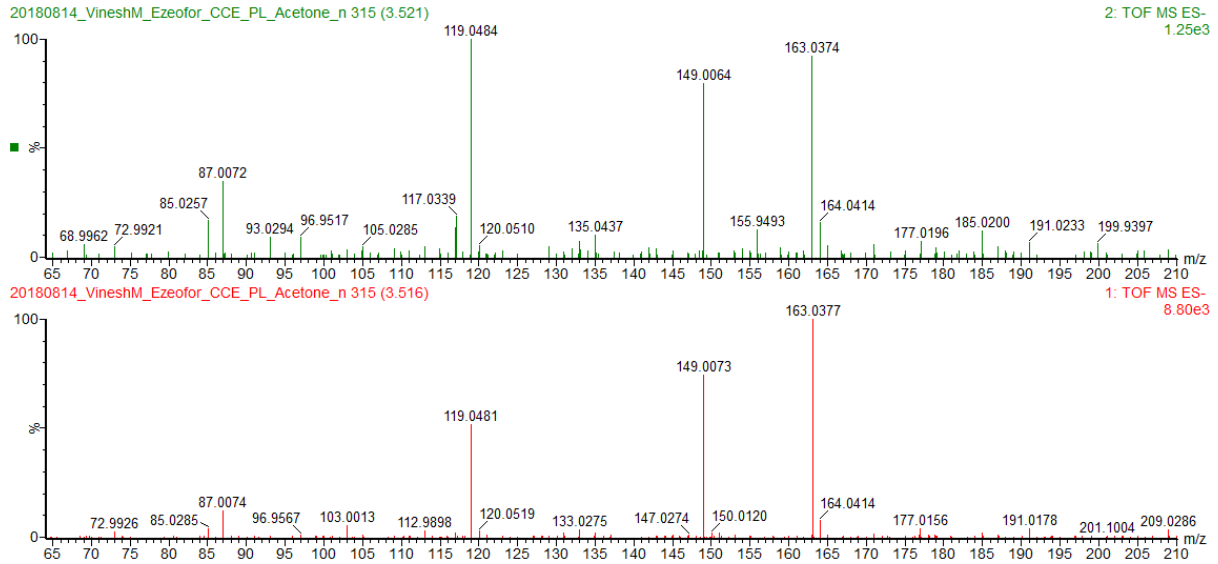
Supplementary data 19: MS and MS/MS data of *p*-coumaric acid (**39**) in the acetone extract of *P. capitatum* leaves.

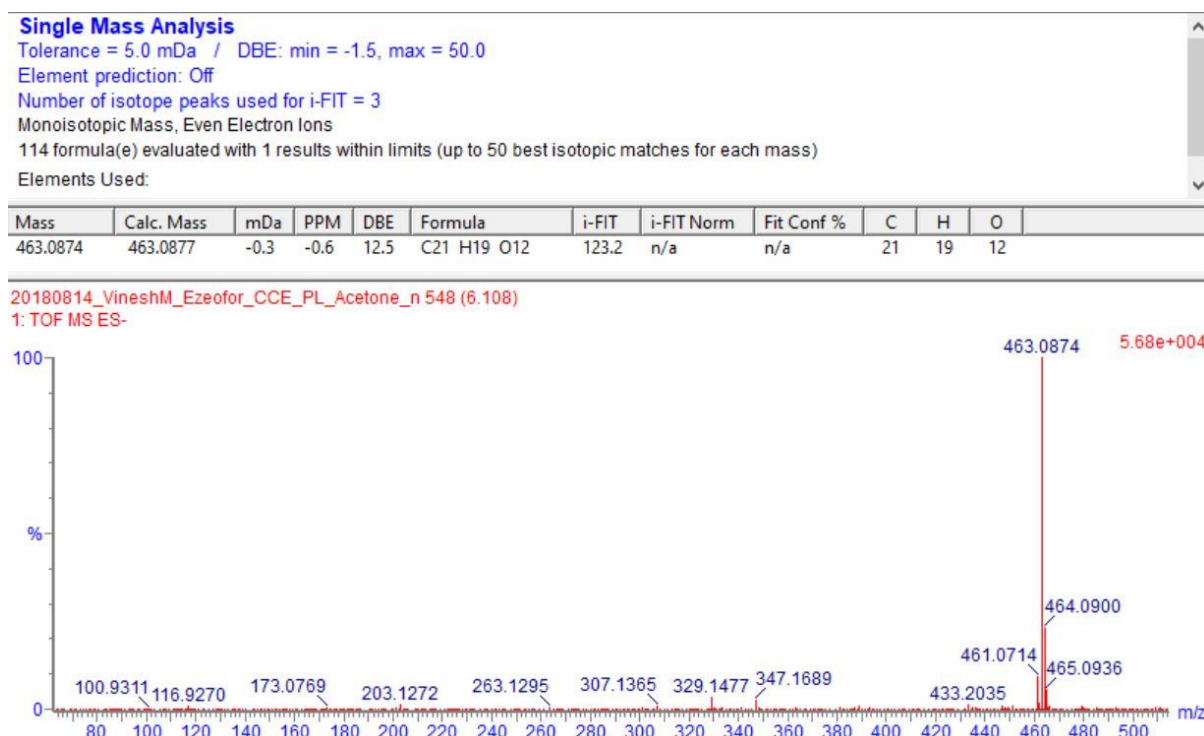**Supplementary data 20:** iFit value of *p*-coumaric acid (**39**) in the acetone extract of *P. capitatum* leaves.

239

Supplementary data 21: MS and MS/MS data of quercetin-3-*O*-sophoroside (**40**) in the acetone extract of *P. capitatum* leaves.

Single Mass Analysis
Tolerance = 5.0 mDa / DBE: min = -1.5, max = 50.0
Element prediction: Off
Number of isotope peaks used for i-FIT = 3
Monoisotopic Mass, Even Electron Ions
187 formula(e) evaluated with 3 results within limits (up to 50 best isotopic matches for each mass)
Elements Used:

| Mass	Calc. Mass	mDa	PPM	DBE	Formula	i-FIT	i-FIT Norm	Fit Conf %	C	H	O
625.1425	625.1405	2.0	3.2	13.5	C27 H29 O17	125.4	0.001	99.86	27	29	17
	625.1463	-3.8	-6.1	4.5	C20 H33 O22	132.0	6.610	0.13	20	33	22
	625.1440	-1.5	-2.4	35.5	C45 H21 O4	135.5	10.178	0.00	45	21	4

Supplementary data 22: iFit value of quercetin-3-*O*-sophoroside (**40**) in the acetone extract of *P. capitatum* leaves.
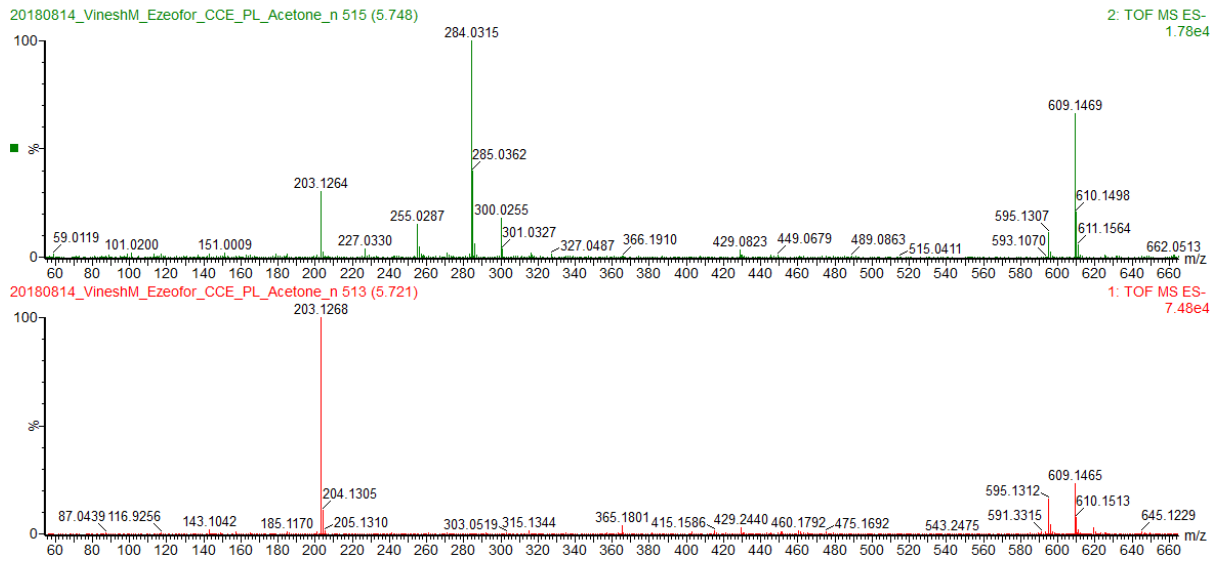
Supplementary data 23: MS and MS/MS data of rutin (**41**) in the acetone extract of *P. capitatum* leaves.

Single Mass Analysis
Tolerance = 5.0 mDa   /   DBE: min = -1.5, max = 50.0
Element prediction: Off
Number of isotope peaks used for i-FIT = 3
Monoisotopic Mass, Even Electron Ions
178 formula(e) evaluated with 3 results within limits (up to 50 best isotopic matches for each mass)
Elements Used:

Mass	Calc. Mass	mDa	PPM	DBE	Formula	i-FIT	i-FIT Norm	Fit Conf %	C	H	O	
609.1465	609.1456	0.9	1.5	13.5	C27 H29 O16	118.2	0.006	99.42	27	29	16	
	609.1514	-4.9	-8.0	4.5	C20 H33 O21	123.5	5.315	0.49	20	33	21	
	609.1491	-2.6	-4.3	35.5	C45 H21 O3	125.2	7.017	0.09	45	21	3	

Supplementary data 24: iFit value of rutin (**41**) in the acetone extract of *P. capitatum* leaves.
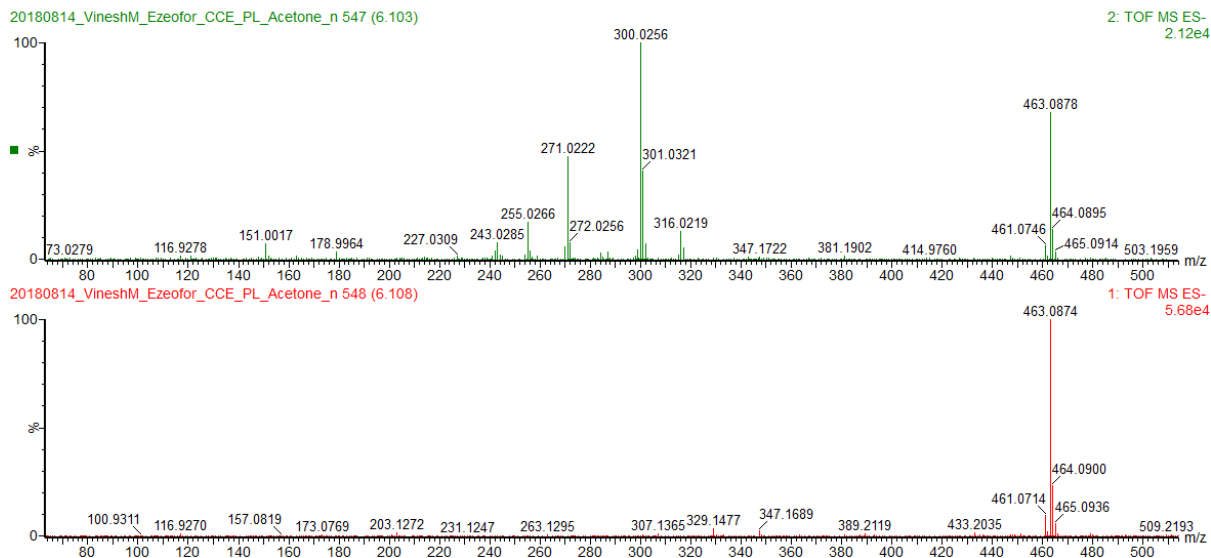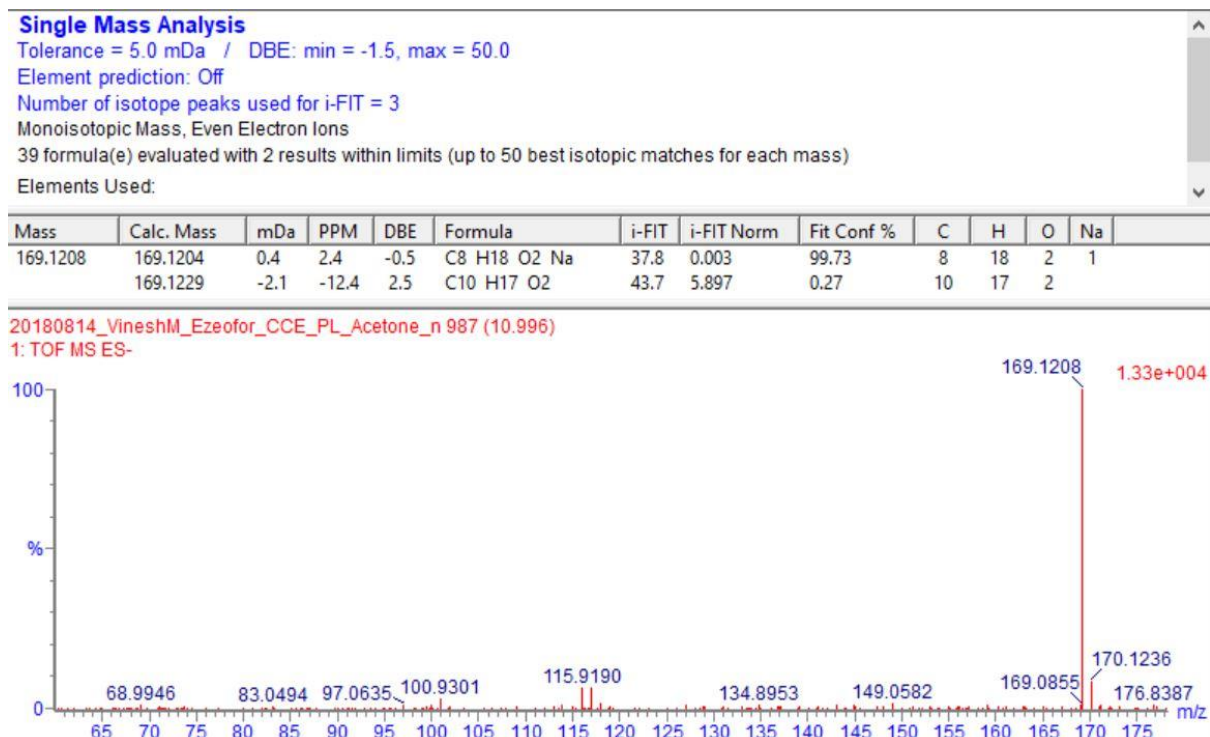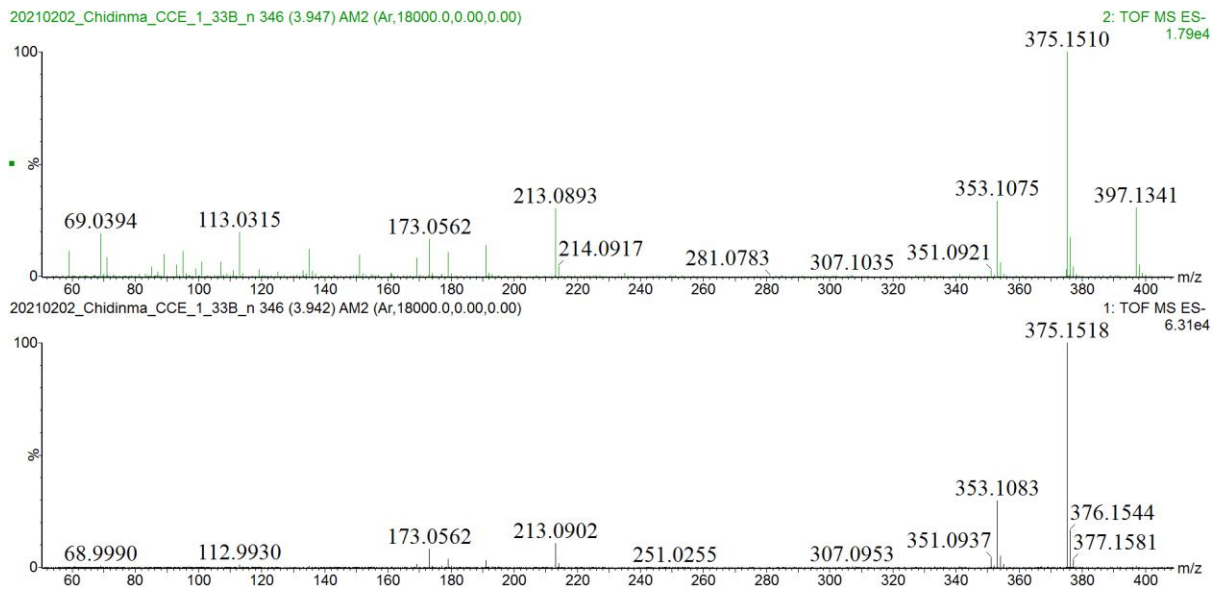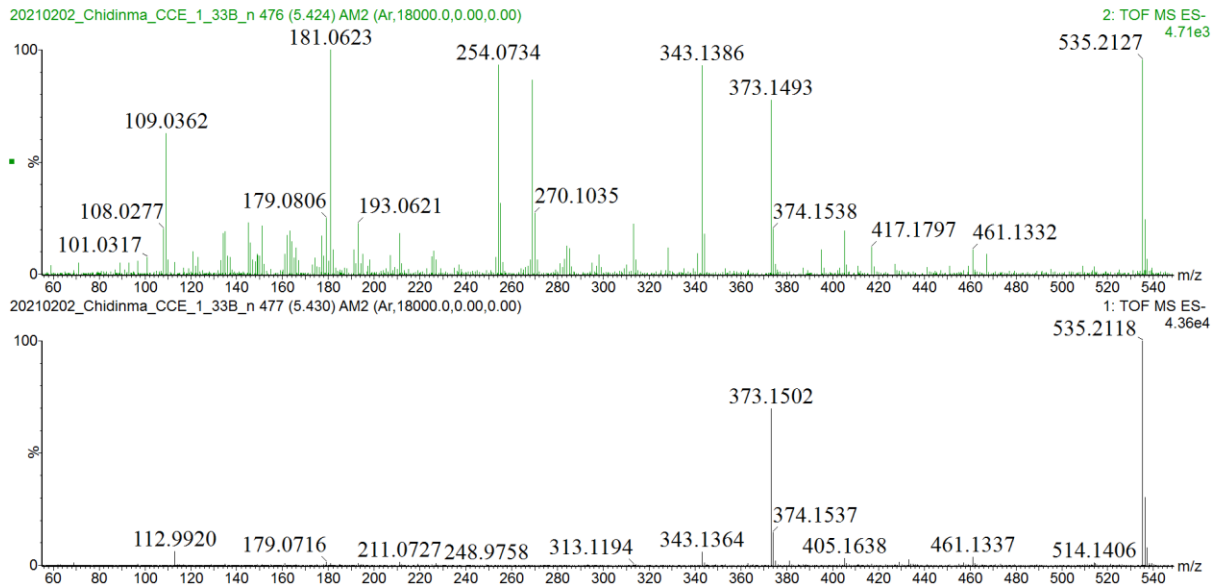
Supplementary data 25: MS and MS/MS data of quercimeritrin (**42**) in the acetone extract of *P. capitatum* leaves.

Supplementary data 26: iFit value of quercimeritrin (**42**) in the acetone extract of *P. capitatum* leaves.
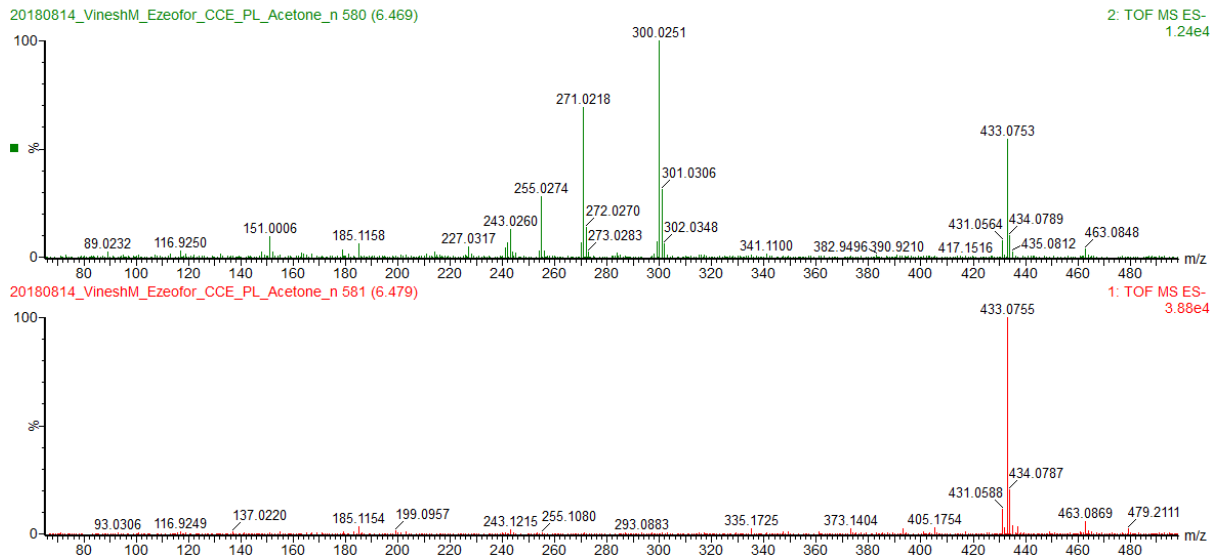
Supplementary data 27: MS and MS/MS data of quercetin-3-*O*-alpha-L-arabinopyranside (**43**) in the acetone extract of *P. capitatum* leaves.

Single Mass Analysis
Tolerance = 5.0 mDa / DBE: min = -1.5, max = 50.0
Element prediction: Off
Number of isotope peaks used for i-FIT = 3
Monoisotopic Mass, Even Electron Ions
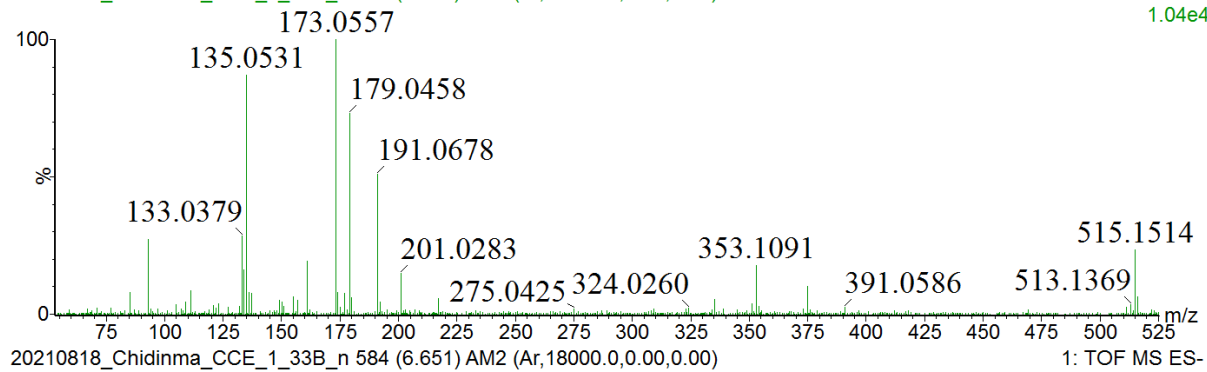99 formula(e) evaluated with 2 results within limits (up to 50 best isotopic matches for each mass)
Elements Used:

Mass	Calc. Mass	mDa	PPM	DBE	Formula	i-FIT	i-FIT Norm	Fit Conf %	C	H	O
433.0755	433.0771	-1.6	-3.7	12.5	C20 H17 O11	123.4	0.003	99.66	20	17	11
	433.0712	4.3	9.9	21.5	C27 H13 O6	129.0	5.687	0.34	27	13	6
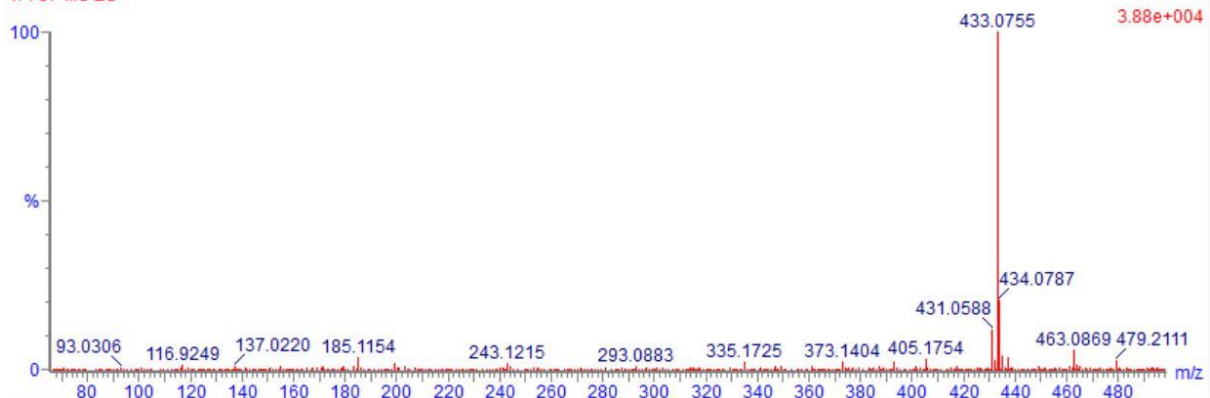
Supplementary data 28: iFit value of quercetin-3-*O*-alpha-L-arabinopyranside (**43**) in the acetone extract of *P. capitatum* leaves.
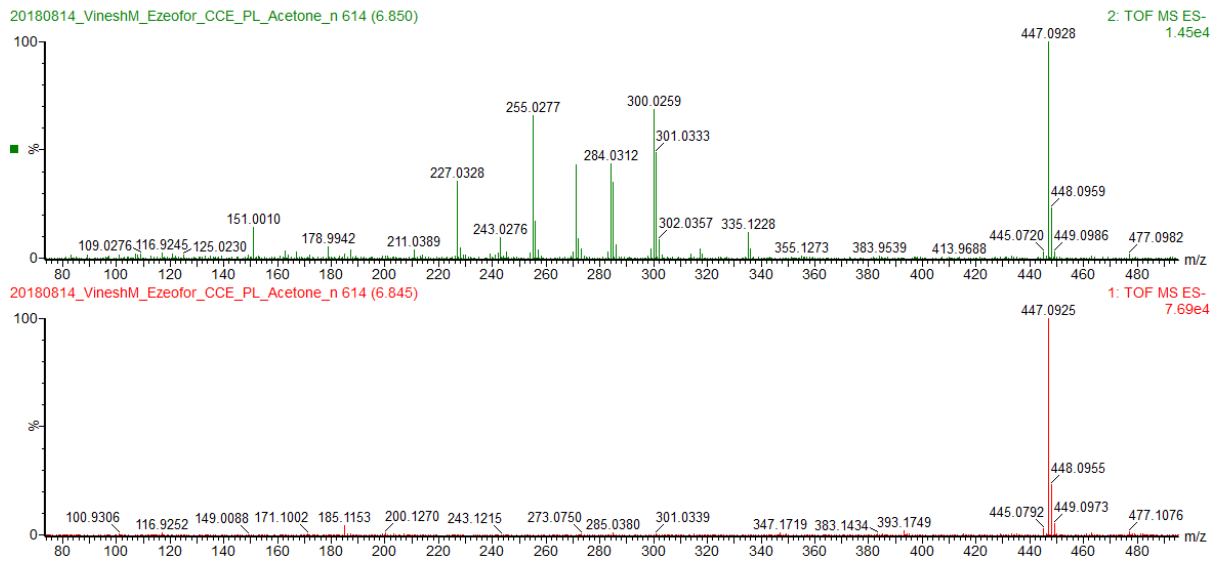
Supplementary data 29: MS and MS/MS data of orientin (**44**) in the acetone extract of *P. capitatum* leaves.
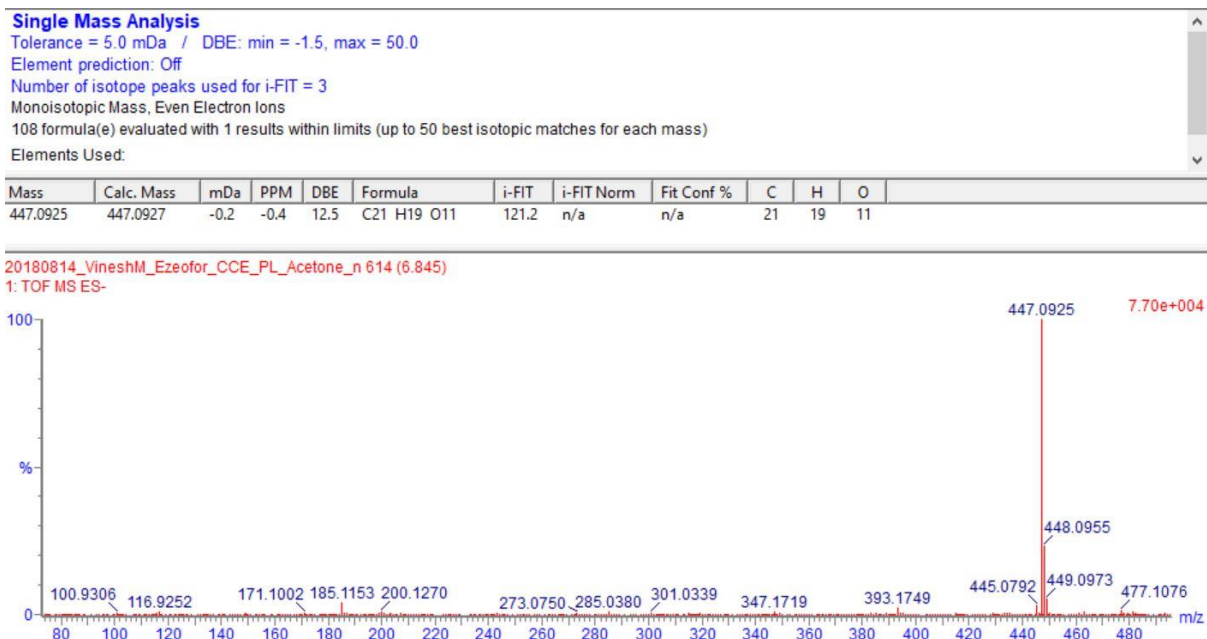
Supplementary data 30: iFit value of orientin (**44**) in the acetone extract of *P. capitatum* leaves.
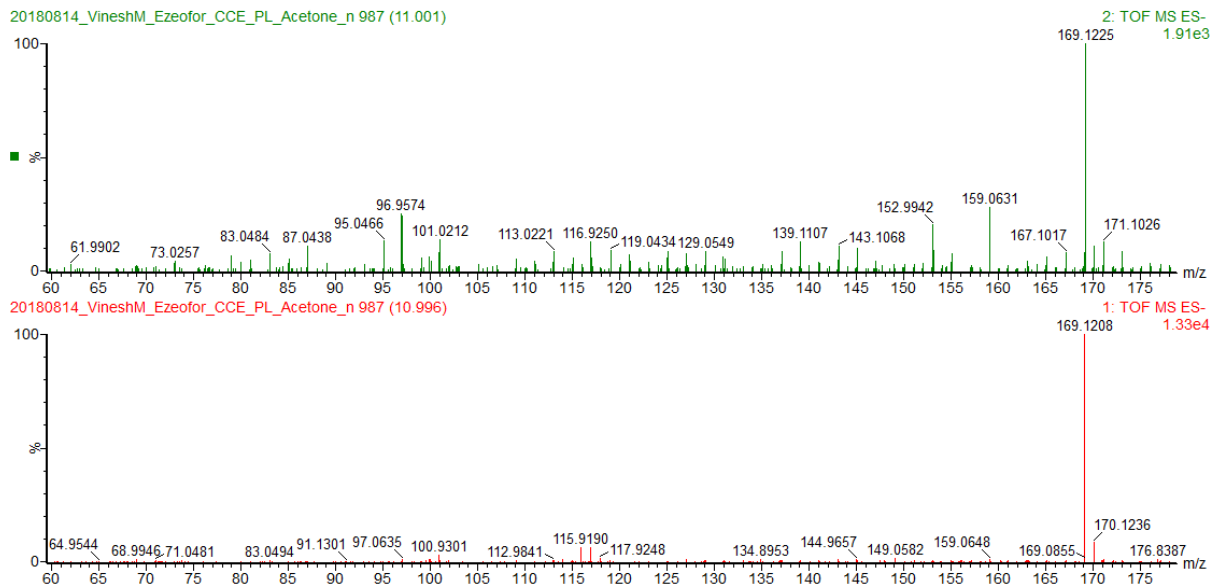
Supplementary data 31: MS and MS/MS data of citronellic acid (**45**) in the acetone extract of *P. capitatum* leaves.

Single Mass Analysis
Tolerance = 5.0 mDa   /   DBE: min = -1.5, max = 50.0
Element prediction: Off
Number of isotope peaks used for i-FIT = 3
Monoisotopic Mass, Even Electron Ions
39 formula(e) evaluated with 2 results within limits (up to 50 best isotopic matches for each mass)
Elements Used:

Mass	Calc. Mass	mDa	PPM	DBE	Formula	i-FIT	i-FIT Norm	Fit Conf %	C	H	O	Na
169.1208	169.1204	0.4	2.4	-0.5	C8 H18 O2 Na	37.8	0.003	99.73	8	18	2	1
	169.1229	-2.1	-12.4	2.5	C10 H17 O2	43.7	5.897	0.27	10	17	2	

Supplementary data 32: iFit value of citronellic acid (**45**) in the acetone extract of *P. capitatum* leaves.

20210202_Chidinma_CCE_1_33B_n 346 (3.947) AM2 (Ar,18000.0,0.00,0.00)
2: TOF MS ES-
1.79e4

20210202_Chidinma_CCE_1_33B_n 346 (3.942) AM2 (Ar,18000.0,0.00,0.00)
1: TOF MS ES-
6.31e4

Supplementary data 33: MS and MS/MS data of loganic acid (**53**) in the ethanol extract of *S. columbaria* roots.

Single Mass Analysis
Tolerance = 15.0 mDa / DBE: min = -1.5, max = 50.0
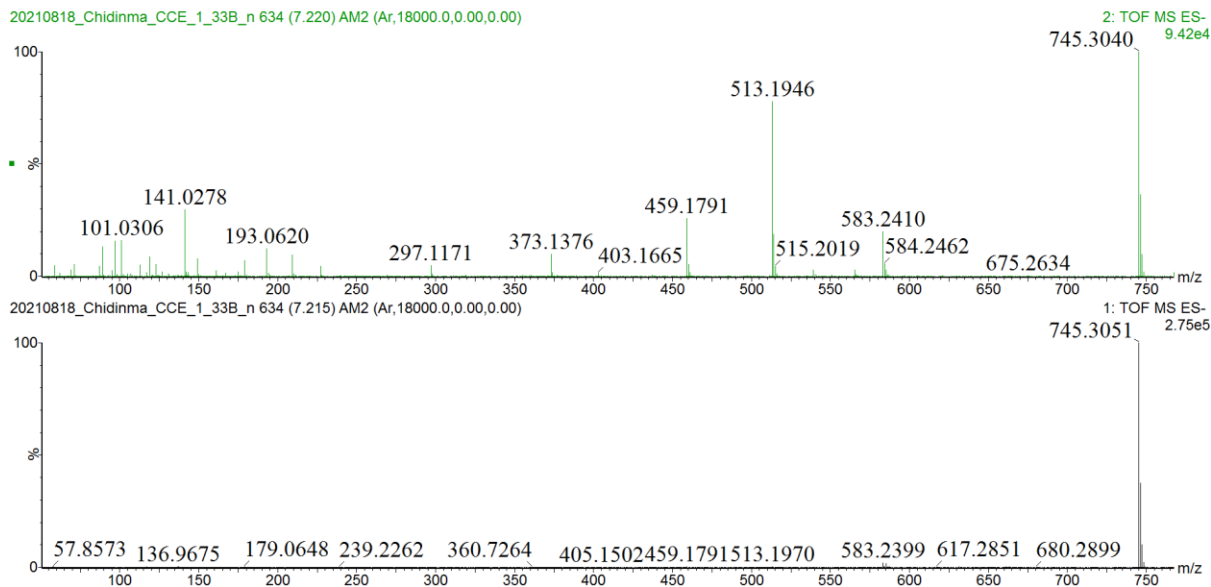Element prediction: Off
Number of isotope peaks used for i-FIT = 3
Monoisotopic Mass, Even Electron Ions
82 formula(e) evaluated with 5 results within limits (up to 50 best isotopic matches for each mass)
Elements Used:

Mass	Calc. Mass	mDa	PPM	DBE	Formula	i-FIT	i-FIT Norm	Fit Conf %	C	H	O
375.1298	375.1291	0.7	1.9	5.5	C16 H23 O10	105.8	0.188	82.82	16	23	10
	375.1444	-14.6	-38.9	9.5	C20 H23 O7	107.8	2.188	11.21	20	23	7
	375.1232	6.6	17.6	14.5	C23 H19 O5	108.5	2.903	5.49	23	19	5
	375.1385	-8.7	-23.2	18.5	C27 H19 O2	111.0	5.442	0.43	27	19	2
	375.1174	12.4	33.1	23.5	C30 H15	113.3	7.685	0.05	30	15	

Supplementary data 34: iFit value of loganic acid (**53**) in the ethanol extract of *S. columbaria* roots.

246

Supplementary data 35: MS and MS/MS data of scrophuloside A_1 (**peak 2**) in the ethanol extract of *S. columbaria* roots.

Single Mass Analysis
Tolerance = 15.0 mDa   /   DBE: min = -1.5, max = 50.0
Element prediction: Off
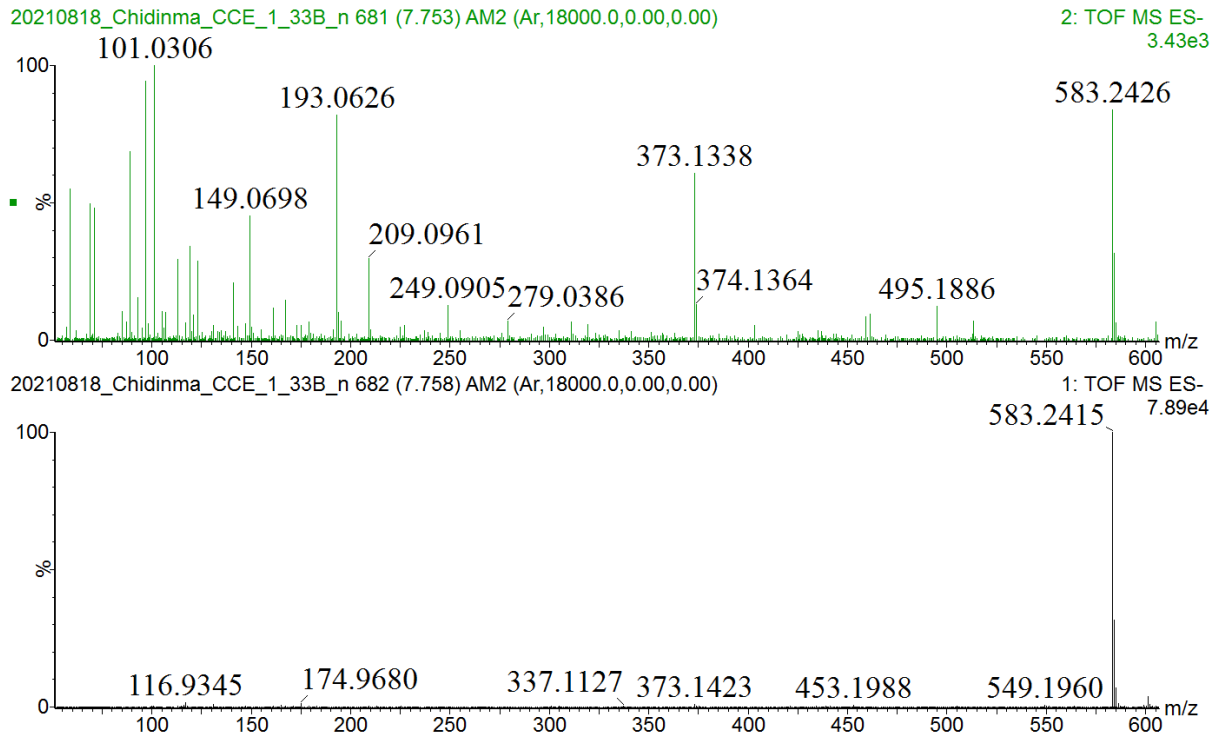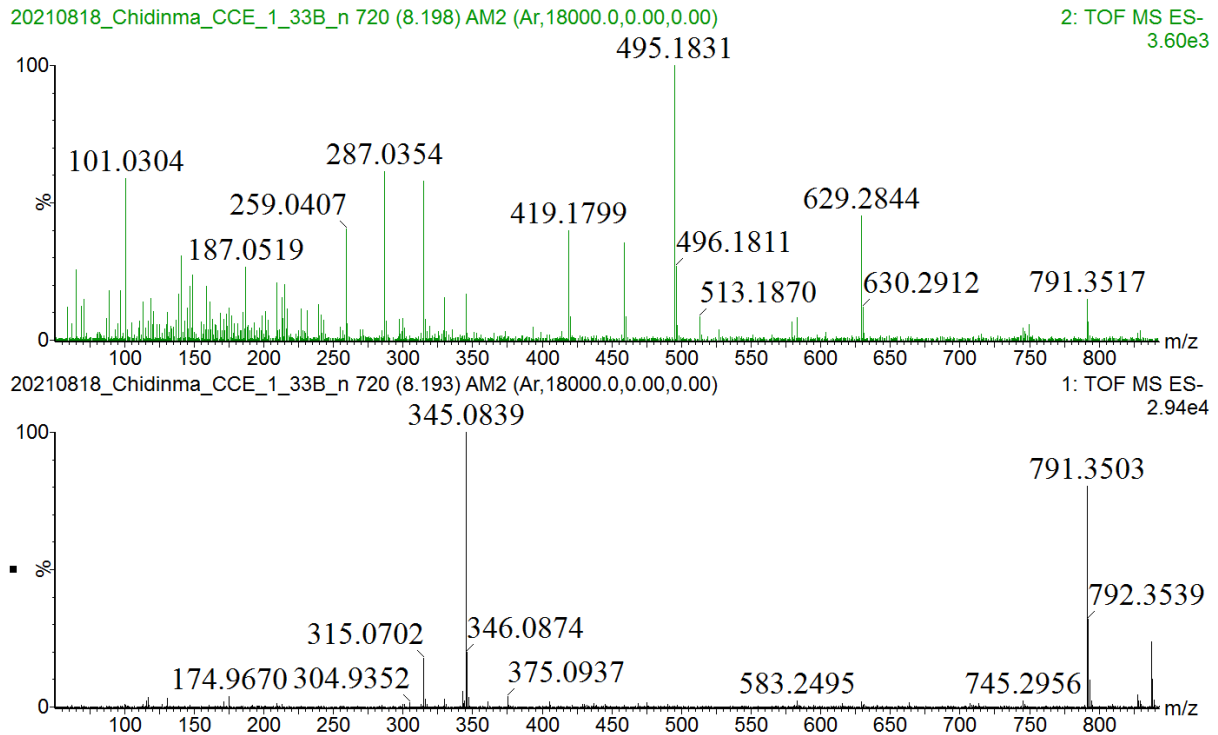Number of isotope peaks used for i-FIT = 3
Monoisotopic Mass, Even Electron Ions
147 formula(e) evaluated with 7 results within limits (up to 50 best isotopic matches for each mass)
Elements Used:

Mass	Calc. Mass	mDa	PPM	DBE	Formula	i-FIT	i-FIT Norm	Fit Conf %	C	H	O
535.1801	535.1816	-1.5	-2.8	11.5	C26 H31 O12	104.2	0.013	98.67	26	31	12
	535.1757	4.4	8.2	20.5	C33 H27 O7	108.7	4.566	1.04	33	27	7
	535.1663	13.8	25.8	7.5	C22 H31 O15	110.8	6.667	0.13	22	31	15
	535.1874	-7.3	-13.6	2.5	C19 H35 O17	111.0	6.821	0.11	19	35	17
	535.1909	-10.8	-20.2	24.5	C37 H27 O4	112.2	8.088	0.03	37	27	4
	535.1722	7.9	14.8	-1.5	C15 H35 O20	113.3	9.190	0.01	15	35	20
	535.1698	10.3	19.2	29.5	C40 H23 O2	113.3	9.191	0.01	40	23	2

Supplementary data 36: iFit value of scrophuloside A_1 (**peak 2**) in the ethanol extract of *S. columbaria* roots.

247
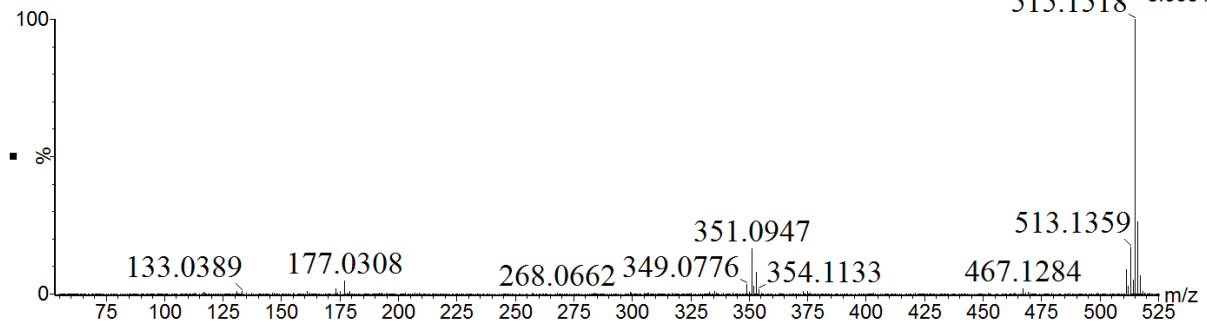
Supplementary data 37: MS and MS/MS data of 3,4-dicaffeoylquinic acid (**peak 3**) in the ethanol extract of *S. columbaria* roots.

Supplementary data 38: iFit value of 3,4-dicaffeoylquinic acid (**peak 3**) in the ethanol extract of *S. columbaria* roots.

Supplementary data 39: MS and MS/MS data of cantleyoside (**peak 4**) in the ethanol extract of *S. columbaria* roots.

Single Mass Analysis
Tolerance = 15.0 mDa / DBE: min = -1.5, max = 50.0
Element prediction: Off
Number of isotope peaks used for i-FIT = 3
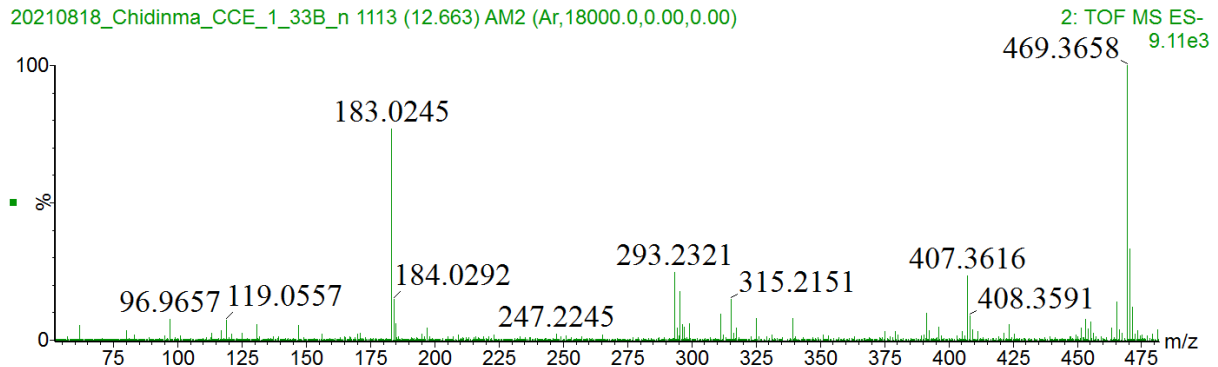Monoisotopic Mass, Even Electron Ions
255 formula(e) evaluated with 8 results within limits (up to 50 best isotopic matches for each mass)
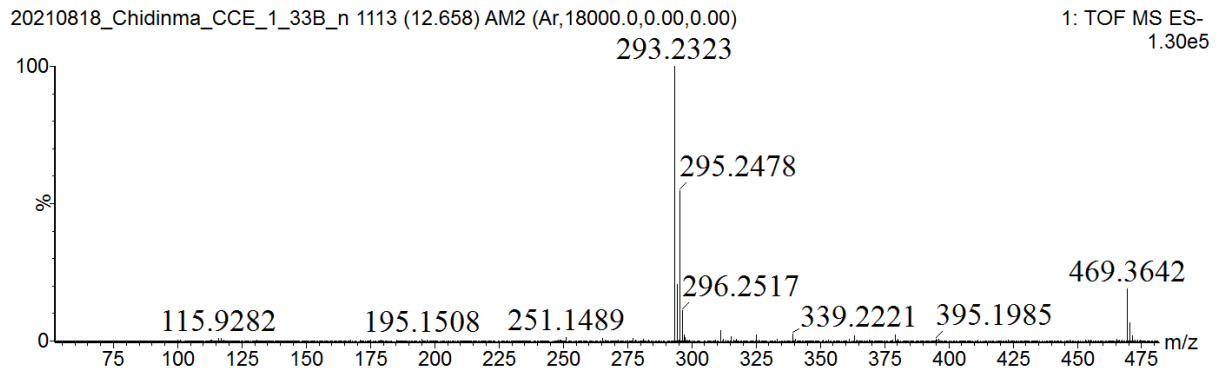Elements Used:

Mass	Calc. Mass	mDa	PPM	DBE	Formula	i-FIT	i-FIT Norm	Fit Conf %	C	H	O
745.2555	745.2555	0.0	0.0	11.5	C33 H45 O19	170.6	0.000	100.00	33	45	19
	745.2496	5.9	7.9	20.5	C40 H41 O14	184.3	13.663	0.00	40	41	14
	745.2614	-5.9	-7.9	2.5	C26 H49 O24	185.5	14.826	0.00	26	49	24
	745.2649	-9.4	-12.6	24.5	C44 H41 O11	186.1	15.467	0.00	44	41	11
	745.2590	-3.5	-4.7	33.5	C51 H37 O6	186.9	16.243	0.00	51	37	6
	745.2438	11.7	15.7	29.5	C47 H37 O9	187.5	16.819	0.00	47	37	9
	745.2531	2.4	3.2	42.5	C58 H33 O	187.6	16.979	0.00	58	33	1
	745.2461	9.4	12.6	-1.5	C22 H49 O27	188.1	17.410	0.00	22	49	27

Supplementary data 40: iFit value of cantleyoside (**peak 4**) in the ethanol extract of *S. columbaria* roots.

Supplementary data 41: MS and MS/MS data of sylvestroside III (**peak 5**) in the ethanol extract of *S. columbaria* roots.

Single Mass Analysis
Tolerance = 15.0 mDa / DBE: min = -1.5, max = 50.0
Element prediction: Off
Number of isotope peaks used for i-FIT = 3
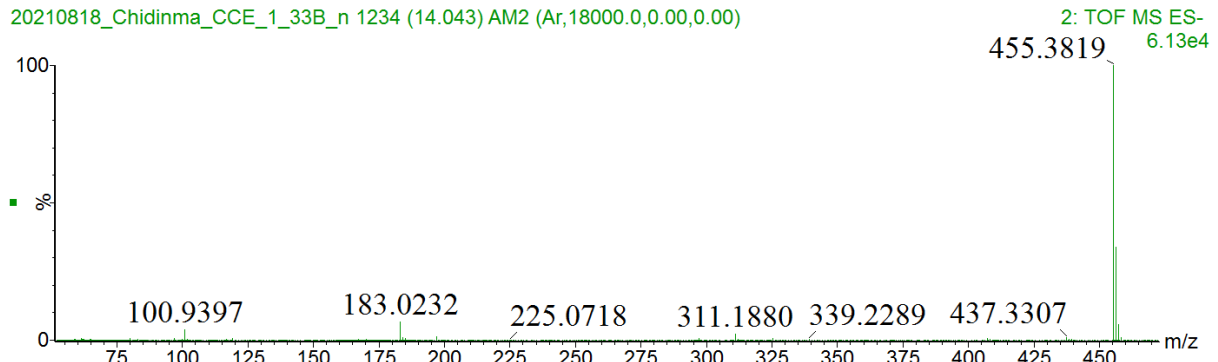Monoisotopic Mass, Even Electron Ions
171 formula(e) evaluated with 7 results within limits (up to 50 best isotopic matches for each mass)
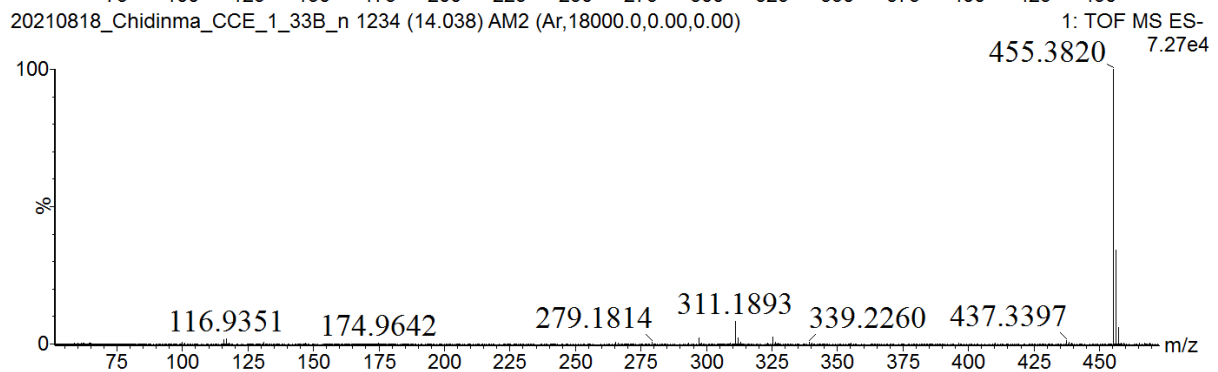Elements Used:

Mass	Calc. Mass	mDa	PPM	DBE	Formula	i-FIT	i-FIT Norm	Fit Conf %	C	H	O
583.2033	583.2027	0.6	1.0	10.5	C27 H35 O14	110.3	0.015	98.51	27	35	14
	583.2179	-14.6	-25.0	14.5	C31 H35 O11	114.8	4.569	1.04	31	35	11
	583.2086	-5.3	-9.1	1.5	C20 H39 O19	116.2	5.932	0.27	20	39	19
	583.1968	6.5	11.1	19.5	C34 H31 O9	116.6	6.376	0.17	34	31	9
	583.2121	-8.8	-15.1	23.5	C38 H31 O6	119.1	8.834	0.01	38	31	6
	583.1909	12.4	21.3	28.5	C41 H27 O4	120.5	10.218	0.00	41	27	4
	583.2062	-2.9	-5.0	32.5	C45 H27 O1	121.0	10.757	0.00	45	27	1

Supplementary data 42: iFit value of sylvestroside III (**peak 5**) in the ethanol extract of *S. columbaria* roots.

Supplementary data 43: MS and MS/MS data of triplostoside A (**54**) in the ethanol extract of *S. columbaria* roots.

Single Mass Analysis
Tolerance = 15.0 mDa   /   DBE: min = -1.5, max = 50.0
Element prediction: Off
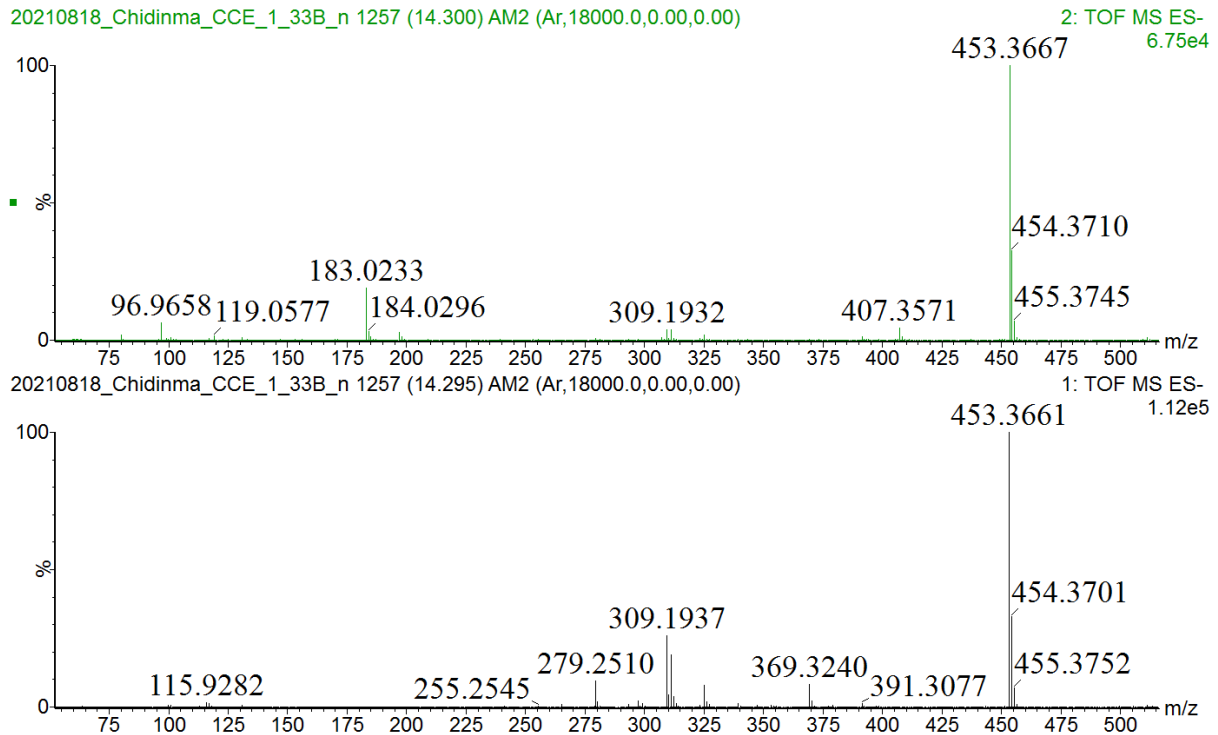Number of isotope peaks used for i-FIT = 3
Monoisotopic Mass, Even Electron Ions
293 formula(e) evaluated with 8 results within limits (up to 50 best isotopic matches for each mass)
Elements Used:

Mass	Calc. Mass	mDa	PPM	DBE	Formula	i-FIT	i-FIT Norm	Fit Conf %	C	H	O
791.2983	791.2974	0.9	1.1	10.5	C35 H51 O20	76.6	0.006	99.43	35	51	20
	791.3126	-14.3	-18.1	14.5	C39 H51 O17	82.2	5.550	0.39	39	51	17
	791.2915	6.8	8.6	19.5	C42 H47 O15	83.3	6.687	0.12	42	47	15
	791.3032	-4.9	-6.2	1.5	C28 H55 O25	85.1	8.447	0.02	28	55	25
	791.3068	-8.5	-10.7	23.5	C46 H47 O12	85.1	8.531	0.02	46	47	12
	791.3009	-2.6	-3.3	32.5	C53 H43 O7	86.0	9.332	0.01	53	43	7
	791.2950	3.3	4.2	41.5	C60 H39 O2	87.1	10.465	0.00	60	39	2
	791.2856	12.7	16.0	28.5	C49 H43 O10	87.1	10.488	0.00	49	43	10

Supplementary data 44: iFit value of triplostoside A (**54**) in the ethanol extract of *S. columbaria* roots.

Supplementary data 45: MS and MS/MS data of hederagenin (**55**) in the ethanol extract of *S. columbaria* roots.

Single Mass Analysis
Tolerance = 15.0 mDa / DBE: min = -1.5, max = 50.0
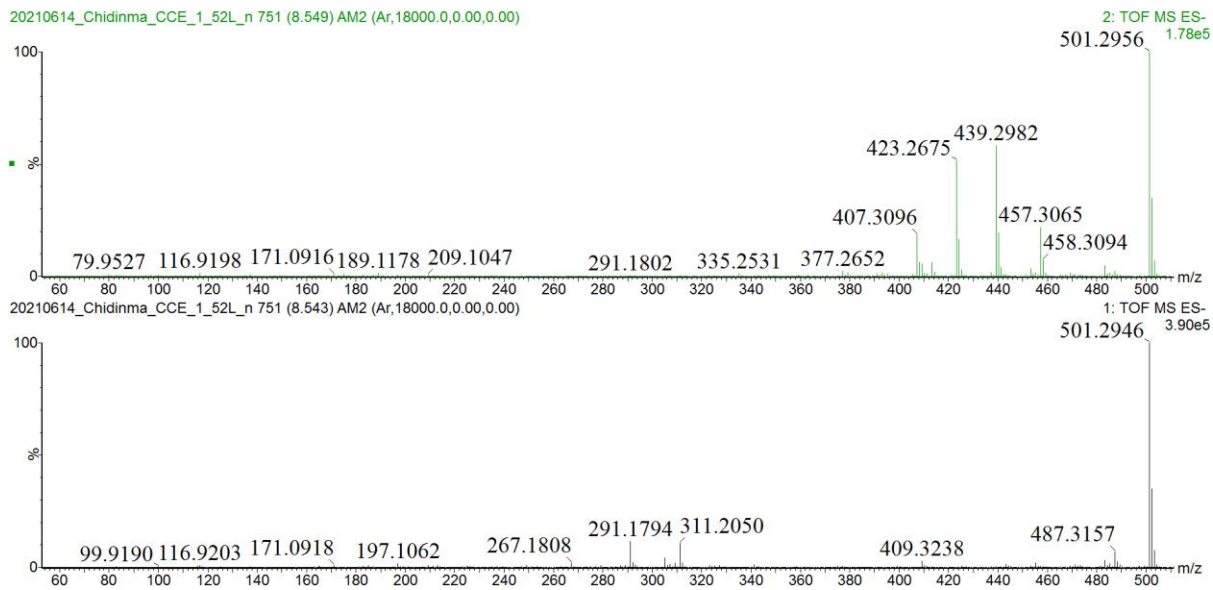Element prediction: Off
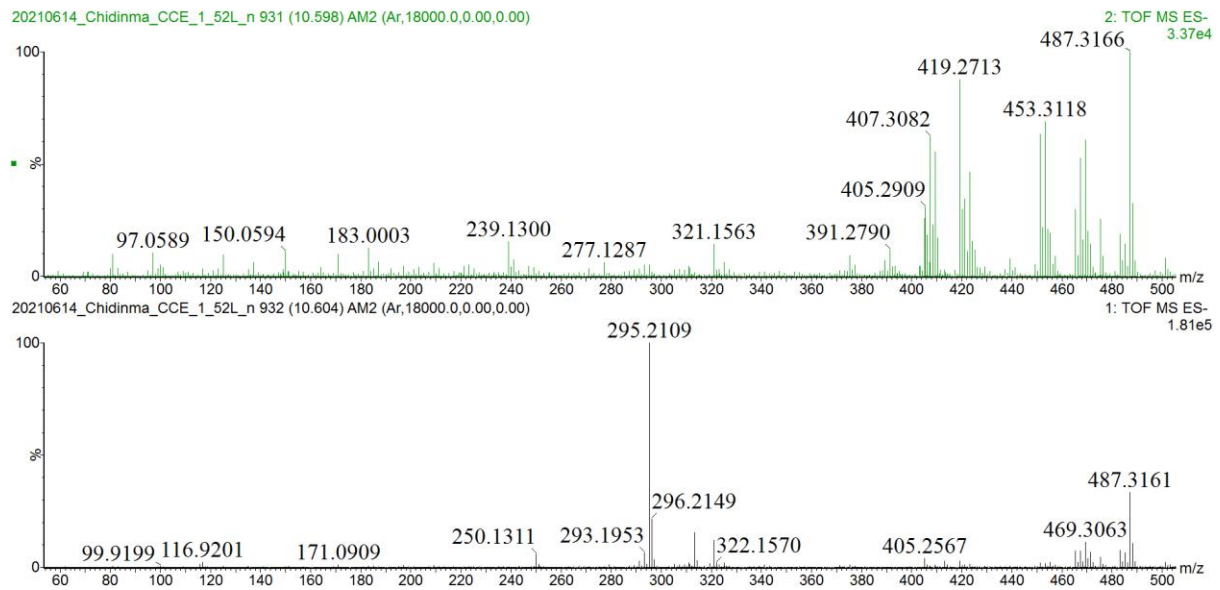Number of isotope peaks used for i-FIT = 3
Monoisotopic Mass, Even Electron Ions
119 formula(e) evaluated with 3 results within limits (up to 50 best isotopic matches for each mass)
Elements Used:

Mass	Calc. Mass	mDa	PPM	DBE	Formula			i-FIT	i-FIT Norm	Fit Conf %	C	H	O
471.3455	471.3322	13.3	28.2	3.5	C26	H47	O7	53.1	0.682	50.57	26	47	7
	471.3474	-1.9	-4.0	7.5	C30	H47	O4	53.2	0.742	47.63	30	47	4
	471.3533	-7.8	-16.5	-1.5	C23	H51	O9	56.4	4.017	1.80	23	51	9

Supplementary data 46: iFit value of hederagenin (**55**) in the ethanol extract of *S. columbaria* roots.

252

2: TOF MS ES-
6.13e4

455.3819

100.9397   183.0232   225.0718   311.1880 339.2289 437.3307

20210818_Chidinma_CCE_1_33B_n 1234 (14.038) AM2 (Ar,18000.0,0.00,0.00)

1: TOF MS ES-
7.27e4

455.3820

116.9351   174.9642   279.1814   311.1893 339.2260 437.3397

Supplementary data 47: MS and MS/MS data of 2-isoursolic acid (**56**) in the ethanol extract of *S. columbaria* roots.

Single Mass Analysis
Tolerance = 15.0 mDa   /   DBE: min = -1.5, max = 50.0
Element prediction: Off
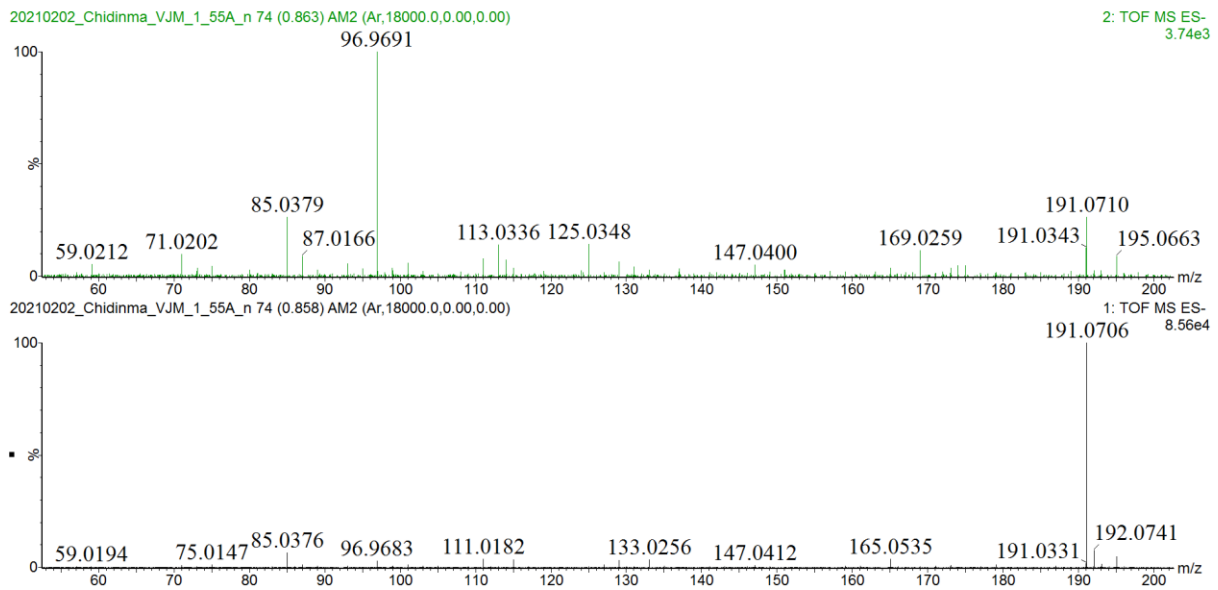Number of isotope peaks used for i-FIT = 3
Monoisotopic Mass, Even Electron Ions
112 formula(e) evaluated with 3 results within limits (up to 50 best isotopic matches for each mass)
Elements Used:

Mass	Calc. Mass	mDa	PPM	DBE	Formula	i-FIT	i-FIT Norm	Fit Conf %	C	H	O
455.3511	455.3525	-1.4	-3.1	7.5	C30 H47 O3	111.2	0.000	99.96	30	47	3
	455.3373	13.8	30.3	3.5	C26 H47 O6	119.4	8.152	0.03	26	47	6
	455.3584	-7.3	-16.0	-1.5	C23 H51 O8	120.8	9.595	0.01	23	51	8

Supplementary data 48: iFit value of 2-isoursolic acid (**56**) in the ethanol extract of *S. columbaria* roots.

453.3667

100

%

454.3710

183.0233
455.3745
96.9658 119.0577
184.0296
309.1932
407.3571

0
m/z
75   100   125   150   175   200   225   250   275   300   325   350   375   400   425   450   475   500

20210818_Chidinma_CCE_1_33B_n 1257 (14.295) AM2 (Ar,18000.0,0.00,0.00)   1: TOF MS ES-
1.12e5

453.3661

100

%

454.3701

309.1937
455.3752
279.2510
115.9282
369.3240
255.2545
391.3077

0
m/z
75   100   125   150   175   200   225   250   275   300   325   350   375   400   425   450   475   500

Supplementary data 49: MS and MS/MS data of glycyrrhetaldehyde (**peak 10**) in the ethanol extract of *S. columbaria* roots.

Single Mass Analysis
Tolerance = 15.0 mDa   /   DBE: min = -1.5, max = 50.0
Element prediction: Off
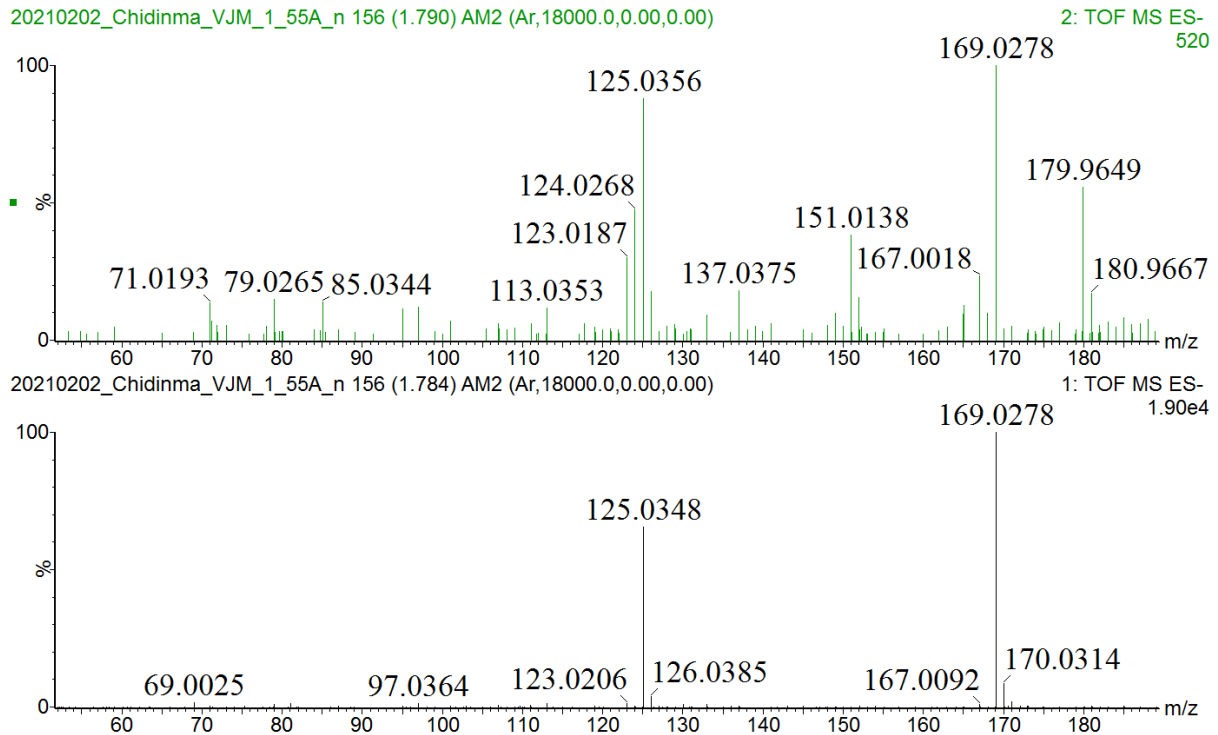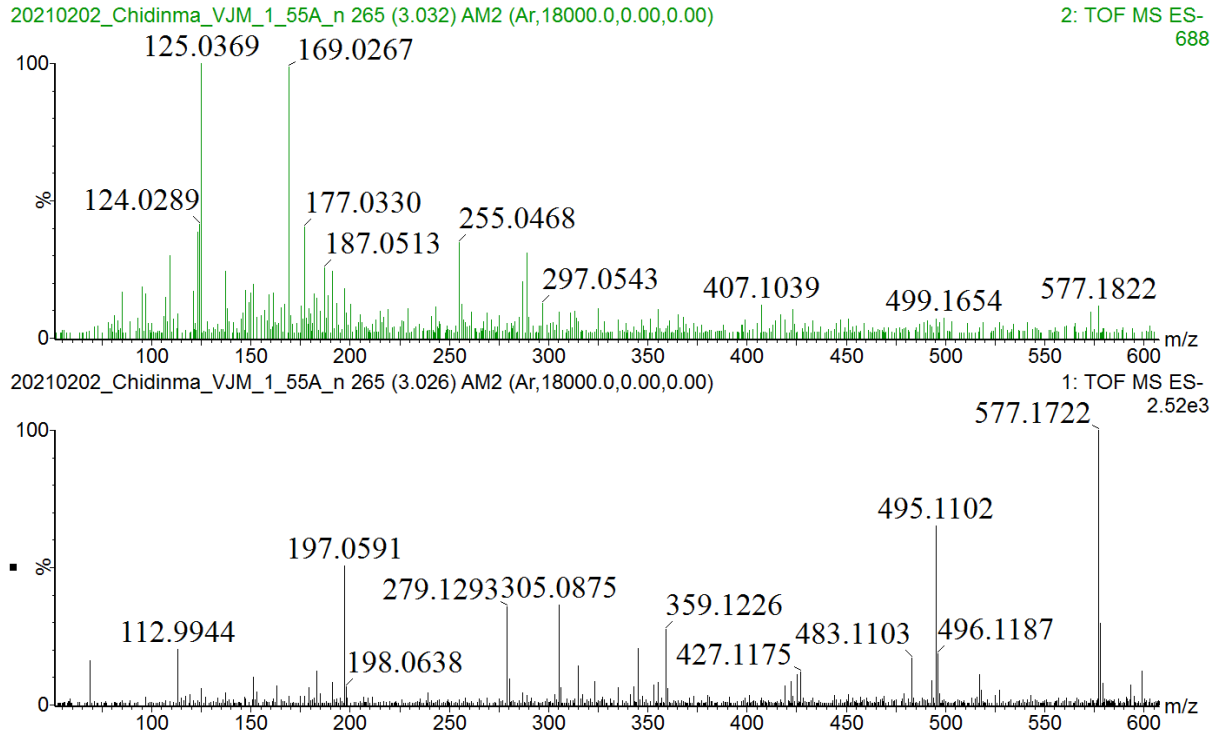Number of isotope peaks used for i-FIT = 3
Monoisotopic Mass, Even Electron Ions
106 formula(e) evaluated with 3 results within limits (up to 50 best isotopic matches for each mass)
Elements Used:

Mass	Calc. Mass	mDa	PPM	DBE	Formula	i-FIT	i-FIT Norm	Fit Conf %	C	H	O
453.3355	453.3369	-1.4	-3.1	8.5	C30 H45 O3	134.5	0.012	98.80	30	45	3
	453.3216	13.9	30.7	4.5	C26 H45 O6	139.1	4.575	1.03	26	45	6
	453.3427	-7.2	-15.9	-0.5	C23 H49 O8	140.9	6.379	0.17	23	49	8

Supplementary data 50: iFit value of glycyrrhetaldehyde (**peak 10**) in the ethanol extract of *S. columbaria* roots.

.

20210614_Chidinma_CCE_1_52L_n 751 (8.549) AM2 (Ar,18000.0,0.00,0.00) 2: TOF MS ES-

20210614_Chidinma_CCE_1_52L_n 751 (8.543) AM2 (Ar,18000.0,0.00,0.00) 1: TOF MS ES-

Supplementary data 51: MS and MS/MS data of pomaceic acid (**57**) in the ethanol extract of *S. columbaria* roots.

Single Mass Analysis
Tolerance = 15.0 mDa / DBE: min = -1.5, max = 50.0
Element prediction: Off
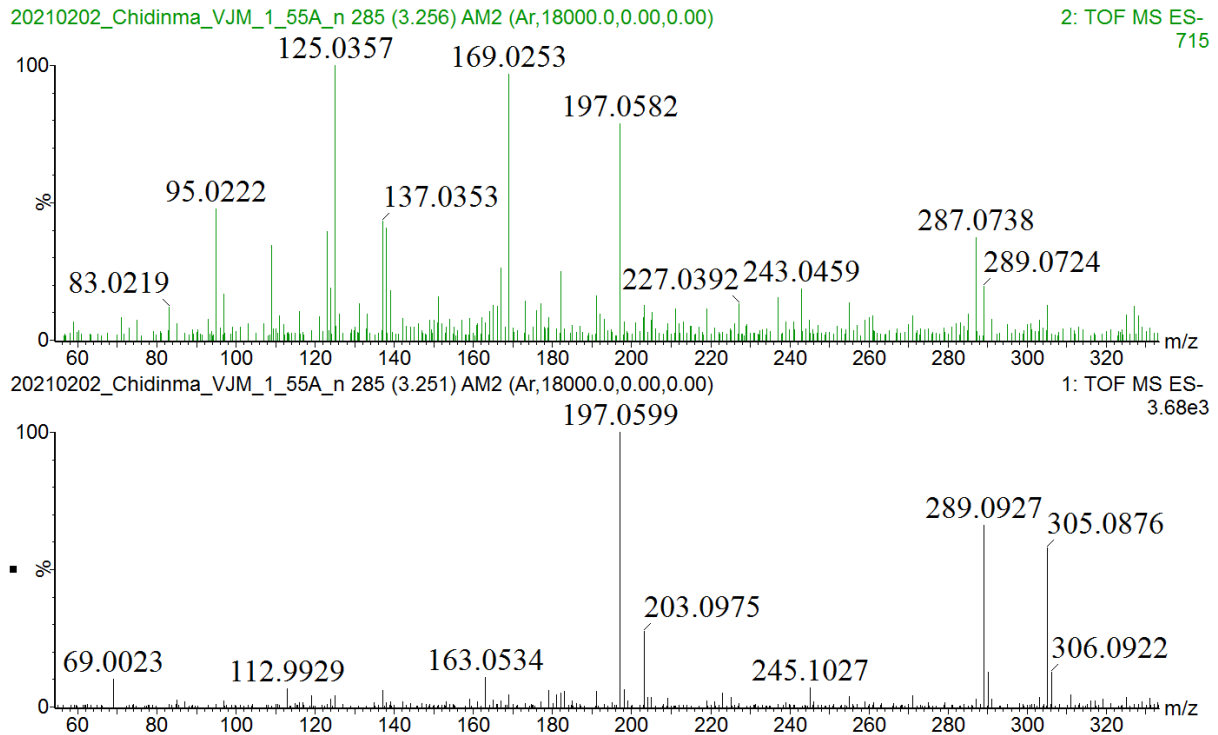Number of isotope peaks used for i-FIT = 3
Monoisotopic Mass, Even Electron Ions
127 formula(e) evaluated with 4 results within limits (up to 50 best isotopic matches for each mass)
Elements Used:

Mass	Calc. Mass	mDa	PPM	DBE	Formula	i-FIT	i-FIT Norm	Fit Conf %	C	H	O
501.3203	501.3216	-1.3	-2.6	8.5	C30 H45 O6	272.3	0.108	89.76	30	45	6
	501.3157	4.6	9.2	17.5	C37 H41 O	274.5	2.296	10.07	37	41	1
	501.3064	13.9	27.7	4.5	C26 H45 O9	278.9	6.762	0.12	26	45	9
	501.3275	-7.2	-14.4	-0.5	C23 H49 O11	279.7	7.553	0.05	23	49	11

Supplementary data 52: iFit value of pomaceic acid (**57**) in the ethanol extract of *S. columbaria* roots.

Supplementary data 53: MS and MS/MS data of euscaphic acid (**58**) in the ethanol extract of *S. columbaria* roots.

Mass	Calc. Mass	mDa	PPM	DBE	Formula	i-FIT	i-FIT Norm	Fit Conf %	C	H	O
487.3418	487.3423	-0.5	-1.0	7.5	C30 H47 O5	141.5	0.023	97.68	30	47	5
	487.3271	14.7	30.2	3.5	C26 H47 O8	145.9	4.492	1.12	26	47	8
	487.3365	5.3	10.9	16.5	C37 H43	146.3	4.885	0.76	37	43	
	487.3482	-6.4	-13.1	-1.5	C23 H51 O10	146.8	5.410	0.45	23	51	10

Supplementary data 54: iFit value of euscaphic acid (**58**) in the ethanol extract of *S. columbaria* roots.

Supplementary data 55: MS and MS/MS data of quinic acid (**peak 1**) in the aqueous extract of *S. birrea* leaves.

Single Mass Analysis
Tolerance = 15.0 mDa / DBE: min = -1.5, max = 50.0
Element prediction: Off
Number of isotope peaks used for i-FIT = 3
Monoisotopic Mass, Even Electron Ions
28 formula(e) evaluated with 3 results within limits (up to 50 best isotopic matches for each mass)
Elements Used:

Mass	Calc. Mass	mDa	PPM	DBE	Formula	i-FIT	i-FIT Norm	Fit Conf %	C	H	O
191.0582	191.0556	2.6	13.6	2.5	C7 H11 O6	156.2	0.001	99.94	7	11	6
	191.0708	-12.6	-65.9	6.5	C11 H11 O3	164.4	8.135	0.03	11	11	3
	191.0497	8.5	44.5	11.5	C14 H7 O	164.5	8.213	0.03	14	7	1

Supplementary data 56: iFit value of quinic acid (**peak 1**) in the aqueous extract of *S. birrea* leaves.

Supplementary data 57: MS and MS/MS data of gallic acid (**peak 2**) in the aqueous extract of *S. birrea* leaves.

Single Mass Analysis
Tolerance = 15.0 mDa / DBE: min = -1.5, max = 50.0
Element prediction: Off
Number of isotope peaks used for i-FIT = 3
Monoisotopic Mass, Even Electron Ions
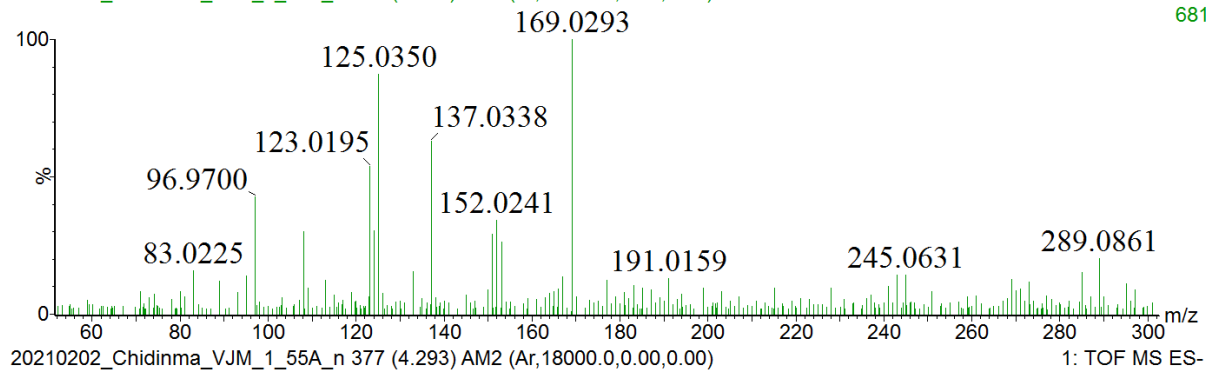22 formula(e) evaluated with 3 results within limits (up to 50 best isotopic matches for each mass)
Elements Used:

Mass	Calc. Mass	mDa	PPM	DBE	Formula	i-FIT	i-FIT Norm	Fit Conf %	C	H	O
169.0166	169.0137	2.9	17.2	5.5	C7 H5 O5	32.7	0.017	98.32	7	5	5
	169.0290	-12.4	-73.4	9.5	C11 H5 O2	36.8	4.126	1.61	11	5	2
	169.0078	8.8	52.1	14.5	C14 H	40.1	7.386	0.06	14	1	

Supplementary data 58: iFit value of gallic acid (**peak 2**) in the aqueous extract of *S. birrea* leaves.

Supplementary data 59: MS and MS/MS data of procyanidin B2 (**peak 3**) in the aqueous extract of *S. birrea* leaves.

Single Mass Analysis
Tolerance = 15.0 mDa / DBE: min = -1.5, max = 50.0
Element prediction: Off
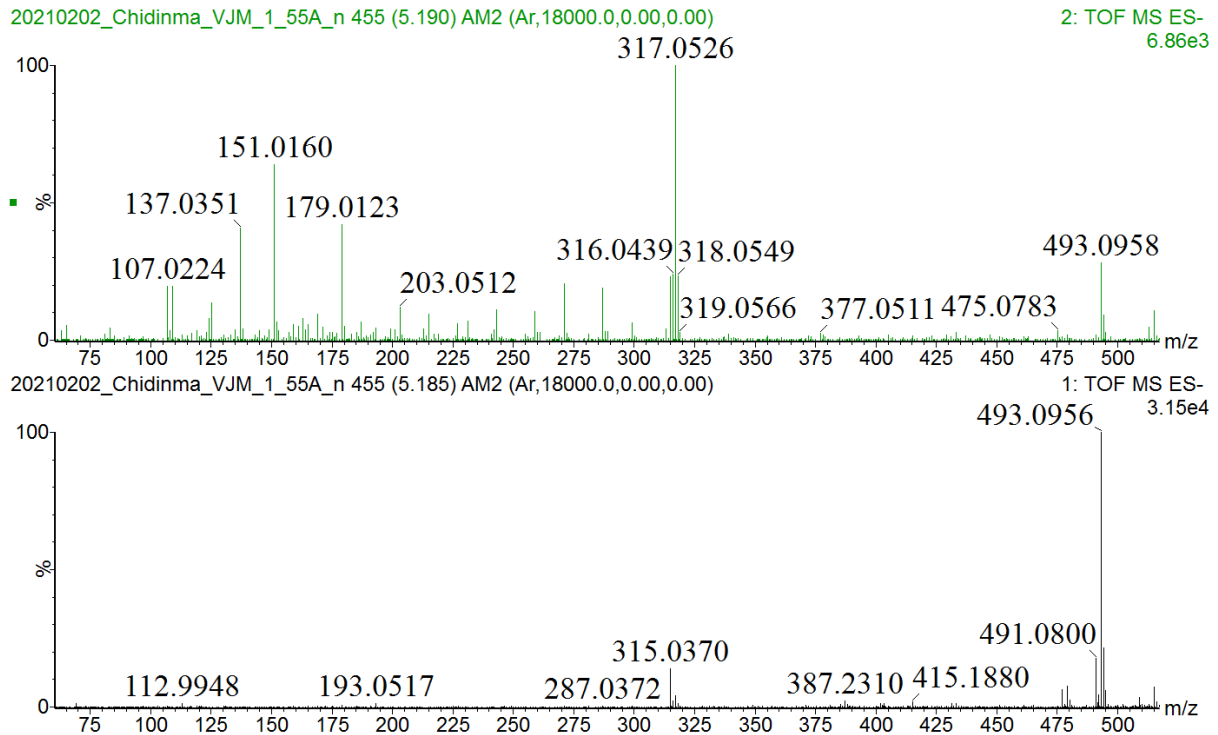Number of isotope peaks used for i-FIT = 3
Monoisotopic Mass, Even Electron Ions
162 formula(e) evaluated with 8 results within limits (up to 50 best isotopic matches for each mass)
Elements Used:

Mass	Calc. Mass	mDa	PPM	DBE	Formula	i-FIT	i-FIT Norm	Fit Conf %	C	H	O
577.1329	577.1346	-1.7	-2.9	18.5	C30 H25 O12	34.3	0.763	46.64	30	25	12
	577.1193	13.6	23.6	14.5	C26 H25 O15	34.3	0.785	45.60	26	25	15
	577.1405	-7.6	-13.2	9.5	C23 H29 O17	36.3	2.752	6.38	23	29	17
	577.1287	4.2	7.3	27.5	C37 H21 O7	38.3	4.751	0.86	37	21	7
	577.1252	7.7	13.3	5.5	C19 H29 O20	39.2	5.738	0.32	19	29	20
	577.1440	-11.1	-19.2	31.5	C41 H21 O4	40.5	6.956	0.10	41	21	4
	577.1229	10.0	17.3	36.5	C44 H17 O2	40.9	7.349	0.06	44	17	2
	577.1463	-13.4	-23.2	0.5	C16 H33 O22	41.3	7.810	0.04	16	33	22

Supplementary data 60: iFit value of procyanidin B2 (**peak 3**) in the aqueous extract of *S. birrea* leaves.

Supplementary data 61: MS and MS/MS data of gallocatechin (**peak 4**) in the aqueous extract of *S. birrea* leaves.

Single Mass Analysis
Tolerance = 15.0 mDa / DBE: min = -1.5, max = 50.0
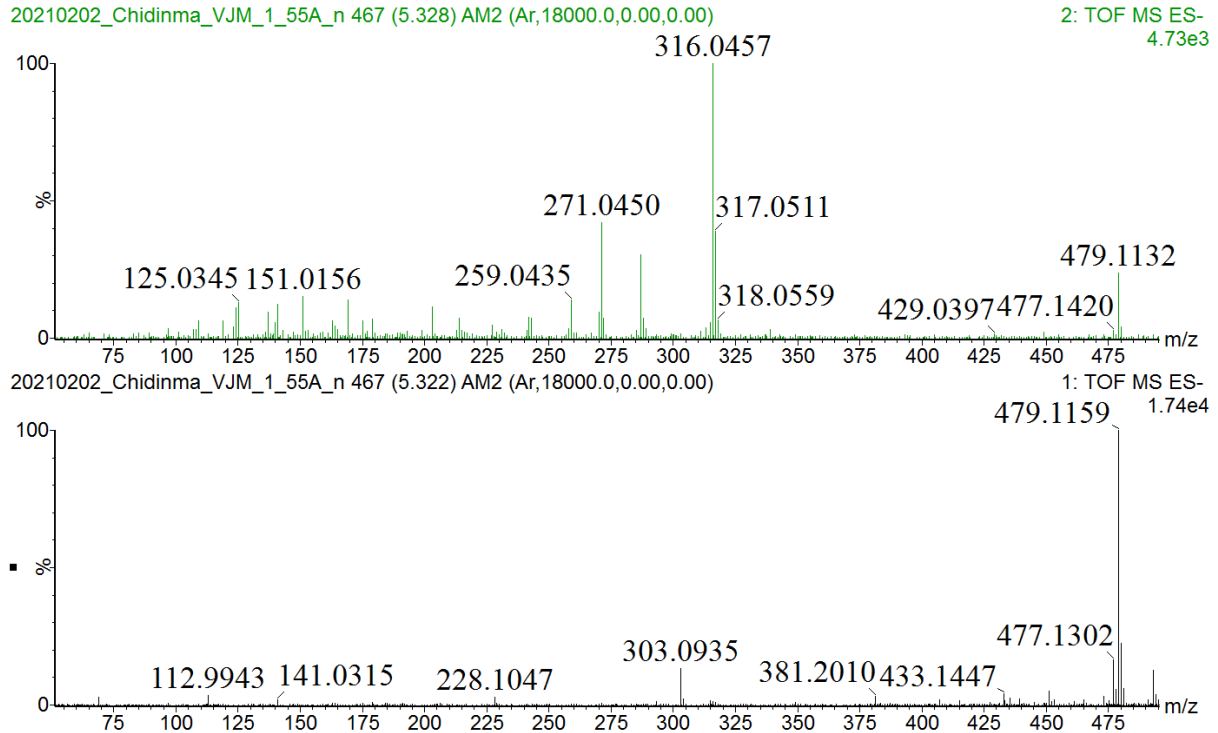Element prediction: Off
Number of isotope peaks used for i-FIT = 3
Monoisotopic Mass, Even Electron Ions
56 formula(e) evaluated with 4 results within limits (up to 50 best isotopic matches for each mass)
Elements Used:

Mass	Calc. Mass	mDa	PPM	DBE	Formula	i-FIT	i-FIT Norm	Fit Conf %	C	H	O
305.0666	305.0661	0.5	1.6	9.5	C15 H13 O7	48.8	0.841	43.13	15	13	7
	305.0603	6.3	20.7	18.5	C22 H9 O2	49.4	1.447	23.52	22	9	2
	305.0814	-14.8	-48.5	13.5	C19 H13 O4	49.7	1.736	17.63	19	13	4
	305.0720	-5.4	-17.7	0.5	C8 H17 O12	49.8	1.850	15.72	8	17	12

Supplementary data 62: iFit value of gallocatechin (**peak 4**) in the aqueous extract of *S. birrea* leaves.
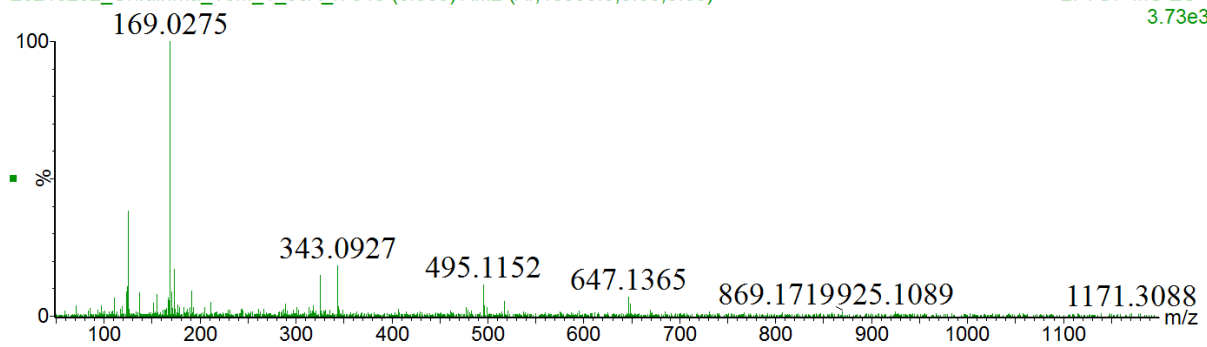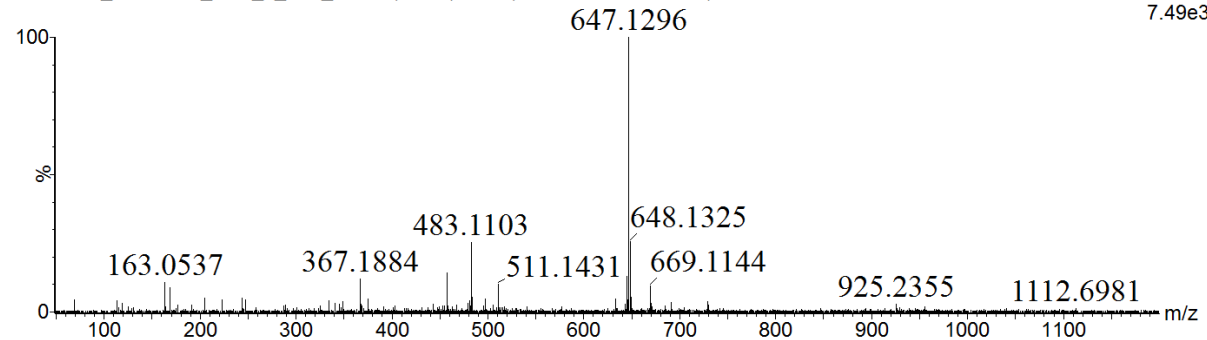
Supplementary data 63: MS and MS/MS data of pistafolin A (**peak 5**) in the aqueous extract of *S. birrea* leaves.

Single Mass Analysis
Tolerance = 15.0 mDa / DBE: min = -1.5, max = 50.0
Element prediction: Off
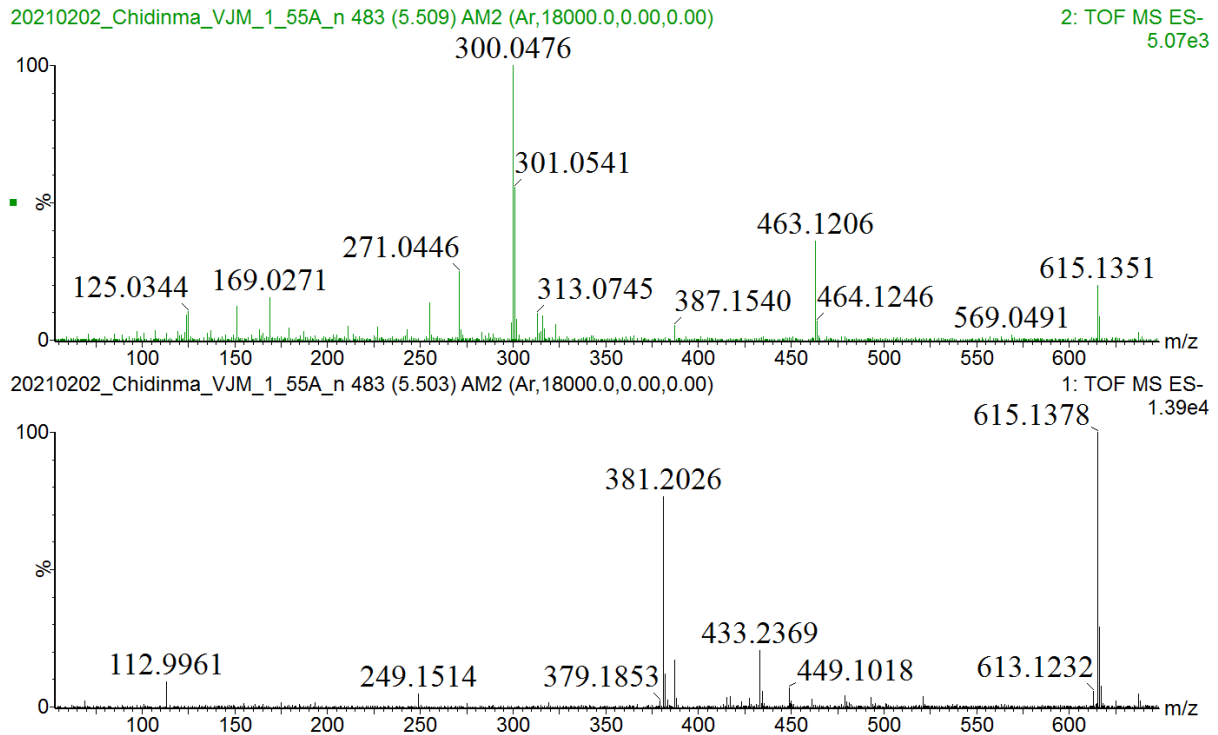Number of isotope peaks used for i-FIT = 3
Monoisotopic Mass, Even Electron Ions
205 formula(e) evaluated with 10 results within limits (up to 50 best isotopic matches for each mass)
Elements Used:

Mass	Calc. Mass	mDa	PPM	DBE	Formula	i-FIT	i-FIT Norm	Fit Conf %	C	H	O
647.0870	647.0943	-7.3	-11.3	8.5	C21 H27 O23	59.6	0.847	42.87	21	27	23
	647.0732	13.8	21.3	13.5	C24 H23 O21	60.0	1.263	28.29	24	23	21
	647.0884	-1.4	-2.2	17.5	C28 H23 O18	60.6	1.932	14.49	28	23	18
	647.0791	7.9	12.2	4.5	C17 H27 O26	61.2	2.485	8.33	17	27	26
	647.0826	4.4	6.8	26.5	C35 H19 O13	62.5	3.846	2.14	35	19	13
	647.1002	-13.2	-20.4	-0.5	C14 H31 O28	62.7	3.966	1.90	14	31	28
	647.0978	-10.8	-16.7	30.5	C39 H19 O10	63.5	4.824	0.80	39	19	10
	647.0767	10.3	15.9	35.5	C42 H15 O8	64.0	5.311	0.49	42	15	8

Supplementary data 64: iFit value of pistafolin A (**peak 5**) in the aqueous extract of *S. birrea* leaves.
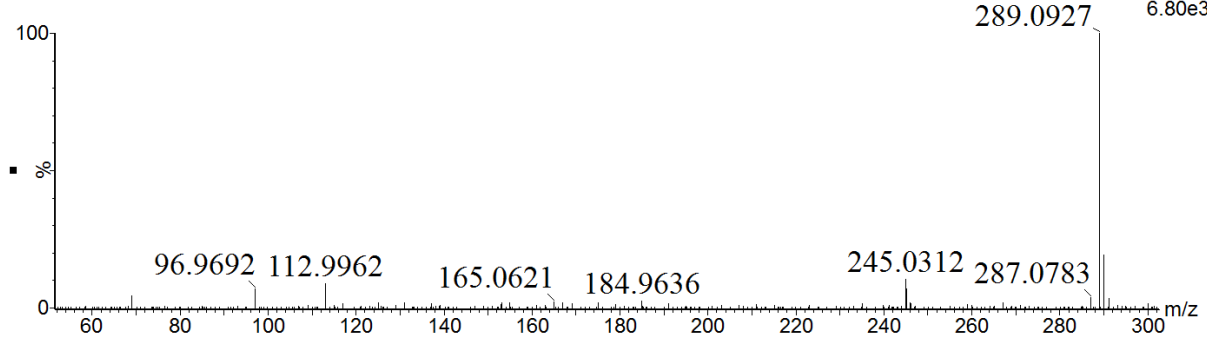
Supplementary data 65: MS and MS/MS data of epicatechin (**peak 6**) in the aqueous extract of *S. birrea* leaves.

Single Mass Analysis
Tolerance = 15.0 mDa   /   DBE: min = -1.5, max = 50.0
Element prediction: Off
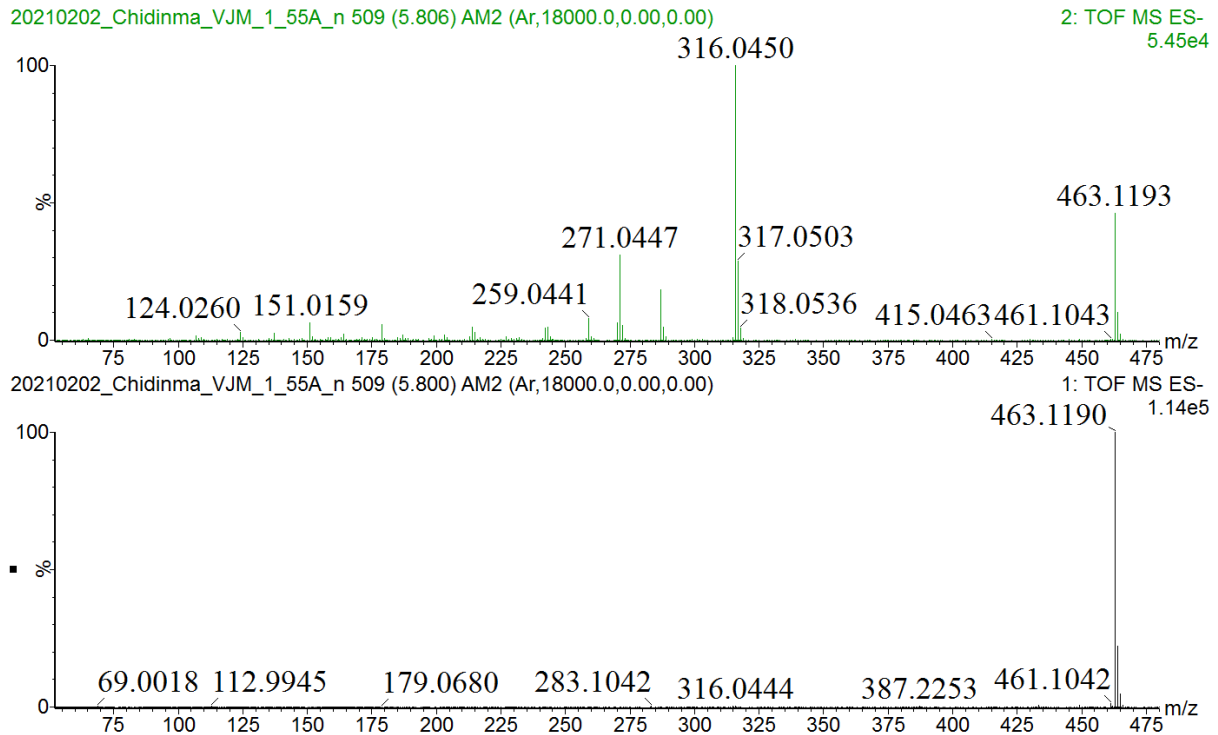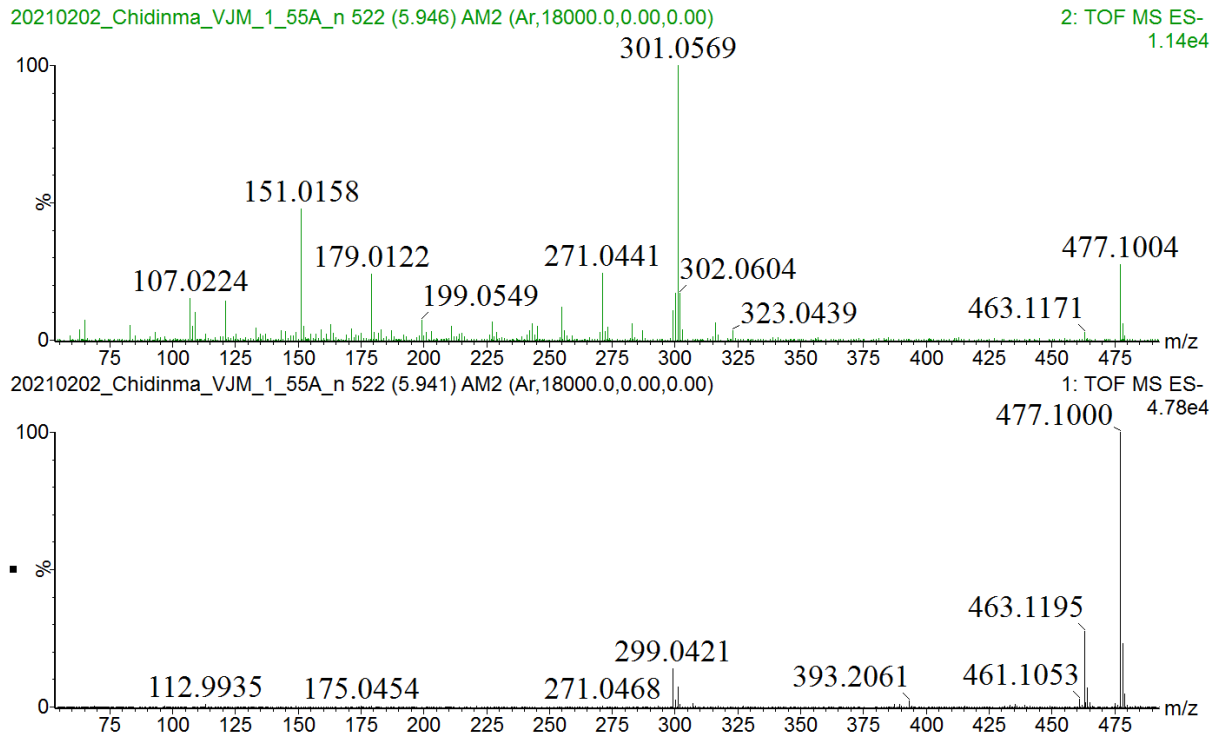Number of isotope peaks used for i-FIT = 3
Monoisotopic Mass, Even Electron Ions
51 formula(e) evaluated with 4 results within limits (up to 50 best isotopic matches for each mass)
Elements Used:

Mass	Calc. Mass	mDa	PPM	DBE	Formula	i-FIT	i-FIT Norm	Fit Conf %	C	H	O	
289.0735	289.0865	-13.0	-45.0	13.5	C19 H13 O3	32.3	0.652	52.09	19	13	3	
	289.0712	2.3	8.0	9.5	C15 H13 O6	32.5	0.844	43.00	15	13	6	
	289.0653	8.2	28.4	18.5	C22 H9 O	35.1	3.441	3.20	22	9	1	
	289.0771	-3.6	-12.5	0.5	C8 H17 O11	35.8	4.070	1.71	8	17	11	

Supplementary data 66: iFit value of epicatechin (**peak 6**) in the aqueous extract of *S. birrea* leaves.

Supplementary data 67: MS and MS/MS data of myricetin 3-*O*-β-D-glucuronide (**88**) in the aqueous extract of *S. birrea* leaves.

Single Mass Analysis
Tolerance = 15.0 mDa / DBE: min = -1.5, max = 50.0
Element prediction: Off
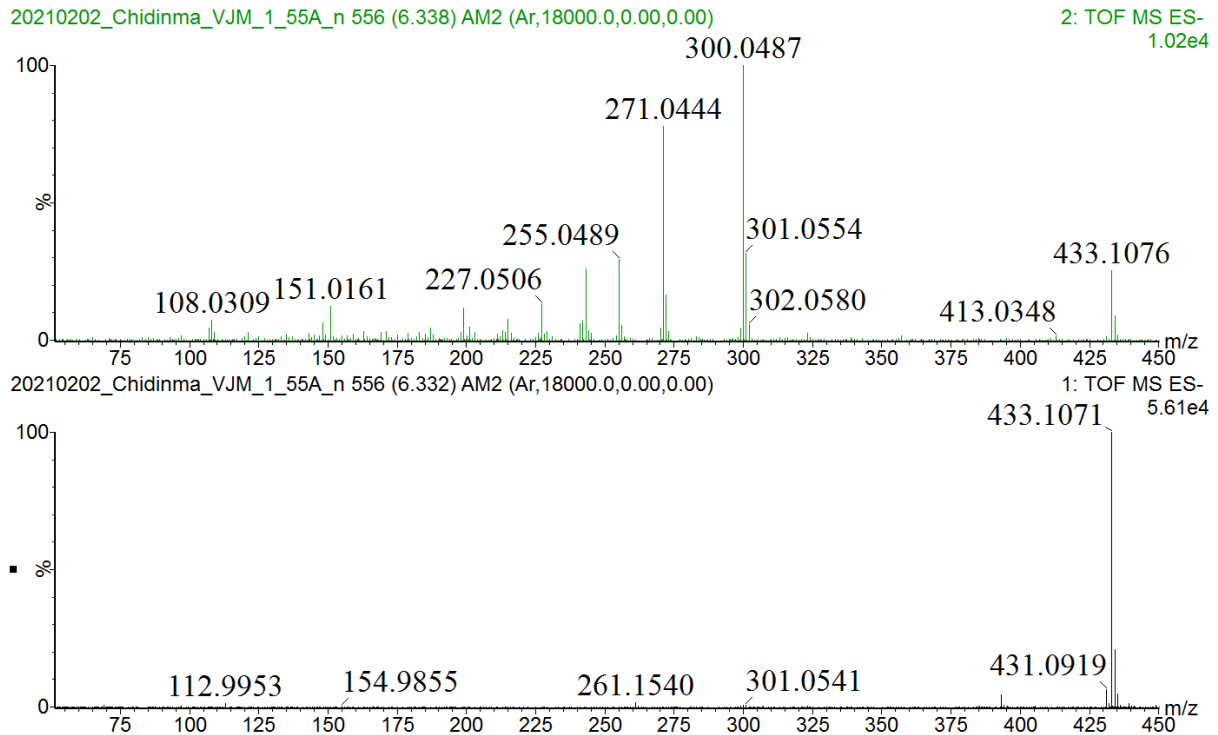Number of isotope peaks used for i-FIT = 3
Monoisotopic Mass, Even Electron Ions
122 formula(e) evaluated with 8 results within limits (up to 50 best isotopic matches for each mass)
Elements Used:

Mass	Calc. Mass	mDa	PPM	DBE	Formula	i-FIT	i-FIT Norm	Fit Conf %	C	H	O
493.0631	493.0618	1.3	2.6	13.5	C21 H17 O14	80.0	0.082	92.14	21	17	14
	493.0677	-4.6	-9.3	4.5	C14 H21 O19	82.7	2.755	6.36	14	21	19
	493.0771	-14.0	-28.4	17.5	C25 H17 O11	84.9	4.948	0.71	25	17	11
	493.0524	10.7	21.7	0.5	C10 H21 O22	85.2	5.248	0.53	10	21	22
	493.0560	7.1	14.4	22.5	C28 H13 O9	86.1	6.185	0.21	28	13	9
	493.0712	-8.1	-16.4	26.5	C32 H13 O6	87.8	7.876	0.04	32	13	6
	493.0501	13.0	26.4	31.5	C35 H9 O4	88.9	8.985	0.01	35	9	4
	493.0653	-2.2	-4.5	35.5	C39 H9 O	89.5	9.606	0.01	39	9	1

Supplementary data 68: iFit value of myricetin 3-*O*-β-D-glucuronide (**88**) in the aqueous extract of *S. birrea* leaves.

263

2: TOF MS ES-
4.73e3

316.0457

317.0511

271.0450

318.0559

125.0345 151.0156

259.0435

429.0397 477.1420

479.1132

m/z

20210202_Chidinma_VJM_1_55A_n 467 (5.322) AM2 (Ar,18000.0,0.00,0.00)

1: TOF MS ES-
1.74e4

479.1159

477.1302

112.9943 141.0315

228.1047

303.0935

381.2010 433.1447

m/z

Supplementary data 69: MS and MS/MS data of gossypin (**peak 8**) in the aqueous extract of *S. birrea* leaves.

Single Mass Analysis
Tolerance = 15.0 mDa / DBE: min = -1.5, max = 50.0
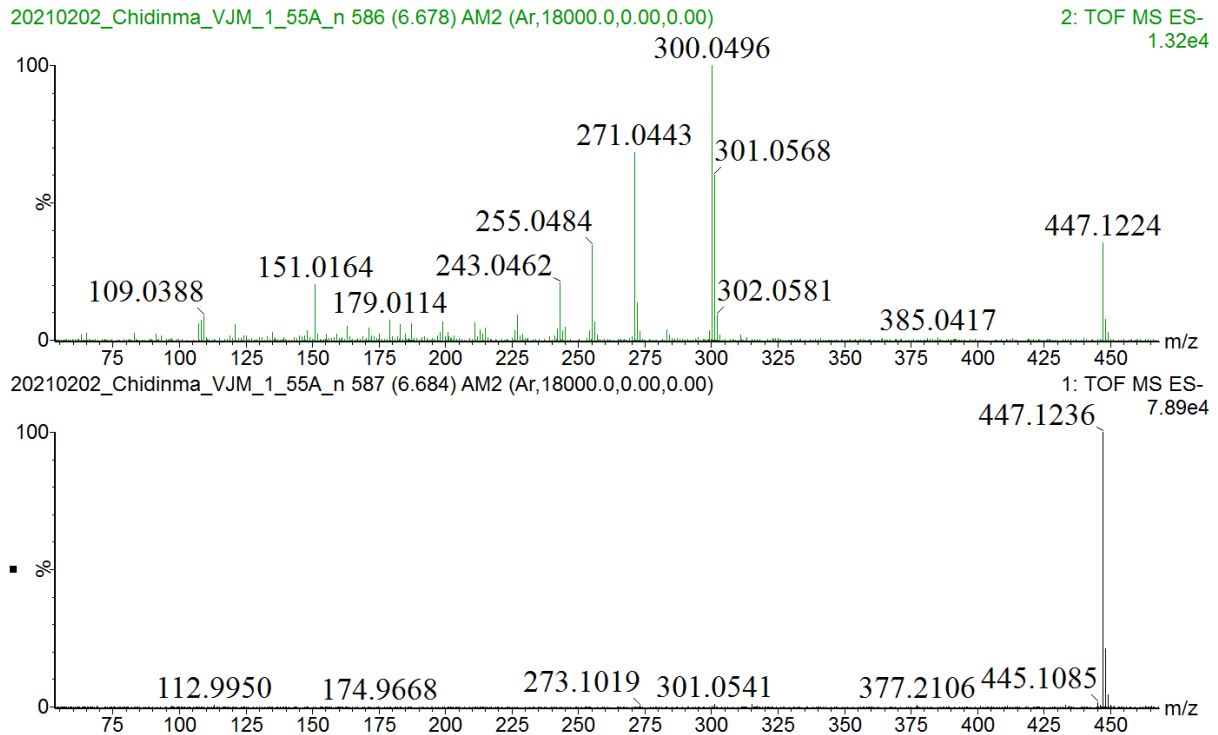Element prediction: Off
Number of isotope peaks used for i-FIT = 3
Monoisotopic Mass, Even Electron Ions
121 formula(e) evaluated with 8 results within limits (up to 50 best isotopic matches for each mass)
Elements Used:

Mass	Calc. Mass	mDa	PPM	DBE	Formula			i-FIT	i-FIT Norm	Fit Conf %	C	H	O
479.0833	479.0826	0.7	1.5	12.5	C21 H19 O13			41.6	0.020	98.07	21	19	13
	479.0767	6.6	13.8	21.5	C28 H15 O8			46.7	5.130	0.59	28	15	8
	479.0884	-5.1	-10.6	3.5	C14 H23 O18			46.7	5.193	0.56	14	23	18
	479.0978	-14.5	-30.3	16.5	C25 H19 O10			47.1	5.527	0.40	25	19	10
	479.0861	-2.8	-5.8	34.5	C39 H11			47.8	6.290	0.19	39	11	
	479.0919	-8.6	-18.0	25.5	C32 H15 O5			48.0	6.502	0.15	32	15	5
	479.0708	12.5	26.1	30.5	C35 H11 O3			49.6	8.029	0.03	35	11	3

Supplementary data 70: iFit value of gossypin (**peak 8**) in the aqueous extract of *S. birrea* leaves.

Supplementary data 71: MS and MS/MS data of quercetin 3-*O*-(6"-galloyl)-Beta-D-glucopyranoside (**peak 9**) in the aqueous extract of *S. birrea* leaves.

Single Mass Analysis
Tolerance = 15.0 mDa / DBE: min = -1.5, max = 50.0
Element prediction: Off
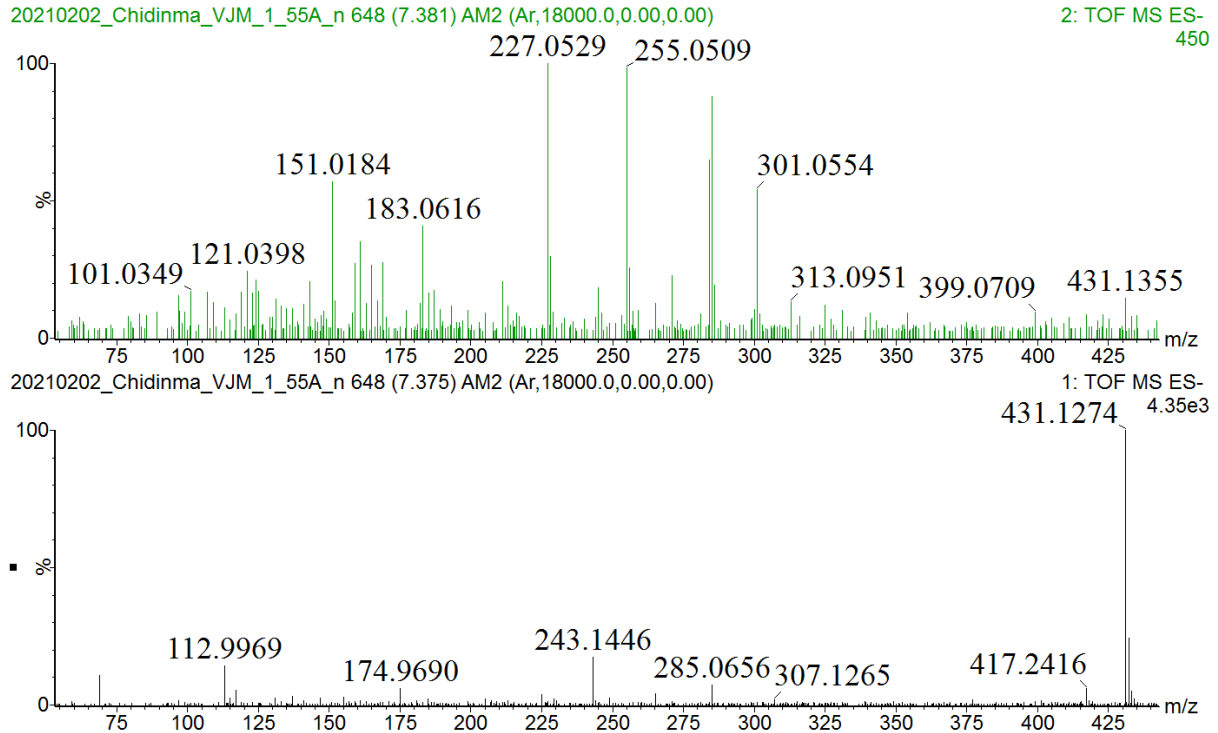Number of isotope peaks used for i-FIT = 3
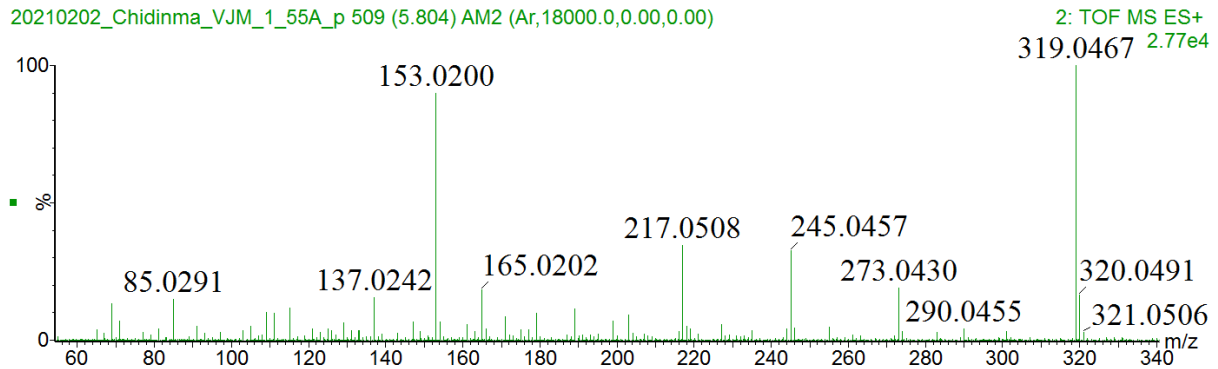Monoisotopic Mass, Even Electron Ions
188 formula(e) evaluated with 9 results within limits (up to 50 best isotopic matches for each mass)
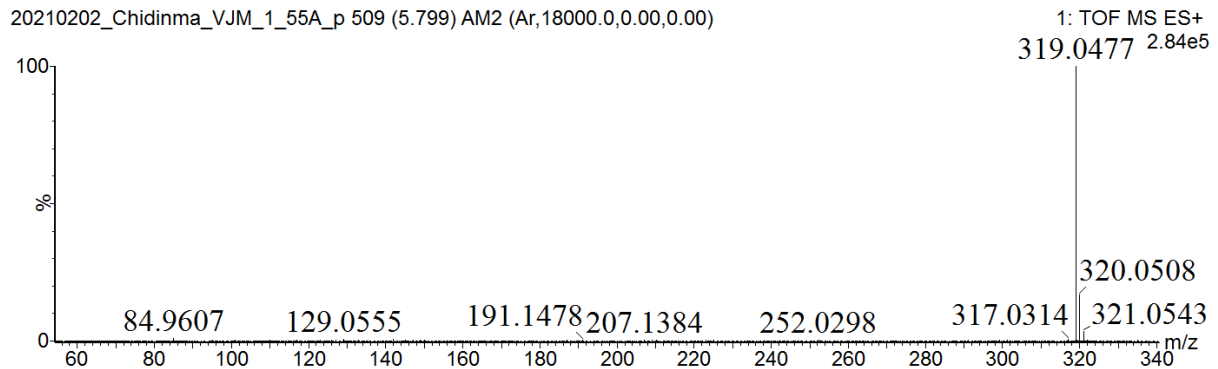Elements Used:

Mass	Calc. Mass	mDa	PPM	DBE	Formula	i-FIT	i-FIT Norm	Fit Conf %	C	H	O
615.0966	615.0986	-2.0	-3.3	17.5	C28 H23 O16	70.5	0.063	93.93	28	23	16
	615.0834	13.2	21.5	13.5	C24 H23 O19	73.4	2.938	5.30	24	23	19
	615.0927	3.9	6.3	26.5	C35 H19 O11	76.1	5.667	0.35	35	19	11
	615.1045	-7.9	-12.8	8.5	C21 H27 O21	76.1	5.683	0.34	21	27	21
	615.1021	-5.5	-8.9	39.5	C46 H15 O3	78.7	8.258	0.03	46	15	3
	615.1080	-11.4	-18.5	30.5	C39 H19 O8	78.9	8.470	0.02	39	19	8
	615.0892	7.4	12.0	4.5	C17 H27 O24	79.0	8.529	0.02	17	27	24
	615.0869	9.7	15.8	35.5	C42 H15 O6	79.3	8.836	0.01	42	15	6

Supplementary data 72: iFit value of quercetin 3-*O*-(6"-galloyl)-Beta-D-glucopyranoside (**peak 9**) in the aqueous extract of *S. birrea* leaves.

265

20210202_Chidinma_VJM_1_55A_n 509 (5.806) AM2 (Ar,18000.0,0.00,0.00)   2: TOF MS ES-
5.45e4

20210202_Chidinma_VJM_1_55A_n 509 (5.800) AM2 (Ar,18000.0,0.00,0.00)   1: TOF MS ES-
1.14e5

Supplementary data 73: MS and MS/MS data of myricetin-3-*O*-alpha-L-rhamnopyranoside (**peak 10**) in the aqueous extract of *S. birrea* leaves.

Single Mass Analysis
Tolerance = 15.0 mDa / DBE: min = -1.5, max = 50.0
Element prediction: Off
Number of isotope peaks used for i-FIT = 3
Monoisotopic Mass, Even Electron Ions
114 formula(e) evaluated with 7 results within limits (up to 50 best isotopic matches for each mass)
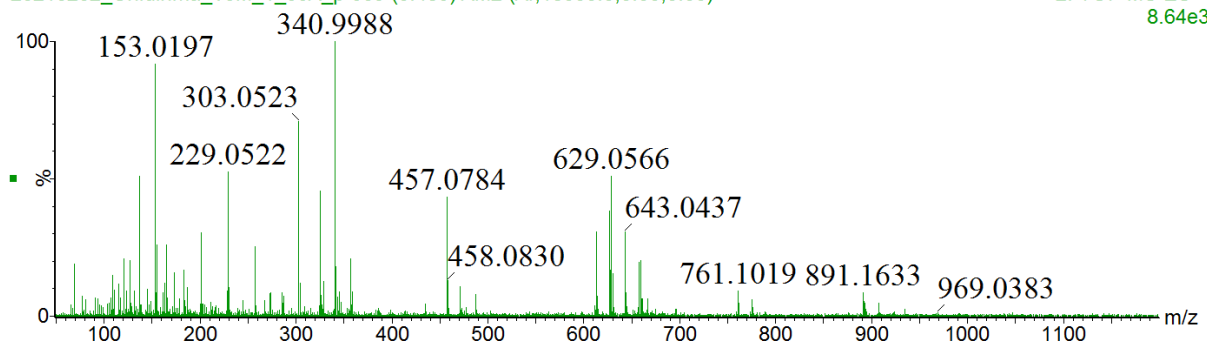Elements Used:

Mass	Calc. Mass	mDa	PPM	DBE	Formula	i-FIT	i-FIT Norm	Fit Conf %	C	H	O
463.0881	463.0877	0.4	0.9	12.5	C21 H19 O12	110.9	0.016	98.43	21	19	12
	463.0935	-5.4	-11.7	3.5	C14 H23 O17	115.1	4.274	1.39	14	23	17
	463.1029	-14.8	-32.0	16.5	C25 H19 O9	118.0	7.156	0.08	25	19	9
	463.0783	9.8	21.2	-0.5	C10 H23 O20	118.2	7.292	0.07	10	23	20
	463.0818	6.3	13.6	21.5	C28 H15 O7	119.1	8.193	0.03	28	15	7
	463.0970	-8.9	-19.2	25.5	C32 H15 O4	121.3	10.382	0.00	32	15	4
	463.0759	12.2	26.3	30.5	C35 H11 O2	122.5	11.626	0.00	35	11	2

Supplementary data 74: iFit value of myricetin-3-*O*-alpha-L-rhamnopyranoside (**peak 10**) in the aqueous extract of *S. birrea* leaves.

20210202_Chidinma_VJM_1_55A_n 522 (5.946) AM2 (Ar,18000.0,0.00,0.00)   2: TOF MS ES-
1.14e4

Peaks: 301.0569, 151.0158, 179.0122, 199.0549, 271.0441, 107.0224, 302.0604, 323.0439, 463.1171, 477.1004

20210202_Chidinma_VJM_1_55A_n 522 (5.941) AM2 (Ar,18000.0,0.00,0.00)   1: TOF MS ES-
4.78e4

Peaks: 477.1000, 463.1195, 299.0421, 112.9935, 175.0454, 271.0468, 393.2061, 461.1053

Supplementary data 75: MS and MS/MS data of quercetin-3-*O*-beta-D-glucuronide (**89**) in the aqueous extract of *S. birrea* leaves.

Single Mass Analysis
Tolerance = 15.0 mDa   /   DBE: min = -1.5, max = 50.0
Element prediction: Off
Number of isotope peaks used for i-FIT = 3
Monoisotopic Mass, Even Electron Ions
115 formula(e) evaluated with 8 results within limits (up to 50 best isotopic matches for each mass)
Elements Used:

Mass	Calc. Mass	mDa	PPM	DBE	Formula	i-FIT	i-FIT Norm	Fit Conf %	C	H	O
477.0679	477.0669	1.0	2.1	13.5	C21 H17 O13	47.8	0.009	99.11	21	17	13
	477.0728	-4.9	-10.3	4.5	C14 H21 O18	53.0	5.172	0.57	14	21	18
	477.0822	-14.3	-30.0	17.5	C25 H17 O10	53.9	6.117	0.22	25	17	10
	477.0575	10.4	21.8	0.5	C10 H21 O21	55.4	7.599	0.05	10	21	21
	477.0610	6.9	14.5	22.5	C28 H13 O8	55.5	7.676	0.05	28	13	8
	477.0763	-8.4	-17.6	26.5	C32 H13 O5	57.5	9.667	0.01	32	13	5
	477.0552	12.7	26.6	31.5	C35 H9 O3	58.8	10.971	0.00	35	9	3
	477.0704	-2.5	-5.2	35.5	C39 H9	59.4	11.578	0.00	39	9	

Supplementary data 76: iFit value of quercetin-3-*O*-beta-D-glucuronide (**89**) in the aqueous extract of *S. birrea* leaves.

100 -
300.0487

271.0444

301.0554

255.0489

%

108.0309 151.0161　　227.0506　　302.0580　　433.1076

413.0348

0 -
75　100　125　150　175　200　225　250　275　300　325　350　375　400　425　450　m/z

20210202_Chidinma_VJM_1_55A_n 556 (6.332) AM2 (Ar,18000.0,0.00,0.00)　　　　1: TOF MS ES-
5.61e4

100 -
433.1071

%

112.9953　154.9855　　261.1540　301.0541　　431.0919

0 -
75　100　125　150　175　200　225　250　275　300　325　350　375　400　425　450　m/z

Supplementary data 77: MS and MS/MS data of quercetin-3-O-arabinoside (**peak 12**) in the aqueous extract of *S. birrea* leaves.

Single Mass Analysis
Tolerance = 15.0 mDa　/　DBE: min = -1.5, max = 50.0
Element prediction: Off
Number of isotope peaks used for i-FIT = 3
Monoisotopic Mass, Even Electron Ions
99 formula(e) evaluated with 7 results within limits (up to 50 best isotopic matches for each mass)
Elements Used:

Mass	Calc. Mass	mDa	PPM	DBE	Formula	i-FIT	i-FIT Norm	Fit Conf %	C	H	O
433.0774	433.0771	0.3	0.7	12.5	C20 H17 O11	103.3	0.005	99.53	20	17	11
	433.0712	6.2	14.3	21.5	C27 H13 O6	109.2	5.853	0.29	27	13	6
	433.0923	-14.9	-34.4	16.5	C24 H17 O8	110.2	6.866	0.10	24	17	8
	433.0830	-5.6	-12.9	3.5	C13 H21 O16	111.0	7.652	0.05	13	21	16
	433.0865	-9.1	-21.0	25.5	C31 H13 O3	111.6	8.252	0.03	31	13	3
	433.0653	12.1	27.9	30.5	C34 H9 O	113.4	10.044	0.00	34	9	1
	433.0677	9.7	22.4	-0.5	C9 H21 O19	114.2	10.871	0.00	9	21	19

Supplementary data 78: iFit value of quercetin-3-O-arabinoside (**peak 12**) in the aqueous extract of *S. birrea* leaves.

268

100

%

300.0496

271.0443 301.0568

255.0484

151.0164　243.0462

109.0388　　179.0114　　　　　　　302.0581

385.0417

447.1224

0
　　75　　100　　125　　150　　175　　200　　225　　250　　275　　300　　325　　350　　375　　400　　425　　450　　m/z

100

447.1236

%

112.9950　　174.9668　　273.1019　301.0541　377.2106　445.1085

0
　　75　　100　　125　　150　　175　　200　　225　　250　　275　　300　　325　　350　　375　　400　　425　　450　　m/z

Supplementary data 79: MS and MS/MS data of quercetin-3-*O*-alpha-L-rhamnopyranoside (**peak 13**) in the aqueous extract of *S. birrea* leaves.

Single Mass Analysis
Tolerance = 15.0 mDa　/　DBE: min = -1.5, max = 50.0
Element prediction: Off
Number of isotope peaks used for i-FIT = 3
Monoisotopic Mass, Even Electron Ions
108 formula(e) evaluated with 6 results within limits (up to 50 best isotopic matches for each mass)
Elements Used:

Mass	Calc. Mass	mDa	PPM	DBE	Formula	i-FIT	i-FIT Norm	Fit Conf %	C	H	O
447.0925	447.0927	-0.2	-0.4	12.5	C21 H19 O11	114.1	0.004	99.61	21	19	11
	447.0869	5.6	12.5	21.5	C28 H15 O6	120.2	6.180	0.21	28	15	6
	447.0986	-6.1	-13.6	3.5	C14 H23 O16	120.5	6.459	0.16	14	23	16
	447.1021	-9.6	-21.5	25.5	C32 H15 O3	123.0	8.951	0.01	32	15	3
	447.0834	9.1	20.4	-0.5	C10 H23 O19	123.9	9.878	0.01	10	23	19
	447.0810	11.5	25.7	30.5	C35 H11 O	124.4	10.315	0.00	35	11	1

Supplementary data 80: iFit value of quercetin-3-*O*-alpha-L-rhamnopyranoside (**peak 13**) in the aqueous extract of *S. birrea* leaves.

Supplementary data 81: MS and MS/MS data of kaempferol-3-*O*-alpha-L-rhamnopyranoside (**peak 14**) in the aqueous extract of *S. birrea* leaves.

Single Mass Analysis
Tolerance = 15.0 mDa   /   DBE: min = -1.5, max = 50.0
Element prediction: Off
Number of isotope peaks used for i-FIT = 3
Monoisotopic Mass, Even Electron Ions
102 formula(e) evaluated with 6 results within limits (up to 50 best isotopic matches for each mass)
Elements Used:

Mass	Calc. Mass	mDa	PPM	DBE	Formula	i-FIT	i-FIT Norm	Fit Conf %	C	H	O
431.0977	431.0978	-0.1	-0.2	12.5	C21 H19 O10	88.4	0.008	99.22	21	19	10
	431.0919	5.8	13.5	21.5	C28 H15 O5	93.6	5.274	0.51	28	15	5
	431.1037	-6.0	-13.9	3.5	C14 H23 O15	94.8	6.488	0.15	14	23	15
	431.1072	-9.5	-22.0	25.5	C32 H15 O2	95.7	7.321	0.07	32	15	2
	431.0884	9.3	21.6	-0.5	C10 H23 O18	96.5	8.111	0.03	10	23	18
	431.0861	11.6	26.9	30.5	C35 H11	96.7	8.340	0.02	35	11	

Supplementary data 82: iFit value of kaempferol-3-*O*-alpha-L-rhamnopyranoside (**peak 14**) in the aqueous extract of *S. birrea* leaves.

Supplementary data 83: MS and MS/MS data of myricetin (**90**) in the aqueous extract of *S. birrea* leaves.

Single Mass Analysis
Tolerance = 15.0 mDa / DBE: min = -1.5, max = 50.0
Element prediction: Off
Number of isotope peaks used for i-FIT = 3
Monoisotopic Mass, Even Electron Ions
62 formula(e) evaluated with 5 results within limits (up to 50 best isotopic matches for each mass)
Elements Used:

Mass	Calc. Mass	mDa	PPM	DBE	Formula	i-FIT	i-FIT Norm	Fit Conf %	C	H	O
319.0461	319.0454	0.7	2.2	10.5	C15 H11 O8	216.1	0.024	97.61	15	11	8
	319.0606	-14.5	-45.4	14.5	C19 H11 O5	220.5	4.437	1.18	19	11	5
	319.0395	6.6	20.7	19.5	C22 H7 O3	220.6	4.464	1.15	22	7	3
	319.0548	-8.7	-27.3	23.5	C26 H7	223.8	7.674	0.05	26	7	
	319.0513	-5.2	-16.3	1.5	C8 H15 O13	225.9	9.754	0.01	8	15	13

Supplementary data 84: iFit value of myricetin (**90**) in the aqueous extract of *S. birrea* leaves.

20210202_Chidinma_VJM_1_55A_p 569 (6.485) AM2 (Ar,18000.0,0.00,0.00)　　　2: TOF MS ES+
8.64e3

153.0197　340.9988
303.0523
229.0522
457.0784
629.0566
643.0437
458.0830
761.1019 891.1633
969.0383

20210202_Chidinma_VJM_1_55A_p 569 (6.480) AM2 (Ar,18000.0,0.00,0.00)　　　1: TOF MS ES+
1.06e5

303.0519
435.0951
84.9604
305.0594 458.0797 671.1127
891.1665
1046.1843
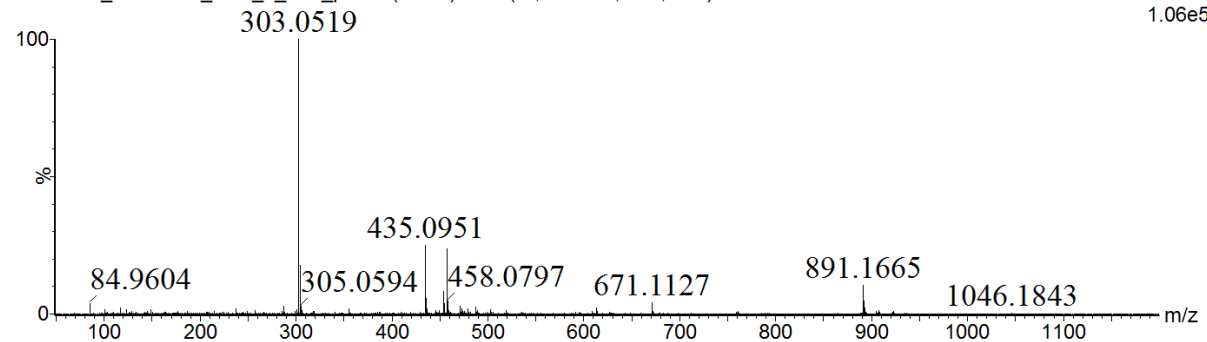
Supplementary data 85: MS and MS/MS data of quercetin (**peak 16**) in the aqueous extract of *S. birrea* leaves.

Single Mass Analysis
Tolerance = 15.0 mDa　/　DBE: min = -1.5, max = 50.0
Element prediction: Off
Number of isotope peaks used for i-FIT = 3
Monoisotopic Mass, Even Electron Ions
57 formula(e) evaluated with 4 results within limits (up to 50 best isotopic matches for each mass)
Elements Used:

Mass	Calc. Mass	mDa	PPM	DBE	Formula	i-FIT	i-FIT Norm	Fit Conf %	C	H	O
303.0501	303.0505	-0.4	-1.3	10.5	C15 H11 O7	213.5	0.019	98.16	15	11	7
	303.0446	5.5	18.1	19.5	C22 H7 O2	217.5	4.026	1.78	22	7	2
	303.0352	14.9	49.2	6.5	C11 H11 O10	221.0	7.570	0.05	11	11	10
	303.0564	-6.3	-20.8	1.5	C8 H15 O12	223.3	9.807	0.01	8	15	12

Supplementary data 86: iFit value of quercetin (**peak 16**) in the aqueous extract of *S. birrea* leaves.
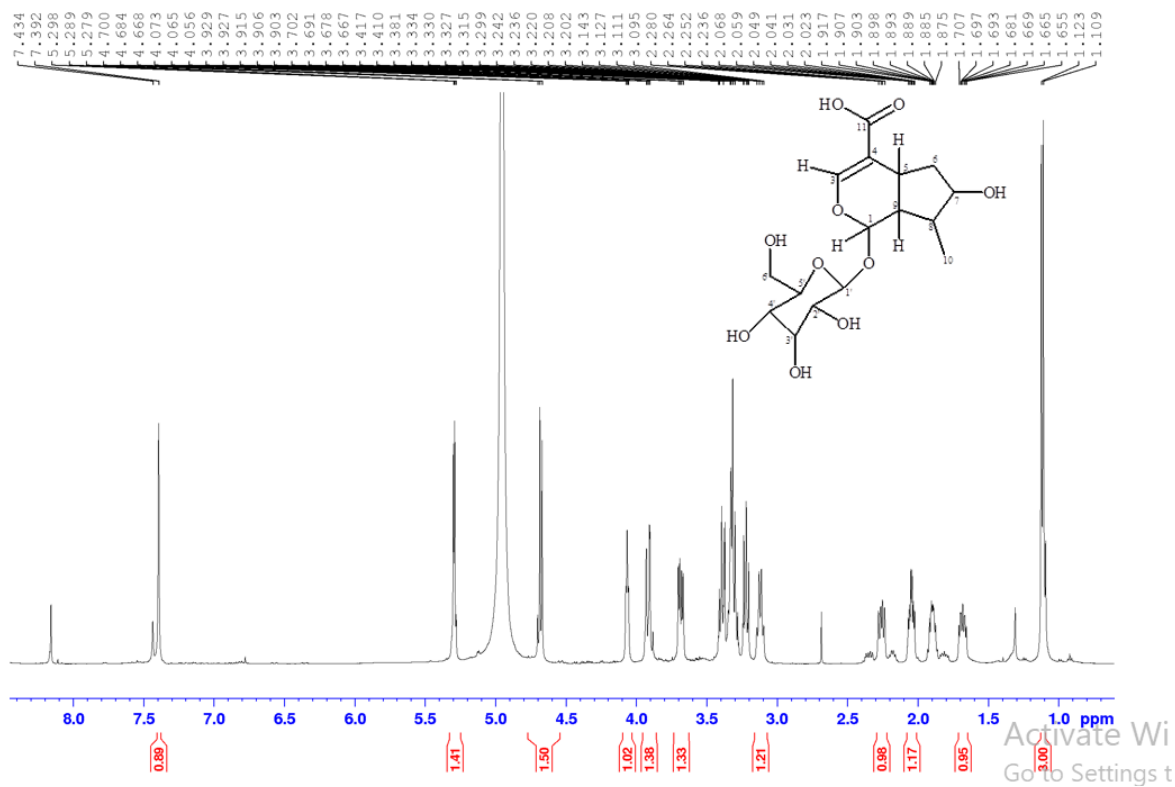
Supplementary data 87: ^{1}H NMR spectrum of loganic acid (**62**) in CD$_3$OD.
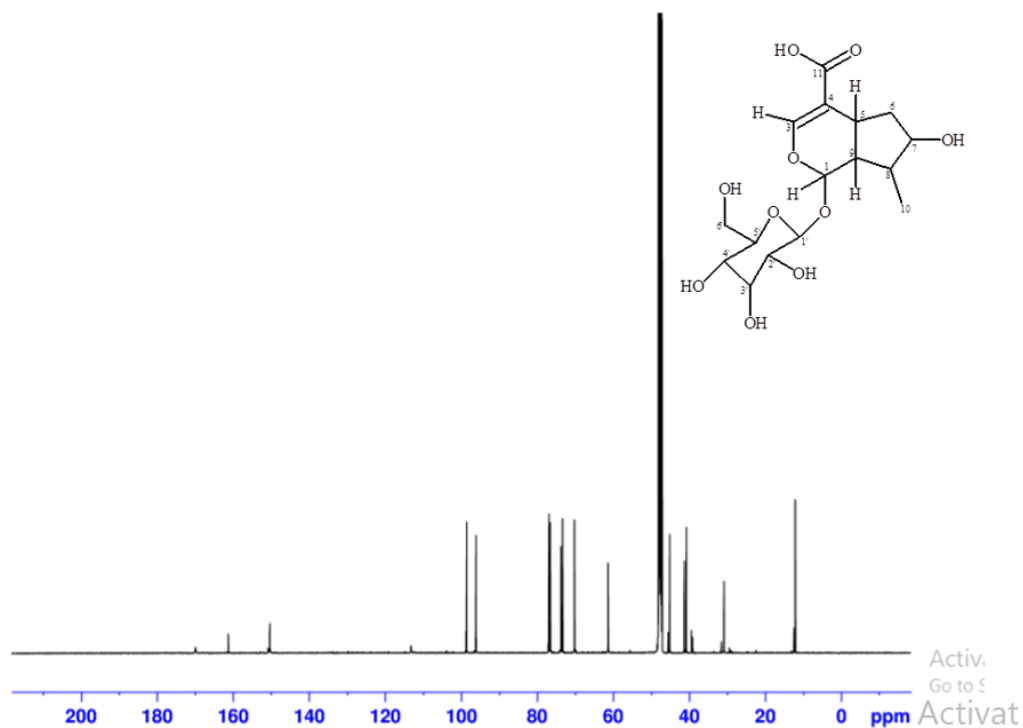
Supplementary data 88: ^{13}C NMR spectrum of loganic acid (**62**) in CD$_3$OD.
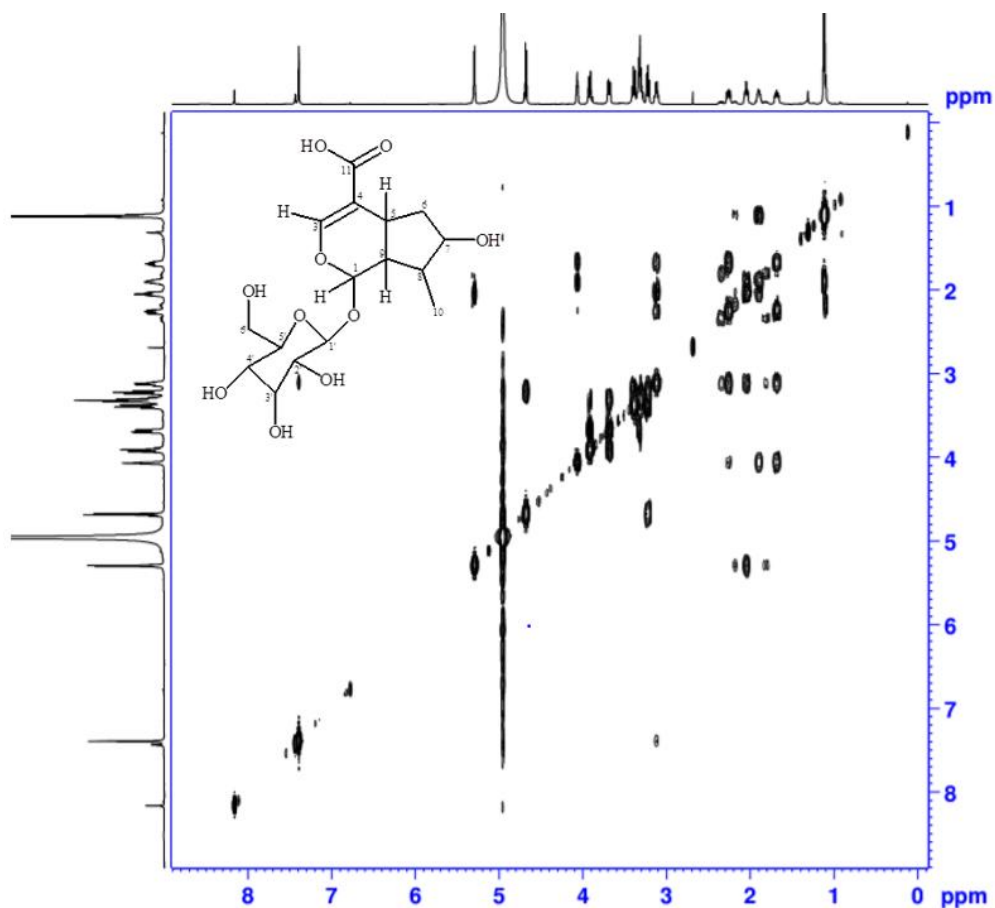
Supplementary data 89: ^{1}H-^{1}H COSY NMR spectrum of loganic acid (**62**) in CD$_3$OD.
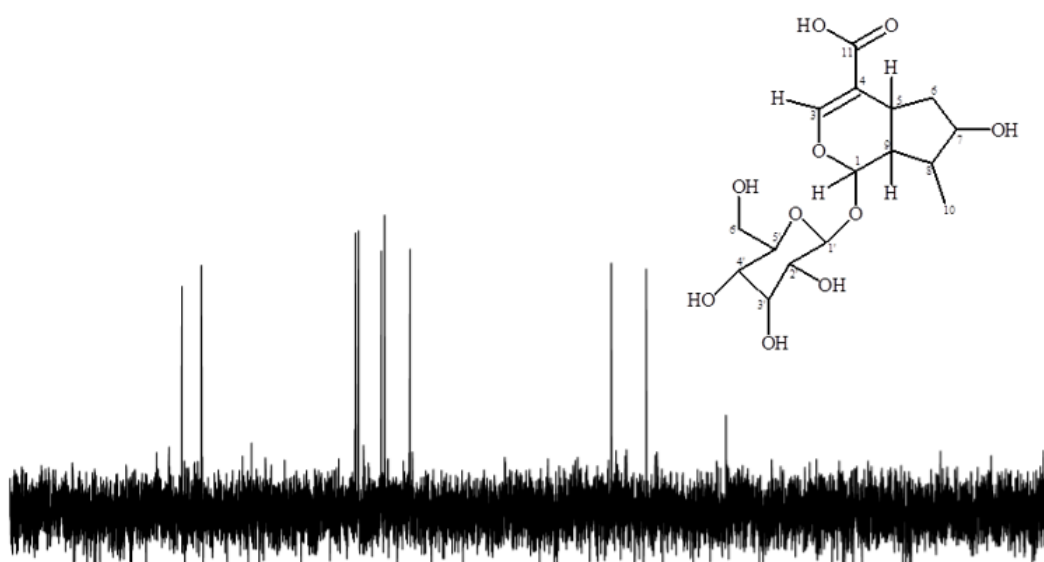
Supplementary data 90: DEPT-90 NMR spectrum of loganic acid (**62**) in CD$_3$OD.

274
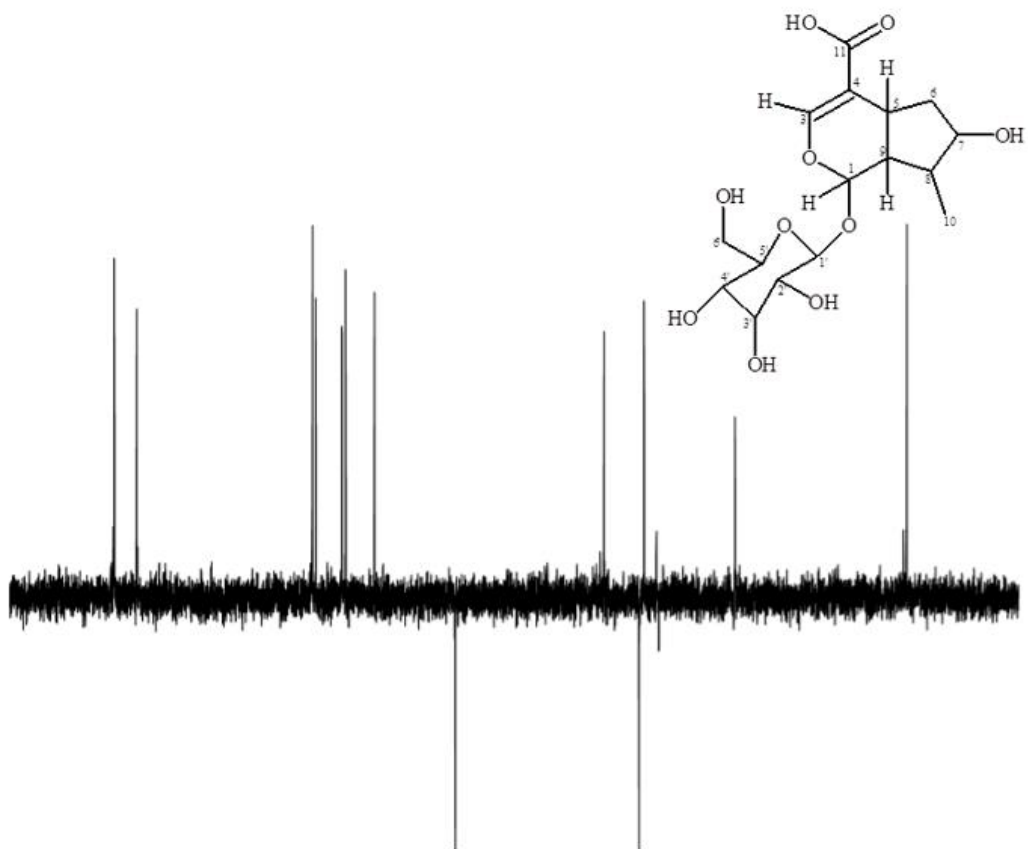
Supplementary data 91: DEPT-135 NMR spectrum of loganic acid (**62**) in CD₃OD.
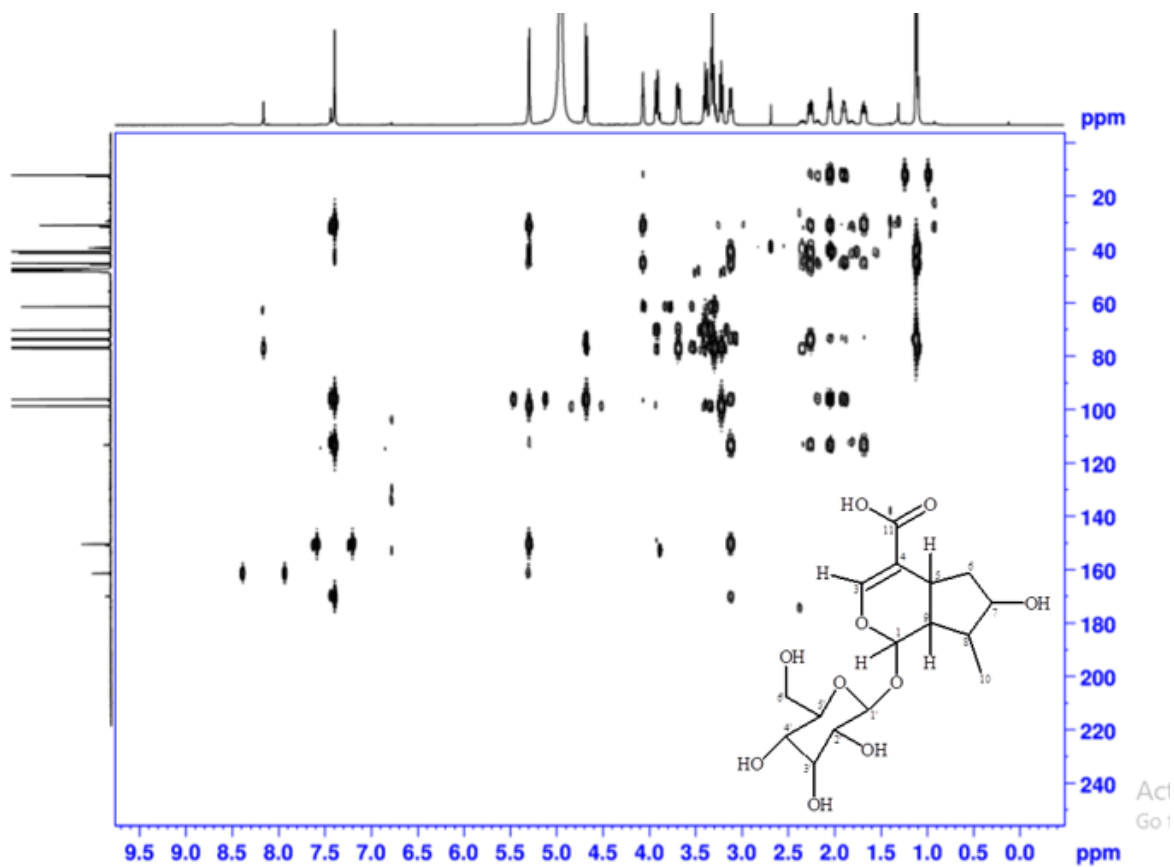
Supplementary data 92: ^{1}H-^{13}C HMBC NMR spectrum of loganic acid (**62**) in CD$_3$OD.
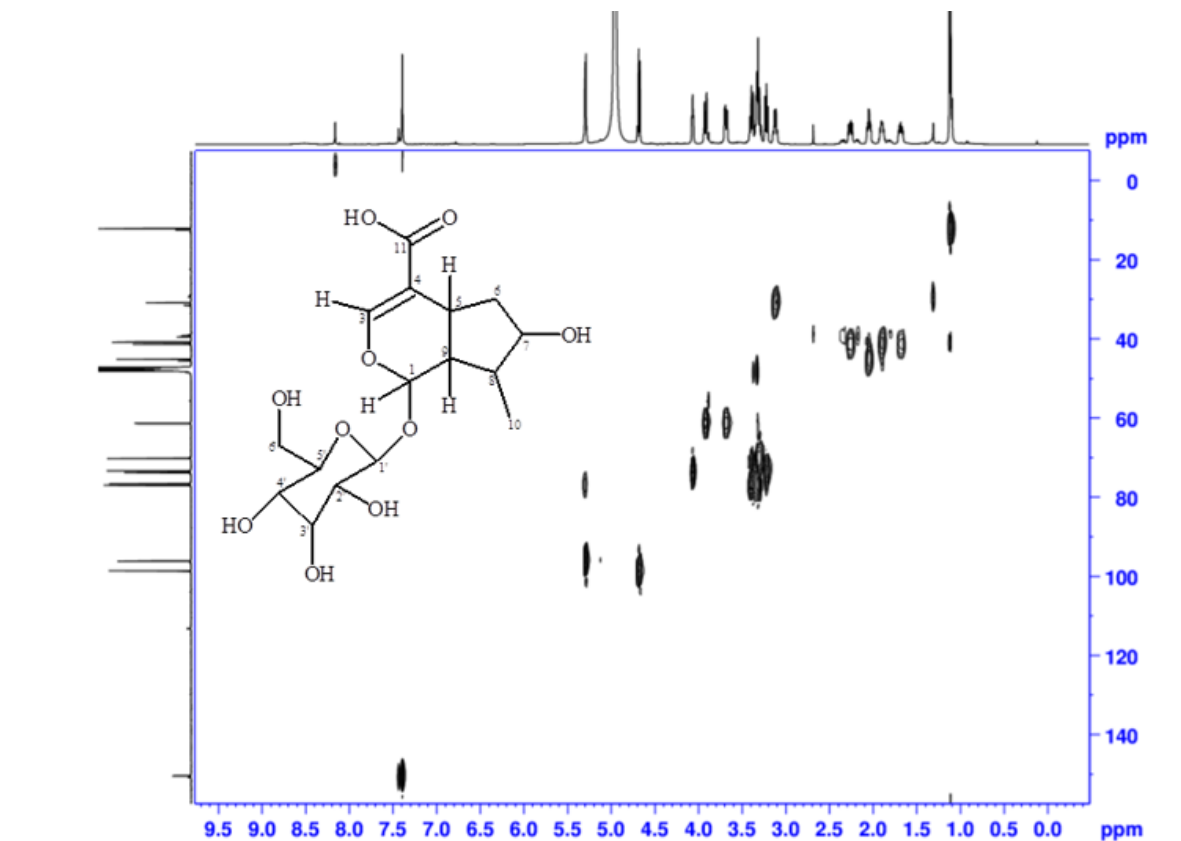
Supplementary data 93: ^1H-^{13}C HSQC NMR spectrum of loganic acid (**62**) in CD$_3$OD.
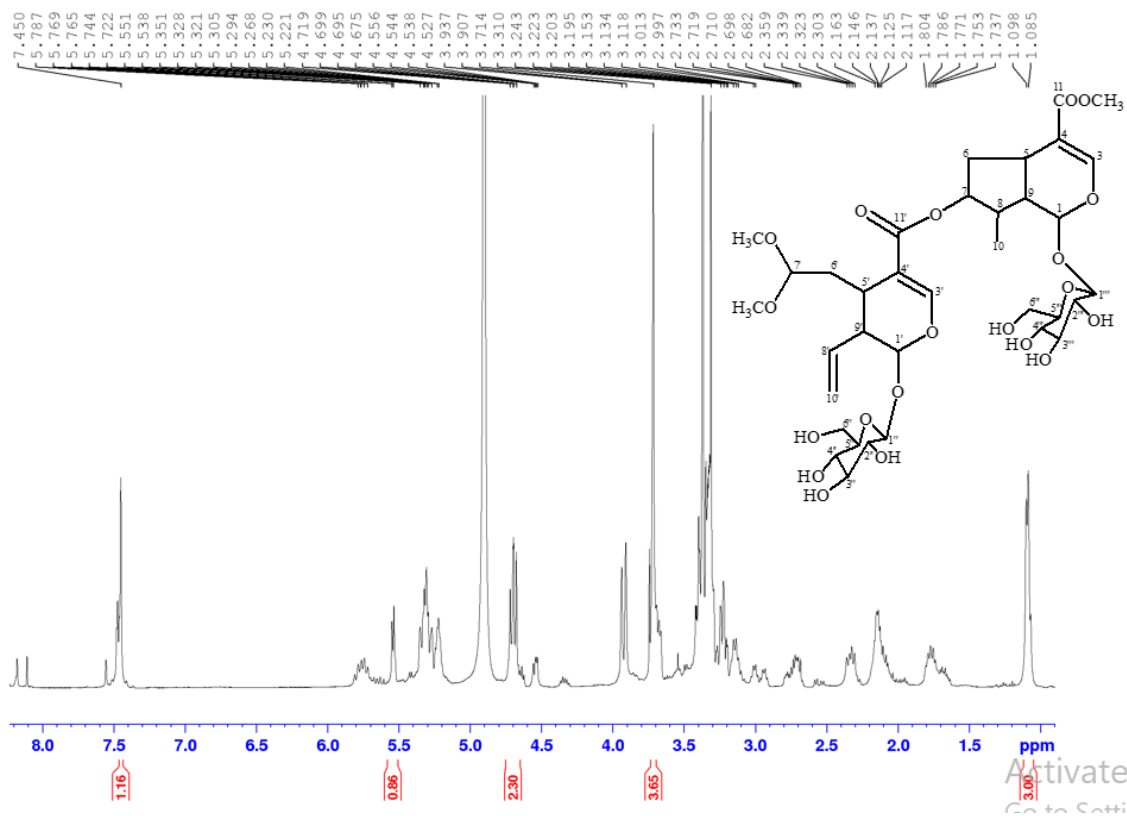
Supplementary data 94: ^{1}H NMR spectrum of cantleyoside-dimethyl-acetal (**63**) in CD$_3$OD.
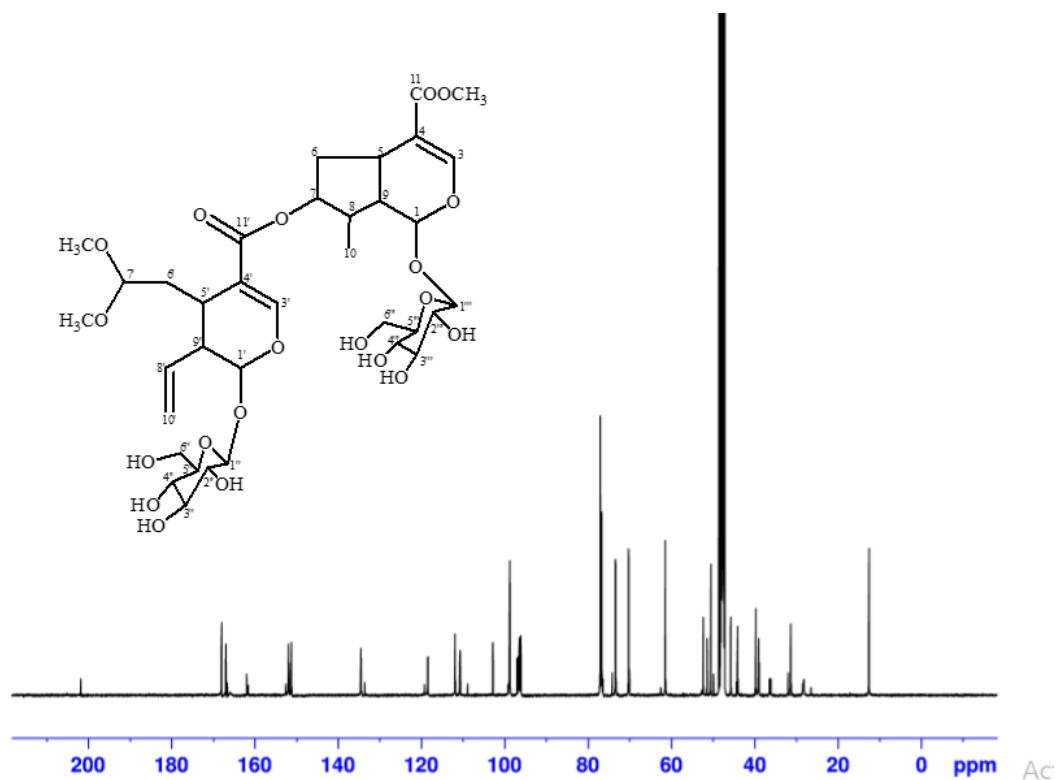
Supplementary data 95: ^{13}C NMR spectrum of cantleyoside-dimethyl-acetal (**63**) in CD$_3$OD.
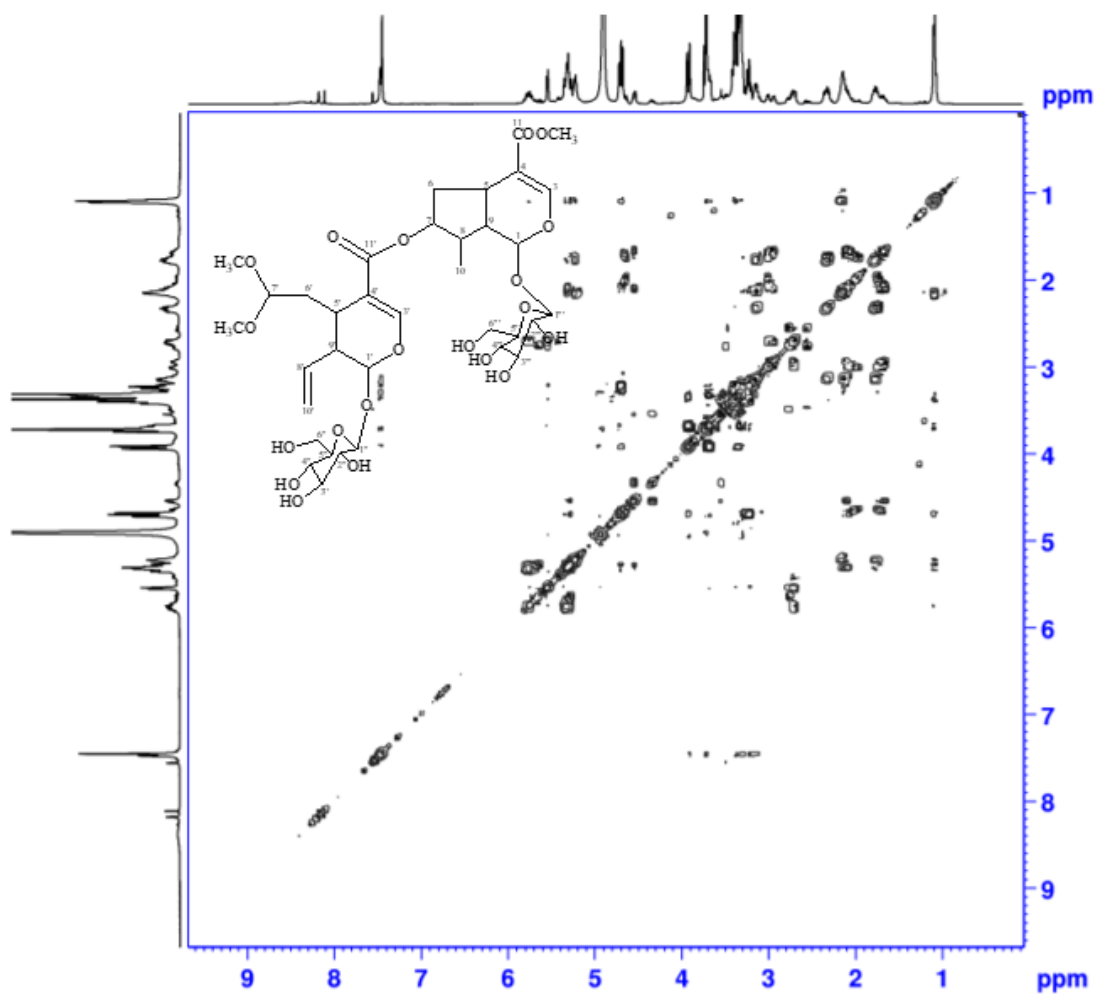
Supplementary data 96: ^{1}H-^{1}H COSY NMR spectrum of cantleyoside-dimethyl-acetal (**63**) in CD$_3$OD.
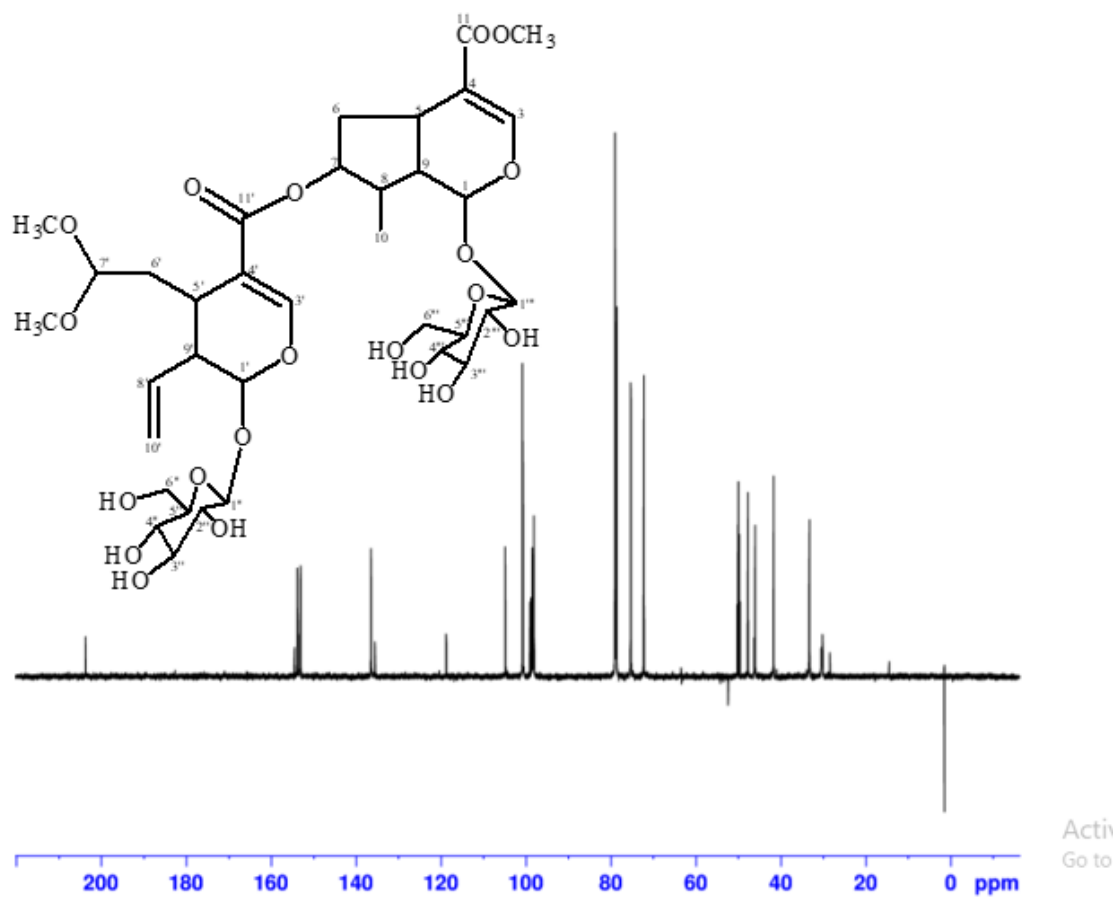
Supplementary data 97: DEPT-90 NMR spectrum of cantleyoside-dimethyl-acetal (**63**) in CD₃OD.
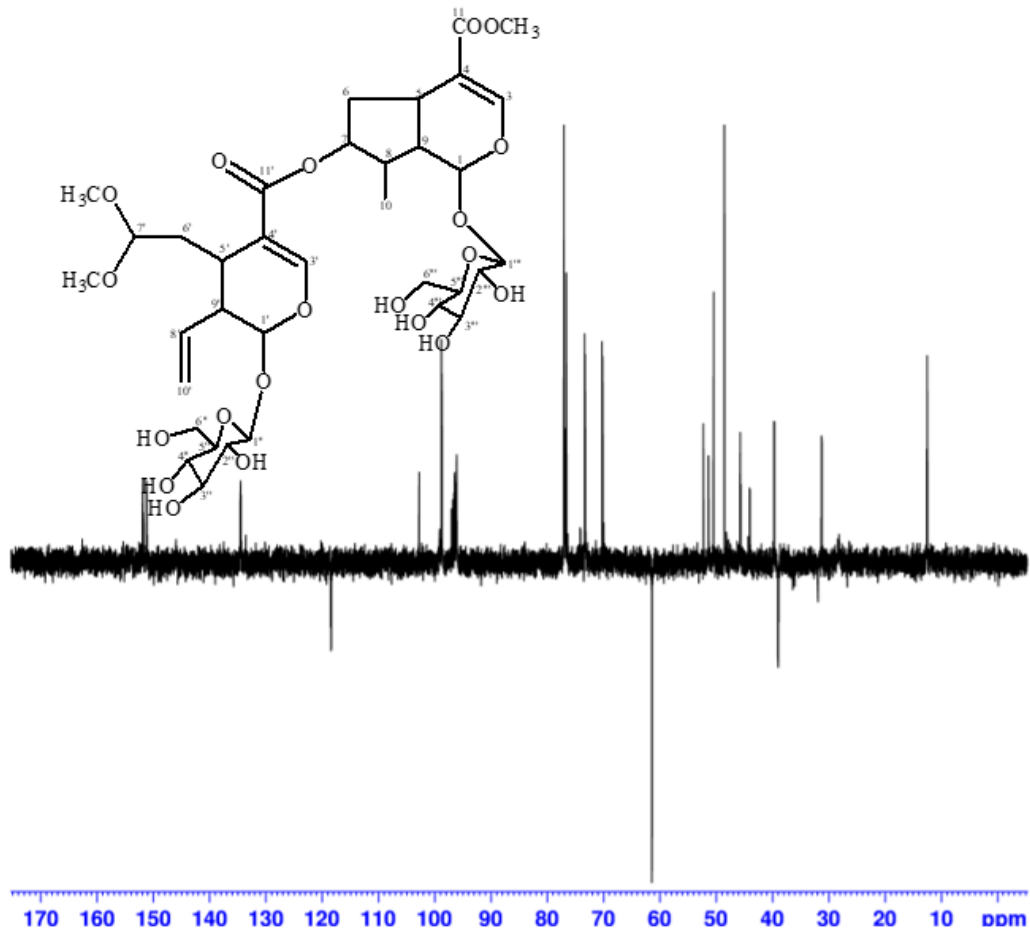
Supplementary data 98: DEPT-135 NMR spectrum of cantleyoside-dimethyl-acetal (**63**) in CD₃OD.
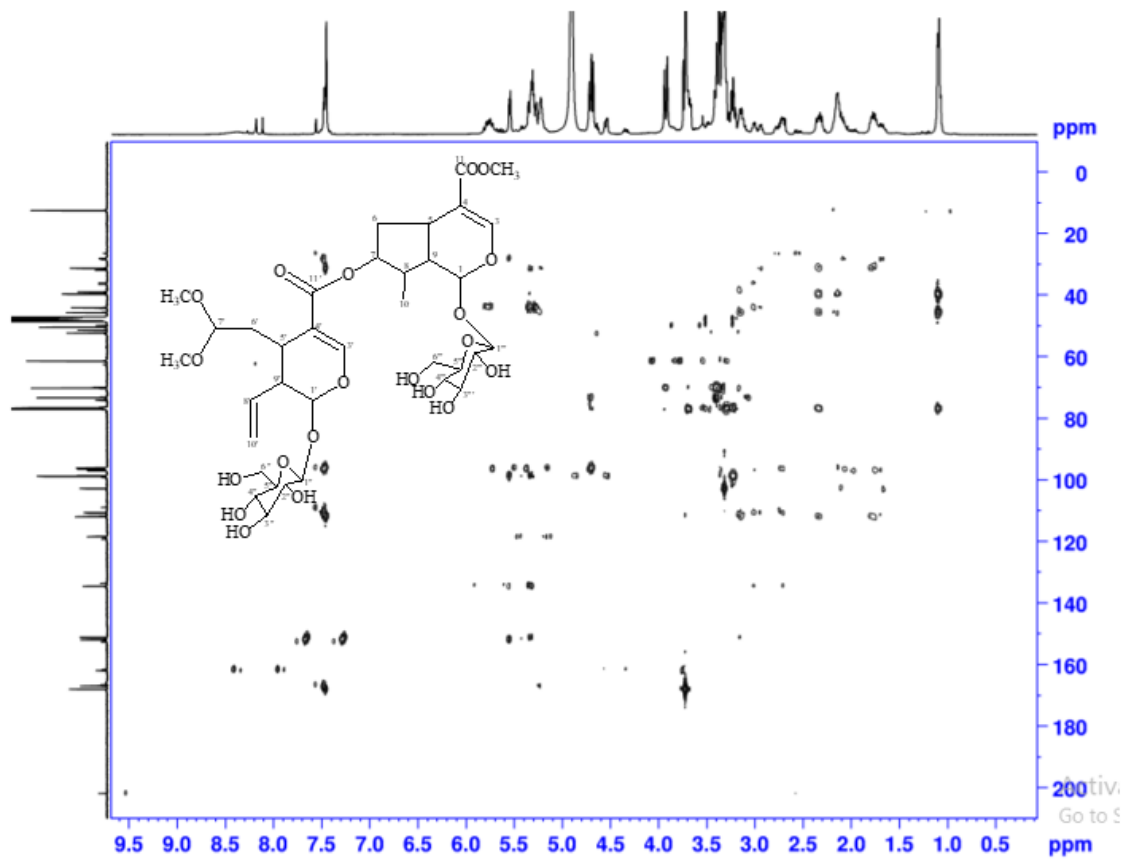
Supplementary data 99: ^{1}H-^{13}C HMBC NMR spectrum of cantleyoside-dimethyl-acetal (**63**) in CD$_3$OD.
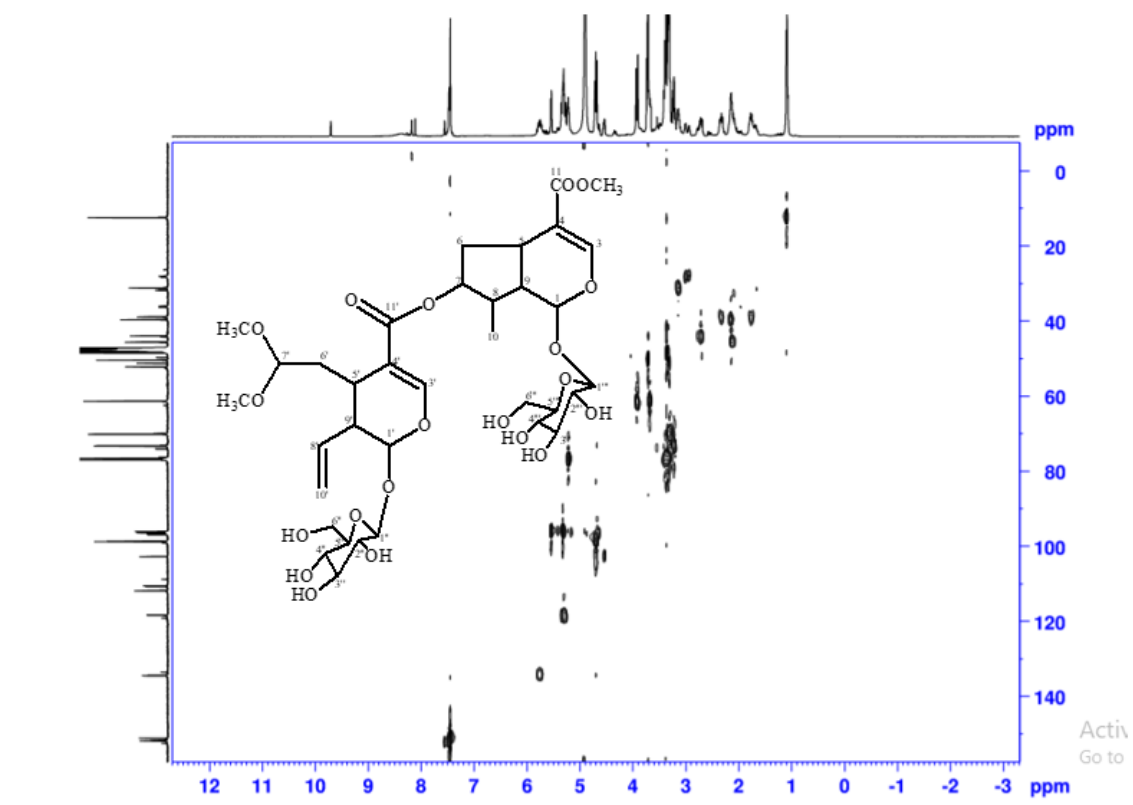
Supplementary data 100: ^{1}H-^{13}C HSQC NMR spectrum of cantleyoside-dimethyl-acetal (**63**) in CD$_3$OD.
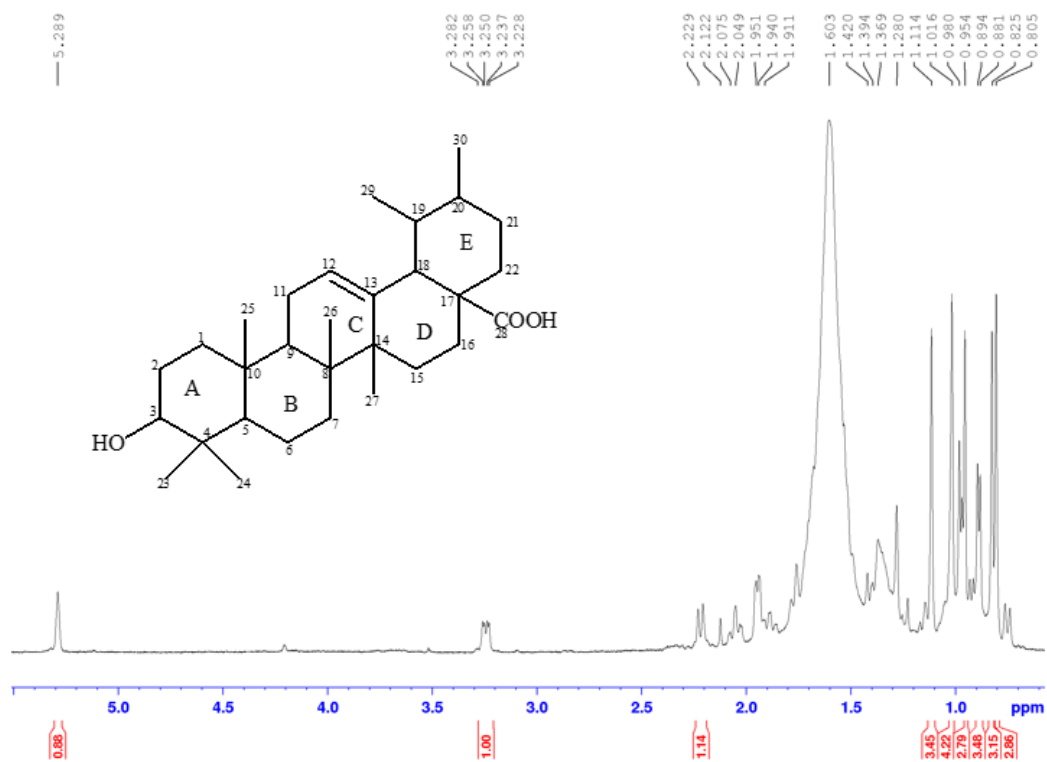
Supplementary data 101: ^{1}H NMR spectrum of ursolic acid (**64**) in CDCl$_3$.
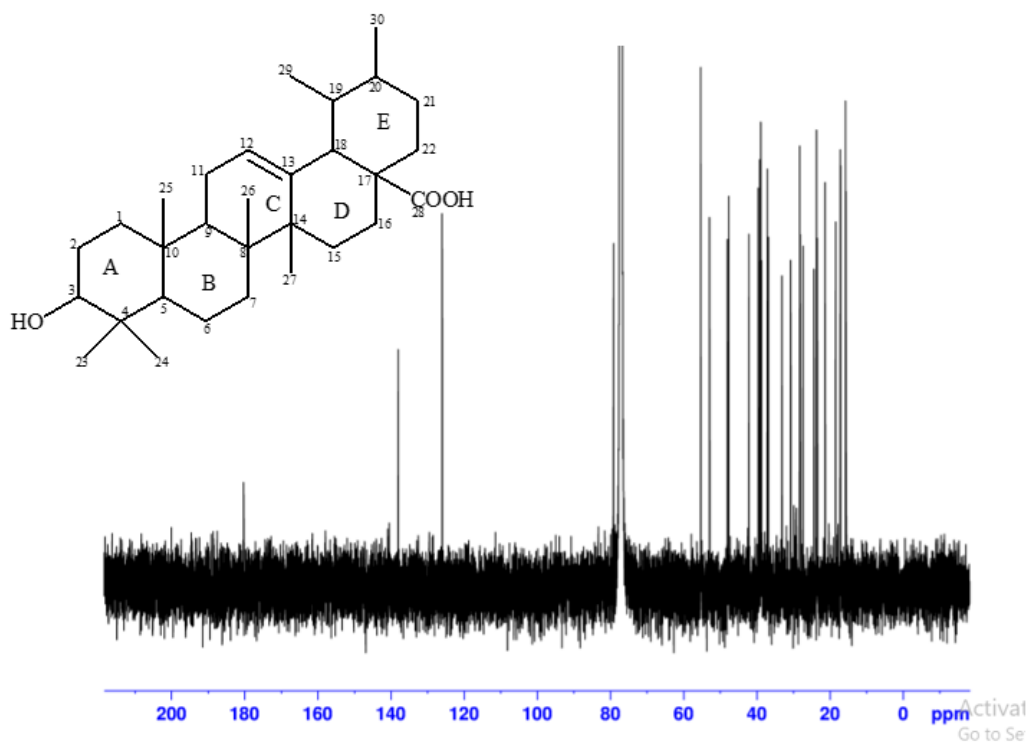
Supplementary data 102: ^{13}C NMR spectrum of ursolic acid (**64**) in CDCl$_3$.

284
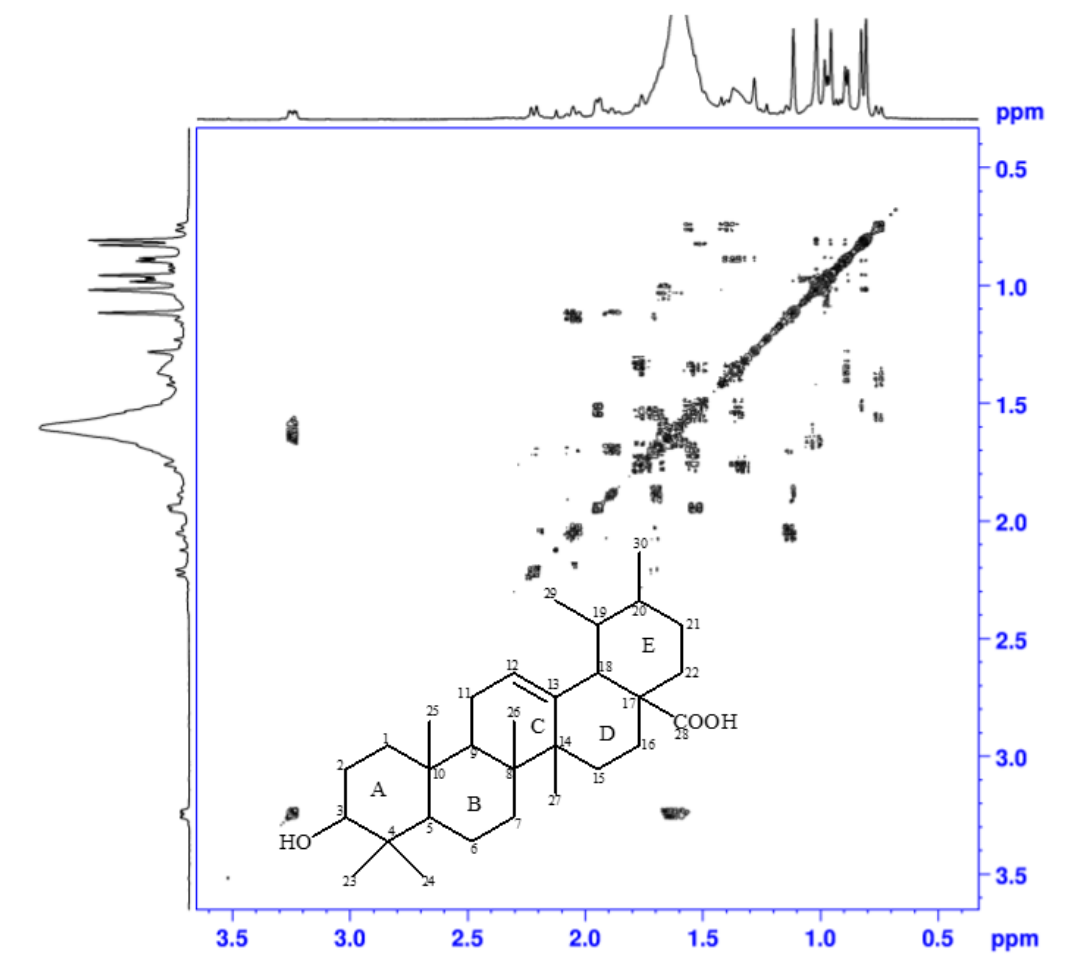
Supplementary data 103: ^{1}H-^{1}H COSY NMR spectrum of ursolic acid (**64**) in CDCl$_3$.
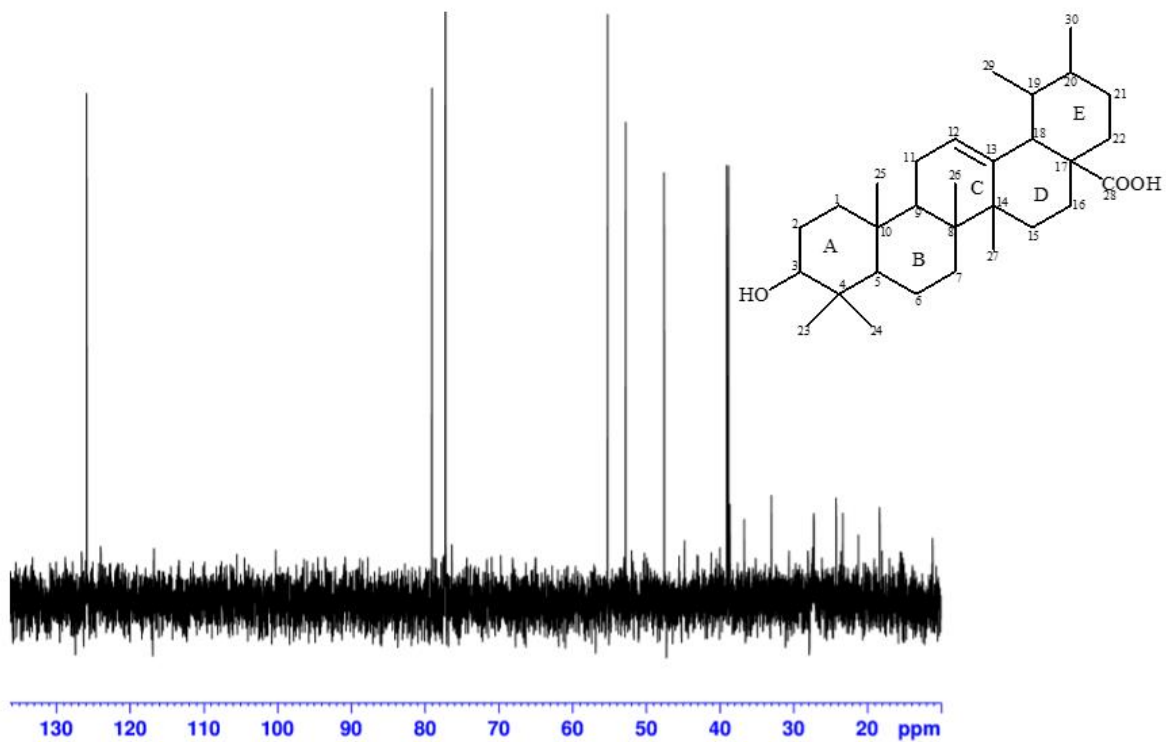
Supplementary data 104: DEPT-90 NMR spectrum of ursolic acid (**64**) in CDCl₃.
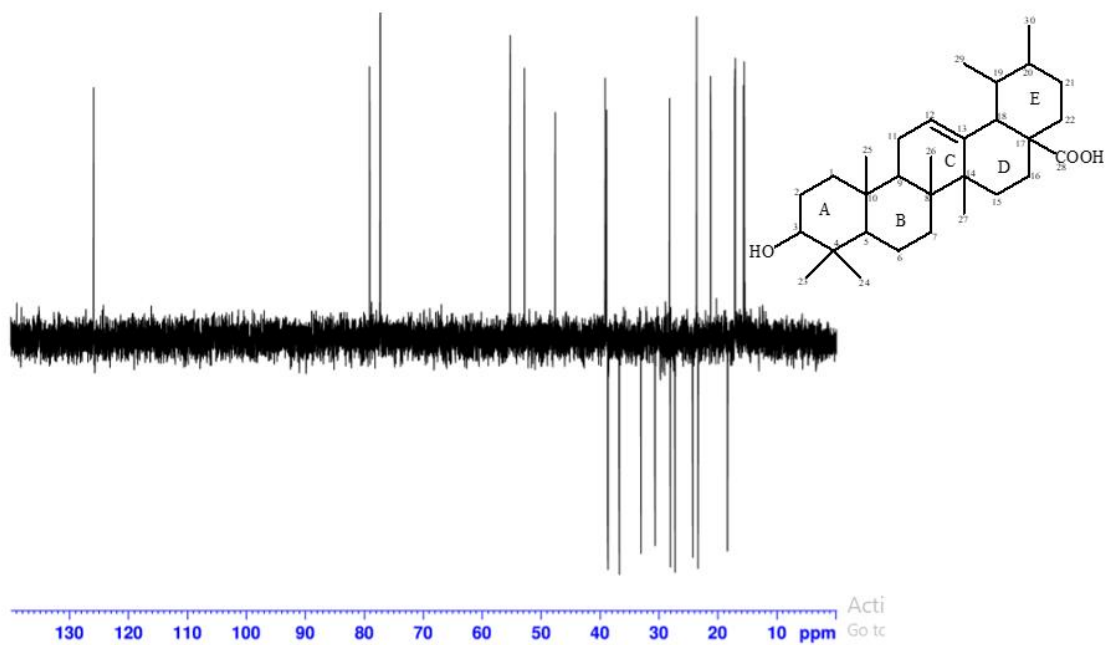
Supplementary data 105: DEPT-135 NMR spectrum of ursolic acid (**64**) in CDCl₃.

286
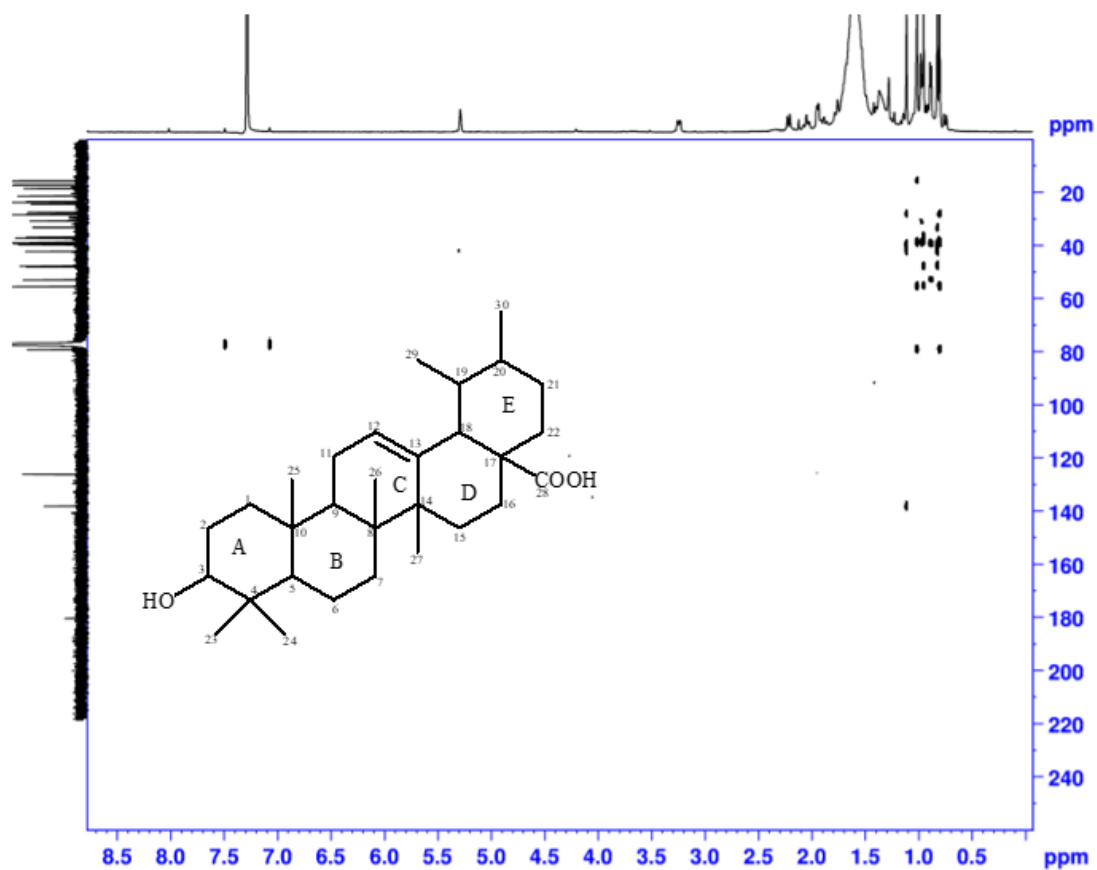
Supplementary data 106: ^{1}H-^{13}C HMBC NMR spectrum of ursolic acid (**64**) in CDCl₃.
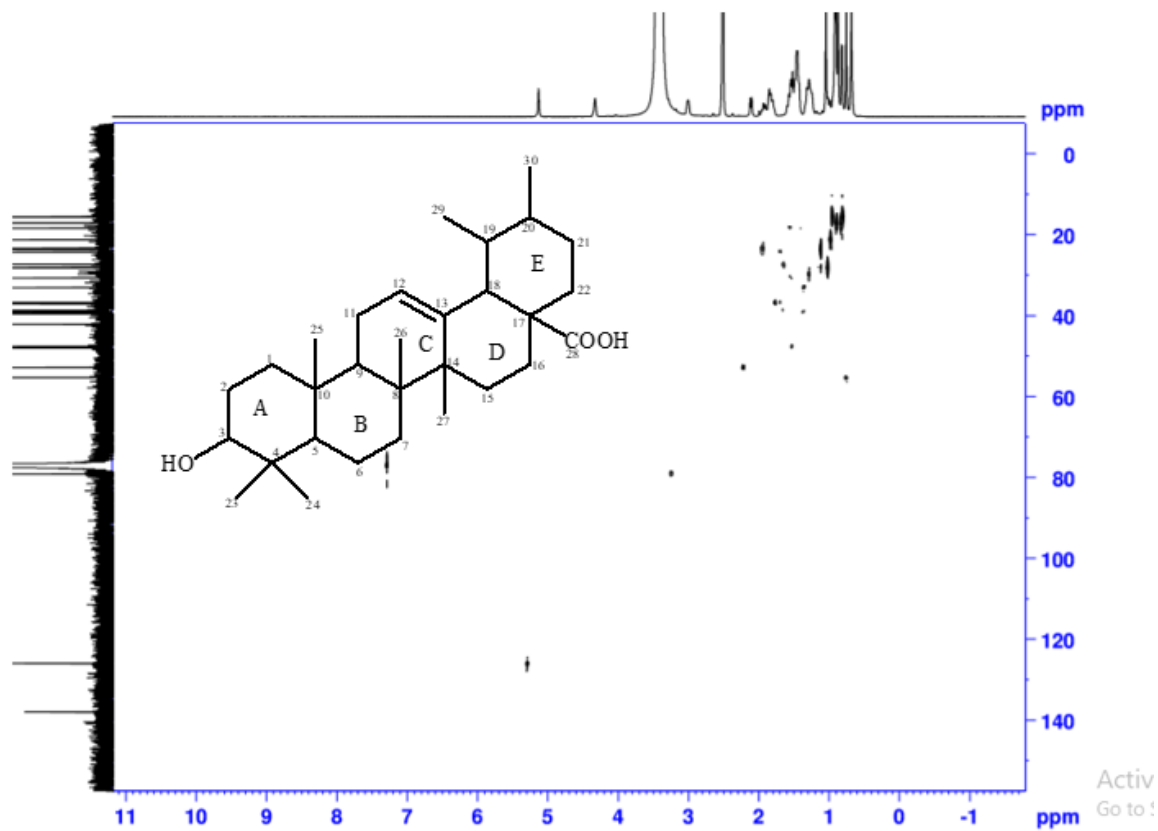
Supplementary data 107: ^{1}H-^{13}C HSQC NMR spectrum of ursolic acid (**64**) in CDCl$_3$.
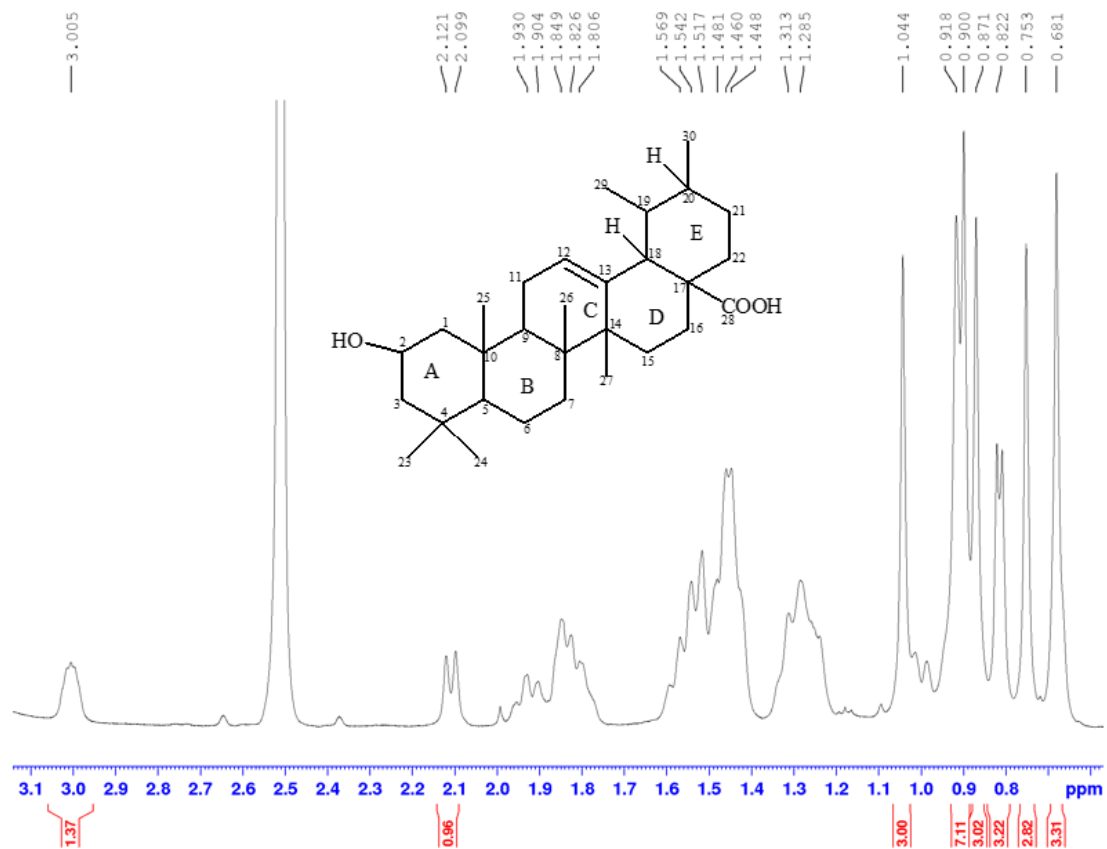
Supplementary data 108: ^{1}H NMR spectrum of 2-isoursolic acid (**65**) in DMSO-d$_6$.
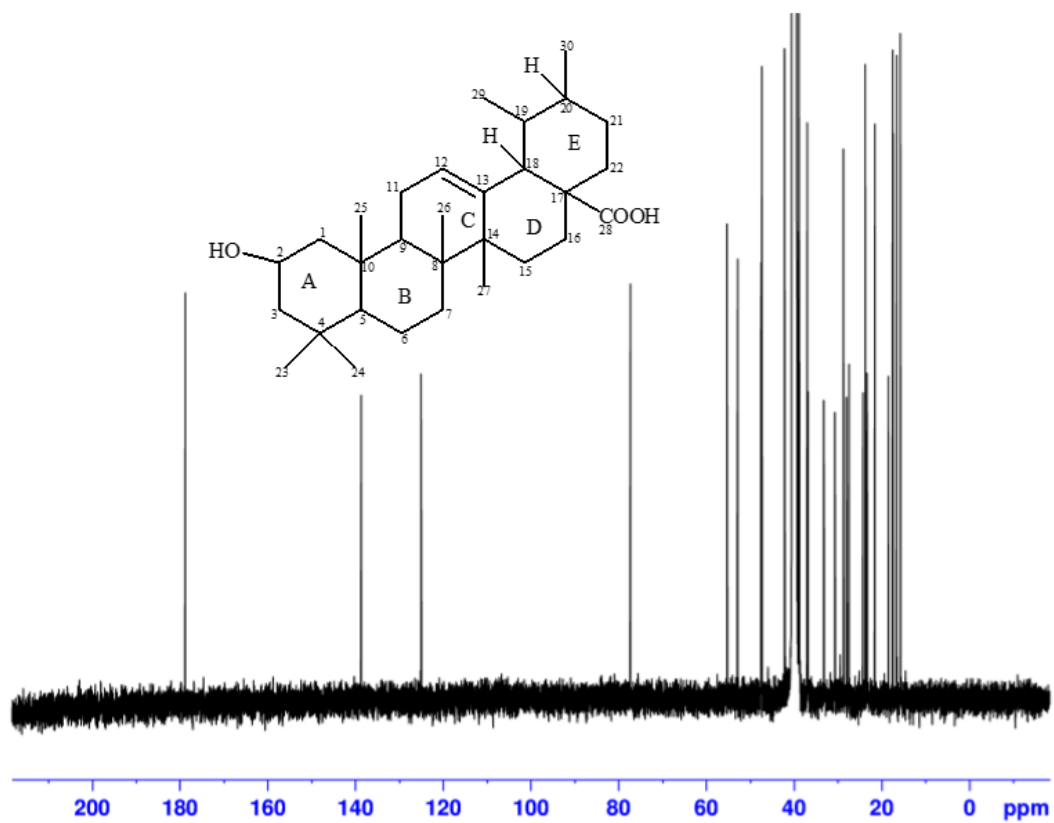
Supplementary data 109: ^{13}C NMR spectrum of 2-isoursolic acid (**65**) in DMSO-d$_6$.
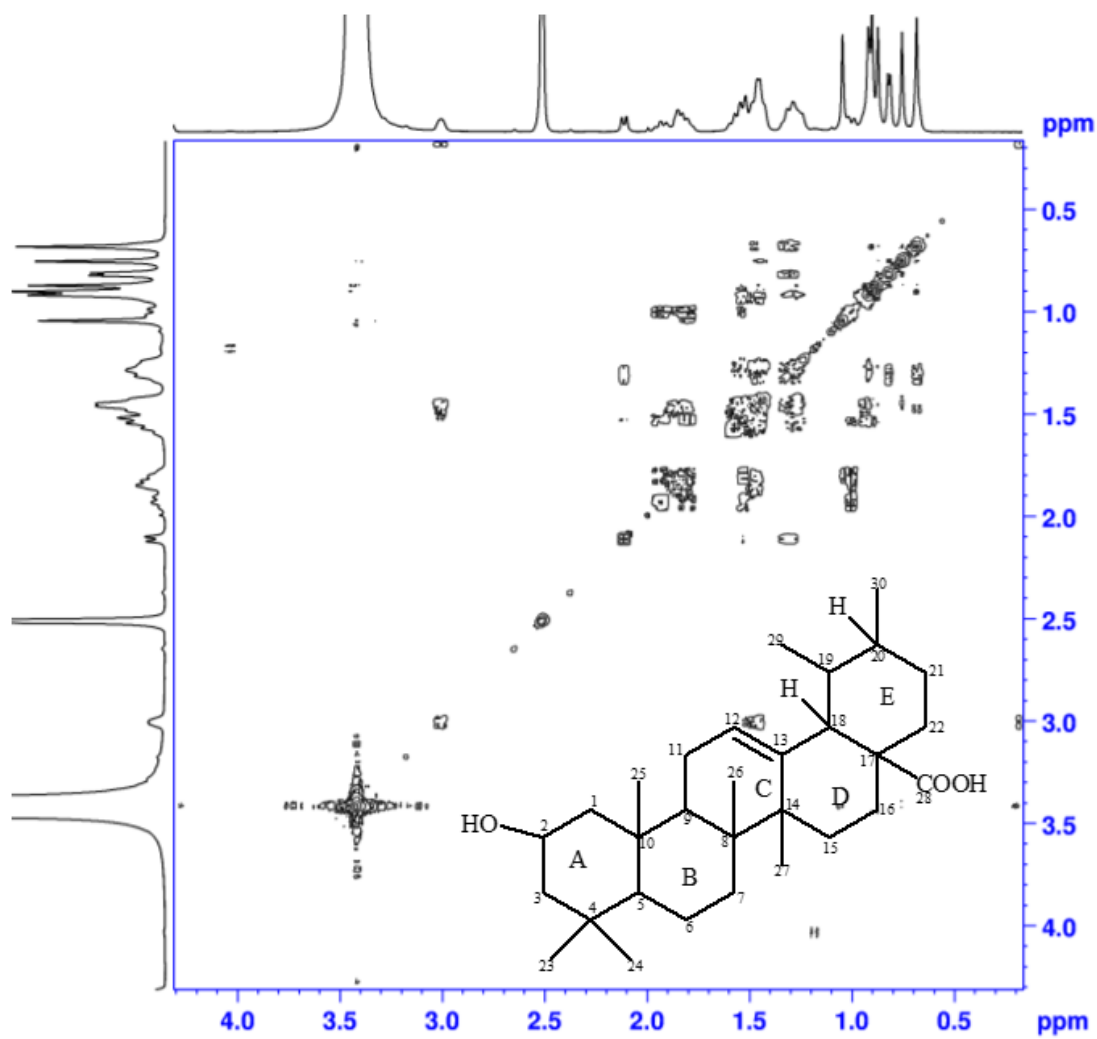
Supplementary data 110: ^{1}H-^{1}H COSY NMR spectrum of 2-isoursolic acid (**65**) in DMSO-d$_6$.
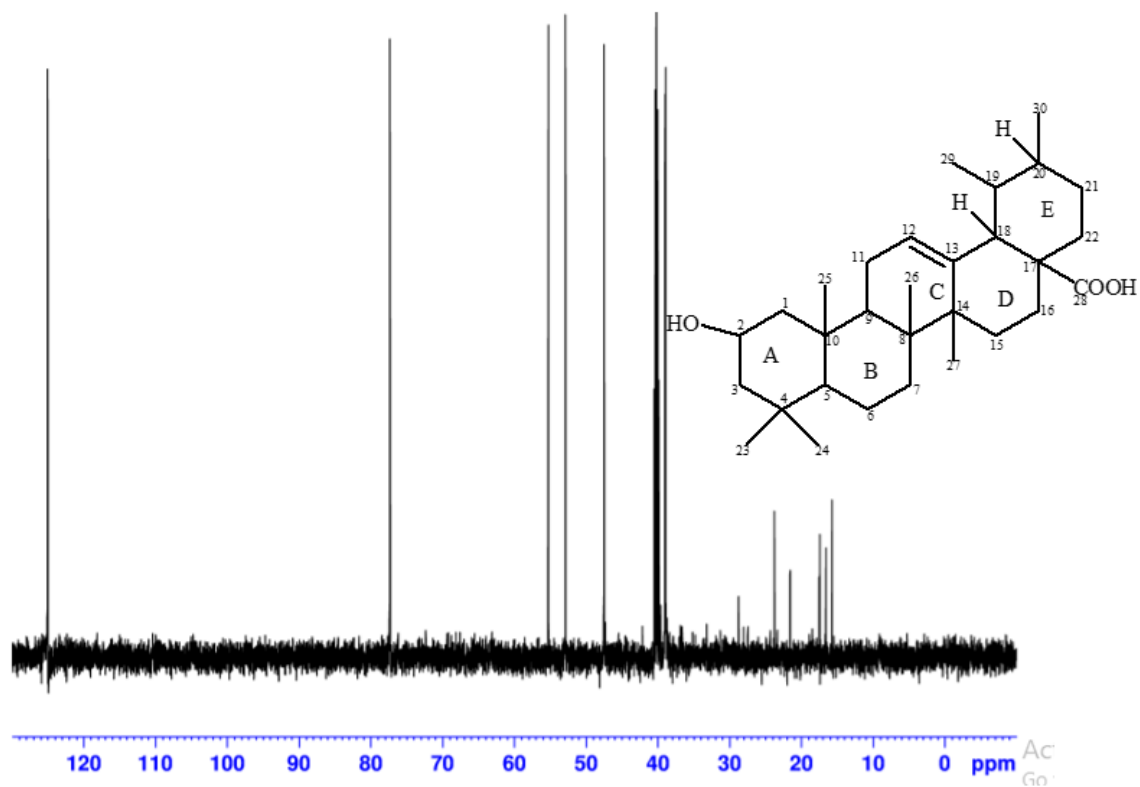
Supplementary data 111: DEPT-90 NMR spectrum of 2-isoursolic acid (**65**) in DMSO-d$_6$.
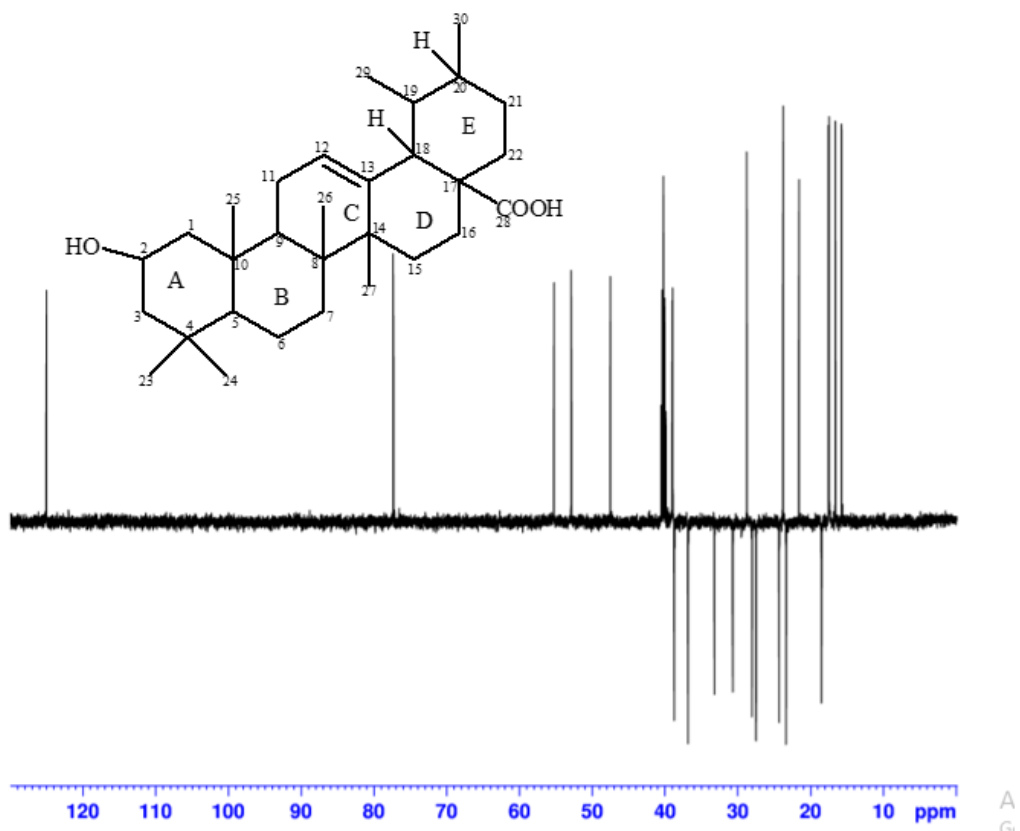
Supplementary data 112: DEPT-135 NMR spectrum of 2-isoursolic acid (**65**) in DMSO-d$_6$.
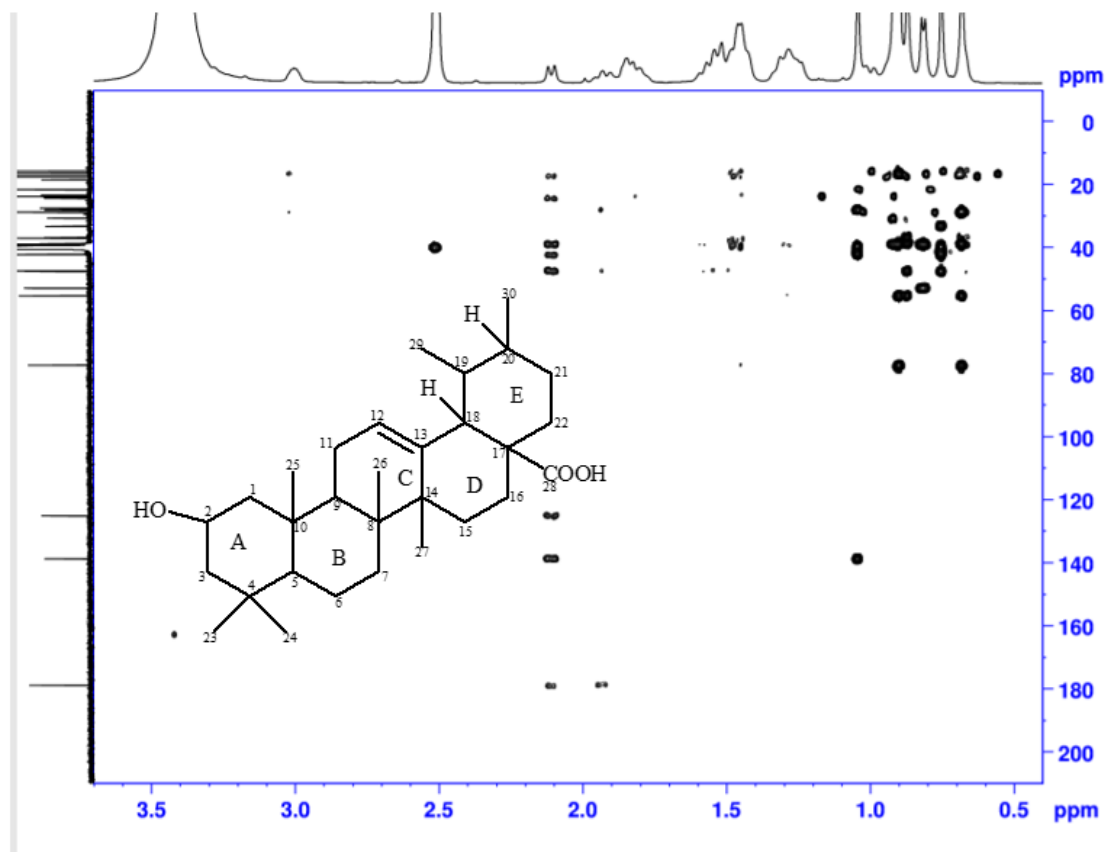
Supplementary data 113: ^1H-^{13}C HMBC NMR spectrum of 2-isoursolic acid (**65**) in DMSO-d_6.
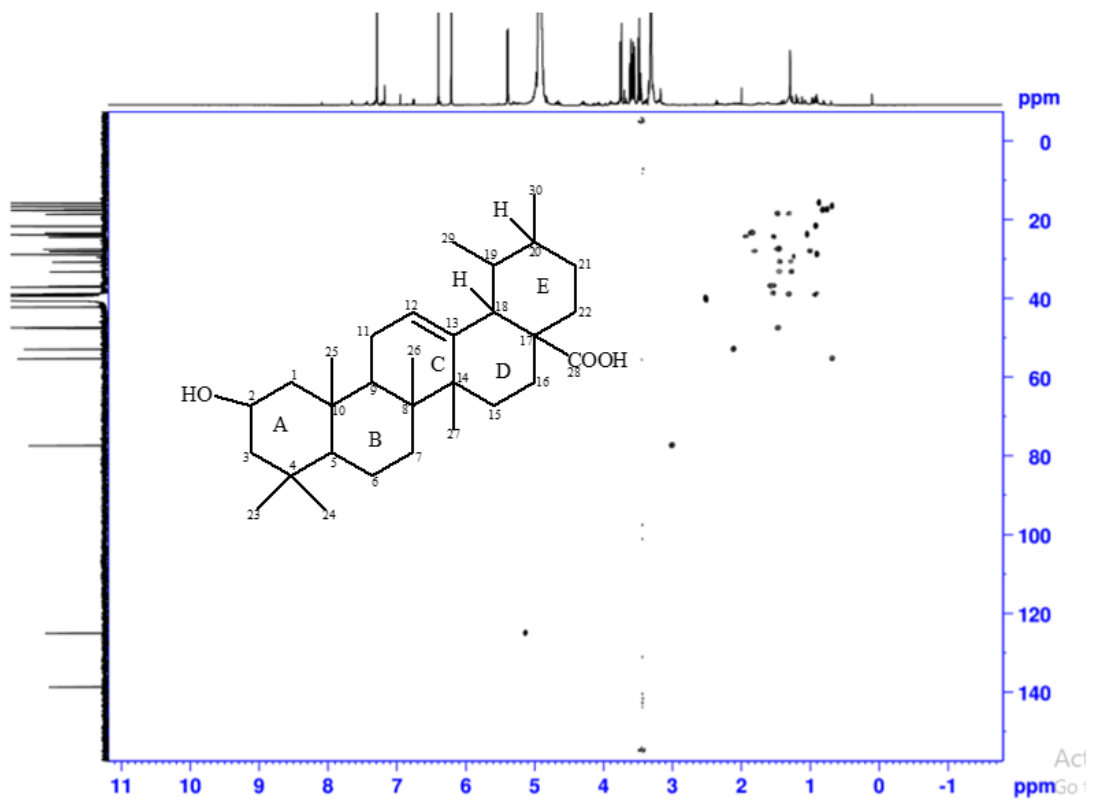
Supplementary data 114: ^{1}H-^{13}C HSQC NMR spectrum of 2-isoursolic acid (**65**) in DMSO-d$_6$.
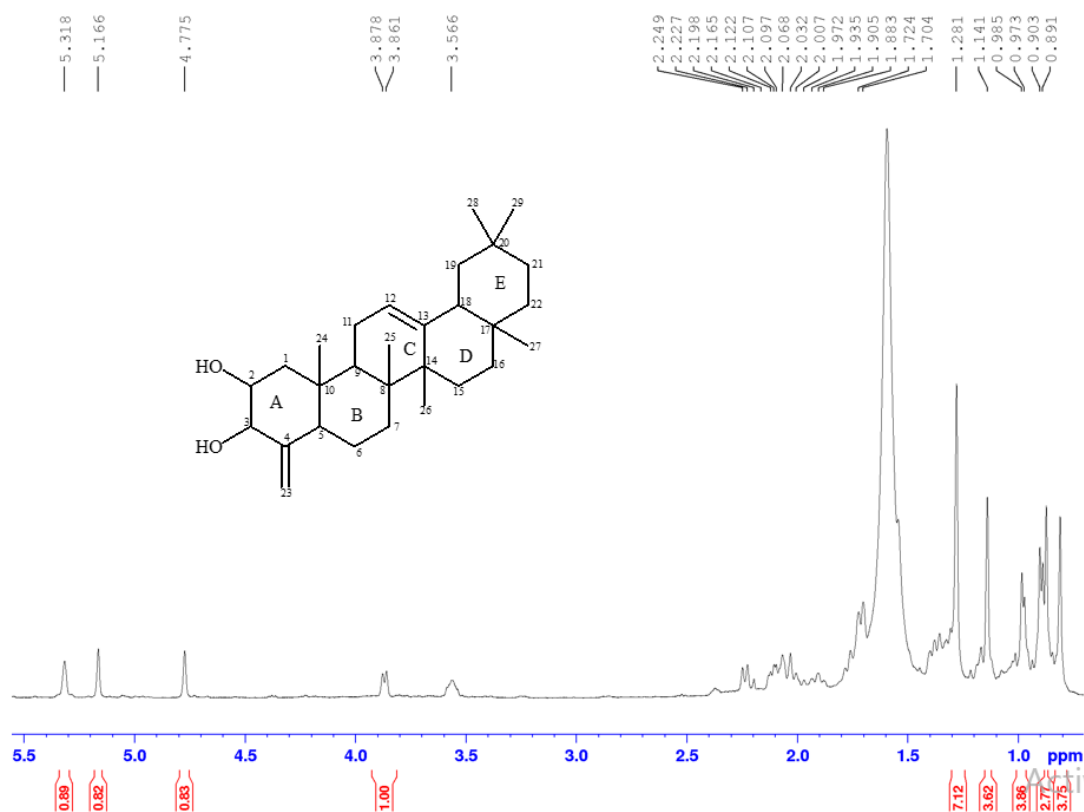
Supplementary data 115: ^{1}H NMR spectrum of 24-nor-2α,3β-dihydroxyolean-4(23)-12-ene (**66**) in CDCl$_3$.

296
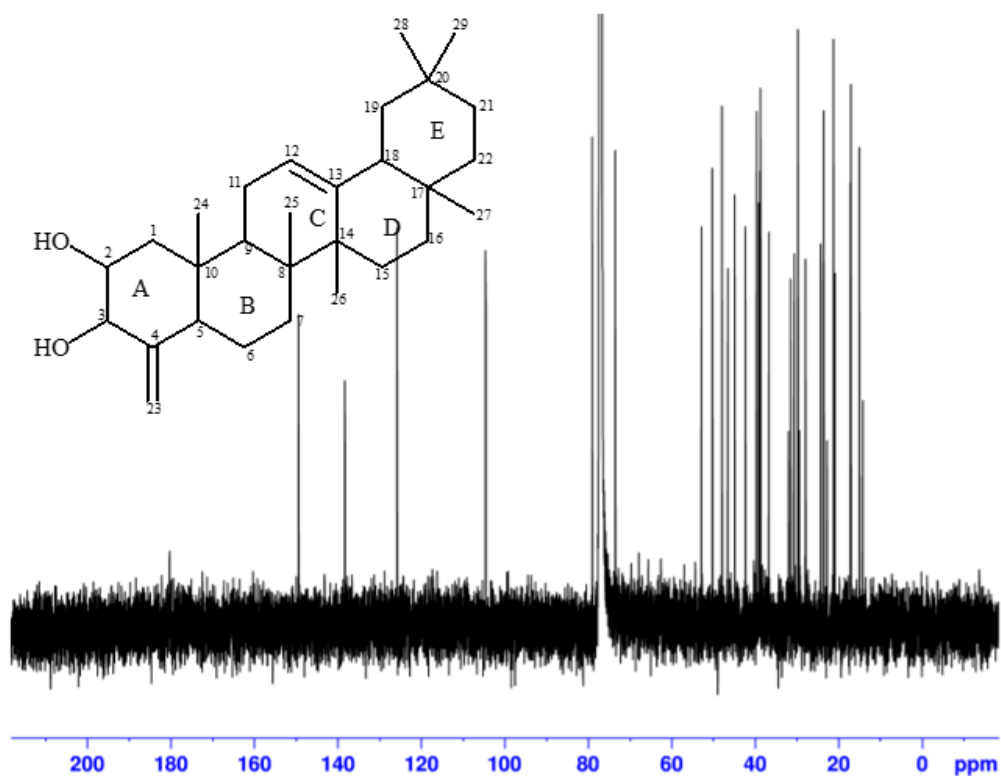
Supplementary data 116: ^{13}C NMR spectrum of 24-nor-2α,3β-dihydroxyolean-4(23)-12-ene (**66**) in CDCl$_3$.
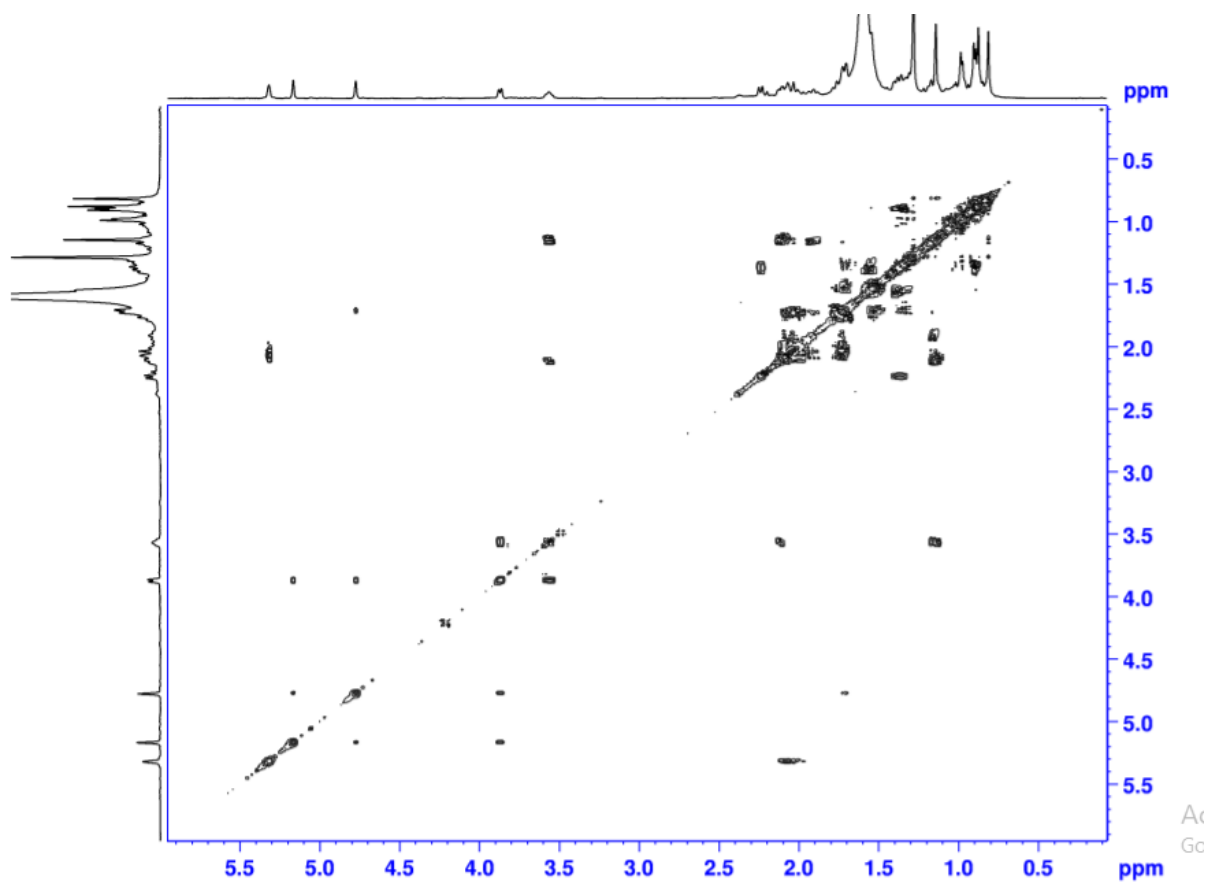
Supplementary data 117: ^{1}H-^{1}H COSY NMR spectrum of 24-nor-2α,3β-dihydroxyolean-4(23)-12-ene (**66**) in CDCl$_3$.

297
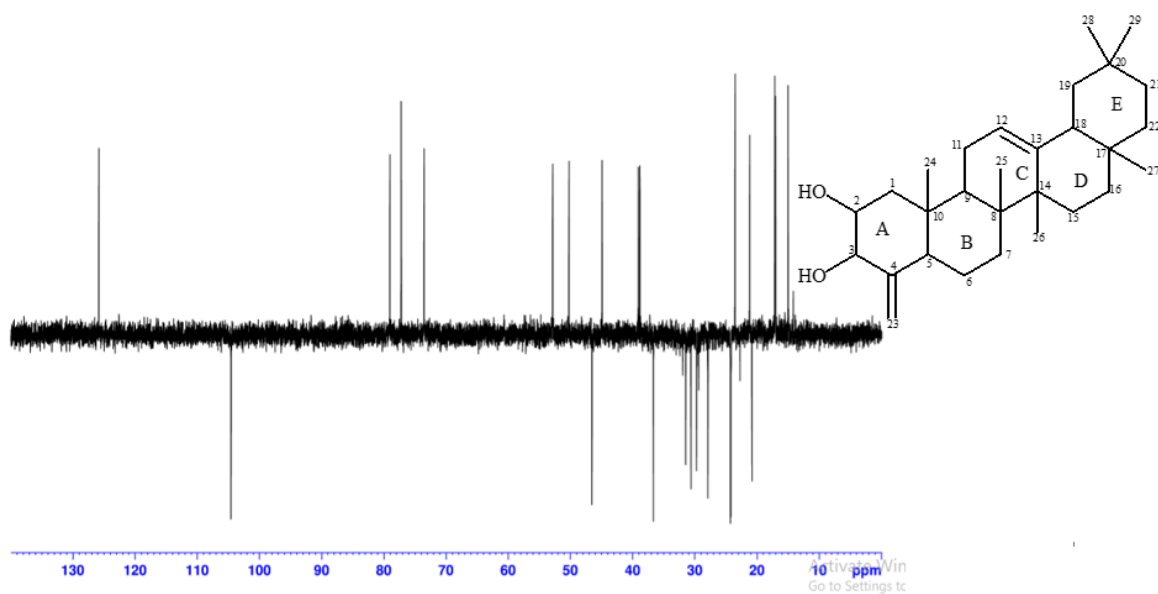
Supplementary data 118: DEPT-135 NMR spectrum of 24-nor-2α,3β-dihydroxyolean-4(23)-12-ene (**66**) in CDCl₃.
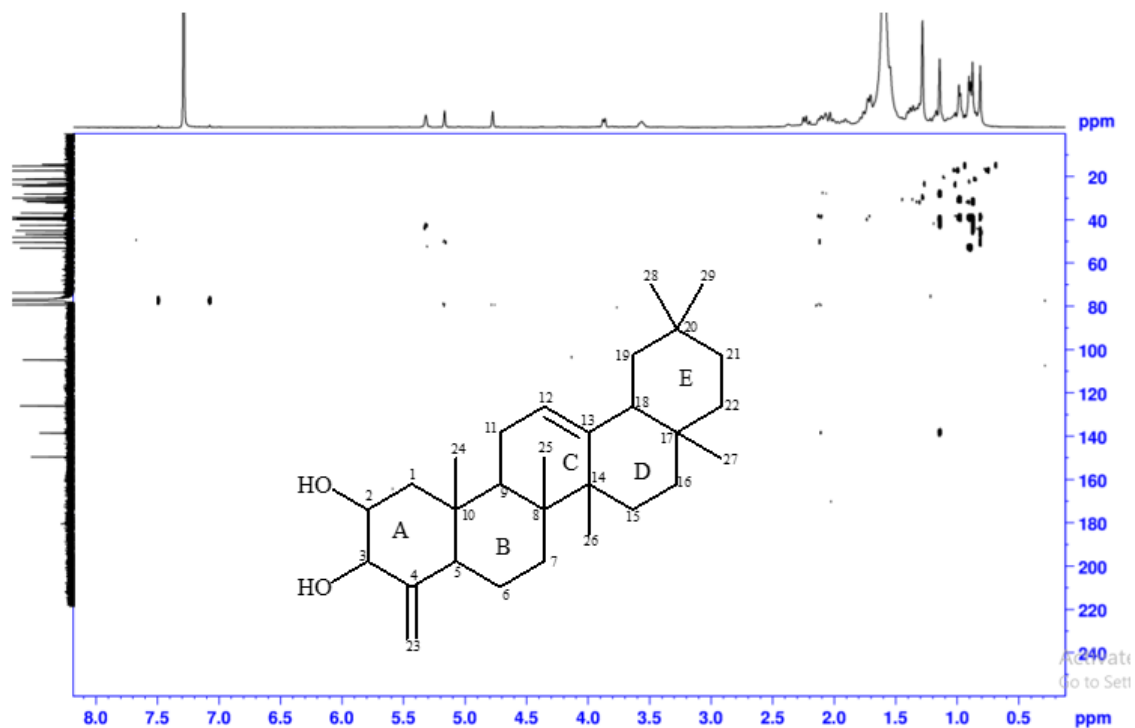
Supplementary data 119: ¹H-¹³C HMBC NMR spectrum of 24-nor-2α,3β-dihydroxyolean-4(23)-12-ene (**66**) in CDCl₃.
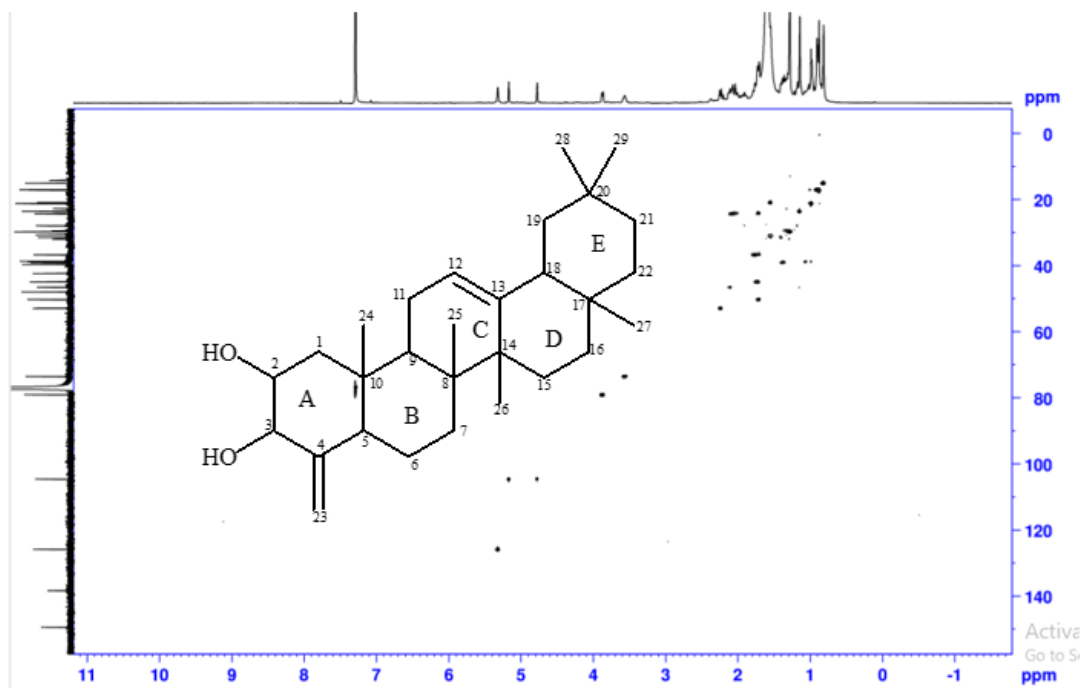
Supplementary data 120: ^{1}H-^{13}C HSQC NMR spectrum of 24-nor-2α,3β-dihydroxyolean-4(23)-12-ene (**66**) in CDCl₃.
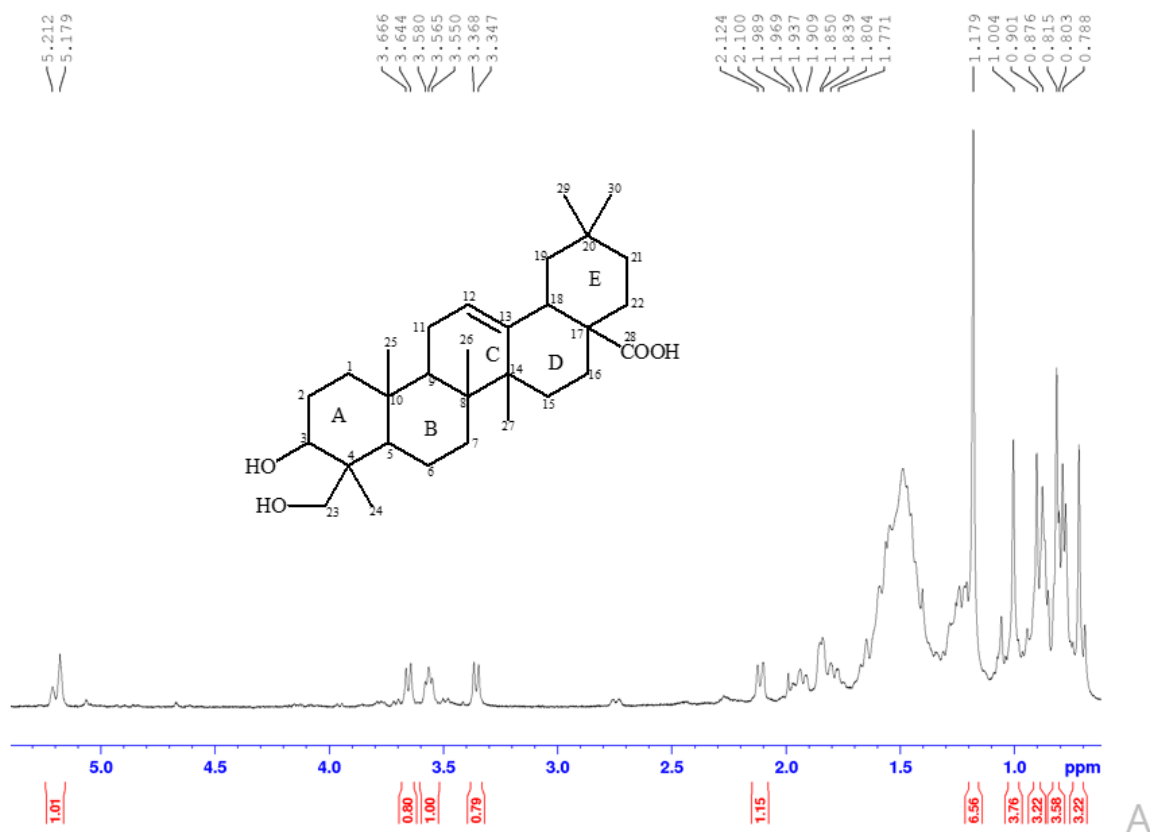
Supplementary data 121: ^{1}H NMR spectrum of hederagenin (**67**) in CDCl₃.

299
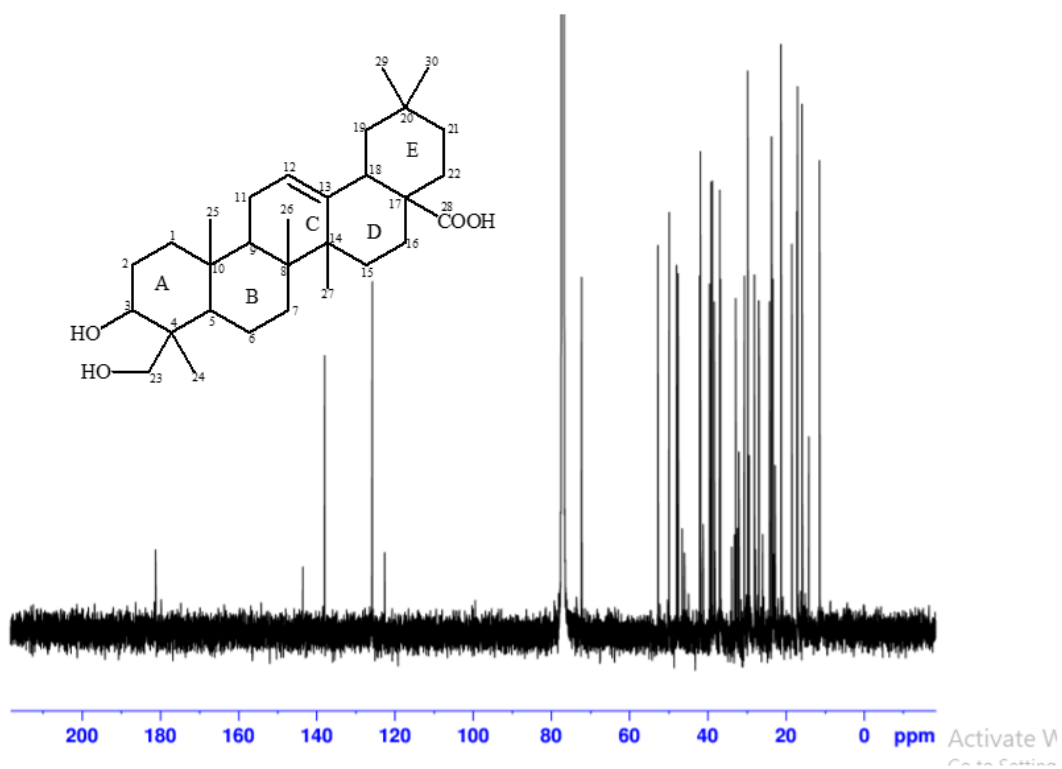
Supplementary data 122: ^{13}C NMR spectrum of hederagenin (**67**) in CDCl$_3$.
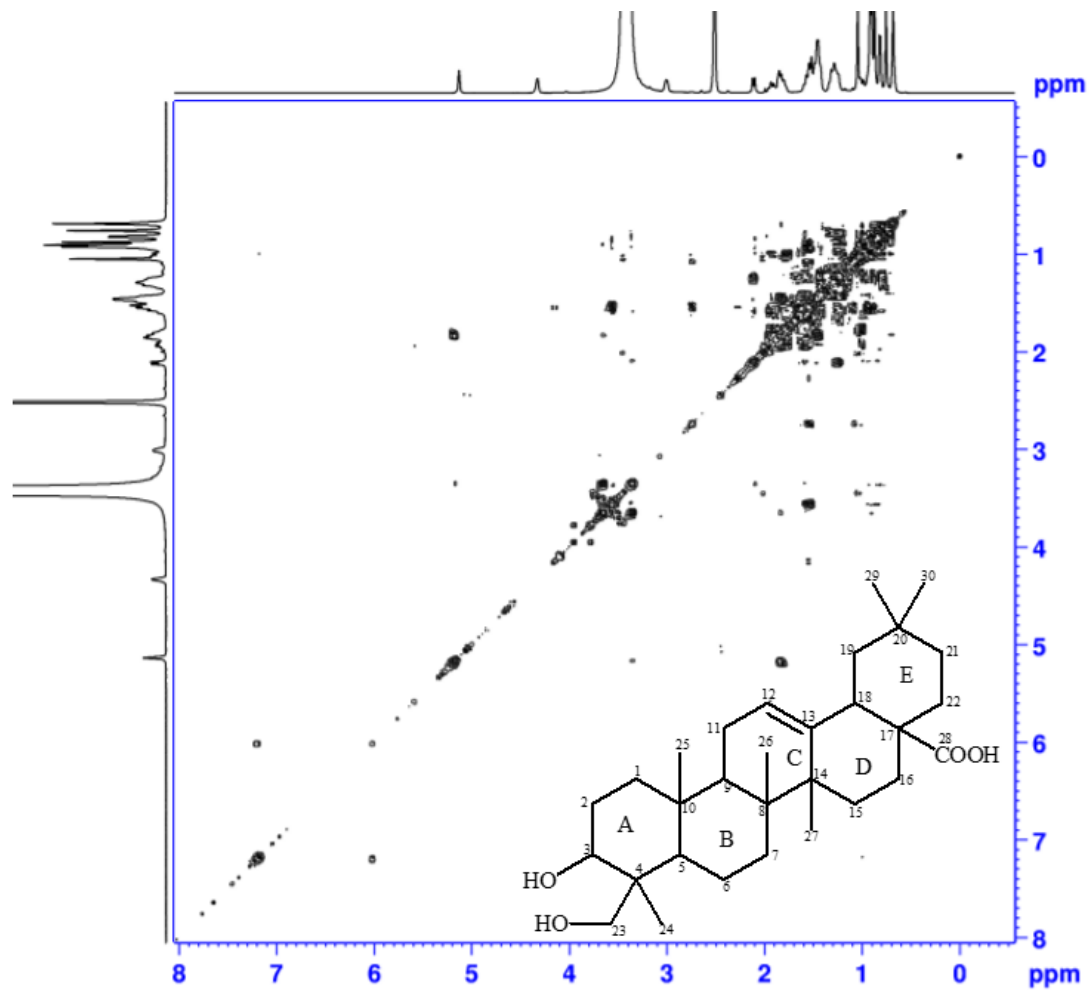
Supplementary data 123: ^{1}H-^{1}H COSY NMR spectrum of hederagenin (**67**) in CDCl$_3$.
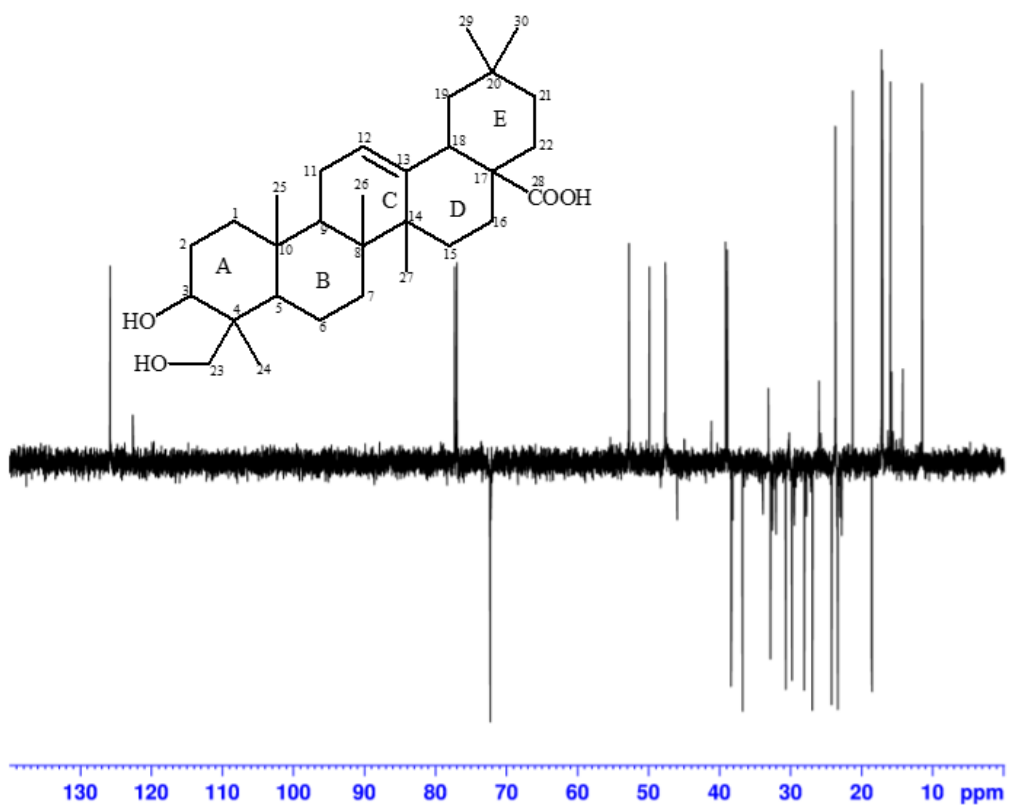
Supplementary data 124: DEPT-135 NMR spectrum of hederagenin (**67**) in CDCl₃.

302
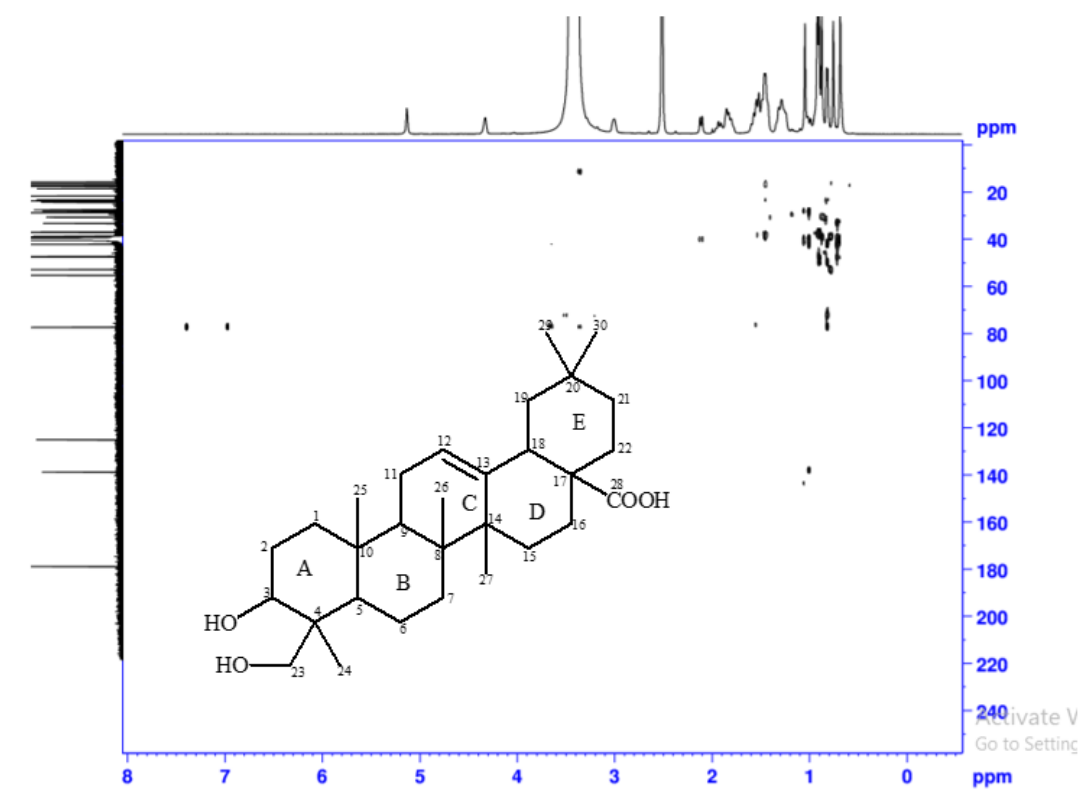
Supplementary data 125: ^{1}H-^{13}C HMBC NMR spectrum of hederagenin (**67**) in CDCl$_3$.
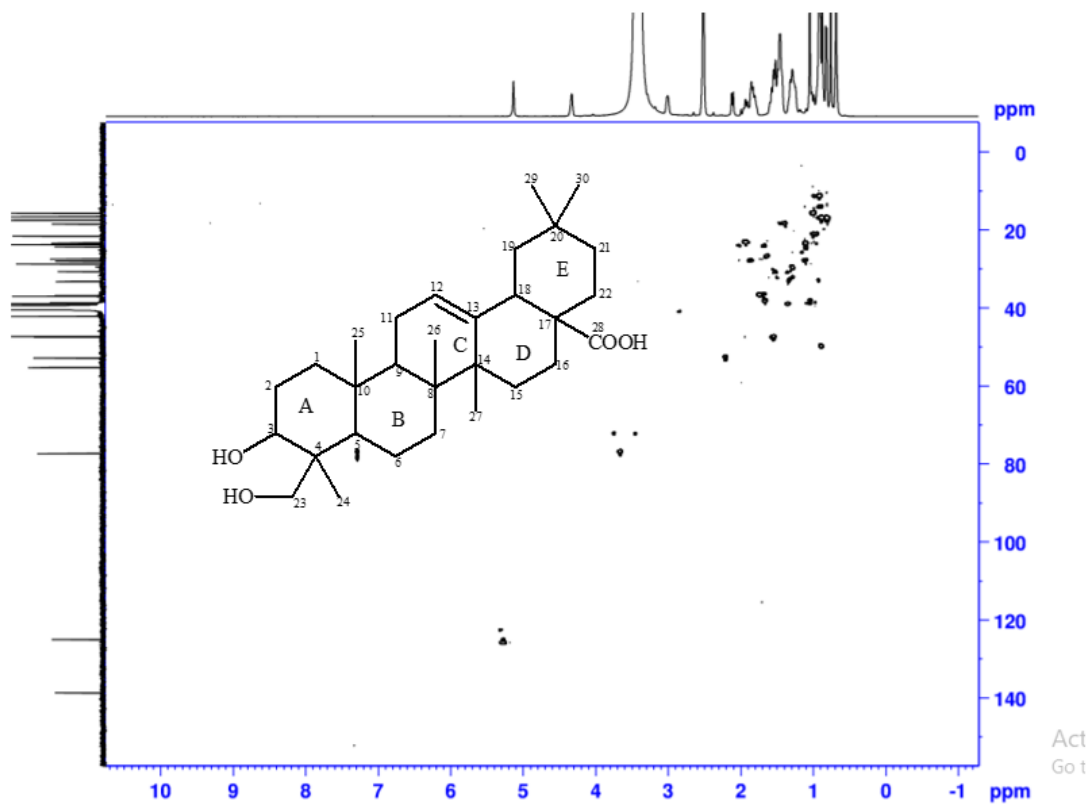
Supplementary data 126: ^{1}H-^{13}C HSQC NMR spectrum of hederagenin (**67**) in CDCl$_3$.
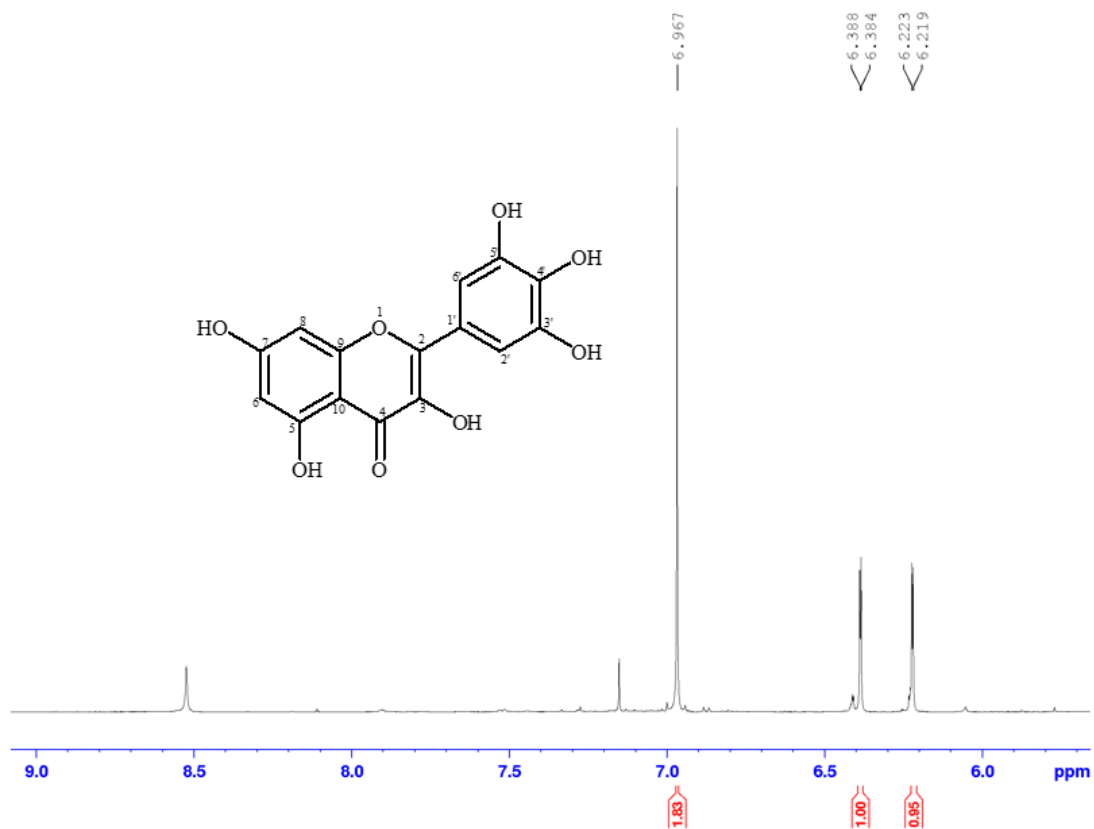
Supplementary data 127: ^{1}H NMR spectrum of myricetin (**91**) in CD$_3$OD.
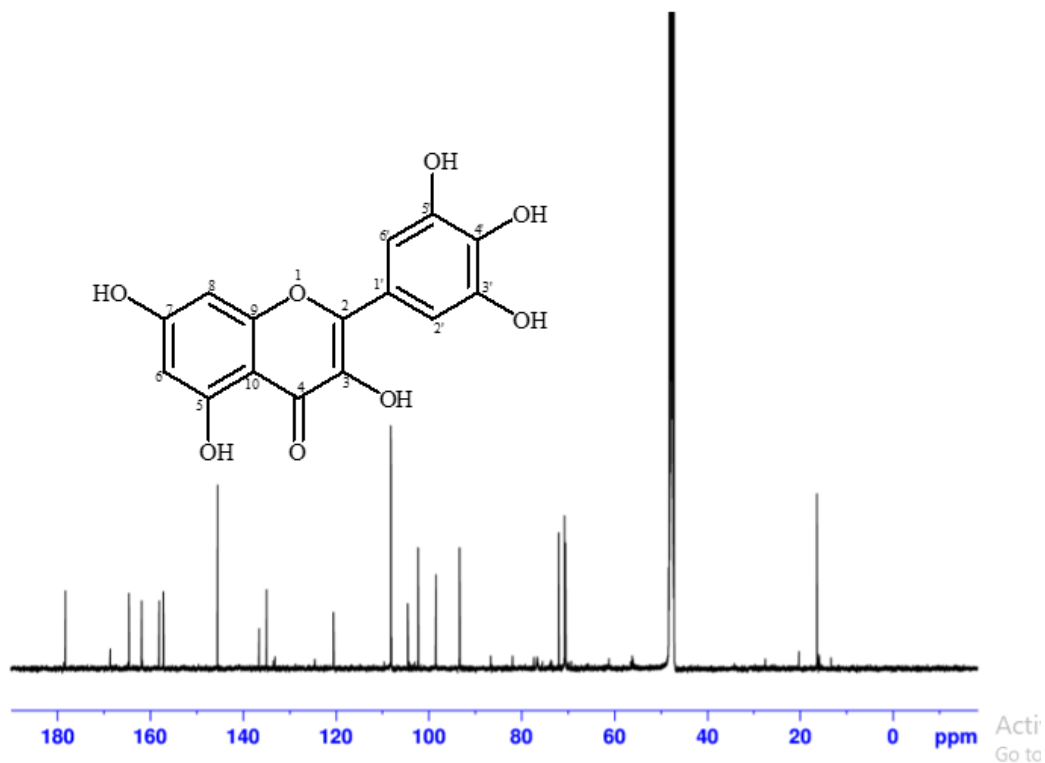
Supplementary data 128: ^{13}C NMR spectrum of myricetin (**91**) in CD_3OD.
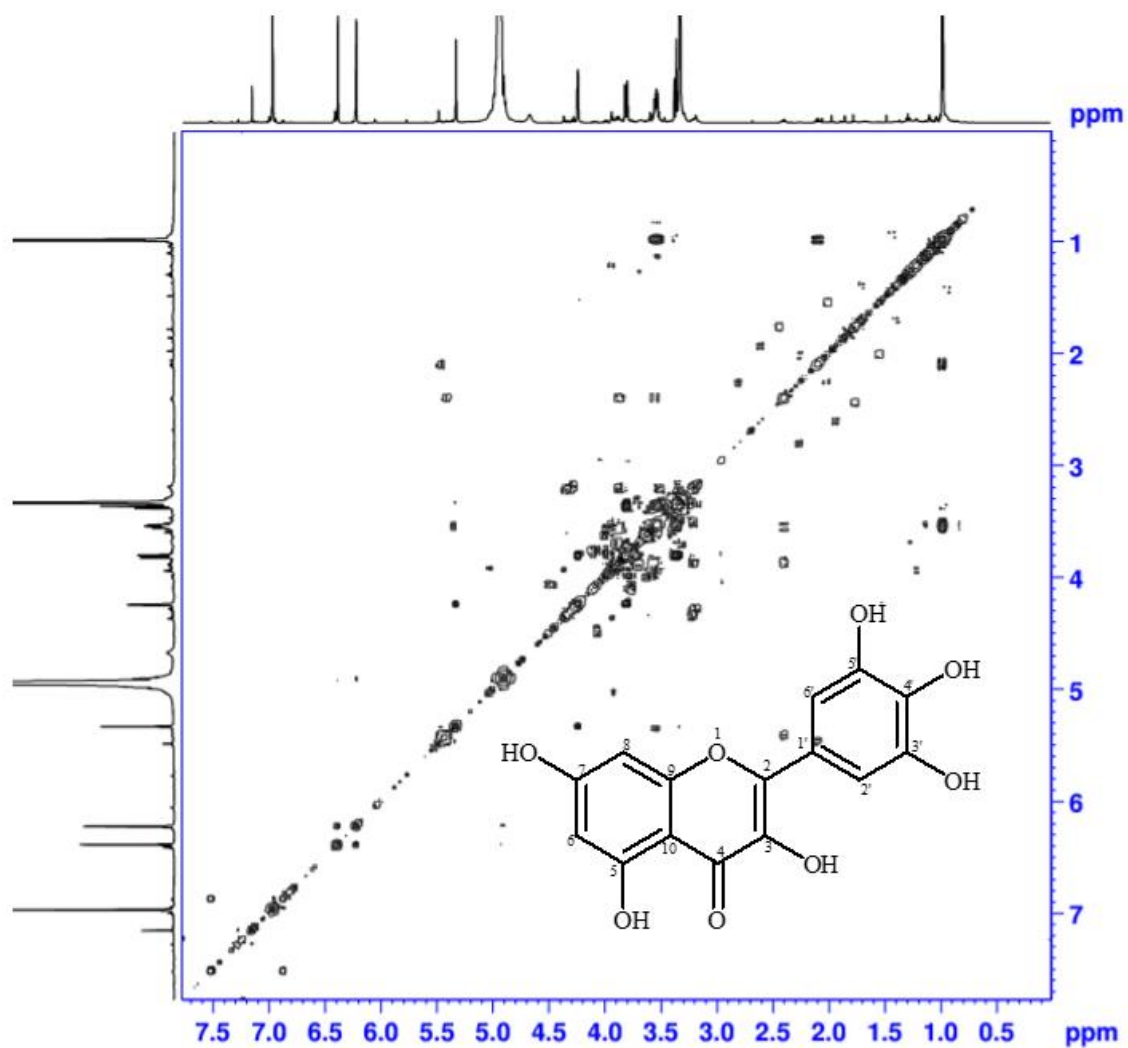
Supplementary data 129: ^{1}H-^{1}H COSY NMR spectrum of myricetin (**91**) in CD$_3$OD.
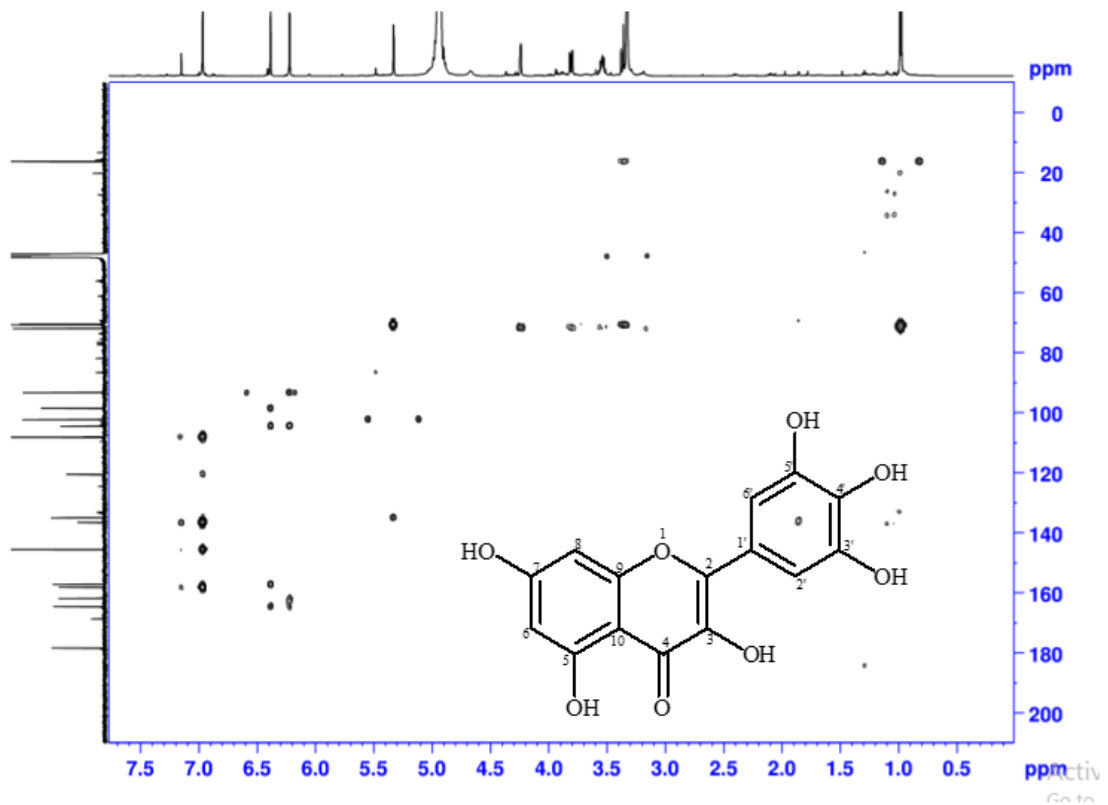
Supplementary data 130: ^{1}H-^{13}C HMBC NMR spectrum of myricetin (**91**) in CD$_3$OD.
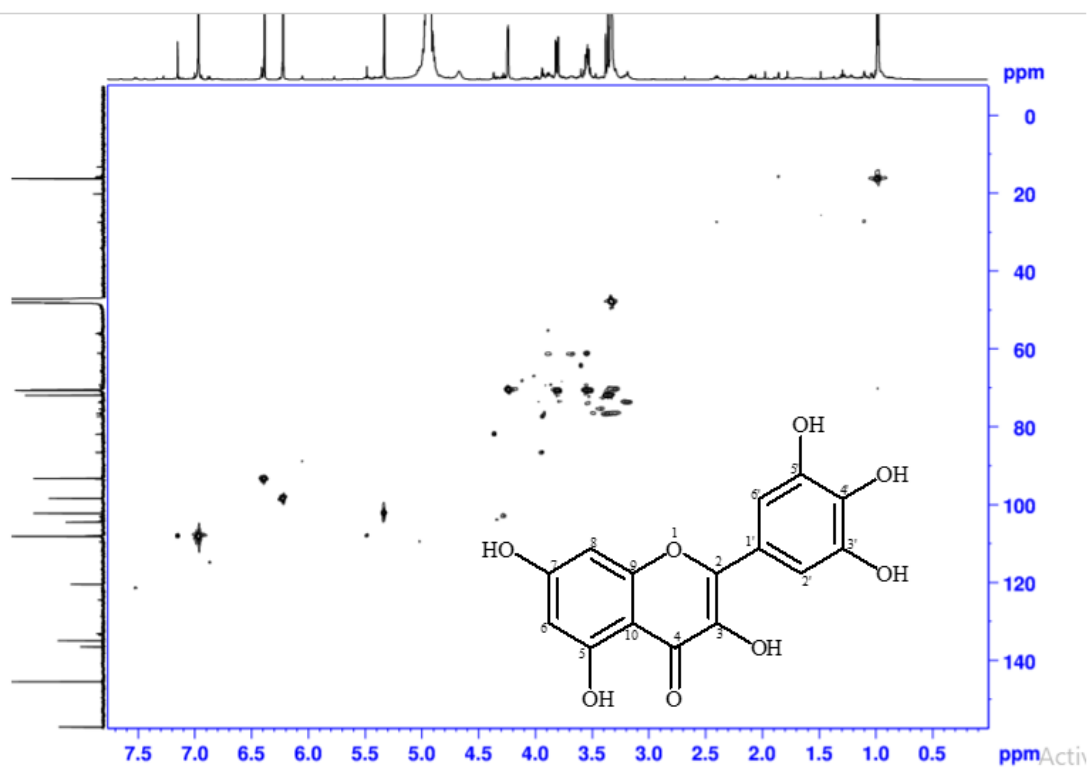
Supplementary data 131: ^{1}H-^{13}C HSQC NMR spectrum of myricetin (**91**) in CD$_3$OD.
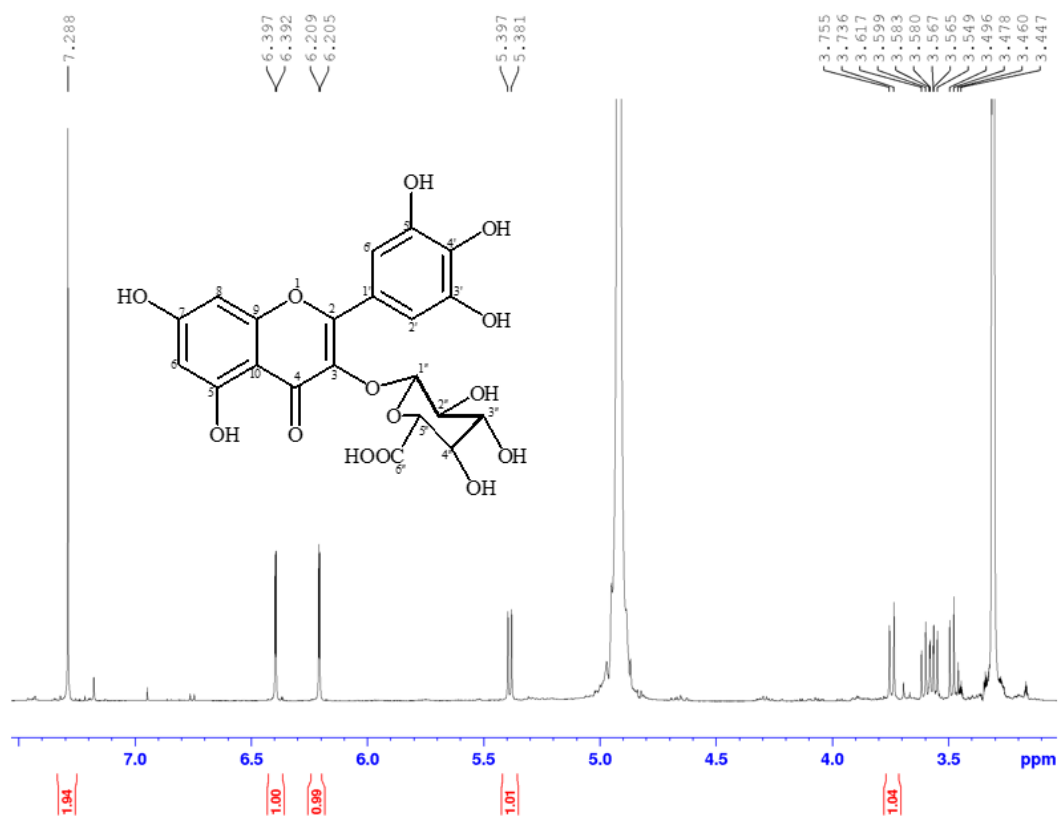
Supplementary data 132: ¹H NMR spectrum of myricetin-3-O-β-D-glucuronide (**92**) in CD₃OD.
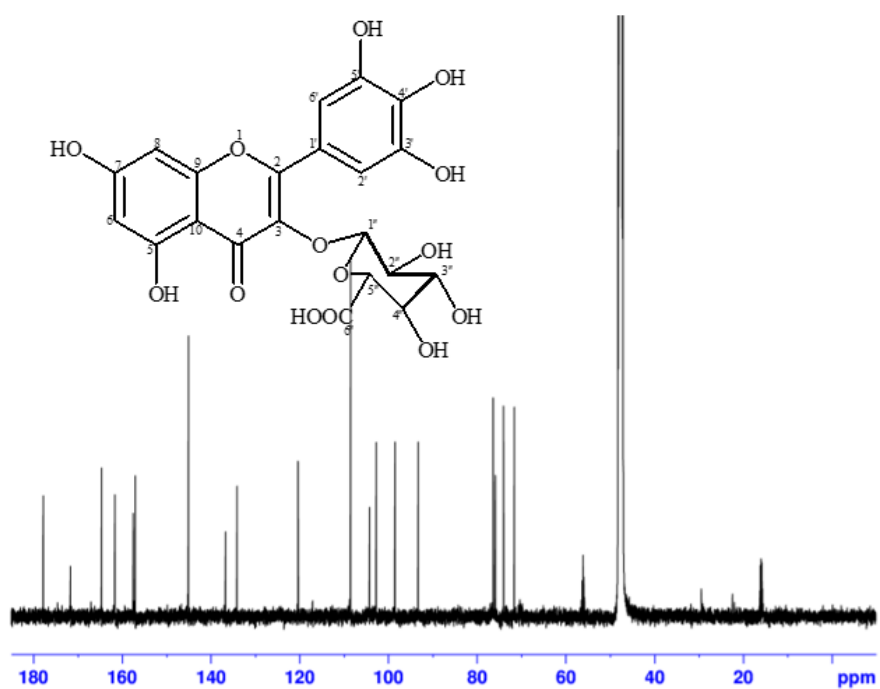
Supplementary data 133: ^{13}C NMR spectrum of myricetin-3-*O*-β-D-glucuronide (**92**) in CD$_3$OD.
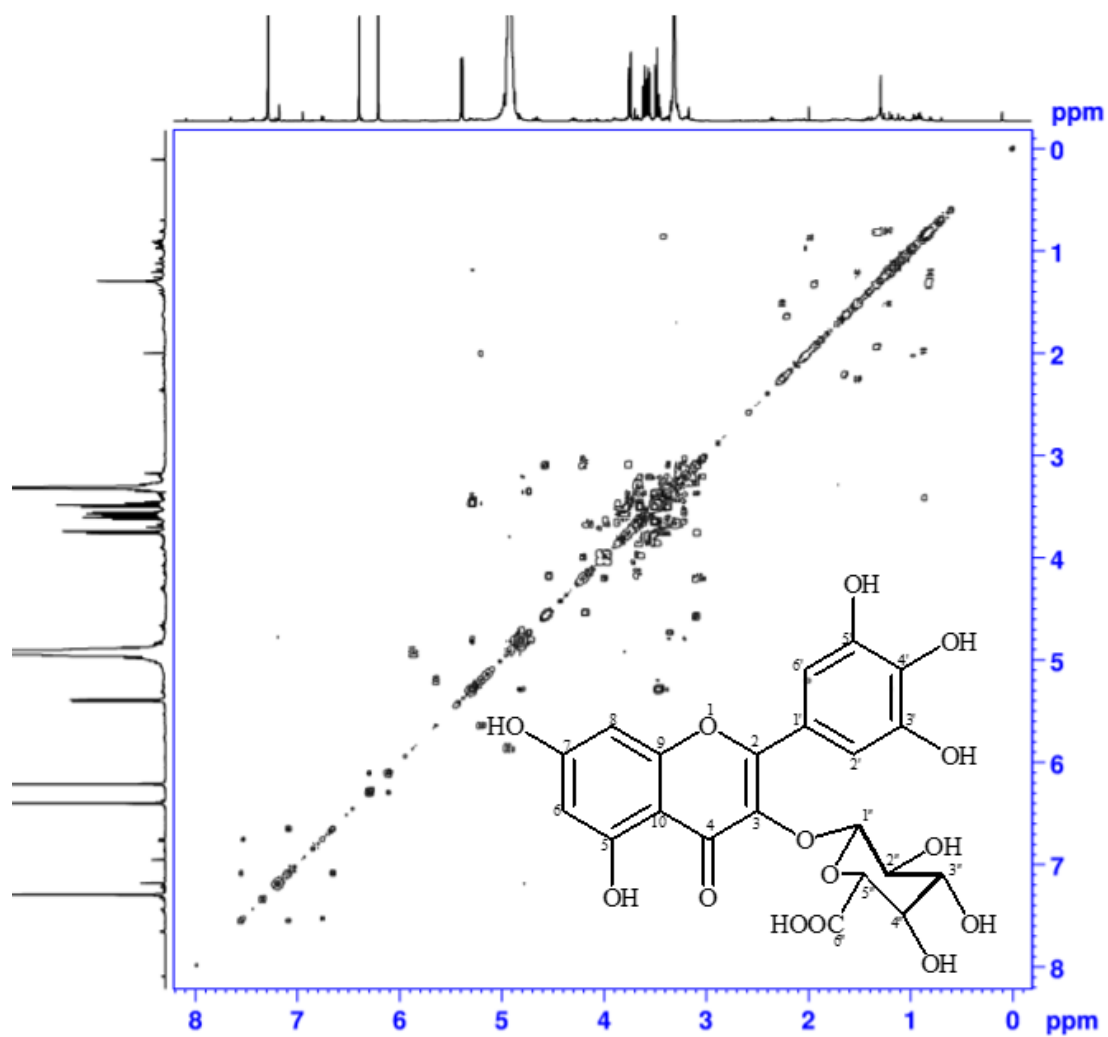
Supplementary data 134: ^{1}H-^{1}H COSY NMR spectrum of myricetin-3-O-β-D-glucuronide (**92**) in CD$_3$OD.
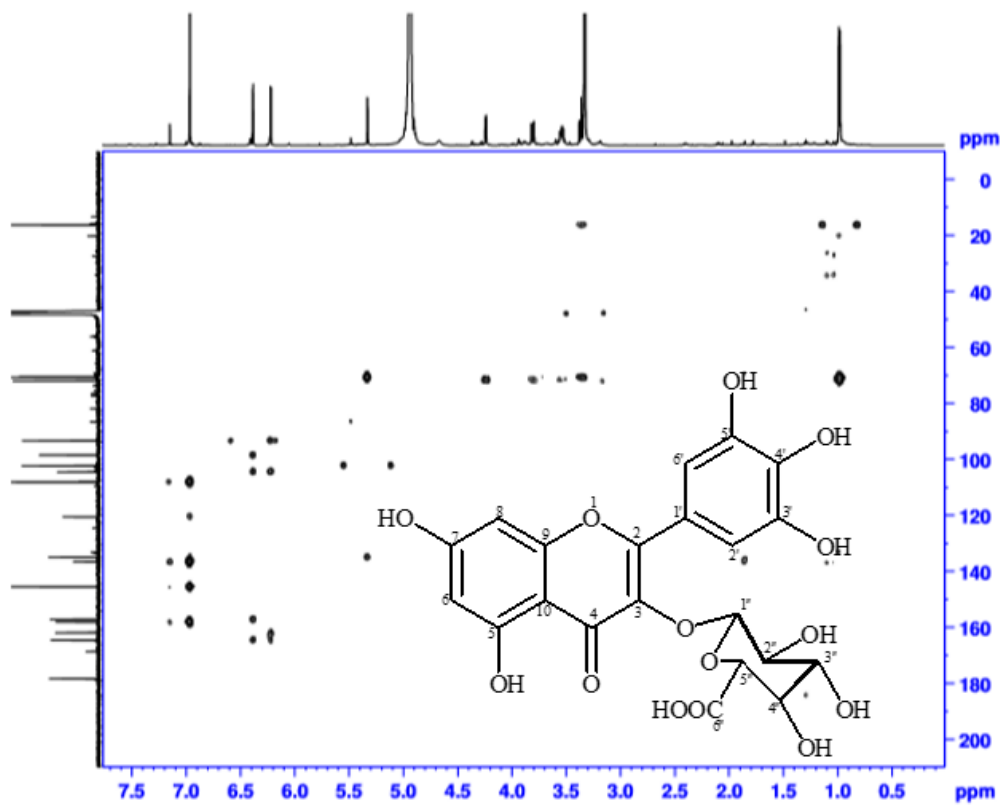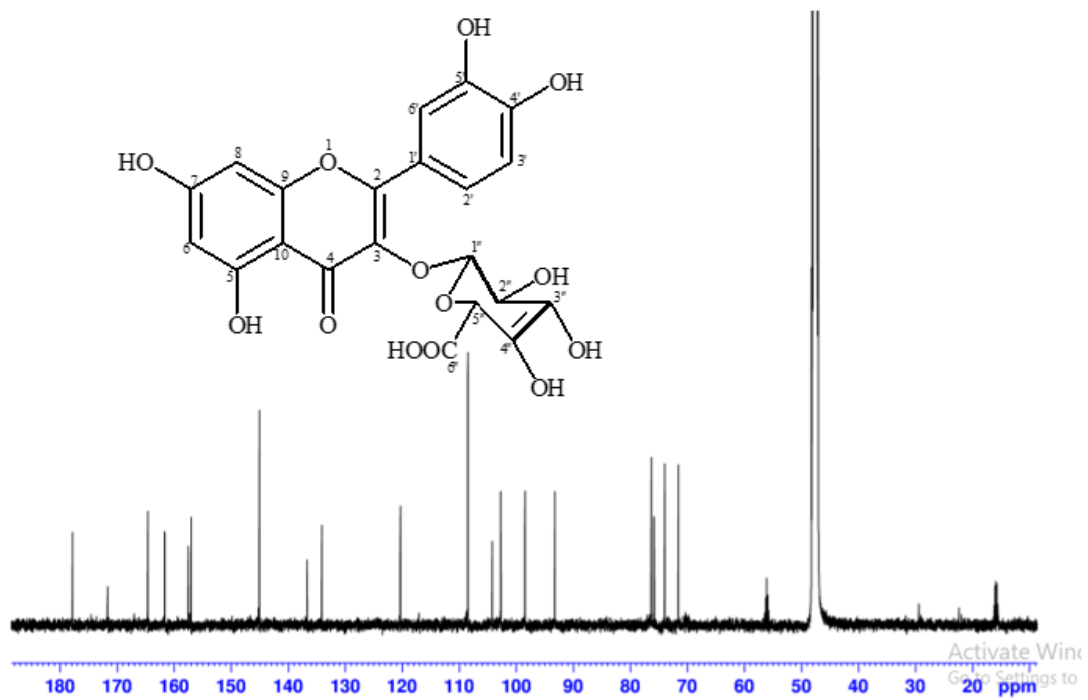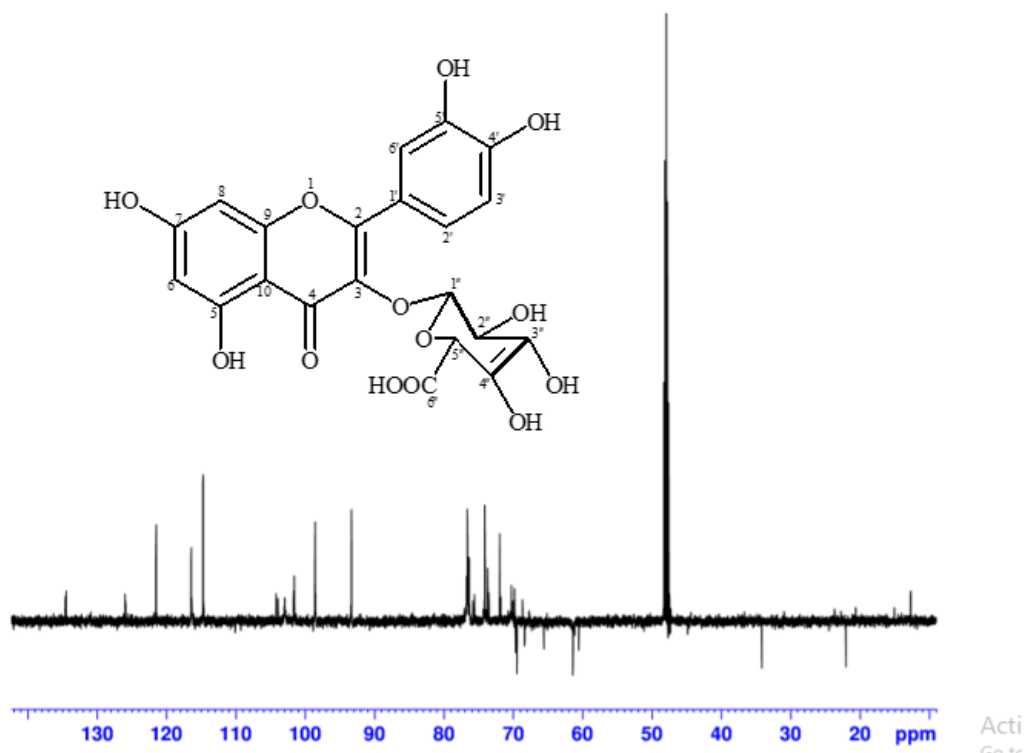
Supplementary data 135: ^{1}H-^{13}C HMBC NMR spectrum of myricetin-3-O-β-D-glucuronide (**92**) in CD$_3$OD.
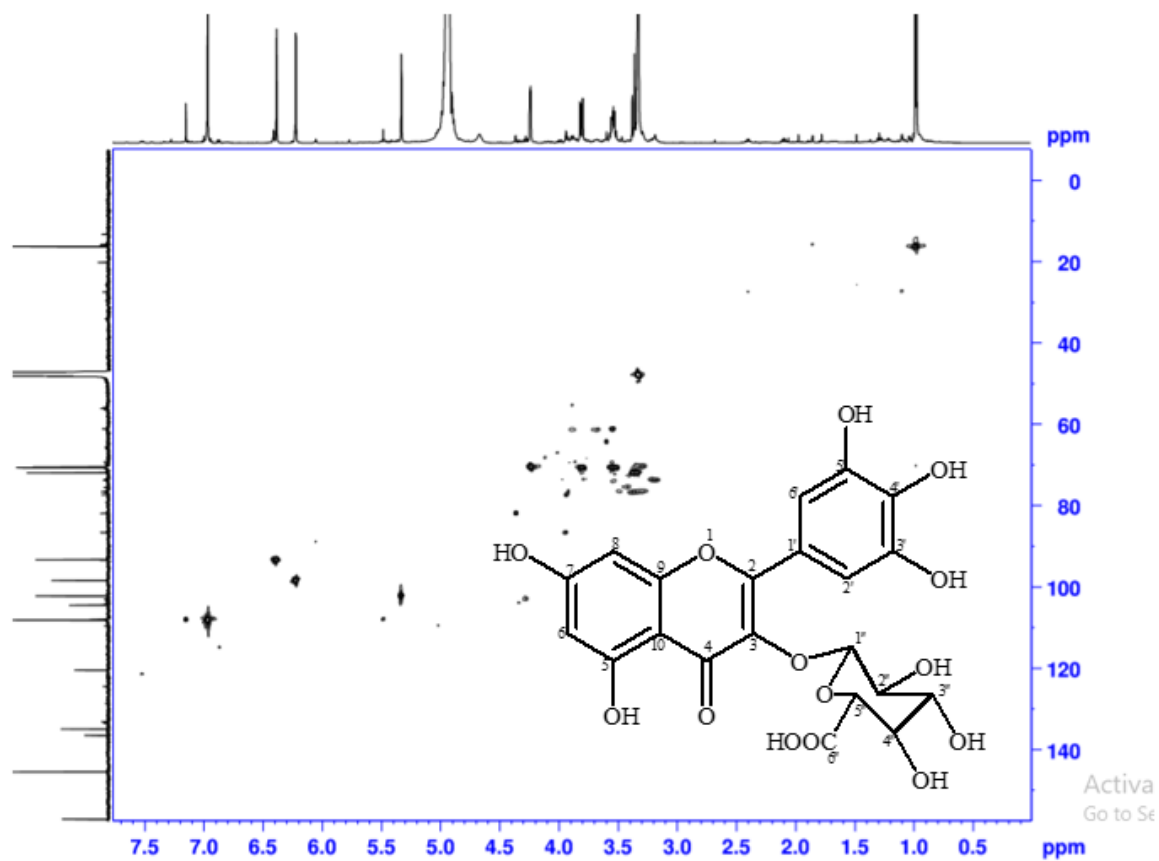
Supplementary data 136: ^{1}H-^{13}C HSQC NMR spectrum of myricetin-3-*O*-β-D-glucuronide (**92**) in CD₃OD.
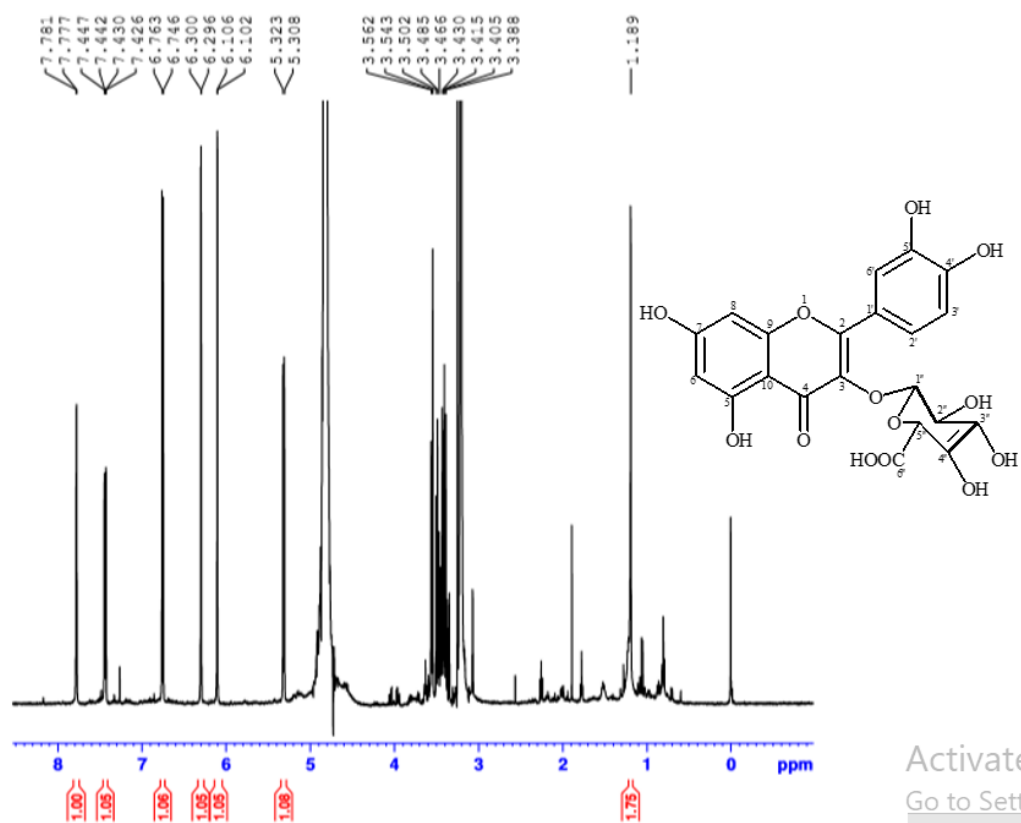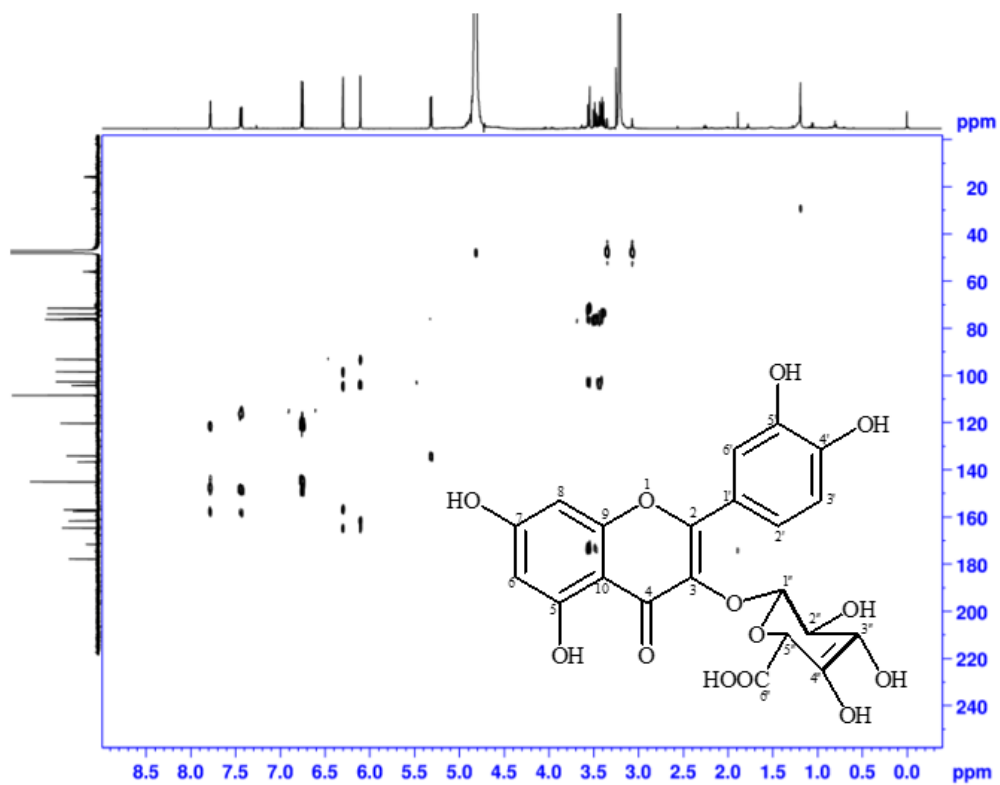
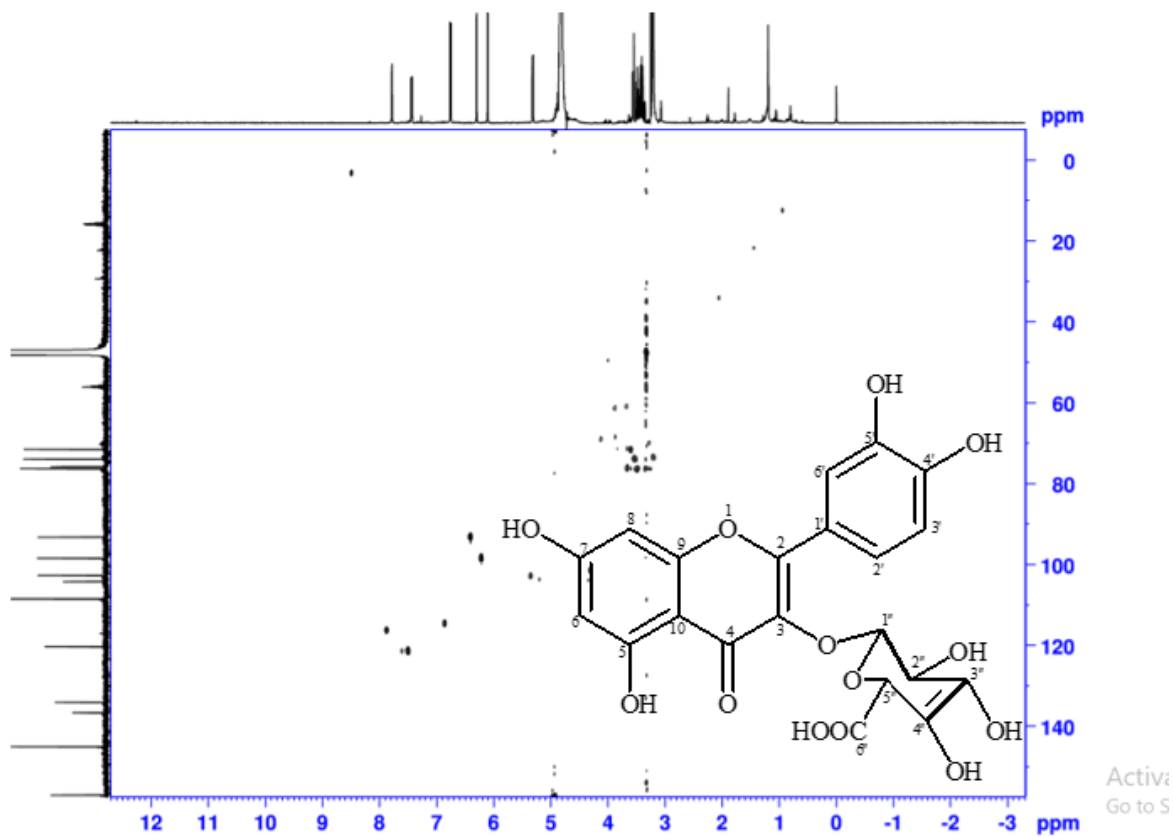**Supplementary data 137:** ^{1}H NMR spectrum of quercetin-3-O-β-D-glucuronide (**93**) in CD$_3$OD.

Supplementary data 138: ^{13}C NMR spectrum of quercetin-3-O-β-D-glucuronide (**93**) in CD$_3$OD.

Supplementary data 139: DEPT-135 NMR spectrum of quercetin-3-*O*-β-D-glucuronide (**93**) in CD₃OD.

Supplementary data 140: ^{1}H-^{13}C HMBC NMR spectrum of quercetin-3-*O*-β-D-glucuronide (**93**) in CD$_3$OD.

Supplementary data 141: ^{1}H-^{13}C HSQC NMR spectrum of quercetin-3-*O*-β-D-glucuronide (**93**) in CD$_3$OD.